ONLINE INTERACTIVE CATALOGUE OF SURVEYING TECHNOLOGIES FOR TRANSPORT INFRASTRUCTURE

IM-SAFE.EU

This project has received funding from the European Union's Horizon 2020 research and innovation programme under grant agreement No 958171.

Document Information

Name	Remark
Document Name	Online interactive catalogue of surveying technologies for transport infrastructure
Version No.	V1.0
Due date Annex I	15/07/2020
Report date	30/04/2022 (last updated in 13/04/2022)
Number of pages	80
Lead Author	Ana Sánchez Rodríguez (UVIGO)
Other Authors	Monica Longo (SAC), Serena Negri (SAC), Patrycja Sanecka (MOW), Juliusz Zach (MOW), Chiara Marchiori (IBM), Mattia Rigotti (IBM), Esra Bektas (TNO), Pablo del Río (UVIGO), Daniel Lamas (UVIGO), Javier Grandío (UVIGO), Ignacio Rodríguez (UVIGO), Mª Mercedes Solla (UVIGO), Joaquín Martínez (UVIGO), Belén Riveiro (UVIGO)
Dissemination level	Public

Document history

Ver.	Date	Remark	Author	Checked by
Rev. 0.1	13/04/2021	Creation of the document	A. Sánchez	M. Longo, S. Negri, J. Zach, C. Marchiori, B. Riveiro
Rev. 0.2	01/10/2021	First draft for revision	All	D. Allaix
Rev. 0.3	15/10/2021	Amendments on structure and content	All	A. Sánchez
Rev. 0.4	31/01/2022	Document for reviewers	All	J. Köhler, K. Bergmeister and D. Allaix
Rev. 0.5	27/03/2022	Amendments from reviewers	All	A. Sánchez
Rev. 0.6	13/04/2022	Document for approval	All	F. Cinquini and A. Bigaj-van Vliet
Rev. 1.0	30/04/2022	Document Uploaded	All	A. Bigaj-van Vliet

Document approval

Ver.	Date	Approval	Project's Role	Beneficiary
Rev. 1.0	30/04/2022	A. Bigaj-van Vliet	Coordinator	TNO

This project has received funding from the European Union's Horizon 2020 research and innovation programme under grant agreement No 958171.

Preface

This deliverable is part of the H2020 CSA IM-SAFE project and is the outcome of the first task of work package 2 (Diagnostics of structures based on inspection, monitoring and testing, task 2.1: Surveying technologies). It will help to set the basis of the proposal for the mandate to the European Committee for Standardization (CEN).

Task leader: Universidade de Vigo (UVIGO)

Contributors: SAFECERTIFIEDSTRUCTURE INGEGNERIA S.R.L (SAC)

MOSTOSTAL WARSZAWA (MOW)

NEDERLANDSE ORGANISATIE VOOR TOEGEPAST NATUURWETENSCHAPPELIJK ONDERZOEK (TNO)

WP2 helps to identify and obtain an inventory of state-of-practice as well as advanced developments with regard to condition survey technologies and data analysis methods that are applicable to transport infrastructure, especially for bridges and tunnels.

This document contains a revision of a particular selection of surveying technologies, including their main characteristics, performance, and performance indicators (PIs) that can measure in some way.

This project has received funding from the European Union's Horizon 2020 research and innovation programme under grant agreement No 958171.

Executive summary

This document aims to offer a detailed description of the surveying technologies considered within this project for condition survey of transport infrastructure, more specifically bridges and tunnels.

The document will be divided into three main sections:

- Surveying technologies, being classified as destructive or non-destructive as the most general classification
- Data analysis methods, studying the most common ones for the selection of surveying technologies made
- Fitness-for-purpose, as the strategy to follow when deciding which surveying technology should be used for each specific case study

From the information gathered in this document, an online interactive catalogue containing the main characteristics for each surveying technology was created.

This project has received funding from the European Union's Horizon 2020 research and innovation programme under grant agreement No 958171.

Table of Content

DOCUMENT INFORMATION 1
DOCUMENT HISTORY 1
DOCUMENT APPROVAL 1
PREFACE 2
EXECUTIVE SUMMARY 0
TABLE OF CONTENT 0
TABLE OF FIGURES 0
TABLE OF TABLES 0

1 PROBLEM STATEMENT 9

1.1 INTRODUCTION 9
1.2 OBJECTIVES OF THE DELIVERABLE 9
1.3 CONTENT 10

2 INFORMATION FLOW IN WP2 11

3 SURVEYING TECHNOLOGIES AND SEMANTIC WIKI 13

3.1 INTRODUCTION 13
3.2 GENERAL CHARACTERISTICS 14
3.2.1 OBJECTIVES OF THE MONITORING ACTIVITIES 14
3.2.2 MAIN CHARACTERISTICS OF THE TECHNOLOGY 14
3.2.3 BACKGROUND 17
3.2.4 PERFORMANCE 17
3.2.5 INTERPRETATION AND VALIDATION OF RESULTS 21
3.2.6 ADVANTAGES AND DISADVANTAGES 21
3.2.7 POSSIBILITY OF AUTOMATISING THE MEASUREMENTS 21
3.2.8 BARRIERS 22
3.2.9 EXISTING STANDARDS 22
3.2.10 APPLICABILITY 22
3.2.11 AVAILABLE KNOWLEDGE 22
3.3 SEMANTIC WIKI 23
3.3.1 WP2 KNOWLEDGE MODEL 23
3.3.2 RESULT 24

4 DATA ANALYSIS 25

4.1 INTRODUCTION 25
4.2 DESCRIPTION OF ANALYSIS METHODS 25
4.2.1 PARAMETRIC-, MODEL- AND PHYSICS-BASED METHODS 25
4.2.2 BAYESIAN VS FREQUENTIST STATISTICS 26
4.2.3 DESCRIPTIVE STATISTICS FOR SCIENTIFIC OBSERVABLES 27
4.2.4 FITTING OF DATA TO PROBABILITY DISTRIBUTIONS 30
4.2.5 OUTLIER DETECTION AND ROBUST REGRESSION 31
4.2.6 METHODS BASED ON CORRELATIONS 31
4.2.7 DIMENSIONALITY REDUCTION METHODS 31
4.2.8 ANALYSIS METHODS FOR TIME DEPENDENT DATA 33
4.2.9 MODAL ANALYSIS 34

This project has received funding from the European Union's Horizon 2020 research and innovation programme under grant agreement No 958171.

4.2.10 ANALYSIS METHODS FOR BIG DATA 37
4.2.11 MACHINE LEARNING 38
4.2.12 DEEP LEARNING 42
4.2.13 CLASSIC COMPUTER VISION TECHNOLOGIES VS DEEP LEARNING METHODS 49

5 FRAMEWORK FOR EVALUATING THE FITNESS-FOR-PURPOSE OF SURVEYING TECHNOLOGIES 54

5.1 TRL VS FIT-FOR-PURPOSE 54
5.2 CRITERIA FOR EVALUATING THE FITNESS-FOR-PURPOSE OF TECHNOLOGIES FOR CONDITION SURVEY 56
5.2.1 FITNESS FOR PURPOSE IN THE BROAD SENSE & IM-SAFE INTERPRETATION 56
5.2.2 FITNESS FOR PURPOSE IN ACHIEVEMENT STANDARD 91610 56
5.2.3 FITNESS-FOR-PURPOSE CONSIDERING THE SUPPLY AND DEMAND CHAIN OF MONITORING AND MANAGEMENT OF STRUCTURES 60
5.3 IM-SAFE APPROACH TO EVALUATE THE FITNESS-FOR-PURPOSE OF TECHNOLOGIES FOR CONDITION SURVEY 62

6 SUMMARY AND CONCLUSIONS 64

7 BIBLIOGRAPHY 65

8 APPENDIXES 80

This project has received funding from the European Union's Horizon 2020 research and innovation programme under grant agreement No 958171.

Table of Figures

Figure 2.1 – Information flow in WP2 11

Figure 3.1 – Classification of surveying technologies and platforms by IM-SAFE 13

Figure 3.2 – Ideal curve and sensitivity error [4] 16

Figure 4.1 – Comparison between parametric and non-parametric methods 26

Figure 4.2 – Process experimental verification of structure dynamic parameters 35

Figure 4.3 – List of techniques for OMA data 36

Figure 4.4 – Overview of modal parameters extraction through FFT-based analysis. 36

Figure 4.5 – Pros and cons of different OMA techniques 37

Figure 4.6 – Examples for parametric and non-parametric methods for nonlinear and non-stationary systems 37

Figure 4.7 – Example of a map reduce job [34] 38

Figure 4.8 – Confusion Matrix for multiclass classification. TP, FP, TN and FN are assigned with respect to class B 40

Figure 4.9 – Single neuron or node 43

Figure 4.10 – Network of layers of neurons or nodes [40] 43

Figure 4.11 – Diagram of a feedforward ANN [41] 44

Figure 4.12 – Architecture elements of CNN [45] 45

Figure 4.13 – Convolutional operation on the RGB channels of an image patch [47] 46

Figure 4.14 – Temporal unfolding of the dynamics of an RNN [44] 47

Figure 4.15 – Classic computer versus Deep Learning approaches 49

Figure 4.16 – Computer vision tasks [67] 50

Figure 4.17 –Timeline of the introduction of instance segmentation DL-based models [68] 51

Figure 4.18 – The architecture in [67] 51

Figure 4.19 – The Fast R-CNN architecture of [69] 52

Figure 4.20 – Feature Pyramid Networks for Object Detection. Visual representation [71] 52

Figure 4.21 – The Mask R-CNN architecture of [72] 53

Figure 5.1 – The valley of death bridging the gap between research and commercial application 54

Figure 5.2 – Representative Schedule for Identifying CTEs [74] 55

Figure 5.3 – Representative Schedule for Assessing CTE Readiness [74] 56

Figure 5.4 – The 7-step diagram used to describe case studies (Adaptation from [83]) 61

This project has received funding from the European Union's Horizon 2020 research and innovation programme under grant agreement No 958171.

Table of Tables

Table 4-1 – Descriptive statistics 27
Table 4-2 – Measures of central tendency in detail 28
Table 4-3 – Measures of variability in detail 29
Table 4-4 – Measures of symmetry in detail 29
Table 4-5 – Definition of multiclass classification metrics 41
Table 4-6 – Common evaluation metrics for regression problems 42
Table 5-1 – Technology Readiness Level scale in current NASA [76] & European Union usage [77] (definitions combined) 55
Table 5-2 – Suggestions to be considered when evaluating the fitness for purpose [78] 57
Table 5-3 – IM-SAFE perspective based on ISO 9001:2015 59
Table 5-4 – Generic terms to be consider in the FFP evaluation (IM-SAFE perspective) [82] 60

This project has received funding from the European Union's Horizon 2020 research and innovation programme under grant agreement No 958171.

1 Problem statement

1.1 Introduction

In recent years, the world has faced a rapid growth of testing, inspection, and monitoring technologies in various sectors. In the domain of transport infrastructure, intensive research has been carried out to enable the use of these technologies to support asset management of bridges and tunnels These technologies allow to conduct condition survey and are therefore referred to as surveying technologies. Condition survey is the process of acquiring data and transforming it into information about the current condition of the structure with regard to its appearance, functionality and/or ability to meet the specified performance requirements. The aim of condition survey is to recognise important limitations, defects, deterioration of the structures and to support decision making regarding the remedial measures to be taken. During condition survey, data may be obtained by activities such as inspection, monitoring and testing through a wide range of data collection technologies and data analysis methods. However, accepted and harmonised approaches to condition survey are lacking until now.

The current state of standardisation on inspection, monitoring and testing of civil structures consists of guidelines published in a limited number of European countries and few ISO standards on dynamic tests of bridges. These documents provide the user with information and guidelines on the technologies, execution of the surveying activities and data analysis. Nevertheless, the current standards and guidelines do not address sufficiently the complex combination of decisions that would result into gathering relevant and sufficient information about the condition of the structure for the purpose of asset management. This hinders asset owners and public authorities in charge of maintenance of the transport infrastructure to apply the latest developments.

If monitoring were to be standardized, some actions should be taken into consideration, such as providing definitions and vocabulary in this context, and developing an approach for decision making regarding the surveying strategy.

This report aims to respond to this challenge by reviewing data collection technologies and data analysis methods used in condition survey and identifying their requirements. Data collection technologies and data analysis methods that are applicable to transport infrastructure, especially for bridges and tunnels, will be discussed. This objective will be achieved taking into consideration the demands of data-informed diagnostics of structures and reviewing the current practice of relevant projects.

All the information gathered regarding surveying technologies will be part of an online catalogue. This catalogue is to be implemented through a semantic wiki, which is a free and open-source extension to the wiki software.

1.2 Objectives of the deliverable

The present report aims to collect information in the context of surveying technologies used for condition survey to meet the requirements specification to support WP5 in drafting the mandate for CEN. The activities of WP2 will provide input for the part of the draft mandate concerning the “new standard on structural monitoring”. Within this context, the objectives of task T2.1 are:

- To review data collection technologies used for condition survey, including devices and platforms. A comprehensive insight will be generated with regards to:
    - Satellite technologies, including optical and radar monitoring
    - Aerial und UAV technologies, including optical and NDT payloads

This project has received funding from the European Union’s Horizon 2020 research and innovation programme under grant agreement No 958171.

- Terrestrial dedicated inspection platforms, including GNSS, IMU, cameras and LiDAR
- IoT and sensor networks/systems for in situ monitoring, including Distributed Optic Fibre Techniques, MEMS, Weight-in-Motion methods
- NDT active or passive testing technologies, including Acoustic Emission Techniques, Guided Wave Techniques, Ground Penetrating Radar, Magnetic and Electrical Methods, Radioactive and Nuclear Methods.
- Destructive and semi-destructive techniques commonly used in practise:
  - Physical methods: mechanical tests on cored samples (compression, tensile, fatigue, torque, etc.), surface measurements (hardness, Schmidt hammer, penetration, pull-out test), boroscopy, endoscopy, water penetration, water resistance, etc.
  - Chemical methods: qualitative methods (pH test, Rainbow test, etc.) and quantitative methods (Alkali test, Chloride tests, Electroanalytical tests).

- To review data analysis methods used in condition survey, such as:
  - Modal Analysis (MA)
  - Statistical analysis methods
  - LSI for satellite, aerial, and terrestrial sensor data
  - Big Data Analytics and Artificial Intelligence (Ref. T4.4).
- To define of procedures for calibration, initialisation, parametrisation, and configuration of data collection in condition survey; and procedures for defining layout, set-up for data collection, and data analysis methods in condition survey. This will be performed in the context of each surveying technology analysed within the project.

1.3 Content

The present report is divided in seven different chapters. In this section, a short description of each of them is provided.

Chapter 2 presents the flow of information between the two tasks of work package 2 (WP2), which are “surveying technologies” and “diagnostics of structures”. Here, this relation is described, giving in T2.2 context to all the information gathered in the present task (T2.1). Then, Chapter 3 provides a general description of the sections included in the reports about each surveying technology described within the project. This has been done following standardised definitions and guidelines when possible. These will be part of the online catalogue of the project (Semantic Wiki).

In Chapter 4, an analysis of the most used data analysis methods for each surveying technology in Chapter 2 has been performed. With that context, a broad description of those data analysis methods is provided, considering that can be used for several types of data. In the next deliverable (ref. D2.2), a context is provided in relation with surveying technology and damage process.

Finally, Chapter 5 describes fitness for purpose in the context of technologies, and provides a criterion for evaluating it on technologies for condition survey. And to sum up, the conclusions and summary of this report are provided in Chapter 6, followed by the list of references (Chapter 7) and Annex A. The latter contains detailed information about each surveying technology analysed within the project.

This project has received funding from the European Union’s Horizon 2020 research and innovation programme under grant agreement No 958171.

2 Information flow in WP2

IM-SAFE proposes the basis for the assessment of the structural condition of an asset based on the integration of inspections, monitoring, and testing. The information gathered from the structure can be used for assessing safety and risk levels of the structure as well as for predicting the future safety and risks. In work package two (WP2), different information regarding surveying technologies, data analysis methods, damage processes to be detected, and the different analysis phases existing is collected. The need for clarification of the relationship between the available information and condition survey has led to the development of the information flow presented in Figure 2.1, and will be further explained along this chapter. This information flow describes the path followed by data in the process of condition surveying and during the lifespan and maintenance process of the structure. The main objective of the work package is to propose a methodology to use when evaluating the health condition of several structures. This flow includes the choice of the most appropriate surveying technologies, the data analysis methods to be used, how to detect all damage processes acting on the structure, and how to relate the information coming from different instruments.

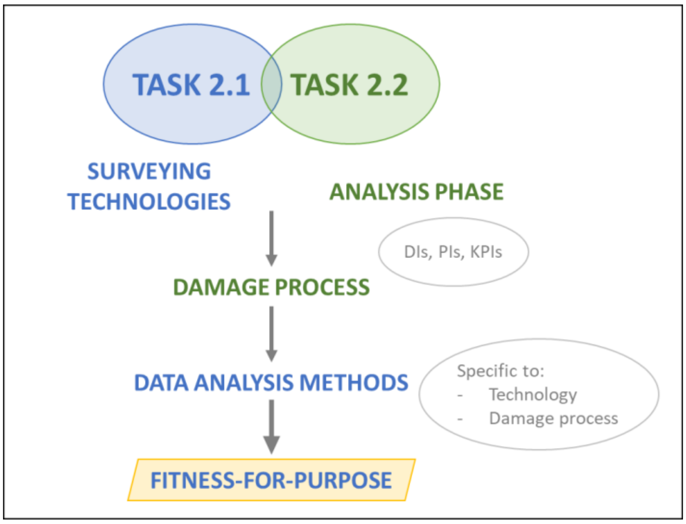

Figure 2.1 – Information flow in WP2

In the first task of this work package (T2.1), which is directly related with the present deliverable (D2.1), the objective was to create an online catalogue containing general information about different surveying technologies used for condition survey (see Chapter 3). It is based on the review of relevant documentation, standards, and guidelines specific for each of them about their performance and general characteristics, among others. This information can also be consulted on Annex A.

Deliverable D2.1 also considers the different data analysis methods that can be used depending on: (i) the type of data used as an input, which directly depends on the surveying technology used for the data gathering; and (ii) the specific application (detection or measuring of a definite damage process, and actions on the structure). While Chapter 4 of D2.1 gives a general overview of the most used data analysis methods for all the surveying technologies considered in the project, Chapter 5 of D2.2 presents the dependency between these two and the specific application. In addition, it is important to highlight the reliance on the analysis phase (Chapter 3, 4, and 6 of D2.2).

Deliverable D2.2 is completed by making an overview of damage and degradation mechanisms for bridges and tunnels, presenting the different processes for damage evaluation. Moreover, the deliverable includes a description of the different damage and

This project has received funding from the European Union's Horizon 2020 research and innovation programme under grant agreement No 958171.

degradation processes that might affect bridges and tunnels. This is in direct relation with surveying technologies and data analysis methods, as explained in the previous paragraph. The document also proposes a relation between the studied damage processes and the damage and performance indicators evaluated in work package three (WP3).

This general review is required to help in the decision-making process to choose among different technologies that share a common application. Apart from the specific characteristics of each surveying technology, this decision-making process is also based on (see Chapter 5):

- Specific application
- Repeatability and reproducibility of measures
- Data collection plan
- Maintenance of the asset/infrastructure
- Cost/benefit evaluation

This project has received funding from the European Union's Horizon 2020 research and innovation programme under grant agreement No 958171.

3 Surveying technologies and semantic wiki

3.1 Introduction

The main contribution of task T2.1 is to create an online interactive catalogue of surveying technologies for transport infrastructure. This catalogue is to be made by using a knowledge model integrated as a wiki of the whole IM-SAFE project, including information from three work packages: WP1, 2 and 3. The information gathered under T2.1 for this catalogue has been recruited with the form of individual reports for each surveying technology considered in the project. These reports can be consulted both online and as Annex to this document (Annex A), and will answer, among other things, to the following main three questions:

- What can be measured?
- Which results can be achieved or expected?
- How fit are the results to describe the health of the structure?

The schema provided in Figure 3.1 is the classification approach chosen in this project, although there are several others that could be chosen. For instance, a more general approach would be to classify the technologies into global or local surveying. In addition, a deeper class would depend on the type of measure (static and/or dynamic).

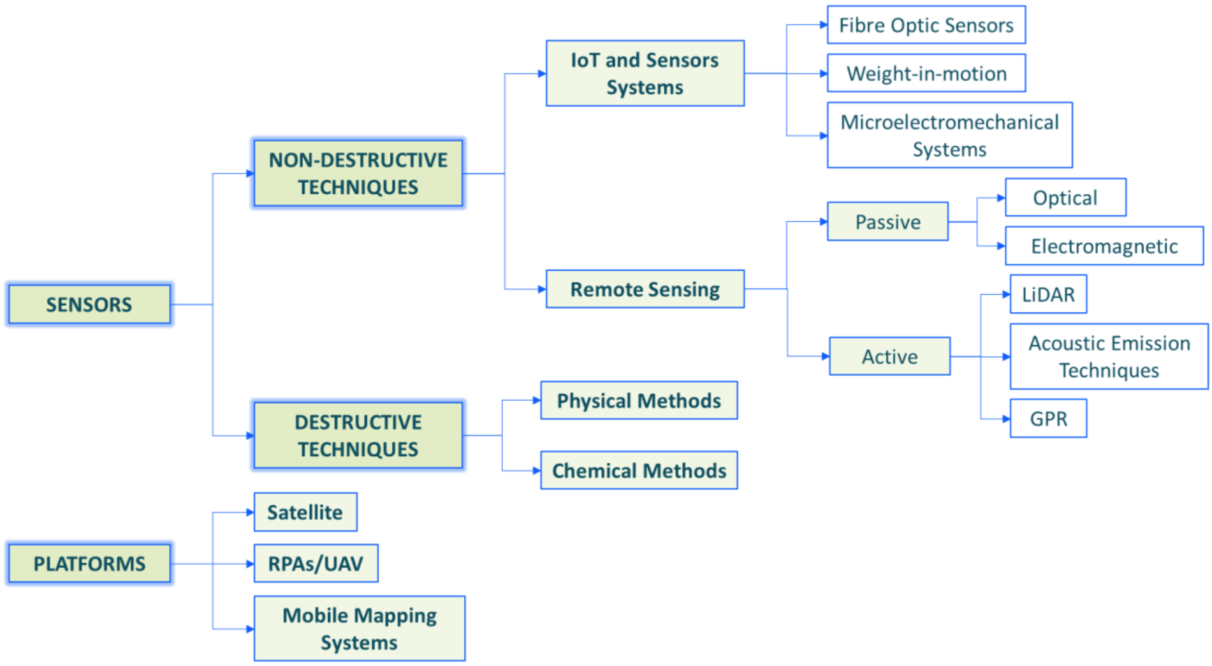

Figure 3.1 – Classification of surveying technologies and platforms by IM-SAFE

These technologies rely on sensors for data acquisition and processing to obtain raw data that support digitalization through data analysis to obtain meaningful information. Sensing technologies are based on transducers that produce an output signal to study and sample a physical phenomenon with the aim of attaining information about the condition of the physical property of interest. To this end, a distinction can be made between: (i) primary sensors, as transducers from a specific physical domain to other physical domain and (ii) sensors that provide a signal in the electrical domain. In certain cases, the physical magnitude of interest cannot be measured directly and it is necessary to use sensors that measure related physical phenomena. This type of indirect measurement is also known as proxy sensors. Low-power electrical signals may need a conditioning step to amplify the signal and filter the noise in the measurements. Conditioned signal can be stored or transmitted to an intelligent device for

This project has received funding from the European Union's Horizon 2020 research and innovation programme under grant agreement No 958171.

processing. Sensors can also be classified depending on their need of energy sources to perform the sampling and can be differentiated as: (i) passive sensors, if they only use an external source of energy (such as a digital camera); and (ii) active sensors, which are those that need an internal source of energy to perform the sampling of the interest phenomenon (e.g., RADAR or SONAR sensors). Both active and passive sensors can be placed in several platforms that support the sampling process in a variety of conditions and locations. These include terrestrial platforms that consist of on-site fixed systems for monitoring and mobile systems for surveying, and, with the lowering access costs, aerial platforms based on unmanned aerial vehicles (UAVs) and satellites. Regardless their classification, the signals that come from a sensor need to be digitized to obtain the so-called raw digital data. This process of Analog-to-Digital conversion is always subjected to quantization error and depends on the digital resolution of the sample but, as a result, a raw digital data can be obtained. This raw data, after a processing step, results in the digital data that can be considered as basis for digitalization.

This chapter provides a general description of the sections included in the report for each surveying technology, following standardised definitions and guidelines when possible.

3.2 General characteristics

3.2.1 Objectives of the monitoring activities

The first section of the report contains information about what is the main objective of performing surveying activities with the technology at hand. Here, a clear statement should be made regarding why the surveying technology being analysed is used for monitoring or inspecting bridges or tunnels, and what are the benefits of using it.

The main goal is to help identifying the appropriate differentiating features to consider when choosing one technology or another while seeking for the same result, whether it is the monitoring, inspection, or testing of a predefined asset.

3.2.2 Main characteristics of the technology

The variety of existing monitoring technologies can be defined attending to certain characteristics, which are described in this section. The definition and important aspects of each technology are also addressed.

3.2.2.1 Functioning mode

This section of the report provides a general description of the surveying technology, including the sensors composing the equipment and the way they interact with the media to obtain the required measurements from them.

3.2.2.2 Types

Some surveying technologies might be categorised attending to different principles. In this section, a short description of the existing types should be provided, including a comparison between them and when to choose one or another.

3.2.2.3 Process/event[1] to be detected or monitored

The event to be detected refers to the purpose of using the surveying technology for monitoring, inspection or testing of the asset. For instance, measuring the displacement of an element, or indicate the presence of flaws. This coincides with physical phenomena that can be measured by the surveying technology, as an event can be defined by several physical quantities, and a physical quantity can define several events. Therefore, a single surveying technology can be used to detect various events.

---

[1] Event: Phenomenon serving as a basis of a measurement [1].

This project has received funding from the European Union's Horizon 2020 research and innovation programme under grant agreement No 958171.

This relationship between events and physical quantity is what makes the comparison between different surveying technologies so important. Many options can be used for the same event, but they might rely on different physical quantities that are not the best approach for the scenario. Therefore, this section is to define the event to be detected.

3.2.2.4 Physical quantity to be measured

One of the most important aspects when selecting a surveying technology is to know what is to be measured (physical quantity) and what results are expected from the measurement. Following the definition given in [1], “a physical quantity is a property of a phenomenon, body, or substance, where the property has a magnitude that can be expressed as a number and a reference”. In most of the cases, it is necessary to further analyse these data to be able to know the damage process or processes acting on an asset.

Different equipment forming a surveying technology can measure different physical quantities depending on their nature. They quantify a property of the object under study and can be expressed as a value with its characteristic units.

1.1.1.1 Induced damage to the structure during the measurement

During the measurement process, the structure could incur damages that adversely affect its structural components. Following the definition given in [2], damage is understood as "an unfavourable change in the condition of a structure that can affect structural performance". According to their induced damage to the structure, surveying techniques can be classified as destructive and non-destructive.

In non-destructive[2] techniques, the equipment does not alter the structure in any way, and therefore avoid inducing damage to it. On the other hand, destructive techniques do induce a certain damage with the objective of better analysing the performance and properties of the materials of the structure. While each technique induces different damages, most of them cause imperceptible damages that do not affect the structural stability.

The aim of this section is to categorise each surveying technology under study into destructive or non-destructive ones. In the case they are destructive technologies, a description of the damage induced to the structure should be provided, together with the related impact on the structural performance (if any).

3.2.2.5 Measurement type

In this section, a general classification of measurements is proposed. This classification is based on the time-dependency of the data acquisition, taking into account both the sampling frequency and the test frequency.

- Static measurement[3]: The output signal of the instrument can be regarded as constant. The measurement is also considered static when the instrument changes after each measure. The test returns a single measurement that is related to a specific point in time.
- Dynamic measurement[4]: The output signal changes over time. This type of measurement is used for synchronized real-time continuous monitoring. Normally, each measurement value is either related to a specific time or position and is continuously stored. The test is performed over a time interval and returns a series of values.

---

[2] Non-destructive test: Technologies used to evaluate the properties of a material, component or system without causing damage [143].

[3] Static measurements: Measurement made with the equipment stationary relative to the product to be tested [140].

[4] Dynamic measurements: Measurements used for synchronized real-time continuous monitoring [140].

This project has received funding from the European Union’s Horizon 2020 research and innovation programme under grant agreement No 958171.

A measurements classification based on the phenomenon description can be made. It is often distinguished global and local measurements.

- Global measurements: Global measures are those measures that provide the complete valuation of an object surveyed or phenomenon [3].
- Local measurements: Local measures provide the overall valuation of one quantity of an object surveyed or phenomenon. Local measurements are typically used in various items to measure all appropriate global features of dimensions [3].

A classification based on measurement collecting data time can be made to differentiate the spatial measurement types. It is often distinguished between continuous and discrete measurements, as follows.

- Continuous measurement: refers to change over time, including complex numbers and varying data values that are measured over a specific time interval [3].
- Discrete measurement: is a numerical type of measurement that includes concrete numbers, with specific and fixed data values in a particular time [3].

3.2.2.6 Measurement range

An important aspect to consider in choosing the proper equipment for each surveying technology is their measurement range[5]. The measurement range comprises the maximum and minimum values of a physical quantity that can be measured by a sensor (see Figure 3.2). This is normally settled down under defined conditions with specified instrumental uncertainty[6].

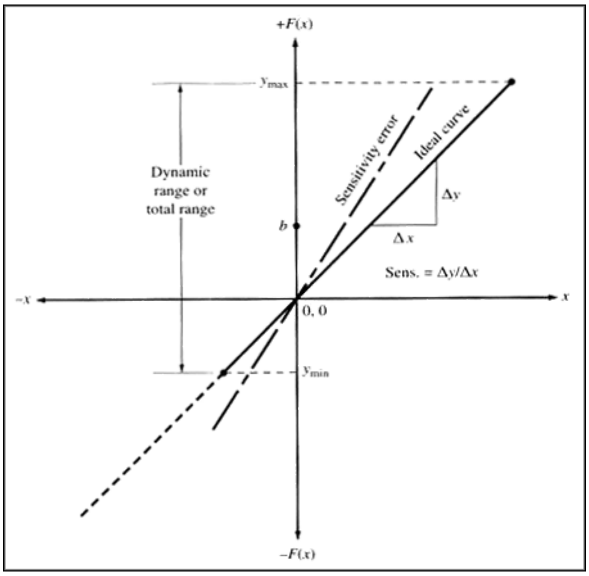

Figure 3.2 – Ideal curve and sensitivity error [4]

[5] Measurement range: Set of values of quantities of the same kind that can be measured by a given measuring instrument or measuring system [147].

[6] Uncertainty (of measurement): Non-negative parameter characterizing the dispersion of the quantity values being attributed to a measurand, based on the information used [1].

This project has received funding from the European Union's Horizon 2020 research and innovation programme under grant agreement No 958171.

3.2.2.7 Measurement accuracy

The accuracy of any measurement tends to be influenced by several factors, including the instruments employed, the methods used, and the skill of the experimenter. The measurement accuracy[7] is defined by ISO 3534, 2006 as the “closeness of agreement between a test result and the accepted reference value”. It can be expressed in absolute terms or as a percentage of full scale. Two types of accuracy can be distinguished:

- Instrument accuracy[8]: Measurement tolerance, or transmission of the instrument (depending on instrument intrinsic properties) that defines the limits of the errors made when the instrument is used in normal operating conditions. This is a numerical quantity, uniquely determinable.
- Test accuracy: Measurement dependence on the test procedure. The ability to measure the true value in a sample.

3.2.3 Background

This section is intended to provide a literature review for each of the surveying technologies being analysed, with an evolution through the years from the invention until today.

3.2.4 Performance

The performance of a surveying technology is a set of practices, processes, that in a scientific and systematic manner help to improve the desired outcomes of the survey [5]. Here, an analysis of the requirements and important aspects to be considered before and during the data gathering is provided.

3.2.4.1 General points of attention and requirements

- Design criteria and requirements for the design of the survey

  This part of the report is to contain a thorough description of the design aspects of the survey, such as:

  - Survey objectives. They should be clearly established, defining its scope, the location where the survey takes place, the asset of interest, the attributes to be assessed regarding that asset, and the length of the monitoring period.
  - Site and structure pre-checking. This includes the steps to assess the suitability of the site where the monitoring activity is taking place, as well as the description of the structure and the relevant details to consider prior to its monitorization. With this, general access constraints and the appropriate areas to place the sensors on the structure, or its surroundings, should be defined.
  - Survey planning. Here, it is intended to describe the general requirements, including safety assessment during the monitoring activity; the definition of the survey layout, composed of location of the instruments and accessory elements, if any; and the installation process.
  - Risk assessment. Enumerate, evaluate, and foresee mitigation measures related to the operation risks. In the case of small sensors requiring installation work to embed them in the structure, indicate if there is a need of disruption that may happen in the affected asset.

[7] Measurement accuracy: Closeness of agreement between a test result and the accepted reference value (ISO 3534, 2006).

[8] Instrument accuracy: Ability of a measuring instrument to give responses close to the true value [150]

This project has received funding from the European Union’s Horizon 2020 research and innovation programme under grant agreement No 958171.

- Permission application. Indicate the permission requirements for the development of the monitoring activity. This includes any regulation constraints or the need to contact the proper authority to communicate the survey plan and obtain the required permits.
- Environmental effects. Specify the need of consideration of the influence of external forces in the survey environment and process (weather, illumination, traffic, etc.).

- Procedures for defining layout of the survey

  In this section of the report, it is important to specify if there are any existing manuals, guidelines, and standard procedures for the design and layout of the surveying technology involved. In the case that the monitoring scenario is not adjusted to previously existing procedures, the survey design must be conveniently described considering the existing special features.

- Design constraints

  The purpose of this section is to include a description of the limitations of the surveying technologies that must be kept in mind during the data gathering. These constraints are both referred to those inherent to the technology itself, considering the requirements of the planned survey; and those regarding the conditions of the site and its environment as identified in the previous section.

- Sensibility of measurements to environmental conditions

  This part of the report is to describe the environmental dependency of the measurement These conditions could decrease the data quality or impede the survey entirely. There are two types of data with respect of how they are influenced by the environment: those related to the absolute values of the conditions, such as temperature or humidity; and those that are susceptible to changes in the environmental parameters during the data gathering.

  The sensitivity of measurement[9] can be a characteristic of an instrument or a nominal metrological characteristic. It can be defined as the slope of the ideal curve (Figure 3.2), or the minimum input necessary to produce a standardized output change [4]. It could be potentially affecting the output value of the measuring due to environmental conditions. The ratio of the change in the measurement mainly depends on the type of equipment used and the measurand target. Apart from that, it is also important to consider the sensitivity error[10], which is a departure from the ideal slope of the characteristic curve [4].

3.2.4.2 Preparation

This section is meant to describe the preparation procedures for data acquisition, which can be categorized as:

- Procedures for calibration, initialisation, and post-installation verification

  Available manuals, standards, and guidelines for the correct development of these tasks must be included in this section. The procedures to be described are:

  - Calibration. Some sensors need to be calibrated before their use. Usually, the objective of the calibration is to settle the sensor's sensitivity at different values. They normally depend on the sensor itself, but the final part of the process consists of comparing sensor and theorical measures, thus obtaining the calibration curve. The

[9] Sensitivity (of measurement): Quotient of the change in an indication of a measuring system and the corresponding change in a value of a quantity being measured [1].

[10] Sensitivity error: Departure from the ideal slope of the characteristic curve [4].

This project has received funding from the European Union's Horizon 2020 research and innovation programme under grant agreement No 958171. © 2021

procedures for calibration are sometimes illustrated in ISO standards, but this is not always the case.

Calibration methods can be divided in two different categories: system calibration, referred as a step of the whole monitoring system setup; and sensor calibration, which is aimed to assure the correct operation and trustworthiness of each sensor present in the monitoring instruments.

- Initialisation. The sensor parameters should be adequately set according to the structure type, the desired measure, and the frequency range of interest. In some cases, signals coming from different sensors should be combined in post-processing analysis, so their synchronization must be guaranteed.
- Post-installation verification. Once the monitoring instruments have been installed, calibrated, and initialised, a trial can be carried out to check if the data is being correctly acquired. This can also be done by supervising the initial period of the actual data acquisition process.

- Procedures for estimating the calibration uncertainty

  Many times, the uncertainty of the quality of a measurement is hardly quantifiable and even more when the parameter of interest is unknown. This section defines basic concepts related to availability and measurement uncertainty[11] with the aim to clarify their role for assessing the quality of a measurement. The ISO 99, 2007 defines the uncertainty of measurement as a "non-negative parameter characterizing the dispersion of the quantity values being attributed to a measurand, based on the information used". Therefore, it is a parameter directly associated with the result of a measurement. Absolute uncertainty depends on the value of the measured physical quantity, for this reason it is not a suitable quantitative characteristic of the measurement accuracy. On the other hand, relative uncertainty does not have this drawback: the inverse of the relative uncertainty expressed as a fraction of the physical quantity is a typical characterization of the measurement accuracy. The ratio in which the system is performing its mission is also called the availability of an equipment. In its simplest form, availability refers to the measure of the actual system's availability over a period of time in a real production environment.

  When the true value of the measurand is unknown, the dispersion of the values could be reduced if the repeatability[12] and reproducibility[13] conditions are used. The repeatability condition influences random errors[14], good repeatability usually indicates that these types of errors are small. On the other hand, systematic errors[15] are only influenced for the reproducibility condition. A good reproducibility during measurements should indicate that systematic and random errors are small.

- Requirements for data acquisition depending on measured physical quantity

---

[11] Measurement uncertainty: Non-negative parameter characterizing the dispersion of the quantity values being attributed to a measurand, based on the information used (ISO 99, 2007).

[12] Repeatability: Condition of measurement, out of a set of conditions that includes the same measurement procedure, same operators, same measuring system, same operating conditions and same location, and replicate measurements on the same or similar objects over a short period of time [1].

[13] Reproducibility: Quality of measurements that reflects the closeness of the results of measurements of the same quantity performed under different conditions [1].

[14] Random Error: Component of measurement error that in replicate measurements varies in an unpredictable manner [149].

[15] Systematic Error: component of measurement error that in replicate measurements remains constant or varies in a predictable manner [149].

This project has received funding from the European Union's Horizon 2020 research and innovation programme under grant agreement No 958171.

This section is meant to include specific requirements for a suitable calibration, initialisation, and post-installation verification of the components of the monitoring system, regarding the particular objectives of the monitoring activities and the characteristics of the technology itself, as described before.

3.2.4.3 Performance

- Requirements and recommendations for maintenance during operation (in case of continuous maintenance)

  This is specifically addressed for continuous monitoring of a bridge or tunnel. Maintenance is of special important in a long-term monitoring system due to non-stop data recordings. In consequence, inspection and maintenance of the equipment is an important process to be implemented between the monitoring station and remote monitoring centre to make sure of the truthfulness of data recordings. In that sense, in this section the importance of maintenance to avoid interrupting long-term monitoring are addressed.

- Criteria for ensuring measurements repeatability and comparability within successive surveying campaigns for updating the sensors

  The objective of this section is to describe the criteria to be followed to set the sensors layout and sensors technical specifications in successive surveys. The reason behind this process is that temporal and spatial consistency of the data is essential when collecting data from multiple sensors on the same infrastructure. In this sense, it is necessary to develop a set of criteria that allow scanning the same parameters of an infrastructure more than once, while maintaining consistency between these data and allowing comparison between successive surveys.

  These successive campaigns conducted to compare sensor data involve the following steps: (i) Georeferenced frame, i.e., global location on the bridge; (ii) Relative alignment of sensor data; (iii) multi-temporal registration with previous campaigns; and (iv) Diagnostics.

  - Georeferenced frame. A common spatial georeferenced frame must be selected prior to the survey so all the measurements acquired can be unambiguously located on the structure. The reference system must be reproducible on successive surveys. If a global coordinate system is employed, either the position of the sensors relative to it or to globally referenced points must be indicated. A reference system can also be defined locally, based on the layout of the survey site and indicating easily identifiable reference points.
  - Relative alignment of sensor data. To assess the correct alignment of sensor data, control points can be acquired. The location of these points relative to the georeferenced frame must be recorded with the best possible precision, so it can be compared with the registered position of measurement points, and therefore evaluate the correct spatial referencing of the latter.
  - Multi-temporal registration with previous campaigns. A temporal reference system must be established to compare successive surveys, so changes on the structure produced over time can be accurately interpreted and evaluated.
  - Diagnostics. How to produce a report of the surveys.

3.2.4.4 Reporting

This section should describe how to present the results of the survey in a meaningful way, depending on each specific surveying technology. This should include information about the existence of guidelines or standards to follow for performing this task. In addition, an indication of the highlights of the survey (for example, from the obstacles encountered to the quality of the results obtained).

This project has received funding from the European Union's Horizon 2020 research and innovation programme under grant agreement No 958171.

3.2.4.5 Lifespan of the technology and required maintenance

This section is in charge of specifying the lifespan[16] of the surveying technology being studied, together with the needed maintenance during operation. This is specifically addressed for continuous monitoring of a bridge or tunnel. Maintenance is of special important in a long-term monitoring system due to non-stop data recordings. In consequence, inspection and maintenance to the equipment is an important process to be implemented between the monitoring station and remote monitoring centre to make sure of the truthfulness of data recordings. In that sense, in this section the importance of maintenance to avoid interrupting long-term monitoring are addressed. The lifespan of the technology includes the evaluation of expected service life to all primary and secondary equipment, data acquisition system, and all necessary to the proper operation of each specific technology. Moreover, aspects that could potentially limit the lifespan of a technology should be also mentioned.

3.2.5 Interpretation and validation of results

This section is to describe the relationship between the result or output of a measurement, and the event that is expected to detect. In a similar manner, this section should also include how the results are validated, meaning that it should describe the procedure followed to ensure that the result or output is correct, including the quantitative and qualitative error evaluation. The subsequent structure is to be followed.

3.2.5.1 Expected output

This section should describe the data format (e.g., numbers in a .txt file).

3.2.5.2 Interpretation

This project is providing a review of different surveying technologies currently in use. Each surveying technology results in the collection of a specific type of data. This section is intended to specify what are those data and how to interpret them (e.g., each number of the file symbolizes the acceleration of a degree of freedom in the bridge).

3.2.5.3 Validation

Once the data gathering is finished, it is necessary to review the obtained data to see if they have an appropriate quality, and to see if any unexpected malfunction occurred during this process. In this section, it is important to specify the following:

- Specific methods used for validation of results depending on the technique
- Quantification of the error
- Quantitative or qualitative evaluation

3.2.6 Advantages and disadvantages

All surveying technologies considered in the project have general advantages and disadvantages, and some specific ones when applied for damage detection on bridges and tunnels. These should be reflected in this part of the report.

3.2.7 Possibility of automatising the measurements

Depending on the surveying technology and the instruments employed, it is feasible that certain steps of the data gathering[17] procedure can be automatized. This section is to include any aspect of the surveying technology that can be automatized, for example:

[16] Lifespan: Maximum number of uses and/or processing cycles as validated by the manufacturer [142].

[17] Data gathering: Collect data from all of the data sources that were identified as relevant for the acquisition objectives.

This project has received funding from the European Union's Horizon 2020 research and innovation programme under grant agreement No 958171.

- Planification of the survey route or the spots/points of the structure to place the measuring instruments (or in the surroundings for the case of remote sensing)
- Setup and calibration of the instruments
- Data gathering, in the case of instruments recording data continuously or taking discrete measurements over time

3.2.8 Barriers

In accordance with Section 3.2.6 regarding the disadvantages of the surveying technology being studied, some barriers can be also identified and should be described here.

3.2.9 Existing standards

Any existing standards or good practice documents that are related to the technology should be described here.

3.2.10 Applicability

Surveying technologies can be easily used to assess and monitor the condition of infrastructures, improving the efficiency of monitoring, inspection, repair, and rehabilitation efforts. In this section, the ease of application of each technology will be covered focusing on aspects as the ease of execution, transportation, need of specialized operators, equipment, costs, etc. This should be addressed in the context of damage detection and/or monitoring in bridges and tunnels.

3.2.10.1 Relevant knowledge fields

In order to provide a better context, and ease the linking of this technology to others, this section is to include a list of all the knowledge fields or fields of study related to the technology (e.g., civil engineering).

3.2.10.2 Performance indicators

This part of the report should list the performance indicators that can be detected or monitored with the surveying technology under evaluation.

3.2.10.3 Type of structure

This section should include all the types of structures where this technology can be used.

3.2.10.4 Spatial scales addressed

Here, the report should state to which state does the surveying technology work, from network level to a specific element.

3.2.10.5 Materials

This section should list all the materials where the technology is applicable, and add any detail that might be of interest when using the technology in said material.

3.2.11 Available knowledge

This section should complement the existing standards. It should include other reference projects that deal with similar scenarios, or any other information that could provide further insight in the workings or application of the technology.

This project has received funding from the European Union's Horizon 2020 research and innovation programme under grant agreement No 958171.

3.3 Semantic wiki

The *Online interactive catalogue of surveying technologies for transport infrastructure* has been created as part of an intuitive wiki. This wiki contains information not only from this deliverable, but also from WP1 and WP3 of IM-SAFE project.

The information coming from deliverable D2.1 has been gathered by experts in the field by doing intensive research about each surveying technology analysed within the project. The collected information needs to be structured to be implemented in the wiki. In this project, a semantic wiki has been used to store all this information. It contains an underlying knowledge model capturing information by means of classes, relationships amongst classes, and their properties. In section 3.3.1, a better explanation is given.

3.3.1 WP2 knowledge model

The knowledge model of WP2 has been created based on the information gathered from the review of the different surveying technologies. Said information has been reviewed to identify the different classes, subclasses, object properties and their relationships to create the knowledge model. The created model was validated by domain experts, and the provided feedback was used to modify the needed aspects of it. Figure 3.3 shows a detailed view of WP2 model.

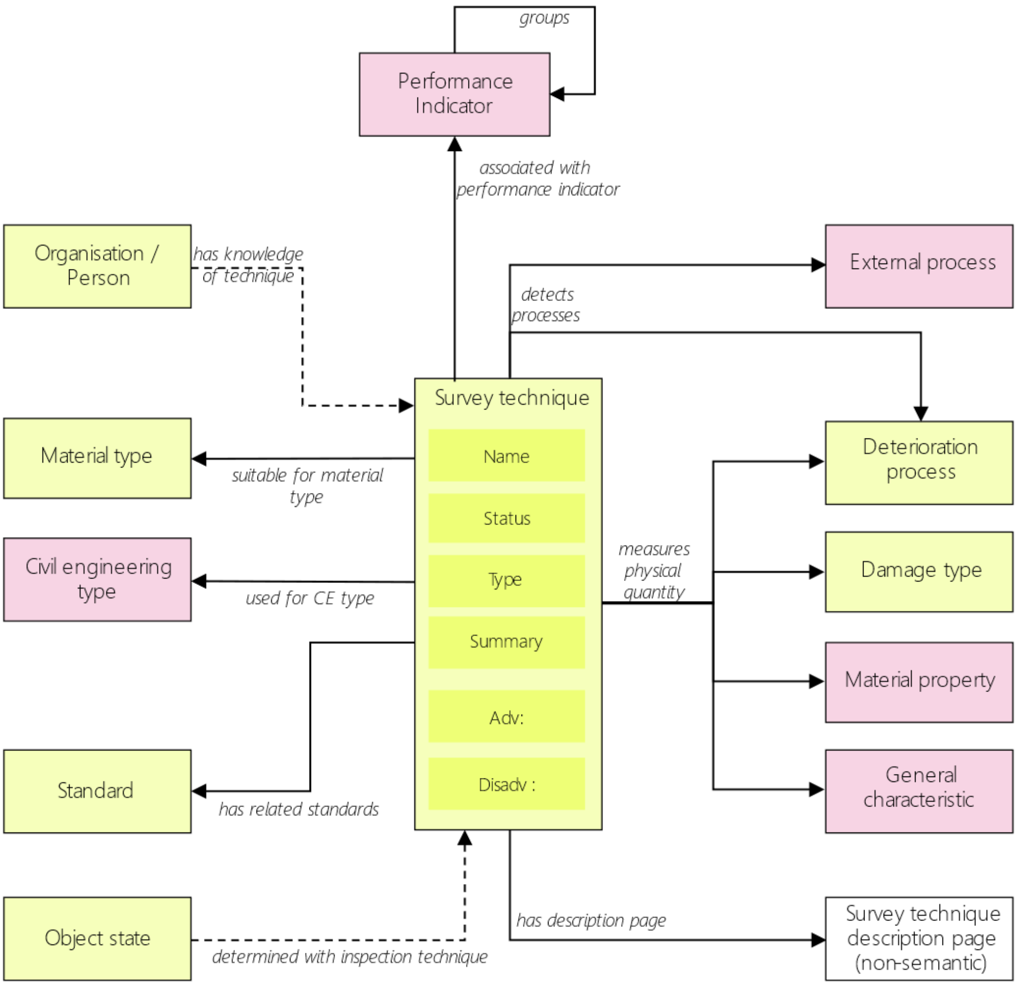

Figure 3.3 – Knowledge model of WP2 (surveying technologies)

Once the knowledge model was created, the information of each surveying technology report could be imported into the semantic wiki. In addition, research and retrieval patterns were created so that end users could navigate the wiki in an easy way.

This project has received funding from the European Union's Horizon 2020 research and innovation programme under grant agreement No 958171.

3.3.2 Result

Lastly, the *online interactive catalogue of surveying technologies for transport infrastructure* is to be delivered as part of the IM-SAFE semantic wiki, which is the main result of task T2.1.

The IM-SAFE Semantic Wiki is operational and publicly available at this location:

https://imsafe.wikixl.nl/

The content of the present deliverable is accessible under the *Surveying Technologies* tab (Figure 3.4).

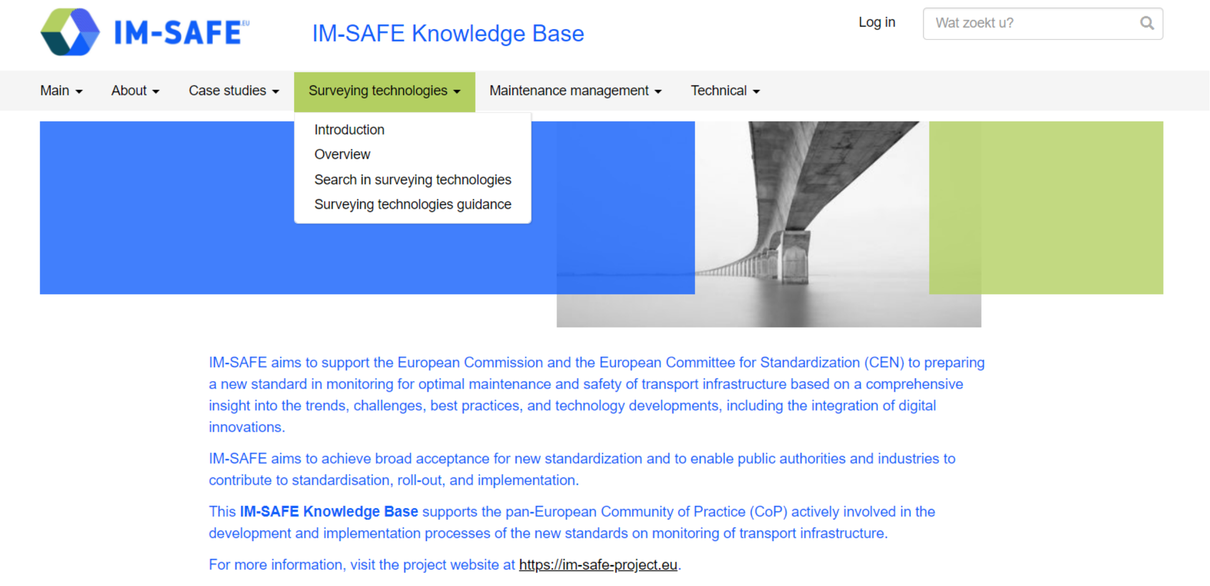

Figure 3.4 – Screenshot of the actual wiki, showing the tabs available on WP2

In case more information is needed, please go to deliverable D1.2 of the present project, where a detailed description of the wiki has been provided.

This project has received funding from the European Union's Horizon 2020 research and innovation programme under grant agreement No 958171.

4 Data analysis

4.1 Introduction

The range of surveying techniques considered in this project is very broad in terms of type, quality, and volume of generated data. The same holds for the complexity and type of information that can be derived from the data. Since for each surveying technology several data analysis approaches can be used, giving a comprehensive overview of all the potentially used data analysis methods is not possible. Therefore, the approach chosen is to focus on the list of the most used data analysis methods for each of the surveying technologies described (see Chapter 3).

The aim of this chapter is to depict at high level the principles on which the different data analysis methods are based. For detailed descriptions and exhaustive mathematical derivations, the reader should refer to the numerous cited sources.

4.2 Description of analysis methods

4.2.1 Parametric-, model- and physics-based methods

Several fields and industries have traditionally relied on empirical and theoretical models to explain reality. Most theoretical methods used are the result of deriving differential equations based on conservation laws, physical principles, and/or phenomenological behaviours for a particular process. Partial differential equations are numerically solved using finite differences, finite elements, spectral and meshless methods. These physics-based approaches assume that a physical model describing the behaviour behind these measurements is available and somehow sufficiently accurate and self-contained to predict future behaviour.

An initial simulation of the expected behaviour is performed by assuming initial model and parameters, then parameters are modified to obtain the best fit of data to model, using either a trial-and-error heuristic process (in the simplest cases) or by minimizing the value of an objective function, which is a measure of the difference between the experimental and simulated data. This data analysis approach is still used for several of the surveying technologies here described, e.g., radioactive and nuclear methods, guided waves techniques, surface measurements, acoustic emission, qualitative and quantitative chemical methods, mechanical tests on cored samples.

However, over the last years, thanks to the availability of a growing wealth of multi-fidelity observations from sensors and instruments, a paradigm shift towards data-driven methods has been observed, with *Machine Learning* (ML) and *Deep Learning* (DL) becoming ubiquitous. These methods can explore massive design spaces, identify multi-dimensional correlations, and manage ill-posed problems. Deep learning approaches naturally provide tools for the automated extraction of features from massive amounts of multi-fidelity observational data that are currently available and characterized by unprecedented spatial and temporal coverage. They can also help to link these features with existing approximate models and exploit them in building new predictive tools.

At the crossroad of the two approaches, physics-informed learning [6] integrates (noisy) data and mathematical models and implements them through neural networks or other kernel-based regression networks. *Physics-informed machine learning* can seamlessly integrate data and the governing physical laws, including models with partially missing physics, in a unified way. This can be expressed compactly using automatic differentiation and neural networks that are designed to produce predictions that respect the underlying physical principles [7]. Although this specific approach is not described in detail in this chapter, it may be an important future direction for the civil engineering.

This project has received funding from the European Union's Horizon 2020 research and innovation programme under grant agreement No 958171.

4.2.1.1 High level considerations for the engineering infrastructure domain

For Structural Health Monitoring (SHM), *parametric techniques*, also called model- or physical-based detection methods, are good for physical conceptualization and for the prediction of infrastructure future behaviour. However, structural models are difficult to create and may not accurately reflect real behaviour. Difficulties and uncertainties increase in presence of complex civil infrastructures so that well-defined and unique behaviour models of structures cannot be clearly identified.

Alternatively, non-parametric algorithms referred to as model-free or data-driven methods are independent of mathematical model and process the data in a way that is free of geometrical and material information. This makes non-parametric damage detection algorithm desirable for long-term monitoring of structures. However, of the several non-parametric damage detection algorithms available, not all are of practical application in the case of long-term monitoring of real-life civil structure. Parameters such as daily and seasonal variation of environmental conditions (temperature), missing data (instrument failure, extreme natural phenomena, power interruptions, removal of erroneous measurements), the presence of large amount of noise and outliers [8] can limit or add some complexity to the non-parametric data interpretation. A summary of advantages and disadvantages of parametric versus non-parametric techniques is reported in [9] and also shown in Figure 4.1.

Data Analysis Approaches	Scenarios for Common Use	Advantages	Disadvantages
Non-parametric Methods also known as • Data-Driven Methods; • Direct Signal Analysis; • Model-free Methods • Non-Physics-Based Methods	• Structure may not be a critical structure • Structural prediction is not critical • Many structures need to be monitored • There is time for training the system	• No need for models, therefore no modeling costs • May detect and localize changes/damage • Many options for signal analysis • Incremental training can track damage accumulation • Good for long-term use on structures for early detection of situations requiring model-based interpretation	• Physical interpretation of the signal may be difficult • Weak support for decisions on rehabilitation and repair • Indirect guidance for structural management activities such as inspection and further measurement • Cannot be used to justify replacement avoidance
Parametric Methods also known as • Structural Methods; • Model-based Methods; • Physics-Based Methods	• Design model is not accurate • Structure has strategic importance • Damage is suspected • There are structural management challenges	• Interpretation is easy when links between measurements and potential causes are explicit • The effects of changes in loading and use can be predicted • Guidance for further inspection and measurement • Consequences of future damage can be estimated • Support for planning rehabilitation and repair • May help justify replacement avoidance	• Modeling is expensive and time consuming • Errors in models and in measurements can lead to identification of the wrong model • Large numbers of candidate models are hard to manage • Identification of the right model could require several interpretation - measurement cycles • Complex structures with many elements have combinatorial challenges

Figure 4.1 – Comparison between parametric and non-parametric methods

4.2.2 Bayesian vs Frequentist statistics

There are two broad classes of inference methods in statistics: frequentist and Bayesian methods. These two approaches are the result of two competing schools of thought on how probabilities should be interpreted.

This project has received funding from the European Union's Horizon 2020 research and innovation programme under grant agreement No 958171. © 2021

Frequentist statisticians have an *objective interpretation* of probabilities as the result of experiments that sample unknown but fixed population values. For instance, the fraction of statistics practitioners who subscribe to the frequentist school as opposed to the Bayesian one is currently unknown but could be estimated by polling people and counting the frequency with which a respondent says that they belong to one school as opposed to the other (hence the term frequentist). Sampling people independently at random would presumably tell us that frequentist are a much larger group as the frequentist view is generally perceived as more pragmatic and by far most of the statistics analyses appearing in scientific publications are based on measures of significance that rely on p-values and confidence intervals, which are frequentist objects (see e.g. [10]).

Ironically, frequentistist approaches would not allow us to incorporate our prior knowledge on the overwhelming popularity of frequentict statistics in our analysis. That is where **Bayesian statistics** comes which is a school of thought supporting a *subjective interpretation of probabilities* as statistical propositions that depend on a posterior belief that is formed by combining prior beliefs and data observations. The measure of significance of provided by Bayesian statistics paralleling p-values and confidence intervals are Bayes factors and credible intervals, i.e. the relative probability of competing models given the data, and an interval of values within which a parameter has a given high probability of being located, respectively.

In light of the mentioned dominance of frequentist statistics in technical domains, in the rest of this chapter we will mostly focus on frequentist methods. However, it is useful to point out that on one hand to stress the value of Bayesian methods when one has a good grasp on the prior distribution of a parameter to be estimated, or when one needs a principled way of comparing competing models of the data. Finally, it is also useful to remember that the frequentist vs Bayesian divide might not be as deep as it might seems (see e.g. Andrew Gelman piece titled "Bayesians are frequentists" [11]).

4.2.3 Descriptive statistics for scientific observables

4.2.3.1 Descriptive statistics

Descriptive statistics is about describing and summarizing data (Table 4-1 to Table 4-4). The quantitative approach describes and summarizes data numerically. The visual approach illustrates data with charts, plots, histograms, and other graphs. It can be applied to one or many datasets or variables. Univariate analysis describes and summarizes a single variable; bivariate analysis is used to search for statistical relationships among a pair of variables; similarly, a multivariate analysis is concerned with multiple variables at once.

Descriptive statistics is used for several of the surveying technologies considered in this project (e.g., Mechanical tests on cored samples, Water resistance, Quantitative chemical methods, Weight-in-Motion).

Measures of Frequency	**Measures of Central Tendency**	**Measures of Dispersion or Variation**	**Measures of Position**
Shows how often something occurs.	Locates the distribution by various points.	Identifies the spread of data points by stating intervals.	Describes how data fall in relation to one another. Relies on standardized scores.
- Count - Percent - Frequency	- Weighted mean - Harmonic mean - Median - Mode	- Range - Variance - Standard Deviation	- Percentile Ranks - Quartile Ranks

Table 4-1 – Descriptive statistics

This project has received funding from the European Union's Horizon 2020 research and innovation programme under grant agreement No 958171.

Mean	The sample mean, also called the sample arithmetic mean or simply the average, is the arithmetic average of all the items in a dataset. The mean of a dataset x is mathematically expressed as $\Sigma_i x_i/n$, where i = 1, 2, …, n. In other words, it's the sum of all the elements x_i divided by the number of items in the dataset x.
Weighted mean	The weighted mean, also called the weighted arithmetic mean or weighted average, is a generalization of the arithmetic mean that enables you to define the relative contribution of each data point to the result. You define one weight w_i for each data point x_i of the dataset x, where i = 1, 2, …, n and n is the number of items in x. Then, you multiply each data point with the corresponding weight, sum all the products, and divide the obtained sum with the sum of weights: $\Sigma_i\,(w_i x_i)/\Sigma_i w_i$. Note: It's convenient (and usually the case) that all weights are nonnegative, $w_i \geq 0$, and that their sum is equal to one, or $\Sigma_i w_i = 1$.
Harmonic mean	The harmonic mean is the reciprocal of the mean of the reciprocals of all items in the dataset: $n/\Sigma_i(1/x_i)$, where i = 1, 2, …, n and n is the number of items in the dataset x.
Geometric mean	The geometric mean is the n-th root of the product of all n elements x_i in a dataset x: $^n\sqrt{(\Pi_i x_i)}$, where i = 1, 2, …, n.
Median	The sample median is the middle element of a sorted dataset. The dataset can be sorted in increasing or decreasing order. If the number of elements n of the dataset is odd, then the median is the value at the middle position: 0.5(n + 1). If n is even, then the median is the arithmetic mean of the two values in the middle, that is, the items at the positions 0.5n and 0.5n + 1. The main difference between the behaviour of the mean and median is related to dataset outliers or extremes. The mean is heavily affected by outliers, but the median only depends on outliers either slightly or not at all. By comparing the mean and median, outliers and asymmetry in data can be detected. Whether the mean value or the median value is more useful depends on the context of a particular problem.
Mode	The sample mode is the value in the dataset that occurs most frequently. If there isn't a single such value, then the set is multimodal since it has multiple modal values.

Table 4-2 – Measures of central tendency in detail

Variance	The sample variance shows numerically how far the data points are from the mean. You can express the sample variance of the dataset x with n elements mathematically as $s^2 = \Sigma_i\big(x_i - mean(x)\big)^2/(n-1)$, where i = 1, 2, …, n and mean(x) is the sample mean of x. To calculate population variance use n in the denominator instead of n − 1: $\Sigma_i\big(x_i - mean(x)\big)^2/n$. In this case, n is the number of items in the entire population.
Standard deviation	The sample standard deviation is another measure of data spread. It's connected to the sample variance, as standard deviation, s, is the positive square root of the sample variance. The standard deviation is often more convenient than the variance because it has the same unit as the data points. The population standard deviation refers to the entire population. It's the positive square root of the population variance.
Coefficient of variation	The coefficient of variation (CV), also known as relative standard deviation (RSD), is a standardized measure of dispersion of a probability distribution or frequency distribution. It is often expressed as a percentage and is defined as the ratio of the standard deviation, s, to the mean (or its absolute value).

This project has received funding from the European Union's Horizon 2020 research and innovation programme under grant agreement No 958171.

Percentiles	The sample p percentile is the element in the dataset such that p% of the elements in the dataset are less than or equal to that value. Also, (100 − p)% of the elements are greater than or equal to that value. If there are two such elements in the dataset, then the sample p percentile is their arithmetic mean. Each dataset has three quartiles, which are the percentiles that divide the dataset into four parts (first quartile is the sample 25th percentile, second quartile is the sample 50th percentile or the median, the third quartile is the sample 75th percentile).
Ranges	The range of data is the difference between the maximum and minimum element in the dataset. The interquartile range is the difference between the first and third quartile.

Table 4-3 – Measures of variability in detail

Skewness	The sample skewness measures the asymmetry of a data sample. There are several mathematical definitions of skewness. One common expression to calculate the skewness of the dataset x with n elements is $\left(n^2/\left((n-1)(n-2)\right)\right)\left(\Sigma_{\mathrm{i}}\left(x_{\mathrm{i}}-mean(x)\right)^3/(ns^3)\right)$. A simpler expression is $\Sigma_{\mathrm{i}}\left(x_{\mathrm{i}}-mean(x)\right)^3 n/\left((n-1)(n-2)s^3\right)$, where i = 1, 2, …, n and mean(x) is the sample mean of x. The skewness defined like this is called the adjusted Fisher-Pearson standardized moment coefficient.
Kurtosis	The kurtosis is a measure of the "tailedness" of the probability distribution of a real-valued random variable which, like skewness, can be quantified in several different ways. The standard measure of a distribution's kurtosis is a scaled version of the fourth moment of the distribution and is defined as $Kurt(x) = E\left[\left(\frac{x-mean(x)}{\sigma}\right)^4\right]$, where σ denotes the standard deviation of x, and E is the expectation operation.
Standardized moments	The moments of a function are quantitative measures related to the shape of the function's graph. They are important quantities in statistics, because if the function under consideration is a probability distribution, the collection of all the moments (of all orders, from 0 to infinity) uniquely determines the distribution. The expected value, the variance, skewness, and kurtosis are directly related to respectively the first, second, third and fourth moments of the probability distribution. The standardized moment of degree k is defined as $\frac{\mu_k}{\sigma^k}$, where $\mu_k = E[(x-\mu)^k]$, $\sigma^k = \left(\sqrt{E[(x-\mu)^2]}\right)^k$, $\mu = mean(x)$ and E is the expectation operator,

Table 4-4 – Measures of symmetry in detail

4.2.3.2 Inferential Statistics

The theory of statistical inference consists of methods by which inferences or generalizations about a population are made. Instead of examining the entire collection called the population, which may be difficult or impossible, we may examine a small part of it called random sample. Statistical inference is the process used to draw certain inferences about the population from results derived from the sample. The process of obtaining samples is called sampling. The distribution of a statistic calculated based on random sample is called sampling distribution and it is basic to all statistical inference. If a measurement is generated in every experiment unit in the entire collection, the resulting data set constitutes the population of interest (i.e., set of all measurements of interest to the investigator). Any smaller subset of measurements is a sample (i.e., subset of measurements selected from the population of interest). The size of the population N is the number of objects or observations in the population. The size of a sample is denoted by n. If n ≥ 30, the sampling is said to be large and if n < 30, the sampling

This project has received funding from the European Union's Horizon 2020 research and innovation programme under grant agreement No 958171.

is customarily considered "small". Statistical measures of the population such as mean, and variance are known as population parameters.

The process of estimating a population parameter by using sample information is called estimation. The processes used to decide whether to accept or reject a set of hypotheses are called basis of hypothesis. There are two types of estimation procedures: Point estimation or Interval estimation. An interval estimator is a rule for calculating two numbers a and b to create an interval that contains with high probability the parameter of interest. The probability that a confidence interval will contain the estimated parameter is called the confidence coefficient, $1-\alpha$. When the sampling distribution of a point estimator is approximately normal, an interval estimator or *confidence interval* can be calculated as:

$$\left(\bar{x} - Z_{\alpha/2}\frac{\sigma}{\sqrt{n}}, \bar{x} + Z_{\alpha/2}\frac{\sigma}{\sqrt{n}}\right) \qquad \textit{Eq. 1}$$

with $\bar{x}$ sample mean, σ standard deviation, n sample size, and $Z_{\alpha/2}$that depends on the confidence coefficient and is 1.96 (2.58) for 95% (98%) large sample confidence interval. In this type of analysis, if the specified value is within the confidence interval, we conclude that there is not a statistically significant difference between that specified value and the actual value for the population or process. If the size of the sample is small ($n < 30$), the actual density function or curve that describes the sampling distribution is called the *t-distribution*. Point and interval estimator formula need then to be updated to this specific distribution [12].

Inferential Statistics is involved in such analyses as ANOM, ANOVA, Chi-Square Tests, F-tests, Regression, t-tests, and z-tests. For more details, the reader is referred to the following books on Probability and Statistics [13].

4.2.3.3 Statistics in Analytical Chemistry

Modern analytical chemistry is concerned with the detection, identification, and measurement of the chemical composition of substances using instrumental techniques. Quantitative results are obtained using instruments that allow the user to determine the concentration of a chemical in a sample from an observable signal. There is *always* some variation in that signal over time due to noise and/or drift within the instrument. The user needs to *calibrate* the response as a function of analyte concentration to obtain meaningful quantitative data. As a result, there is *always* an *error*, a deviation from the *true* value, inherent in that measurement. One of the uses of statistics in analytical chemistry is therefore to provide an *estimate* of the likely value of that error, hence, to establish the *uncertainty* associated with the measurement. Two terms of importance in any measurement are *accuracy* and *precision*. Accuracy is defined as the closeness of a result to the *true value*. This can be applied to a single measurement but is more commonly applied to the mean value of several repeated measurements, or replicates. Precision is defined as the extent to which results agree with one another. In other words, it is a measure of *consistency*, and is usually evaluated in terms of the range or spread of results. Practically, this means that precision is inherently related to the standard deviation of the repeated measurements. When referring to the consistency between individual values amongst a set of replicate measurements performed by the same person, at the same time on the same sample, using the same method, this is termed the measurement *repeatability*. When referring to the consistency of a method as used by different analysts, laboratories, and/or over an extended time, this is termed the *reproducibility*. For a comprehensive tutorial please read [14].

4.2.4 Fitting of data to probability distributions

Measurement processes usually introduce a certain amount of variability or randomness into the results, and this randomness can affect the conclusions drawn from measurements. The same holds for naturally occurring random phenomena or uncertainties caused by incomplete knowledge. Randomness in measured variables can be accounted for by their probability density functions (PDF). In order to find the density function of continuous measured data, one

This project has received funding from the European Union's Horizon 2020 research and innovation programme under grant agreement No 958171.

can simply determine the best fit of selected PDFs to the observational data. The selection of candidates PDF must be done considering the nature of the random process, the domain or support of the distribution, and the shape of the observational data. For a list of probability distributions please see [15].

4.2.5 Outlier detection and robust regression

4.2.5.1 Outlier detection

An outlier is a data point that differs significantly from other observations and may be due to variability in the measurement or to experimental error. When outliers originate from measurement error, they can be discarded using statistics that are robust to outliers. If they originate from heavy-tailed distribution (high skewness) one should be very cautious in using tools or intuitions that assume a normal distribution. A frequent cause of outliers is a mixture of two distributions, which may be two distinct sub-populations, or may correspond to the correct versus erroneous measurement.

Outlier detection is sometimes also called novelty detection, anomaly detection, noise detection, deviation detection or exception mining. For a recent overview of outlier detection methodologies [16]. For outlier detection in local feature matching of computer vision pipelines, the reader is referred to [17].

4.2.5.2 Robust Regression Analysis (RRA)

Least squares estimate for regression models are highly sensitive to outliers. Robust Regression Analysis methods aim to develop procedures that give a good fit to the bulk of the data without being perturbed by a small proportion of outliers, and that do not require deciding in advance which observations are outliers. Whether an estimator is robust can be studied with two simple measurements: Influence function and Breakdown point. Both measurements are based on the idea of studying the behaviour of an estimation function under the influence of gross errors, i.e. arbitrary included data. A well-established technique is the one of M-estimators. The M-estimator is essentially a weighted mean, wherein the weights are designed to prevent the influence of outliers on the estimator as much as possible.

4.2.6 Methods based on correlations

4.2.6.1 Cross-Correlation Analysis (CCA)

In signal processing, cross-correlation (also known as a *sliding dot product* or *sliding inner-product*) is a measure of similarity of two series as a function of their relative displacement. It is commonly used for searching a long signal for a shorter known feature and is similar in nature to the convolution of two functions. For mathematical derivation please read [18].

4.2.6.2 Magnitude Squared Coherence

The magnitude-squared coherence (MSC) is a measure that estimates the extent to which one real- or complex-valued signal can be predicted from another real- or complex-valued signal using a linear model. When used as a measure of the similarities in the frequency content of two signals, it returns real values between 0 and 1 to indicate how well two-time domain signals $x(t)$ and $y(t)$ match each other at various frequencies.

4.2.7 Dimensionality reduction methods

Dimensionality reduction is the transformation of high-dimensional data into a meaningful representation of reduced dimensionality. There is a very long list of linear and nonlinear dimensionality reduction techniques, but we will review only the most used techniques, related to the surveying technologies considered in the project. For an interesting comparison between linear and nonlinear methods, the reader can refer to [19].

This project has received funding from the European Union's Horizon 2020 research and innovation programme under grant agreement No 958171.

4.2.7.1 Factor analysis

Factor analysis attempts to identify underlying variables, or **factors**, that explain the pattern of correlations within a set of observed variables. Factor analysis is often used in data reduction to identify a small number of factors that explain most of the variance that is observed in a much larger number of manifest variables. Factor analysis can also be used to generate hypotheses regarding causal mechanisms or to screen variables for subsequent analysis. It may help to deal with data sets where there are large numbers of observed variables that are thought to reflect a smaller number of underlying/latent variables. It is one of the most commonly used inter-dependency techniques and is used when the relevant set of variables shows a systematic inter-dependence and the objective is to find out the latent factors that create a commonality. To reduce the number of variables to explain and to interpret the results, FA relies on two steps, *factor extraction* followed by *factor rotation*. Factor extraction involves making a choice about the type of model as well the number of factors to extract. Factor rotation comes after the factors are extracted, with the goal of achieving *simple structure* in order to improve interpretability.

The two main factor analysis techniques are Exploratory Factor Analysis (EFA) and Confirmatory Factor Analysis (CFA) [20]. CFA attempts to confirm hypotheses and uses path analysis diagrams to represent variables and factors, whereas EFA tries to uncover complex patterns by exploring the dataset and testing predictions. For a detailed yet simple tutorial on FA the reader is referred to [21]. For permutation methods for Factor Analysis [22].

4.2.7.2 Principal component Analysis (PCA)

Principal component analysis (PCA) is the process of computing the principal components and using them to perform a change of basis on the data. The analysis includes the transformation of the data with respect to a current coordinate space to a new space, to re-express the original data reducing, filtering or eliminating the noise and possible redundancies. These redundancies are measured by means of the correlation between the variables.

In other words, PCA is defined as an orthogonal *linear* transformation that transforms the data to a new coordinate system such, that the greatest variance by some scalar projection of the data comes to lie on the first coordinate (called the first principal component), the second greatest variance on the second coordinate, and so on. The first principal component can equivalently be defined as a direction that maximizes the variance of the projected data (and by assumption the signal-to-noise-ratio). The i-th principal component can be taken as a direction orthogonal to the first i-1principal components that maximizes the variance of the projected data. It can be shown that the principal components are eigenvectors of the data's covariance matrix. Thus, the principal components are often computed by eigendecomposition of the data covariance matrix or singular value decomposition (SVD) of the data matrix. Since the results of PCA depend on the scaling of the variables, it is important to scale each feature by its standard deviation, hence use the derived dimensionless features with unital variance. In summary, the process is as follows: 1) Organize data as an $m \times n$ matrix, where m is the number of measurement types (for example different sensors) and n is the number of samples, 2) Subtract off the mean for each measurement type; 3) Calculate the SVD or the eigenvectors of the covariance. For a complete mathematical description of deriving PCA and the linear algebra solutions, using the above-mentioned techniques, please read [23].

PCA is commonly used for dimensionality reduction by projecting each data point onto only the first few principal components to obtain lower-dimensional data while preserving as much of the data's variation as possible. Such dimensionality reduction can be a very useful step for visualising and processing high-dimensional datasets, while still retaining as much of the variance in the dataset as possible. For example, keeping only the first two principal components finds the two-dimensional plane through the high-dimensional dataset in which the data is most spread out, so if the data contains clusters these too may be most spread out, and therefore most visible to be plotted out in a two-dimensional diagram. Instead, if two

This project has received funding from the European Union's Horizon 2020 research and innovation programme under grant agreement No 958171. © 2021

directions through the data (or two of the original variables) are chosen at random, the clusters may be much less spread apart from each other and may in fact be much more likely to substantially overlay each other, making them indistinguishable. One approach, especially when there are strong correlations between different possible explanatory variables, is to reduce them to a few principal components and then run the regression against them, a method called principal component regression.

There are some limitations and disadvantages. Standard PCA can capture linear correlations between the features but fails when the linearity assumption is violated. To overcome this problem, kernel PCA was introduced, based on constructing nonlinear mappings that maximize the variance in the data. Another limitation is the mean-removal process before constructing the covariance matrix for PCA. PCA is at a disadvantage if the data has not been standardized before applying the algorithm to it. PCA transforms original data into data that is relevant to the principal components of that data, which means that the new data variables cannot be interpreted in the same ways that the originals were. They are linear interpretations of the original variables. While PCA finds the mathematically optimal method (as in minimizing the squared error), it is still sensitive to outliers in the data that produce large errors, something that the method tries to avoid in the first place. It is therefore common practice to remove outliers before computing PCA. However, in some contexts, outliers can be difficult to identify. Robust principal component analysis (RPCA) via decomposition in low-rank and sparse matrices is a modification of PCA that works well with respect to grossly corrupted observations. The objective of *sparse principal component analysis* (sparse PCA) is to find a reasonable trade-off between statistical fidelity and interpretability [24]. For additional recent development, please refer to [25].

4.2.7.3 Independent component analysis (ICA)

ICA is a computational method for separating a multivariate signal into additive sub-components, by assuming that the sub-components are non-Gaussian signals and that they are statistically independent from each other [26]. ICA corresponds to a general framework for solving Blind Source Separation (BSS) problems based on statistical independence of the unknown sources. ICA finds the independent components (also called factors, latent variables, or sources) by maximizing the statistical independence of the estimated components. This is achieved either by minimization of mutual information or the maximization of non-Gaussianity. Typical algorithms for ICA use centering (subtract the mean to create a zero-mean signal), whitening (usually with the eigenvalue decomposition), and dimensionality reduction as preprocessing steps to simplify and reduce the complexity of the problem for the actual iterative algorithm. Whitening and dimension reduction can be achieved with principal component analysis or singular value decomposition. Whitening ensures that all dimensions are treated equally a priori before the algorithm is run. For a relatively recent tutorial on ICA please read [27].

Well-known algorithms for ICA include infomax, FastICA [28], JADE, and kernel-independent component analysis. In general, ICA cannot identify the actual number of source signals, a uniquely correct ordering of the source signals, nor the proper scaling (including sign) of the source signals. While PCA identifies an orthogonal linear basis which maximizes the variance of the data, ICA is not restricted to an orthogonal basis because statistical independence makes no such requirement.

4.2.8 Analysis methods for time dependent data

A time series is a series of data points indexed in time order and, most commonly, it is a sequence of data points taken at successive equally-spaced points in time. Time series analysis comprises methods for analysing time series data in order to extract meaningful statistics and other characteristics of the data. Time series forecasting is the use of a model to predict future values based on previously observed values. While regression analysis is often employed in such a way as to test relationships between one or more different

This project has received funding from the European Union's Horizon 2020 research and innovation programme under grant agreement No 958171.

time series, this type of analysis is not usually called "time series analysis", which refers in particular to relationships between different points in time within a single series.

4.2.8.1 Time frequency analysis techniques: Fourier Transforms and Wavelets

A wavelet is a mathematical function used to decompose a given function or continuous-time signal into components of different scale. Each scale component has an assigned frequency range and can be studied with a resolution that matches its scale. A wavelet transform is the representation of a function by wavelets, scaled and translated copies (known as "daughter wavelets") of a finite-length or fast-decaying oscillating waveform (known as the "mother wavelet"). Wavelet transforms have advantages over traditional Fourier transforms for representing functions that have discontinuities and sharp peaks, and for accurately deconstructing and reconstructing finite, non-periodic and/or non-stationary signals. Wavelet transforms are classified into discrete wavelet transforms (DWTs) and continuous wavelet transforms (CWTs). Both DWT and CWT are continuous time (analog) transforms and can be used to represent analog signals. CWTs operate over every possible scale and translation whereas DWTs use a specific subset of scale and translation values or representation grid.

4.2.8.2 ARIMA

ARIMA is an acronym for "Auto Regressive Integrated Moving Average", which are a general class of linear models for one-dimensional time series. The main idea is to explain the current value of the time series based on its own past values, that is, its own lags and the lagged forecast errors, so that equation can be used to forecast future values. In practice an ARIMA model assumes that the current value of the time series is explained as a sum of three terms (explaining also the name of the model):

1. an Auto Regressive term: $AR(p) = \alpha + \beta_1 X_{t-1} + \cdots + \beta_p X_{t-p} + \epsilon_1$, where α, β_1, ..., β_p are parameters to be fit and ε_1 is a noise term assumed to be sampled from a Gaussian;

2. a Moving Average term: $MA(q) = \alpha + \varepsilon_t + \phi_1 \varepsilon_{t-1} + \cdots + \phi_q \varepsilon_{t-q}$;

3. and an Integrated (or differencing) term that can be defined as: for and $I_t(0) = X_t$, where m is the seasonality of the signal X_t.

Setting corresponds to the special case of an ARMA (Autoregressive Moving-Average) model: which works for stationary signals and can be estimated by using the Box-Jenkins method (see e.g. [@Ngo2013]). In case of non-stationary signals, the term of the general ARIMA model for can be used to remove the seasonality of the signal in order to recover a situation that can be handled by the ARMA model.

4.2.8.3 Deep learning methods for time series (see chapter Best DL-models for time series)

Because of their capability to model time-dependent signals, recurrent neural networks like the neural architectures of choice to model time series. Among these architectures based on LSTMs and GRUs units are the typical choice, since the designed to combat the problem of vanishing gradients, which is otherwise ubiquitous when training recurrent neural networks on long time horizons (see later paragraph on recurrent neural networks).

4.2.9 Modal Analysis

Modal analysis aims to determine the dynamic properties (natural frequencies, damping ratios and mode shapes) of a structure, directly related to their mass and stiffness. It is based on the principle that the dynamic behaviour of a structure depends only on its intrinsic characteristics. Degradation processes can significantly affect material properties, geometric properties and/or boundary conditions, and, consequently, modify stiffness and modal parameters. The whole process of experimental identification of a structure dynamic parameters can be synthetically illustrated in Figure 4.2.

This project has received funding from the European Union's Horizon 2020 research and innovation programme under grant agreement No 958171. © 2021

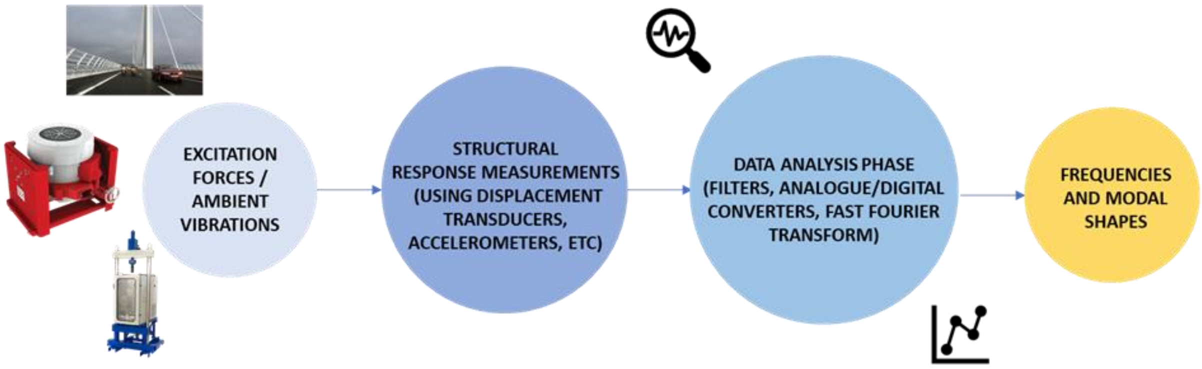

Figure 4.2 – Process experimental verification of structure dynamic parameters

Two different categories of modal analysis can be distinguished: Operational Modal Analysis (OMA) and Experimental Modal Analysis (EMA). OMA processes output signals extracted from monitored structures during their ambient operation (the structure is excited by ambient excitations like wind or traffic). EMA is an experimental procedure that comprises a testing protocol in which the structure is excited by one or several known dynamic excitation forces. Thus, while EMA procedures are developed in a deterministic framework, OMA methods can be seen as their stochastic counterpart. EMA methods are known as *input-output* modal analysis, while OMA methods are known as *output-only* modal analysis.

The dynamic behaviour of a structure can be represented either by a set of differential equations in time domain, or by a set of algebraic equations in frequency domain. The techniques of dynamic identification can, therefore, be classified into time domain and frequency domain techniques. For a thorough mathematical discussion to which the reader is referred.

There is a wide variety of input-output modal identification methods whose application relies either on estimates of a set of Frequency Response Functions (FRF) or on the corresponding impulse response functions (IRFs), which can be obtained through the inverse Fourier transform [29]. The FRF matrix carries all the information about the inertial, elastic, and energy dissipating properties of the structure. These methods attempt to perform some fitting between measured and theoretical functions and employ different optimization procedures and different levels of simplification. They are usually classified according to the following criteria: Domain of application (time or frequency), Type of formulation (indirect or modal and direct), Number of modes analysed (single degree or multi degree of freedom- SDOF or MDOF), Number of inputs and type of estimates (single-input single-output, single-input multi-output, multi-input multi-output, multi-input single-output, SISO, SIMO, MIMO, MISO). Two categories of methods can be also distinguished: parametric methods (algorithms that include the consideration of a parametrized system model) and non-parametric methods (comparison of measured data with some threshold and direct identification of some metric). In the context of parametric identification methods, the intermediate step of estimating the parameters of a system model is called system identification.

Several techniques are available to analyse OMA data and summarized in Figure 4.3.

This project has received funding from the European Union's Horizon 2020 research and innovation programme under grant agreement No 958171.

Analysis domain	Parametric methods	Non-parametric methods
Time domain	Poly-reference least square exponential (p-LSCE) (39)	Ibrahim time-domain (ITD) method (43)
	Auto-regressive moving average (40) (ARMA) methods	Random decrement technique (RDT) (44)
	Covariance-driven stochastic subspace identification (SSI-cov) (41)	Principal Component Analysis (PCA)/Blind Source Separation Methods
	Data-driven stochastic subspace identification (SSI-data) (42)	
	Natural Excitation Technique (NExT)/Eigensystem Realization Algorithm (ERA)	
Frequency domain	Poly-reference least square frequency domain (p-LSCF) method (45)	Frequency Response Function estimation
	Stochastic frequency-domain subspace method (46)	Peak picking or Circle Fitting methods
		Least Squares Frequency Domain (LSFD)
		Frequency domain decomposition (FDD) method (47)

Figure 4.3 – List of techniques for OMA data

The richness and complexity of the OMA methods with the five different types of numerical techniques employed in their development is depicted in [30]. A peculiar aspect of output-only modal identification based on the fitting of response correlation functions is the possibility to use methods that stem from classical input-output identification methods based on impulse response functions. Some of these methods are the Ibrahim time domain (ITD), the multiple reference Ibrahim time domain (MRITD), the least-squares complex exponential (LSCE), the polyreference complex exponential (PRCE) or the covariance-driven stochastic subspace identification (SSI-COV).

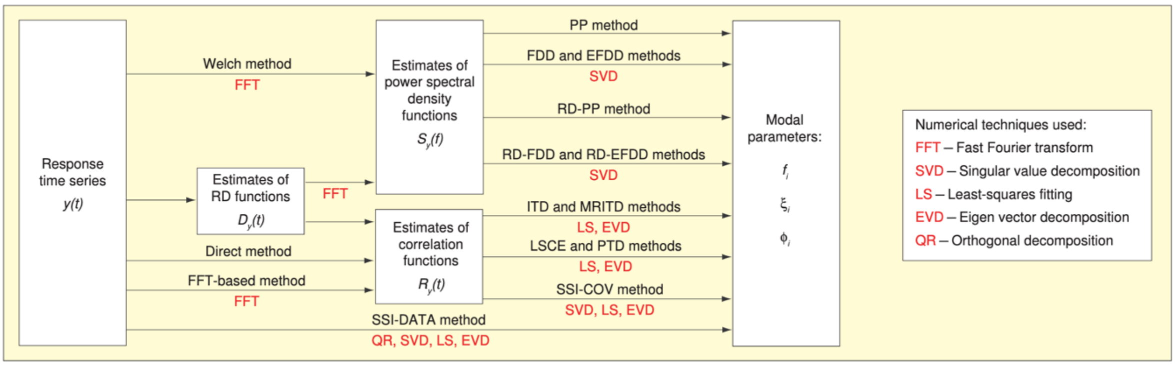

Figure 4.4 – Overview of modal parameters extraction through FFT-based analysis.

Advantages and disadvantages of the most used OMA techniques are summarized in this interesting report [31], and the table contained in Figure 4.5, extracted from the same source.

This project has received funding from the European Union's Horizon 2020 research and innovation programme under grant agreement No 958171. © 2021
IM-SAFE-Project | TNO, The Netherlands, All right reserved |

Method	Type	Pros	Cons
PP	Frequency domain	Simplest, easiest and computationally most undemanding method	Inaccurate if a system has closely spaced modes which is the case in most real structures
FDD	Frequency domain	Can identify natural frequencies and closely spaced mode shapes accurately	Cannot estimate damping ratios
EFDD	Frequency domain	User-friendly and fast processing method Can identify damping ratios along with mode shapes and natural frequencies with higher accuracy than FDD	Exact computation of modal damping is still an issue which may often lead to biased estimates
TDD	Time domain	Computationally efficient method. Reduces operator interaction greatly during modal analysis process	Difficult to extract modal parameters from closely spaced modes
NExT	Time domain	Provides a good ground to extend EMA techniques in OMA	Nature of the data in OMA is stochastic, while NExT methods have deterministic framework
ARMA	Time domain	Output measurements can be utilized directly	Computationally intensive method
SSI	Time domain	High parameter estimation accuracy and high computational efficiency compared to other OMA methods	Mathematically complex method

Figure 4.5 – Pros and cons of different OMA techniques

In case of structures characterised by non-linear behaviour, a suite of methods is available for tackling such higher order complexities, which are listed in Figure 4.6 separated into parametric and non-parametric methods.

Parametric methods (primarily in time domain)	**Non-parametric methods (primarily in a transformed domain)**
Linear parameter Varying Models (40)	Short-time Fourier Transform (Spectrogram)
Nonlinear Auto-regressive models with eXogenous input (ARMA) methods (44)	Wavelet based Analysis (54)
Smoothness Priors Time-Varying AR models (SP-TAR) (49)	Hilbert–Huang transform (HHT)/ Empirical Mode Decomposition (EMD) (55)
	Kernel PCA (56)

Figure 4.6 – Examples for parametric and non-parametric methods for nonlinear and non-stationary systems

Recently some machine learning approaches have been suggested for OMA [32] and for nonlinear modal analysis [33].

4.2.10 Analysis methods for Big Data

4.2.10.1 Big data definition

Nowadays it is common to speak about the seven Vs that characterize the properties of big data: Variety, Velocity, Volume, Veracity, Variability, Visualization, Value.

The concept of big data has received remarkable attention when dealing with complex engineering problems, also within the civil engineering community. Big data may arise for SHM in the case of long-term monitoring strategies, use of dense sensor networks, exploitation of multiple dynamic tests on the structure and high sampling rates [Reference sensors-20-02328].

This project has received funding from the European Union's Horizon 2020 research and innovation programme under grant agreement No 958171. © 2021

4.2.10.2 Big data analysis technologies and methods

The Hadoop Distributed File System (HDFS) is a distributed file system designed to run on commodity hardware. It has many similarities with existing distributed file systems, but the differences are significant. HDFS is highly fault-tolerant, designed to be deployed on low-cost hardware, provides high throughput access to application data and is suitable for applications that have large data sets.

Hadoop MapReduce is a software framework for easily writing applications which process vast amounts of data (multi-terabyte datasets) in-parallel on large clusters (thousands of nodes) of commodity hardware in a reliable, fault-tolerant manner.

A MapReduce *job* usually splits the input dataset into independent chunks which are processed by the *map tasks* in a completely parallel manner. The framework sorts the outputs of the maps, which are then input to the *reduce tasks*. Typically, both the input and the output of the job are stored in a filesystem. The framework takes care of scheduling tasks, monitoring them and re-executes the failed tasks.

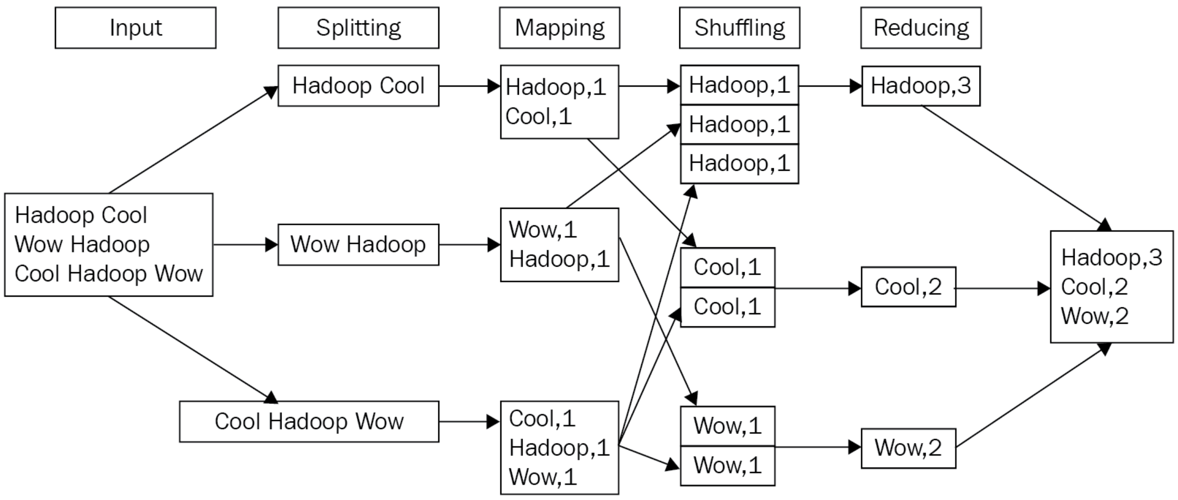

Figure 4.7 – Example of a map reduce job [34]

4.2.11 Machine learning

4.2.11.1 Introduction

Machine learning algorithms build a model based on sample data, known as *training data*, to make predictions or decisions without being explicitly programmed to do so. Machine learning methods can be divided into three broad categories, depending on the nature of the signal or feedback available to the learning system:

- Supervised learning: The computer is presented with example inputs and their desired outputs (*labels*), and the goal is to learn a general rule that maps inputs to outputs.
- Unsupervised learning: No labels are given to the learning algorithm, leaving it on its own to find structure in its input. Unsupervised learning can be a goal (discovering hidden patterns in data) or a means towards an end (feature learning).
- Reinforcement learning: A computer program interacts with a dynamic environment in which it must perform a certain goal (such as driving a vehicle or playing a game against an opponent). As it navigates its problem space, the program is provided feedback that's analogous to rewards, which it tries to maximize.

Supervised learning algorithms build a mathematical model of a set of data that contains both the inputs (features) and the corresponding outputs (labels). In other words, the learned model defines the relationship between features and label. *Training* means creating or learning the

This project has received funding from the European Union's Horizon 2020 research and innovation programme under grant agreement No 958171. © 2021

model, *inference* means applying the trained model to unlabelled examples, hence, using the trained model to make useful predictions. *Regression* models predicts continuous values. *Classification* models handle dependent variables that are classes and is focused on estimating the probability of an observation belonging to each class. Dependent variables in classification problem are discrete and mutually exclusive groups or classes.

In supervised learning, the data has one or more inputs and the desired output, also known as a *label*. In the mathematical model, each example is represented by an array or vector, sometimes called a *feature vector*, and the data is represented by a matrix. The data are split in three portions: the *training set* is used to train the algorithm, the *development set* is used to choose the best performing algorithms or the best hyperparameter values, the *test set* is used as a proxy for new data and serves to evaluate how the chosen algorithm would perform on unseen examples. Examples of commonly used ratios between the training, dev and test sets are 80:10:10 or 70:15:15, but these ratios strictly depend on the amount of available data and may be task specifics. The test set should be large enough to yield statistically meaningful results and be representative of the data set as a whole. Ideally, training, development and test set should all come from the same distribution. If this is not possible, at least development and test sets should meet this requirement. Each sample should be present in one and only one of the training, development, and test portion, so as to allow for appropriate *cross-validation* of the model performance on a test data set that is independent from the training data set. Optimization of the objective function

Through iterative *optimization* of an *objective function*, supervised learning algorithms learn a function that can be used to predict the output associated with *new*, *unseen* inputs. The *objective function* is either a loss function, in which case it must be minimized or its opposite (e.g., a reward function in reinforcement learning), in which case it is to be maximized. The purpose of loss functions is to compute the quantity that a model should seek to minimize during training. There are various factors involved in choosing a loss function for a specific problem, such as the type of machine learning algorithm chosen, the ease of calculating the derivatives and to some degree the percentage of outliers in the data set. Broadly, loss functions can be classified into two major categories, depending upon the type of learning task, *Regression losses* and *Classification losses*. For a list of several available loss functions, the reader is referred to the following sources: Keras API (https://keras.io/api/losses/).

There are many different types of *optimization algorithms* that can be used for continuous function optimization problems. Usually, they are classified into two main groups, depending on whether the target function that is being optimized (in this case the objective function) is differentiable or non-differentiable. First-order optimization algorithms explicitly involve using the first derivative (gradient) to choose the direction to move in the search space. The procedures involve first calculating the gradient of the function, then following the gradient in the opposite direction (e.g., downhill to the minimum for minimization problems) using a step size (also called the *learning rate*). The step size is a hyperparameter that controls how far to move in the search space. A step size that is too small results in a search that takes a long time and can get stuck, whereas a step size that is too large will result in zig-zagging or bouncing around the search space, missing the optima completely. First-order algorithms are generally referred to as *gradient descent*, with more specific names referring to minor extensions to the procedure, e.g. Gradient Descent, Momentum, Adagrad, RMSProp, Adam. The *gradient descent algorithm* also provides the template for the popular stochastic version of the algorithm, named Stochastic Gradient Descent (SGD) that is used to train artificial neural networks (deep learning) models. The important difference is that the gradient is approximated rather than calculated directly, using prediction error on training data, such as one sample (stochastic), all examples (batch), or a small subset of training data (mini-batch). The extensions designed to accelerate the gradient descent algorithm (momentum, etc.) can be and are commonly used with SGD, e.g., Stochastic Gradient Descent, Batch Gradient Descent and Mini-Batch Gradient Descent.

This project has received funding from the European Union's Horizon 2020 research and innovation programme under grant agreement No 958171.

4.2.11.2 Evaluation metrics in classification

A classification model returns the probability for each sample of belonging to a specific class. Starting from the probability assigned by the model, in the two-class classification task a threshold is applied to decide which class must be predicted for each sample data. While in the multi-class task, one can choose amongst various possibilities: the *highest probability value* and the *softmax* are the most used techniques.

Classes	Predicted A	Predicted B	Predicted C	Predicted D
Actual A	TN	FP	TN	TN
Actual B	FN	TP	FN	FN
Actual C	TN	FP	TN	TN
Actual D	TN	FP	TN	TN

Figure 4.8 – Confusion Matrix for multiclass classification. TP, FP, TN and FN are assigned with respect to class B

Performance indicators are very useful when the aim is to evaluate and compare different classification models or machine learning techniques. Many metrics are based on the *confusion matrix*. The confusion matrix is a cross table that records the number of occurrences between two raters, the true/actual classification and the predicted classification [35], similarly to the table in Confusion Matrix for multiclass classification. TP, FP, TN and FN are assigned with respect to class B. There the columns stand for model prediction whereas the rows for the true classification. We focus on class B and consider True Positive (TP) as the only correctly classified units for our class, False Positive (FP) and False Negative (FN) are the wrongly classified elements on the column and the row of the class respectively, while True Negative (TN) are all the other tiles.

Precision for class *i* is the fraction of pertinent instances among all the instances assigned to class *i*. *Recall* (also known as sensitivity) for class *i* is the fraction of relevant instances of class *i* that were retrieved. *Macro averaged precision* and *recall* of the classifier are the arithmetic means of the per-class precision and recall, respectively. *F-score* is a measure that combines precision and recall (their harmonic mean). The *macro-averaged F-score* is computed as the arithmetic mean of the per-class F-scores [36]. In *weighted-average F-score*, the F-score of each class is weighted by the number of samples from that class.

Precision of generic class i	$Precision_i = \frac{TP_i}{(TP_i + FP_i)}$
Recall or True Positive Rate of generic class i	$Recall_i = \frac{TP_i}{(TP_i + FN_i)}$
False Positive Rate	$FalsePositiveRate_i = \frac{FP_i}{(FP_i + TN_i)}$
Macro Average Precision for n classes	$MacroPrecision = \frac{1}{n}\sum_i Precision_i$
Macro Average Recall for n classes	$MacroRecall = \frac{1}{n}\sum_i Recall_i$

This project has received funding from the European Union's Horizon 2020 research and innovation programme under grant agreement No 958171.

Macro F-score for n classes*	$$MacroF-score=\frac{1}{n}\sum_{i}(1+b^2)\frac{Precision_i * Recall_i}{b^2 * Precision_i + Recall_i}$$ F1-score, if b =1 F05-score, if b =0.5, more emphasis on precision than recall F2-score, if b =2, weights recall higher than precision
Micro Average Precision for n classes	$$Micro-\Pr e cision=\frac{\sum_i^n TP_i}{\sum_i^n (TP_i+FP_i)}$$
Micro Average Recall for n classes	$$Micro-Recall=\frac{\sum_i^n TP_i}{\sum_i^n (TP_i+FN_i)}$$
Micro Average F-score for n classes	$$Micro-F-score=\frac{1}{n}\sum_{i}^{n}(1+b^2)\frac{\Pr e cision_i \cdot Recall_i}{b^2 \cdot \Pr e cision_i + Recall_i}$$
Accuracy	$$Accuracy=\frac{TP+TN}{TP+FP+TN+FN}$$

Table 4-5 – Definition of multiclass classification metrics

Another way to evaluate classification performance is to use the area under the receiver operating characteristic (ROC) curve. A ROC curve for a binary classifier plots true positive rates (TPR) vs. false positive rates (FPR) at different classification thresholds. Lowering the classification threshold classifies more items as positive, thus increasing both FP and TP. The Area Under the ROC Curve (AUC) measures the entire two-dimensional area underneath the entire ROC curve (ranges in value from 0 to 1). AUC provides an aggregate measure of performance across all possible classification thresholds, is scale- and classification-threshold-invariant. A model whose predictions are 100% wrong has an AUC of 0.0; one whose predictions are 100% correct has an AUC of 1.0. More on AUC can be found in [37].

4.2.11.3 Evaluation metrics for regression models

Three error metrics that are commonly used for evaluating and reporting the performance of regression models. If we define *n* as the sample number, y_i the real value and $\hat{y}_i$ the predicted value, these metrics can be expressed as presented in Table 4-6.

Mean Squared Error (MSE)	$$\frac{1}{n}\sum_{1}^{n}(y_i-\hat{y}_i)^2$$
Root Mean Squared Error (RMSE)	$$\sqrt{\frac{1}{n}\sum_1^n (y_i-\hat{y}_i)^2}=\sqrt{MSE}$$

This project has received funding from the European Union's Horizon 2020 research and innovation programme under grant agreement No 958171. © 2021

Mean Absolute Error (MAE)	$\frac{1}{n}\sum_{1}^{n}\lvert y_i - \hat{y}_i\rvert$

Table 4-6 – Common evaluation metrics for regression problems

4.2.11.4 Bias vs variance and overfitting

The *bias* error is an error from erroneous assumptions in the learning algorithm. High bias can cause an algorithm to miss the relevant relations between features and target outputs, hence to *underfit*. The *variance* is an error from sensitivity to small fluctuations in the training set. High variance may result from an algorithm learning the random noise in the training data, hence to overfit. *Overfitting* happens when the trained network fits the training dataset perfectly (low training error) but fails to generalize to other data samples that it hasn't seen before (high validation error).

4.2.11.5 Class unbalance

Most standard algorithms assume or expect balanced class distributions or equal misclassification costs per class. Therefore, when presented with complex imbalanced data sets, these algorithms fail to properly represent the distributive characteristics of the data and resultantly provide unfavourable accuracies across the classes of the data. With *imbalanced dataset* it is usually referred to *between-class imbalance*, where some classes are represented by many examples, while other classes by very few (i.e., some classes severely out represent others). The imbalance may be a direct result of the nature of the dataspace (*intrinsic imbalance)*, or rather be a consequence of how the data are collected and stored (*extrinsic imbalance)*. Imbalance due to *rare instances* is representative of domains where minority class examples are very limited, i.e., where the target concept is rare. In this situation, the lack of representative data will make learning difficult regardless of the between-class imbalance. Furthermore, the minority concept may additionally contain a subconcept with limited instances, amounting to diverging degrees of classification difficulty. This is defined as *within-class imbalance*. When standard learning algorithms are applied to imbalanced data, the induction rules that describe the minority concepts are often fewer and weaker than those of majority concepts, since the minority class is often both outnumbered and underrepresented.

In case of imbalance, it is important to apply some specific solutions but also to use the most appropriate evaluation metrics [38]. Typically, the use of *sampling methods* in imbalanced learning applications consists of the modification of an imbalanced data set by some mechanisms in order to provide a balanced distribution. The most popular are *random oversampling* (augment the original dataset by replicating randomly selected minority examples), *random undersampling* (removes randomly selected majority class examples from the original data set), *informed undersampling*. While sampling methods attempt to balance distributions by considering the representative proportions of class examples in the distribution, *cost-sensitive learning methods* consider the costs associated with misclassifying examples.

4.2.11.6 Leakage

Leakage is essentially the introduction of information about the data mining target, which should not be legitimately available to mine from [39]. Usually, the introduction of illegitimate information is unintentional, and a consequence of data collection, aggregation, and preparation process. It is mostly subtle and indirect, therefore hard to detect and eliminate.

4.2.12 Deep learning

4.2.12.1 Artificial neural networks (ANNs)

- ANN Structure

This project has received funding from the European Union's Horizon 2020 research and innovation programme under grant agreement No 958171.

ANNs are composed of artificial neurons which are conceptually derived from biological neurons. The neurons are typically organized into multiple layers: neurons of one layer connect only to neurons of the immediately preceding and immediately following layers. The layer that receives external data is the *input layer*. The layer that produces the ultimate result is the *output layer*. In between them, are zero or more *hidden layers*. If there is more than one hidden layer, then such a network is a *deep neural network*. With each layer, the network transforms the data, creating a new *representation*. Between two layers, multiple connection patterns are possible. Adjacent layers can be *fully connected*, with every neuron in one layer connecting to *every* neuron in the *next* layer or can be *pooling*, where a group of neurons in one layer connect to a single neuron in the next layer, thereby reducing the number of neurons in that layer. Neurons with only such connections form a directed acyclic graph and are known as *feedforward networks*. Alternatively, networks that allow connections between neurons in the same or previous layers are known as *recurrent networks.*

Each artificial neuron has inputs (x_i) and produces a single output which can be sent to other neurons. Each neuron is assigned a *bias*, *b,* and each of its connections to other neurons is assigned a *weight*, w_i. The output of each neuron is then calculated applying a non-linear-transformation or *activation function* σ to the weighted sum of its inputs, i.e., $\sigma(b + \sum w_i \cdot x_i)$. For the nodes in the input layer, the inputs are feature values of a sample of external data, such as images or documents. For the nodes in the hidden and output layers, the inputs are the outputs of other neurons. The outputs of the neurons in the output layer accomplish the task.

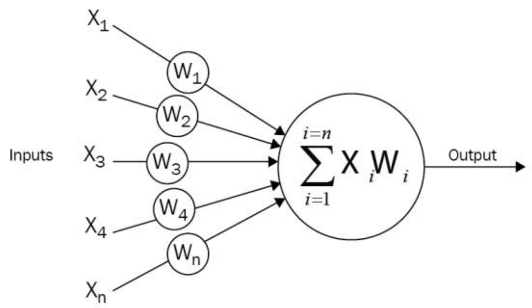

Figure 4.9 – Single neuron or node

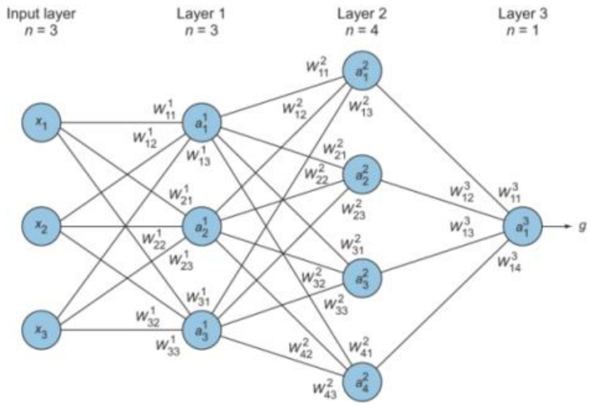

Figure 4.10 – Network of layers of neurons or nodes [40]

The most important feature in an activation function is its ability to add non-linearity into a neural network, hence, to enable the modelling of complex non-linear problems. Different layers may have different activation functions. Activation functions must be differentiable and ideally should be zero-centred, robust against the vanishing gradient problem, and computationally inexpensive. The most known are Sigmoid and Softmax, Rectified Linear Unit

This project has received funding from the European Union's Horizon 2020 research and innovation programme under grant agreement No 958171.

(ReLu), Hyperbolic tangent function (Tanh). For a list of activation functions and how to choose them please read:

- ANN Training

Neural networks can automatically discover combinations of the original features that are important through their training process. Random combinations of the original features are initially created by multiplying the feature by a random weight matrix. During training, the neural network learns to refine combinations that are helpful and discard those that are not. This process of learning which combinations of features are important is known as *representation learning* and makes neural networks successful across different domains.

Training ANNs is performed by backward propagation of errors. It is a common method of training ANNs used in conjunction with an optimization method such as gradient descent. First, the output values of each node are calculated and cached in a forward pass. Then, the partial derivative of the error with respect to each parameter is calculated in a backward pass through the graph. The optimization method is fed with the gradient and uses it to get the weights updated to reduce the loss function.

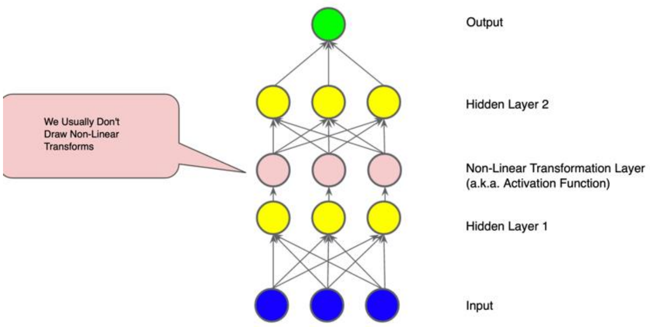

Figure 4.11 – Diagram of a feedforward ANN [41]

To reduce overfitting [42], one can either train the network on more examples (by acquiring more data or by *data augmentation* techniques) or reduce network complexity. As the capacity of a ANN model is defined by both, its structure in terms of number of nodes and layers, and its parameters, in terms of weight values, the complexity of a neural network can be reduced by changing the numbers or the values of weights. It is very common to focus on methods that constrain the size of the weights. Typically used techniques are dropout, *weight regularizations* such *L1* and *L2 regularization*, and *early stopping*. For a complete overview of the regularization taxonomy and method description the reader should refer to [43].

Dropout consists in randomly choosing some proportion *p* of the neurons in a layer and setting them equal to 0 during each forward pass of training. This reduces the capacity of the network, but can prevent overfitting, especially in deeper networks, where the features being learned are multiple layers of abstraction removed from the original features. The percentage *p* is an hyperparameter to be tuned when building the network. Dropout helps reduce interdependent learning among the neurons. L1 and L2 regularization methods add a cost to the loss function. The L2 approach is perhaps the most used and is traditionally referred to as weight decay in the field of neural networks. For additional detailed reading please refer to [44].

4.2.12.2 Convolutional Neural Networks (CNN)

CNNs and their multichannel convolution operations are mostly commonly applied to images, but the more general idea of representing data that is arranged along some spatial dimension with multiple “channels” is applicable beyond images.

CNNs mainly consist of three type of layers: i) convolutional layers, where a kernel (or filter) of weights is convolved in order to extract features; ii) nonlinear layers, which apply an activation function on feature maps (usually element- wise) in order to enable the modelling of

This project has received funding from the European Union’s Horizon 2020 research and innovation programme under grant agreement No 958171. © 2021

non-linear functions by the network; and iii) pooling layers, which replace a small neighbourhood of a feature map with some statistical information (mean, max, etc.) about the neighbourhood and reduce spatial resolution. The units in layers are locally connected; that is, each unit receives weighted inputs from a small neighbourhood, known as the receptive field, of units in the previous layer. By stacking layers to form multi-resolution pyramids, the higher-level layers learn features from increasingly wider receptive fields. The main computational advantage of CNNs is that all the receptive fields in a layer share weights, resulting in a significantly smaller number of parameters than fully-connected neural networks.

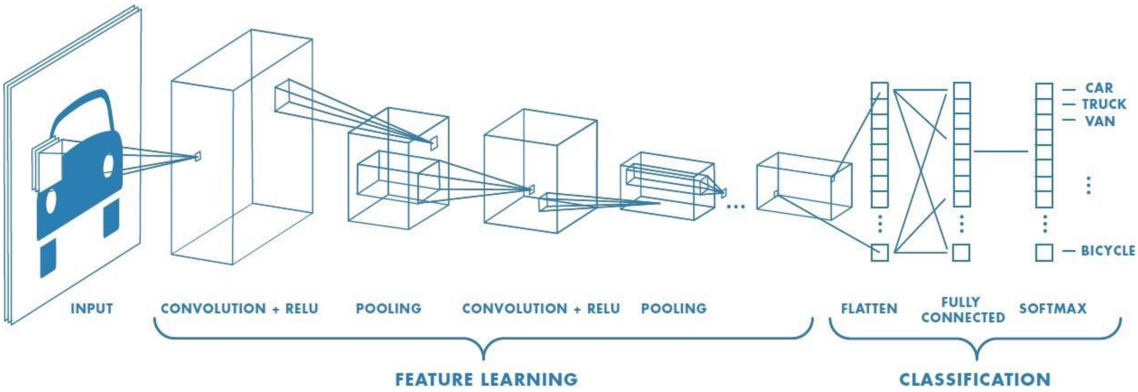

Figure 4.12 – Architecture elements of CNN [45]

In machine learning, linear combinations of the original features are needed to effectively predict the target. In images, the interesting combinations of features mostly come from pixels close together in the image. In an image, it is much less likely that an interesting feature will result from a combination of n^2 randomly selected pixels throughout the image than from a n × n patch of adjacent pixels. The order of the features matters since it tells us which pixels are near each other spatially. To compute many combinations of the pixels from local patches of the input image we use the convolution operation. Convolution is the process of adding each element of the image to its local neighbours, weighted by a small matrix of weights *W* called *kernel, convolution matrix, or mask*. The values of a given pixel in the output image are calculated by multiplying each kernel value by the corresponding input image pixel values. This value is then treated like the other computed features in neural networks: it may have a bias added to it and be fed through an activation function, to represent a “neuron” or “learned feature” that can be passed along to subsequent layers of the network. Thus, features are defined as functions of small patches of an input image. The fact that 3 × 3 or 5 × 5 arrays of numbers can represent “pattern detectors” when their dot product is taken with the pixel values at each location of an image has been well known in the field of computer vision for a long time. If we *slide* W over the input image, by taking the dot product of W with the pixels at each location of the image, we end up with a new image *O* of almost identical size to the original image *I* (it may be slightly different, depending on how we handle the edges). This image *O* is a kind of *feature map* that shows the locations in the input image where the pattern defined by *W* was present. This operation is in fact what happens in convolutional neural networks; it is called a convolution, and its output is indeed called a *feature* map. To read more about the relationship between input shape, kernel shape, zero padding, strides and output shape in convolutional layers, please refer to [46].

Starting with *n* input pixels, the convolution operation creates a feature map with *n* output features, one for each location in the input image. With *f* filters, the convolution operations are repeated *f* times to create *f* sets of *n* features, each set with a corresponding (initially random) set of weights defining a visual pattern whose detection at each location in the input image will be captured in the feature map. This is called *multichannel convolution operation*.

This project has received funding from the European Union’s Horizon 2020 research and innovation programme under grant agreement No 958171. © 2021

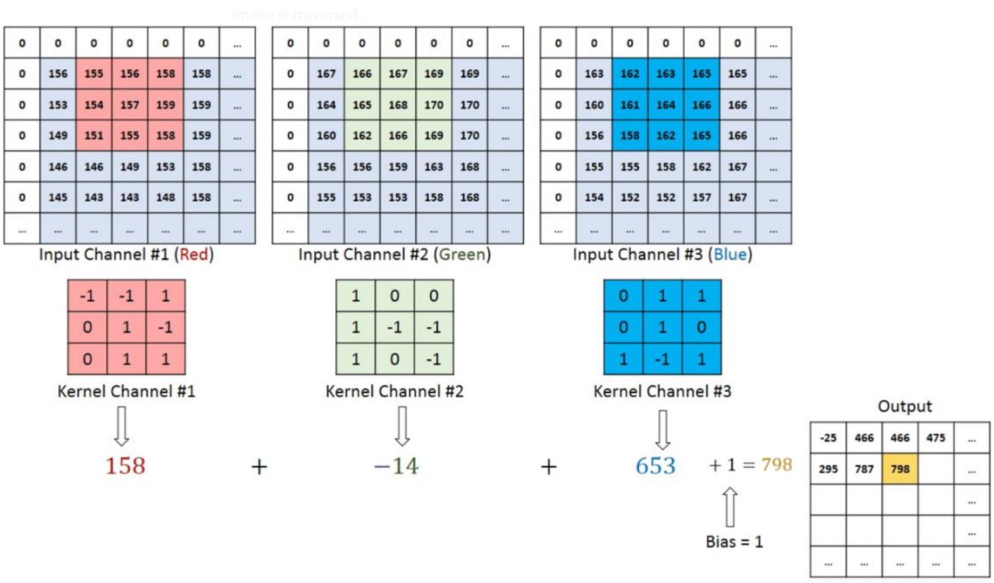

Figure 4.13 – Convolutional operation on the RGB channels of an image patch [47]

Pooling layers are used in convolutional neural networks to down sample each of the feature maps created by a convolution operation. Assuming a pooling size of *p*, this involves mapping each p × p section of each feature map either to the maximum value of that section (*max-pooling*) or to the average value of that section (*average-pooling*). The resulting output has donwsampled dimension $\frac{n}{p} \times \frac{n}{p}$.

Together, the convolutional layer and the pooling layer, form the *i*-th layer of a CNN. Depending on the complexities in the images, the number of such layers may be increased for further capturing low-levels details, at the cost of more computational power. To make predictions with convolutional layers, the feature maps of the last layer must be *flattened* into a one-dimensional vector and then simple matrix multiplication used to make the final predictions. The flattened output is fed to a feed-forward neural network and backpropagation applied to every iteration of training. Some of the most well-known CNN architectures include: AlexNet [48], VGGNet [49], ResNet [50], GoogLeNet [51], MobileNet [52], and DenseNet [53].

- Fully convolutional neural networks

Fully convolutional neural networks are used for semantic segmentation. The key ideas consist in replacing the fully connected layers with 1x1 convolutional layers and in up-sampling the output of the fully-convolutional network to obtain a pixel-wise classification [54].

4.2.12.3 Recurrent Neural Networks

While CNNs can efficiently process spatial information, recurrent neural networks (RNNs) are designed to better handle sequential information. RNNs introduce state variables to store past information, together with the current inputs, to determine the current outputs. A recurrent neural network (RNN) is a special type of an artificial neural network adapted to work for time series data or data that involves sequences. Ordinary feed-forward neural networks are only meant for data points, which are independent of each other. However, if we have data in a sequence such that one data point depends upon the previous data point, we need to modify the neural network to incorporate the dependencies between these data points. RNNs have the concept of 'memory' that helps them store the states or information of previous inputs to generate the next output of the sequence.

This project has received funding from the European Union's Horizon 2020 research and innovation programme under grant agreement No 958171. © 2021

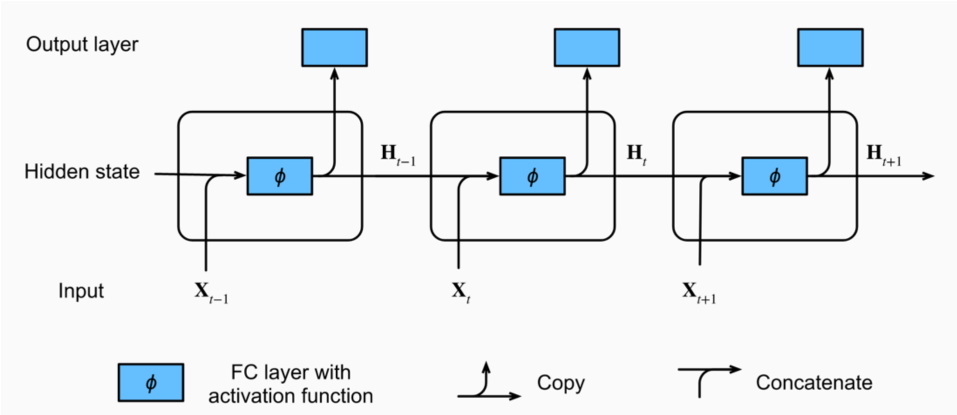

Figure 4.14 – Temporal unfolding of the dynamics of an RNN [44]

Figure 4.14 illustrates the computational logic of an RNN at three adjacent time steps (t-1, t, t+1). At any time step *t*, the computation of the hidden state can be treated as: (i) concatenating the input X_t at the current time step *t* and the hidden state H_{t-1} at the previous time step $t-1$; (ii) feeding the concatenation result into a fully-connected layer with the activation function ϕ. The output of such a fully-connected layer is the hidden state H_t of the current time step t. In this case, the model parameters are the concatenation of W_{xh} and W_{hh}, and a bias of $\mathbf{b}_h$. The hidden state of the current time step t, H_t, will participate in computing the hidden state H_{t+1} of the next time step $t+1$. What is more, H_t will also be fed into the fully-connected output layer to compute the output O_t of the current time step t.

- Long Short Term Memory (LSTM) and GRU

Gated RNNs such as *gated recurrent units* (GRUs) and *long short-term memory* (LSTM) are more common in practice. Gating of the hidden states means that we have dedicated mechanisms for when a hidden state should be *updated* and when it should be *reset*. These mechanisms are learned. If the first token is of great importance, the network will learn not to update the hidden state after the first observation. Likewise, the network will learn to skip irrelevant temporary observations or to reset the latent state whenever needed.

The LSTM [55] introduces a *memory cell* (or *cell* for short) that has the same shape as the hidden state, engineered to record additional information (stores values over arbitrary time intervals). To control the memory cell, hence, to regulates the flow of information into and out, three gates are needed. The *output gate* is needed to read out the entries from the cell. The *input gate* is needed to decide when to read data into the cell. The *forget gate* will be used to reset the content of the cell. The motivation for such a design is the same as that of GRUs, namely to be able to decide when to remember and when to ignore inputs in the hidden state via a dedicated mechanism.

4.2.12.4 Encoder-decoder and autoencoder

Encoder-Decoder models are a family of models which learn to map data-points from an input domain to an output domain via a two-stage network: The encoder, represented by an encoding function z = f(x), compresses the input into a latent-space representation; the decoder, y = g(z), aims to predict the output from the latent space representation. The latent representation here essentially refers to a feature vector representation, which can capture the underlying semantic information of the input that is useful for predicting the output. These models are extremely popular in image-to-image translation problems, as well as for sequence-to-sequence models in NLP. These models are usually trained by minimizing the reconstruction loss $L(y, \hat{y})$ which measures the differences between the ground-truth output y and the subsequent reconstruction $\hat{y}$. The output here could be an enhanced version of the image (such as in image de-blurring, or super-resolution), or a segmentation map. Auto-

This project has received funding from the European Union's Horizon 2020 research and innovation programme under grant agreement No 958171. © 2021
IM-SAFE-Project | TNO, The Netherlands, All right reserved |

encoders are special case of encoder-decoder models in which the input and output are the same.

4.2.12.5 Attention and Transformers

Transformers are a recent class of deep learning layers that are heavily based on the idea of self- and cross-attention [56] Since their introduction in 2017 [56] they've been setting the state-of-the-art in Natural Language Processing tasks, as they are at the basis of Large Language Models like GPT-3 and BERT-based neural networks. Interestingly, recently they've also been introduced in architectures for computer vision, like the Vision Transformer, which are starting to chip away at the dominance of Convolutional Neural Network in the vision domain.

4.2.12.6 Generative models

GANs are deep learning models that consist of two networks, a *generator G* and a *discriminator D*. The generator network $G = z \rightarrow y$ in the conventional GAN learns a mapping from noise z (with a prior distribution) to a target distribution y, which is like the real samples. The discriminator network D attempts to distinguish the generated samples or fakes from the real ones. GAN is defined as a *minimax game* between G and D, where D is trying to minimize its classification error in distinguishing fake samples from real ones (hence maximizing the loss function), and G is trying to maximize the discriminator network's error (hence minimizing the loss function). For additional details, we refer the reader to the original paper [57], the following open AI contribution [58], and a code repository with many generative models [59].

4.2.12.7 Best DL-models for time series

In the past few years, many notable architectures have been published such as the *Multi-Horizon Quantile Recurrent Forecaster (MQRNN) and the Deep Space-State Models (DSSM).* Amongst the latest best models for time series forecasting are N-BEATS [60], DeepAR [61], Spacetimeformer, Temporal Fusion Transformer [62] or TFT. Temporal Fusion Transformer (TFT) is an attention-based DNN architecture for multi-horizon forecasting that achieves high performance while enabling new forms of interpretability.

4.2.12.8 Transfer learning

When enough labelled training data is available, the DL models can be trained from scratch on new the available new datasets for the required applications. When this is not the case, transfer learning can be used to re-purpose a model previously trained on one task (for which a large amount of training data is available) on a new but related task (for which only a limited number of training data is available), usually by some adaptation process toward the new task. In image segmentation case, many people use a model trained on ImageNet (give numbers about ImageNet), as the encoder part of the network, and re-train their model from those initial weights. The assumption here is that those pre-trained models should be able to capture the semantic information of the image required for segmentation, and therefore enabling them to train the model with less labelled samples.

4.2.12.9 AutoML

AutoML frameworks offer the potential of implementing best ML practices only once (including strategies for model selection, ensembling, hyperparameter tuning, feature engineering, data preprocessing, data splitting, etc.), and then being able to repeatedly deploy them. This allows experts to scale their knowledge to many problems without the need for frequent manual intervention. The aim of such frameworks is to robustly take raw data and deliver high-quality predictions without any user input and without software errors. For a review, please refer to [63].

This project has received funding from the European Union's Horizon 2020 research and innovation programme under grant agreement No 958171.

4.2.13 Classic Computer Vision technologies vs Deep Learning methods

4.2.13.1 Computer vision tasks

Since several of the surveying technologies rely on image analysis (Boroscopy, Endoscopy, Visual inspection), we devote a whole paragraph on this type of data analysis.

4.2.13.2 Traditional computer vision approaches

The traditional Computer Vision (CV) approach relies on the use of well-established techniques of feature detection, feature descriptors and feature matching.

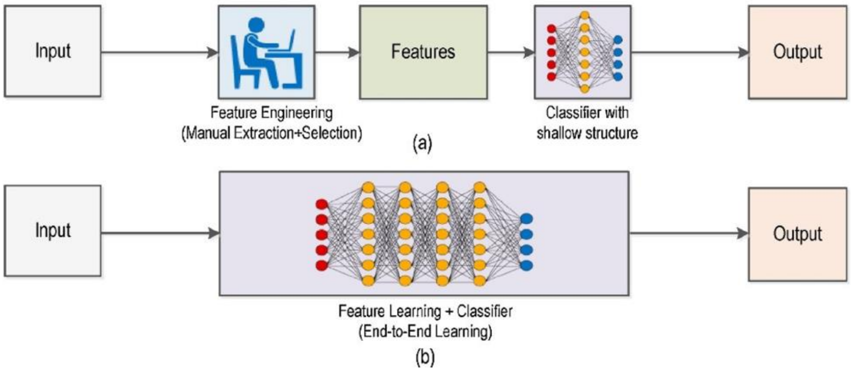

Figure 4.15 – Classic computer versus Deep Learning approaches

In CV and image processing, a feature is a piece of information about the content of an image; typically about whether a certain region of the image has certain properties. Features may be specific structures in the image such as points, edges or objects. Feature detection includes methods for computing abstractions of image information and making local decisions whether there is an image feature of a given type at that specific image point. Several CV algorithms, such as edge detection, corner detection or threshold segmentation may be involved in this step. The resulting features will be subsets of the image domain, often in the form of isolated points, continuous curves or connected regions. Once features have been detected, a local image patch around the feature can be extracted. This extraction may involve quite considerable amounts of image processing. The result is known as a feature descriptor or feature vector. The feature detection step by itself may also provide complementary attributes, such as the edge orientation and gradient magnitude in edge detection and the polarity and the strength of the blob in blob detection. Features detected in each image can be matched across multiple images to establish *corresponding features* such as *corresponding points*.

Amongst the most known feature detection algorithms are Scale-invariant Feature Transform (SIFT) [64], Speeded-up Robust Features (SURF) [65], Features from Accelerated Segment Test (FAST), Oriented FAST and Rotated BRIEF (ORB), Binary Robust Independent Elementary Features (BRIEF), KAZE [66].

To perform CV tasks, as many features as practicable are extracted from images and these features form a definition (known as a bag-of-words) of each object class. At the deployment stage, these definitions are searched for in the new images. If a significant number of features from one bag-of-words are in the new image, the image is classified as containing that specific object (i.e. chair, horse, etc.).

The difficulty with this traditional approach is that it is necessary to choose which features are important in each given image. As the number of classes to classify increases, feature extraction becomes more and more cumbersome. It is up to the CV engineer's judgment and a long trial and error process to decide which features best describe different classes of objects. Moreover, each feature definition requires dealing with a plethora of parameters, all of which must be fine-tuned by the CV engineer. Algorithms like SIFT and even simple colour thresholding and pixel counting algorithms are not class-specific, that is, they are very general

This project has received funding from the European Union's Horizon 2020 research and innovation programme under grant agreement No 958171. © 2021

and perform the same for any image. Therefore, SIFT and other algorithms are often used for applications such as image stitching/3D mesh reconstruction which don't require specific class knowledge. Today, the traditional techniques are used when the problem can be simplified so that they can be deployed on low-cost microcontrollers or to limit the problem for deep learning techniques by highlighting certain features in data, augmenting data or aiding in dataset annotation.

4.2.13.3 Deep learning for computer vision

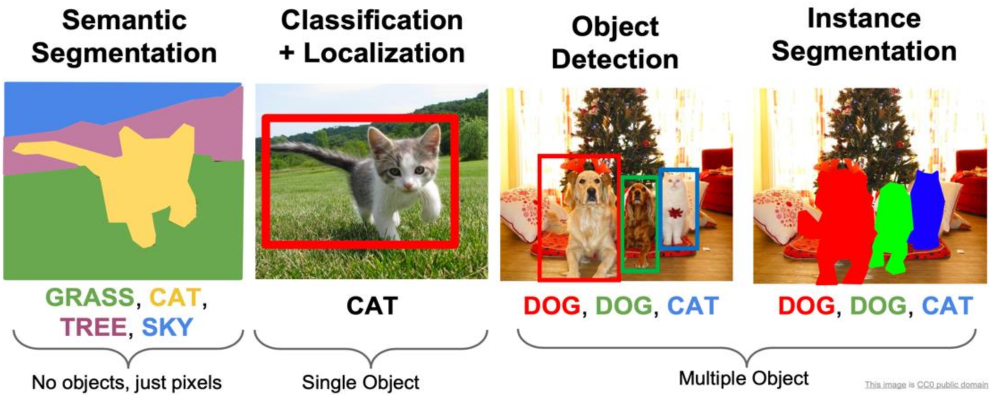

Figure 4.16 – Computer vision tasks [67]

Object detection is a task that involves two main tasks: localizing one or more objects within an image and classifying each object in the image. At high level object detection comprises the following steps:

- Region proposal: an algorithm or a DL model is used to generate regions of interest (RoIs), regions that the network believes might contain an object. The output is many bounding boxes, each with an objectness score. Boxes with large objectness scores are then passed along the network layers for further processing.
- Feature extraction and network predictions: visual features are extracted for each of the bounding boxes and evaluated. It is determined whether and which objects are present in the proposals based on visual features.
- Non-maximum suppression (NMS): in this step, the model has likely found multiple bounding boxes for the same object. NMS combines overlapping boxes into a single bounding box for each object.
- Evaluation metrics: object detection systems have their own metrics to evaluate their detection performance, the most popular metrics are the mean average precision (mAP), precision-recall curve (PR curve), and intersection over union (IoU).

Image segmentation involves partitioning images into multiple segments or objects and can be formulated as a classification problem of pixels with semantic labels (semantic segmentation) or partitioning of individual objects (instance segmentation). *Semantic segmentation* performs pixel-level labelling with a set of object categories (e.g., person, animal, vehicle or crack, spalling, casting defect) for all pixels of the image, thus it is generally a more difficult task than image classification, which predicts a single label for the entire image. *Instance segmentation* extends semantic segmentation scope further by *detecting and delineating* each object of interest in the image (e.g., partitioning of individual defects).

- Models for instance segmentation

Over the years, many deep learning solutions for image segmentation have been developed as seen in the following Figure 4.17.

This project has received funding from the European Union's Horizon 2020 research and innovation programme under grant agreement No 958171.

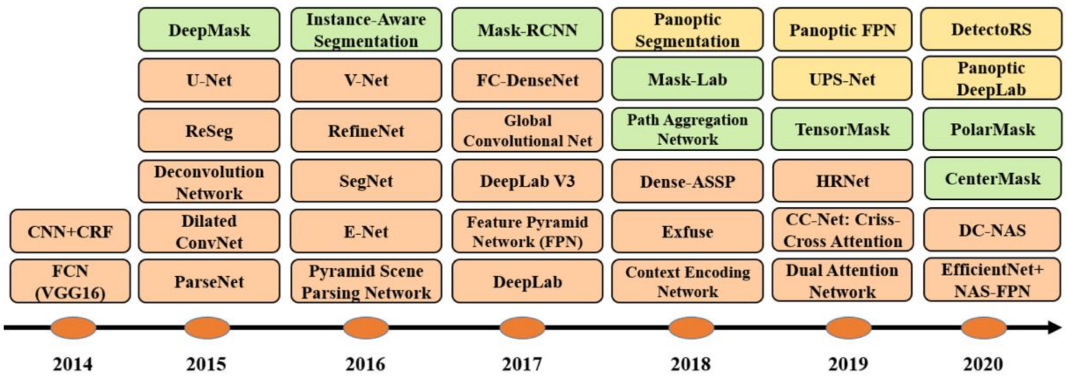

Figure 4.17 –Timeline of the introduction of instance segmentation DL-based models [68]

The regional convolutional network (R-CNN) and its extensions (Fast R-CNN, Faster R-CNN, Masked-RCNN) have proven successful in object detection applications. Some of the extensions have been also widely used to address instance segmentation, hence the task of simultaneously performing object detection and semantic segmentation. Here we report short descriptions and images depicting their high-level architectures, so that the reader can appreciate the main differences. For a detailed description of each model, we refer the reader to the original papers.

Regions with CNN features or *R-CNN* [67] method takes an input image and extracts around 2000 bottom-up region proposals. It then computes features for each proposal using a large CNN and finally classifies each region using class-specific linear SVMs.

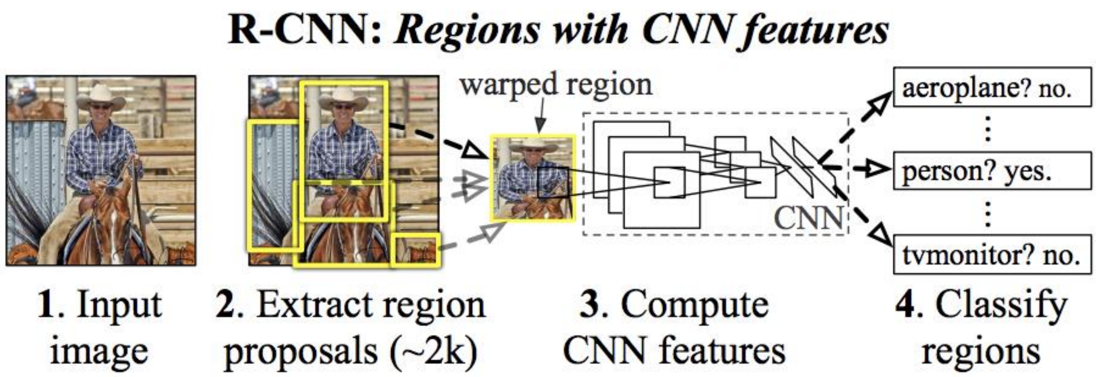

Figure 4.18 – The architecture in [67]

In the *Fast R-CNN* approach [69], instead of feeding the region proposals to the CNN, the input image is directly fed into the CNN to generate a convolutional feature map. From the convolutional feature map, the region of proposals is identified, warped into squares, and reshaped into a fixed size by using a RoI pooling layer, so that it can be fed into a fully connected layer. From the RoI feature vector, a softmax layer predicts the class of the proposed region and the offset values for its corresponding bounding box.

This project has received funding from the European Union's Horizon 2020 research and innovation programme under grant agreement No 958171. © 2021

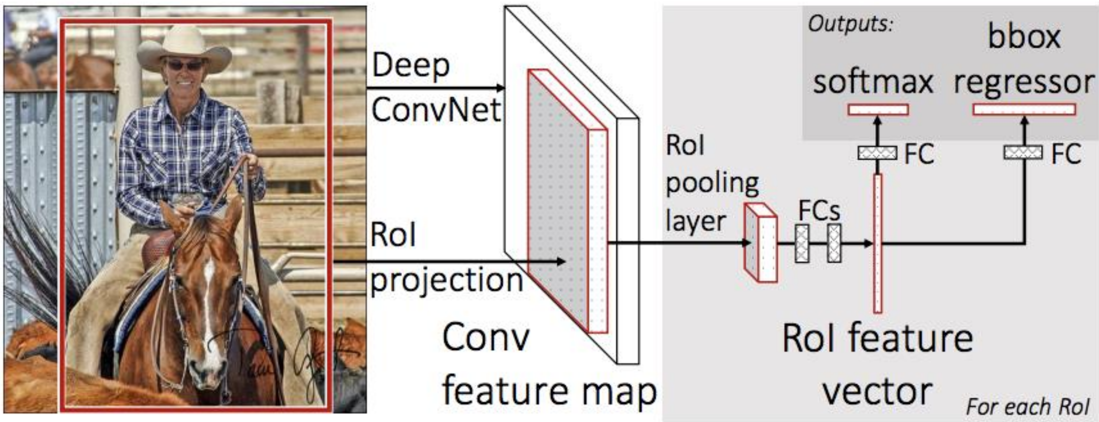

Figure 4.19 – The Fast R-CNN architecture of [69]

Fast R-CNN is faster than R-CNN because it does not require feeding 2000 region proposals to the CNN every time. Instead, the convolution operation is done only once per image and a feature map is generated from it.

The Faster R-CNN architecture [70] developed for object detection uses a region proposal network (RPN) to propose bounding box candidates. The RPN extracts a Region of Interest (RoI), and a RoIPool layer computes features from these proposals to infer the bounding box coordinates and the class of the object.

Feature pyramids are a basic component in recognition systems for detecting objects at different scales. A top-down architecture with lateral connections was developed for building high-level semantic feature maps at all scales. This architecture, called a Feature Pyramid Network (FPN) [71], showed significant improvement as a generic feature extractor in several applications. Using FPN in a basic Faster R-CNN system, it was possible to achieves state-of-the-art single-model results on the COCO detection benchmark surpassing all existing single-model entries.

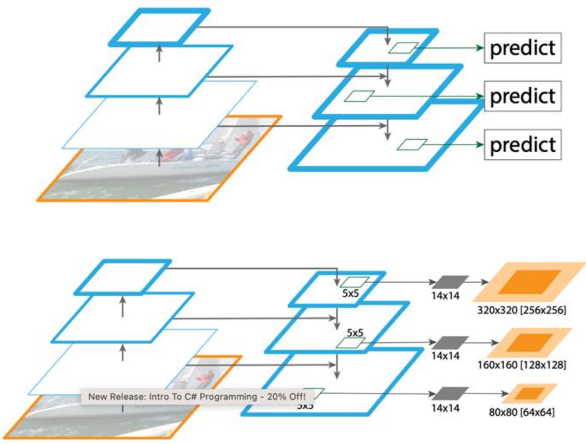

Figure 4.20 – Feature Pyramid Networks for Object Detection. Visual representation [71]

Mask R-CNN [72], extends Faster R-CNN by adding a branch for predicting segmentation masks on each Region of Interest (RoI), in parallel with the existing branch for classification and bounding box regression. The mask branch is a small FCN applied to each RoI, predicting a segmentation mask in a pixel-to-pixel manner. In contrast to the segmentation-first strategy of previous methods, Mask R-CNN is based on an instance-first strategy.

This project has received funding from the European Union's Horizon 2020 research and innovation programme under grant agreement No 958171.

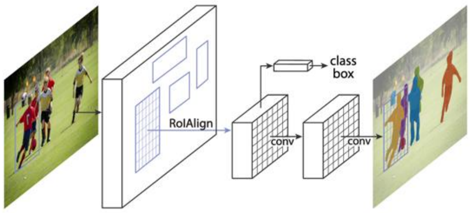

Figure 4.21 – The Mask R-CNN architecture of [72]

- Evaluation Metrics

The most common evaluation metric for object recognition tasks is the mean average precision (mAP). It is expressed as percentage, and while higher values are typically better, its value is different from the accuracy used in standard classification. Intersection over Union (IoU) evaluates the overlap between the ground truth bounding box (B_{ground_truth}) and the predicted bounding box ($B_{predicted}$) and is used to decide whether a detection is valid (True Positive, TP) or not (False Positive, FP). IoU is calculated by dividing the area of overlap (I) by the area of the union (U), as in the following equation:

$$IoU = \frac{B_{ground_{truth}} \cap B_{predicted}}{B_{ground_{truth}} \cup B_{predicted}} = \frac{truepositive}{truepositive + falsepositive + falsenegative} \qquad \textit{Eq. 2}$$

IoU values range from 0 (no overlap at all) to 1 (the two bounding boxes overlap each other 100%). A prediction is defined as a correct prediction or TP, if its IoU value is greater than a specific threshold. The threshold value is tuneable depending on the task, but 0.5 is a standard value. first computes the IOU for each semantic class and then computes the average over classes. Once TP and FP are defined, AP can be calculated as area under the Precision-Recall Curve (AUC) and mAP as the AP averaged over all classes.

This project has received funding from the European Union's Horizon 2020 research and innovation programme under grant agreement No 958171. © 2021

5 Framework for evaluating the fitness-for-purpose18 of surveying technologies

5.1 TRL vs fit-for-purpose

The IM-SAFE project takes into consideration the efforts from the European Commission to develop a strategy to make Europe more attractive for investments in research, technology, innovation, and manufacturing. At present, the biggest challenge in this sense seems to be transferring excellent research and development results into innovative solutions for the markets, bridging the so called 'Valley of Death' that causes many would-be innovations to wither and die [73] (Figure 5.1). This lays in the acceptance by the users, ease and effectiveness of implementation in the process, and the maturity of the technology itself. The latter is dealt with by evaluating the fitness-for-purpose of the technology.

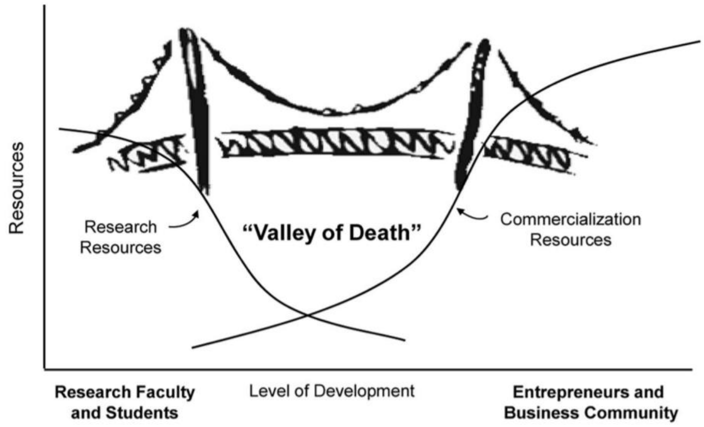

Figure 5.1 – The valley of death bridging the gap between research and commercial application

To analyse the maturity of a technology, the TRA Deskbook [74] defines the concept of technology readiness assessment (TRA) as "a formal, systematic, metrics-based process and accompanying report that assesses the maturity of critical hardware and software technologies to be used in systems". These technologies are called critical technology elements (CTEs) "if the system being acquired depends on this technology element to meet operational requirements (within acceptable cost and schedule limits) and if the technology element or its application is either new or novel or in an area that poses major technological risk during detailed design or demonstration". To assess the maturity of CTEs, the technology readiness level (TRL) is used. Nowadays, the TRL scale (Table 5-1) is the most widely used tool for technology maturity assessment and allows for a consistent comparison of maturity between different types of technologies. The concept was developed by NASA during the 1970's for acquisition phase of a program and was widely adopted to examine concepts and technology requirements, and to demonstrate technology capabilities. In 2010, the European Commission advised European-funded research and innovation projects to adopt the scale for universal usage in context of technology development [75]. In the TRA Deskbook [74], guidance for assessing technology maturity is provided.

[18] Fitness-for-purpose: Degree of suitability (or relevance) of a technique or technology and its associated data analysis methods, in providing reliable information for the structural evaluation in a particular application.

This project has received funding from the European Union's Horizon 2020 research and innovation programme under grant agreement No 958171.

TRL 1	Basic principles observed and reported
TRL 2	Technology concept and/or application formulated
TRL 3	Analytical and Experimental critical function and/or characteristic proof of concept
TRL 4	Technology (component and/or breadboard) validated in lab
TRL 5	Technology (component and/or breadboard) validated in relevant environment (industrially relevant environment in the case of key enabling technologies)
TRL 6	Technology (system/subsystem model or prototype) demonstrated in relevant environment (industrially relevant environment in the case of key enabling technologies)
TRL 7	System prototype demonstration in operational environment
TRL 8	Actual system completed and qualified through test and demonstration
TRL 9	Actual system proven in operational environment (competitive manufacturing in the case of key enabling technologies; or in space)

Table 5-1 – Technology Readiness Level scale in current NASA [76] & European Union usage [77] (definitions combined)

The main two steps in the technology readiness assessment process are: (i) identifying critical technology elements; and (ii) assessing CTE readiness/submitting the TRA report.

(i) Identifying CTEs: Figure 5.2 shows a representative time schedule of the activities to be developed for the critical technology elements identification. For clarification, IRT stands for independent review team, composed by subject matter experts (SME).

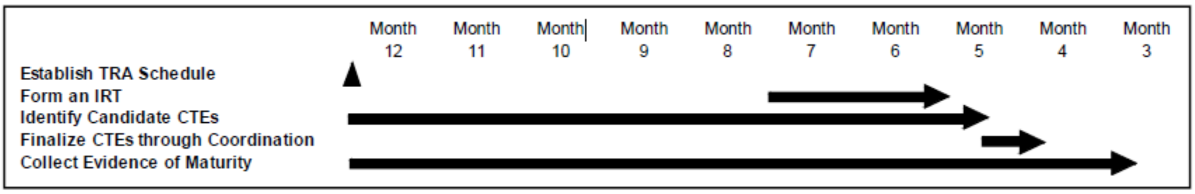

Figure 5.2 – Representative Schedule for Identifying CTEs [74]

(ii) Assessing CTE readiness/submitting the TRA Report. Continuing with the schedule in Figure 5.2, Figure 5.3 presents chronologically the list of activities to be done for the assessment of readiness of a critical technology element. This also includes the submission of the TRA report.

This project has received funding from the European Union's Horizon 2020 research and innovation programme under grant agreement No 958171. © 2021

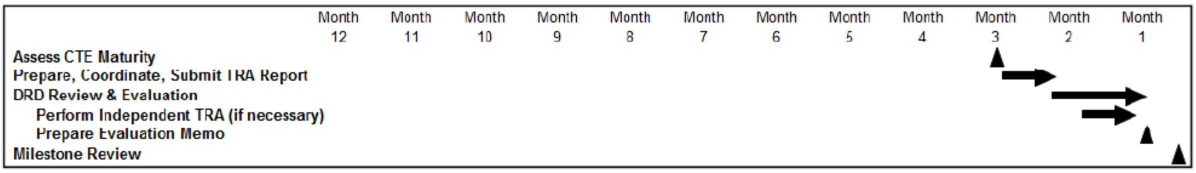

Figure 5.3 – Representative Schedule for Assessing CTE Readiness [74]

For a more detailed explanation of this process, please see the recommendations in [74].

In the IM-SAFE project, the challenge is a different one than in TRA, as it refers to assessing fitness for purpose of the technology rather than its technology development stage (TRL). Hence, it focuses on the already mature technologies, intended for a specific application, such as e.g., the measurement of cracks or displacements, and being supported by application-specific data analysis methods for the purpose of obtaining reliable results.

This chapter addresses this matter on how to know in an objective way if a technology meets fitness for purpose requirements in the current practice. The answer is to be given by using the concept 'fitness-for-purpose of surveying technology', which is defined as the *degree of suitability (or relevance) of a technique or technology and its associated data analysis methods, in providing reliable information for the structural evaluation in a particular application*. The main objective of introducing such concept is that the 'fitness-for-purpose' concept can serve to evaluate if a surveying technology is capable of meeting its objectives or service levels and, based on the outcomes for multiple technologies allows to choose the most appropriate one for performing a specific survey, and for obtaining specific results (i.e., detection and/or measuring a damage process with the required quality).

5.2 Criteria for evaluating the fitness-for-purpose of technologies for condition survey

5.2.1 Fitness for purpose in the broad sense & IM-SAFE interpretation

This section introduces the conception of fitness-for-purpose from different perspectives. In addition, a comparison between the definitions of monitoring and measuring from ISO 9001:2015 and IM-SAFE interpretation is also given.

5.2.2 Fitness for purpose in Achievement Standard 91610

Fitness for purpose is described by the Achievement Standard 91610 as "the ability of a technological outcome to serve its intended purpose (*do the job*) within its intended context, where the *job to be done* is clearly defined by the brief" [78]. In the context of IM-SAFE project, this could mean that the processed result of a survey campaign is usable for its purpose, which would be to detect or monitor a specific damage process and to identify the time dependent evaluation.

But the fitness for purpose in its broadest sense is wider than this, extending the context to the practices involved in the performance of the survey. Some areas that could be considered when demonstrating this concept are shown in Table 5-2, where the information extracted from the reference material is taken as basis for what could be applied under the IM-SAFE perspective. These should be taken as suggestions since other ideas would relate to particular outcomes. The authors of the guidelines considered also important to study the fitness for purpose in its broad sense during the design and planning of the survey.

For conceptual design	For IM-SAFE
Sustainability of resources	The definition considered in IM-SAFE is the ability of a structure or structural element to contribute positively to the fulfilment of the present needs of humankind with respect to nature, society, economy and well-being, without compromising the ability of future

This project has received funding from the European Union's Horizon 2020 research and innovation programme under grant agreement No 958171.

	generations to meet their needs in a similar manner. This is, considering if the technology used to obtain the outcome (detection and characterization of damage and processes) meets the needs without compromising the ability to repeat the process in the future.
Maintainability	Maintainability in IM-SAFE context is to be classified based on the probability that a failed component or system will be restored or repaired to a specified condition within a specified period or time when maintenance is performed in accordance with prescribed procedures. Hence it includes: - Maintainability of the sensors when continuous/periodic monitoring is applied. - Ease of execution of maintenance interventions of critical/non-critical components (see Section 5.1). - Cost of the execution maintenance interventions of critical/non-critical components - Duration and time-constrains of the execution of maintenance interventions
Determination of life cycle	Study the life cycle stages of the surveying technology under revision, being life-cycle defined in COST TU1402 as the “lifespan of the structure, from the construction until the decommissioning or dismantling”.
Ultimate disposal	Being this “the process of returning waste materials to the environment in a form which will have the minimal environmental impacts” [79]. Under IM-SAFE project, this could lead to the question: for how long the outcomes are valid considering the characteristics of the survey?
Practices used in manufacturing	In the context of IM-SAFE, “manufacturing” would be referring to surveying, and here a survey is defined as the “procedure related to collecting quantitative information about network, object, component or element, performed in order to determine or identify change of its status of the items in population”. For the case that is under analysis, “practices used in manufacturing” would mean to check if there are international/national guidelines and standards that should be applied when performing a survey.
Cultural appropriateness of trialling procedures	Not applicable.
Ethical nature of testing procedures	Considering and testing for security and privacy of data when relevant.
Health and safety	Considering safety issues when performing a survey (from the operator and from the asset users).

Table 5-2 – Suggestions to be considered when evaluating the fitness for purpose [78]

5.2.2.1 Monitoring and measurement in ISO 9001:2015

The standard ISO 9001:2015 [80] is relevant when discussing fitness for purpose of surveying technologies. Here, monitoring and measurement are addressed separately as key elements, differently as it was done in the previous 2008 standard, and are defined as follows:

- monitoring: the status of a system, process, or activity
- measuring: the process to determine a value

It is highlightable that these terms are described in the context of the standard, which is based on describing *quality management systems* for improving the global performance strategies of a company or business. The fundamental principle of ISO 9001:2015 [80] is that in order to

This project has received funding from the European Union’s Horizon 2020 research and innovation programme under grant agreement No 958171.

continuously provide products and services that address customer requirements, it is important to implement the quality management system (QMS) and base the decision-making process in evidence. Said evidence shall be gathered through the processes of monitoring and measuring. Thus, consistent with the aspiration of continual improvement that underpins ISO 9001, it is necessary to have a plan, review, and take action on monitoring and measuring processes to guarantee their success [81]. In addition, in the ISO 9001:2015 standard, section 7, it is mentioned that the organization must "ensure that the resources provided:

a) Are suitable for the specific type of monitoring and measurement activities being undertaken;

b) Are maintained to ensure their continuing fitness for their purpose."

Although these concepts are described in a completely different sense than in IM-SAFE project, it is possible to extrapolate and use them adapting the perspective when necessary.

As a continuation of the previous, section 9 of the standard highlights several factors that the organization in charge of performing the survey should determine and can be taken as basis for what could be applied under the IM-SAFE perception. In addition, this standard also addresses the analysis and evaluation that should be performed to data and information resulting from monitoring and measuring. Table 5-3 shows a summary of these aspects in contrast to IM-SAFE perspective.

General considerations	**ISO 9001:2015 Perspective**	**IM-SAFE Perspective**
Before the survey	What needs to be monitored and measured.	Identify the damage process to be monitored and measured using surveying technologies.
	Methods for monitoring, measurement, analysis, and evaluation needed to ensure valid results.	Planning of the surveying campaign. Decision making to choose the best surveying technology for each case study.
	When the monitoring and measuring shall be performed.	Considerations to be made regarding the weather, traffic, risk, and safety conditions, needed to ensure good quality of results.
	When the results from monitoring and measurement shall be analysed and evaluated.	Quality check of the obtained results from the monitoring or measurement. Preparation of raw data to be transformed into usable data. To be perform before the data analysis process.
After the survey (what should be analysed and evaluated)	Conformity of products and services.	Ensure that the data gathered in the survey comply with their intended purpose.
	The degree of customer satisfaction.	Reliability of the results obtained.
	The performance and effectiveness of the quality management system.	*The performance and effectiveness of the* surveying technology chosen for the specific case study.

This project has received funding from the European Union's Horizon 2020 research and innovation programme under grant agreement No 958171.

	If planning has been implemented effectively.	*If planning has been implemented effectively.*
	The effectiveness of actions taken to address risks and opportunities.	*The effectiveness of actions taken to address risks and opportunities.*
	The performance of external providers.	Performance of external actors (i.e., asset managers) and influence on the monitoring and measuring process.
	The need for improvements to the quality management system.	Improvements to be performed in successive surveying campaigns.

Table 5-3 – IM-SAFE perspective based on ISO 9001:2015

As a summary, and considering the continual improvement reinforced by ISO 9001, it is clear the importance of [81]:

- Planning the resources to guarantee the quality of measuring and monitoring tasks
- Use clear evidence for the decision-making process
- Continuously improve and maintain the QMS

5.2.2.2 Generic systems design philosophies: a fitness-for-purpose IT infrastructure strategy

There are some generic terms that are important to be considered when working on generic system design philosophies. These will help to choose the appropriate surveying technology for a specific application and to be aware of the cost of the service. The most important (generic) aspects to be considered are presented in Table 5-4.

Generic term	Definition	IM-SAFE interpretation
Stability	Total variation in measurements of the same part measured over time.	Capacity of repeating the performed measurements or monitoring and obtaining the same result.
Scalability	Capacity for scaling up or down depending on the demand.	
Agility	Processes that can reduce the time expend on obtaining the final result.	Good practices guide specific for every surveying technology.
Data retention	Increased storage and management capabilities to handle large amounts of data, often unstructured.	Resources needed to handle data generated in each survey.
Security	Disaster/interruption recovery measures.	Actions to be taken beforehand that can prevent information loss.
Efficiency	Cost-effectiveness.	Analysis of the cost/benefit of performing a survey with a specific surveying technology, and capacity

This project has received funding from the European Union's Horizon 2020 research and innovation programme under grant agreement No 958171. © 2021

		of conducting data analysis in a later step.

Table 5-4 – Generic terms to be consider in the FFP evaluation (IM-SAFE perspective) [82]

5.2.3 Fitness-for-purpose considering the supply and demand chain of monitoring and management of structures

Generally speaking, there are three different types of monitoring projects to be performed on a structure:

- Operational: Choosing, deciding in a specific project
- Scientific: Validating, calibrating, improving models, testing hypotheses
- Legal: Complying with legal obligation, obtaining licence

In the operational impulse, a further distinction is made between:

- Managerial impulse: Choices, decisions to properly manage the construction management
- Quality assurance impulse: Choices, decisions to guarantee the quality of the execution of the construction (during building)

Next, monitoring can take place in two contexts:

(i) Decision context: The information obtained through monitoring serves to support certain decisions that must be taken during construction or management of the structure.

(ii) Inference context: Monitoring data is used to develop performance models, on the basis of which initial performance analyses are conducted. In this context, data obtained through monitoring is used to draw up or test and adjust design models from which initial (performance) analyses have been or are being made and adjusted.

Taking this into consideration, and in the context of IM-SAFE, monitoring the behaviour of a structure can be used for performing an adequate maintenance and management of the assets. A good example on how to deal with this was presented by SBRCURnet committee [83]. The aim of the project was to learn from practical cases and share those experiences with the sector. In the project, they do this by using the 7-step scheme of Figure 5.4 for monitoring structures. It shows how supply and demand are technically related. Steps (b) to (f) form the supply side of the process. During this process, continuous consultation between the demand and supply side is necessary.

This project has received funding from the European Union's Horizon 2020 research and innovation programme under grant agreement No 958171. © 2021

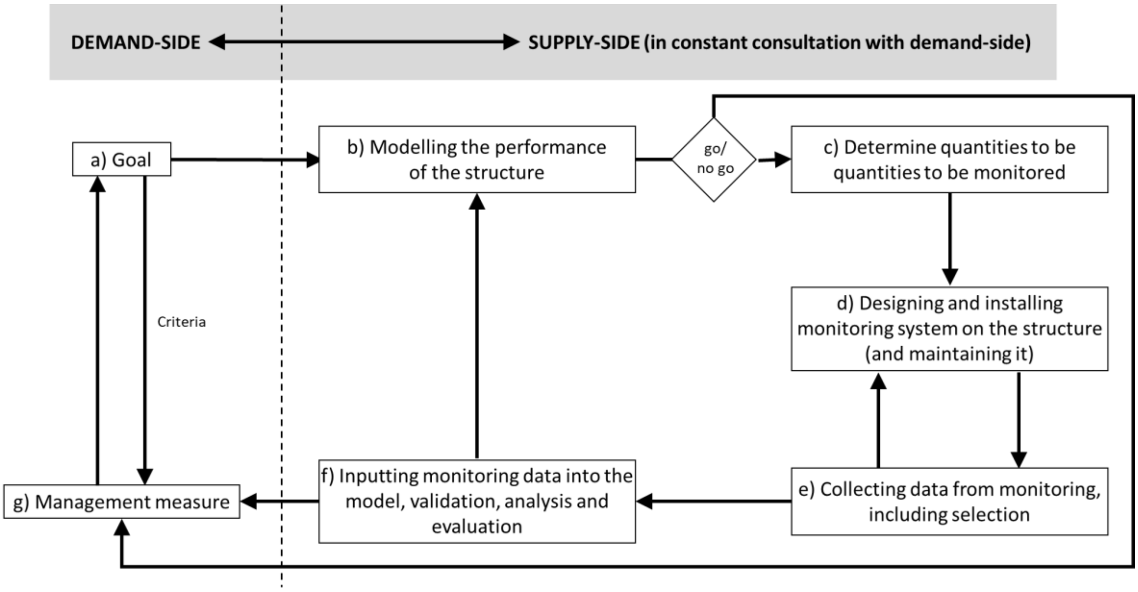

Figure 5.4 – The 7-step diagram used to describe case studies (Adaptation from [83])

The methodology consists of the following steps:

a) Purpose: The initiator has a particular purpose in mind with the monitoring project. For example, a manager wants to optimise the maintenance of the structure or control its lifespan.
b) Modelling the behaviour of the structure: In this step, the behaviour of the structure is modelled for a specific scope. The results of this step are used to determine whether monitoring is really necessary to achieve the intended goal. In case of a 'no go', one can proceed directly to step (g). In the case of a 'go', the next step is the design of the system (step (c), and further).
c) Determine quantities to be measured: In this step, the parties involved identify the quantity or quantities they wish to measure.
d) Design and install measuring system on the structure (and maintain it): The measuring system that can measure the quantities mentioned in step (c) is designed, installed in the structure, and maintained.
e) Collecting measurement data, including selection: From the measurement system (step (d)) raw data comes as output. The relevant data are selected from these raw data.
f) Input of measurement data into model, validation, analysis, and evaluation: The data from step (e) is then validated and analysed using the model established in step (b). If the validation step (f) is successful, the manager applies a management measure based on the results (g). If the data obtained does not correspond well with the model set up, the modelling of the structure can be adapted, and the cycle starts again at point (b).
g) Management measure: In this step, a decision is made on the possible management measure following the measurements and the analysis, based on the results from the previous steps.

In addition to this, the project from SBRCURnet committee considered six aspects to allow to create an idea of the fitness-for-purpose of a surveying technology [83]:

- Purpose of monitoring, including who has interest in it and the goals behind it.
- Opportunities and threats: description of the processes benefiting from the applied technology and the factors that stand in the way of applying it.
- Time horizon, in relation with the distinction between permanent and periodic monitoring and the lifespan of the technology.

This project has received funding from the European Union's Horizon 2020 research and innovation programme under grant agreement No 958171.

- Costs/benefits, including initial cost, maintenance, and benefits (cash and qualitative).
- Data management: information about how the data is processed and stored, and ink with existing information supply.
- Technology Readiness Level (TRL): indication of the TRL of the measuring system.

5.3 IM-SAFE approach to evaluate the fitness-for-purpose of technologies for condition survey

Considering all the different approaches that have been presented throughout this chapter for evaluating fitness-for-purpose, it can be said that the fitness-for-purpose evaluation strategy in the context of IM-SAFE helps to choose the most appropriate surveying technology for each case study. Said strategy considers also the importance of obtaining reliable results through the service that they support. It is also highlightable that critical assets receive greater spending and higher service levels, while non-critical assets receive less [82]. Applying this strategy, some direct benefits arise: First, a better view of priorities when using a specific surveying technology, which leads to a more effective planification of the overall strategy (from design of the monitoring campaign to the analysis of the obtained data). In addition, a better sense of the total cost is obtained. And finally, a good organisation of the required maintenance of the equipment during the survey, and actions to be taken when the sensors fail (in case of continuous monitoring).

Based on the existing references to this regard, IM-SAFE project gathered a list containing the criteria to be used for evaluating the fitness-for-purpose of technologies for condition survey (the following characteristics have been fully described previously under Section 3.2):

- Objectives of the monitoring activities
- Physical quantity to be measured
- Process/event to be detected or monitored
- Measurement type
- Measurement range
- Measurement accuracy
- Sensitivity of measurements to environmental conditions
- Availability and uncertainty of relationships between measured quantity and parameter of interest
- Robustness of the measurement
- Lifespan of the technology and required maintenance
- Possibility of automatising the measurements
- Ease of application of the technology
- Induced damage to the structure during the measurement

As a summary for this chapter, implementing a fitness-for-purpose strategy will also require more general considerations. In the following list, a selection of the most important criteria extracted from references studied in previous sections is shown:

- Planning the surveying campaign:
  - Identify what needs to be monitored and measured
  - Apply a level of suitability for different surveying technologies and their associated applications and assets

This project has received funding from the European Union's Horizon 2020 research and innovation programme under grant agreement No 958171.

  - Importance of the sensor placement (data collection plan) considering the most vulnerable elements of the structure, and depending on the damage process to be measured or monitored (priority levels)
  - Study the life cycle stages of the surveying technology under revision
  - Repeatability and reproducibility of measures
  - Develop a strategy for maintenance and disaster recovery
  - Time dependence of the measures. Validity after a period of time
  - Considerations to be made regarding weather, traffic, risk, and safety conditions
  - Develop a better understanding of the technology costs for specific applications, including cost from the design of the data collection plan to the final data analysis
  - Constant adaptation to changing market (evolving survey strategies and new or improved technologies)
- Data treatment (evaluation):
  - Consider security and privacy of data, when relevant
  - Ensure data quality
  - Reliability of the results obtained

The solution is a fitness-for-purpose strategy, which will optimize data collection to the specific requirements and priorities of the application. This helps to perform a better decision-making for condition survey.

This project has received funding from the European Union's Horizon 2020 research and innovation programme under grant agreement No 958171. © 2021

6 Summary and conclusions

This document describes different surveying technologies to be used for condition survey in a way that meets the requirements specification to support work package 5 (WP5) in drafting the mandate for the European Committee for Standardization (CEN). It presents in form of reports the different characteristics that define the surveying technologies studied in IM-SAFE project. The description of each surveying technology has been oriented to produce a semantic wiki, which has the shape of an online interactive catalogue of surveying technologies for transport infrastructure.

In addition, different data analysis methods used to evaluate the data obtained from sensors are summarised (the most used ones). A large number of references have been provided to this respect, and the ones specific to each surveying technology form part of deliverable D2.2.

The final goal of this deliverable is to help the user to choose the most appropriate surveying technique depending on the specific damage process or action that is to be measured in the structure. To help in this process, this document contains a chapter about the fitness-for-purpose of a technology to fulfil with a specific action. The advantages of applying this strategy before performing a survey are: (i) effective planification (from the monitoring campaign to the data analysis phase); (ii) better analysis of costs; and (iii) good organization of the required maintenance of the sensors (and what to do in case of sensor failure).

The present deliverable complies with the objectives proposed in the Grant Agreement of IM-SAFE for task T2.1, and can be summarised as:

- To review data collection technologies used for condition survey, including devices and platforms
    - → This objective has been accomplished through the creation of the online catalogue of surveying technologies, specifically for bridges and tunnels (Annex A).
- To review data analysis methods used in condition survey
    - → Chapter 4 of this document tackles the part on data analysis methods.
- To identify requirements for data collection technologies and data analysis methods used for condition survey to be considered in guidelines and standards
    - → This is specifically addressed for each surveying technology in the semantic wiki and has been further developed in deliverable D2.2.

This project has received funding from the European Union's Horizon 2020 research and innovation programme under grant agreement No 958171.

7 Bibliography

[1] ISO 99, "International vocabulary of metrology - Basic and general concepts and associated terms (VIM)," *Technical Committee of Management Board*, p. 92, 2007.

[2] ISO 13822, "Bases for design of structures - Assessment of existing structures," *Technical Committee of Reliability of structures*, 2010.

[3] G. Semyon, Evaluating Measurement Accuracy: A Practical Approach, Springer, 2018.

[4] J. J Carr, "Sensors & Circuits: Sensors, Transducers, & Supporting Circuits for Electronic Instrumentation Measurement and Control," *Prentice Hall*, 1993.

[5] D. W. Surry and A. K. Stanfield, "Performance technology," in *The Foundations of Instructional Technology*, M. K. Barbour & M. Orey, 2008.

[6] G. E. Karniadakis, I. G. Kevrekidis, L. Lu, P. Perdikaris, S. Wang and L. Yang, "Physics-Informed Machine Learning," *Nature Reviews Physics*, vol. 3, p. 422–440, 2021.

[7] A. Ourmazd, "Science in the Age of Machine Learning," *Nature Reviews Physics*, vol. 2, p. 342–343, 2020.

[8] D. Posenato, P. Kripakaran, D. Inaudi and I. F. C. Smith, "Methodologies for Model-Free Data Interpretation of Civil Engineering Structures," *Computers & structures*, vol. 88, p. 467–482, 2010.

[9] F. N. Çatbaş, T. Kijewski-Correa and A. E. Aktan, "Structural Identification of Constructed Systems," *Reston (VI): American Society of Civil Engineers*, 2013.

[10] J. M. Bland and D. G. Altman, "Bayesians and Frequentists," *Bmj*, vol. 317, p. 1151–1160, 1998.

[11] A. Gelman, "Bayesians Are Frequentists | Statistical Modeling, Causal Inference, and Social Science," [Online].

[12] R. S. Witte and J. S. Witte, Statistics, Wiley Global Education, 2013.

[13] M. H. DeGroot and M. J. Schervish, Probability and Statistics, Pearson Education, 2012.

[14] "Statistics in Analytical Chemistry - Summary," [Online]. [Accessed 19 January 2022].

[15] "List of Probability Distributions," *Wikipedia*, October 2021.

[16] A. Zimek and P. Filzmoser, "There and Back Again: Outlier Detection between Statistical Reasoning and Data Mining Algorithms," *Wiley Interdisciplinary Reviews: Data Mining and Knowledge Discovery*, vol. 8, p. e1280, 2018.

[17] L. Cavalli, V. Larsson, M. R. Oswald, T. Sattler and M. Pollefeys, "Handcrafted Outlier Detection Revisited," in *European Conference on Computer Vision*, 2020.

[18] E. W. Weisstein, *Cross-Correlation*, Wolfram Research, Inc..

This project has received funding from the European Union's Horizon 2020 research and innovation programme under grant agreement No 958171. © 2021

[19] L. Van Der Maaten, E. Postma and J. van den Herik, “Dimensionality Reduction: A Comparative Review,” vol. 10, no. 13, 2009.

[20] “A Practical Introduction to Factor Analysis: Exploratory Factor Analysis,” [Online]. [Accessed 19 January 2022].

[21] A. G. Yong and S. Pearce, “A Beginner's Guide to Factor Analysis: Focusing on Exploratory Factor Analysis,” *Tutorials in quantitative methods for psychology,* vol. 9, p. 79–94, 2013.

[22] E. Dobriban, “Permutation Methods for Factor Analysis and PCA,” *The Annals of Statistics,* vol. 48, p. 2824–2847, 2020.

[23] J. Shlens, “A Tutorial on Principal Component Analysis,” *arXiv preprint arXiv:1404.1100,* 2014.

[24] M. Journée, Y. Nesterov, P. Richtárik and R. Sepulchre, “Generalized Power Method for Sparse Principal Component Analysis.,” *Journal of Machine Learning Research,* vol. 11, 2010.

[25] I. T. Jolliffe and J. Cadima, “Principal Component Analysis: A Review and Recent Developments,” *Philosophical Transactions of the Royal Society A: Mathematical, Physical and Engineering Sciences,* vol. 374, p. 20150202, 2016.

[26] J. V. Stone, “Independent Component Analysis: A Tutorial Introduction,” 2004.

[27] J. Shlens, “A Tutorial on Independent Component Analysis,” 2014.

[28] A. Hyvärinen, J. Karhunen and E. Oja, “Independent Component Analysis,” 2001.

[29] H. Van der Auweraer, “Structural Dynamics Modeling Using Modal Analysis: Applications, Trends and Challenges,” in *IMTC 2001. Proceedings of the 18th IEEE Instrumentation and Measurement Technology Conference. Rediscovering Measurement in the Age of Informatics (Cat. No. 01CH 37188),* 2001.

[30] Á. Cunha and E. Caetano, “Experimental Modal Analysis of Civil Engineering Structures,” 2006.

[31] F. B. Zahid, Z. C. Ong and S. Y. Khoo, “A Review of Operational Modal Analysis Techniques for In-Service Modal Identification,” *Journal of the Brazilian Society of Mechanical Sciences and Engineering,* vol. 42, p. 1–18, 2020.

[32] D. Liu, Z. Tang, Y. Bao and H. Li, “Machine-Learning-Based Methods for Output-Only Structural Modal Identification,” *Structural Control and Health Monitoring,* vol. 28, p. e2843, 2021.

[33] K. Worden and P. L. Green, “A Machine Learning Approach to Nonlinear Modal Analysis,” vol. 84, 2017.

[34] S. Alla, Big Data Analytics with Hadoop 3: Build Highly Effective Analytics Solutions to Gain Valuable Insight into Your Big Data, Packt Publishing Ltd, 2018.

[35] M. Grandini, E. Bagli and G. Visani, “Metrics for Multi-Class Classification: An Overview,” *arXiv preprint arXiv:2008.05756,* 2020.

This project has received funding from the European Union’s Horizon 2020 research and innovation programme under grant agreement No 958171.

[36] J. Opitz and S. Burst, “Macro F1 and Macro F1,” *arXiv preprint arXiv:1911.03347*, 2019.

[37] J. Hernández-Orallo, P. Flach and C. Ferri Ramírez, “A Unified View of Performance Metrics: Translating Threshold Choice into Expected Classification Loss,” *Journal of Machine Learning Research*, vol. 13, p. 2813–2869, 2012.

[38] H. He and E. A. Garcia, “Learning from Imbalanced Data,” *IEEE Transactions on knowledge and data engineering*, vol. 21, p. 1041–4347, 2009.

[39] S. Kaufman, S. Rosset, C. Perlich and O. Stitelman, “Leakage in Data Mining: Formulation, Detection, and Avoidance,” *ACM Transactions on Knowledge Discovery from Data (TKDD)*, vol. 6, p. 1–21, 2012.

[40] M. Elgendy, Deep Learning for Vision Systems, Simon and Schuster, 2020.

[41] “Introduction to Neural Networks,” [Online].

[42] X. Ying, “An Overview of Overfitting and Its Solutions,” in *Journal of Physics: Conference Series*, 2019.

[43] J. Kukačka, V. Golkov and D. Cremers, “Regularization for Deep Learning: A Taxonomy,” *arXiv preprint arXiv:1710.10686*, 2017.

[44] *Dive into Deep Learning — Dive into Deep Learning 0.17.5 Documentation.*

[45] “Understanding of Convolutional Neural Networks,” [Online].

[46] V. Dumoulin and F. Visin, “A Guide to Convolution Arithmetic for Deep Learning,” *arXiv preprint arXiv:1603.07285*, 2016.

[47] S. Saha, “A Comprehensive Guide to Convolutional Neural Networks— the ELI5 Way,” *Towards data science*, vol. 15, 2018.

[48] A. Krizhevsky, I. Sutskever and G. E. Hinton, “Imagenet Classification with Deep Convolutional Neural Networks,” *Advances in neural information processing systems*, vol. 25, 2012.

[49] K. Simonyan and A. Zisserman, “Very Deep Convolutional Networks for Large-Scale Image Recognition,” *arXiv preprint arXiv:1409.1556*, 2014.

[50] K. He, X. Zhang, S. Ren and J. Sun, “Deep Residual Learning for Image Recognition,” in *Proceedings of the IEEE Conference on Computer Vision and Pattern Recognition*, 2016.

[51] C. Szegedy, W. Liu, Y. Jia, P. Sermanet, S. Reed, D. Anguelov, D. Erhan, V. Vanhoucke and A. Rabinovich, “Going Deeper with Convolutions,” in *Proceedings of the IEEE Conference on Computer Vision and Pattern Recognition*, 2015.

[52] A. G. Howard, M. Zhu, B. Chen, D. Kalenichenko, W. Wang, T. Weyand, M. Andreetto and H. Adam, “Mobilenets: Efficient Convolutional Neural Networks for Mobile Vision Applications,” *arXiv preprint arXiv:1704.04861*, 2017.

[53] G. Huang, Z. Liu and K. Q. Weinberger, *Densely Connected Convolutional Networks. CoRR Abs/1608.06993 (2016)*, 2015.

[54] E. Shelhamer, J. Long and T. Darrell, “Fully Convolutional Networks for Semantic Segmentation,” *IEEE transactions on pattern analysis and machine intelligence*, vol. 39, p. 640–651, 2016.

This project has received funding from the European Union’s Horizon 2020 research and innovation programme under grant agreement No 958171.

[55] S. Hochreiter and J. Schmidhuber, "Long Short-Term Memory," *Neural computation,* vol. 9, p. 1735–1780, 1997.

[56] A. Vaswani, N. Shazeer, N. Parmar, J. Uszkoreit, L. Jones, A. N. Gomez, \. Kaiser and I. Polosukhin, "Attention Is All You Need," *Advances in neural information processing systems,* vol. 30, 2017.

[57] I. Goodfellow, J. Pouget-Abadie, M. Mirza, B. Xu, D. Warde-Farley, S. Ozair, A. Courville and Y. Bengio, "Generative Adversarial Nets," *Advances in neural information processing systems,* vol. 27, 2014.

[58] *Generative Models,* 2016.

[59] A. Hindupur, *The GAN Zoo,* 2022.

[60] B. N. Oreshkin, D. Carpov, N. Chapados and Y. Bengio, "N-BEATS: Neural Basis Expansion Analysis for Interpretable Time Series Forecasting," *arXiv preprint arXiv:1905.10437,* 2019.

[61] D. Salinas, V. Flunkert, J. Gasthaus and T. Januschowski, "DeepAR: Probabilistic Forecasting with Autoregressive Recurrent Networks," *International Journal of Forecasting,* vol. 36, p. 1181–1191, 2020.

[62] B. Lim, S. O. Arik, N. Loeff and T. Pfister, "Temporal Fusion Transformers for Interpretable Multi-Horizon Time Series Forecasting," *arXiv preprint arXiv:1912.09363,* 2019.

[63] N. Erickson, J. Mueller, A. Shirkov, H. Zhang, P. Larroy, M. Li and A. Smola, "Autogluon-Tabular: Robust and Accurate Automl for Structured Data," *arXiv preprint arXiv:2003.06505,* 2020.

[64] D. G. Lowe, "Distinctive Image Features from Scale-Invariant Keypoints," *International journal of computer vision,* vol. 60, p. 91–110, 2004.

[65] H. Bay, T. Tuytelaars and L. V. Gool, "Surf: Speeded up Robust Features," in *European Conference on Computer Vision,* 2006.

[66] P. F. Alcantarilla, A. Bartoli and A. J. Davison, "KAZE Features," in *European Conference on Computer Vision,* 2012.

[67] R. Girshick, J. Donahue, T. Darrell and J. Malik, "Rich Feature Hierarchies for Accurate Object Detection and Semantic Segmentation," in *Proceedings of the IEEE Conference on Computer Vision and Pattern Recognition,* 2014.

[68] S. Minaee, Y. Y. Boykov, F. Porikli, A. J. Plaza, N. Kehtarnavaz and D. Terzopoulos, "Image Segmentation Using Deep Learning: A Survey," *IEEE transactions on pattern analysis and machine intelligence,* 2021.

[69] R. Girshick, "Fast R-Cnn," in *Proceedings of the IEEE International Conference on Computer Vision,* 2015.

[70] S. Ren, K. He, R. Girshick and J. Sun, "Faster R-Cnn: Towards Real-Time Object Detection with Region Proposal Networks," *Advances in neural information processing systems,* vol. 28, 2015.

[71] T.-Y. Lin, P. Dollár, R. Girshick, K. He, B. Hariharan and S. Belongie, "Feature Pyramid Networks for Object Detection," in *Proceedings of the IEEE Conference on Computer Vision and Pattern Recognition,* 2017.

This project has received funding from the European Union's Horizon 2020 research and innovation programme under grant agreement No 958171. © 2021

[72] K. He, G. Gkioxari, P. Dollár and R. Girshick, “Mask R-Cnn,” in *Proceedings of the IEEE International Conference on Computer Vision*, 2017.

[73] S. H. a. B. T. a. M. S. K. a. K. A. I. Barr, “Bridging the valley of death: Lessons learned from 14 years of commercialization of technology education,” *Academy of management learning & education*, vol. 8, no. 3, pp. 370-388, 2009.

[74] U. Department of defense, Technology Readiness Assessment (TRA) Deskbook, 2005.

[75] M. Héder, “From NASA to EU: the evolution of the TRL scale in Public Sector Innovation,” *The Innovation Journal*, vol. 22, no. 2, pp. 1-23, 2017.

[76] I. Tzinis, “Technology Readiness Level,” NASA, 2012. [Online]. Available: https://www.nasa.gov/directorates/heo/scan/engineering/technology/technology_readiness_level.

[77] “Technology Readiness Level (TRL),” European Union. [Online].

[78] *Achievement Standard 91610.*

[79] C. &. A. M. Park, A dictionary of environment and conservation, vol. 21, Oxford University Press, 2007, p. 12.

[80] *ISO 9001:2015.*

[81] J. Nolan, “Analysis of measuring and monitoring requirements in ISO 9001:2015,” [Online]. Available: https://advisera.com/9001academy/knowledgebase/analysis-of-measuring-and-monitoring-requirements-in-iso-90012015/.

[82] C. M. K. M. M. N. S. Hugener, ““Fit-for-purpose” infrastructure strategy. How companies can manage increasing IT demands,” pwc, 2014. [Online]. Available: https://www.strategyand.pwc.com/gx/en/insights/2014/fit-for-purpose-infrastructure-strategy/strategyand-fit-for-purpose-infrastructure-strategy.pdf.

[83] SBRCURnet, “Kennispaper: Slimme constructies voor slim beheer en onderhoud – praktijkcases,” Delft, The Netherlands, 2015.

[84] P. Regtien, Measurement science for engineers, Elsevier, 20014.

[85] ISO 19159, Geographic information - Calibration and validation of remote sensing imagery sensors and data - Part 1: Optical sensors, Technical Committee of Geographic information, 2014.

[86] ISO 7078, Buildings and civil engineering works - Procedures for setting out, measurement and surveying - Vocabulary, Technical Committee of Terminology and harmonization of languages, 2020.

[87] ISO 17123, Optics and optical instruments - Field procedures for testing geodetic and surveying instruments - Part 1: Theory, Technical Committee of Geodetic and surveying instruments, 2014.

[88] V. Khatereh, “Evaluation of commercially available remote sensors for highway bridge condition assessment,” *ournal of Bridge Engineering*, p. 10, 2012.

[89] T. Ahlborn, “An Evaluation of Commercially Available Remote Sensors for Assessing Highway Bridge Condition,” *Michigan Tech Transportation Institute*, p. 73, 2010.

This project has received funding from the European Union’s Horizon 2020 research and innovation programme under grant agreement No 958171.

[90] H. Park, "Convolutional neural network-based safety evaluation method for structures with dynamic responses," *xpert Systems with Applications,* p. 14, 2020.

[91] R. Chang, "IEEE Intelligent TranSPOrtation Systems," *San Diego, USA, October 3-6,* p. 971, 2004.

[92] L. Qiang, "Research on Data Correlation in Structural Health Monitoring System," *Advanced Materials Research,* p. 11, 2013.

[93] A. Radoi, "Static and Dynamic Structural Health," *Romanian Journal of Transport Infraestructure,* p. 16, 2021.

[94] W. Rücker, "Guideline for Structural Health Monitoring," *Federal Institute of Materials Research and Testing,* p. 63, 2006.

[95] ISO 13372, "Condition monitoring and diagnostics of machines - Vocabulary," *Technical Committee of Condition monitoring and diagnostics of machine systems,* p. 15, 2012.

[96] ISO 12718, "Non-destructive testing - Eddy current testing - Vocabulary," *Technical Committee of Eddy current testing,* p. 39, 2019.

[97] ISO 3534, "Statistics - Vocabulary and symbols - Part 1: General statistical terms and terms used in probability," *Applications of statistical methods,* p. 105, 2006.

[98] ISO 23907, "Sharps injury protection - Requirements and test methods - Part 2: Reusable sharps containers," *Technical Committee of devices for administration of medicinal products and catheters,* p. 17, 2019.

[99] ISO 19345, "Petroleum and natural gas industry - Pipeline transportation systems - Pipeline integrity management specification," *Technical Committee of Pipeline transportation systems,* p. 108, 2019.

[100] I. 27892, "Vacuum technology - Turbomolecular pumps - Measurement of rapid shutdown torque," *Technical Committee of Vacuum technology,* p. 16, 2010.

[101] ISO 27892, "Vacuum technology - Turbomolecular pumps - Measurement of rapid shutdown torque," *Technical Committee of Vacuum technology,* p. 16, 2010.

[102] ISO 19262, "Photography — Archiving Systems — Vocabulary," *Technical Committee of Photography,* p. 44, 2015.

[103] ISO 7078, "Buildings and civil engineering works — Procedures for setting out, measurement and surveying — Vocabulary," *Technical Committee of Terminology and harmonization of languages,* p. 34, 2020.

[104] I. Bazovsky, Reliability theory and practice, Courier Corporation, 2004.

[105] ISO 11352, "Water quality — Estimation of measurement uncertainty based on validation and quality control data," *Technical Committee of Physical, chemical and biochemical methods,* p. 26, 2021.

[106] ISO 1998, "Petroleum industry — Terminology — Part 1: Raw materials and products," *Technical Committee of Petroleum and related products, fuels and lubricants from natural or synthetic sources,* 1998.

[107] D. W. Surry.

This project has received funding from the European Union's Horizon 2020 research and innovation programme under grant agreement No 958171. © 2021

[108] D. I. K. B. U. S. A. Grosso, “Monitoring of bridges and concrete structures with Fibre Optic Sensors in Europe,” *IABSE Symposium, Seoul 2001: Cable-Supported Bridges - Challenging Technical Limits,* January 2001.

[109] Ł. B. Rafał Sieńko, “Monitorowanie obiektów budowlanych w sąsiedztwie budowy,” *Geoinzynieria* , pp. 60-65, 2016.

[110] D. I. J. -. M. D. Samuel Vurpillot, *Smart Structures and Materials vol. 2719,* San Diego : Society of Photo-Optical Instrumentation Engineers, 1996.

[111] F. F. Jose Luis Santos, Handbook of Optical Sensors, Boca Raton: CRC Press Taylor & Francis Group, 2015.

[112] R. S. Romaniuk, Miernictwo Światłowodowe Wydanie II Uzupełnione, Warszawa: Instytut Systemów elektronicznych Politechnika Warszawska, 2001.

[113] B. Glisic, *Fibre optic sensors and behaviour in concrete at early age*, Laboratory of Stress Analysis (IMAC) Swiss Federal Institute of Technology , 2000.

[114] A. H.Hartog, "An Introduction to Distributed Optical Fibre Sensors," in *An Introduction to Distributed Optical Fibre Sensors*, Boca Raton, CRC Press Taylor & Francis Group, 2017, pp. 115-128.

[115] E. Udd, Fiber Optic Sensors And Introduction for Engineers and Scientists, New Jersey : John Wiley & Sons, Inc. , 2006.

[116] R. M. Measures, Structural Monitoring with Fiber Optic Technology, Ontario: Institute of Aerospace Studies , 2001.

[117] T. M. A. M. David Krohn, Fiber Optic Sensors Fundamentals and Applications, Washington: SPIE PRESS , 2014.

[118] T. G. Alexis Mendez, “Overview of fiber optic sensors for NDT applications,” in *IV NDT Panamerican Conference Buenos Aires*, Buenos Aires, 2012.

[119] KEYENCE, "Fibre optic sensors FS-N40 Series," 30 11 2021. [Online]. Available: https://www.keyence.co.uk/products/sensor/fiber-optic/fs-n40/downloads/.

[120] NERVE-SENSORS, "NERVE SENSORS Epsilon Rebar strain sensor," 30 11 2021. [Online]. Available: www.nerve-sensors.com. [Accessed 30 11 2021].

[121] R. S. T. H. Łukasz Bednarski, “Wybrane zagadnienia monitorowania konstrukcji,” in *XXX Jubileuszowe Ogólnopolskie Warsztaty Pracy Projektanta Konstrukcji*, Szczyrk , 2015.

[122] S. V. G. M. G. S. D. Inaudi, "SOFO: Structural Monitoring with Fiber Optic Sensors," *FIB, Monitoring and Safety Evaluation of Existing Concrete Structures,* 12-13 February 1999.

[123] K. E. H. Fidanboylu, “Fiber Optic Sensors and their applications,” in *5th Intenrational Advanced Technologies Symposium* , Karabuk, 2009.

[124] K. B. D. I. U. S. Andrea del Grosso, "Monitoring of Bridges and Concrete Structures with Fibre Optic Sensors in Europe," IABSE Symposium Report , 2001.

[125] Y. Mei, *Error analysis for distributed fibre optic sensing tehcnology based on Brillouin scattering*, University of Cambridge, Department of Philosophy , 2018.

This project has received funding from the European Union’s Horizon 2020 research and innovation programme under grant agreement No 958171.

[126] BAUMER, “BAUMER,” 10 12 2021. [Online]. Available: https://www.baumer.com/medias/__secure__/Baumer_Fiber-optic-sensors-to-detect-liquid-levels-and-leakage-of-fluids_EN_0610_AR.pdf?mediaPK=8837757272094.

[127] C. J. R. S. P. A. S. J. R. B. Figuera, "Development of Advanced Fibre Optic Sensors to Monitor the Durability of Concrete and Reinforced Concrete Structures - SolSensors," Universidade do Minho, INESC-TEC and Engiprojects, Lda, 2021.

[128] T. V. S. C. T. S. T. H. Nguyen, "Fluorescence based fibre optic pH sensor for the pH 10–13 range suitable for corrosion monitoring in concrete structures," *Sensors and Actuators B Chemical 191,* pp. 498-507, February 2014.

[129] SHM SYSTEMS, “SHM Systems Projects,” 7 12 2021. [Online]. Available: https://www.shmsystem.pl/projects/. [Accessed 7 12 2021].

[130] Narodowe Centurm Badań i Rozwoju, Politechnika Rzeszowska, , “OptiDeck,” 08 12 2021. [Online]. Available: https://optideck.prz.edu.pl/.

[131] W. B. R. J. Biliszczuk, “System monitorowania mostu w Puławach,” *Mosty 4 ,* pp. 12-17, 2009.

[132] R. S. J. B. W. Barcik, “System monitorowania konstrukcji Mostu Rędzińskiego we Wrocławiu,” *Mosty 2,* pp. 56-62, 2012.

[133] K. B. D. I. U. S. Andrea Del Groso, “IABSE Symposium Report: Monitoring of bridges and concrete structures with Fibre optic sensors in Europe,” International Association for Bridge and Structural Engineering, 2001.

[134] B. J. Mathew kautzman, “Calibration and testing of distributed fiber optic sensors for detection of high energy radiation,” *Journal of Directed Energy ,* 2018.

[135] SMARTEC SA, Branko Glisic, Daniele Posenato, Daniele Inaudi, "Integrity monitoring of old steel bridge using fiber optic distributed sensors based on Brillouin scattering," in *Proceedings of SPIE,* 2007.

[136] SMARTEC SA Branko Glisic, Daniele Inaudi, Sensing tape for easy integration of optical fiber sensors in composite structures, Manno: SMARTEC SA, 2007.

[137] Instytut Maszyn Przepływowych im. Roberta Szewalskiego PAN, *Specyfikacja Istotnych warunków zamówienia (SIWZ),* Gdańsk , 2011.

[138] R. S. Ł. B. Tomasz Siwowski, "System monitorowania mostów kompozytowych z wykorzystaniem światłowodowych czujników odkształceń," in *PROJECT COM-BRIDGE, DEMONSTRATOR+,* 2017.

[139] Annan, 2023.

[140] P. Annan, GPR.

[141] P. Annan, GPR Principles, Procedures & Applications, Mississauga, ON, Canada: Sensors and Software Inc., 2003, p. 278.

[142] P. Annan, GPR Principles, Procedures & Applications, Mississauga, ON, Canada: Sensors and Software Inc., 2003.

[143] D. J. Daniels , Ground Penetrating Radar, London, UK: The institution of Electrical Engineers, 2004.

This project has received funding from the European Union’s Horizon 2020 research and innovation programme under grant agreement No 958171. © 2021

[144] H. M. Jol, Ground Penetrating Radar: Theory and Applications, Amsterdam, The Netherlands: Elsevier Science, 2009.

[145] M. Solla, H. Lorenzo and V. Pérez-Gracia, "Ground Penetrating Radar: Fundamentals, Methodologies and Applications in Structures and Infrastructures," in *Non-Destructive Techniques for the Evaluation of Structures and Infrastructures*, EH Leiden, The Netherlands, CRC Press/Balkema, 2016.

[146] L. Pajewski, S. Fontul and M. Solla, "Ground-penetrating radar for the evaluation and monitoring of transport infrastructures," in *Innovation in Near-Surface Geophysics. Instrumentation, Application, and Data Processing Methods*, Amsterdam, The Netherlands, Elsevier, 2019.

[147] A. Benedetto and L. Pajewski, Civil Engineering Applications of Ground Penetrating Radar, New York, NY, USA: Springer International, 2015.

[148] W. Wai-Lok Lai, X. Dérobert and P. Annan, "A Review of Ground Penetrating Radar Application in Civil Engineering: A 30-Year Journey from Locating and Testing to Imaging and Diagnosis," *NDT E Int.*, vol. 96, p. 58–78, 2018.

[149] M. Solla, V. Pérez-Gracia and S. Fontul, "A review of GPR application on transport infrastructures: troubleshooting and best practices," *Remote Sensing*, vol. 13, no. 672, 2021.

[150] M. Solla, H. González-Jorge, H. Lorenzo and P. Arias, "Uncertainty evaluation of the 1 GHz GPR antenna for the estimation of concrete asphalt thickness," *Measurement*, vol. 46, p. 3032–3040, 2013.

[151] C. Plati, A. Loizos and K. Gkyrtis, "Assessment of modern roadways using non-destructive geophysical surveying techniques," *Surveys in Geophysics*, vol. 41, pp. 395-430, 2020.

[152] F. Xie, W. Lai and X. Dérobert, "GPR uncertainty modelling and analysis of object depth based on constrained least squares," *Measurement*, no. 109799, 2021.

[153] G. Leimbach and H. Löwy, "Verfahren zur systematischen Erforschung desErdinnern größerer Gebiete mittels elektrischer Wellen". Germany Patent 237944, 1910.

[154] G. Leimbach and H. Löwy, "Verfahren zum Nachweis unterirdischer Erzlager oder von Grundwasser mittels elektrischer Wellen". Germany Patent 246836, 1910.

[155] Hülsenbeck, "Prospector Inst Fuer Praktisch Geol, Huelsenbeck&Co Dr". Germany Patent 489434, 1926.

[156] M. Solla, H. Lorenzo and V. Pérez-Gracia, "Ground Penetrating Radar: Fundamentals, Methodologies and Applications in Structures and Infrastructures," in *Non-Destructive Techniques for the Evaluation of Structures and Infrastructures*, EH Leiden, The Netherlands, CRC Press/Balkema, 2016.

[157] N. Linford, P. Linford, L. Martin and A. Payne, "Stepped frequency ground-penetrating radar survey with a multi-element array antenna: Results from field application on archaeological sites," *Archaeological Prospection*, 2010.

This project has received funding from the European Union's Horizon 2020 research and innovation programme under grant agreement No 958171.

[158] A. Simi, G. Manacorda, M. Miniati, S. Bracciali and A. Buonaccorsi, "Underground asset mapping with dualfrequency dual-polarized GPR massive array," in *Proceedings 13rd International Conference on Ground-Penetrating Radar*, Lecce, Italy, 2010.

[159] J. Hugenschmidt, A. Kalogeropoulos, F. Soldovieri and G. Prisco, "Processing strategies for high-resolution GPR concrete inspections," *NDT E Int.*, vol. 43, p. 334–342, 2010.

[160] M. Garcia-Fernandez, Y. Alvarez-Lopez and F. Las Heras, "Autonomous airborne 3D SAR imaging system for subsurface sensing: UWB-GPR on board a UAV for landmine and IED detection," *Remote Sens.*, vol. 11, no. 2357, 2019.

[161] K. Wu, G. Rodriguez, M. Zajc, E. Jacquemin, M. Clément, A. De Coster and S. Lambot, "A new drone-borne GPR for soil moisture mapping," *Remote Sens. Environ.*, vol. 235, no. 111456, 2019.

[162] C. Balaguer, R. Montero, J. Victores, S. Martínez and A. Jardón, "Towards fully automated tunnel inspection: A survey and future trends," in *Proceedings of the 31st International Symposium on Automation and Robotics in Construction and Mining*, Sydney, Australia, 2014.

[163] X. Xie, Y. Chen and B. Zhou, "Data processing of backfill grouting detected by GPR in shield tunnel and research on equipment of GPR antenna," in *Proceedings of the 16th International Conference on Ground Penetrating Radar*, Hong Kong, China, 2016.

[164] Y. Zan, G. Su and Z. Li, "A Train-mounted GPR System for Fast and Efficient Monitoring of Tunnel Health Conditions," in *Proceedings of the 16th International Conference on Ground Penetrating Radar*, Hong Kong, China, 2016.

[165] R. Persico, A. Provenzano, C. Trela, M. Sato, K. Takahashi, S. Arcone, S. Koppenjan, L. Stolarczyk, E. Utsi and K. W. E. P. L. P. S. Ebihara, Recommendations for the safety of people and instruments in ground-penetrating radar and near-surface geophysical prospecting, European Association of Geoscientists and Engineers, EAGE Publications, 2015.

[166] E. Jafarov, A. Parsekian, K. Schaefer, L. Liu, A. Chen, S. Panda and T. Zhang, "Estimating active layer thickness and volumetric water content from ground penetrating radar measurements in Barrow, Alaska," *Geoscience Data Journal*, vol. 4(2), pp. 72-79, 2017.

[167] J. Stryk, R. Matula, K. Pospíšil, X. Dérobert, J. Simonin and A. Alani, "Comparative measurements of ground penetrating radars used for road and bridge diagnostics in the Czech Republic and France," *Constr. Build. Mater.*, vol. 154, p. 1199–1206, 2017.

[168] T. Saarenketo, "Recommendations for guidelines for the use of GPR in asphalt air voids content measurement. Mara Nord Project; Europeiska Unionen," Brussels, Belgium, 2012.

[169] DMRB3.1.7., "Department for Transport, Highway Agency. DMRB 3.1.7.: Design Manual for Roads and Bridges, Advice Notes on the Non-Destructive Testing of Highway Structures—Advice Note 3.5 BA 86/2006: Ground

This project has received funding from the European Union's Horizon 2020 research and innovation programme under grant agreement No 958171.

Penetrating Radar (GPR)," Department for Transport, Highway Agency, Birmingham, UK, 2006.

[170] DMRB7.3.2., "DMRB 7.3.2.: Design Manual for Roads and Bridges, Data for Pavement Assessment—Annex 6 HD 29/2008: Ground-Penetrating Radar (GPR)," Highway Agency, Birmingham, UK, 2008.

[171] ME91/16, "ME91/16: Methodologies for the Use of Ground-Penetrating Radar in Pavement Condition Surveys," Belgian Road 445 Research Centre, Brussels, Belgium, 2016.

[172] ASTM, "Standard Test Method for Determining the Thickness of Bound Pavement Layers Using Short-Pulse Radar; Non-destructive testing of pavement structures; ASTM D4748," ASTM, West Conshohocken, PA, USA, 2004.

[173] L. Pajewski, M. Vrtunski, Ž. Bugarinovic, A. Ristic, M. Govedarica, A. Van der Wielen, C. Grégoire, C. Van Geem, X. Dérobert, V. Borecky and e. al., "GPR system performance compliance according to COST Action TU1208 guidelines," *Ground Penetrating Radar,* vol. 1, p. 104–122, 2018.

[174] ASTM, "ASTM D6087-08(2015)e1. In Standard Test Method for Evaluating Asphalt-Covered Concrete Bridge Decks Using Ground Penetrating Radar," ASTM, West Conshohocken, PA, USA, 2015.

[175] J. Hugenschmidt, A. Kalogeropoulos, F. Soldovieri and G. Prisco, "Processing strategies for high-resolution GPR concrete inspections," *NDT E Int.,* vol. 43, p. 334–342, 2010.

[176] M. Garcia-Fernandez, Y. Alvarez-Lopez and F. Las Heras, "Autonomous airborne 3D SAR imaging system for subsurface sensing: UWB-GPR on board a UAV for landmine and IED detection," *Remote Sens,* vol. 11, no. 2357, 2019.

[177] M. Howlader, T. Sattar and S. Dudley, "Development of a Wall Climbing Robotic Ground Penetrating Radar System for Inspection of Vertical Concrete Structures.," *Int. J. Mech. Mechatron. Eng.,* vol. 10, p. 1382–1388, 2016.

[178] L. Yangí, G. Yang, Z. Liu, Y. Chang, B. Jiang, Y. Awad and J. Xiao, "Wall-climbing robot for visual and GPR inspection," in *Proceedings of the 2018 13th IEEE Conference on Industrial Electronics and Applications (ICIEA),* Wuhan, China, 2018.

[179] M. Bertolino and T. Tanzi, "Towards 3D Simulation for Disaster Intervention Robot Behaviour Assessment," *Adv. Radio Sci.,* vol. 18, p. 23–32, 2020.

[180] S. Gibb, H. La, T. Le, L. Nguyen, R. Schmid and H. Pham, "Nondestructive evaluation sensor fusion with autonomous robotic system for civil infrastructure inspection.," *J. Field Robot.,* vol. 35, p. 988–1004, 2018.

[181] SHRP, "SHRP 2- report S2-R06A-RR-1. In Nondestructive Testing to Identify Concrete Bridge Deck Deterioration," Transportation Research Board, Washington, DC, USA, 2013.

[182] T. Saarenketo, P. Maijala and A. Leppäl¨, "Recommendations for Guidelines for the Use of GPR in Bridge Deck Surveys," Publications of Mara Nord Project, 2011.

This project has received funding from the European Union's Horizon 2020 research and innovation programme under grant agreement No 958171.

[183] BASt, “BASt-Report B55. Examination of GPR in Combination with Magnetic Techniques for the Determination of Moisture and Salinity of Concrete Bridge Decks with Asphalt Cover,” Federal Highway Research Institute, Bundesanstalt für Straßenwesen, 2007.

[184] B10, “Document B10—Recommendation for Nondestructive Testing of Civil Engineering Structures by GPR,” German Society for Non- Destructive Testing (DGZfP), Berlin, Germany, 2008.

[185] AASHTO, “AASHTO R 37-04. Standard Practice for Application of Ground Penetrating Radar (GPR) to Highways,” American Association of State and Highway Transportation Officials, Washington, DC, USA, 2004.

[186] ACI, “ACI 228.2R-98 (Reapproved 2004). Nondestructive Test Methods for Evaluation of Concrete in Structures,” American Concrete Institute, Farmington Hills, MI, USA, 1998.

[187] NCHRP, “NCHRP Research Report 848. In Inspection Guidelines for Bridge Post-Tensioning and Stay Cable Systems Using NDE Methods,” TRB’s National Cooperative Highway Research Program, Washington, DC, USA, 2017.

[188] L. Pajewski, S. Fontul and M. Solla, “Ground-penetrating radar for the evaluation and monitoring of transport infrastructures,” in *Innovation in Near-Surface Geophysics. Instrumentation, Application, and Data Processing Methods,* Amsterdam, The Netherlands, Elsevier, 2019.

[189] [Online]. Available: http://www.bibliotecacpa.org.ar/greenstone/collect/facagr/index/assoc/HASH42bc.dir/doc.pdf. [Accessed 24 junio 2021].

[190] "“Plataformas, sensores y canales.”," [Online]. Available: https://www.um.es/geograf/sigmur/teledet/tema03.pdf. [Accessed 24 Junio 2021].

[191] T. Pultarova, “The Evolution Of Earth Observation,” December 2018. [Online]. Available: https://www.ingenia.org.uk/ingenia/issue-77/the-evolution-of-earth-observation. [Accessed 22 Oct 2021].

[192] M. Zotti and C. La Mantia, “"Open data from earth observation: From big data to linked open data, through INSPIRE",” *Journal of e-Learning and Knowledge Society,* vol. 10, no. 2, 2014.

[193] J. R. Elliott, . R. J. Walters and . T. J. Wright, “The role of space-based observation in understanding and responding to active tectonics and earthquakes.,” *Nature communications,* vol. 7, no. 1, pp. 1-16, 2016.

[194] "NASA's Earth Science Data Systems (ESDS)," [Online]. Available: https://earthdata.nasa.gov/esdis/esco/standards-and-references#deprecated. [Accessed 24 Junio 2021].

[195] W. Yang, “A review of remote sensing data formats for earth system observations.,” *Earth Science Satellite Remote Sensing,* pp. 120-145, 2006.

[196] M. Berger, J. Moreno, J. A. Johannessen, P. F. Levelt and R. F. Hanssen, “ESA's sentinel missions in support of Earth system science.,” *Remote Sensing of Environment,* vol. 120, pp. 84-90, 2012.

This project has received funding from the European Union’s Horizon 2020 research and innovation programme under grant agreement No 958171.

[197] A. Loew, W. Bell, L. Brocca, C. E. Bulgin, J. Burdanowitz, X. Calbet and T. Verhoelst, “Validation practices for satellite-based Earth observation data across communities.,” *Reviews of Geophysics,* vol. 55, no. 3, pp. 779-817, 2017.

[198] S. Sterckx, I. Brown, A. Kääb, M. Krol, R. Morrow, P. Veefkind and P. Thorne, “Towards a European Cal/Val service for earth observation,” *International Journal of Remote Sensing,* vol. 41, no. 12, pp. 4496-4511, 2020.

[199] mapwaredev, “Understanding Errors and Distortion in Remote Sensing,” 4 Jun 2020. [Online]. Available: https://mapware.ai/blog/understanding-errors-and-distortion-in-remote-sensing/. [Accessed 24 Jun 2021].

[200] E. Setyawan, “Intermap,” 12 August 2019. [Online]. Available: https://www.intermap.com/blog/satellite-imagery-resolution-vs.-accuracy. [Accessed 15 Dec 2021].

[201] L. Di, “Standards, Critical Evaluation of Remote Sensing,” *Encyclopedia of GIS, Springer International Publishing,* p. 2187–2196, 2017.

[208] B. Riveiro, H. González-Jorge, B. Conde and I. Puente, “Laser Scanning Technology: Fundamentals, Principles and Applications in Infrastructure,” *Non-Destructive Techniques for the Evaluation of Structures and Infrastructure,* pp. 53-80, 4 2016.

[209] “Digital technologies can enhance climate resilience of critical infrastructure – infrastructuResilience,” 17 12 2021. [Online]. Available: http://www.infrastructuresilience.com/lake-polyfytos-bridge/.

[210] M. Soilán, A. Sánchez-Rodríguez, P. Del Río-Barral, C. Perez-Collazo, P. Arias and B. Riveiro, “Review of Laser Scanning Technologies and Their Applications for Road and Railway Infrastructure Monitoring,” *Infrastructures 2019, Vol. 4, Page 58,* vol. 4, no. 4, p. 58, 9 2019.

[211] S. Paulus, T. Eichert, H. E. Goldbach and H. Kuhlmann, “Limits of Active Laser Triangulation as an Instrument for High Precision Plant Imaging,” *Sensors 2014, Vol. 14, Pages 2489-2509,* vol. 14, no. 2, pp. 2489-2509, 2 2014.

[212] L. LINK, C. J. G and C. J. J, “AIRBORNE LASER SYSTEMS USE IN TERRAIN MAPPING,” 1981.

[213] B. Riveiro, M. J. DeJong and B. Conde, “Automated processing of large point clouds for structural health monitoring of masonry arch bridges,” *Automation in Construction,* vol. 72, pp. 258-268, 12 2016.

[214] D. Kang, H. Lee, H. S. Park and I. Lee, “Computing Method for Estimating Strain and Stress of Steel Beams Using Terrestrial Laser Scanning and FEM,” *Key Engineering Materials,* vol. 347, pp. 517-522, 9 2007.

[215] D. F. Laefer, L. Truong-Hong, H. Carr and M. Singh, “Crack detection limits in unit based masonry with terrestrial laser scanning,” *Ndt & E International,* vol. 62, pp. 66-76, 2014.

[216] D. F. Laefer, J. Gannon and E. Deely, “Reliability of crack detection methods for baseline condition assessments,” *Journal of Infrastructure Systems,* vol. 16, no. 2, pp. 129-137, 2010.

This project has received funding from the European Union’s Horizon 2020 research and innovation programme under grant agreement No 958171. © 2021

[217] A. Sánchez, B. Riveiro, I. Puente, B. Conde, N. Mendes, M. Cabaleiro and P. B. Lourenço, “Parameterization of Structural Faults in Large Historical Constructions for Further Structural Modelling Thanks to Laser Scanning Technology and Computer Vision Algorithms,” *RILEM Bookseries,* vol. 18, pp. 351-359, 2019.

[218] S. Chen, L. Truong-Hong, D. Laefer and E. Mangina, “Automated Bridge Deck Evaluation through UAV Derived Point Cloud,” *undefined,* 2018.

[219] Q. Li and X. Cheng, “DAMAGE DETECTION FOR HISTORICAL ARCHITECTURES BASED ON TLS INTENSITY DATA,” *The International Archives of the Photogrammetry, Remote Sensing and Spatial Information Sciences,* Vols. XLII-3, no. 3, pp. 915-921, 4 2018.

[220] B. Conde, S. Del Pozo, B. Riveiro and D. González-Aguilera, “Automatic mapping of moisture affectation in exposed concrete structures by fusing different wavelength remote sensors,” *Structural Control and Health Monitoring,* vol. 23, no. 6, pp. 923-937, 6 2016.

[221] J. S. Yoon, M. Sagong, J. S. Lee and K. s. Lee, “Feature extraction of a concrete tunnel liner from 3D laser scanning data,” *NDT & E International,* vol. 42, no. 2, pp. 97-105, 3 2009.

[222] Y. Zhou, S. Wang, X. Mei, W. Yin, C. Lin, Q. Hu and Q. Mao, “Railway tunnel clearance inspection method based on 3D point cloud from mobile laser scanning,” *Sensors,* vol. 17, no. 9, 2017.

[223] P. G. Asteris and V. Plevris, “Handbook of research on seismic assessment and rehabilitation of historic structures,” *Handbook of Research on Seismic Assessment and Rehabilitation of Historic Structures,* pp. 1-867, 7 2015.

[224] American Society for Photogrammetry & Remote Sensing, *LAS SPECIFICATION VERSION 1.4 – R13,* 2013.

[225] “BIN File Extension - What is .bin and how to open? - ReviverSoft,” 17 12 2021. [Online]. Available: https://www.reviversoft.com/file-extensions/bin.

[226] “RIEGL - RIEGL Laser Measurement Systems,” 17 12 2021. [Online]. Available: http://www.riegl.com/.

[227] A. Filgueira, H. González-Jorge, S. Lagüela, L. Díaz-Vilariño and P. Arias, “Quantifying the influence of rain in LiDAR performance,” *Measurement,* vol. 95, pp. 143-148, 1 2017.

[228] I. Puente, H. González-Jorge, B. Riveiro and P. Arias, “Accuracy verification of the Lynx Mobile Mapper system,” *Optics & Laser Technology,* vol. 45, no. 1, pp. 578-586, 2 2013.

[229] USGS, *Lidar Base Specification.*

[230] H. Jiang, Q. Li, Q. Jiao, X. Wang and L. Wu, “Extraction of Wall Cracks on Earthquake-Damaged Buildings Based on TLS Point Clouds,” *IEEE Journal of Selected Topics in Applied Earth Observations and Remote Sensing,* vol. 11, no. 9, pp. 3088-3096, 9 2018.

This project has received funding from the European Union’s Horizon 2020 research and innovation programme under grant agreement No 958171.

[231] H. Wu, X. Ao, Z. Chen, C. Liu, Z. Xu and P. Yu, “Concrete spalling detection for metro tunnel from point cloud based on roughness descriptor,” *Journal of Sensors,* vol. 2019, 2019.

[232] A. Kazi, A. Sausthanmath, S. M. Meena, S. V. Gurlahosur and U. Kulkarni, “Detection of holes in 3D architectural models using shape classification based Bubblegum algorithm,” *Procedia Computer Science,* vol. 167, pp. 1684-1695, 1 2020.

[233] H. C. Jo, J. Kim, K. Lee, H.-G. Sohn and Y. M. Lim, “Non-contact strain measurement for laterally loaded steel plate using LiDAR point cloud displacement data,” *Sensors and Actuators A: Physical,* vol. 283, pp. 362-374, 2018.

[234] M. Soilán, B. Riveiro, A. Sánchez-Rodríguez and P. Arias, “Safety assessment on pedestrian crossing environments using MLS data,” *Accident; analysis and prevention,* vol. 111, pp. 328-337, 2 2018.

[235] J. Balado, L. Díaz-Vilariño, P. Arias and H. Lorenzo, “Point clouds for direct pedestrian pathfinding in urban environments,” *ISPRS Journal of Photogrammetry and Remote Sensing,* vol. 148, pp. 184-196, 2 2019.

[236] H. S. Park, H. Lee, H. Adeli and I. Lee, “A new approach for health monitoring of structures: terrestrial laser scanning,” *Computer-Aided Civil and Infrastructure Engineering,* vol. 22, no. 1, pp. 19-30, 2007.

[237] A. Sanchez-Rodríguez, B. Riveiro, B. Conde and M. Soilán, “Detection of structural faults in piers of masonry arch bridges through automated processing of laser scanning data,” *Structural Control and Health Monitoring,* vol. 25, no. 3, p. e2126, 3 2018.

This project has received funding from the European Union’s Horizon 2020 research and innovation programme under grant agreement No 958171. © 2021

8 Appendixes

Appendix A1. Acoustic Emission (AE)

Appendix A2. Aerial UAV with optical payloads

Appendix A3. Optical and visual testing - Boroscopy and Endoscopy

Appendix A4. Fibre optic sensors

Appendix A5. Ground Penetrating Radar (GPR)

Appendix A6. Guided waves propagation (GW) techniques

Appendix A7. Light detection and ranging or laser imaging detection and ranging (LiDAR)

Appendix A8. Magnetic and electrical methods

Appendix A9. Mechanical tests on cored samples

Appendix A10. Micro Electro-Mechanical Systems (MEMS) - Accelerometers

Appendix A11. Micro Electro-Mechanical Systems (MEMS) - Clinometers

Appendix A12. Qualitative Chemical Methods

Appendix A13. Quantitative Chemical Methods

Appendix A14. Radiological and Nuclear Methods

Appendix A15. Satellite remote sensing

Appendix A16. Surface measurements

Appendix A17. Water penetration test – Permeability test

Appendix A18. Water resistance – Absorption test

Appendix A19. Weight-in-motion Systems

This project has received funding from the European Union's Horizon 2020 research and innovation programme under grant agreement No 958171.

ONLINE INTERACTIVE CATALOGUE OF SURVEYING TECHNOLOGIES FOR TRANSPORT INFRASTRUCTURE APPENDIXES

IM-SAFE.EU

This project has received funding from the European Union's Horizon 2020 research and innovation programme under grant agreement No 958171.

APPENDIX A1. Acoustic Emission Techniques (AE)

1.1 Goal(s)

1.1.1 Main objective

The acoustic emission method provides information about possible catastrophic failures or evaluation of the level of damage in different materials and industries. Concrete structures are subjected to many environmental factors during the life-cycle and for this reason, advanced AE techniques are used to provide monitoring of the internal failures progressing in time. The aim is to link the degree of damage in the structure with the operating conditions of the facility. As one of the non-destructive testing methods with an increasing number of produced equipment modifications has a great potential for bridge monitoring as well as quality control and structural integrity assessment. Deformation of the bridge structure element can be real-time monitored with the use of acoustic emission means as it is known that under loads in the life cycle of the bridge the structural elements from concrete and steel emit elastic waves due to different damage processes. As sensing technology is a fast-developing industry branch and therefore there is a growing number of possibilities of system configuration adjusted for a specific purpose. For long-term monitoring aspects, this is an important factor to the future of the application of AE in structural health monitoring of bridges and other constructions (International Atomic Energy Agency, 2002) (E.Tsangouri, 2019).
Currently, there is a need for improvement of the AE systems in aspects of practicality, and economic issues. Despite that - information collected from the Acoustic Emission Monitoring System is successfully used for overall evaluation of the actual quality of the bridge and can help with planning and prioritization of further repairs and maintenance.

1.2 Description

1.2.1 Functioning mode

The basis of the method lies in the analysis of the acoustic waves generated by active, destructive processes developed during the operational loads. Elastic waves are generated in a material when it is subjected to stress, which causes deformation or stress field. When the material is subjected to load, the elastic limit can be crossed. This is known as the acoustic emission, which is inaudible but can be detected by sensors attached to the surface of the tested object. Waves are produced in the tested area and then, those waves can be detected, and their corresponding intensity is linked with the existence of the defect in the studied structures.

Acoustic emission system consists of one to several acoustic sensors, a preamplifier, the main amplifier, and a computer-based data acquisition device. Other accessories are necessary such as couplant and connecting cables. Piezoelectric transducers are used for the detection of the signals,

This project has received funding from the European Union's Horizon 2020 research and innovation programme under grant agreement No 958171.

which transform mechanical waves into electrical signals. When the material is loaded, the elastic limit can be crossed. This is known as the acoustic emission, which is inaudible but can be detected by sensors attached to the surface of the test object.

There are two approaches for the measurement mode:

- the parameter-based technique – only extracting parameters from received signals without saving the waveforms. Crucial parameters such as hit, amplitude, count, rise time, duration are recorded to assess AE activities.

- the signal-based technique – characterized by transforming analog signals to electrical signals for quantitative analysis (Zhou, 2011) (International Atomic Energy Agency, 2002) (Masayasu Ohtsu, 2007).

Acoustic sensors can be mounted in four ways, which is shown below:

- through clearance hole:

Figure 1.1 – Clearance hole mounting (SIEMENS , 2021)

- through drill and tap:

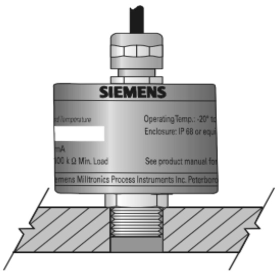

Figure 1.2 – Drill and tap mounting (SIEMENS , 2021)

- with the mounting disc:

This project has received funding from the European Union's Horizon 2020 research and innovation programme under grant agreement No 958171.

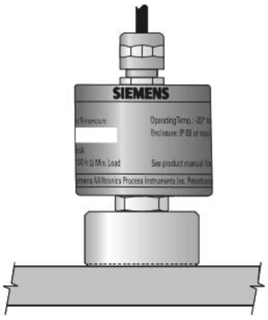

Figure 1.3 – Mounting with disc (SIEMENS , 2021)

- with extension tab.

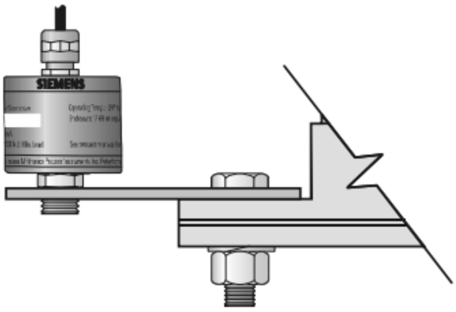

Figure 1.4 – Mounting with extension tab (SIEMENS , 2021).

The transducers can be directed oppositely, parallel, or diagonally.

Systems designed for structural monitoring usually work in the following manner:

- As a transmitting unit – processed data are transmitted to remote locations, where it is possible to analyze information from computer or mobile interface in real-time;
- As a collector unit – processed data are stored in the memory card for further analysis (Masayasu Ohtsu, 2007) (The Vallen Systeme , 2021) (SIEMENS , 2021).

The general working principle is shown below in the scheme:

This project has received funding from the European Union's Horizon 2020 research and innovation programme under grant agreement No 958171.

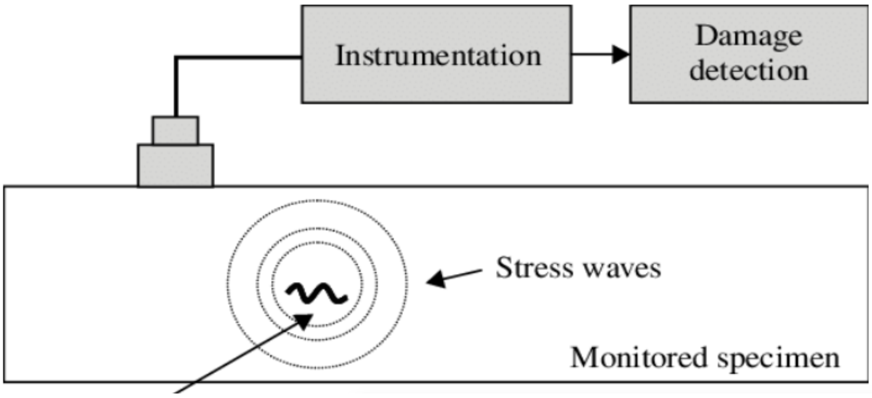

Figure 1.5 – Working scheme of AE technique

1.2.2 Types

Depending on the application there are different types of equipment used for acoustic emission measurements:

- compact, small, usually dual-channel, portable handheld unit optimal for use as a field survey tool with permanent data collection which can be stored on the memory card and then analysed on the computer; use same functioning mode as monitoring systems, but does not allow continuous monitoring for longer periods; useful for the fast in field and laboratory testing – battery last for few hours; good for areas difficult to reach; composed with two passive sensors, memory card, parametric cable, and battery,
- multi-channel instruments with wireless data transmission for long-term monitoring purposes; composed with at least four acoustic channels, two power supplies, wireless module, memory card and adjusted software for analysis of the collected data, start and termination of the monitoring activities as well as transfer to the base station; allow collecting information about behavior and responses to in-service loads, include alarming system after analysis of the data collected from the baseline and eventual damages (International Atomic Energy Agency, 2002) (Mix, 2005).

From the point of view of sensors applied, several options can be used, depending on the application, for instance:

- high sensitivity sensors with integral preamplifier
- frequency differential sensors
- wideband differential sensors
- high sensitivity intrinsically safe wideband differential sensors
- low-frequency sensors
- flat frequency response sensors
- lightweight miniature sensors
- underground sensors

This project has received funding from the European Union's Horizon 2020 research and innovation programme under grant agreement No 958171. © 2021

- epoxy coated underwater sensors (The Vallen Systeme , 2021)

1.2.3 Process/event to be detected or monitored

Processes that can be monitored by means of acoustic emission sensors are:

- detection of dynamic processes in materials,
- detection of leaks,
- detection of flaws,
- tracking of degradation processes in concrete,
- detection of damage mechanisms related to corrosion – cracking, debonding,
- level of intensity of cracking processes,
- integrity testing of metallic structures,
- integrity testing of composite materials,
- integrity testing of concrete structures.

Examples of the detection in concrete elements performed with acoustic emission techniques can be found in (E.Tsangouri, 2019) (Y. Kawasaki, 2013) (D.G. Aggelis, 2013) (B. Goszczyńska, 2015).

1.2.4 Physical quantity to be measured (e.g. actions, displacements, deformations, dynamic structural properties, material properties including mechanical, electrical and chemical properties, relative displacements of the two sides of a crack, etc.).

The time of passage of the elastic wave between the transducers should be monitored on the measurement device and recorded. Time of the elastic pulse path from the transmitting to the receiving transducer through the concrete. Wavefront is recorded by measuring device.

1.2.5 Induced damage to the structure during the measurement

The registration of signals of elastic waves is non-destructive for the structures.

1.2.6 General characteristics

1.2.6.1 Measurement type (static or dynamic, local or global, short-term or continuous, etc.)

An acoustic emission sensor is designed for both global and local measurements. For global purposes helps with assessing the structural integrity, while in local uses – detecting specific areas of damage. It is possible to perform an inspection for short periods as well as long term. Static and dynamic load tests can be carried out with an acoustic sensors system (Tae-Min Oh, 2020).

1.2.6.2 Measurement range

- high sensitivity range is obtained when signal level are up to 40 dB,
- low sensitivity range applies when signals are in 28 – 68 dB,
- typical signals frequency range: 1 kHz up to 1MHz, usually divided into three categories – low-frequency range (20 kHz – 100 kHz), standard (100 – 400 kHz), and high (>400 kHz).
- data sets rate: 80 hits/sec per channel,

This project has received funding from the European Union's Horizon 2020 research and innovation programme under grant agreement No 958171.

- up to 310 m line of site (The Vallen Systeme , 2021).

1.2.6.3 Measurement accuracy

- Measurement path can be recorded with +/- 1% accuracy. The sensitivity of acoustic emission is affected by temperature. In most applications, this is not a concern when considering the much greater changes in signal level due to changes in flow.
- If the temperature of the standard Sensor increased from 20 °C to 50 °C, its sensitivity would decrease by 15%. If the Sensor were to be used to monitor flow changes over such a temperature range, you should set an associated alarm set point at least 30% away from the normal operating level measured at 20 °C.

1.3 Background (evolution through the years)

B.H Schofield firstly named sound-emitting phenomenon as 'Acoustic Emission' in his publication. Important works on the method has been made in 1970 by monitoring of the portable military bridge. First analysis of the amplitude distribution has been performed back then. In 1980 first investigations had been carried out to see if it is possible to use acoustic emission techniques for continuous and long-term monitoring. The next advance was made by the performance of the monitoring crack activity in steel bridges. Physical Acoustic Corporation performed many experiments to study different types of sensors and use of additional guard sensors to eliminate unwanted signals from the consideration (International Atomic Energy Agency, 2002). (Kaphle, 2012) (E.Tsangouri, 2019) (Mix, 2005) (Tae-Min Oh, 2020) (Zhou, 2011) (Ohtsu, 1996).

1.4 Performance

1.4.1 General points of attention and requirements

1.4.1.1 Design criteria and requirements for the design of the survey

For transducers recommended working frequency is 20 kHz to 150 kHz. The instrument should be able to determine the time of arrival of the wave front with the lowest possible amplitude level. The excited pulse generated in the transmitting head should have a rise time of no more than a quarter of its natural period of vibration so that the onset of the received wave is free from the influence of disturbances. The sensors should be installed at using high-vacuum grease with adhesive tape to enhance the coupling performance at the interface between the concrete and the sensor.

1.4.1.2 Procedures for defining layout of the survey

No specific guidelines.

1.4.1.3 Design constraints (e.g. related to the measurement principles of the monitoring technologies)

The performed tests suffer from the presence of other sources that give rise to other unwanted signals that can mask the ones from cracks, wire breaks or other defects.

This project has received funding from the European Union's Horizon 2020 research and innovation programme under grant agreement No 958171. © 2021

1.4.1.4 Sensibility of measurements to environmental conditions

The sensitivity of acoustic emission is affected by temperature. In most applications this is not a concern when considering the much greater changes in signal level due to changes in flow. However it is important to be aware of the effect. For standard sensor the sensitivity decreases with increasing temperatures at a rate of approximately 0,5% per degree Celsius. For example, if the temperature of the standard sensor increased from 20°C to 50°C, its sensitivity would decrease by 15%. However modern sensors are adjusted to work in temperatures from 20 °C up to 120 °C with a sufficient accuracy.

1.4.2 Preparation

1.4.2.1 Procedures for calibration, initialisation, and post-installation verification

Calibration involves probing with an oscilloscope to set gain and threshold levels. The sensors are installed at the points of the sample using high-vacuum grease with adhesive tape to enhance the coupling performance at the interface between the concrete and the sensor.

1.4.2.2 Procedures for estimating the component of measurement uncertainty resulting from calibration of the data acquisition system (calibration uncertainty)

Calibration uncertainty depends on the configuration of the system, influenced by transducer sensitivity and background noise.

1.4.2.3 Requirements for data acquisition depending on measured physical quantity (e.g. based on the variation rate)

Right before the measurement, initial inspection of the construction should be carried out. Sensors should be attached to the cleaned surface. Calibrating the EA sensors is just as important as the appropriate setting of hardware parameters. Calibration consists of reading the values of the parameters of the EA signals, generated by the standard source.

1.4.3 Performance

1.4.3.1 Requirements and recommendations for maintenance during operation (in case of continuous maintenance)

There is no uniform standard or procedure for maintenance during operation, however available guidelines for short-term bridge monitoring can be found in ASTM E1932-02.

1.4.3.2 Criteria for the successive surveying campaigns for updating the sensors.

Not applicable.

1.4.4 Reporting

Report should include:

- identification of concrete sample and construction,
- date,
- localization,
- age of the concrete,

This project has received funding from the European Union's Horizon 2020 research and innovation programme under grant agreement No 958171.

- temperature,
- localization of the transducers,
- identification of the apparatus used,
- velocity of the elastic wave on each measurement path.

1.4.5 Lifespan of the technology (if applied for continuous monitoring)

Specially designed wireless systems give the possibility for continuous monitoring longer than one year.

1.5 Interpretation and validation of results

1.5.1 Expected output (Format, e.g. numbers in a .txt file)

Graph with a discrete electrical signal at the output of a sensor, amplitude on the sensors [dB] vs time [s]. List of measured times necessary to overcome the path between transducers for each length. Other parameters:

- number of signals,
- signal amplitude is given in mV or dB,
- signal energy,
- burst signal energy: the energy of the electrical signal caused by a detected burst,
- burst signal peak amplitude: the highest voltage excursion of the detected burst signal,
- rise time: the time difference of the peak occurrence to the start of the hit,
- duration: the time difference between the end of hit and start of the hit,
- counts: the number of positive threshold crossings in the time period between start of hit and end of.

An example of the output on one of the sensor responses is shown below:

This project has received funding from the European Union's Horizon 2020 research and innovation programme under grant agreement No 958171. © 2021

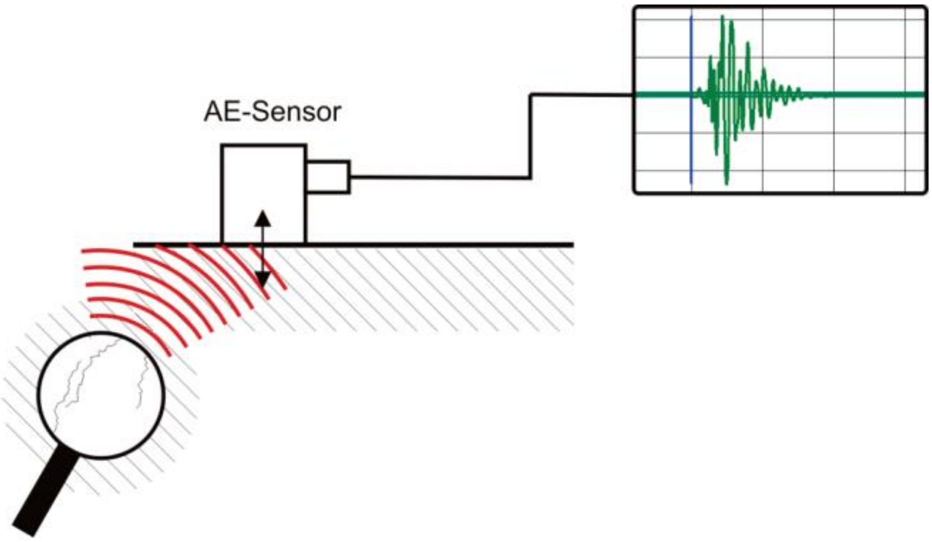

Figure 1.6 – Cracks emitting the elastic wave - acoustic emission measurement (Vallen Systeme GmbH, 2019)

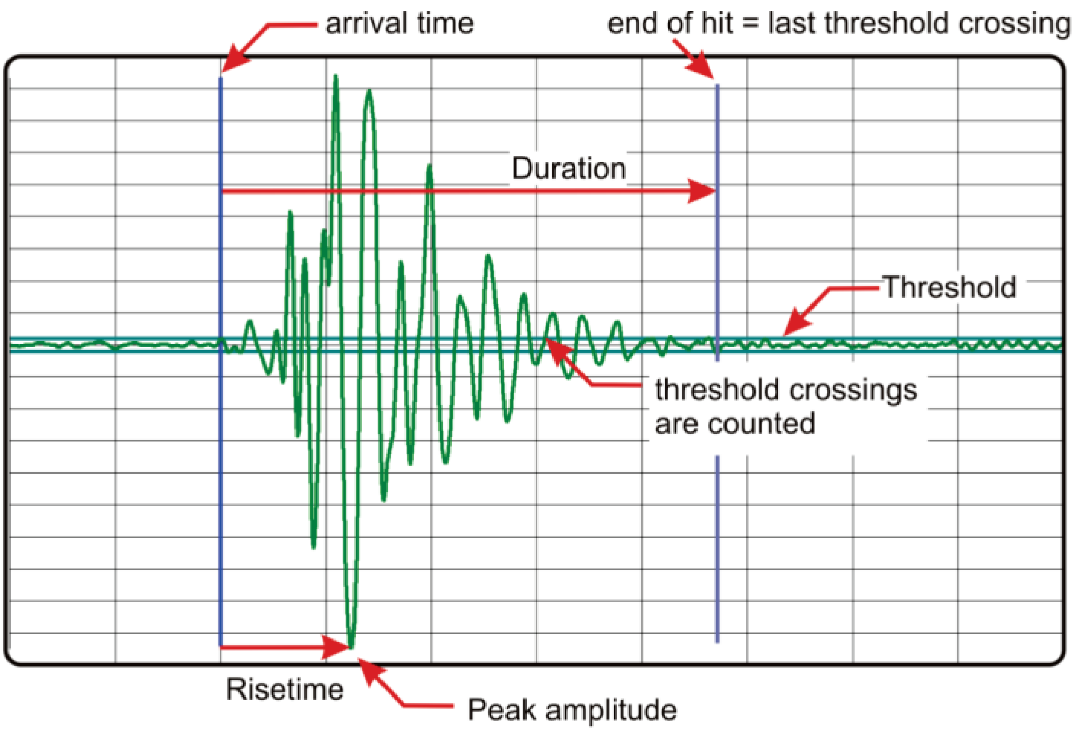

Figure 1.7 – Extracted features from a hit (Vallen Systeme GmbH, 2019).

1.5.2 Interpretation (e.g. each number of the file symbolizes the acceleration of a degree of freedom in the bridge)

TR diagrams show waveforms (transient data) in the time and/or frequency domain. AE diagrams are used to plot any of the available AE attributes, time, or parametric data against each other. AE diagrams can be 2D or 3D.

Comparative analysis of the emission signals recorded during the test of the object with the created model database of destructive signals allows for the identification and location of active destructive processes. Measured time is used to calculate the velocity of the ultrasonic wave, where the length of

This project has received funding from the European Union's Horizon 2020 research and innovation programme under grant agreement No 958171.

the measuring path in meters is divided by the time needed to transmit to wave on a selected path in seconds. An intensity analysis technique has to be performed to accumulate obtained data and use it for characterization of the damages. Comparison of the intensity of the signals on each sensor gives information about potential failure risk in the structure.

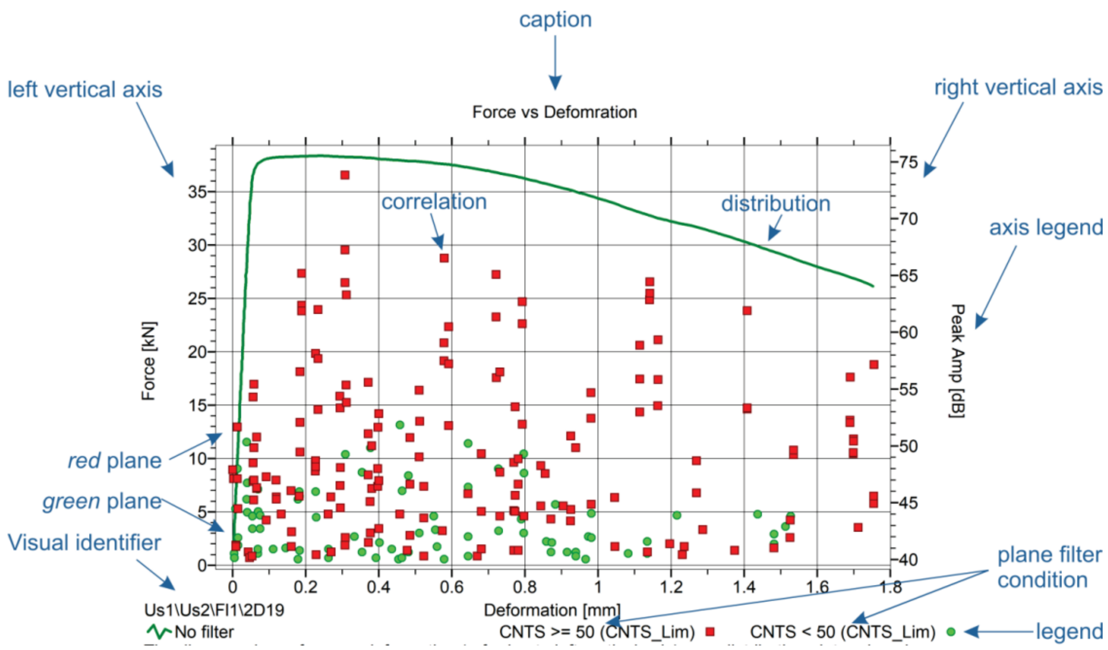

Figure 1.8 – Distribution plot and peak amplitude vs deformation (Vallen Systeme GmbH, 2019).

1.5.3 Validation

1.5.3.1 Specific methods used for validation of results depending on the technique

Validations of AE techniques are based on tests carried out in laboratory conditions on specimens or individual structural elements.

1.5.3.2 Quantification of the error

Quantification of the error by root mean square error method mainly or automatically in the software provided by the manufacturer.

1.5.3.3 Quantitative or qualitative evaluation

Quantitative evaluation can be performed by analysis of the AE signals with AE waveforms.

1.5.4 Detection accuracy

Specific correlations between the different factors influencing the accuracy of results are described in the norms: EN13477-1, Non-destructive testing – Acoustic emission testing – Equipment characterization – Part 1: Equipment description and that can be verified according to EN 13477-2, Non-destructive testing – Acoustic emission testing – Equipment characterization – Part 2: Verification of operating characteristics.

Cracks can be detected with 0,01 mm accuracy.

This project has received funding from the European Union's Horizon 2020 research and innovation programme under grant agreement No 958171. © 2021

1.6 Advantages

Acoustic emission can be particularly effective for monitoring damages in foundations, which are not visible using a typical monitoring system. It is capable of detecting the onset of failure and locating the source of possible failure. Since acoustical signals come from defects throughout the structures a few transducers are enough to detect and locate defects over large areas. Enables localization of the particularly dangerous areas and quantification of the issue.

Taking into consideration systems needed for bridge monitoring:

- both local and global measurement possible
- no interference with the traffic on the bridge
- remote navigation and analysis of the data
- customized alarm system upon reaching user-defined damage thresholds
- internal storage of the data
- power saving options
- compatibility with different power sources and batteries
- simple connection to the base station.

1.7 Disadvantages

Disadvantages of the method include:

- requirement of two-sided access to a given measurement site,
- sensitivity to the differences in the moisture content of the concrete surface,
- sensitivity to the presence of reinforcing bars,
- difficulty with measurements, when complex geometry is given,
- difficulty with measurements when large number of defects is present,
- more suitable for new bridges and construction as a supplement for standard inspection.

1.8 Possibility of automatizing the measurements

Rapid progress of microchips causes immediate appearance new, more compact, convenient and informational - capacious AE instruments.

1.9 Barriers

The main barrier is the technological need for decreasing the power level consumption to extend the lifetime of the battery used.

1.10 Existing standards

- EN 13554:2011 Non-destructive testing - Acoustic emission testing - General principles,
- EN 473 The European Standard for Qualification and Certification of NDT Personnel,

This project has received funding from the European Union's Horizon 2020 research and innovation programme under grant agreement No 958171.

- EN 1330-9, Non-destructive testing —Terminology — Part 9: Terms used in acoustic emission testing,
- ASTM E3100 – 17 - Standard Guide for Acoustic Emission Examination of Concrete Structures,
- ISO 16836:2019, Non-destructive testing — Acoustic emission testing — Measurement method for acoustic emission signals in concrete,
- ASTM E650, Standard guide for mounting piezoelectric acoustic emission sensors,
- ASTM E1106, Standard method for primary calibration of acoustic emission sensors.

1.11 Applicability

1.11.1 Relevant knowledge fields

1.12.1 Industry:

- machine condition monitoring,
- cavitation monitoring,
- leak detection,
- production quality control.

1.12.2 Chemical industry:

- reactor vessels testing,
- offshore testing,
- drill pipe testing,
- pipelines testing,
- transformers testing,
- valves testing,
- hydro treaters.

1.12.3 Aerospace technology:

- aging aircraft's evaluation,
- rocket motor testing,
- fatigue cracks detection.

1.12.4 Energy industry:

- nuclear reactors testing,
- steam generators testing,
- ceramics insulators,
- transformers,
- aerial devices.

This project has received funding from the European Union's Horizon 2020 research and innovation programme under grant agreement No 958171. © 2021

1.11.2 Performance Indicators

Relate the surveying technology being studied with PIs from WP3, provided in the document of the TU1406 COST ACTION.

- delamination,
- cracks,
- rupture,
- displacement,
- reinforcement bar failure/bending,
- loss of section,
- debonding,
- deformation,
- holes,
- wire breaks.

1.11.3 Type of structure

- bridges,
- tunnels,
- walls,
- viaducts.

1.11.4 Spatial scales addressed (whole structure vs specific asset elements)

- knots and stringers,
- hanger connections,
- link pin connection,
- copes and stringers,
- stiffener to weld connection.

1.11.5 Materials

- concrete,
- steel,
- composites,
- ceramics,
- polymers.

1.12 Available knowledge

1.12.1 Reference projects

WI-HEALTH: Wireless network for total SHM of bridges (EU FP7 2011-2013).

This project has received funding from the European Union's Horizon 2020 research and innovation programme under grant agreement No 958171.

1.12.2 Other

Examples of use of acoustic emission uses:

- use of the acoustic emission and base of reference signals for viaduct located in Kielce, Poland.
- use of acoustic emission for assessment of the technical condition of the bolted bridge in Sandomierz, Poland.
- self-powered Sensor Network for Bridge Health Prognosis, sponsored by the National Institute of Standards and Technology (NIST) through the Technology Innovation Project Grant (TIP).
- Wireless Acoustic Emission Systems – overview in a publication

Manufacturers websites:

- Acoustic Emission Sensing System
- Physical Acoustic
- Physical Acoustic – overview of the products and system elements
- MARPOSS Acoustic Emission Sensors
- Vallen Systeme GmbH
- Vallen Systeme – Acoustic Emission Sensors and preamplifiers.
- FUJI CERAMICS CORPORATION

1.13 Bibliography

B. Goszczyńska, G. Ś. (2015). Analysis of the microcracking process with the Acoustic Emission method with respect to the service life of reinforced concrete structures with the example of the RC beams. *Civil Engineering*, pp. 55-63.

D. Robert Hay, J. A. (2009). Monitoring The Civil Infrastructure with Acoustic Emission: Bridge Case Studies. *J. Acoustic Emission*, pp. 1-10.

D.G. Aggelis, S. V. (2013). Characterization of mechanical performance of concrete beams with external reinforcement by acoustic emission and digital correlation . *Construction and Building Materials 47* , pp. 1037-1045.

E.Tsangouri, D. A. (2019). A review of acoustic emission as indicator of reinforcement effectiveness in concrete and cementitious composites. *Construction and Building Materials 224* , pp. 198-205.

International Atomic Energy Agency. (2002). *Guidebook on non-destructive testing of concrete structures. Training Course No.17.* Vienna: IAEA.

Kaphle, M. (2012). Analysis of Acoustic Emission Data for Accurate Damage Assessment for Structural Health Monitoring Applications. Brisbane, Australia: Queensland University of Technology.

Masayasu Ohtsu, T. I. (2007). Acoustic Emission Techniques Standardized for Concrete Structures. *J. Acoustic Emission*, pp. 21-32.

Mix, P. E. (2005). *Introduction to Nondestructive Testing - A Training Guide* . New Jersey: John Wiley & Sons,Inc. .

This project has received funding from the European Union's Horizon 2020 research and innovation programme under grant agreement No 958171.

Ohtsu, M. (1996). The history and development of acoustic emission in concrete engineering. *Mag. Concrete Res. 49*, pp. 321-330.

SIEMENS . (2021, 12 14). *SIEMENS Acoustic Sensors* . Retrieved from Siemens Operating Instructions SIT Trans AS100: https://adegis.com/media/asset/981b1fab3911f86718855fb811cc55a8ce6ece66f0e5f730aaf297fca9f45200.pdf

SIEMENS . (2021, 12 14). *SIEMENS support industry* . Retrieved from https://support.industry.siemens.com/cs/products?dtp=Catalog&mfn=ps&pnid=17666&lc=en-WW

Tae-Min Oh, M.-K. K.-W.-J. (2020, August 23). Experimental Investigation on Effective Distances of Acoustic Emission in Concrete Structures. *applied sciences*, pp. 1-18.

The Vallen Systeme . (2021, 12 14). *Acoustic Emission Sensors and Preamplifiers.* Retrieved from The Vallen Systeme - The Acoustic Emission Company: https://www.vallen.de/zdownload/pdf/Sensor_Preamplifier_Description.pdf

Vallen Systeme GmbH. (2019, 07). AMSY-6 System description. Retrieved 12 15, 2021, from https://www.vallen.de/zdownload/pdf/AMSY-6_Description.pdf

Y. Kawasaki, T. W. (2013). Corrosion mechanisms in reinferced concrete by acoustic emission . *Construction and Building Materials 48*, pp. 1240-1247.

Zhou, J. (2011). *A Study Of Acoustic Emission Technique For Concrete Damage Detection.* Michigan: Michigan Technological University.

This project has received funding from the European Union's Horizon 2020 research and innovation programme under grant agreement No 958171.

APPENDIX A2. Aerial UAV. Optical Payloads

2.1 Goal(s)

2.1.1 Main objective

An unmanned aircraft vehicle (UAV) is defined as a powered aerial vehicle that does not carry a human operator, making use of aerodynamic forces to fly, being piloted remotely or by means of an autonomous control (González-Jorge et al., 2017).

In order to measure and monitor the environment, these vehicles can carry optical imaging sensors, such as Light Detection and Ranging (LiDAR), Synthetic Aperture Radar (SAR) and NDT payloads. The measurements can be georeferenced by the navigation system and the attitude sensors of the vehicle, generally based on Global Navigation Satellite Systems (GNSS) and Inertial Measurement Units (IMU).

The main contribution of UAVs technology consists of their capability to fly in difficult and inaccessible areas, lowering the risks to the crews of manned aircraft.

In the last years, these systems have enabled for the so-called Aerial Robotics, that can obtain measurements and perform inspection tasks in bridges to obtain georeferenced images and raw data from onboard sensors.

This technology consists of a platform that acts as the carrier for multiple sensors that have been widely used for bridge diagnosis, such LiDAR, GPR, and other sensors. We refer interested readers to the reports on specific sensor technologies.

2.1 Description

2.1.1 Functioning mode

UAVs behavior mainly depends on system properties and, in general, their functioning mode heavily depends on their subsystems, that briefly consist of:

Frame

The frame is the main structural element of UASs. The frame is the support for the rest of the components such as motors, electronic subsystems, batteries, and payload.

The frame should obey a trade-off between a smooth geometry with little aerodynamic resistance to fly and the need for actuating and hovering in the air. Accordingly, Aerodynamics is more important in fixed-wing than in rotary-wing UASs.

The classification of frames depends also on the aerospace materials used to create the UAV: from foam frames used in low-end fixed-wing UAVs carbon fiber and expensive materials used for high-end vehicles. For rotary-wing UAVs plastic, aluminum, and carbon fiber frames, are frequent materials depending on the quality of the aircraft.

Motors and batteries

This project has received funding from the European Union's Horizon 2020 research and innovation programme under grant agreement No 958171.

The strong adoption of rotary-wing UAVs is partly caused by the performance and popularization of brushless motors. These motors can be controlled straightforward based on off-the-shelf electronics and are very efficient in energy consumption, being powered by light batteries that use an integrated inverter to obtain AC electric signals that control and drive the motor. For heavy UAVs, there is a need to use combustion motors powered by solid combustible that can carry the payload and are more complex to use and maintain.

Propellers

The propellers convert the rotational motion of the motors into thrust following the Bernoulli's principle. Depending on the type and size of the UAV, different size, pitch, number of blades, and type of material are used. For professional small UAVs, carbon fiber propellers are preferred because they are more rigid and produce less vibration when spinning.

Flight control

The flight of the UAV is controlled by the so-called autopilot that performs a mission based on a planned path. This is a challenging task and the basis for the different applications of the UAVs beyond the use of remote controls by a human operator.

Path planning must consider several procedures and constrains such as obstacle avoidance, maximum coverage, sensor limitations, and vehicle motions, as well as time and cost efficiency. For optimal flight path, several algorithms have being proposed based on spanning trees or Neural Networks (Bolourian et al., 2017).

The flight control strongly depends on the Navigation (GNSS) and attitude (IMU) sensors of the aircraft.

Payloads and Data Processing

Payload is defined as all the components that are not used to fly but are specific to perform the mission and its objectives. Payloads of civil UAS are mainly classified into optical payloads that enable for remote sensing of the environment and NDT payloads that support aerial robotics (González-Jorge et al., 2017).

OPTICAL PAYLOADS

Optical payloads are the basis for remote inspection, one of the key features enabled by UAVs. Typical payloads that support a wide range of inspection tasks, include (Greenwood et al., 2019):

- Passive sensors: These sensors (mainly cameras) use the ambient light to record the reflection of that light on the object to be imaged and include the different ranges of the spectrum.
    - RGB cameras. These are the most frequent cameras and may be considered as a ubiquitous sensors, since a high number of modern devices include cameras. Depending on their applicability to measurement tasks, we can distinguish metric, semi-metric and non-metric cameras (Mart\'\inez-Sánchez et al., 2016).
    - Multispectral and hyperspectral cameras. These cameras can capture images in visible and non-visible parts of the spectrum from the Ultraviolet (UV) to the long wave infrared (LWIR), passing through optical frequencies, Near Infrared (NIR), infrared and short wave infrared (SWIR). Depending on the number of wavelengths that the camera is able to capture we distinguish multispectral (up-to 10 wavelengths) of hyperspectral cameras (tenths of hundreds of wavelengths)

This project has received funding from the European Union's Horizon 2020 research and innovation programme under grant agreement No 958171.

    - Thermal camera. Given their application, we distinguish this type of cameras based on sensors that are sensible to long infrared spectra, the so called Thermal Infrared (TIR) that covers from 8 to 14 micrometers (Lagüela et al., 2011).

- Active sensors: These sensors use an internal source of energy to illuminate the object to be inspected and record the reflection to that specific signal. As a consequence, these sensors are sensible only for an specific range of the spectrum, being monochromatic in the case of Laser-based systems. Active sensors include (Dorafshan & Maguire, 2018):
    - Light detection and ranging (LiDAR) is probably the most up-to-date system for object inspection and monitoring. More information in Laser Scanning report.
    - Radio detection and ranging (RADAR)/synthetic aperture RADAR (SAR). In this case, the source of energy is a pulsed radio wave. More information in GPR report.
    - Sound navigation and ranging (SONAR) Using pressure waves, one of the applications of SONAR consists of underwater measurements providing underwater object information, but not limited to because of their capability to detect objects.

2.1.2 Types

There are several types of UAVs and they can be classified depending on a number of their characteristics as developed in the following tables(Hassanalian & Abdelkefi, 2017) and paragraphs.

Depending on the weight:

Class	Type	Weight range
Class I(a)	Nano drones	W≤200 g
Class I(b)	Micro drones	200 g <W≤2 kg
Class I(c)	Mini drones	2 kg <W≤20 kg
Class I(d)	Small drones	20 kg <W≤150 kg
Class II	Tactical drones	150 kg <W≤600 kg
Class III	MALE/HALE/Strike drones	W> 600 kg

Table 2-1 – Classification of UAVs depending on their weight

Depending on the application:

- Military
- Civilian
- Agriculture and forestry
- Disaster monitoring and management
- Surveillance
- Environmental monitoring
- 3D mapping
- Atmospheric

This project has received funding from the European Union's Horizon 2020 research and innovation programme under grant agreement No 958171.

- Wildlife monitoring

Depending on the flying principle

Type	Description
Fixed wing	Airfoil that generates the lift of the plane. These frames are controlled making use of surfaces built on the wing (ailerons, elevators, and rudder)
Flapping wing	Inspired from insects, and small birds consist of the flexible and flapper wings which use an actuation mechanism for their flapping motion. Most of the flapping wings have flexible and light wings as observed in birds and insects which indicate that the flexibility and weight of wings are important for their aerodynamic proficiency and flight stability
Fixed/flapping wing	Hybrid designs which use fixed wings for lift and flapping wings for propulsion
Rotary wing	These systems are based on the control of the motors and propellers that provide the force to lift. Their manoeuvrability is very high and allows them to hover and subsequently, to fly in and inspect confined spaces. These characteristics make rotary wings the key UAV type for surveying hardly-accessible areas and components in high-rise applications]

Table 2-2 UAV classification based on flying principle

2.1.3 Process/event to be detected or monitored

UAV support the combined advantages of robot inspection and remote sensor inspection. As such, the use of these systems for documentation, inspection, and monitoring, has gained a significant focus. Even though RPAS/UAVs platforms can help practitioners to make measurements in difficult environments, the detection of damages and failures depends on the specific sensors onboard the platform. Please refer to the templates about sensor technologies for more information.

2.1.4 Physical quantity to be measured

The quantities to be measured using UAVs depends mainly on the payload sensors attached to the frame. The most frequent sensors include:

- Optical cameras for visual inspection through image processing
- Multispectral and thermographic cameras
- LiDAR for collecting points clouds
- RADAR payloads

Please review the other templates regarding specific sensors for a more detailed description about measurement techniques

Visual inspection

This project has received funding from the European Union's Horizon 2020 research and innovation programme under grant agreement No 958171.

Traditional visual bridge inspection methods are time-consuming and unsafe for practitioners because of the height works and falling risk. The use of UAS for visual inspection is a mitigation measure to reduce the risk and improve the efficiency of the field inspection. As a general feasible procedure, UAS are able to obtain high-quality image data to be analysed by inspectors.

In this context, the visual inspection of the assets is based on optical payloads onboard the frame of the UAV and is dependent on the image acquisition system and surveying process in the field and the trajectory followed by the system. In order to limit the dependence on the field work, UAS can include control algorithm based on computer vision to navigate an unknown 3D environment and saturation functions to maintain the object to be inspected in the camera's field of view.

Unattended or automatized image processing can contribute to detect a range of damages on the surface of the asset, such as moderate crack thickness ranging from 0.5 mm to several mm. The extension of the crack can be achieved with statistical analysis and sufficient data to cover a representative inspection area. Depending on the thickness, the standard photogrammetric survey can be a useful tool for quantifying the damage.

In order to detect smaller thickness cracks, higher quality images (in terms of resolution, sharpness and entropy) followed by image postprocessing treatment can reveal cracks with a small thickness of 0.1 mm.

In addition, the UAS can help to easily access structural components at high altitudes, such as girders, putting together optical cameras, infrared, motion, and modelling sensors.

Other damages, such as gaps between the end of kerf plate and sawn kerf in the brace, can be identified on the bridge components.

In general and due to the higher resolution of optical cameras, image processing techniques may be preferred over other sensors such as LiDAR or RADAR, to detect the boundaries of the defects.

2.1.5 Induced damage to the structure during the measurement

Not Applicable.

2.1.6 General characteristics

2.1.1.1 Measurement type (static or dynamic, local or global, short-term or continuous, etc.)

Depending on the payload that is attached to the system and subject to the flight time of the framework. The flight time for typical UAVs ranges from 15-45 minutes for multirotor systems to more than one hour (or more) for fixed wing aircrafts.

Given that multirotor UAVs are more adequate for bridge inspection, the typical measurement time could be considered as 30 minutes, restricted by the autonomy of the UAV and the payload.

2.1.1.2 Measurement range

Depending on the payload that is attached to the system and subject to the flight time of the framework.

This project has received funding from the European Union's Horizon 2020 research and innovation programme under grant agreement No 958171.

For optical systems (i.e. cameras) onboard the UAV, the range is restricted by the optical scale of the images.

The optical scale is the relation between the distance to the object and the principal distance (*focal length*) of the camera. This optical scale is a limit for the expected accuracy of the measurements and, in general, can be considered that the higher the principal distance the higher the expected accuracy.

The drawback of the *optical scale* consists of the *field of view* (FoV) of the camera: for each body and sensor, a larger principal distance would reduce the FoV and, thus, increase the time needed for measurement in the field and a more complex planification of the operation.

For more information on active sensors (LiDAR and RADAR) please refer to the technology documentation.

2.1.1.3 Measurement accuracy

Regarding the accuracy of the data with optical payloads, two main sources of issues should be taken into consideration:

- The quality of the collected images

The accuracy of the data processing procedure, mainly, the photogrammetric process.

Image quality assessment

After the inspection, there is a need of completing the image quality assessment in the field in order to limit the number of visits to the inspection site.

In order to speed up the process the entire dataset should be analysed. This is a drawback for photogrammetric projects because the number of pictures is very high.

The quality of the images must be quantified calculating sharpness and entropy of the images and comparing the results to the average value for the image dataset. This analysis can be carried out with image processing tools included in photogrammetric software bundles. Higher quality images consist of the portion of the dataset presenting improved sharpness without a variation in entropy.

The quality of the images largely depends on lighting conditions. A sufficient illumination in the images would lead to sharpness and increased entropy (Duque et al., 2018)(Seo et al., 2018)

Accuracy of the photogrammetric process

Beyond the quality of each single image, when dealing with a photogrammetric project, it is important to quantify the accuracy of the final 3D measurements. The internal and external accuracy of the measurements is one of results of the photogrammetric data processing and, thus, a surveying of control and test points is mandatory to obtain both. Moreover, the final accuracy depends on the image photogrammetric network, that should be defined previously to the field work, as described in the next sections.

To summarize, the photogrammetric process is based on a number of procedures that affect the accuracy of the measurements and should be considered:

This project has received funding from the European Union's Horizon 2020 research and innovation programme under grant agreement No 958171.

- Alignment of the images. In the current state of the art, the alignment solves the relative orientation of the images and the absolute orientation to a global frame (ie. Global coordinate system). This is based on a bundle block adjustment that solves the unknowns for certain 3D points on the inspection site that are considered *interest points* based on the calculation of salient features on the images. As a result, the alignment provides the precision figures based on redundant information on the images about this interest points, that are classified on *Key points* and *Tie points*.
- A dense point cloud can be calculated based on the alignment of the images. In this procedure, the disparity map of the images is transformed into a depth map and a 3D point cloud. The accuracy of this procedure depends not only on the image network and the overall accuracy of the images to obtain the *interest points* but on the reliability of *each pixel* in the image. This is related to the image quality assessment. Nevertheless, there are a number of methods to detect the outliers in the point cloud calculation and, accordingly, to filter the points with a lower precision.
- Depending on the inspection task, obtaining a mesh of the surface is mandatory to model the site. This process is subject to the filtering of unknowns and may result on lower frequency models. A visual inspection of such models is mandatory to solve the trade-off between number of triangles in the surface and the actual optical resolution of the model. The correction of the texture of this triangulation could lead to a more accurate model in terms of radiometric properties.
- The most frequently used method for the assessment of the photogrammetric results consists of a classical surveying using a GPS and depending on the accuracy objectives. The points in the GPS surveying must be divided into *control points* and *check points* to clarify the internal and external accuracy figures of the photogrammetric process.

2.2 Background (evolution through the years)

Military applications

The drones or UAS are an example of how military systems can be applied to civil requirements after a long time.

The first UAS attempts started during World War I when the Dayton-Wright Airplane Company invented an unmanned aerial torpedo that would explode at a pre-set time.

During World War II, Reginald Denny Industries' first large-scale production drone appeared. They made about 15,000 drones to be used as targets for anti-aircraft gunner training.

The first target drone converted for an unmanned aerial photographic reconnaissance mission on the battlefield was a version of the MQM-57 Falconer (first flown in 1955).

UASs were not applied until the 1980s when the coordinated use of UASs with manned aircraft became popular with applications such as electronic decoys, electronic jammers, and reconnaissance tools.

Military UAS as the Predator RQ-1L were deployed from the Balkan war in the 1990s to current war conflicts.

Civil applications in recent times

Recent improvements in the field of Aerial Robots have enabled the use of various multi-rotor platforms (for example, four- and eight-rotor platforms) in the field of SHM, with various implementations focusing on inspection and maintenance of bridges, mostly based on visual inspection methods. However, some

This project has received funding from the European Union's Horizon 2020 research and innovation programme under grant agreement No 958171.

of the recent studies have attempted to explore different ways in which aerial robots can be modified to provide contact and perch-based inspection capabilities.

Several recent studies have also proposed the development of hybrid robots, which can provide multiple functionalities (for example, mechanisms for flying and walking and a number of different approaches based on contact and flight).

Some of these platforms have provided a proof of concept with considerable potential for successful use for future bridge inspection.

This is a relatively new field of research to take full advantage of the flexibility and versatility of aerial robotic platforms to access and monitor different components of the bridge infrastructure.

Trends for Aerial Robotics

The trends for the UAS is their evolution to Aerial Robotic System to use UAV for bridge inspection tasks that require physical contact between the aerial platform and bridge surfaces[13,14], such as beam deflection analysis or crack depth measurement with an ultrasonic sensor.

These systems take advantage of the aerodynamic ceiling effect when the multirotor approaches the bridge surface. As a consequence, a UAV can be used as a sensor capable of flying and touching the bridge to take measurements during a contact inspection. The numerous practical applications of these systems include measuring beam girder deflection from a bridge using a laser tracking station.

Other common approach is UAS design based on aerial manipulators composed of an aerial platform and an articulated robotic arm attached to the top of the multirotor, which was used to perform inspection tasks that require contact with the bridge. However, the payload requirements for this type of manipulator are high, resulting in large, heavy platforms that are slower and more complex to control.

2.3 Performance

2.1.7 General points of attention and requirements

2.3.1.1 Design criteria and requirements for the design of the survey

Depending on the sensors to be mounted on the platform see 4.4.1.3 below

2.3.1.2 Procedures for defining layout of the survey

Depending on the sensors to be mounted on the platform see 4.4.1.3 below

2.3.1.3 Design constraints (e.g. related to the measurement principles of the monitoring technologies)

Data collection and surveying using UAV needs for specific measures to prevent risky situations and obtain useful data.

Workflow	Steps
Survey objectives	Determine the objective areas and data

This project has received funding from the European Union's Horizon 2020 research and innovation programme under grant agreement No 958171.

Site prechecking	Revise available geographical information of the location and the operational constraints of the environment
Fight planning	Offline flight planning, including: ▪ take-off and landing locations, ▪ flight speeds and heights, ▪ image scale constraints (distance vs focal length) ▪ Preliminary Operation Safety study
Risk assessment	Enumerate, evaluate, and foresee mitigation measures related to the operation risks.
Permission application	Study Regulation constraints to depending on the risk-level of the operation: ▪ Obtain permission for the flight and/or ▪ Communicate authority the specified flight plan
Data collection	Notify any potentially impacted populations about when the aerial survey will start; follow the devised flight plan for data collection, and if any emergency occurs, land the UAV safely

Table 2-3 Workflow for the planning of a UAV-based survey. Following (Chen et al., 2019)

The field work for bridge inspection must be clearly defined and scheduled in order to reduce the time spent in the field, especially for risky operations. The process consists of conducting the following steps:

1. Path planning. It consists of defining the six Degrees of Freedom of the system during the trajectory for the inspection. It is dependent on the payload sensor because the field of view of the object must be maintained and the distance to the structure is critical. It can be considered a collection of Poses (Position and Orientation)
    a. Defining critical sections: potential location of cracks or other surface defects, which could be estimated using structural analysis or based on experience. These sections define the Regions of Interest (RoI) during the inspection.
    b. Define critical waypoints: Depending on the critical section and the payload sensor, these are the POSES of the best locations for surveying to likely detect the damage in the RoI.
    c. Select optimal path
        i. Generate paths. Taking into account the RoI and the Waypoints, a number of trajectories are proposed.
        ii. Calculate coverage and cost.
        iii. Select the optimal trajectory or path in terms of cost, including the energy cost of the flight and the coverage to obtain a good image quality.
2. Data collection and image quality assessment.

This project has received funding from the European Union's Horizon 2020 research and innovation programme under grant agreement No 958171.

3. Data analysis and overall accuracy assessment

2.3.1.4 Sensibility of measurements to environmental conditions

Taking into consideration UAVs consist of a platform to carry sensors as the so called payload, the environmental conditions affect the trajectory followed by the vehicle and we should consider:

- Wind speed: the maximum speed the UAV can maintain the sustainability and flight capabilities. It depends mainly on the type of frame, the size and weight of the platform and the power of the propellers and motors. The flight controller should account for variations in wind speed, particularly, for sureying with a high accuracy requirement.
- Visibility: even though UAVs can perform the mission with a very high degree of autonomy, safety issues and normative requires that a pilot is the person in charge of the operation. Low visibility also affects optical payloads that are the most applicable in the state of the practise.
- IP protection grade with respect to rain and water. Robustness of the system depends on the ambient moisture/rain.

2.3.2 Preparation

2.3.2.1 Procedures for calibration, initialisation, and post-installation verification

Data collection by UAV is highly dependent on the aircraft's navigation system, which is mainly comprised of a GNSS solution for location and an IMU for measuring drone attitude. A lack of proper calibration of the navigation system would result in incorrect or useless data.

The process to perform the pre-calibration of the navigation system consists of confirming that the flight is going to be carried out safely and efficiently, in the Pre-Flight Setup. [9]

Components to be inspected include motors, propellers, batteries, ground station and / or remote control, payload gimbal, and communications. The components to be calibrated are mainly focused on the IMU and, specifically, on the magnetometers and compass. To calibrate the compass, several rotations must be made around the three axes of the aircraft.

Regarding image quality and image processing, the state of the Technique permits to perform the so-called self-calibration of the camera during the alignment of the images in the photogrammetric process.

Self-calibration takes advantage of automated Interest Point detection based on different techniques to obtain feature descriptors, such as SIFT, SURF or ORB. Using these methods, thousands of points can be detected and matched on different images. This database can be used to model the properties of the camera during the data collection, outperforming traditional calibration based on laboratory or in field calibration using a known pattern of points.

The components of the calibration model for optical cameras consist of the principal distance (ie. focal length), the principal point and the distortion parameters of the camera.

This project has received funding from the European Union's Horizon 2020 research and innovation programme under grant agreement No 958171.

2.3.2.2 Procedures for estimating the component of measurement uncertainty resulting from calibration of the data acquisition system (calibration uncertainty)

Not Applicable. The operational uncertainty in navigation position and attitude of the UAV is higher than the calibration uncertainty and strongly depends on surveying conditions.

2.3.2.3 Requirements for data acquisition depending on measured physical quantity (e.g. based on the variation rate)

The operational uncertainty in navigation position and attitude strongly depends on surveying conditions.

2.3.3 Performance

2.3.3.1 Requirements and recommendations for maintenance during operation (in case of continuous maintenance)

Not applicable.

2.3.3.2 Criteria for the successive surveying campaigns for updating the sensors. The campaigns include: (i) Georeferenced frame, i.e. the global location on the bridge; (ii) Alignment of sensor data, relative alignment of the data collected in a surveying; (iii) Multi-temporal registration to previous campaigns; and (iv) Diagnostics.

General constraints

The sensors onboard UAS can obtain their Position and Orientation (POSE) from the navigation sensors used by the UAV platform. Consequently, the absolute accuracy of the data will largely depend on UAV navigation system.

The positioning provided by standard GPS units is generally adequate for navigation of small RPAS that entail a lower risk during the navigation. There are a number of applications, including that based on visual inspection, the image quality is more important that the POSE accuracy and, thus, standard coarse GPS is correct.

If we focus on photogrammetric applications where the dimensional surveying of the bridge is a key, the general workflow consists of complementing coarse navigation GPS with survey-grade GPS in the field. As described in the photogrammetric discussion, these accurate GPS points must be divided into *control points* and *test points* in order to quantify the internal and external accuracy of the data.

This GPS surveying increase the cost of the inspection and is time consuming and in recent times, small RPAS systems include RTK positioning systems that can provide centimetric positioning accuracy. As a result, manually surveyed checkpoints are no longer necessary for a number of applications that don't need very high precision, increasing the cost-effectiveness of UAV platforms.

Nevertheless, although Network-based RTK GNSS positioning can improve the precision of surveying if needed, the altitude component of the measurements is worse than the planimetric surveying due to the nature of satellite navigation.

This project has received funding from the European Union's Horizon 2020 research and innovation programme under grant agreement No 958171. © 2021

The POSE of the UAV will affect the different sensors onboard the platform. In this document we focus on image-based surveying and we refer the reader to the specific document for other sensors, such as LiDAR and RADAR.

(i) Georeferenced frame

The use of GNSS based POSE makes UAS based surveying a repeatable method, subject to the accuracy of the positioning system.

The general framework for traditional surveying based on external GPS consists of selecting a number of control points with a minimum of three (to know the internal precision) and perform a transformation to the Global Reference Frame or Global Coordinate System (GCS).

Global coordinates can be achieved from the local 3D photogrammetric coordinates through a conformal 3D Helmert or 7-parameter transformation.

For the transformation between GCS the is a need for changing both datum and projection system.

(ii) Alignment of sensor data

The alignment of sensor data or *relative orientation* is possible if there is a redundancy in the spatial distribution of data.

In the case of the photogrammetric process, we described this alignment based on redundant points on the images. This process can be automatized through *interest point* detection and matching using feature descriptors.

Even though the POSE of the UAV during data collection is not mandatory for the alignment of data, it can largely speed-up the process, providing initial guesses for the solution in a non-linear bundle adjustment that includes the POSE for the cameras and the 3D coordinates of the thousands of points detected in the images.

(iii) Multi-temporal registration to previous campaigns.

Multi-temporal registration of successive data collection campaigns is based on the control points gathered during the GPS surveying phase. Having the results of the photogrammetric process (Points clouds, Images and Orthomosaics) in a GCS enables for direct multi-temporal analysis and change detection.

In the case that the UAV platform includes a RTK positioning system and the GNSS survey is not performed, the registration must be based on points that remain fixed between campaigns. These points can be used as initial guess for image alignment, as fixed points in a Helmert 3D transformation or as control points in a Iterative Closest Point (ICP) process to register Point Clouds.

Previous knowledge about fixed points can speed up the process for GNSS surveying, using these points as *control points* and reducing the data acquisition to *test points* that can be analysed to obtain the *external accuracy* of the final data.

This project has received funding from the European Union's Horizon 2020 research and innovation programme under grant agreement No 958171.

(iv) Diagnostics

Not Applicable

2.3.4 Reporting

Not Applicable. Depending on the sensors to be mounted on the platform.

2.3.5 Lifespan of the technology (if applied for continuous monitoring)

Not Applicable.

2.2 Interpretation and validation of results

2.3.6 Expected output (Format, e.g. numbers in a .txt file)

Not Applicable. Depending on the sensors to be mounted on the platform.

2.3.7 Interpretation (e.g. each number of the file symbolizes the acceleration of a degree of freedom in the bridge)

Not Applicable. Depending on the sensors to be mounted on the platform.

2.3.8 Validation

Not Applicable. Depending on the sensors to be mounted on the platform.

2.3.8.1 Specific methods used for validation of results depending on the technique

Not Applicable. Depending on the sensors to be mounted on the platform.

2.3.8.2 Quantification of the error

Not Applicable. Depending on the sensors to be mounted on the platform.

2.3.8.3 Quantitative or qualitative evaluation

Not Applicable. Depending on the sensors to be mounted on the platform.

2.3.9 Detection accuracy

Not Applicable. Depending on the sensors to be mounted on the platform.

2.4 Advantages

- Lower risk for practitioners and operators
- Access to hard-to-reach areas such as deck bottoms
- Robust Data acquisition in high components
- Better site visibility and aerial point of view of the system
- Cost-effective technique for surveying
- Speed-up the process in field compared to manual data acquisition
- Pre-defined risk scenarios for the operation that simplify the planification phase.

This project has received funding from the European Union's Horizon 2020 research and innovation programme under grant agreement No 958171.

2.5 Disadvantages

The main disadvantage in the use of drones consist of the Regulations related to Aviation safety and the operational constraints

- Limited flight time -Autonomy of the system
- Payload weight limited by Maximum Take Off Weight and regulations.
- Even though there is a EU regulation defined by European Aviation Safety Agency (EASA), the National regulation and local permissions are not standardized.
    - Mixed between operational safety and System Certification
- Operational constraints including
    - Visual Line of Sight (VLOS) restrictions.
    - Subject to field conditions, including weather condition
    - Navigation solutions for interesting areas, such as deck bottoms
- More complex planification phase.
- Low Readiness Level for a number of inspection applications, such as Aerial Robotics
- Limitation for Real-Time data and postprocessing procedures.

2.6 Possibility of automatising the measurements

Although current regulations require that a pilot be in charge of the operation of remotely piloted aerial systems (RPAS), technology allows the consideration of autonomous aerial systems (UAS) that include vehicles (UAVs) and other subsystems. and components that allow the sensing of bridge properties automatically.

The measurement procedure using UAVs includes the definition of a precise path that the vehicle will follow thanks to its navigation system, based on GNSS and IMU, which is known as mission planning. The precision of the components included in the navigation system will determine the adjustment of the real trajectory followed by the vehicle to the one defined in the mission planning. The missions include the planning of infrastructure sampling, which is determined by the position and orientation (POSE) of the sensors involved. When the UAV reaches the marked position, the flight controller will send a trigger signal to the sensor to collect data. Optionally, the sensor is oriented towards the area of the asset to be monitored thanks to the use of so-called gimbals.

The georeferencing of the data obtained is done automatically at that time, being able to relate each individual measurement to the vehicle's pose. The accuracy of this automatic georeferencing depends on the accuracy of the navigation subsystem. There are solutions on the market based on real-time differential kinematic GNSS systems (RTK) that allow obtaining centimetric precision in the positioning of the measurements.

Automatic data georeferencing can speed up the photogrammetric process: since the positioning of the images is known, it is easier to establish neighbourhood relationships between the images to be

This project has received funding from the European Union's Horizon 2020 research and innovation programme under grant agreement No 958171. © 2021

processed. In this way, the automatic calculation of the relative orientation, or alignment, of the images can start from an initial solution and many checks of the geometry of the images to be processed are avoided.
Today, most of the photogrammetric process is automated. The automatic detection of points of interest (PoI) or KeyPoints in the images allows obtaining the alignment of the images and the coordinates of such Keypoints through the intersection of their projection rays. The application of automatic image processing techniques also supports the calculation of disparity maps between each pair of images and, therefore, the depth for each pixel of the photo in the real world. In this way, a dense point cloud is calculated, with precision and resolution figures that are comparable to those obtained by a LiDAR system.

2.7 Barriers

- Assessment of the cost-effectiveness
- Safety
- Lack of harmonized Regulation.
    - Reactiveness in Traffic Control of UAS that difficult the operations.
- Applicability and Robustness of the Results
- TRL of well-knowns applications on UAS and Aerial Robotics.
- Results subject to field conditions, including weather condition and remotely sensed data.

2.8 Existing standards

2.8.1 International Standards

Standardization in the field of unmanned aircraft systems (UAS) including, but not limited to, classification, design, manufacture, operation (including maintenance) and safety management of UAS operations.

Code	Topic
ISO/TC 20/SC 16/AG 5	Detect And Avoid (DAA)
ISO/TC 20/SC 16/AHG 1	Counter UAS
ISO/TC 20/SC 16/JWG 7	Joint ISO/TC 20/SC 16 - ISO/TC 43/SC 1 WG: Noise measurements for UAS (Unmanned Aircraft systems)
ISO/TC 20/SC 16/WG 1	General
ISO/TC 20/SC 16/WG 2	Product manufacturing and maintenance
ISO/TC 20/SC 16/WG 3	**Operations and procedures**
ISO/TC 20/SC 16/WG 4	UAS Traffic Management
ISO/TC 20/SC 16/WG 5	Testing and evaluation
ISO/TC 20/SC 16/WG 6	UAS subsystems

This project has received funding from the European Union's Horizon 2020 research and innovation programme under grant agreement No 958171. © 2021

Table 2-4 Working groups in SO/TC 20/SC 16

CEN - PREN 4709-Aerospace series - Unmanned Aircraft Systems

Part 001: Product requirements and verification

Part 002: Direct Remote identification

Part 003: Geo-awareness requirements

Part 004: Lighting requirements

2.8.2 National Standards

Spain - CTN 028/SC 02 "SISTEMAS AÉREOS NO TRIPULADOS (UAS)"

2.9 Applicability

2.9.1 Relevant knowledge fields

2.9.2 Performance Indicators

2.9.3 Type of structure

2.9.4 Spatial scales addressed (whole structure vs specific asset elements)

2.9.5 Materials

2.10 Available knowledge

2.10.1 Reference projects

- GIS-Based Infrastructure Management System for Optimized Response to Extreme Events of Terrestrial Transport Networks - SAFEWAY. 2018 - 2022 | European Union | H2020-MG-2016-2017 Ref. 769255-2
- Healthy and Efficient Routes In Massive Open-Data Based Smart Cities: Smart 3D Modelling: HERMES-S3D. 2014 - 2016 | MINECO | Ref. TIN2013-46801-C4-4-R
- SITEGI project: Application of Geotechnologies to Infrastructure Management and Inspection. 2011 - 2013 | Technology Centre for Industrial Development, CDTI.

2.10.2 Other

2.11 Bibliography

Bolourian, N., Soltani, M. M., Albahri, A. H., & Hammad, A. (2017). High level framework for bridge inspection using LiDAR-equipped UAV. ISARC 2017 - Proceedings of the 34th International Symposium on Automation and Robotics in Construction, July, 683–

This project has received funding from the European Union's Horizon 2020 research and innovation programme under grant agreement No 958171.

688. https://doi.org/10.22260/isarc2017/0095

Chen, S., Laefer, D. F., Mangina, E., Zolanvari, S. M. I., & Byrne, J. (2019). UAV Bridge Inspection through Evaluated 3D Reconstructions. Journal of Bridge Engineering, 24(4), 05019001. https://doi.org/10.1061/(asce)be.1943-5592.0001343

Dorafshan, S., & Maguire, M. (2018). Bridge inspection: human performance, unmanned aerial systems and automation. In Journal of Civil Structural Health Monitoring (Vol. 8, Issue 3). Springer Berlin Heidelberg. https://doi.org/10.1007/s13349-018-0285-4

Duque, L., Seo, J., & Wacker, J. (2018). Synthesis of Unmanned Aerial Vehicle Applications for Infrastructures. Journal of Performance of Constructed Facilities, 32(4), 04018046. https://doi.org/10.1061/(asce)cf.1943-5509.0001185

González-Jorge, H., Martínez-Sánchez, J., Bueno, M., & Arias, P. (2017). Unmanned aerial systems for civil applications: A review. Drones, 1(1), 1–19. https://doi.org/10.3390/drones1010002

Greenwood, W. W., Lynch, J. P., & Zekkos, D. (2019). Applications of UAVs in Civil Infrastructure. Journal of Infrastructure Systems, 25(2), 04019002. https://doi.org/10.1061/(asce)is.1943-555x.0000464

Hassanalian, M., & Abdelkefi, A. (2017). Classifications, applications, and design challenges of drones: A review. Progress in Aerospace Sciences, 91(April), 99–131. https://doi.org/10.1016/j.paerosci.2017.04.003

Lagüela, S., Martínez, J., Armesto, J., & Arias, P. (2011). Energy efficiency studies through 3D laser scanning and thermographic technologies. Energy and Buildings, 43(6). https://doi.org/10.1016/j.enbuild.2010.12.031

Martinez-Sánchez, J., Arias, P., & Caamaño, J. C. (2016). Close Range Photogrammetry: Fundamentals, Principles and Applications in Structures. Non-Destructive Techniques for the Evaluation of Structures and Infrastructure, 11, 35.

Seo, J., Duque, L., & Wacker, J. P. (2018). Field Application of UAS-Based Bridge Inspection. Transportation Research Record, 2672(12), 72–81. https://doi.org/10.1177/0361198118780825

This project has received funding from the European Union's Horizon 2020 research and innovation programme under grant agreement No 958171.

APPENDIX A3. Optical and visual testing: Boroscopy and Endoscopy

3.1 Goal(s)

3.1.1 Main objective

Optical and visual testing have been widely known in the diagnostics of civil engineer structures, since methods are easily available and do not require large expenditures and effort in application. In literature both methods are assigned mostly in category of non-destructive testing, however sometimes they fall into destructive category, since in some particular cases there is a need of inducing minor damages in case of difficult to reach areas (Mix, 2005).

However, historically, when developed technology and equipment was not existing - usefulness of this methods was highly limited and not accurate. Especially due to high subjectivity and no possibility of recording hardcopy documentation. Final analysis of the inspected damages or structures was highly dependent on the operator., quality of tested object and optical instrument.

Nowadays there are available very advanced optical technologies and as a result borescope's and endoscope's popularity has increased in diagnostics of bridge or tunnels as a routine operational equipment. Currently assessment of the structure behaviour is also affected by the operator, however the quality of imaging is much more developed, which simplifies the task.

Despite its advantages and disadvantages – both boroscopy and endoscopy cannot be used as a sole method of verification and should be coupled with other non-destructive or destructive surveying technologies in order to receive accurate answer on the structural behaviour and state of the infrastructure.

3.2 Description

3.2.1 Functioning mode

Borescopes and endoscopes are devices used to inspect hard-to-reach, dark places. It can be the inside of the profile or the engine compartment, elements of the vehicle suspension or an air conditioning system. They allow the observation of very complex devices without the need to disassemble. In case of civil engineering structures inspection this is also a main advantage of the equipment allowing to test difficult to reach areas with no source of light or at night. Endoscopes/videoscopes are a more advanced types of the borescope that has video and still image recording capabilities. Main components of the borescope and endoscope are objective lens system, relay lens system, eyepiece. The eyepiece determines the magnification. At the end of the tool there are objective lens which works similarly to a camera lens. First image of the object is created at the back of the lens and relay lens reform it along the length of the borescope or endoscope. The last set of lenses produce the final image, which can be seen through the eyepiece. The magnification of the

This project has received funding from the European Union's Horizon 2020 research and innovation programme under grant agreement No 958171. © 2021

lens and eyepiece are determined by the manufacturer and is referred to magnification at a specific distance and mathematically it is a logarithmic function. Modern equipment allows to have a complete video processing system (closed-circuit television) with computerized video enhancement and high-resolution display. Other important elements are – video output terminal (in case of endoscopes), insertion tube, handle, remote control (e.g. brightness/center button, live/gain button, measurement joystick or freeze button) (Mix, 2005) (International Atomic Energy Agency, 2002).

3.2.2 Types

Borescopes:

- rigid/half rigid borescopes – usually in diameter 4 to 19 mm with different types of light sources (UV,VIS,LED); extendable versions available on the market as well – in that case the diameter can vary between 9,5 mm up to 44 mm,
- flexible borescopes – diameter range from 3 mm to 10 mm,
- micro borescopes – usually in diameter of 1 mm to 3,5 mm.
- periscopes – for use in underwater or high/low pressure conditions.

Endoscopes:

- rigid endoscopes
- flexible endoscopes

The parameters are usually similar for borescopes and endoscopes, in both cases there is USB interface and built-in memory of, for instance, 64Mb. The cable of the borescope or endoscope has usually length of 1 m.

Technical specifications, availability and prices of different types of borescopes and endoscopes can be found on the websites of the manufacturers as well with the operational manuals (AXIO MET, 2021) (Olympus, 2021).

3.2.3 Process/event to be detected or monitored

By means of borescopes and endoscopes it is possible to detect and photograph abnormal sections on the structural elements of the bridge or tunnel with cracks or deformations. Moreover it is possible to detect areas affected by different types of corrosion or chemical attack. Typical defects observed on the concrete structures can be found in Guidebook on non-destructive testing of concrete structures (International Atomic Energy Agency, 2002).

3.2.4 Physical quantity to be measured (e.g. actions, displacements, deformations, dynamic structural properties, material properties including mechanical, electrical and chemical properties, relative displacements of the two sides of a crack, etc.).

No physical quantity is directly measured in case of boroscopy or endoscopy, however as stated in section 1.3.3. it is possible to detect visible effects of the degradation processes occurring on structural elements of the bridge or tunnel.

This project has received funding from the European Union's Horizon 2020 research and innovation programme under grant agreement No 958171.

3.2.5 Induced damage to the structure during the measurement

Inspection of concrete often require using a drill hole for inserting the structural inspection endoscope, this method causes minor damage to the structure. Despite this, in most cases, both boroscopy and endoscopy are non-destructive to the structure.

3.2.6 General characteristics

3.2.6.1 Measurement type (static or dynamic, local or global, short-term or continuous, etc.)

Inspection with borescopes and endoscopes is static and performed locally in a short-term conditions.

3.2.6.2 Measurement range

Not applicable.

3.2.6.3 Measurement accuracy

Depends on the magnification of the lens and adjustment of the camera to the inspected element or area.

3.3 Background (evolution through the years)

Borescopes and endoscopes were primarily used in inspection of the pipes and tubing. Lenox Instrument Company, was a pioneer in the development of borescopes for a various applications around the world. First borescope for turbine rotor inspections was found in 1921. Lenox Instrument Company supplied borescopes for inspecting hard to reach, often dark, locations. Applications included power turbines, oil refinery piping, gas mains, soft drink tanks, and many other remote locations. After 1944 Lenox improved its borescope with radiation resistant optics and a swivel-joint eyepiece, which permitted the operator to work from any angle. This newer instrument was also capable of considerable bending to snake through the tubes in the reactor. Lenox supplied a total of three borescopes with radiation resistant optics; they were the first optical instruments to be used in a nuclear environment. (Lenox Instrument Company, 2021) (D. Mężyk, 2016). (Davis, 1998)

Endoscopes have mainly experienced four stages of development, from the initial rigid tube endoscope, semi-flexed endoscope to fiber endoscope, and now electronic endoscope. With the continuous improvement of the endoscope structure, the image quality is also undergoing a qualitative leap. The original endoscope used candle light as the light source. Later, Edison invented the electric light bulb, and the endoscope was changed to the light bulb as the light source. Today's endoscopes mainly use optical fibers or LED lights as light sources. Shenzhen Coantec Technology focuses on the research of endoscopes. It has been carefully thinking about the choice of light source and the improvement of image quality (The Nippon Communications Foundation, 2021). (Mężyk, 2010) (Davis, 1998)

This project has received funding from the European Union's Horizon 2020 research and innovation programme under grant agreement No 958171.

3.4 Performance

3.4.1 General points of attention and requirements

3.4.1.1 Design criteria and requirements for the design of the survey

Before the survey with use of the borescope or the endoscope there should be few issues considered when performing an inspection. In the first place – what kind of defects could be present and in what elements of the bridge or tunnel structure. Secondly – what would be the nature of the defect and if the tested area is reachable by the operator without any risk. Regarding the equipment itself care should be taken while use – LCD monitor should not be subjected to impact, pressure or scratching.

3.4.1.2 Procedures for defining layout of the survey

Details on general rules of the survey with visual testing can be found in norm EN 13018:2016 - Non-destructive testing - Visual testing - General principles. Standard specify the general principles and requirements for direct and remote testing and can be used as a guide, however it applies to the determination of a product with specified requirements, so attention is required, and should not be treated as an only source of information.

3.4.1.3 Design constraints (e.g. related to the measurement principles of the monitoring technologies)

Most important issue that shall be considered is the access to the tested element and if inspection will not induce the risk for operator's safety.

3.4.1.4 Sensibility of measurements to environmental conditions.

Measurement with borescope and endoscope is not influenced by environmental conditions.

3.4.2 Preparation

3.4.2.1 Procedures for calibration, initialisation, and post-installation verification

Adjustment of the equipment should be performed depending on the objective of the inspection. The inspector should be trained and qualified. Details on the equipment adjustment can be found in manufacturers manual (Olympus, 2021) (AXIO MET, 2021)

3.4.2.2 Procedures for estimating the component of measurement uncertainty resulting from calibration of the data acquisition system (calibration uncertainty)

Not applicable.

3.4.2.3 Requirements for data acquisition depending on measured physical quantity (e.g. based on the variation rate)

Not applicable.

3.4.3 Performance

3.4.3.1 Requirements and recommendations for maintenance during operation (in case of continuous maintenance)

Not applicable for continuous maintenance. Details on the equipment use recommendations can be found in manufacturers manuals (Olympus, 2021) (AXIO MET, 2021).

3.4.3.2 Criteria for the successive surveying campaigns for updating the sensors. The campaigns include: (i) Georeferenced frame, i.e. the global location on the bridge; (ii) Alignment of sensor data, relative alignment of the data collected in a surveying; (iii) Multi-temporal registration to previous campaigns; and (iv) Diagnostics.

Not applicable.

3.4.4 Reporting

Report should include:

- identification of the equipment used,

This project has received funding from the European Union's Horizon 2020 research and innovation programme under grant agreement No 958171. © 2021

- inspected area, element,
- scope of research,
- date of survey,
- photos and/or videos adequately labelled and described with date/hour/description of the place of inspection and surrounding conditions.

3.4.5 Lifespan of the technology (if applied for continuous monitoring)

Boroscopy and endoscopy are not used in continuous monitoring.

3.5 Interpretation and validation of results

3.5.1 Expected output (Format, e.g. numbers in a .txt file)

Photos and videos collected on the memory card as jpg files etc.

3.5.2 Interpretation (e.g. each number of the file symbolizes the acceleration of a degree of freedom in the bridge)

Visual evaluation based on the photos and videos recorded.

3.5.3 Validation

3.5.3.1 Specific methods used for validation of results depending on the technique

No specific guidelines available.

3.5.3.2 Quantification of the error

Not applicable.

3.5.3.3 Quantitative or qualitative evaluation

Boroscopy and endoscopy are used in qualitative evaluation.

3.5.4 Detection accuracy

Primarily depends on the resolution of camera and experience of the operator.

3.6 Advantages

- Recording directly on the memory card.
- Small diameter of the camera to pass through the tiniest holes.
- Various photo resolution settings and low cost.
- The durability guaranteed by stainless steel construction of the device.

3.7 Disadvantages

Experience of the operator required to properly understand observed issues.

3.8 Possibility of automatising the measurements

Live video inspections can now be viewed in real time from a computer, tablet or smartphone across the room or around the world.

This project has received funding from the European Union's Horizon 2020 research and innovation programme under grant agreement No 958171. © 2021

3.9 Barriers

The main barrier in the survey includes the access to the tested areas for the operator, which can be limited.

3.10 Existing standards

EN 13018:2016 - Non-destructive testing - Visual testing - General principles.

ACI 201.1R, ACI 207.3R, ACI 224.1R, ACI 362R.

3.11 Applicability

3.11.1 Relevant knowledge fields

- Construction diagnostics,
- Construction appraisal,
- Design studies of facilities subjected to dynamic loads,
- Technical expertise regarding assessment of impact of vibrations on buildings,
- Analysis of the reliability of shell structures.

3.11.2 Performance Indicators

Relate the surveying technology being studied with PIs from WP3, provided in the document of the TU1406 COST ACTION.

- cracks,
- holes,
- deformation,
- obstruction/impeding,
- rupture.

3.11.3 Type of structure

- bridges,
- tunnels,
- walls,
- buildings,
- viaducts,
- marine hydrotechnical structures,
- lining of tunnels and mining shafts,
- foundations.

3.11.4 Spatial scales addressed (whole structure vs specific asset elements)

Boroscopy and Endoscopy can be used to inspect specific elements of bridges or tunnels which are primarily subjected to corrosion risk and mechanical damages and accessible for the operator.

This project has received funding from the European Union's Horizon 2020 research and innovation programme under grant agreement No 958171.

3.11.5 Materials

- concrete,
- steel,
- composites,
- polymers,
- ceramics.

3.12 Available knowledge

3.12.1 Reference projects

No reference projects.

3.12.2 Other

Examples of application of borescopes and endoscopes in real case studies:

- Assessment of the technical condition of selected buildings on the premises of PGE GiEK S.A. Turów Power Plant Branch, Poland; (PGE, 2021)
- Assessment of the technical condition along with material tests of the structural elements of the Electrolytic Baths Hall on the area of KGHM Polska Miedź S.A., Poland;
- Technical expertise of the steel supporting structure of the hall with a cubature in Łazy, Poland.

Borescope Inspection Training and Certification

3.13 Bibliography

AXIO MET. (2021, 12 10). *Borescopes — inspection in harsh conditions.* Retrieved from AXIO MET Instruments with a digital Soul: https://axiomet.eu/pl/en/page/1127/borescopes-inspection-in-harsh-conditions-en/

D. Mężyk, P. S. (2016). Wprowadzenie do zaawansowanych technik pomiarowych 3D stosowanych w wideoboroskopowych zdalnych badaniach wizualnych. *Przegląd Spawalnictwa - Welding Technology Review vol 88 No 10*.

Davis, A. (1998). *Nondestructive Test Methods for Evaluation of Concrete in Structures/ACI 228.2R-98.* American Concrete Institute.

International Atomic Energy Agency. (2002). *Guidebook on non-destructive testing of concrete structures. Training Course No.17.* Vienna: IAEA.

Lenox Instrument Company. (2021, 12 11). *History of borescopes*. Retrieved from Lenox Instruments: https://www.lenoxinst.com/About_History_2_Borescopes.html

Mężyk, D. (2010, 3). Zastosowanie endoskopii przemysłowej w procesie badań wizualnych jako metody diagnostyki obiektów przemysłowych. *Dozór Techniczny*.

Mix, P. E. (2005). *Introduction to Nondestructive Testing - A Training Guide* . New Jersey: John Wiley & Sons,Inc. .

Olympus. (2021, 12 10). *Olympus Instructions - Industrial Endoscope*. Retrieved from Olympus Support Downloads : https://www.olympus-ims.com/en/.downloads/download/?file=285218824&fl=en_US&inline

This project has received funding from the European Union's Horizon 2020 research and innovation programme under grant agreement No 958171.

PGE. (2021, 12 10). *PGE Polska Grupa Energetyczna SA*. Retrieved from https://elturow.pgegiek.pl/strona-glowna

The Nippon Communications Foundation. (2021, 12 10). *Olympus Endoscopes: The Inside Story*. Retrieved from https://www.nippon.com/en/features/c00513/

This project has received funding from the European Union's Horizon 2020 research and innovation programme under grant agreement No 958171.

APPENDIX A4. Fibre Optic Sensors (FOS)

4.1 Goal(s)

4.1.1 Main objective

One of the relatively new technologies that have found many applications in different industries, including civil engineering, is the sensing with use of fibre optics. It is quite a new tool for the assessment of the structural integrity or performance of civil structures such as bridges or tunnels in comparison with the techniques present in European Union standards. However with a great perspective in long-term monitoring and remote control of the condition of facilities. FOS technology allows to measure the bridge/tunnel performance under traffic loads and store the information globally with expanding modern data storage solutions. At the moment it is still not widely used as a diagnostic tool across the European Union for maintenance of the existing civil structures (A. Grosso, 2001).

It is worth mentioning that FOS can be also useful in situations, where there is a need for control of the surrounding civil engineering structures in the vicinity of the construction site. In such a case it is possible to control the impact of the construction works/vibrations on the existing civil structures and therefore prevent serious accidents (Rafał Sieńko, 2016).

4.2 Description

4.2.1 Functioning mode

The light source (an LED) transmits the light beam down the fibre optic cable by repeatedly reflecting the light off the boundary between the fibre core and its sheath. When it reaches the end of the fibre the light is dispersed at the end. When the light is dispersed it spreads out and forms a beam much like that of other sensors.

The first element that must be considered in the system for FOS monitoring is the optical fibre used as sensor adjusted to be sensitive to their state and environment. Standard optic fibre is made of silica and can transmit light with very high efficiency over long distances. Considered technology used with fibre optics there are following functioning modes:

- Fabry-Perot Interferometers – point sensors, a single measurement point at the end of the fibre optic connection cable, similarly to most electrical sensors;
- Low-Coherence Interferometers – long base sensors, sensors integrate the measurement over a long measurement base, known as long-gage sensors;
- Fibre Bragg Grating sensors – quasi distributed sensors, microstructure of Bragg Grating causes periodic changes in the refractive index of the laser beam. As light travels along the fibre, the Bragg grating reflects a very narrow range of wavelengths. All other wavelengths pass through the mesh. The centre of the band of reflected wavelengths is known as the Bragg wavelength. Due to the deformation of the structure, the wavelength is modified due to the

This project has received funding from the European Union's Horizon 2020 research and innovation programme under grant agreement No 958171.

physical stretching or compression of the optical fibre. This change causes a wavelength shift which is then detected and recorded by the interrogator or optical data acquisition system.

- Distributed Raman/Brillouin Scattering sensors – sensing at any point along a single fibre line, typically every meter over many kilometres of length (Samuel Vurpillot, 1996) (Jose Luis Santos, 2015) (Romaniuk, 2001).

The physical quantity measured by optic fibre is changed into modulation of the light wave. In general, the studied physical quantities can influence the light wave in a different way – externally in the measurement chamber or directly, internally through the fibre optic structure. Depending on the type of modulation of the light wave parameter there are different categories of the sensors such as:

- sensors with wave intensity modulation,
- sensors with wavelength modulation – with Bragg grating to measure temperature changes, deformation, acceleration, inclination,
- sensors with light wave phase modulation – interferometers and fibre optic gyroscopes
- sensors with wave polarization modulation

Details on the mechanisms for the selected functioning mode can be found in (Glisic, 2000) (H.Hartog, 2017) (Udd, 2006) (Measures, 2001) (David Krohn, 2014) (Alexis Mendez, 2012).

4.2.2 Types

The fibre optics are small and can be mounted in places where other sensors could not fit. Fibre optic sensor heads can be used in areas that standard sensors are unable to operate, for instance hazardous areas. This is because no electric current flows through them. This also means they are totally unaffected by electrical noise (provided the amplifier is suitably positioned). By using glass fibres instead of plastic they can be used in areas of up to 350°C.

There are different classifications of the sensoring technology with fibre optic sensors. It is worth to start with types of heads of the sensors available on the market:

- standard cylindrical shape
- square shape
- miniature shape
- long distance shape

Taking into account number of fibres used can be divided into:

- Single-mode optical fibres, which are used especially in telecommunication, in this case, the diameter is typically from 5 to 10 µm, depending on the light wavelength that is designed for (Measures, 2001)
- Multi-mode optical fibres, which are used mostly in the medical field, and the diameter core up above 100 µm (Measures, 2001)

This project has received funding from the European Union's Horizon 2020 research and innovation programme under grant agreement No 958171.

Due to mounting location of the optic fibres:

- Intrinsic sensors
- Extrinsic sensors

In civil engineering structures monitoring there are used single-mode extrinsic sensors for measurements of relative displacement, deformation, pressure, stress load.

4.2.3 Process/event to be detected or monitored

Due to the deformation of the structure, the wavelength is modified because of physical stretching or compression of the optical fibre. This change causes a wavelength shift which is then detected and recorded by the interrogator or optical data acquisition system.

Inspection of stresses and deformation inside a reinforced concrete structure. Strain and crack analysis – distribution of the measured quantity along a given line.

4.2.4 Physical quantity to be measured (e.g. actions, displacements, deformations, dynamic structural properties, material properties including mechanical, electrical and chemical properties, relative displacements of the two sides of a crack, etc.).

- Depending on the application and used type of optical fibre sensor it is possible to measure: Strain
- Deformation
- Temperature
- Vibration
- Pressure
- Acceleration
- Inclination

4.2.5 Induced damage to the structure during the measurement

No damage induced to the structure. For bridge monitoring sensors are mounted on the surfaces without interference in the structure integrity.

4.2.6 General characteristics

4.2.6.1 Measurement type (static or dynamic, local or global, short-term or continuous, etc.)

Depending on the technology used there is possibility to measure selected parameters dynamically in local variations or globally for the whole structures if proper sensors arrangement is implemented. Depending on the type of the sensoring technology there are different possibilities:

- for Fabry Perot Interferometers (FISO) – local measurements of temperature, strain or displacement in long-term adjustment,

This project has received funding from the European Union's Horizon 2020 research and innovation programme under grant agreement No 958171.

- for Low-Coherence Interferometers (SOFO) – global and continuous measurements of the concrete and geotechnical structures, also working as references,
- for Fibre Bragg Grating Sensors (FBG) – geometrically continuous measurements in long-term adjustment,
- for Distributed Raman Scattering Sensors – local average temperature for fibre lengths up to ten of kilometres – detection of hold/cold points, leaks etc.
- for Distributed Brillouin Scattering Sensors – possibility to measure distributed strain in contrary to Raman Scattering sensors and therefore detection of cracks, movements, deformations, settlements

4.2.6.2 Measurement range

Measurement path of deformation for each sensor can be varying from 1 to 2 m path.

On the market there are available various types of fibre optic sensors heads and amplifiers. As an example below are presented some measurement ranges for different sensors given by the producers and available on their websites (KEYENCE, 2021) (NERVE-SENSORS, 2021):

- displacement sensor for monitoring applications (HBM), suitable for bridge piles, sustaining walls and whole buildings) has a following specification: measurement range +/- 40 mm, resolution of 20 µm,
- static and dynamic strain sensor for structural health monitoring applications (HBM), with range of strain measured between +/- 2500, +/- 5000 +/- 20000 µm/m, resistant to temperature up to 100°C,
- temperature sensor (HBM), (e.g. weldable for metallic structures, for laboratory use etc.) with measurement range between -20°C to 80°C, with aramid cables for difficult environments,
- fibre optic piezometer for pressure measurement (Roctest) with range from 200 to 7000 kPa and resolution up to 0,0025%.
- fibre optic strain sensors (NERVE-SENSOR) – for strain and crack measurements – strain measurement range - 4% and resolution up to 1,0 µe.

4.2.6.3 Measurement accuracy

Details with different technical specifications of the fibre optic sensors can be found in product brochures of manufacturers. As an example:

- For displacement sensors, depending on the producer measurement accuracy is on the level of 0,1% and resolution of 0,002 mm (Roctest)

This project has received funding from the European Union's Horizon 2020 research and innovation programme under grant agreement No 958171. © 2021

- For temperature sensors as well accuracy vary on the producer, typically on the level of 0,1 °C (Roctest)
- For piezometric sensors Roctest) accuracy is usually on the level 0,1% with resolution 0,025%.

4.3 Background (evolution through the years)

Fibre Optic Sensoring technology would not exist without the finding and description of the phenomenon of propagation of the light in water in 1870 made by John Tyndall (Łukasz Bednarski, 2015). In ten years from that discovery there was a patent released by William Wheeling, where fibre optics supposed to be used as a source of light inside the buildings, however did not replace the Edison bulb for economic reasons. High development of the technology has started after 1950s, since a lot of new scientific papers has been released at that time, describing the phenomena in details. For the first time the concept called optic fibre cable has been used by Brian O'Brien and Narinder Kapany, however their research was focused on the application of optic fibres in endoscopy for human body investigation (Measures, 2001). In the beginning the technology were designed mostly for very simple types of sensors such as card readers for computers and then rapidly developed (David Krohn, 2014).

Further development of the fibre optic sensors focused on different types of measurements and by now the technology is quite universal for various detections – strains, structural deformations, vibration, pressure, temperature, frequencies (Measures, 2001) (Łukasz Bednarski, 2015).

The first optical fibres had attenuation at the level up to 100 dB/km. Recent optical fibres have a high purity of glass material and their attenuation is very low at the level under 0.2 dB/km.

In past decades various devices, including fibre optic gyroscopes; sensors of temperature, pressure and vibration have been under the development of FOS technology. (H.Hartog, 2017).

4.4 Performance

4.4.1 General points of attention and requirements

4.4.1.1 Design criteria and requirements for the design of the survey

Used optic fibres should be dedicated for the measurements on long measuring distances in difficult operating conditions. In places where sensors will be mounted it is necessary to remove the paint covers and to clean the surface. After placement of sensors – epoxy paint is applied for safety.

4.4.1.2 Procedures for defining layout of the survey

There are no uniform guidelines specifying the layout of the survey for fibre optic sensors methodology, however there are few issues that have to be considered:

Design of the survey should be preceded by following considerations:

- determination of the measured quantities,

This project has received funding from the European Union's Horizon 2020 research and innovation programme under grant agreement No 958171.

- localization of the measurement points, arrangement of the sensors,
- frequency of the measurement (depending on the technology),
- limit levels for the measured physical quantities, the exceeding of which requires a decision making process,
- choice of the technique – types of sensors, installation method,
- desired accuracy,
- data analysis methods to be included and theoretical models if necessary.

4.4.1.3 Design constraints (e.g. related to the measurement principles of the monitoring technologies)

For different applications with use of fibre optic sensors special attention is required: in outdoor use, potential chemical contamination and environmental conditions that will be having major influence on the system performance during service life. In applications of fibre optic sensors such as nuclear energy control systems, railroad systems, aviation systems there should be taken into account safety and/or government regulations additionally. The risk should be assessed before implementation of the system in order to avoid any serious injuries and accidents.

Regarding the sensor itself and arrangement of the arrays in real cases, clearly varying on the producer specification, there are few key points that should be considered when mounting the monitoring system, such as:

- amplifier cable should be separated from power lines and high voltage lines – otherwise if they are placed in the same conduit, detection error will occur from the noise interference or the sensors will be damaged
- sensitivity setting may fluctuate and units can heat up if incorrectly wired
- direct lightening should be avoided
- sensors should not be used in atmosphere where inflammable gas, powder, liquid is present since they are not explosion-proof
- when several units are connected the ambient temperature should be confirmed; depending on the number of units the range is different for instance in case of 3-10 units it is as follows: -10°C – +50°C, while for more than 10 units - -10°C – +45°C (KEYENCE, 2021)

4.4.1.4 Sensibility of measurements to environmental conditions

Fibre Optic Sensors are insensitive to humidity, corrosion, vibration and electromagnetic fields. Variation on the data graph during the measurement can result from thermal elongation of the bridge,

This project has received funding from the European Union's Horizon 2020 research and innovation programme under grant agreement No 958171.

change of the temperature and drying shrinkage. However those influences are controlled by the monitoring systems (D. Inaudi, 1999).

4.4.2 Preparation

4.4.2.1 Procedures for calibration, initialisation, and post-installation verification

Depending on the manufacturer there can be some modifications to the calibration process and initialisation setup, which also depends on the software utilized. Due to this variations in this section there will be described briefly some examples of the sensitivity calibration procedures given by the manufacturer (KEYENCE, 2021) on its website:

- 2 – point calibration – setting value established by pressing the set button on the amplifier when the object to detect is present and once when I absent. The setting value is set to the middle of the values between both of this measurements,
- Maximum sensitivity calibration - method suitable when the received light intensity is expected to be reduced by dirt, the setting value is set slightly higher than the received light intensity when the setting was executed,
- Full Auto Calibration – the sensitivity is set automatically using a moving object. The setting value is determined as the middle value between the maximum and minimum received light intensity received while holding down the set button,
- Positioning Calibration – used when precise position detection is needed and in this case center of the projecting beams must align with the center of the object.

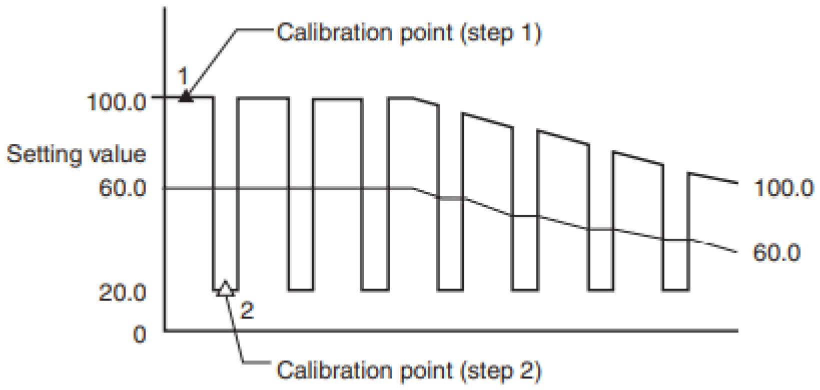

Figure 4.1 – Sensitivity Calibration

4.4.2.2 Procedures for estimating the component of measurement uncertainty resulting from calibration of the data acquisition system (calibration uncertainty)

Calibration and measurement themselves introduce a certain amount of variability and randomness that can affect the conclusions drawn. This randomness in measured variables can be quantified by their probability density functions. In order to find the density function of continuously measured data, the so-called evaluation strategy (or genetic algorithms) may be applied (A. Grosso, 2001)

This project has received funding from the European Union's Horizon 2020 research and innovation programme under grant agreement No 958171.

4.4.2.3 Requirements for data acquisition depending on measured physical quantity (e.g. based on the variation rate)

No specific guidelines available.

4.4.3 Performance

4.4.3.1 Requirements and recommendations for maintenance during operation (in case of continuous maintenance)

During the service life of the monitoring system, except the regular control of the operational parameters and registered signals, generally performance diagnostics there are some remarks, usually given by the producer on how to prolong the service life minimizing the risk of failures:

- stray light should be avoided, which makes the sensor works incorrectly and the sensitivity will be influenced, basically this should be considered as well when deciding on the types of sensors selected in the first place,
- any dirt, dust should be repeatedly removed from the surface of the sensor since the sensitivity will be as well changed due to its presence, however for some types of the sensors there are mechanisms which automatically correct the sensitivity and maintain at fixed ratio when sensor detecting surface has become dirty,
- workpiece colour variation should be avoided, since this changes influence the ability to obtain the expected light intensity – sensitivity should be adjusted that the output is on the presence of the colour with the lowest reflectance,
- regular calibration should be performed.

4.4.4 Reporting

Reporting and visualization of the data is done automatically in the software given by the producer. Depending on the manufacturers the layout can be different and adjusted for specific purpose. Always there are present information such as date and hour, localization of the measurement points on the bridge for example, recorded values and statistical analysis. However, the final output depends on the settings of the end user.

4.4.5 Lifespan of the technology (if applied for continuous monitoring)

The lifespan of the systems with sensors is characterized as the minimum length of time over which the sensor will operate, either continuously or over a number of cycles without changing performance characteristics beyond specified tolerances. The continuous measurement system with fibre optic sensors has a high durability - over 30 years. For telecommunication applications for instance the service life of the fibre optic is greater than 20 years without any failure. It is important to know that environment can greatly influence the expected service life of the optic fibres, especially when the coating is damaged and the fibres are subjected to moisture. Inspection of the coating has to be carried out in different intervals especially in the places where there are various and changing climatic

This project has received funding from the European Union's Horizon 2020 research and innovation programme under grant agreement No 958171.

conditions to ensure their performance for long period of time. Also stress load applied to the fibres during their service life is highly influencing the lifespan of the technology itself. (Measures, 2001). (Fidanboylu, 2009) (Samuel Vurpillot, 1996).

4.5 Interpretation and validation of results

4.5.1 Expected output (Format, e.g. numbers in a .txt file)

Raw data registered in the software depending on the measured physical quantities defined by the operator/end user (for example temperatures/frequencies measured in different channels), which can be exported to csv/Excel file:

A	B	C	D	E	F	G	H	I	J	K	L
id	R2_CH001_f	R2_CH001_T	R2_CH002_f	R2_CH002_T	R2_CH003_f	R2_CH003_T	R2_CH004_f	ł2_CH004_	date	device_id	notes_num
29246	1918.4410	-3.6260	2112.9010	-3.6750	1853.9090	-3.7310	2027.8460	-3.6820	2021-12-07 12:45	246	0
29247	1916.0840	-3.6630	2116.2600	-3.7170	1848.0440	-3.7810	2029.2770	-3.7240	2021-12-07 13:00	246	0
29248	1914.6340	-3.6740	2119.6350	-3.7340	1842.4940	-3.7670	2034.0880	-3.7200	2021-12-07 13:15	246	0
29249	1918.5750	-3.6710	2111.7340	-3.7370	1852.9840	-3.7740	2030.8170	-3.7300	2021-12-07 13:30	246	0
29258	1914.6420	-3.6440	2117.5690	-3.7080	1850.0820	-3.7440	2028.0950	-3.6980	2021-12-07 13:45	246	0
29259	1910.5460	-3.7800	2127.0680	-3.8450	1854.4480	-3.9070	2021.9180	-3.8310	2021-12-07 14:00	246	0
29260	1917.2910	-3.6800	2114.7150	-3.7600	1850.2620	-3.7790	2030.2370	-3.7320	2021-12-07 14:15	246	0
29261	1917.7310	-3.8030	2115.4910	-3.8720	1851.5090	-3.9250	2029.3950	-3.8770	2021-12-07 14:30	246	0
29262	1914.4860	-3.7170	2116.5890	-3.7930	1848.5810	-3.8330	2029.1840	-3.7730	2021-12-07 14:45	246	0
29263	1916.8860	-3.7310	2115.6930	-3.7990	1846.7460	-3.8310	2030.9050	-3.7920	2021-12-07 15:00	246	0
29264	1914.8980	-3.7820	2125.1950	-3.8750	1832.2980	-3.9110	2036.2150	-3.8640	2021-12-07 15:15	246	0
29265	1917.5210	-3.8940	2115.5680	-3.9750	1848.8330	-4.0170	2030.0940	-3.9550	2021-12-07 15:30	246	0
29266	1915.6850	-4.0040	2118.0370	-4.0640	1846.4220	-4.1390	2031.2530	-4.0420	2021-12-07 15:45	246	0
29267	1918.4920	-4.0320	2115.3950	-4.0990	1848.1720	-4.1750	2031.0650	-4.0920	2021-12-07 16:00	246	0
29268	1915.8930	-4.1540	2115.7380	-4.2340	1846.7800	-4.2900	2030.3250	-4.2180	2021-12-07 16:15	246	0
29269	1916.4710	-4.0760	2115.2350	-4.1660	1851.3230	-4.1810	2029.0940	-4.1120	2021-12-07 16:30	246	0
29270	1917.0020	-4.0200	2115.5240	-4.0770	1850.2310	-4.1190	2030.3970	-4.0710	2021-12-07 16:45	246	0
29271	1916.2170	-4.2730	2116.1670	-4.3450	1848.2880	-4.4100	2029.1340	-4.3120	2021-12-07 17:00	246	0
29272	1917.0660	-4.2980	2113.3200	-4.3670	1856.7980	-4.4200	2023.4660	-4.3160	2021-12-07 17:15	246	0
29273	1917.3090	-4.3440	2116.1520	-4.4340	1847.7440	-4.4790	2031.0670	-4.4270	2021-12-07 17:30	246	0
29274	1909.8440	-4.5210	2126.6140	-4.6550	1837.0090	-4.6650	2026.6530	-4.6090	2021-12-07 17:45	246	0
29275	1916.8500	-4.6100	2116.9680	-4.6970	1848.5700	-4.7240	2030.4280	-4.6640	2021-12-07 18:00	246	0
29276	1914.2340	-4.6190	2119.8650	-4.7240	1842.8390	-4.7590	2033.6540	-4.6940	2021-12-07 18:15	246	0
29277	1916.3290	-4.5520	2117.0970	-4.6360	1847.1820	-4.6670	2030.9200	-4.6090	2021-12-07 18:30	246	0
29278	1915.5770	-4.6690	2119.2230	-4.7370	1845.6880	-4.7800	2030.9090	-4.6990	2021-12-07 18:45	246	0
29279	1908.2150	-4.6760	2126.3610	-4.7490	1852.4920	-4.8040	2022.7060	-4.7220	2021-12-07 19:00	246	0

Figure 4.2 – Exported table with raw data after one day cycle of measurement on the bridge

4.5.2 Interpretation (e.g. each number of the file symbolizes the acceleration of a degree of freedom in the bridge)

As a result of deformation, the length of the optical fibre changes, and thus the distance between local defects of the structure changes. The appearance of the dissipation profile before and after mechanical stress are compared with each other. On this basis, the distribution of mechanical deformations is determined.

Raw data are cleaned and processed automatically in the software and there are presented statistic/graphs/ abnormal signal information about the measured quantities, depending on the settings of the user. For example – when deformation and temperature on the bridge is registered in real-time, after automatic data analysis, there can be presented graphical dependence of the deformation in με and temperature in °C in time for different measurement locations on the bridge, as below:

This project has received funding from the European Union's Horizon 2020 research and innovation programme under grant agreement No 958171.

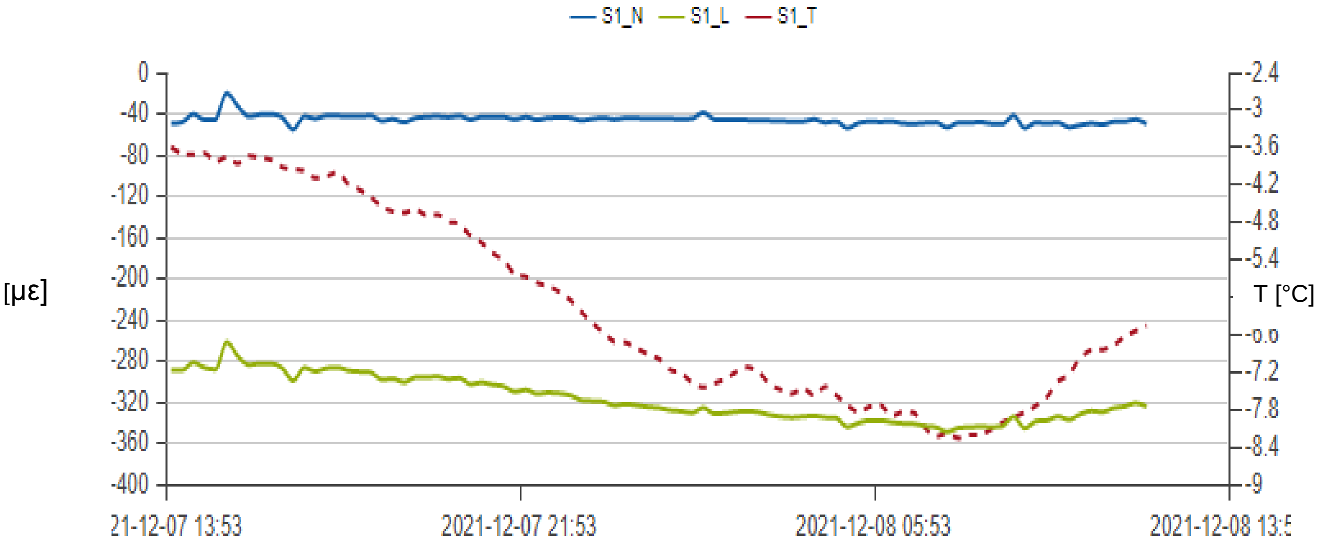

Figure 4.3

Figure 4.4 – Processed data at one measurement point on the South part of the investigated bridge

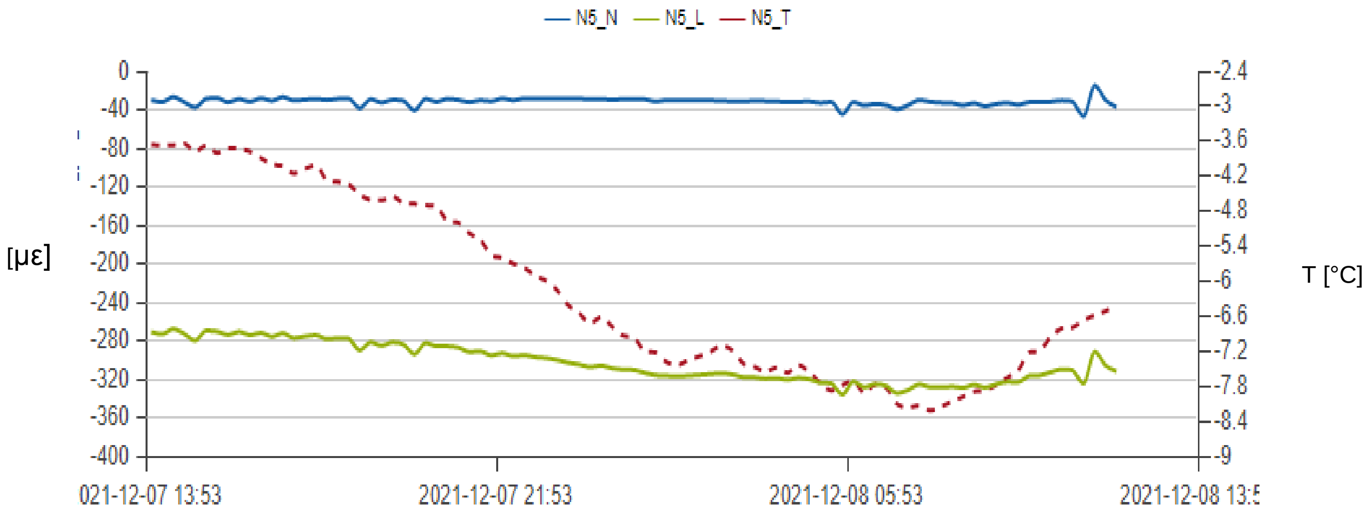

Figure 4.5 – Processed data at one measurement point on the North part of investigated bridge

4.5.3 Validation

4.5.3.1 Specific methods used for validation of results depending on the technique

The methods for validation can be varying depending on the theoretical model assumptions. Typically to verify and assess the effectiveness of the monitoring system it is necessary to compare the measured data with calculated data. For this case Finite Element Model of the monitored structure based on a linear or non-linear approach. However it is only an example, there are different numerical methods that can be used, model should be adjusted for the purpose or theoretical background (Andrea del Grosso, 2001) (Mei, 2018).

This project has received funding from the European Union's Horizon 2020 research and innovation programme under grant agreement No 958171.

4.5.3.2 Quantification of the error

Error quantification methodology should be given by the producer of monitoring system of the software for measured data. Usually the software enable to automatically perform the error calculation and statistical analysis within ensemble of data. (Mei, 2018)

4.5.3.3 Quantitative or qualitative evaluation

With use of different types of fibre optic sensors technologies it is possible to perform both quantitative and qualitative evaluation.

4.5.4 Detection accuracy

Examples of the accuracy of the fibre optic sensors available on the market:

- Sensors for detection of the non-conductive liquids – fluid level can be detected accurately up to 1 mm (BAUMER, 2021),
- Sensors for temperature measurements – detection between -50°C to 100°C and resolution 0,02 to 0,05°C of range,
- Sensors for pressure measurements – detection in range 10, 20, 100 bar, maximum pressure – 150% of range and resolution 0,001 to 0,002% of range. Sensitivity: 450 up to 3000 pm/ZP (SmartFibres),
- Sensors for strain measurements – µstrain range - ±9, sensitivity pm/µstrain -1,2, resolution 0,4 (EC Test System),
- Sensors for vibration measurements – bandwith 0- 1000 Hz or 0-350 Hz (SmartFibres),
- Sensors for deformations measurements –-1,5% for compressing to +1,5% for stretching of measurement range DiTeSt SMARTube).
- Sensors for displacement measurements -

4.6 Advantages

- Possibility of continuous measurement along the length of the monofilament, and therefore also along the length of the structural element to which the fibre has been attached;
- Allows replacement of plenty of traditional sensors with one single optical fibre;
- Longer lifetime compared to conventional resistance strain sensors;
- Long-term signal stability under unfavorable conditions;
- Possibility of placing several sensors on the same fibre;
- Resistance to interference;

This project has received funding from the European Union's Horizon 2020 research and innovation programme under grant agreement No 958171.

- Cost of the measurement system is relatively low, easy to install, highly sensitive, compact in size.

4.7 Disadvantages

Optical fibres are fragile and prone to damage during use. Care should be taken while use.

4.8 Possibility of automatiing the measurements

Remote server includes the software for data analysis, results presentation and automatic alerting. Manufacturers offer sensors compatible with different open networks for advanced traceability, and maintenance. Different networks are available EtherNet/IPtm , DeviceNet, PROFIBUS, EtherCAT, CC-Link. Advanced visualisation and analysis can be performed with real-time data transferred over IO-link. (KEYENCE, 2021).

Actual developments on FOS systems consist of use of new materials to produce fibre optic sensors, such as hybrid sol-gel materials and development to simultaneously monitor moisture, pH, chloride ions, alkali-silica reactions in concrete (R. B. Figuera, 2021) (T. H. Nguyen, 2014).

4.9 Barriers

Technical problems such as adhesion between the measuring fibre and the surrounding medium. Problems with installation of thin optical fibres into the analysed medium.

4.10 Existing standards

EN IEC 61757-1-1:2020-12 - FIBRE OPTIC SENSORS - PART 1-1: STRAIN MEASUREMENT - STRAIN SENSORS BASED ON FIBRE BRAGG GRATINGS

4.11 Applicability

4.11.1 Relevant knowledge fields

Civil engineering:

- smart structures, where sensors are used to detect vibration, temperature, and stress, detection of anomalies of electromagnetic fields in power distribution systems, leak detection, temperature and stress monitors, gripping mechanisms, and other applications in industrial manipulators and mobile robots, multi-point measurement systems of one quantity and measurement systems of several quantities at different measurement points.

Energetics:

- wind turbines, pipelines, nuclear reactors, generators inspection

Marine Transportation:

- cabins, decks inspection

Aviation:

This project has received funding from the European Union's Horizon 2020 research and innovation programme under grant agreement No 958171. © 2021

- composite structures
- wind tunnels

Internal Security:

- security gate monitoring.

Other applications can be found in - (Udd, 2006) (David Krohn, 2014) (Fidanboylu, 2009).

4.11.2 Performance Indicators

Relate the surveying technology being studied with PIs from WP3, provided in the document of the TU1406 COST ACTION.

- cracks
- rupture
- holes
- wire break
- loss of section
- displacement
- deformation
- obstruction/impeding
- stirrup rupture
- deteriorated mortar joints
- tensioning force deficiency
- delamination
- debonding

4.11.3 Type of structure

- bridges,
- tunnels.

4.11.4 Spatial scales addressed (whole structure vs specific asset elements)

Suitable for specific elements such as cross brace on the bridge or whole reinforced concrete structures.

4.11.5 Materials

- concrete,

This project has received funding from the European Union's Horizon 2020 research and innovation programme under grant agreement No 958171.

- reinforced concrete,
- composites,
- steel,
- wood.

4.12 Available knowledge

4.12.1 Reference projects

- SUSTAINABLE BRIDGES – Assessment for future traffic demands and longer lives.
- Com-Bridge" (program DEMONSTRATOR+)
- ISTIMES – Integrated System Transport Infrastructure surveillance and Monitoring by Electromagnetic Sensing, WP4: Sensing Technology.

4.12.2 Other

Examples of the application of monitoring systems with the use of fibre optic sensors:

- Design of diaphragm walls made of fibreglass concrete, Poland (SHM SYSTEMS, 2021),
- Laboratorial intelligent bridge system made of polymer composites (OptiDeck project), Poland (Narodowe Centurm Badań i Rozwoju, Politechnika Rzeszowska, , 2021),
- Monitoring of a bridge over the Vistula in Puławy, Poland (J. Biliszczuk, 2009)
- Monitoring of a composite bridge in Nowa Wieś near Rzeszów, Poland (SHM SYSTEMS, 2021),
- Monitoring of the two composite bridges located along public roads in Podkarpacie constructed within project "Com-Bridge" (program DEMONSTRATOR+),
- Monitoring of a composite footbridge in Nowy Sącz, Poland (SHM SYSTEMS, 2021),
- Monitoring of the Rędziński bridge in Wrocław, Poland (W. Barcik, 2012),
- Monitoring of a pedestrian bridge over the river Malý Dunaj in Bratislava, Slovakia,
- Steel bridges monitoring: "Przemyska Gate" in Przemyśl and Tadeusz Mazowiecki bridge in Rzeszów, Poland,
- Measurements on the concrete road bridges in Naples and Potenza, in Italy,
- Monitoring in the Venoge bridge with sensors covered with polyimide coated fibres,

Manufacturers websites:

- EC Test Systems
- Omron Electronics
- Roctest
- HBM FibreSensing
- SHM Systems

This project has received funding from the European Union's Horizon 2020 research and innovation programme under grant agreement No 958171. © 2021

- LiComm – amplifiers, analog optical transceivers
- MicronOptics
- NPPhotonics

4.13 Bibliography

SMARTEC SA Branko Glisic, Daniele Inaudi. (2007). *Sensing tape for easy integration of optical fiber sensors in composite structures.* Manno, Switzerland : SMARTEC SA.

A. Grosso, D. I. (2001, January). Monitoring of bridges and concrete structures with Fibre Optic Sensors in Europe. *IABSE Symposium, Seoul 2001: Cable-Supported Bridges - Challenging Technical Limits*.

Alexis Mendez, T. G. (2012). Overview of fiber optic sensors for NDT applications. *IV NDT Panamerican Conference Buenos Aires.* Buenos Aires. Retrieved from https://www.researchgate.net/publication/228340034_Overview_of_fiber_optic_sensors_for_NDT_applications

Andrea Del Groso, K. B. (2001). *IABSE Symposium Report: Monitoring of bridges and concrete structures with Fibre optic sensors in Europe.* International Association for Bridge and Structural Engineering.

Andrea del Grosso, K. B. (2001). *Monitoring of Bridges and Concrete Structures with Fibre Optic Sensors in Europe.* IABSE Symposium Report .

BAUMER. (2021, 12 10). *BAUMER* . Retrieved from Passion for sensors : https://www.baumer.com/medias/__secure__/Baumer_Fiber-optic-sensors-to-detect-liquid-levels-and-leakage-of-fluids_EN_0610_AR.pdf?mediaPK=8837757272094

D. Inaudi, S. V. (1999, February 12-13). SOFO: Structural Monitoring with Fiber Optic Sensors . *FIB, Monitoring and Safety Evaluation of Existing Concrete Structures*.

David Krohn, T. M. (2014). *Fiber Optic Sensors Fundamentals and Applications* . Washington: SPIE PRESS .

Fidanboylu, K. E. (2009). Fiber Optic Sensors and their applications. *5th Intenrational Advanced Technologies Symposium* . Karabuk: Fauniversity .

Glisic, B. (2000). Fibre optic sensors and behaviour in concrete at early age . *PhD thesis*. Switzerland: Laboratory of Stress Analysis (IMAC) Swiss Federal Institute of Technology .

H.Hartog, A. (2017). An Introduction to Distributed Optical Fibre Sensors. In A. H.Hartog, *An Introduction to Distributed Optical Fibre Sensors* (pp. 115-128). Boca Raton, United States: CRC Press Taylor & Francis Group.

Instytut Maszyn Przepływowych im. Roberta Szewalskiego PAN. (2011, March). Specyfikacja Istotnych warunków zamówienia (SIWZ). *Dostawa czujników światłowodowych i przetworników* . Gdańsk , Polska .

J. Biliszczuk, W. B. (2009). System monitorowania mostu w Puławach. *Mosty 4* , pp. 12-17.

Jose Luis Santos, F. F. (2015). *Handbook of Optical Sensors.* Boca Raton: CRC Press Taylor & Francis Group.

KEYENCE. (2021, 11 30). *Fibre optic sensors FS-N40 Series*. Retrieved from Digital Fibre optic Sensor: https://www.keyence.co.uk/products/sensor/fiber-optic/fs-n40/downloads/

This project has received funding from the European Union's Horizon 2020 research and innovation programme under grant agreement No 958171.

Łukasz Bednarski, R. S. (2015). Wybrane zagadnienia monitorowania konstrukcji. *XXX Jubileuszowe Ogólnopolskie Warsztaty Pracy Projektanta Konstrukcji* (pp. 28-30). Szczyrk : Politechnika Krakowska, Akademia Górniczo-Hutnicza.

Mathew kautzman, B. J. (2018). Calibration and testing of distributed fiber optic sensors for detection of high energy radiation . *Journal of Directed Energy* .

Measures, R. M. (2001). *Structural Monitoring with Fiber Optic Technology* . Ontario: Institute of Aerospace Studies .

Mei, Y. (2018, August). Error analysis for distributed fibre optic sensing tehcnology based on Brillouin scattering. USA: University of Cambridge, Department of Philosophy .

Narodowe Centurm Badań i Rozwoju, Politechnika Rzeszowska, . (2021, 12 08). *OptiDeck*. Retrieved from Inteligentny system pomostowy z kompozytów polimerowych do budowy i modernizacji drogowych obiektów mostowych: https://optideck.prz.edu.pl/

NERVE-SENSORS. (2021, 11 30). *NERVE SENSORS Epsilon Rebar strain sensor*. Retrieved 11 30, 2021, from NERVE SENSORS: www.nerve-sensors.com

R. B. Figuera, C. J. (2021). *Development of Advanced Fibre Optic Sensors to Monitor the Durability of Concrete and Reinforced Concrete Structures - SolSensors.* Universidade do Minho, INESC-TEC and Engiprojects, Lda.

Rafał Sieńko, Ł. B. (2016). Monitorowanie obiektów budowlanych w sąsiedztwie budowy . *Geoinzynieria* , pp. 60-65.

Romaniuk, R. S. (2001). *Miernictwo Światłowodowe Wydanie II Uzupełnione.* Warszawa: Instytut Systemów elektronicznych Politechnika Warszawska.

Samuel Vurpillot, D. I.-M. (1996, April 22). Smart Structures and Materials vol. 2719. *Bridge Monitoring by fiber optic deformation sensors: design, emplacemnet and results*. San Diego , USA: Society of Photo-Optical Instrumentation Engineers.

SHM SYSTEMS. (2021, 12 7). *SHM Systems Projects*. Retrieved 12 7, 2021, from SHM Systems: https://www.shmsystem.pl/projects/

SMARTEC SA, Branko Glisic, Daniele Posenato, Daniele Inaudi. (2007, May). Integrity monitoring of old steel bridge using fiber optic distributed sensors based on Brillouin scattering. *Proceedings of SPIE.* The International Society for Optical Engineering. doi:10.1117/12.716055

T. H. Nguyen, T. V. (2014, February). Fluorescence based fibre optic pH sensor for the pH 10–13 range suitable for corrosion monitoring in concrete structures. *Sensors and Actuators B Chemical 191*, pp. 498-507.

Tomasz Siwowski, R. S. (2017, May). System monitorowania mostów kompozytowych z wykorzystaniem światłowodowych czujników odkształceń. *PROJECT COM-BRIDGE, DEMONSTRATOR+*, (pp. 50-53).

Udd, E. (2006). *Fiber Optic Sensors And Introduction for Engineers and Scientists.* New Jersey : John Wiley & Sons, Inc. .

W. Barcik, R. S. (2012). System monitorowania konstrukcji Mostu Rędzińskiego we Wrocławiu. *Mosty 2*, pp. 56-62.

This project has received funding from the European Union's Horizon 2020 research and innovation programme under grant agreement No 958171.

APPENDIX A5. Ground Penetrating Radar (GPR)

5.1 Goal(s)

5.1.1 Main objective

GPR is a geophysical method that allows for the analysis of the propagation capacity of electromagnetic waves through media with different dielectric constants. This is a non-destructive testing technique widely used in the inspection of masonry and concrete bridges; thus, previously unknown information about the internal condition of structures can be provided, such as material zoning, thicknesses, corrosion, moisture content, etc.

A detailed description of the methodology along with a deep theoretical background can be found in (Annan, 2003) (Daniels , 2004) (Jol, 2009).

5.2 Description

5.2.1 Functioning mode

A transmitting antenna emits an electromagnetic signal into the ground, which is partly reflected at the interface between two different media with sufficient dielectric contrast and partly transmitted into deeper layers. Then, the reflections produced are recorded from the receiving antenna, which is either in a separate antenna box or in the same antenna box as the transmitter. The strength (amplitude) of the reflected fields is proportional to the change in the magnitude of the dielectric constant. If the time required to propagate to a reflector and back is measured, and the velocity of the signal propagation in the medium is known, the depth of the reflector can therefore be determined.

GPR applications in structures and infrastructures depend highly on the characteristics of the studied elements and on the problems that must be studied. Radar data can be acquired with a single antenna or with an array of antennas moved on the surface of the medium. The first case is usual in narrow and small zones or in inaccessible areas for large equipment (walls, columns, etc.), while the second one is used in wide areas without obstacles (during road/pavement inspections). GPR data is also used in boreholes with antennas designed for this purpose. The study of walls or small size construction elements is sometimes done with transillumination and radar tomography, but in the majority of the cases the results are provided as depth slides and pseudo 3D models.

The different GPR data acquisition modes (*Figure 5.1*) are briefly described:

- Common-Offset Mode

The most prevalent data acquisition methodology is Common-Offset (CO), also called single-fold or single-offset. This is the common reflection mode, the simplest and fastest way of acquiring data with a GPR system. Using the CO mode, one or two antennas are moved by keeping constant the distance between transmitter and receiver. Generally, survey lines should be designed to run perpendicular to the preferred strike direction of the features under investigation. Regarding the polarization of the

This project has received funding from the European Union's Horizon 2020 research and innovation programme under grant agreement No 958171. © 2021

antennas, they should be Bow-tie and Vivaldi antennas with linear polarization (most commonly perpendicular to the direction of data collection).

- 3D Common-Offset Mode

In some GPR surveys, particularly in wide areas, the CO procedure is repeated at regular intervals and for a number of survey lines, which are usually located parallel to each other. Using 3D CO, more realistic images of the underground space are provided, which allows not only for the location, but also for the reconstruction of buried structures. These 3D images (or time-slices) provide accurate and intuitive display of the underground distribution, and appropriate spatial correlations between reflectors in depth.

- Common-Mid-Point Mode

In the CMP configuration, also known Multi-Offset, multifold or wide-aperture, the separation between transmitter and receiver increases at each survey location. Both the transmitting and receiving antennas are moved apart about a common fixed center point along the survey line at a constant step. The antenna spacing is varied at a fixed location and the change of the two-way travel time of the electromagnetic wave from the reflectors is measured. The CMP mode can be used to calculate the velocity of propagation.

- Transillumination Mode

Another possible survey mode is the transillumination (more commonly known as borehole radar) used for borehole and tomography studies. Employing this mode, the transmitting antenna is kept stable at a fixed location while the receiving antenna is moved along a survey line in constant step intervals. While in the CO mode the reflected signal is received, the CDP mode receives the direct wave produced.

This project has received funding from the European Union's Horizon 2020 research and innovation programme under grant agreement No 958171.

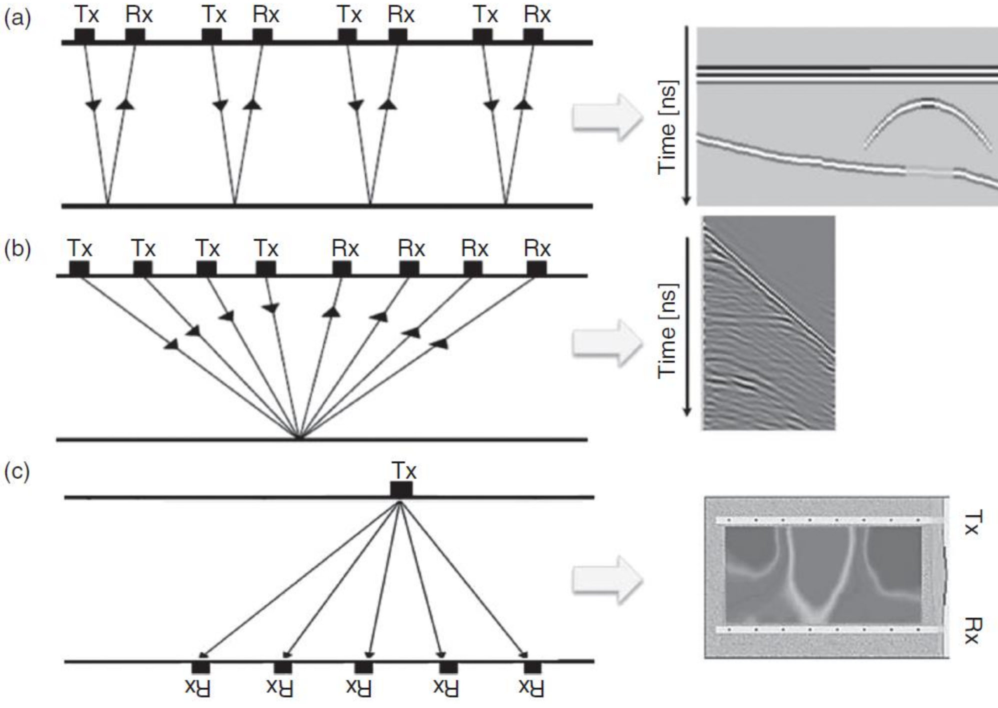

Figure 5.1. GPR data acquisition modes: (a) Common-Offset mode, (b) Common-Mid-Point (CMP) mode and (c) Transillumination mode (Solla, Lorenzo, & Pérez-Gracia, 2016).

5.2.2 Types

There are GPR systems operating in the frequency and in the time domain. However, their principles are not different, only differ the approaches of capturing wide band transient signals.

In the time domain, all the frequencies are emitted at the same time to give pulses. The signal capture uses synchronous detection of the signals. Common names for time domain GPR systems are: impulse and UWB (Ultra-Wide Band) impulse radars. UWB impulse radar systems transmit signals across a wider frequency (wide band signals) than conventional systems.

In the frequency domain, the signals are emitted as a sinusoidal wave. Common names for frequency domain systems are FMCW (Frequency-Modulated Continuous Wave) and SFCW (Step-Frequency Continuous Wave) radars. They provide wide bandwidth and their operating frequency can change during the measurement.

There are several GPR manufacturers and commercial equipment available, and some experimental prototypes also exist. Different GPR systems have different capabilities according to the type of antennas and their frequency, which affect the operating speed, the resolution, the penetration and the sampling rate (Pajewski, Fontul, & Solla, Ground-penetrating radar for the evaluation and monitoring of transport infrastructures, 2019). The frequency and depth of penetration are related, with higher frequency pulses achieving lower penetration, but better resolution. Impulse GPR systems are the most widely used, with two main groups of GPR antennas, dipole and horn antennas, and with frequencies nowadays ranging from 10 MHz to 6 GHz. Currently, the most commonly used technology is the time-

This project has received funding from the European Union's Horizon 2020 research and innovation programme under grant agreement No 958171.

domain impulse radar. Additionally, several investigations point to the step-frequency radar as a potential technology for broad resolution range, although these systems do not allow real-time visualization of data during acquisition.

- GPR with horn antennas

GPR horn antennas were specifically designed for use in transport infrastructures evaluation, since they can operate at traffic speeds. In the last ten years, this type of equipment has evolved from prototype status to routine use in pavement evaluation studies.

Horn antennas have frequencies ranging from 1 to 2.5 GHz, corresponding to penetration depths in the order of 1 m to 0.4 m, respectively. The minimum layer thickness that can be detected is about 50 mm, for 1 GHz antennas and 25 mm, for the higher frequencies.

The antennas are “air-coupled”, and normally they work mounted on a mobile vehicle and are suspended at a certain distance from the surface, typically ranging from 0.4 to 0.6 m. They perform measurements at traffic speeds (up to 80–120 km/h) without any interference with traffic, and therefore they are suitable for the evaluation of in-service pavements and bridge decks without major disturbance to road users.

- GPR with dipole antennas

Dipole antennas were primarily developed for use in geological survey, normally ground-coupled. They have frequencies ranging between 10 MHz and 6 GHz. For transport infrastructure applications, the best results are obtained with antennas from 400 MHz to 2.5 GHz central frequency. In general, the higher the frequency, the lower the penetration depth and the higher the resolution is. For example, 1.5 GHz dipole antennas will give a penetration depth of 0.50 m, while the 400 MHz will give a penetration of 2.00 m. *Figure 5.2* illustrates the simplified GPR-antenna footprint for bistatic dipole antennas.

Dipole antennas were mainly developed for use in contact with the surface, or suspended just above it (2–5 cm), and they are suitable for testing at maximum speeds of 20–30 km/h. In this condition, the radar signal is “ground-coupled”. Ground coupling introduces a stronger signal into the pavement, and therefore these antennas are normally employed for detailed studies over limited areas, as they allow one to obtain higher resolution.

This project has received funding from the European Union’s Horizon 2020 research and innovation programme under grant agreement No 958171.

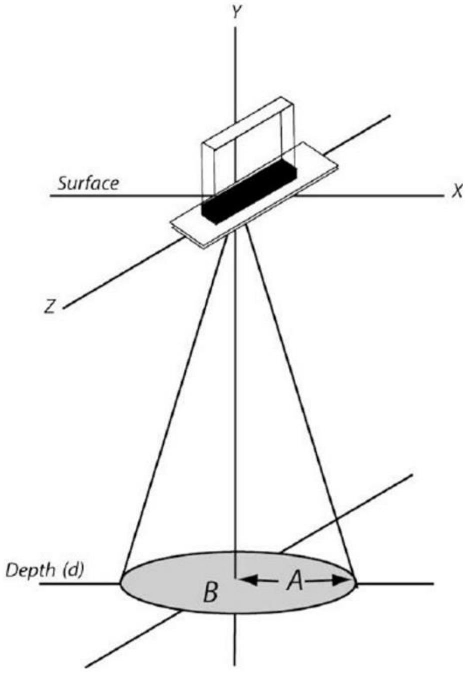

$$A = \frac{\lambda}{4} + \frac{d}{\sqrt{k+1}}$$

A – approximate long dimension radius of footprint

λ – center frequency wavelength of radar energy

d – depth from ground Surface to reflection Surface

K – average relative dielectric permittivity of material from ground surface to depth

Figure 5.2. Simplified GPR-antenna footprint (Fresnel zone) for bistatic dipole antennas.

- GPR with antennas array multi-channel

GPR array multi-channel systems consist of a large number of closely-spaced antennas recording at the same time. Different multi-channel prototypes have recently been provided with different configurations, and they can include both air- and ground-coupled antennas. Commonly, such multi-static systems are composed of 4–16 couples of transmitting and receiving channels mounted in a parallel broadside configuration with a cross-line trace spacing of 4–12 cm, depending on the manufacturer. The main advantage is that they enable faster data collection by increasing the extension of the investigated area per time unit, and they make it easier for the operator to produce 3D images.

Generally, in transport infrastructure inspection, the antennas are mounted on a mobile vehicle to minimize traffic disruption. Mobile GPR is positioned connected to an external real-time kinematic (RTK) global navigation satellite system (GNSS) for trace tagging (georeferenced data) or to a distance measurement indicator (DMI) to control the distance trace-interval and to measure the travelled distance. The system also uses a computer navigation guided system to correctly follow profile direction and keep a constant overlap among parallel profiles without any physical marker on the ground surface.

- Bore-hole antennas

Bore-hole antenna systems are often applied to GPR investigations of deeper formations. The applications of such systems include fracture characterization, foundation investigations, cavity and crack detection, as well as tunnelling inspection. Measurement methods include single-hole reflection mode, crosshole mode (tomography) and surface-to-borehole mode. Available bore-hole antenna

This project has received funding from the European Union's Horizon 2020 research and innovation programme under grant agreement No 958171. © 2021

frequencies are 100 MHz, 150 MHz, 250MHz and 300 MHz, and the system can perform surveys deeper than 30 m, with special BH equipment and accessories capable of measuring as deep as 2500 m. The area of investigation has a radius of about 10–100m depending on the dielectric properties of the propagation media.

5.2.3 Process/event to be detected or monitored

The detection of discontinuities (changes in the dielectric properties of media) in subsoil/subsurface. Particularly for the diagnosis of bridges and tunnels, the GPR method has been demonstrated as effective for the detection of the following characteristics:

Masonry arch bridges

- Unknown geometries remaining in the interior of the bridge such as hidden arches and ancient profiles (shape) of the structure
- Evidence of restorations and/or reconstructions in the stonework
- Existence of cavities and fractures/cracking in masonry
- Moisture in masonry
- Inventory of bridge foundations
- Filling distribution in masonry
- Thickness of ashlars (pavement, ring arch, spandrel walls, etc.)

Concrete bridges

- Estimation of concrete cover depth.
- Mapping reinforcing bars (deck and beams).
- Location of cable ducts and other utilities such as deck joints or drain grate.
- Damage detection on concrete (corrosion, cracking, spall, delamination, etc.).
- Moisture detection and water content estimation.

Tunnels

- Thickness of concrete segment/lining.
- Thickness of the backfill grouting layer.
- Damages in concrete lining and grouting layer.
- Damages (e.g., cracks/fissures, fractures and voids) behind tunnel linings.
- Moisture/water content.
- Depth and location of reinforcement (rebar).
- Inspection of other reinforced concrete structures (e.g., steel arch and shotcrete layer).

This project has received funding from the European Union's Horizon 2020 research and innovation programme under grant agreement No 958171.

- Location of immersion joints.
- Identification of depth and presence of insulation material.

More information about the application of the GPR method on transport infrastructures inspection can be found in (Benedetto & Pajewski, 2015) (Wai-Lok Lai, Dérobert, & Annan, 2018) (Solla, Pérez-Gracia, & Fontul, 2021).

5.2.4 Physical quantity to be measured (e.g. actions, displacements, deformations, dynamic structural properties, material properties including mechanical, electrical and chemical properties, relative displacements of the two sides of a crack, etc.).

The method is based on measuring the time arrival and amplitude of the reflected waves. The magnitude of the measured amplitudes and the propagation time depend on the dielectric properties of the medium materials that can be inferred analysing the arrival time, the amplitude and the frequency of the received signals. The amplitude value is the strength or intensity of the reflected fields that is proportional to the magnitude of the dielectric contrast between adjacent media. But the amplitude of the received signals depends on different factors apart from the strength of the field reflected on the discontinuity: (i) distance between the target and the antenna and (ii) dielectric properties of the medium; hence, these factors determines the geometrical spreading and the attenuation of the radar waves.

5.2.5 Induced damage to the structure during the measurement

Non-destructive Testing

5.2.6 General characteristics

5.2.6.1 Measurement type (static or dynamic, local or global, short-term or continuous, etc.)

The GPR data acquisition with air-launched antennas allows for a dynamic measurement at traffic speeds (up to 80–120 km/h). The measurement is continuous (each a certain distance or scan/m interval) through the GPR profile line. This configuration is most typically used for pavement and bridge deck monitoring (e.g. thicknesses, cracking, rebar, etc.).
The GPR data acquisition with ground-coupled antennas allows for both a dynamic or a static measurement (up to 60–80 Km/h). The measurement is continuous (every certain distance or time interval) through the GPR profile line. This configuration can be used for pavement and bridge deck monitoring (e.g. thicknesses, cracking, rebar, etc.), as well as for more local or punctual surveying such as piers. The ground-coupled antennas provide a deeper range of penetration and better resolution (better signal-to-noise ratio) when compared with air-coupled antennas.
Finally, the GPR data acquisition with ground-coupled array systems allows for both a dynamic measurement (up to 15 Km/h). This configuration is most commonly focused on pavement and bridge deck monitoring (e.g. 3D mapping of rebar, delamination/corrosion maps, etc.).

5.2.6.2 Measurement range

The higher the frequency, the lower the penetration depth and the higher the resolution is. Resolution is commonly referred to by its horizontal (or lateral) and vertical (longitudinal or range) resolution. The vertical resolution allows the differentiation of two adjacent signals in the time axis (or in depth) like different events, while the horizontal resolution indicates the minimum distance between two adjacent

This project has received funding from the European Union's Horizon 2020 research and innovation programme under grant agreement No 958171. © 2021

targets at the same depth to be detected as separate events. Nevertheless, the measurement range provided by the GPR is somewhat like uncertainty because these parameters are highly dependent on the bandwidth used and, thus, on the dominant frequency of the antenna with determines pulse duration, as well as on the wave velocity of propagation (dielectric permittivity of media) and signal attenuation.

The 500 MHz antennas have limited ground penetration, but they give a very high-resolution map of the subsurface in the first 2–3 meters. Below this depth, lower frequency antennas work better (with signal penetration up to 10-15 m), but those with a central frequency below 100 MHz may have insufficient vertical resolution. Frequencies in the order of GHz are suited for very shallow studies (< 1 m), and they are an especially effective tool for structure inspection: detection of cracks, estimation of wall thickness, moisture content inside structures, rebar detection, etc. Regarding to horizontal resolution, the HF band provides data with a range resolution from 0.5 to 0.1 m, while the LF band is limited to a resolution ranging from 0.5 m up to 2.5 m. On the other hand, the vertical resolution ranges between 4 cm and 1 cm for HF band, and between 5 cm and 0.5 m for LF band.

5.2.6.3 Measurement accuracy

The optimal depth/thickness estimation from GPR data requires a correct calibration process by determining accurate dielectric permittivity and wave velocity of propagation in media.
GPR manufactures mainly focuses on system accuracy, but measurements of unknown quantities should be accompanied by the uncertainty assessment (Solla, González-Jorge, Lorenzo, & Arias, 2013) (Plati, Loizos, & Gkyrtis, 2020) (Xie, Lai, & Dérobert, 2021).

5.3 Background (evolution through the years)

The first application of radio waves in detecting buried targets was proposed in two German patents by Leimbach and Lowy in 1910 (Germany Patent No. 237944, 1910) (Germany Patent No. 246836, 1910), as a methodology for shallow geological surveys. One of the patents was based on using the analysis of signals amplitude transmitted and received by dipole antennas placed in boreholes. The other patent described the use of surface antennas to detect underground ore and water deposits. This application was based on the previous German patent of the 'telemobiloskop' by Huelsmeyer in 1904, which allowed the detection of distant metallic objects by using electromagnetic waves. The method was improved in 1926 with the development of pulsed systems (Germany Patent No. 489434, 1926), based on the detection of reflections occurring in buried targets, allowing best depth resolution. The technique was developed during the following decades; the first applications being used to determine the thickness of a glacier in 1930. However, the method did not seem to generate enough interest during this first period, and commercially available devices appeared during the 1970s. This pioneer equipment was firstly used to analyse the radio waves' penetration in ice and in different rocks and soil materials. Some of the first GPR studies in civil engineering appeared in mid 1970s, and were devoted to the detection of hidden utilities. Simultaneously, some first applications in pavements were also described. From these first works, the number of applications and developments of the methodology increased remarkably. GPR became a useful tool in the analysis of many structures and infrastructures, and nowadays it is successfully applied in a large number of cases: road and pavement analysis, detection of voids and cavities, study of bridges and tunnels, assessment of actual buildings and cultural heritage, archaeological surveys, forensics and mining detection, geotechnical evaluations and water management analysis.

In the last 10 years, thanks to different multi-channel prototypes and complex data analysis, manufacturers have provided with robust full-resolution GPR imaging solutions where the antenna responses of individual elements are much closer resulting in streamlined methodologies and consistent results (Linford, Linford, Martin, & Payne, 2010) (Simi, Manacorda, Miniati, Bracciali, & Buonaccorsi, 2010). GPR array multi-channel systems consisting of a large number of closely-spaced antennas represented a new evolution for 3D mapping. These multi-channel systems speed up data acquisition and allow full wave-field recording at the same time, thus increasing the extension of the investigated area.

This project has received funding from the European Union's Horizon 2020 research and innovation programme under grant agreement No 958171. © 2021

More recent research is focused on the design of innovative devices that facilitates surveying in complex or inaccessible structures such as columns, walls and roofs (e.g. a device consisting of a support for the antenna in rails moved with an electric motor (Hugenschmidt, Kalogeropoulos, Soldovieri, & Prisco, Processing strategies for high-resolution GPR concrete inspections, 2010)). In this way, in some cases, the use of drones has been also proposed and tested (Garcia-Fernandez, Alvarez-Lopez, & Las Heras, Autonomous airborne 3D SAR imaging system for subsurface sensing: UWB-GPR on board a UAV for landmine and IED detection, 2019) (Wu, et al., 2019), although further progress could be focused on the development of antennas and UAV (unmanned aerial vehicle) systems for surveying structures or parts of the structures with poor accessibility and large structures. With respect to tunnelling inspection, new GPR devices are being developed for higher speed data collection and complete cross section scanning towards fully automated tunnel inspection (Balaguer, Montero, Victores, Martínez, & Jardón, 2014) (Xie, Chen, & Zhou, 2016) (Zan, Su, & Li, 2016).

5.4 Performance

5.4.1 General points of attention and requirements

5.4.1.1 Design criteria and requirements for the design of the survey

The most significant performance limitation of GPR is in highly conductive materials such as clay soils and salt contaminated soils. Performance is also limited by signal attenuation under moisture conditions and signal dispersion under heterogeneous conditions. Another limitation is the fact that the electromagnetic signal is fully reflected in metal, and the radar waves do not penetrate.

Therefore, GPR surveys should be performed under dry soil condition to avoid signal attenuation due to water content, as well as far from any object causing signal disturbance (typically called air-waves events), such as metallic objects (fences, manholes or vehicles), power lines, walls, etc. Moreover, as the ground-coupled GPR antennas are moved in contact with the ground surface, the profile line should be conducted in open areas free of obstacles like stones, trees, etc.

5.4.1.2 Procedures for defining layout of the survey

Generally, the profile lines are gathered in perpendicular to the trend of the features under investigation.

It should be noted that there are technical standards regulating the electromagnetic emissions of GPR equipment. The following are the main standards in Europe, USA and Canada: European Telecommunications Standard Institute (ETSI) EN 203 066-1, ETSI EN 203 066-2,
ETSI EN 203 489-32 and ETSI EG 202 730, USA regulations on UWB-GPR: Part 15 of Federal Communications Commission (FCC) Regulations, and Industry Canada Radio Standards Specification RSS-220 (Issue 1) “Devices Using Ultra-Wideband (UWB) Technology.

Useful recommendations for planning safe GPR surveys are given in (Persico, et al., 2015).

5.4.1.3 Design constraints (e.g. related to the measurement principles of the monitoring technologies)

Since water content in soils significantly attenuates the GPR signal, the GPR survey should be conducted at least 1-2 days without rain/snow weather conditions.

5.4.1.4 Sensibility of measuring to environmental conditions.

In wet or saturated media, the capacity of signal penetration can be reduced by 10 or even totally lost in wet clays or salt media.

This project has received funding from the European Union’s Horizon 2020 research and innovation programme under grant agreement No 958171. © 2021

5.4.2 Preparation

5.4.2.1 Procedures for calibration, initialisation, and post-installation verification

In some cases, for both air-launched and ground-coupled systems, calibration consists of comparing GPR data with cores. In other cases, and more particularly for air-launched antennas, calibration consists of comparing the amplitude of the reflected wave with the amplitude of the wave reflected on a metallic plate. Moreover, the dielectric permittivity of the media can be also determined with the common-mid-point (CMP) operating mode.
In Europe, there are no specific common guidelines about the application of GPR in pavement surveys, even though some proposals are developed in different countries (Stryk, et al., 2017).
Examples of those guidelines are in the Mara Nord Project (Saarenketo, Recommendations for guidelines for the use of GPR in asphalt air voids content measurement. Mara Nord Project; Europeiska Unionen, 2012) and in the British (DMRB3.1.7., 2006) (DMRB7.3.2., 2008) and Belgian (ME91/16, 2016) regulations. The studies demonstrate that the correct calibration causes an extreme decrease in the error on the estimation of thickness measurements.
The guide ASTM D4748-98 (ASTM, Standard Test Method for Determining the Thickness of Bound Pavement Layers Using Short-Pulse Radar; Non-destructive testing of pavement structures; ASTM D4748, 2004) presents the procedures for the inspection of the upper layers of both bituminous and concrete pavements, using a short-pulse GPR. The methods included in this international standard are focused on the thickness evaluation of pavement layers. The guide includes technical topics such as calibration and standardization, procedures, calculation and reliability of the results.
The COST Action TU1208 has published some tests and recommendations for suitable GPR system performance compliance, obtained by scientists from Belgium (Belgium Road Research Center), Czech Republic (University of Pardubice), Portugal (National Laboratory for Civil Engineering), and Serbia (Faculty of Technical Sciences, Novi Sad) (Pajewski, et al., 2018). The D6087-08 standard (ASTM, 2015), describes four procedures for the calibration of GPR systems equipped with air-coupled antennas. After a critical analysis of those procedures, four improved tests were proposed in (Jafarov, et al., 2017), which can be carried out to evaluate the signal-to-noise ratio, short-term stability, linearity in the time axis, and long-term stability of the GPR signal.

5.4.2.2 Procedures for estimating the component of measurement uncertainty resulting from calibration of the data acquisition system (calibration uncertainty)

There is no standardization or guidelines regarding measurement (calibration) uncertainty. Only very few scientific papers in the literature have approached the uncertainty issue in GPR data (Solla, González-Jorge, Lorenzo, & Arias, 2013) (Plati, Loizos, & Gkyrtis, 2020) (Xie, Lai, & Dérobert, 2021) (Jafarov, et al., 2017).

5.4.2.3 Requirements for data acquisition depending on measured physical quantity (e.g. based on the variation rate)

Soil type and soil water content. Soil water content is highly determined by weather conditions and has a large effect on the dielectric permittivity and electric conductivity of the soil medium.

The most important parameters in designing GPR data acquisition are:

- Operating frequency. The selection of the optimal operating frequency should provide a good compromise between resolution and depth of penetration.
- Time window. Time length between two transmitted pulses for which the reflected signals are recorded.
- Temporal sampling interval. Time interval between points on a recorded waveform. This parameter is controlled by the Nyquist sampling concept and should be at most half the period of the highest frequency signal in the record.

This project has received funding from the European Union's Horizon 2020 research and innovation programme under grant agreement No 958171. © 2021

The sampling rate should be approximately six times the centre frequency of the antenna.

- Spatial sampling interval. This interval should not exceed the Nyquist sampling intervals, which is one quarter of the wavelength in the host medium.

  Normally, the sampling interval in GPR surveys should be at least 10 scan /m in longitudinal survey profiles and at least 40 scans /m in cross section profiles.

More definition and rules to configure these parameters can be found in (Annan, 2003) (Benedetto & Pajewski, 2015).

Regarding the design of a survey grid, the line spacing should be less than the antenna footprint.

5.4.3 Performance

5.4.3.1 Requirements and recommendations for maintenance during operation (in case of continuous maintenance)

Not applicable.

5.4.3.2 Criteria for the successive surveying campaigns for updating the sensors. The campaigns include: (i) Georeferenced frame, i.e. the global location on the bridge; (ii) Alignment of sensor data, relative alignment of the data collected in surveying; (iii) Multi-temporal registration to previous campaigns; and (iv) Diagnostics.

Georeferenced grid or profile lines (at least the starting corner or initial point, respectively) in case of multi-temporal registration.

5.4.4 Reporting

Not applicable.

5.4.5 Lifespan of the technology (if applied for continuous monitoring)

Not applicable. The GPR method does not offer continuous (long-term) monitoring.

5.5 Interpretation and validation of results

5.5.1 Expected output (Format, e.g. numbers in a .txt file)

The GPR data is a binary file format, that varies depending on the manufacturer:

- Sensors & Software: *.dt1, *.hd, *.gps
- MALA geoscience: *.rd3, *.rd7, *.rad, *.cor
- Impulse radar: *.iprb, *.iprh, *.cor, *.time, *.mrk
- GSSI: *.dzt, *.dzx
- IDS: *.dt, *.gec
- SEG-Y: *.sgy
- Radar systems, Inc.: *.sgy
- 3dradar: *.3dra, *.vol
- ASCII: *.txt (3 column format; X, t, amplitude)
- etc.

This project has received funding from the European Union's Horizon 2020 research and innovation programme under grant agreement No 958171. © 2021

5.5.2 Interpretation (e.g. each number of the file symbolizes the acceleration of a degree of freedom in the bridge)

Each number in the GPR binary data file represents an amplitude value. It consists of a matrix, composed by many sequentially stacked traces in the horizontal dimensions and samples in the vertical dimensions (trace data recorded sample by sample), which display individual amplitudes for each position in the matrix. Thus, the x axis represents the distance (number of trace) on the profile line, and the z axis represents the distance-time (number of sample) in which the reflection occurs.

Thus, the vertical axis of a radargram indicates the travel-time in which the propagated wave reflects the target or discontinuity. Knowing the exact medium, dielectric properties, and wave velocity of propagation, these travel-time scales can be converted into depths, which allows estimating thicknesses in a quantitative manner. The horizontal axis indicates the length or distance in the profile line, which gives an estimation of the spatial target dimensions. A GPR system typically operates with an odometer wheel attached to control the trace interval distance and the length of the profile line.

The interpretation of the GPR imaging is basically based on qualitative aspects and reflection patter recognition (geometry, signal polarity, etc.).

5.5.3 Validation

5.5.3.1 Specific methods used for validation of results depending on the technique

5.5.3.2 Quantification of the error

5.5.3.3 Quantitative or qualitative evaluation

The combination of GPR with complementary geophysical techniques is highly recommended to validate interpretation. Each particular method provides different information owing to the physical properties of the construction material, which allows for a more detailed investigation in the diagnosis of structures. In the case of reinforced concrete structures, GPR is widely complemented with seismic and ultrasonic pulse-echo technology, but also with profoscope (rebar detector), half-cell potential (corrosion analysis) and hammer sounding resistivity (concrete strength properties). Regarding the validation of quantitative measurements (thicknesses), the calibration and error estimation consists of comparing GPR data with cores. normally reference coring should be made at 2–3 km intervals, with a minimum 1/10 km road section (Benedetto & Pajewski, 2015).

5.5.4 Detection accuracy

Detecting boundary between layers or discontinuities requires enough dielectric permittivity contrast between adjacent media.

When the dielectric contrast is enough between two adjacent media to ensure detection, the other parameter controlling the detection accuracy is the spatial resolution and zone of influence around the propagation path of the GPR signal. In general, the higher the frequency, the lower the penetration depth and the higher the resolution is.

This project has received funding from the European Union’s Horizon 2020 research and innovation programme under grant agreement No 958171.

Resolution is commonly referred to by its horizontal (or lateral) and vertical (longitudinal or range) resolution. The vertical resolution, which allows the differentiation of two adjacent signals in the time axis (or in depth) like different events, mainly depends on the bandwidth used and, therefore, on the dominant frequency of the antenna which determines pulse duration (quarter of the wavelength criteria). On the other hand, horizontal resolution indicates the minimum distance between two adjacent targets at the same depth to be detected as separate events. This parameter mainly depends on the number of traces recorded that is directly adjusted before data acquisition, the bandwidth, and the depth of the reflector.

In general, low frequencies (50 – 200 MHz) are capable to reach a penetrating depth ranging from 10 to 3 m. The high frequency band (500 – 2000 GHz) provides a penetrating depth ranging from 3 to 0.5 m. Regarding to horizontal resolution, the HF band provides data with a range resolution from 0.5 to 0.1 m, while the LF band is limited to a resolution ranging from 0.5 m up to 2.5 m. The vertical resolution ranges between 4 cm and 1 cm for HF band, and between 5 cm and 0.5 m for LF band.

5.6 Advantages

The main advantages of the GPR method are:

- Non-destructive and non-invasive method.
- Easy transportation.
- Fast data acquisition compared with other geophysical methods.
- Imaging of the subsoil with high resolution.
- Precise vertical and horizontal positioning.
- Results are displayed in real-time.

5.7 Disadvantages

- The interpretation of radargrams is generally non-intuitive and requires considerable expertise to properly process and understand the measurements.
- Uncertainty/inaccuracy in depth/thickness estimation (pre-calibrated media characterization and accurate wave velocity of propagation are needed).

5.8 Possibility of automatizing the measurements

Regarding the possibility of automatizing the measurements, innovative devices start to emerge aiming to facilitate surveying in complex or inaccessible structures such as columns, walls and roofs. One example is the device designed and tested by (Hugenschmidt, Kalogeropoulos, Soldovieri, & Prisco, 2010) that consists of a support for the antenna in rails moved with an electric motor. Other developments include prototypes to mount the GPR on an UAV (Garcia-Fernandez, Alvarez-Lopez, & Las Heras, 2019), a climbing robot supporting a GPR antenna for wall inspection (Howlader, Sattar, & Dudley, 2016) (Yangí, et al., 2018) or robots specifically designed for disaster management that could integrated different sensors (GPR, LiDAR, cameras, etc.) on the platform (Bertolino & Tanzi, 2020). Moreover, the recent proposal of a big robotic platform with a large number of sensors for autonomous

This project has received funding from the European Union's Horizon 2020 research and innovation programme under grant agreement No 958171. © 2021

pavement assessment (Gibb, et al., 2018) opens an interesting line of research in the field of structures assessment.

5.9 Barriers

The main limitations occur in the presence of high-conductivity materials (such as wet clay) and in heterogeneous conditions causing signal attenuation and complex scattering phenomena, respectively.

The following limitations and drawbacks can occur during concrete bridge inspections:

(1) The steel/metal is a quasi-perfect reflector of the radar-waves, which facilitates the rebar detection, but deeper targets can be masked if it is a tight mesh. In this regard, collecting data in both polarizations (with the dipoles perpendicular and parallel to data collection direction) has benefits because the reflections produced by metallic targets perpendicular to the data collection direction are weakly seen in data collected with dipoles parallel to the scanning direction, so that other potential targets below them can be more easily detected.

(2) Overlapping reflections are usually observed between consecutive bars that is dependent on the spatial resolution of the antenna (higher frequencies provide a higher resolution), which may lead to the misinterpretation of closest or smaller-diameter bars. Resolution problems can also occur in sections with a too small concrete cover when measuring pavement thickness. The selection of the most appropriate central frequency of the antenna is therefore crucial herein.

(3) Another important parameter affecting the location accuracy is the horizontal sampling. Dense horizontal sampling (scan spacing), gives more accuracy on positioning and good quality data for further amplitude analysis, although its main consequence is a decrease in the survey speed. Conversely, using a low sampling rate may limit data visibility in the field and cause inaccurate adjustments of hyperbolas peaks when processing.

(4) The 3D data acquisition (especially with single GPR antennas) may incur an incorrect distance encoder calibration due to variations in topography, position of the antenna on starting/ending grid lines, improperly configured survey grid, georeferencing, etc. The use of antenna arrays or automatic scanner systems makes the acquisition of 3D data easier and thus encourages a wider use of 3D techniques although, in practice, these systems usually have an excessive cost. For example, a higher sampling rate (higher number of traces recorded) decreases a survey speed, which could result in higher survey costs and, more importantly, could interrupt the traffic flow.

(5) The amplitude value is highly dependent on various factors such as different depth to the top mat of the reinforcing steel, weather conditions (e.g., humidity) during data acquisition, and concrete properties (e.g., density, porosity, etc.), which makes the detection of corrosion and delamination only difficult from the analysis of amplitude maps. Confirmation with the additional

This project has received funding from the European Union's Horizon 2020 research and innovation programme under grant agreement No 958171. © 2021

analysis of other signal attributes (e.g., signal attenuation, signal-to-noise ratio and velocity of propagation) or complementary NDT should be part of the process whenever possible.

With respect to tunnelling inspection, the following limitations and drawbacks can occur:

(1) Generally, tunnels are inspected manually, by manoeuvring the GPR antenna over the surface of the tunnel, with single ground-coupled antennas using the mode of continuous acquisition, which is very slow and inefficient. In the process of tunnel inspection, longitudinal survey lines are most commonly arranged, with a range of three to six serial lines located at the vault, the left hance, the right hance, the left sidewall, the right sidewall and the inflected arch.

(2) The connection with external GPS devices for data referencing is obviously limited when surveying the interior of a tunnel structure. Therefore, wheel encoders are used during data acquisition to ensure the accuracy of ranging (trace interval) and location. So far, the following practical problems that typically occur are: (i) loss of contact between the antenna and the surface (the operator should ensure both the antenna and the survey wheel are in contact with the surface, while keeping a constant (uniform speed) and continuous rotation); (ii) deviation of the antenna with respect to the radar line (the operator should ensure the antenna position is consistent with the location of the acquisition line); and (iii) the presence of cables and conduits on the walls of the tunnel that makes it impossible to collect data in those areas.

(3) There are so many noisy signals from utilities (e.g., power cables) or metal (reinforcement) in the tunnel. Shotcrete-containing steel fibers cannot be inspected because fibers generate random electromagnetic scattering.

5.10 Existing standards

- The American standard ASTM D6087-08 “Standard Test Method for Evaluating Asphalt-Covered Concrete Bridge Deck Using Ground Penetrating Radar” (ASTM, 2015).
- The American SHRP 2- report S2-R06A-RR-1 “Nondestructive Testing to Identify Concrete Bridge Deck Deterioration” (SHRP, 2013).
- The Mara Nord Project “Recommendations for guidelines for the use of GPR in bridge deck surveys” (Saarenketo, Maijala, & Leppäl¨, 2011).
- The British technical specifications DMRB 3.1.7 “Design Manual for Roads and Bridges, Advice notes on the non-destructive testing of highway structures—advice note 3.5 BA 86/2006: Ground Penetrating Radar (GPR)” (DMRB3.1.7., 2006).
- The German BASt-report B55 “Examination of GPR in combination with magnetic techniques for the determination of moisture and salinity of concrete bridge decks with asphalt cover” (BASt, 2007).
- The German document B10 “Recommendation for nondestructive testing of civil engineering structures by GPR” (B10, 2008).

This project has received funding from the European Union’s Horizon 2020 research and innovation programme under grant agreement No 958171.

- The American AASHTO R 37-04 “Standard Practice for Application of Ground Penetrating Radar (GPR) to Highways” (AASHTO, 2004).
- The American ACI 228.2R-98 “Nondestructive Test Methods for Evaluation of Concrete in Structures” (ACI, 1998).
- The American NCHRP RR 848 “Inspection Guidelines for Bridge Post-Tensioning and Stay Cable Systems Using NDE Methods” (NCHRP, 2017).

5.11 Applicability

5.11.1 Relevant knowledge fields

- Civil Engineering.
    - Rebar, linear metallic targets.
    - Utilities.
    - Roads and pavements.
    - Railways, ballast and tunnels
    - Concrete structures and buildings.
    - Bridges.
    - Foundations.
- Environmental investigations.
    - Waste and pollution.
    - Hydrology and water detection.
    - Soil texture characterization.
    - Root biomass.
    - Ice sounding.
    - Mining.
- Geology investigations.
    - Fractures, faults.
    - Stratigraphic studies.
    - Bathymetry (freshwater).
    - Dunes/sand environments.
    - Volcanics.

This project has received funding from the European Union’s Horizon 2020 research and innovation programme under grant agreement No 958171.

- Archaeology and Cultural Heritage.
  - Archaeology remains.
  - Palaeontology.
  - Painting.
  - Monuments.
  - Statues.
  - Ancient structures/buildings.
- Humanitarian assistance and forensics.
  - Landmines/UXO/IED detection.
  - Locating trapped people (avalanche, earthquake, etc.).
  - Buried remains.
- Other emerging fields.
  - Planetary exploration.
  - Precision farming.

5.11.2 Performance Indicators

- Cracks
- Delamination
- Spalling
- Holes
- Debonding
- Reinforcement bar / corrosion
- Loss of section

5.11.3 Type of structure

- Masonry bridges.
- Concrete bridges.
- Tunnels.

5.11.4 Spatial scales addressed (whole structure vs specific asset elements)

Air-coupled antennas were specifically developed for pavement (bridge deck) monitoring, allowing for measurements at traffic speed. Conversely, the ground-coupled antennas are most commonly used in specific parts of the bridge structure (e.g. beams, piers, etc.). Moreover, the ground-coupled array systems, are focused on 3D pavement/deck surveying.

This project has received funding from the European Union's Horizon 2020 research and innovation programme under grant agreement No 958171.

5.11.5 Materials

Stone, brick, concrete/reinforced concrete, rock, wood.

5.12 Available knowledge

5.12.1 Reference projects

Assets4Rail "Measuring, Monitoring and Data Handling for Railway Assets; Bridges, Tunnels, Tracks and Safety Systems" EU H2020 Project (Grant Agreement ID 826250).

COST Action TU1208 "Civil engineering applications of Ground Penetrating Radar".

LASTING-RTI2018-095893-B-C1. Life-Cycle Assessment of Existing Bridge Structures using Multiscale and Multisource Data. Spanish Ministry of Science and Innovation.

OPAF-SIG: Observatory of masonry arch bridges. Integrated Management System (BIA2009-08012). Spanish Ministry of Science and Innovation.

Geomatic techniques for the structural and dimensional analysis of historical bridges and their conservation (BIA2006-10259). Spanish Ministry of Education and Science.

ESA-approved project "MOBI: Monitoring Bridges and Infrastructure Networks" (EOhops proposal 2045 (id 52479)).

5.12.2 Other

Not applicable.

5.13 Bibliography

AASHTO. (2004). AASHTO R 37-04. Standard Practice for Application of Ground Penetrating Radar (GPR) to Highways. Washington, DC, USA: American Association of State and Highway Transportation Officials.

ACI. (1998). ACI 228.2R-98 (Reapproved 2004). Nondestructive Test Methods for Evaluation of Concrete in Structures. Farmington Hills, MI, USA: American Concrete Institute.

Annan, P. (2003). GPR Principles, Procedures & Applications. Mississauga, ON, Canada: Sensors and Software Inc.

ASTM. (2004). Standard Test Method for Determining the Thickness of Bound Pavement Layers Using Short-Pulse Radar; Non-destructive testing of pavement structures; ASTM D4748. West Conshohocken, PA, USA: ASTM.

ASTM. (2015). ASTM D6087-08(2015)e1. In Standard Test Method for Evaluating Asphalt-Covered Concrete Bridge Decks Using Ground Penetrating Radar. West Conshohocken, PA, USA: ASTM.

B10. (2008). Document B10—Recommendation for Nondestructive Testing of Civil Engineering Structures by GPR. Berlin, Germany: German Society for Non- Destructive Testing (DGZfP).

Balaguer, C., Montero, R., Victores, J., Martínez, S., & Jardón, A. (2014). Towards fully automated tunnel inspection: A survey and future trends. Proceedings of the 31st International Symposium on Automation and Robotics in Construction and Mining. Sydney, Australia.

BASt. (2007). BASt-Report B55. Examination of GPR in Combination with Magnetic Techniques for the Determination of Moisture and Salinity of Concrete Bridge Decks

This project has received funding from the European Union's Horizon 2020 research and innovation programme under grant agreement No 958171.

with Asphalt Cover. Bundesanstalt für Straßenwesen: Federal Highway Research Institute.

Benedetto, A., & Pajewski, L. (2015). Civil Engineering Applications of Ground Penetrating Radar. New York, NY, USA: Springer International.

Bertolino, M., & Tanzi, T. (2020). Towards 3D Simulation for Disaster Intervention Robot Behaviour Assessment. Adv. Radio Sci., 18, 23–32.

Daniels , D. J. (2004). Ground Penetrating Radar. London, UK: The institution of Electrical Engineers.

DMRB3.1.7. (2006). Department for Transport, Highway Agency. DMRB 3.1.7.: Design Manual for Roads and Bridges, Advice Notes on the Non-Destructive Testing of Highway Structures—Advice Note 3.5 BA 86/2006: Ground Penetrating Radar (GPR). Birmingham, UK: Department for Transport, Highway Agency.

DMRB7.3.2. (2008). DMRB 7.3.2.: Design Manual for Roads and Bridges, Data for Pavement Assessment—Annex 6 HD 29/2008: Ground-Penetrating Radar (GPR). Birmingham, UK: Highway Agency.

Garcia-Fernandez, M., Alvarez-Lopez, Y., & Las Heras, F. (2019). Autonomous airborne 3D SAR imaging system for subsurface sensing: UWB-GPR on board a UAV for landmine and IED detection. Remote Sens., 11(2357).

Garcia-Fernandez, M., Alvarez-Lopez, Y., & Las Heras, F. (2019). Autonomous airborne 3D SAR imaging system for subsurface sensing: UWB-GPR on board a UAV for landmine and IED detection. Remote Sens, 11(2357).

Gibb, S., La, H., Le, T., Nguyen, L., Schmid, R., & Pham, H. (2018). Nondestructive evaluation sensor fusion with autonomous robotic system for civil infrastructure inspection. J. Field Robot., 35, 988–1004.

Howlader, M., Sattar, T., & Dudley, S. (2016). Development of a Wall Climbing Robotic Ground Penetrating Radar System for Inspection of Vertical Concrete Structures. Int. J. Mech. Mechatron. Eng., 10, 1382–1388.

Hugenschmidt, J., Kalogeropoulos, A., Soldovieri, F., & Prisco, G. (2010). Processing strategies for high-resolution GPR concrete inspections. NDT E Int., 43, 334–342.

Hugenschmidt, J., Kalogeropoulos, A., Soldovieri, F., & Prisco, G. (2010). Processing strategies for high-resolution GPR concrete inspections. NDT E Int., 43, 334–342.

Hülsenbeck. (1926). Germany Patent No. 489434.

Jafarov, E., Parsekian, A., Schaefer, K., Liu, L., Chen, A., Panda, S., & Zhang, T. (2017). Estimating active layer thickness and volumetric water content from ground penetrating radar measurements in Barrow, Alaska. Geoscience Data Journal, 4(2), 72-79.

Jol, H. M. (2009). Ground Penetrating Radar: Theory and Applications. Amsterdam, The Netherlands: Elsevier Science.

Leimbach, G., & Löwy, H. (1910). Germany Patent No. 237944.

Leimbach, G., & Löwy, H. (1910). Germany Patent No. 246836.

Linford, N., Linford, P., Martin, L., & Payne, A. (2010). Stepped frequency ground-penetrating radar survey with a multi-element array antenna: Results from field application on archaeological sites. Archaeological Prospection.

ME91/16. (2016). ME91/16: Methodologies for the Use of Ground-Penetrating Radar in Pavement Condition Surveys. Brussels, Belgium: Belgian Road 445 Research Centre.

NCHRP. (2017). NCHRP Research Report 848. In Inspection Guidelines for Bridge Post-Tensioning and Stay Cable Systems Using NDE Methods. Washington, DC, USA: TRB's National Cooperative Highway Research Program.

This project has received funding from the European Union's Horizon 2020 research and innovation programme under grant agreement No 958171. © 2021

Pajewski, L., Fontul, S., & Solla, M. (2019). Ground-penetrating radar for the evaluation and monitoring of transport infrastructures. In Innovation in Near-Surface Geophysics. Instrumentation, Application, and Data Processing Methods. Amsterdam, The Netherlands: Elsevier.

Pajewski, L., Vrtunski, M., Bugarinovic, Ž., Ristic, A., Govedarica, M., Van der Wielen, A., . . . al., e. (2018). GPR system performance compliance according to COST Action TU1208 guidelines. Ground Penetrating Radar, 1, 104–122.

Persico, R., Provenzano, A., Trela, C., Sato, M., Takahashi, K., Arcone, S., . . . S. Ebihara, K. W. (2015). Recommendations for the safety of people and instruments in ground-penetrating radar and near-surface geophysical prospecting. European Association of Geoscientists and Engineers, EAGE Publications.

Plati, C., Loizos, A., & Gkyrtis, K. (2020). Assessment of modern roadways using non-destructive geophysical surveying techniques. Surveys in Geophysics, 41, 395-430.

Saarenketo, T. (2012). Recommendations for guidelines for the use of GPR in asphalt air voids content measurement. Mara Nord Project; Europeiska Unionen. Brussels, Belgium.

Saarenketo, T., Maijala, P., & Leppäl¨, A. (2011). Recommendations for Guidelines for the Use of GPR in Bridge Deck Surveys. Publications of Mara Nord Project.

SHRP. (2013). SHRP 2- report S2-R06A-RR-1. In Nondestructive Testing to Identify Concrete Bridge Deck Deterioration. Washington, DC, USA: Transportation Research Board.

Simi, A., Manacorda, G., Miniati, M., Bracciali, S., & Buonaccorsi, A. (2010). Underground asset mapping with dualfrequency dual-polarized GPR massive array. Proceedings 13rd International Conference on Ground-Penetrating Radar, (pp. 1001-1005). Lecce, Italy.

Solla, M., González-Jorge, H., Lorenzo, H., & Arias, P. (2013). Uncertainty evaluation of the 1 GHz GPR antenna for the estimation of concrete asphalt thickness. Measurement, 46, 3032–3040.

Solla, M., Lorenzo, H., & Pérez-Gracia, V. (2016). Ground Penetrating Radar: Fundamentals, Methodologies and Applications in Structures and Infrastructures. In B. Riveiro, & M. Solla, Non-Destructive Techniques for the Evaluation of Structures and Infrastructures. EH Leiden, The Netherlands: CRC Press/Balkema.

Solla, M., Pérez-Gracia, V., & Fontul, S. (2021). A review of GPR application on transport infrastructures: troubleshooting and best practices. Remote Sensing, 13(672).

Stryk, J., Matula, R., Pospíšil, K., Dérobert, X., Simonin, J., & Alani, A. (2017). Comparative measurements of ground penetrating radars used for road and bridge diagnostics in the Czech Republic and France. Constr. Build. Mater., 154, 1199–1206.

Wai-Lok Lai, W., Dérobert, X., & Annan, P. (2018). A Review of Ground Penetrating Radar Application in Civil Engineering: A 30-Year Journey from Locating and Testing to Imaging and Diagnosis. NDT E Int., 96, 58–78.

Wu, K., Rodriguez, G., Zajc, M., Jacquemin, E., Clément, M., De Coster, A., & Lambot, S. (2019). A new drone-borne GPR for soil moisture mapping. Remote Sens. Environ., 235(111456).

Xie, F., Lai, W., & Dérobert, X. (2021). GPR uncertainty modelling and analysis of object depth based on constrained least squares. Measurement(109799).

Xie, X., Chen, Y., & Zhou, B. (2016). Data processing of backfill grouting detected by GPR in shield tunnel and research on equipment of GPR antenna. Proceedings of the 16th International Conference on Ground Penetrating Radar. Hong Kong, China.

This project has received funding from the European Union's Horizon 2020 research and innovation programme under grant agreement No 958171.

Yangí, L., Yang, G., Liu, Z., Chang, Y., Jiang, B., Awad, Y., & Xiao, J. (2018). Wall-climbing robot for visual and GPR inspection. Proceedings of the 2018 13th IEEE Conference on Industrial Electronics and Applications (ICIEA), (pp. 1004–1009). Wuhan, China.

Zan, Y., Su, G., & Li, Z. (2016). A Train-mounted GPR System for Fast and Efficient Monitoring of Tunnel Health Conditions. Proceedings of the 16th International Conference on Ground Penetrating Radar. Hong Kong, China.

Zan, Y., Su, G., & Li, Z. (2016). A Train-mounted GPR System for Fast and Efficient Monitoring of Tunnel Health Conditions. Proceedings of the 16th International Conference on Ground Penetrating Radar. Hong Kong, China.

This project has received funding from the European Union's Horizon 2020 research and innovation programme under grant agreement No 958171.

APPENDIX A6. Guided Waves Propagation (GW)

6.1 Goal(s)

6.1.1 Main objective

Detection of the damage in structural health monitoring of the reinforced concrete can be studied with guided waves propagation survey as a promising and non-destructive testing. Guided waves technique enables examination within seconds on large areas and with limited number of sensors mounted on the structure. Guided waves can propagate over many tens of meters therefore it is possible to monitor areas that are very costly to inspect using other methods; for instance, insulated pipelines or buried sections of road crossings.

In variety of fields guided waves can be used for inspection of reinforcement and other metal structures, because of sensitivity greater than other conventional non-destructive methods. Guided waves techniques give possibility to inspect the state of the structure for destructive changes in a semi-automated way. Used in rapid testing or screening tools to detect, locate, and classify corrosion defects. Permanently installed sensors allow critical sections of infrastructures, such as bridges, to be regularly and efficiently monitored. Regular data collection from fixed positions greatly enhances the usefulness of guided waves.

6.2 Description

6.2.1 Functioning mode

Guided waves technique can be performed in two modes of wave generator frequency:

- high frequency mode – used for continuous monitoring
- low frequency mode – used for short-term measurements

From the point of methodology there are two important approaches:

- pulse-echo based mode – structure is excited with narrow pulse and the sensors detect the echo of the pulse coming from discontinuities; signals from the defects are filtered out and defect location can be obtained by use of the wave speed; reflected signal associated with the damage detected,
- pitch-catch based mode – pulse is sent across the sample and the sensor at the other end receives the signal; studying various characteristics of the received signal such as amplitude, frequency content, delay in time of transmit information about damage can be extracted; diffracted signal associated with the damage detected.

Guided waves propagation system includes device for wave generation and acquisition system of spring waves.

There are few transducer technology used:

This project has received funding from the European Union's Horizon 2020 research and innovation programme under grant agreement No 958171. © 2021

- *Systems with piezoelectric transducers*

The sensors are embedded or mounted on the surface of the inspected element. Piezoelectric sensors are inexpensive and available in different thicknesses. Materials used in production of piezoelectric are mostly zirconium titanate ceramics and polymer film made from polyvinylidene fluoride.

- *Systems with piezocomposite transducers*

Piezocomposite transducers were introduced mostly to overcome the issue with brittleness of standard ceramic piezoelectric transducers.

- *Systems with non-piezoelectric transducers:*
    - fibre optic sensors,
    - flat magnetostrictive sensors.

Fiber optic sensors are taken into consideration where comes to long term structural monitoring with guided waves, however to acquire the associated support equipment higher cost will be generated. Flat magnetostrictive sensors consist of a thin nickel foil with a coil which can be permanently bonded to the surface of inspected element (Victor Giurgiutiu, 2010) (Ye Lu, 2013).

6.2.2 Types

- Impact-Echo test (IE) – general working principle is shown on the Fig.1. Instrumentation consists of:
    - a mechanical impactor capable of producing short-duration impacts, the duration of which can be varied,
    - a high fidelity receiver to measure the surface response,
    - data acquisition – signal analysis system to capture, process and store the waveforms of surface motion.

The duration of the impact is critical for success of an impact-echo test. The impact gives rise to modes of vibration and the frequency of these modes is related to the geometry of the test object and the presence of flaws.

This project has received funding from the European Union's Horizon 2020 research and innovation programme under grant agreement No 958171. © 2021

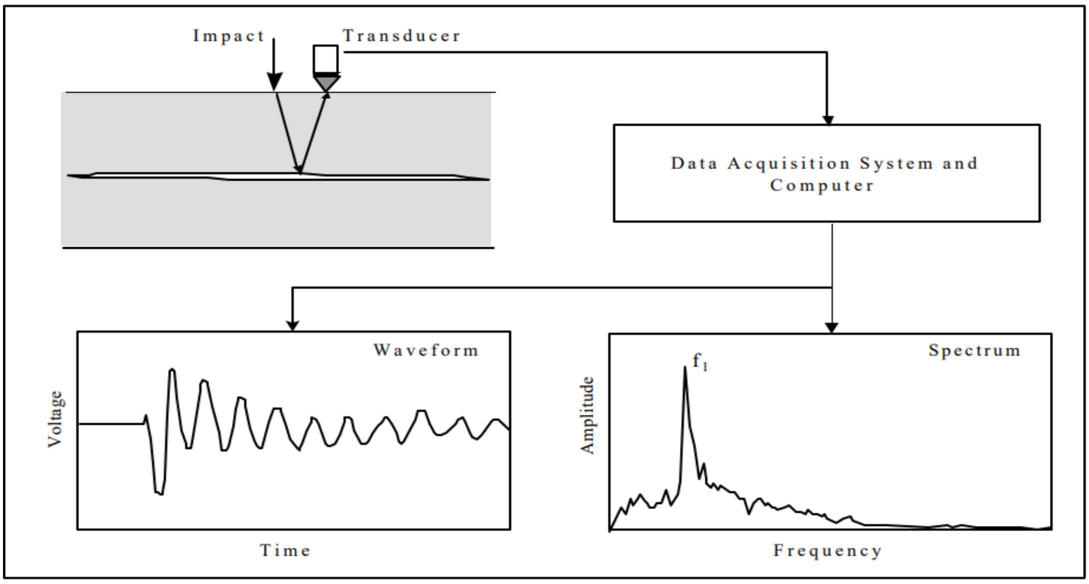

Figure 6.1 – Scheme of the method

- Ultrasonic Pulse Velocity Test (UPV) – a pulse of longitudinal vibrations is produced by an electro−acoustical transducer, which is held in contact with one surface of the concrete under test. When the pulse generated is transmitted into the concrete using a liquid coupling material such as grease or cellulose paste, it undergoes multiple reflections at the boundaries of the different material phases within the concrete. A complex system of stress waves develops, which include both longitudinal and shear waves, and propagates through the concrete. The first waves to reach the receiving transducer are the longitudinal waves, which are converted into an electrical signal by a second transducer. Three modes are generally used:
  - Opposite faces (direct transmission) mode
  - Adjacent faces (semi−direct transmission) mode
  - The same face (indirect or surface transmission) mode.

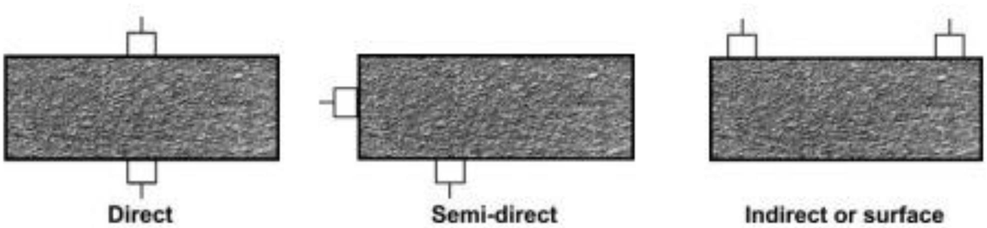

Figure 6.2 – Transducers arrangement

- Spectral Analysis of Surface Waves (SASW) - uses the dispersive characteristics of surface waves to determine the variation of the surface wave velocity (stiffness) of layered systems with depth.

6.2.3 Process/event to be detected or monitored

Guided waves techniques can be generally applied to detect:

This project has received funding from the European Union's Horizon 2020 research and innovation programme under grant agreement No 958171.

- the presence of discontinuity from the wave signal diffracted by the crack.
- detection of delamination and debonding of the concrete structures.
- surface cracks depth
- homogeneity of concrete
- quality variation of concrete
- detection of voids, imperfections
- determination of the age of concrete.

Impact Echo investigations are performed to assess the condition of slabs, beams, columns, walls, pavements, runways, tunnels, dams, and other structures. voids, honeycomb, cracks, delamination and other damage in concrete, wood, stone, and masonry materials can be found utilizing the IE method. IE investigations are also performed to predict the strength of early age concrete if the member thickness is known, and to measure the thickness of structural members.

Spectral Surface Waves Analysis can be applied for:

• determination of pavement system profiles including the surface layer, base and subgrade materials

• determination of surface opening crack depths

• freeze-Thaw damage depth measurement

• fire damage depth measurement

• determination of abutment depths of bridges

• condition assessments of concrete liners in tunnels, and other structural concrete conditions

6.2.4 Physical quantity to be measured (e.g. actions, displacements, deformations, dynamic structural properties, material properties including mechanical, electrical and chemical properties, relative displacements of the two sides of a crack, etc.).

Strength of longitudinal and/or flexural wave transmission along a rebar:

- amplitude of the signals [mv],
- amplitude of the noise [mV],
- ringing zone duration [µs],
- speed of the wave [m/s],
- thickness of elements [mm].

6.2.5 Induced damage to the structure during the measurement

No damage is induced during the measurement.

6.2.6 General characteristics

6.2.6.1 Measurement type (static or dynamic, local or global, short-term or continuous, etc.)

Guided waves techniques are dynamic and both local and global measurement, which offers both short-term and continuous monitoring.

This project has received funding from the European Union’s Horizon 2020 research and innovation programme under grant agreement No 958171. © 2021

6.2.6.2 Measurement range

- Guided Wave propagation:

  Range depends on the thickness of the sample and the test method. For 5 mm specimen the maximum frequency range is around 250 kHz with a 10 mm minimum wavelength. Transducers working frequency usually lies between 100 up to 240 kHz.

  Wave generator – work parameters and example of ranges:

  - range of work frequencies: usually from a few ten to several hundred hertz, 30 – 350 kHz
  - number of transmitting/measuring channels - 1/15 (16) or 1/7 (8)
  - number of periods of lambda waves packs: 1-16
  - modulation of wave packets: Hanning window, triangular, rectangular
  - delay between generated packets: 1-4095 ms;
  - amplifier output voltage: ±100 V
  - regulation of the receiving circuit: .1, ½, ¼, ⅛, 1/10, 1/20, 1/40, 1/80
  - sampling frequency of the measurement path: 2,5 MHz
  - analog-to-digital converter: 24 bit.

- Ultrasonic Pulse Velocity Test (UPV):
  - transit time measurement Range 0.1 – 9999 µs + auto-ranging.
  - resolution 0.1 µs.

- Impact-echo method:

Parameters		**Examples**	
Symbol	**Description**	**Example 1**	**Example 2**
Δt	Sampling interval; time between successive points in waveform.	2 µs	4 µs
f_s	Sampling frequency; inverse of Δt.	500 kHz	250 kHz
f_{max}	Maximum frequency in amplitude spectrum; one-half of f_s.	250 kHz	125 kHz
N	Number of points in waveform (record).	1024	2048
$N\,\Delta t$	Record length; duration of waveform.	2.048 ms	8.192 ms
Δf	Frequency resolution in amplitude spectrum; equal to inverse of record length.	0.488 kHz	0.122 kHz

Table 6-1 – Data acquisition parameters

6.2.6.3 Measurement accuracy

- Impact-echo method - the defect depth determination is possible with accuracy ranging from 60.00 - 99.05%. Stronger concrete gives better accuracy in determining the depth of defect. The size of the smallest flaw that can be detected increases as the flaw depth increases.

This project has received funding from the European Union's Horizon 2020 research and innovation programme under grant agreement No 958171. © 2021

- Ultrasonic Pulse Velocity – the compressive strength evaluation by means of UPV can be performed with up to 94% accuracy.
- SASW measurements are accurate to within 5% for the determination of the thickness and stiffness of the top layer during pavement layer analysis or of the concrete liner of a tunnel.

6.3 Background (evolution through the years)

First studies over guided waves propagating were performed in the seismology domain in early 1920. Guided wave technique was developed in 1990 for the rapid survey of pipes, for the detection of both internal and external corrosion. The main area of application has been to pipes and pipelines (Mix, 2005) (International Atomic Energy Agency, 2002).

6.4 Performance

6.4.1 General points of attention and requirements

6.4.1.1 Design criteria and requirements for the design of the survey

The wave should propagate in a spiral - a necessary condition that various types of reflected waves do not disturb the measurement and the attenuation along the way should be small enough to be able to record the returning wave (too much attenuation extinguishes the wave energy). For proper analysis of the failures there should be noted some information about the structure in undamaged state or stage when the inspection is planned. Surface should be prepared before mounting the sensors – evened with sandpaper and degreased.

6.4.1.2 Procedures for defining layout of the survey

No specific procedures.

6.4.1.3 Design constraints (e.g. related to the measurement principles of the monitoring technologies)

The SASW method can be performed when an accessible surface is available for receiver mounting and impacting.

6.4.1.4 Sensibility of measurements to environmental conditions

In case of Impact-Echo method special attention should be given to the surrounding environment. If the stiffness of bedrock or underlying slab is very close to those of the main concrete element, the accuracy of the method will be affected.

When testing with SASW, in inclement weather, receivers must be protected against rain drops. Care should be taken when lateral variations might be expected at the site because they may more easily affect long arrays. Passive methods may face difficulties in very quiet sites where the level of ambient vibrations is very low or in case of stiff soil to rock conditions, where the mechanism of generation and propagation of surface waves is less efficient.

This project has received funding from the European Union’s Horizon 2020 research and innovation programme under grant agreement No 958171.

6.4.2 Preparation

6.4.2.1 Procedures for calibration, initialisation, and post-installation verification

For accurate results it is necessary to have good practice and theoretical knowledge of the effects of damage on the wave characteristics. Base signal line should be obtained in the healthy state for use as reference in comparison with results in time. Optimization of the wave propagation in initial phase can be done by adjusting frequency and number of cycles. Data cleansing should be performed before the actual measurement.

- Ultrasonic Pulse Velocity Test (UPV)

  The distance (path length) between the transducers should be measured as accurately as possible. It is very important to ensure adequate acoustic coupling of the transducers to the surface under test. A thin layer of couplant should be applied to the transducer and the test surface. In some cases it may be necessary to prepare the surface by smoothing it. For compound measurements and uniformity testing a test grid should be drawn out on the surface. Rebars affect the ultrasonic measurements as the signal will travel faster through the rebar than through the concrete. The location of rebars should be determined using a rebar locator.

6.4.2.2 Procedures for estimating the component of measurement uncertainty resulting from calibration of the data acquisition system (calibration uncertainty)

Guided wave behaviour is directly affected by thickness of the specimen and frequency used. Measurement uncertainty can be evaluated with statistical methods.

6.4.2.3 Requirements for data acquisition depending on measured physical quantity (e.g. based on the variation rate)

Data processing algorithm pass the signals along the same radial line.

6.4.3 Performance

6.4.3.1 Requirements and recommendations for maintenance during operation (in case of continuous maintenance)

Signal processing algorithm should be capable of running in real-time and frequent intervals, possibly during operation of the structure. System should be able to distinguish between signal changes due to damage processes and changes to environmental conditions. These environmental changes should be compensated with efficient signal-processing methods. Elimination of the sensitivity to temperature changes.

6.4.3.2 Criteria for the successive surveying campaigns for updating the sensors. The campaigns include: (i) Georeferenced frame, i.e. the global location on the bridge; (ii) Alignment of sensor data, relative alignment of the data collected in a surveying; (iii) Multi-temporal registration to previous campaigns; and (iv) Diagnostics.

No data available.

6.4.4 Reporting

The inspection report should include:

- date of the inspection,

This project has received funding from the European Union's Horizon 2020 research and innovation programme under grant agreement No 958171.

- dimensions of the investigated area or sketch of the structure,
- ambient temperature,
- registered signals.

In case of continuous monitoring usually the system is equipped with a software and reports are generated automatically with scans, reflection annotations and operator notes are stored in the cloud.

6.4.5 Lifespan of the technology (if applied for continuous monitoring)

The guided waves technique can be used in short-term inspection and continuous monitoring over large volumes with mounted sensors. Continuous measurement can take from few hours to years.

6.5 Interpretation and validation of results

6.5.1 Expected output (Format, e.g. numbers in a .txt file)

- Guided Wave Propagation method:

Time domain response vs amplitude of piezo sensors in a graphical form on the computer.

An example of base signal with the recorded signal from a rebar in concrete structure is shown below:

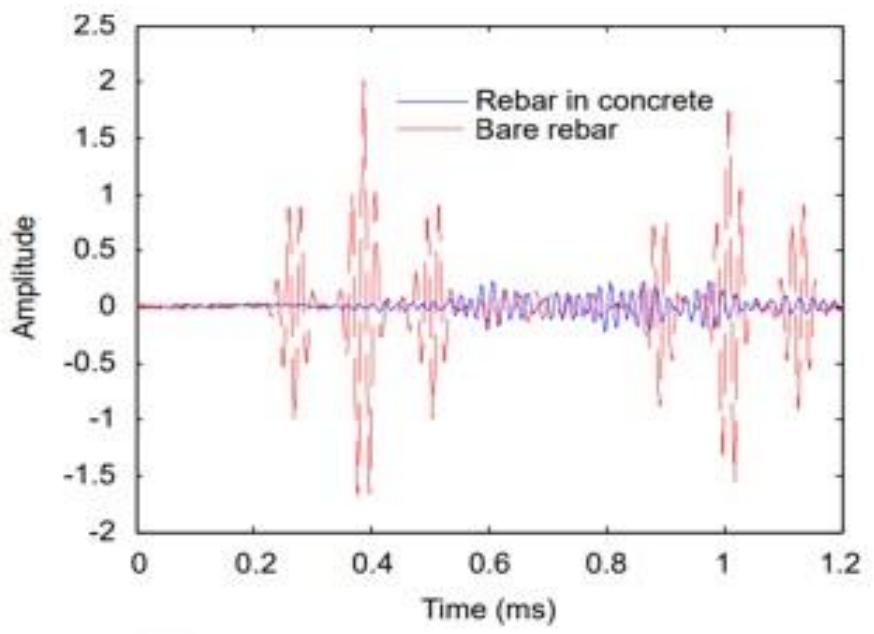

Figure 6.3 – Time domain response from the inspected concrete area

In the pictures below there is visible an output without any damage detected and additional signal with lower amplitude in the middle on the second graph resulted from crack in the damaged rebar.

This project has received funding from the European Union's Horizon 2020 research and innovation programme under grant agreement No 958171. © 2021

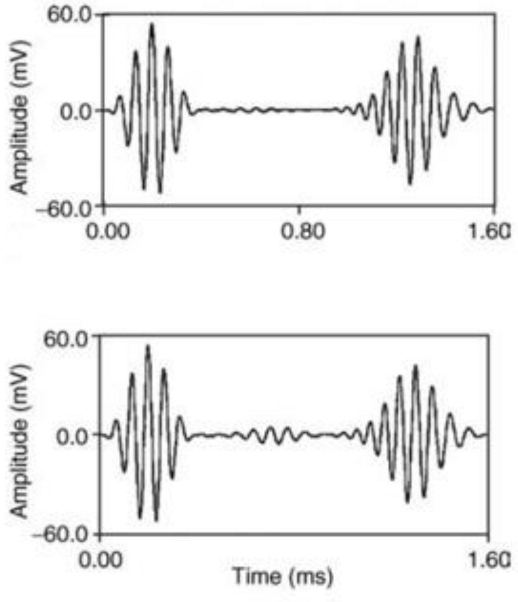

Figure 6.4 – Time domain response for healthy and damaged structure

- Impact - Echo Method

Test results can be saved to a file in the computer for later examination and analysis, and for printing copies of test results. The results of a single test are stored as a unique record in a random access file. The file can be on the hard disk or on a floppy disk or another storage device connected the computer.

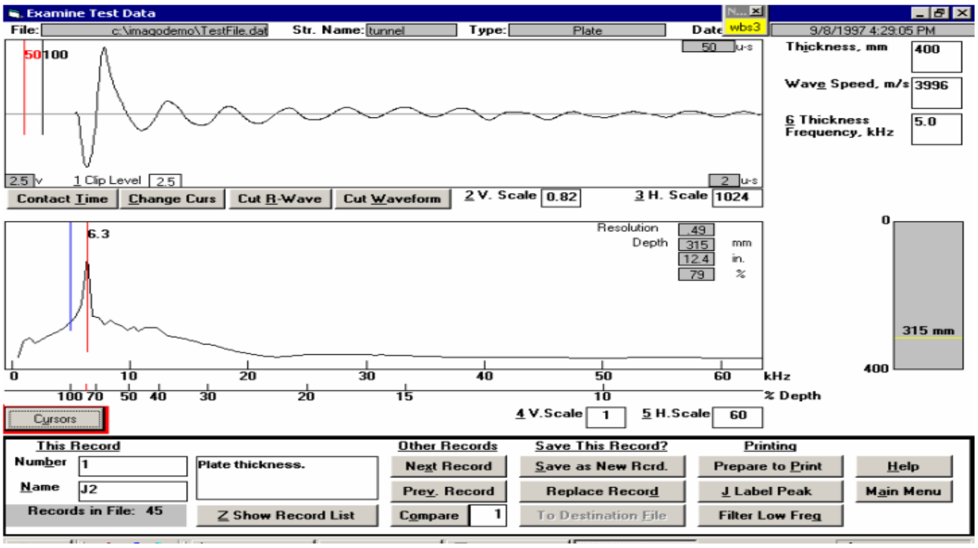

Figure 6.5 – Test Record (Impact-Echo Instruments, LLC, 2001)

- Ultrasonic Pulse Velocity Test :

This project has received funding from the European Union's Horizon 2020 research and innovation programme under grant agreement No 958171.

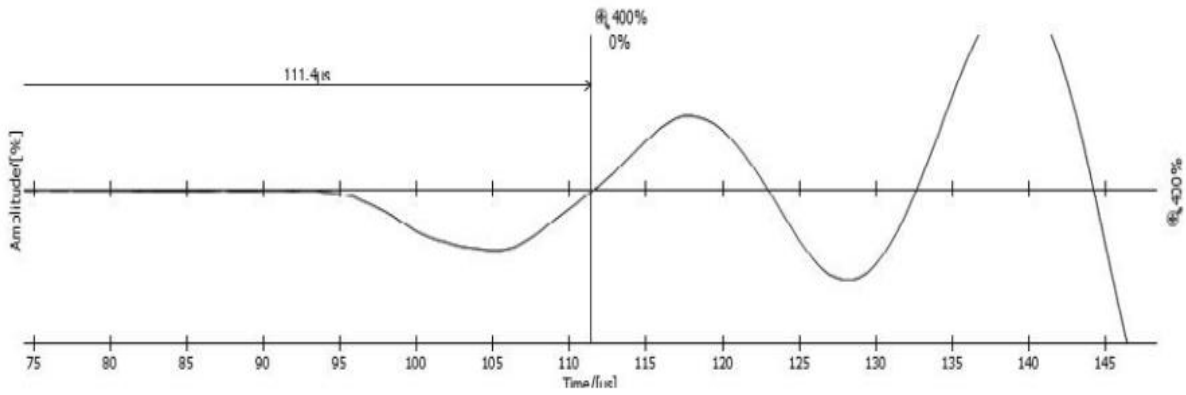

Figure 6.6 – Ultrasonic test output

- Spectral Analysis of Surface Waves (SASW)

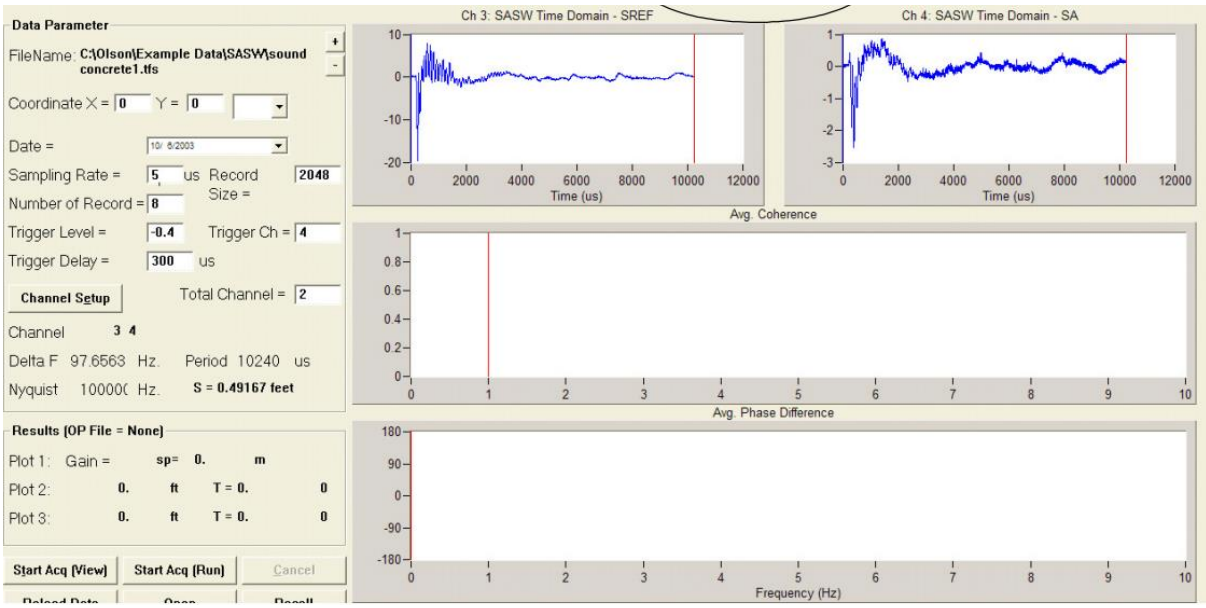

Figure 6.7 – SASW Output

6.5.2 Interpretation (e.g. each number of the file symbolizes the acceleration of a degree of freedom in the bridge)

Wave propagation characteristics corresponds to different structural conditions. The results of the experiment show measured excitation vibrations and then reflected mechanical waves from the defects. Knowing the material and dimensions of the object, it is possible to calculate whether the given reflection comes from damage to the structure. Higher signal strength at the receiving end indicates debonding and corrosion.

- Impact - Echo Method – example response of the concrete slab with detected voids:

This project has received funding from the European Union's Horizon 2020 research and innovation programme under grant agreement No 958171. © 2021

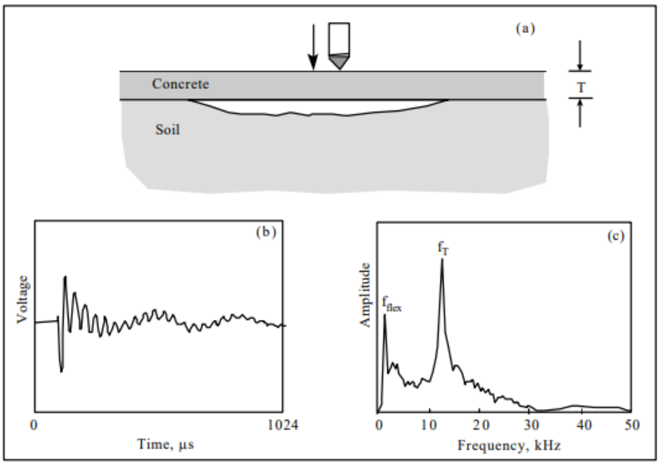

Figure 6.8 – Concrete slab with voids

6.5.3 Validation

6.5.3.1 Specific methods used for validation of results depending on the technique

Numerical methods used for studies on relationship between arrival time, amplitude of waves – models used for fitting with experimental data. To extract effective information on damages from received signals it is usually necessary to perform a simulation of the issue by numerical method.

selective verification of key conclusions after Impact-Echo test should be undertaken by drilling cores or drilling holes in combination with visual inspection using a borescope. Verification is especially important when evaluating a complex structure.

6.5.3.2 Quantification of the error

Numerical simulations of wave propagation, Finite Element Method, Boundary Element Method are used, and models are compared with experimental data.

6.5.3.3 Quantitative or qualitative evaluation

The global matrix approach is applied for quantification of the reflection and transmission coefficients of discontinuities from measured data.

6.5.4 Detection accuracy

Detection accuracy depends on the signal-to-noise ratio which can be enhanced depending on the system configuration and environmental conditions. Statistical averaging is used to reduce global noise and improve the accuracy. For Ultrasonic Pulse Velocity (UPV) depending on the detected quantity – the accuracy level can be on the level of 97,0 % (Sutan, 2002).

6.6 Advantages

- propagation over long distances
- sensitivity to different type of flaws
- detection of damages from remote position, with use of surface-mounted sensors

This project has received funding from the European Union's Horizon 2020 research and innovation programme under grant agreement No 958171.

- combined with ultrasonic tomography give information such as localization of the damages in the cross-section, degree of degradation, determination of which rebars are damaged
- performance over long range with an accurate sensitivity
- testing of multi-layered structures
- fully automated data collection

6.7 Disadvantages

- different damage configurations require numerical analysis
- difficulties in extracting desired wave modes
- dependence on the thickness and shape
- interpretation of the results highly dependent on the operator.

6.8 Possibility of automatising the measurements

In case of impact- echo method there are some attempts for automatization of the whole measurement and an example can be found in - (B. Sawicki, 2021). However, data collection in all guided waves techniques is fully automated.

6.9 Barriers

High power requirements for the system used for structural health monitoring in real-time for excitation of guided waves with an accurate scan range.

6.10 Existing standards

- BS 9690-1:2011, Non-destructive testing. Guided wave testing. General guidance and principles,
- BS 9690-2:2011, Non-destructive testing. Guided wave testing. Basic requirements for guided wave testing of pipes, pipelines and structural tubulars,
- ASTM E2775 – 16, Standard Practice for Guided Wave Testing of Above Ground Steel Pipework Using Piezoelectric Effect Transduction,
- E2929 – 13, Standard Practice for Guided Wave Testing of Above Ground Steel Piping with Magnetostrictive Transduction,
- ISO 18211:2016, Non-destructive testing — Long-range inspection of aboveground pipelines and plant piping using guided wave testing with axial propagation,
- PCN/GEN GUIDED WAVE TESTING ISSUE, 1 Rev A, 1st January 2013 – General requirements for qualification and PCN Certification of Guided Wave testing personnel.

This project has received funding from the European Union's Horizon 2020 research and innovation programme under grant agreement No 958171.

6.11 Applicability

6.11.1 Relevant knowledge fields

1.12.1.1 Civil engineering:

- adhesive bonding
- diagnostics of screw connections
- insulated, underground pipelines.

1.12.1.2 Geotechnics:

- diagnostics of rock and ground anchors
- strengthening of slopes and tunnels walls
- seismic exploration
- erosion process.

1.12.1.3. Aerospace structures:

- aircraft fuselage structures
- rocket motors
- fuel tanks.

6.11.2 Performance Indicators

Relate the surveying technology being studied with PIs from WP3, provided in the document of the TU1406 COST ACTION.

- cracks
- holes
- wire break
- loss of section
- frequency
- vibrations/oscillation
- obstruction/impeding
- displacement
- reinforcement bar failure/bending
- stirrup rupture
- debonding
- delamination
- spalling
- tensioning force deficiency.

This project has received funding from the European Union's Horizon 2020 research and innovation programme under grant agreement No 958171.

6.11.3 Type of structure

- suspension bridges
- wind turbine blade
- metallic structures
- adhesive joints

6.11.4 Spatial scales addressed (whole structure vs specific asset elements)

Guided waves propagation inspection is addressed to whole structures since wave excited at one end of the structure propagate through the volume and the waveforms can be registered at place.

6.11.5 Materials

- steel
- concrete
- glass fibres
- polymers
- composites.

6.12 Available knowledge

6.12.1 Reference projects

WI-HEALTH: Wireless network for total SHM of bridges (EU FP7 2011-2013).

6.12.2 Other

Future considerations on development of systems for structural health monitoring concern use of carbon and boron nanotubes as transducers. High cost and other problems are limiting use of nanocomposites in monitoring for now.

Manufacturers websites:

Guided Ultrasonics LTD.

Guided Ultrasonics LTD. WavePro4tm analysis software

Guided Ultrasonics LTD. Training Descriptions

IMPACT ECHO INSTRUMENTS

Mistras Hellas A.B.E.E. – Impact-echo technology overview, products, software

ACS-Solutions GmbH Science – Ultrasonic test equipment

Olson Instruments – Spectral Analysis of Surface Waves - Products

Olson Instruments – Impact Echo Scanning

General information:

Ultrasonics Pulse Velocity test methods – overview

Ultrasonic Pulse Velocity Test for Concrete - video

Guided Wave Ultrasonic Inspection – video

This project has received funding from the European Union's Horizon 2020 research and innovation programme under grant agreement No 958171.

Impact – Echo method – how to test concrete - video

Impact-Echo – User's Manual

6.13 Bibliography

Ajay Raghavan, C. E. (2007, March). Review of Guided-wave Structural Health Monitoring. *The Shock and Vibration Digest*, pp. 90-114.

B. L. Ervin, J. .. (2006). Estimation of general corrosion damage to steel reinforced mortar using frequency sweeps of guided mechanical waves. Insight, vol. 48, no. 11, (2006): 682–692. *Insight, vol. 48, no. 11*, pp. 682–692.

B. Sawicki, T. P. (2021, March 23). Development of Impact-Echo method Multitransducer Device for Automated Concrete Homogeneity Assessment . *Materials 14{9}*.

Beata Zima, M. R. (2017). Guided wave propagation for assessment of adhesive bonding between steel and concrete. *Procedia Engineering*, pp. 2300-2305.

Clements, M.-Á., Miró, M., Carbajo, J., Poveda-Martínez, P., Almenar, G., & Ramis, J. (2019). Use of Non-Linear Ultrasonic Techniques to Detect Cracks Due to Steel Corrosion in Reinforced Concrete Structures. *Materials 12*.

Evelyne El Masri, T. W. (2020, 09 27). Guided Wave Inspection of Bars in Reinforced-Concrete Beams Using Surface-Mounted Vibration Sensors. *vibration*, pp. 343-356.

Impact-Echo Instruments, LLC. (2001, October). Impact-Echo User's Manual - A Self-Teaching Course and Reference for the Impact-Echo Method and Software. New York, USA.

International Atomic Energy Agency. (2002). *Guidebook on non-destructive testing of concrete structures. Training Course No.17.* Vienna: IAEA.

Li, D., Ruan, T., & J., Y. (2012). Inspection of reinforced concrete interface delamination using ultrasonic guided wave non-destructive test technique. . *Sci. China Ser. E Technol.*, p. 2893=2901.

M. Krawczuk, J. G.—c.–5.–4. (2006). Longitudinal wave propagation. Part I—comparison of rod theories,. *Journal of Sound and Vibration 295 (3–5)* , pp. 461–478.

M. Rheinfurth, F. S. (2010, 12 9). Air-coupled guided waves combined with thermography for monitoring fatigue in biaxially loaded composite tubes. *Composites Science and Technology*, pp. 600-608.

Masri, E. (2020). Guided Wave Inspection of Bars in Reinforced Concrete Beams Using Surface Mounted Vibration Sensor. . Hampshire, United Kingdom: University of Southampton.

Miller, T., Kundu, T., Huang, J., & Grill, J. (2012). A new guided wave–based technique for corrosion monitoring in reinforced concrete. . *Structural Health Monitoring 12*, pp. 35-47.

Mix, P. E. (2005). *Introduction to Nondestructive Testing - A Training Guide* . New Jersey: John Wiley & Sons,Inc. .

Paul Fromme, P. D. (2006, Kwiecień). On the Development and Testing of a Guided Ultrasonic Wave Array for Structural Integrity Monitoring. pp. 777-785.

Rucka, M. (2009, grudzień 3). Experimental and numerical study on damage detection in an L-joint using guided wave propagation. *Journal of Sound and Vibration*, pp. 1760-1779.

This project has received funding from the European Union's Horizon 2020 research and innovation programme under grant agreement No 958171.

Sharma, A., Sharma, S., Sharma, S., & Mukherjee, A. (2018). Monitoring invisible corrosion in concrete using a combination of wave propagation techniques. *Cem. Concr. Compos. 90*, pp. 89-99.

Sriramadasu, R., Lu, Y., & Banerjee, S. (2018). Identification of incipient pitting corrosion in reinforced concrete structures using guided waves and piezoelectric wafer transducers. . *Struct. Health Monit. 18*, pp. 164-171.

Sutan, N. M. (2002). The Accuracy of Ultrasonic Pulse Velocity Method in the Detection of Distress for Reinforced Concrete Structure. . *Pakistan Journal of Information and Technology* , pp. 233-237.

V. Giurgiutiu, A. C. (2005). Embedded non-destructive evaluation for structural health monitoring, damage detection, and failure prevention. *The Shock and Vibration Digest 37 (2)*, pp. 83-105.

Victor Giurgiutiu, C. S. (2010). Guided Wave Methods for Structural Health Monitoring. *Encyclopedia of Aerospace Engineering*, pp. 1-20.

W. Na, T. K. (2002). Ultrasonic guided waves for steel bar concrete interface testing. *Material. Evaluation., vol. 60, no. 3.* , pp. 437-444.

Ye Lu, J. L. (2013, 05 12). Guided waves for damage detection in rebar-reinforced concrete beams. *Construction and Building Materials*, pp. 370-378.

Zhupeng Zheng, Y. L. (2014, August 27). Effects of Concrete on Propagation Characteristics of Guided Wave in Steel Bar Embedded in Concrete. *Hindawi Publishing Corporation Shock and Vibration*, pp. 1-15.

This project has received funding from the European Union's Horizon 2020 research and innovation programme under grant agreement No 958171.

APPENDIX A7. Light Detection And Ranging or Laser Imaging Detection And Ranging (LiDAR)

7.1 Goal(s)

7.1.1 Main objective

LiDAR technology is used to obtain three-dimensional (3D) representations of objects or structures. This representation is a set of many measures. Each measure is applied to a point on a surface. The information recorded depends on the sensor, which may be the coordinates of each point or its reflectivity, among others.

7.2 Description

7.2.1 Functioning mode

Laser scanning uses a laser beam to generate a 3D model of the object's surface to which it is pointing at. This object is represented in the space by its 3D coordinates, which are obtained by computing the distance between the LiDAR system and the target object. This, therefore, classifies remote sensing as an active technology. When the distance measurement device is combined with optomechanical systems or mirrors, which deflect the laser beam and measure the deflection angle, a 3D point cloud is obtained.

The Euclidian coordinates of each point of the cloud are defined by its distance (range) to the sensor and the angles relative to it as in *Figure 7.1*.

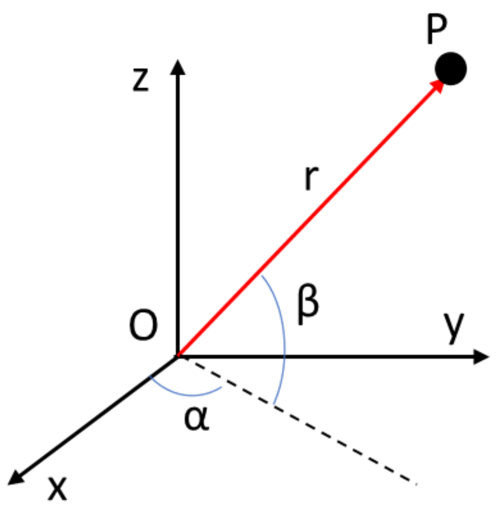

Figure 7.1 – Point position calculation.

- Range measurement:
    - Time-of-Flight (TOF):

This project has received funding from the European Union's Horizon 2020 research and innovation programme under grant agreement No 958171.

The time that it takes to a laser beam to reflect on an object and return back to the instrument. Knowing the velocity of the light waves in a given medium (C), the TOF (round trip, τ) allows to evaluate the range D, as shown in *Figure 7.2*. Measuring this time delay, the distances may be obtained directly by using short repetitive laser pulses, or indirectly by modulating the power of the wavelength of the laser beam and using phase difference.

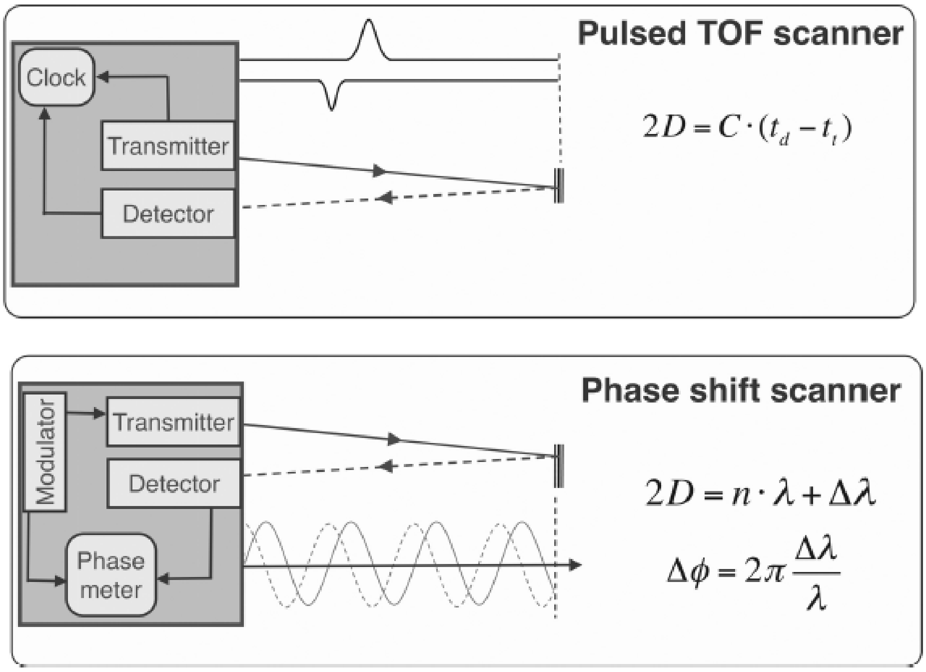

Figure 7.2 – Principles of measurement for TOF scanners. (a) Pulsed laser scanners; (b) Phase shift scanners. (Riveiro, González-Jorge, Conde, & Puente, 2016)

- Phase Measurement

This method measures the TOF by amplitude modulation (AM) using phase difference. A lower-frequency signal modulates the amplitude of the laser wave. Using low frequency signal to modulate the optical signal, AMCW can provide high-accuracy measurements compared to that obtained using the optical signal only.

In phase measurement instruments, the distance (D) is obtained by comparing the emitted laser beam and the collected laser light. The phase difference (Δϕ) yields the time delay and the range is found. The scanners using this method are not suitable for long distances. Their main advantage is the low nominal error when estimating distances compared with TOF scanners.

- Triangulation

The light scattered from the laser's impact surface is collected from a vantage point distinct from the projected light beam. This light is focused onto a position-sensitive detector. The knowledge of both projection and collection angles relative to a baseline determines the dimensions of a triangle, and hence the (x, y, z) coordinates of a point on a surface.

This method is suitable for close-range applications, providing very accurate measurement results.

This project has received funding from the European Union's Horizon 2020 research and innovation programme under grant agreement No 958171. © 2021
IM-SAFE-Project | TNO, The Netherlands, All right reserved |

- Angle Measurement

The transmitted laser beam must be deflected all around the FOV of the scanner. In order to achieve that, optomechanical scanners are implemented. In TLS, horizontal deflection (around vertical axis) is achieved using of optomechanical devices, while vertical deflection (around horizontal axis) is based on using spinning or oscillating mirrors. The scanning process must be fast enough to compensate the rotation around the vertical axis. In case of mobile devices, it must be done to compensate the forward velocity of the vehicle for achieving the desired point cloud density. Oscillating mirrors rotate back and forth and their scanning speed depends on the inertia of the moving parts and the available power of the scanner drives because the mirrors experience accelerated movements.
Another solution is the use of mirror scanners. These can develop the scan rotating constantly and in the same direction or in oscillating mode. The first one is more suitable for achieving a greater FOV.

7.2.2 Types

To carry out surveys on ground, there are two types of laser scanner systems: Terrestrial Laser Scanner, Mobile Laser Scanner and Aerial Laser Scanner.

- Terrestrial Laser Scanner (TLS)

Static scanners, also known as Terrestrial Laser Scanners, were the first type of laser scanners used as surveying for measuring 3D point coordinates. These scanners use high-speed rotating mirrors to deflect the laser beam in the vertical plane, measuring elevation angles. With motors rotating the head around the vertical axis, they can provide measurements at different azimuth angles. Normally, these mirrors can rotate 360º. After performing the survey, a very dense point cloud is obtained in the spherical coordinate system, which will be turned into Cartesian coordinates by most of the scans. The point clouds will be formed by the mentioned coordinates (x, y, z) for each single point, as well as by some other attributes, described later in this document (Riveiro, González-Jorge, Conde, & Puente, 2016). A representation of this can be seen in *Figure 7.3*.

This project has received funding from the European Union's Horizon 2020 research and innovation programme under grant agreement No 958171.

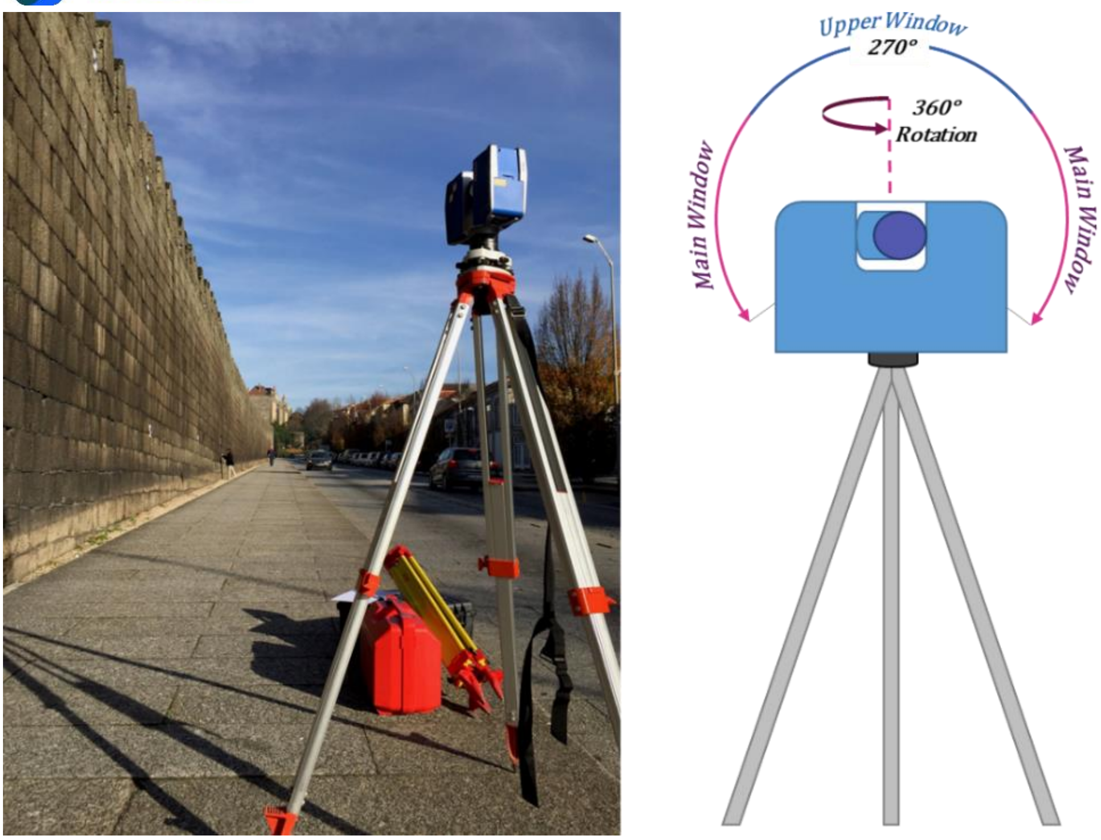

Figure 7.3 – FARO Focus3D X 330 (left); TLS rotation angles (right)

- Mobile Laser Scanner (MLS)

Mobile Laser Scanners are the more appropriate platforms for scanning large infrastructures since TLS required too much time to create their 3D models. Yet, there are two different modes of performing this type of surveys, differing in the imaging procedure, even though the sensors are identical:

- Stop-and-go mode (SAG)

At least one laser scanner is placed on a vehicle-borne platform. During the scanning process, the position and orientation of the scanner does not change, remaining static. After every scan, the vehicle changes its position, and the next scan is performed. For each temporary position of the scanner reference point together with the orientation of the scanner axes a new coordinate system is defined. In this way, each point cloud results to be geometrically consistent with the others. With respect to a unique coordinate system there are six geometric degrees of freedom: the three coordinates of the scanner reference point and the three rotation angles of the scanner axes.

- On-the-fly mode

The vehicle moves along a predefined trajectory while the laser scanner is continuously working. In order to do that, the Mobile Mapping System (MMS) is formed by the vehicle itself (car) and the laser scanner. Also, the monitoring of the position of the scanning system is possible thanks to the use of a Global Navigation Satellite System (GNSS), combined with an Inertial Measurement System (IMS) and Distance Measurement Indicators (DMI). With this, the so-called trajectory followed by the platform is

This project has received funding from the European Union's Horizon 2020 research and innovation programme under grant agreement No 958171.

registered into a global coordinate system. The 3D point cloud is created when the laser scanner is synchronized with the navigation system. In contrast with the previous instruments, in MLS the laser beam is deflected only in one axis, so that the point cloud being recorded is contained in one plane. Thanks to the vehicle motion, a dense 3D point cloud is obtained as the scanned profiles are ranged along the trajectory. Nowadays, most of the systems cover a field of view (FOV) of 360º.

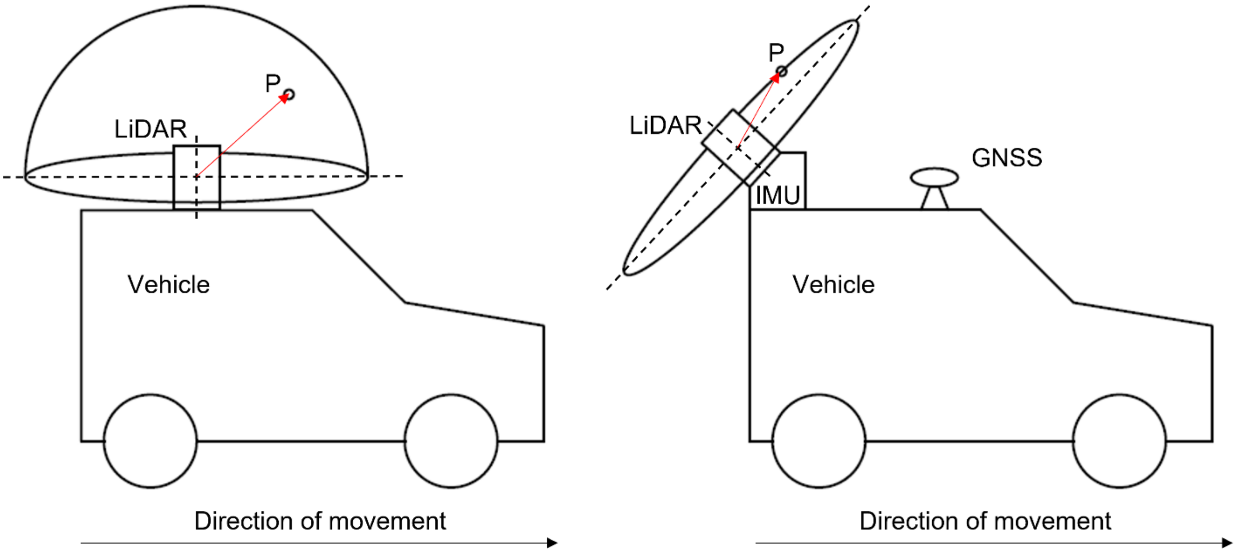

Figure 7.4 – Acquisition modes: Stop-and-go (left) and on-the-fly (right)

The difference between these two surveying modes, as shown in *Figure 7.4*, lies in the registration process. While in the first case, the registration between the different scans performed needs from tie points referenced externally (e.g. GPS), in the second case this is done thanks to the GPS/IMU module already part of the equipment (Riveiro, González-Jorge, Conde, & Puente, 2016).

7.2.3 Process/event to be detected or monitored

Laser scanner technology is employed to acquire comprehensive data about a real site, namely its layout, shape and other information regarding its general appearance, and use it to produce a virtual representation of the scene. A single scan is discrete and thus limited to a particular time, so in order to record the effects of an event or some process that occurred on the site, several scans must be acquired at different times to be compared.

7.2.4 Physical quantity to be measured

- Geometric information

This project has received funding from the European Union's Horizon 2020 research and innovation programme under grant agreement No 958171. © 2021

Laser scanning is used to capture the geometry of the structure. This geometry is represented by 3D Euclidean coordinates that constitute a 3D point cloud. An example of a point cloud is shown in *Figure 7.5*.

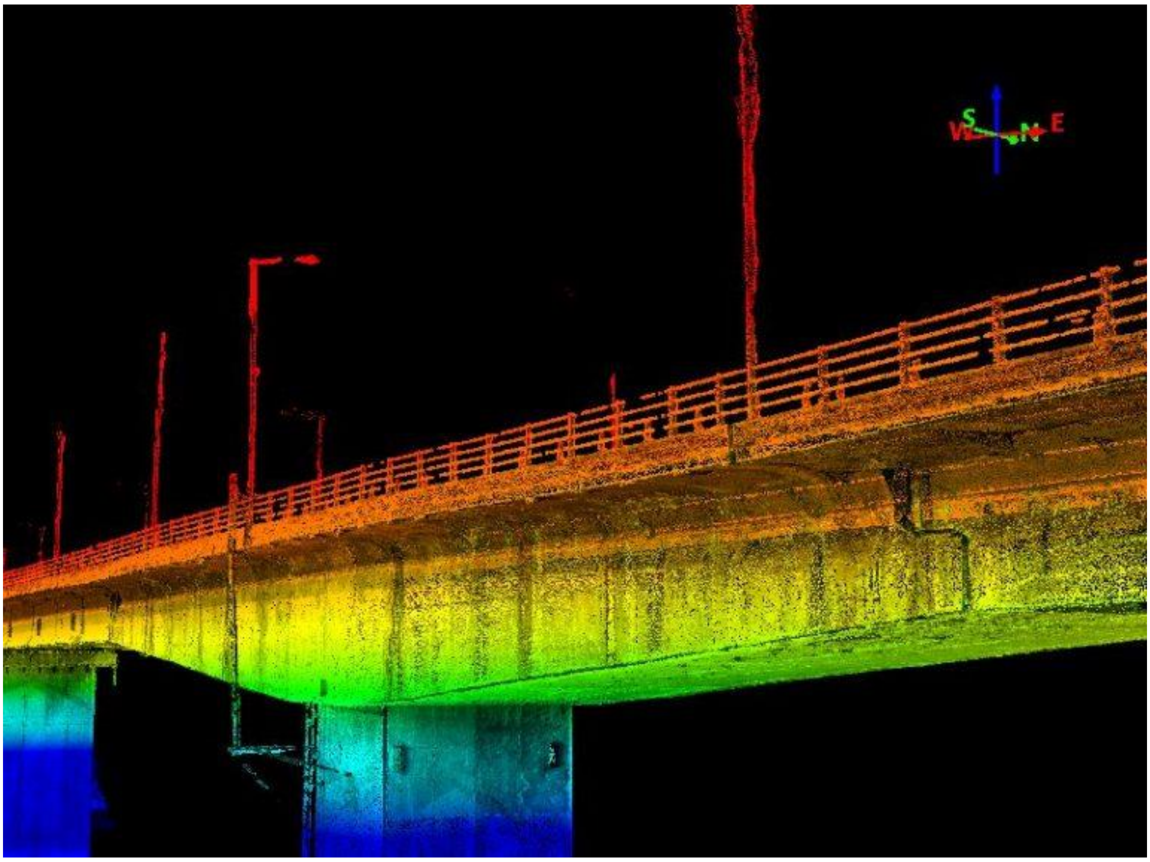

Figure 7.5 – Point cloud example. (Digital technologies can enhance climate resilience of critical infrastructure – infrastructuResilience, 2021)

Aside from the 3D geometry obtained with laser scanners, additional physical characteristics, such as those described below, are calculated and assigned to the individual points of the point cloud.

Radiometric information:

- Intensity data

Laser scanners are active and remote sensors. They can emit the laser beam at a specific wavelength in the electromagnetic spectrum. Depending on the instrument, green or near infrared wavelengths are used. Recently, systems including several lasers at different wavelengths have been developed to provide multispectral measurements.

The spectral reflectance (intensity data) is the amount of energy reflected by an object's surface when receiving a laser beam depending on the characteristics of the material. This backscatter generated after the collision is recorded by most LiDAR instruments as a function of time (Riveiro, González-Jorge, Conde, & Puente, 2016), (Soilán, y otros, 2019). Depending on the objects' surface there might be several function peaks, each of them representing an object measured at a different range.

This project has received funding from the European Union's Horizon 2020 research and innovation programme under grant agreement No 958171.

Also, it is important to highlight that LiDAR intensity values can vary depending on the weather circumstances.

- Pulse Returns

The return power is recorded as a function of time after the transmission. The return number is the number of times the emitted laser pulse returns to the LiDAR sensor. The transmission function will be recorded with as many peaks as objects reached by the laser beam, located at different ranges.

- Waveform

The LiDAR pulse can be recorded as separate returns (discrete return LiDAR), or as one continuous wave saving the whole return (full-waveform LiDAR). In this way, many objects can be measured from a single emission.

7.2.5 Induced damage to the structure during the measurement

Laser scanning is a non-destructive and non-contact technology. In consequence, it does not induce any damage to the structure.

7.2.6 General characteristics

7.2.6.1 Measurement type (static or dynamic, local or global, short-term or continuous, etc.)

The captures recorded with laser scanning belong to a given point in time, so they can be described as discrete measurements. Also, the model generated may represent the whole structure or just a given part depending on the method used.

7.2.6.2 Measurement range

- Time-of-Flight (TOF): Up to several kilometres (Soilán, y otros, 2019).
- Phase Measurement: Up to 300 meters (Soilán, y otros, 2019).
- Triangulation: Up to 5-10 meters

7.2.6.3 Measurement accuracy

- Time-of-Flight (TOF): 5 mm
- Phase Measurement: 2-3 mm
- Triangulation: 20μm (Paulus, Eichert, Goldbach, & Kuhlmann, 2014).

7.3 Background (evolution through the years)

LiDAR technology started to grow in the 1960s with several applications in geosciences. Years later, land surveying applications appeared in the picture thanks to the use of airborne profilometers. This equipment resulted to be useful for deriving the vegetation height evaluating the returned signal (LINK, G, & J, 1981). During the 1980s and 1990s, the use of laser scanning for environmental and land surveying applications increased. In the second part of the 1990s, civil engineering related applications

This project has received funding from the European Union's Horizon 2020 research and innovation programme under grant agreement No 958171.

started to arise, but it was not until the last part of the century and the beginning of the new one when the first terrestrial devices for 3D digitalization performance appeared. From this point, numerous applications for different fields quickly raised (Riveiro, DeJong, & Conde, Automated processing of large point clouds for structural health monitoring of masonry arch bridges, 2016), and TLS proved to be the appropriate technology to use when detailed 3D models were required. With the evolution of technology, the resolution and quality of data given by laser scanning devices have been improved. And so, in these final years, mobile mapping systems are arising in order to perform high resolution surveys of large infrastructures (tunnels, roads, urban modelling…) in a short period of time.

Nowadays, the main bottleneck for LiDAR technology is processing the large amounts of data acquired with laser scanning devices. Throughout the years, many tools have been developed for point cloud data processing. Most of them depend on manual or semi-automatic operations that have to be performed by a specialist in the field of geomatics. The challenge now is to develop tools for the efficient automation of data processing, using the information provided by ALS, MLS or TLS devices.

With the emergence of machine learning algorithms, tedious and hard processing tends to disappear. These tools allow not only the development of advanced, efficient and intelligent processing but also interpretation of data. One of the main objectives exploited is obtaining inventories for road, railway or urban management. Now, this has evolved and the trend is to obtain spatial models of infrastructures based on the fusion of geometric and radiometric data and monitoring the infrastructure behaviour and changes through the years. These models can be used as a geometrical basis for BIM (Building Information Modelling) and AIM (Asset Information Model) applications, allowing to have not only as-design representations of the asset but also as-built and as-operate models and update these over time.

An example of a segmented point cloud is shown in *Figure 7.6*.

This project has received funding from the European Union's Horizon 2020 research and innovation programme under grant agreement No 958171.

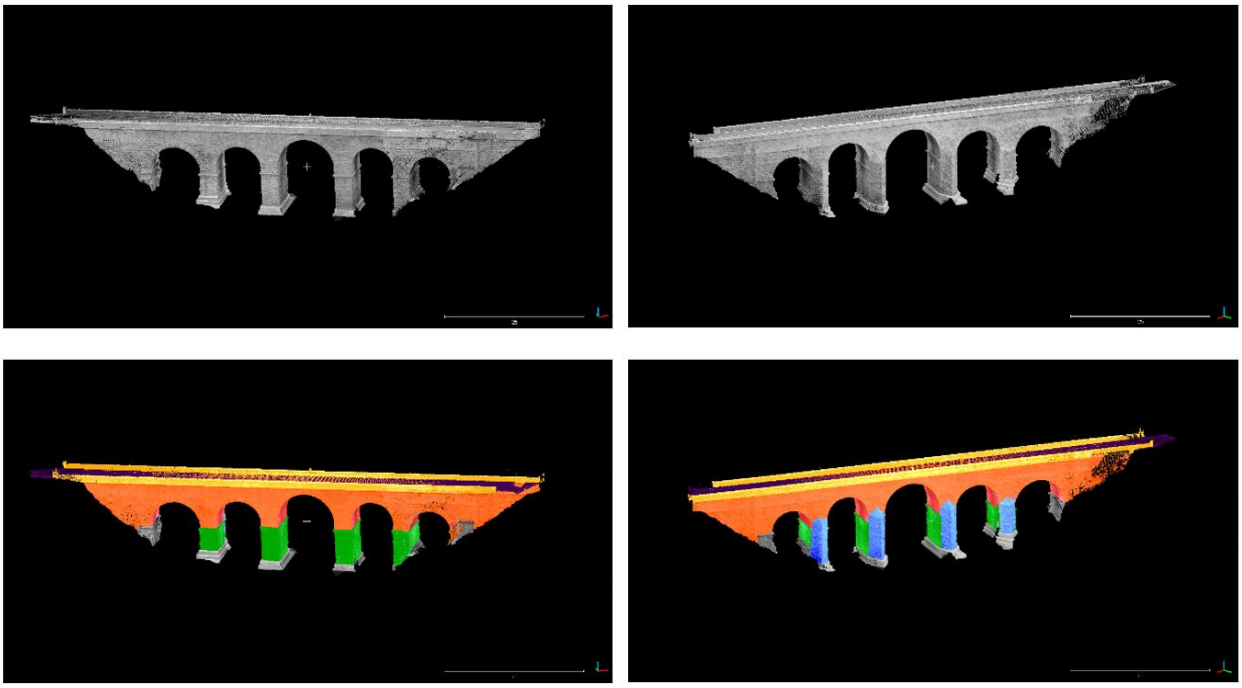

Figure 7.6 – Segura's roman bridge segmentation (Downstream and Upstream) (LINK, G, & J, 1981)

Thanks to the information extracted with LiDAR systems, existing deformations in the structures can also be detected and later related with their causing loads in their virtual model. This will help to monitor the structural integrity and the origin of damage (LINK, G, & J, 1981). LiDAR data can be used in finite-element analysis (Kang, Lee, Park, & Lee, 2007), (Park, Lee, Adeli, & Lee, 2007), but the data can also be processed directly. To this end, new algorithms for pathology or damage detection need to be developed. Some of the applications are crack detection (Laefer, Gannon, & Deely, Reliability of crack detection methods for baseline condition assessments, 2010), (Laefer, Truong-Hong, Carr, & Singh, 2014), general damage identification (Sanchez-Rodríguez, Riveiro, Conde, & Soilán, 2018), (Sánchez, y otros, 2019), (Chen, Truong-Hong, Laefer, & Mangina, 2018), (Li & Cheng, 2018), (Conde, Del Pozo, Riveiro, & González-Aguilera, 2016), geometrical variations (Yoon, Sagong, Lee, & Lee, 2009), (Zhou, y otros, 2017) and many others to be developed from now and with the evolution of technology.

Although research is continuously updating about automation of data processing, a general and robust methodology is still needed in order to definitely implement LiDAR as a basic tool for civil engineering purposes. As Petrie and Toth (2008) said, laser scanning is probably "the most important geospatial data acquisition technology that has been introduced since the last millennium'' (Riveiro, DeJong, & Conde, Automated processing of large point clouds for structural health monitoring of masonry arch bridges, 2016).

This project has received funding from the European Union's Horizon 2020 research and innovation programme under grant agreement No 958171.

7.4 Performance

7.4.1 General points of attention and requirements

7.4.1.1 Design criteria and requirements for the design of the survey

Survey planning with laser scanner involves: selection of the suitable device (TLS, MLS or ALS); definition of the suitable scanning positions or trajectory; preparation and calibration of the equipment; definition of the working parameters (Maximum range, Pulse repetition frequency…).

Laser scanners are an active remote sensing technology, so surveys can be performed at night. Nevertheless, most of the surveys are planned during the day due to the use of optical cameras along with LS. In any case, it is important to consider the benefits of nightly surveying (less pedestrian and/or roadway traffic, less impact if interrupting the service of any infrastructure…).

A more detailed explanation on how to plan a survey may be consulted following reference (Asteris & Plevris, 2015).

7.4.1.2 Procedures for defining layout of the survey

The environment of the survey location must be thoroughly studied prior to the operation to identify the best positions for the equipment (in the case of TLS systems) or trajectory to follow (MLS) in order to register the sections of interest on the infrastructure and other assets that are object of the monitoring activity.

7.4.1.3 Design constraints (e.g. related to the measurement principles of the monitoring technologies)

It is important to take into account the vegetation in the survey area. This could be both a good and a bad issue when performing a survey. In some cases, vegetation would provoke occlusions of important areas in the infrastructure, so it would be better to acquire the data in leaf-off conditions. However, in some cases, it would be better to perform the survey during leaf-on campaigns to obtain better ground measurements (ALS).

Low reflectivity surfaces, glass and other transparent or translucent materials can also cause issues on laser detections, such as signal losses or multiple, conflicting signal returns.

7.4.1.4 Sensibility of measurements to environmental conditions

Since most of the LiDAR systems work with lasers in the NIR range, dust and vapor can severely affect the results of the measurements. Moreover, some sensors are sensitive to direct sunlight. These factors should be considered when choosing a date for performing the survey, since the weather conditions need to be specific.

7.4.2 Preparation

7.4.2.1 Procedures for calibration, initialization, and post-installation verification

Calibration procedures are carried out with the objective of adjusting the sensitivity of the sensor at different values.

This project has received funding from the European Union's Horizon 2020 research and innovation programme under grant agreement No 958171.

LiDAR sensors must be calibrated in terms of measured range to the target object and the angle of the rotating mirrors that deflect the laser beam in different directions, which are determined by encoders. The intensity of the returned beam measured by the receiver must be calibrated as well. The manufacturer is usually in charge of carrying out the calibration of this equipment.

The geometric calibration of the offsets measured between the different devices (LiDAR sensors, GNSS antennas, IMU, DMI) must be carried out as well to guarantee a correct point cloud referencing. For such task, a total station can be used.

In the case of MLS scanners, as they work as a component of a Mobile Mapping System, the navigation instruments must be calibrated and initialized as well. For each type of device, the procedures include:

- GNSS (Global Navigation Satellite Systems, such as GPS, Galileo or GLONASS): the MMS vehicle must initialize the recording of the trajectory. Depending on the navigation system, this must be done either by maintaining a static position for a minimum period of time or moving the vehicle, in both cases in a clear area to avoid obstacles that could interfere with the satellites' line of sight.
- IMU (Inertial Measurement Unit): the MMS vehicle has to be subjected to sudden movements so the IMU can record accelerations high enough to calibrate the system.
- DMI (Distance Measurement Instrument): to calibrate the device, the odometer is installed on one of the wheels of the vehicle, moving it then along a straight line of a known longitude.

7.4.2.2 Procedures for estimating the component of measurement uncertainty resulting from calibration of the data acquisition system (calibration uncertainty)

These parameters are determined by the system manufacturer.

7.4.2.3 Requirements for data acquisition depending on measured physical quantity (e.g. based on the variation rate)

These parameters are determined by the system manufacturer.

A more detailed explanation of these aspects can be found in (Riveiro, González-Jorge, Conde, & Puente, 2016), (Asteris & Plevris, 2015).

7.4.3 Performance

The surveys are taken in successive campaigns, so certain preparations and processing steps must be taken into account to perform the task correctly, and they must be always followed for the measurements to be coherent along the time.

- Global reference system (i.e.: Datum, reference ellipsoid, reference geoid for altitude)
- Sensor positions. (TLS case)
- Follow the same trajectory. (MMS case)
- Use same sensor to avoid discrepancies due to the quality of the measurement.

This project has received funding from the European Union's Horizon 2020 research and innovation programme under grant agreement No 958171.

- Make sure weather conditions are adequate in all cases.
- Remove mobile objects that may cause occlusions.
- Repeatability.

7.4.4 Reporting

Surveying campaign report usually include the following sections:

- Technical and performance specifications of the employed equipment.
- Description of the different phases/steps of the acquisition process
    - Assembling and of the equipment
    - Planification of the areas/scenes to be captured and the spots to place the LiDAR (in the case of TLS) or the route to follow (in the case of MLS)
    - Marking and measuring of control/support points, consisting of highly visible targets that are individually geo-referenced for later precision assessment and data adjustment.
    - Data acquisition, including:
        - Initialization and set-up of the equipment carried out prior to the survey.
        - Creation of files to store the survey results.
    - Data processing and verification:
        - For MLS, correction of the trajectory data according to a reference positioning station.
        - Point cloud adjustment according to control/support points.
- Results reporting
    - For MLS, trajectory calculation precision expressed as RMS error in meters for North, East and Down positions.
    - Differences in control/support positions when measured individually and in the point cloud.
    - Point density and distribution metrics.
- Conclusions

7.4.5 Lifespan of the technology (if applied for continuous monitoring)

Does not apply.

7.5 Interpretation and validation of results

7.5.1 Expected output (Format, e.g. numbers in a .txt file)

Point cloud with the values obtained in the survey. There are different formats, depending on the sensor, and several standards such as .las, .laz (American Society for Photogrammetry & Remote Sensing, 2013) or .bin (BIN File Extension - What is .bin and how to open? - ReviverSoft, 2021).

Point clouds are organized in such a way that each point has as many attributes as the LiDAR used is able to acquire. Some of these are:

- Coordinates of the points expressed in a reference axis.
- Intensity data
- Number of recorded pulse returns and/or waveform
- LiDAR ID that collected the point
- Scanning angle

This project has received funding from the European Union's Horizon 2020 research and innovation programme under grant agreement No 958171.

- Timestamp

7.5.2 Interpretation

- Coordinates: location in the space of the measured point.
- Intensity data: reflectivity of the measured point.
- Pulse returns and waveform: energy intensity belongs to a single beam returned to the sensor over time. Pulse returns are the maximums of this curve energy intensity over time.
- LiDAR ID: ID of the LiDAR that made the measurement of the point.
- Scanning angle: position register by the decoder when the measurement was made.
- Timestamp: time at which the measurement was made.

7.5.3 Validation

7.5.3.1 Specific methods used for validation of results depending on the technique

Distances between the data and a reference. Visual supervision.

7.5.3.2 Quantification of the error

The error is quantified by analysing the characteristic points of the point cloud. These points are compared with reference points, quantifying their differences.

7.5.3.3 Quantitative or qualitative evaluation

Quantitative and qualitative evaluation is applicable.

The qualitative validation consists of human visual supervision of the point cloud recorded. This point cloud is compared with the real environment to check if the data obtained is visually correct.

The quantitative validation requires the usage of a more precise sensor to measure characteristic points of the scene. This allows to have high fidelity measures of those points and use them to quantify the error and make the validation.

7.5.4 Detection accuracy

Changes in the accuracy of point clouds are noticeable regarding the equipment with which they were acquired. Depending on the source of data, the errors registered with laser scanners can vary from 2 mm to 200 cm.

There are three types of errors leading to low accuracy (in general) in laser scanners:

- Laser range error: Error when measuring the distance to an object. It is different for every scanner and can be corrected by recalibrating the scanner (by the manufacturer or a specialist in the field).

This project has received funding from the European Union's Horizon 2020 research and innovation programme under grant agreement No 958171.

- Range noise: Measure of the deviation of single readings from the real value within a sample of measurements. It is conditioned by the distance to the object to be scanned and the reflectivity of the object's material.
- Mechanical error: Difference between the measured and actual horizontal and vertical angles (angular error). It is caused by the mechanical devices forming the laser scanner (mirrors and servos).

The georeferencing devices in charge of the positioning of the 3D data are also a key issue when performing a laser scanning survey. This is supported by GNSS (Global Navigation Satellite System) and INS (Inertial Navigation System) systems that require a specific planning for every measurement campaign. These systems may result in invalid coordinates for the GNSS base station(s), misalignment of the INS with the LiDAR scanner, or a software failure at coordinate conversions. These cause systematic errors that may be identified by sensor calibration, comparing LiDAR with known reference data or additional control operations (RIEGL - RIEGL Laser Measurement Systems, 2021).

It is important to highlight that accuracy depends not only on the equipment, but also on the geometry of the 3D scenario under study and on the environmental conditions. This affects to the performance of the trajectory and point cloud computation algorithms, and so a specific value of accuracy cannot be given as an answer. The atmospheric condition can also have undesired effects in the LiDAR performance that could lead to noisy measurements (Filgueira, González-Jorge, Lagüela, Díaz-Vilariño, & Arias, 2017).

An example of a MLS is shown in *Figure 7.7*.

Figure 7.7. Lynx Mobile Mapper system (Puente, González-Jorge, Riveiro, & Arias, 2013)

7.6 Advantages

- Big amounts of data (Big Data)
- Short data acquisition time
- High accuracy
- Day and night operation (active sensor)
- Easy integration with other technologies (RGB, Thermography…)

This project has received funding from the European Union's Horizon 2020 research and innovation programme under grant agreement No 958171. © 2021

- Access to unreachable areas
- [MLS] Continuous data acquisition

7.7 Disadvantages

- Need of experts for surveys' performing
- Need for large data storage
- Not many automated process
- High processing time
- Sensitive to other reflections (e.g. sunlight)
- [MLS] Reliance on navigation system performance for point referencing
- [TLS] Limited to a single standpoint per acquisition
- Expensive data collection for small areas
- No international protocols

7.8 Possibility of automatising the measurements

Currently, it is not possible to automate the survey because an operator is needed to either transport/drive MLS platform or place the TLS at different spots.

7.9 Barriers

- Weather conditions must be favorable. It is not possible to make a survey on rainy or foggy days.
- Accessibility. Some places are not accessible for mobile mapping systems, so aerial mapping systems are needed for those cases.

7.10 Existing standards

Techniques and Methods 11–B4 (USGS).

7.11 Applicability

7.11.1 Relevant knowledge fields

- Civil Engineering
- Architectural heritage
- Geosciences
- Archaeology

This project has received funding from the European Union's Horizon 2020 research and innovation programme under grant agreement No 958171. © 2021

7.11.2 Performance Indicators

- Cracks (Jiang, Li, Jiao, Wang, & Wu, 2018).
- Crushing.
- Rupture (Riveiro, González-Jorge, Conde, & Puente, 2016).
- Spalling (Wu, y otros, 2019).
- Holes (Kazi, Sausthanmath, Meena, Gurlahosur, & Kulkarni, 2020).
- Displacement (Jo, Kim, Lee, Sohn, & Lim, 2018).
- Deformation (Jo, Kim, Lee, Sohn, & Lim, 2018).

7.11.3 Type of structure

- Bridges
- Buildings
  - Façade and annexed elements
  - Indoor spaces
- Walls
- Heritage sites
- Roads
- Urban environment
  - Street furniture
  - Sign posts and markers, traffic lights
  - Elements regarding accessibility for people with reduced mobility (Soilán, Riveiro, Sánchez-Rodríguez, & Arias, 2018), (Balado, Díaz-Vilariño, Arias, & Lorenzo, 2019).
- Railway network

7.11.4 Spatial scales addressed (whole structure vs specific asset elements)

With laser scanner all the area within the limits established by the maximum range of the system is registered in the point cloud, so the type of technology, either TLS or MLS, the specifications of the system employed (Field-of-View, range, accuracy, etc.) and its location in the site to be captured must be taken into account. Therefore, due planification is necessary to delimit the elements to be included in the scan, which can be either the whole structure or the parts of it that are of interest for the survey. For the case of the monitoring of specific asset elements, if it is not possible to scan them individually, the point cloud can be processed and segmented to isolate the elements of interest and create a new cloud including only them.

7.11.5 Materials

- Stone
- Concrete

This project has received funding from the European Union's Horizon 2020 research and innovation programme under grant agreement No 958171.

- Steel (high difficulty, under development)
- Glass and other transparent/translucent materials
- Wood
- Forests and other vegetation
- Environment in general

7.12 Available knowledge

7.12.1 Reference projects

- GIS-Based Infrastructure Management System for Optimized Response to Extreme Events of Terrestrial Transport Networks - SAFEWAY.

2018 - 2022 | European Union | H2020-MG-2016-2017 Ref. 769255-2

- Healthy and Efficient Routes In Massive Open-Data Based Smart Cities: Smart 3D Modelling: HERMES-S3D.

2014 - 2016 | MINECO | Ref. TIN2013-46801-C4-4-R

- SITEGI project: Application of Geotechnologies to Infrastructure Management and Inspection.

2011 - 2013 | Technology Centre for Industrial Development, CDTI.

7.12.2 Other

7.13 Bibliography

(n.d.). Retrieved junio 24, 2021, from http://www.bibliotecacpa.org.ar/greenstone/collect/facagr/index/assoc/HASH42bc.dir/doc.pdf

SMARTEC SA Branko Glisic, Daniele Inaudi. (2007). *Sensing tape for easy integration of optical fiber sensors in composite structures.* Manno, Switzerland : SMARTEC SA.

“Plataformas, sensores y canales.”. (n.d.). Retrieved Junio 24, 2021, from https://www.um.es/geograf/sigmur/teledet/tema03.pdf

27892, I. (2010). Vacuum technology - Turbomolecular pumps - Measurement of rapid shutdown torque. *Technical Committee of Vacuum technology*, 16.

A. Grosso, D. I. (2001, January). Monitoring of bridges and concrete structures with Fibre Optic Sensors in Europe. *IABSE Symposium, Seoul 2001: Cable-Supported Bridges - Challenging Technical Limits*.

AASHTO. (2004). *AASHTO R 37-04. Standard Practice for Application of Ground Penetrating Radar (GPR) to Highways.* Washington, DC, USA: American Association of State and Highway Transportation Officials.

Achievement Standard 91610. (n.d.). *Developing a conceptual design considering fitness for purpose in the broadest sense.* Retrieved from https://es.calameo.com/read/003415039afdc4054de72

This project has received funding from the European Union’s Horizon 2020 research and innovation programme under grant agreement No 958171.

ACI. (1998). *ACI 228.2R-98 (Reapproved 2004). Nondestructive Test Methods for Evaluation of Concrete in Structures.* Farmington Hills, MI, USA: American Concrete Institute.

Ahlborn, T. (2010). An Evaluation of Commercially Available Remote Sensors for Assessing Highway Bridge Condition. *Michigan Tech Transportation Institute*, 73.

Alexis Mendez, T. G. (2012). Overview of fiber optic sensors for NDT applications. *IV NDT Panamerican Conference Buenos Aires.* Buenos Aires. Retrieved from https://www.researchgate.net/publication/228340034_Overview_of_fiber_optic_sensors_for_NDT_applications

American Society for Photogrammetry & Remote Sensing. (2013). LAS SPECIFICATION VERSION 1.4 – R13.

Andrea Del Groso, K. B. (2001). *IABSE Symposium Report: Monitoring of bridges and concrete structures with Fibre optic sensors in Europe.* International Association for Bridge and Structural Engineering.

Andrea del Grosso, K. B. (2001). *Monitoring of Bridges and Concrete Structures with Fibre Optic Sensors in Europe.* IABSE Symposium Report .

Annan. (2023).

Annan, P. (2003). *GPR Principles, Procedures & Applications.* Mississauga, ON, Canada: Sensors and Software Inc.

Annan, P. (2003). *GPR Principles, Procedures & Applications.* Mississauga, ON, Canada: Sensors and Software Inc.

Annan, P. (n.d.). *GPR* .

Asteris, P., & Plevris, V. (2015, 7). Handbook of research on seismic assessment and rehabilitation of historic structures. *Handbook of Research on Seismic Assessment and Rehabilitation of Historic Structures*, 1-867.

ASTM. (2004). *Standard Test Method for Determining the Thickness of Bound Pavement Layers Using Short-Pulse Radar; Non-destructive testing of pavement structures; ASTM D4748.* West Conshohocken, PA, USA: ASTM.

ASTM. (2015). *ASTM D6087-08(2015)e1. In Standard Test Method for Evaluating Asphalt-Covered Concrete Bridge Decks Using Ground Penetrating Radar.* West Conshohocken, PA, USA: ASTM.

B10. (2008). *Document B10—Recommendation for Nondestructive Testing of Civil Engineering Structures by GPR.* Berlin, Germany: German Society for Non-Destructive Testing (DGZfP).

Balado, J., Díaz-Vilariño, L., Arias, P., & Lorenzo, H. (2019, 2). Point clouds for direct pedestrian pathfinding in urban environments. *ISPRS Journal of Photogrammetry and Remote Sensing, 148*, 184-196.

Balaguer, C., Montero, R., Victores, J., Martínez, S., & Jardón, A. (2014). Towards fully automated tunnel inspection: A survey and future trends. *Proceedings of the 31st International Symposium on Automation and Robotics in Construction and Mining.* Sydney, Australia.

Barr, S. H. (2009). Bridging the valley of death: Lessons learned from 14 years of commercialization of technology education. *Academy of management learning & education, 8*(3), 370-388.

BASt. (2007). *BASt-Report B55. Examination of GPR in Combination with Magnetic Techniques for the Determination of Moisture and Salinity of Concrete Bridge Decks*

This project has received funding from the European Union's Horizon 2020 research and innovation programme under grant agreement No 958171.

with Asphalt Cover. Bundesanstalt für Straßenwesen: Federal Highway Research Institute.

BAUMER. (2021, 12 10). *BAUMER* . Retrieved from Passion for sensors : https://www.baumer.com/medias/__secure__/Baumer_Fiber-optic-sensors-to-detect-liquid-levels-and-leakage-of-fluids_EN_0610_AR.pdf?mediaPK=8837757272094

Bazovsky, I. (2004). *Reliability theory and practice.* Courier Corporation.

Benedetto, A., & Pajewski, L. (2015). *Civil Engineering Applications of Ground Penetrating Radar.* New York, NY, USA: Springer International.

Berger, M., Moreno, J., Johannessen, J., Levelt, P., & Hanssen, R. (2012). ESA's sentinel missions in support of Earth system science. *Remote Sensing of Environment, 120*, 84-90.

Bertolino, M., & Tanzi, T. (2020). Towards 3D Simulation for Disaster Intervention Robot Behaviour Assessment. *Adv. Radio Sci., 18*, 23–32.

BIN File Extension - What is .bin and how to open? - ReviverSoft. (2021, 12 17). Retrieved from https://www.reviversoft.com/file-extensions/bin

Chang, R. (2004). IEEE Intelligent TranSPOrtation Systems. *San Diego, USA, October 3-6*, 971.

Chen, S., Truong-Hong, L., Laefer, D., & Mangina, E. (2018). Automated Bridge Deck Evaluation through UAV Derived Point Cloud. *undefined*.

Conde, B., Del Pozo, S., Riveiro, B., & González-Aguilera, D. (2016, 6). Automatic mapping of moisture affectation in exposed concrete structures by fusing different wavelength remote sensors. *Structural Control and Health Monitoring, 23*(6), 923-937. Retrieved from https://onlinelibrary.wiley.com/doi/full/10.1002/stc.1814

D. Inaudi, S. V. (1999, February 12-13). SOFO: Structural Monitoring with Fiber Optic Sensors . *FIB, Monitoring and Safety Evaluation of Existing Concrete Structures*.

Daniels , D. J. (2004). *Ground Penetrating Radar.* London, UK: The institution of Electrical Engineers.

David Krohn, T. M. (2014). *Fiber Optic Sensors Fundamentals and Applications* . Washington: SPIE PRESS .

Di, L. (2017). Standards, Critical Evaluation of Remote Sensing. *Encyclopedia of GIS, Springer International Publishing*, 2187–2196.

Digital technologies can enhance climate resilience of critical infrastructure – infrastructuResilience. (2021, 12 17). Retrieved from http://www.infrastructuresilience.com/lake-polyfytos-bridge/

DMRB3.1.7. (2006). *Department for Transport, Highway Agency. DMRB 3.1.7.: Design Manual for Roads and Bridges, Advice Notes on the Non-Destructive Testing of Highway Structures—Advice Note 3.5 BA 86/2006: Ground Penetrating Radar (GPR).* Birmingham, UK: Department for Transport, Highway Agency.

DMRB7.3.2. (2008). *DMRB 7.3.2.: Design Manual for Roads and Bridges, Data for Pavement Assessment—Annex 6 HD 29/2008: Ground-Penetrating Radar (GPR).* Birmingham, UK: Highway Agency.

Elliott, J., Walters, R., & Wright, T. (2016). The role of space-based observation in understanding and responding to active tectonics and earthquakes. *Nature communications, 7*(1), 1-16.

This project has received funding from the European Union's Horizon 2020 research and innovation programme under grant agreement No 958171. © 2021

Fidanboylu, K. E. (2009). Fiber Optic Sensors and their applications. *5th Intenrational Advanced Technologies Symposium* . Karabuk: Fauniversity .

Filgueira, A., González-Jorge, H., Lagüela, S., Díaz-Vilariño, L., & Arias, P. (2017, 1). Quantifying the influence of rain in LiDAR performance. *Measurement, 95*, 143-148.

Garcia-Fernandez, M., Alvarez-Lopez, Y., & Las Heras, F. (2019). Autonomous airborne 3D SAR imaging system for subsurface sensing: UWB-GPR on board a UAV for landmine and IED detection. *Remote Sens., 11*(2357).

Garcia-Fernandez, M., Alvarez-Lopez, Y., & Las Heras, F. (2019). Autonomous airborne 3D SAR imaging system for subsurface sensing: UWB-GPR on board a UAV for landmine and IED detection. *Remote Sens, 11*(2357).

Gibb, S., La, H., Le, T., Nguyen, L., Schmid, R., & Pham, H. (2018). Nondestructive evaluation sensor fusion with autonomous robotic system for civil infrastructure inspection. *J. Field Robot., 35*, 988–1004.

Glisic, B. (2000). Fibre optic sensors and behaviour in concrete at early age . *PhD thesis*. Switzerland: Laboratory of Stress Analysis (IMAC) Swiss Federal Institute of Technology .

H.Hartog, A. (2017). An Introduction to Distributed Optical Fibre Sensors. In A. H.Hartog, *An Introduction to Distributed Optical Fibre Sensors* (pp. 115-128). Boca Raton, United States: CRC Press Taylor & Francis Group.

Héder, M. (2017). From NASA to EU: the evolution of the TRL scale in Public Sector Innovation. *The Innovation Journal, 22*(2), 1-23.

Howlader, M., Sattar, T., & Dudley, S. (2016). Development of a Wall Climbing Robotic Ground Penetrating Radar System for Inspection of Vertical Concrete Structures. *Int. J. Mech. Mechatron. Eng., 10*, 1382–1388.

Hugener, C. M. (2014). *"Fit-for-purpose" infrastructure strategy. How companies can manage increasing IT demands.* Retrieved from https://www.strategyand.pwc.com/gx/en/insights/2014/fit-for-purpose-infrastructure-strategy/strategyand-fit-for-purpose-infrastructure-strategy.pdf

Hugenschmidt, J., Kalogeropoulos, A., Soldovieri, F., & Prisco, G. (2010). Processing strategies for high-resolution GPR concrete inspections. *NDT E Int., 43*, 334–342.

Hugenschmidt, J., Kalogeropoulos, A., Soldovieri, F., & Prisco, G. (2010). Processing strategies for high-resolution GPR concrete inspections. *NDT E Int., 43*, 334–342.

Hülsenbeck. (1926). *Germany Patent No. 489434.*

Instytut Maszyn Przepływowych im. Roberta Szewalskiego PAN. (2011, March). Specyfikacja Istotnych warunków zamówienia (SIWZ). *Dostawa czujników światłowodowych i przetworników* . Gdańsk , Polska .

ISO 11352. (2021). Water quality — Estimation of measurement uncertainty based on validation and quality control data. *Technical Committee of Physical, chemical and biochemical methods*, 26.

ISO 12718. (2019). Non-destructive testing - Eddy current testing - Vocabulary. *Technical Committee of Eddy current testing*, 39.

ISO 13372. (2012). Condition monitoring and diagnostics of machines - Vocabulary. *Technical Committee of Condition monitoring and diagnostics of machine systems*, 15.

ISO 13822. (2010). Bases for design of structures - Assessment of existing structures. *Technical Committee of Reliability of structures*.

This project has received funding from the European Union's Horizon 2020 research and innovation programme under grant agreement No 958171. © 2021

ISO 17123. (2014). *Optics and optical instruments - Field procedures for testing geodetic and surveying instruments - Part 1: Theory.* Technical Committee of Geodetic and surveying instruments.
ISO 19159. (2014). *Geographic information - Calibration and validation of remote sensing imagery sensors and data - Part 1: Optical sensors.* Technical Committee of Geographic information.
ISO 19262. (2015). Photography — Archiving Systems — Vocabulary. *Technical Committee of Photography*, 44.
ISO 19345. (2019). Petroleum and natural gas industry - Pipeline transportation systems - Pipeline integrity management specification . *Technical Committee of Pipeline transportation systems*, 108.
ISO 1998. (1998). Petroleum industry — Terminology — Part 1: Raw materials and products. *Technical Committee of Petroleum and related products, fuels and lubricants from natural or synthetic sources*.
ISO 23907. (2019). Sharps injury protection - Requirements and test methods - Part 2: Reusable sharps containers. *Technical Committee of devices for administration of medicinal products and catheters*, 17.
ISO 27892. (2010). Vacuum technology - Turbomolecular pumps - Measurement of rapid shutdown torque. *Technical Committee of Vacuum technology*, 16.
ISO 3534. (2006). Statistics - Vocabulary and symbols - Part 1: General statistical terms and terms used in probability. *Applications of statistical methods*, 105.
ISO 7078. (2020). *Buildings and civil engineering works - Procedures for setting out, measurement and surveying - Vocabulary.* Technical Committee of Terminology and harmonization of languages.
ISO 7078. (2020). Buildings and civil engineering works — Procedures for setting out, measurement and surveying — Vocabulary. *Technical Committee of Terminology and harmonization of languages*, 34.
ISO 9001:2015. (n.d.). *Quality management systems — Requirements*.
ISO 99. (2007). International vocabulary of metrology - Basic and general concepts and associated terms (VIM). *Technical Committee of Management Board*, 92.
J Carr, J. (1993). Sensors & Circuits: Sensors, Transducers, & Supporting Circuits for Electronic Instrumentation Measurement and Control. *Prentice Hall*.
J. Biliszczuk, W. B. (2009). System monitorowania mostu w Puławach. *Mosty 4* , pp. 12-17.
Jafarov, E., Parsekian, A., Schaefer, K., Liu, L., Chen, A., Panda, S., & Zhang, T. (2017). Estimating active layer thickness and volumetric water content from ground penetrating radar measurements in Barrow, Alaska. *Geoscience Data Journal*, *4(2)*, 72-79.
Jiang, H., Li, Q., Jiao, Q., Wang, X., & Wu, L. (2018, 9). Extraction of Wall Cracks on Earthquake-Damaged Buildings Based on TLS Point Clouds. *IEEE Journal of Selected Topics in Applied Earth Observations and Remote Sensing, 11*(9), 3088-3096.
Jo, H. C., Kim, J., Lee, K., Sohn, H.-G., & Lim, Y. M. (2018). Non-contact strain measurement for laterally loaded steel plate using LiDAR point cloud displacement data. *Sensors and Actuators A: Physical, 283*, 362-374.
Jol, H. M. (2009). *Ground Penetrating Radar: Theory and Applications.* Amsterdam, The Netherlands: Elsevier Science.

This project has received funding from the European Union's Horizon 2020 research and innovation programme under grant agreement No 958171.

Jose Luis Santos, F. F. (2015). *Handbook of Optical Sensors.* Boca Raton: CRC Press Taylor & Francis Group.

Kang, D., Lee, H., Park, H., & Lee, I. (2007, 9). Computing Method for Estimating Strain and Stress of Steel Beams Using Terrestrial Laser Scanning and FEM. *Key Engineering Materials, 347*, 517-522. Retrieved from https://www.scientific.net/KEM.347.517

Kazi, A., Sausthanmath, A., Meena, S., Gurlahosur, S., & Kulkarni, U. (2020, 1). Detection of holes in 3D architectural models using shape classification based Bubblegum algorithm. *Procedia Computer Science, 167*, 1684-1695.

KEYENCE. (2021, 11 30). *Fibre optic sensors FS-N40 Series*. Retrieved from Digital Fibre optic Sensor: https://www.keyence.co.uk/products/sensor/fiber-optic/fs-n40/downloads/

Khatereh, V. (2012). Evaluation of commercially available remote sensors for highway bridge condition assessment. *ournal of Bridge Engineering*, 10.

Laefer, D. F., Gannon, J., & Deely, E. (2010). Reliability of crack detection methods for baseline condition assessments. *Journal of Infrastructure Systems, 16*(2), 129-137.

Laefer, D. F., Truong-Hong, L., Carr, H., & Singh, M. (2014). Crack detection limits in unit based masonry with terrestrial laser scanning. *Ndt & E International, 62*, 66-76.

Leimbach, G., & Löwy, H. (1910). *Germany Patent No. 237944.*

Leimbach, G., & Löwy, H. (1910). *Germany Patent No. 246836.*

Li, Q., & Cheng, X. (2018, 4). DAMAGE DETECTION FOR HISTORICAL ARCHITECTURES BASED ON TLS INTENSITY DATA. *The International Archives of the Photogrammetry, Remote Sensing and Spatial Information Sciences, XLII-3*(3), 915-921. Retrieved from https://doi.org/10.5194/isprs-archives-XLII-3-915-2018

Linford, N., Linford, P., Martin, L., & Payne, A. (2010). Stepped frequency ground-penetrating radar survey with a multi-element array antenna: Results from field application on archaeological sites. *Archaeological Prospection*.

LINK, L., G, C., & J, C. (1981). AIRBORNE LASER SYSTEMS USE IN TERRAIN MAPPING.

Loew, A., Bell, W., Brocca, L., Bulgin, C., Burdanowitz, J., Calbet, X., & Verhoelst, T. (2017). Validation practices for satellite-based Earth observation data across communities. *Reviews of Geophysics, 55*(3), 779-817.

Łukasz Bednarski, R. S. (2015). Wybrane zagadnienia monitorowania konstrukcji. *XXX Jubileuszowe Ogólnopolskie Warsztaty Pracy Projektanta Konstrukcji* (pp. 28-30). Szczyrk : Politechnika Krakowska, Akademia Górniczo-Hutnicza.

mapwaredev. (2020, Jun 4). *Understanding Errors and Distortion in Remote Sensing*. Retrieved Jun 24, 2021, from https://mapware.ai/blog/understanding-errors-and-distortion-in-remote-sensing/

Mathew kautzman, B. J. (2018). Calibration and testing of distributed fiber optic sensors for detection of high energy radiation . *Journal of Directed Energy* .

ME91/16. (2016). *ME91/16: Methodologies for the Use of Ground-Penetrating Radar in Pavement Condition Surveys.* Brussels, Belgium: Belgian Road 445 Research Centre.

Measures, R. M. (2001). *Structural Monitoring with Fiber Optic Technology* . Ontario: Institute of Aerospace Studies .

This project has received funding from the European Union's Horizon 2020 research and innovation programme under grant agreement No 958171.

Mei, Y. (2018, August). Error analysis for distributed fibre optic sensing tehcnology based on Brillouin scattering. USA: University of Cambridge, Department of Philosophy .

Narodowe Centurm Badań i Rozwoju, Politechnika Rzeszowska, . (2021, 12 08). *OptiDeck*. Retrieved from Inteligentny system pomostowy z kompozytów polimerowych do budowy i modernizacji drogowych obiektów mostowych: https://optideck.prz.edu.pl/

NASA's Earth Science Data Systems (ESDS). (n.d.). Retrieved Junio 24, 2021, from Standards and Practices: https://earthdata.nasa.gov/esdis/esco/standards-and-references#deprecated

NCHRP. (2017). *NCHRP Research Report 848. In Inspection Guidelines for Bridge Post-Tensioning and Stay Cable Systems Using NDE Methods.* Washington, DC, USA: TRB's National Cooperative Highway Research Program.

NERVE-SENSORS. (2021, 11 30). *NERVE SENSORS Epsilon Rebar strain sensor*. Retrieved 11 30, 2021, from NERVE SENSORS: www.nerve-sensors.com

Nolan, J. (n.d.). *Analysis of measuring and monitoring requirements in ISO 9001:2015*. Retrieved from 9001 Academy: https://advisera.com/9001academy/knowledgebase/analysis-of-measuring-and-monitoring-requirements-in-iso-90012015/

Pajewski, L., Fontul, S., & Solla, M. (2019). Ground-penetrating radar for the evaluation and monitoring of transport infrastructures. In *Innovation in Near-Surface Geophysics. Instrumentation, Application, and Data Processing Methods.* Amsterdam, The Netherlands: Elsevier.

Pajewski, L., Fontul, S., & Solla, M. (2019). Ground-penetrating radar for the evaluation and monitoring of transport infrastructures. In *Innovation in Near-Surface Geophysics. Instrumentation, Application, and Data Processing Methods.* Amsterdam, The Netherlands: Elsevier.

Pajewski, L., Vrtunski, M., Bugarinovic, Ž., Ristic, A., Govedarica, M., Van der Wielen, A., . . . al., e. (2018). GPR system performance compliance according to COST Action TU1208 guidelines. *Ground Penetrating Radar*, *1*, 104–122.

Park, H. (2020). Convolutional neural network-based safety evaluation method for structures with dynamic responses. *xpert Systems with Applications*, 14.

Park, H. S., Lee, H., Adeli, H., & Lee, I. (2007). A new approach for health monitoring of structures: terrestrial laser scanning. *Computer-Aided Civil and Infrastructure Engineering, 22*(1), 19-30.

Paulus, S., Eichert, T., Goldbach, H., & Kuhlmann, H. (2014, 2). Limits of Active Laser Triangulation as an Instrument for High Precision Plant Imaging. *Sensors 2014, Vol. 14, Pages 2489-2509, 14*(2), 2489-2509. Retrieved from https://www.mdpi.com/1424-8220/14/2/2489/htm

Persico, R., Provenzano, A., Trela, C., Sato, M., Takahashi, K., Arcone, S., . . . S. Ebihara, K. W. (2015). *Recommendations for the safety of people and instruments in ground-penetrating radar and near-surface geophysical prospecting.* European Association of Geoscientists and Engineers, EAGE Publications.

Plati, C., Loizos, A., & Gkyrtis, K. (2020). Assessment of modern roadways using non-destructive geophysical surveying techniques. *Surveys in Geophysics, 41*, 395-430.

Puente, I., González-Jorge, H., Riveiro, B., & Arias, P. (2013, 2). Accuracy verification of the Lynx Mobile Mapper system. *Optics & Laser Technology*, *45*(1), 578-586.

This project has received funding from the European Union's Horizon 2020 research and innovation programme under grant agreement No 958171.

Pultarova, T. (2018, December). *The Evolution Of Earth Observation*. Retrieved Oct 22, 2021, from The Evolution Of Earth Observation: https://www.ingenia.org.uk/ingenia/issue-77/the-evolution-of-earth-observation

Qiang, L. (2013). Research on Data Correlation in Structural Health Monitoring System. *Advanced Materials Research*, 11.

R. B. Figuera, C. J. (2021). *Development of Advanced Fibre Optic Sensors to Monitor the Durability of Concrete and Reinforced Concrete Structures - SolSensors.* Universidade do Minho, INESC-TEC and Engiprojects, Lda.

Retrieved from http://www.eurosdr.net/

Radoi, A. (2021). Static and Dynamic Structural Health. *Romanian Journal of Transport Infraestructure*, 16.

Rafał Sieńko, Ł. B. (2016). Monitorowanie obiektów budowlanych w sąsiedztwie budowy . *Geoinzynieria* , pp. 60-65.

Regtien, P. (20014). *Measurement science for engineers.* Elsevier.

RIEGL - RIEGL Laser Measurement Systems. (2021, 12 17). Retrieved from http://www.riegl.com/

Riveiro, B., DeJong, M., & Conde, B. (2016, 12). Automated processing of large point clouds for structural health monitoring of masonry arch bridges. *Automation in Construction, 72*, 258-268.

Riveiro, B., González-Jorge, H., Conde, B., & Puente, I. (2016, 4). Laser Scanning Technology: Fundamentals, Principles and Applications in Infrastructure. *Non-Destructive Techniques for the Evaluation of Structures and Infrastructure*, 53-80. Retrieved from https://www.taylorfrancis.com/chapters/edit/10.1201/b19024-12/laser-scanning-technology-fundamentals-principles-applications-infrastructure-riveiro-gonzález-jorge-conde-puente

Romaniuk, R. S. (2001). *Miernictwo Światłowodowe Wydanie II Uzupełnione.* Warszawa: Instytut Systemów elektronicznych Politechnika Warszawska.

Rücker, W. (2006). Guideline for Structural Health Monitoring. *Federal Institute of Materials Research and Testing*, 63.

Saarenketo, T. (2012). *Recommendations for guidelines for the use of GPR in asphalt air voids content measurement. Mara Nord Project; Europeiska Unionen.* Brussels, Belgium.

Saarenketo, T., Maijala, P., & Leppäl¨, A. (2011). *Recommendations for Guidelines for the Use of GPR in Bridge Deck Surveys.* Publications of Mara Nord Project.

Samuel Vurpillot, D. I.-M. (1996, April 22). Smart Structures and Materials vol. 2719. *Bridge Monitoring by fiber optic deformation sensors: design, emplacemnet and results*. San Diego , USA: Society of Photo-Optical Instrumentation Engineers.

Sánchez, A., Riveiro, B., Puente, I., Conde, B., Mendes, N., Cabaleiro, M., & Lourenço, P. (2019). Parameterization of Structural Faults in Large Historical Constructions for Further Structural Modelling Thanks to Laser Scanning Technology and Computer Vision Algorithms. *RILEM Bookseries, 18,* 351-359. Retrieved from https://link.springer.com/chapter/10.1007/978-3-319-99441-3_37

Sanchez-Rodríguez, A., Riveiro, B., Conde, B., & Soilán, M. (2018, 3). Detection of structural faults in piers of masonry arch bridges through automated processing of laser scanning

This project has received funding from the European Union's Horizon 2020 research and innovation programme under grant agreement No 958171.

data. *Structural Control and Health Monitoring, 25*(3), e2126. Retrieved from https://onlinelibrary.wiley.com/doi/full/10.1002/stc.2126

SBRCURnet. (2015). *Kennispaper: Slimme constructies voor slim beheer en onderhoud – praktijkcases.* Delft, The Netherlands.

Semyon, G. (2018). *Evaluating Measurement Accuracy: A Practical Approach.* Springer.

Setyawan, E. (2019, August 12). *Intermap*. Retrieved Dec 15, 2021, from Satellite Imagery: Resolution vs. Accuracy: https://www.intermap.com/blog/satellite-imagery-resolution-vs.-accuracy

SHM SYSTEMS. (2021, 12 7). *SHM Systems Projects*. Retrieved 12 7, 2021, from SHM Systems: https://www.shmsystem.pl/projects/

SHRP. (2013). *SHRP 2- report S2-R06A-RR-1. In Nondestructive Testing to Identify Concrete Bridge Deck Deterioration.* Washington, DC, USA: Transportation Research Board.

Simi, A., Manacorda, G., Miniati, M., Bracciali, S., & Buonaccorsi, A. (2010). Underground asset mapping with dualfrequency dual-polarized GPR massive array. *Proceedings 13rd International Conference on Ground-Penetrating Radar*, (pp. 1001-1005). Lecce, Italy.

SMARTEC SA, Branko Glisic, Daniele Posenato, Daniele Inaudi. (2007, May). Integrity monitoring of old steel bridge using fiber optic distributed sensors based on Brillouin scattering. *Proceedings of SPIE.* The International Society for Optical Engineering. doi:10.1117/12.716055

Soilán, M., Riveiro, B., Sánchez-Rodríguez, A., & Arias, P. (2018, 2). Safety assessment on pedestrian crossing environments using MLS data. *Accident; analysis and prevention, 111*, 328-337. Retrieved from https://pubmed.ncbi.nlm.nih.gov/29272790/

Soilán, M., Sánchez-Rodríguez, A., Del Río-Barral, P., Perez-Collazo, C., Arias, P., & Riveiro, B. (2019, 9). Review of Laser Scanning Technologies and Their Applications for Road and Railway Infrastructure Monitoring. *Infrastructures 2019, Vol. 4, Page 58, 4*(4), 58. Retrieved from https://www.mdpi.com/2412-3811/4/4/58/htm

Solla, M., González-Jorge, H., Lorenzo, H., & Arias, P. (2013). Uncertainty evaluation of the 1 GHz GPR antenna for the estimation of concrete asphalt thickness. *Measurement, 46*, 3032–3040.

Solla, M., Lorenzo, H., & Pérez-Gracia, V. (2016). Ground Penetrating Radar: Fundamentals, Methodologies and Applications in Structures and Infrastructures. In B. Riveiro, & M. Solla, *Non-Destructive Techniques for the Evaluation of Structures and Infrastructures.* EH Leiden, The Netherlands: CRC Press/Balkema.

Solla, M., Lorenzo, H., & Pérez-Gracia, V. (2016). Ground Penetrating Radar: Fundamentals, Methodologies and Applications in Structures and Infrastructures. In B. Riveiro, & M. Solla, *Non-Destructive Techniques for the Evaluation of Structures and Infrastructures.* EH Leiden, The Netherlands: CRC Press/Balkema.

Solla, M., Pérez-Gracia, V., & Fontul, S. (2021). A review of GPR application on transport infrastructures: troubleshooting and best practices. *Remote Sensing, 13*(672).

Sterckx, S., Brown, I., Kääb, A., Krol, M., Morrow, R., Veefkind, P., & Thorne, P. (2020). Towards a European Cal/Val service for earth observation. *International Journal of Remote Sensing, 41*(12), 4496-4511.

This project has received funding from the European Union's Horizon 2020 research and innovation programme under grant agreement No 958171.

Stryk, J., Matula, R., Pospíšil, K., Dérobert, X., Simonin, J., & Alani, A. (2017). Comparative measurements of ground penetrating radars used for road and bridge diagnostics in the Czech Republic and France. *Constr. Build. Mater.*, *154*, 1199–1206.

Surry, D. W. (n.d.).

Surry, D., & Stanfield, A. (2008). Performance technology. In J. M. Spector, *The Foundations of Instructional Technology*. M. K. Barbour & M. Orey.

T. H. Nguyen, T. V. (2014, February). Fluorescence based fibre optic pH sensor for the pH 10–13 range suitable for corrosion monitoring in concrete structures. *Sensors and Actuators B Chemical 191*, pp. 498-507.

Technology Readiness Level (TRL). (n.d.). Retrieved from HORIZON 2020 – WORK PROGRAMME 2014-2015.

Tomasz Siwowski, R. S. (2017, May). System monitorowania mostów kompozytowych z wykorzystaniem światłowodowych czujników odkształceń. *PROJECT COM-BRIDGE, DEMONSTRATOR+*, (pp. 50-53).

Tzinis, I. (2012). *Technology Readiness Level*. (NASA) Retrieved from National Aeronautics and Space Administration (NASA): https://www.nasa.gov/directorates/heo/scan/engineering/technology/technology_readiness_level

Udd, E. (2006). *Fiber Optic Sensors And Introduction for Engineers and Scientists.* New Jersey : John Wiley & Sons, Inc. .

USGS. (n.d.). Lidar Base Specification. Retrieved from moz-extension://d5b2584d-3b96-42e7-ab74-19371b183693/enhanced-reader.html?openApp&pdf=https%3A%2F%2Fpubs.usgs.gov%2Ftm%2F11b4%2Fpdf%2Ftm11-B4.pdf

W. Barcik, R. S. (2012). System monitorowania konstrukcji Mostu Rędzińskiego we Wrocławiu. *Mosty 2*, pp. 56-62.

Wai-Lok Lai, W., Dérobert, X., & Annan, P. (2018). A Review of Ground Penetrating Radar Application in Civil Engineering: A 30-Year Journey from Locating and Testing to Imaging and Diagnosis. *NDT E Int.*, *96*, 58–78.

Wu, H., Ao, X., Chen, Z., Liu, C., Xu, Z., & Yu, P. (2019). Concrete spalling detection for metro tunnel from point cloud based on roughness descriptor. *Journal of Sensors, 2019*.

Wu, K., Rodriguez, G., Zajc, M., Jacquemin, E., Clément, M., De Coster, A., & Lambot, S. (2019). A new drone-borne GPR for soil moisture mapping. *Remote Sens. Environ., 235*(111456).

Xie, F., Lai, W., & Dérobert, X. (2021). GPR uncertainty modelling and analysis of object depth based on constrained least squares. *Measurement*(109799).

Xie, X., Chen, Y., & Zhou, B. (2016). Data processing of backfill grouting detected by GPR in shield tunnel and research on equipment of GPR antenna. *Proceedings of the 16th International Conference on Ground Penetrating Radar*. Hong Kong, China.

Yang, W. (2006). A review of remote sensing data formats for earth system observations. *Earth Science Satellite Remote Sensing*, 120-145.

Yangí, L., Yang, G., Liu, Z., Chang, Y., Jiang, B., Awad, Y., & Xiao, J. (2018). Wall-climbing robot for visual and GPR inspection. *Proceedings of the 2018 13th IEEE Conference on Industrial Electronics and Applications (ICIEA)*, (pp. 1004–1009). Wuhan, China.

This project has received funding from the European Union's Horizon 2020 research and innovation programme under grant agreement No 958171.

Yoon, J., Sagong, M., Lee, J., & Lee, K. (2009, 3). Feature extraction of a concrete tunnel liner from 3D laser scanning data. *NDT & E International*, *42*(2), 97-105.

Zan, Y., Su, G., & Li, Z. (2016). A Train-mounted GPR System for Fast and Efficient Monitoring of Tunnel Health Conditions. *Proceedings of the 16th International Conference on Ground Penetrating Radar.* Hong Kong, China.

Zhou, Y., Wang, S., Mei, X., Yin, W., Lin, C., Hu, Q., & Mao, Q. (2017). Railway tunnel clearance inspection method based on 3D point cloud from mobile laser scanning. *Sensors*, *17*(9).

Zotti, M., & La Mantia, C. (2014). "Open data from earth observation: From big data to linked open data, through INSPIRE". *Journal of e-Learning and Knowledge Society, 10*(2).

This project has received funding from the European Union's Horizon 2020 research and innovation programme under grant agreement No 958171.

APPENDIX A8. Magnetic and electrical methods

8.1 Goal(s)

8.1.1 Main objective

Electromagnetic methods have been widely used in detection of corrosion in post-tensioned concrete elements. In case of bridge infrastructure management, the most used techniques are based on the electromagnetic pulse induction technology. Structural performance of concrete is affected by the arrangement of the rebars and their dimensions. Those include especially on-site tests with simple or advanced covermeters. In the future their functioning mode can be extended with detailed tomography of the structure with more advanced software. Pulse induction technologies are exploited primarily for qualitative analysis, such as localization of the rebars in structure, determination of their dimensions and diameter of cover.

On the other hand, there is another group of quantitative magnetic methods basing on magnetic field fluctuations and inverse magnetostrictive effect (Villary effect). From the point of view of bridge maintenance, the significant ones are methods based on magnetic field variation due to prestressing such as Magnetic Memory Method (MMM) or Pulsed Eddy Current Method (PEC). Those are also known in energy industry for determination of the most critical areas and equipment having stress concentration. The magnetic flux leakage method can be also used in structural health monitoring. One of the promising technology in area of magnetic methods is the iCAMM – Infrastructure Corrosion Assessment Magnetic Method, which is currently under studies and development. Details can be found in - (M. Mosharfari, 2020) (M. Mosharafi, 2018) (S.B. Mahbaz, 2017).

There are quite a few modifications of magnetic methods such as:

- Eddy Current Array Method (ECA), (D. C. Hurley, 1992) (Pelkner, Pohl, Erthner, Stegemann, & Kreutzbruc, 2015)
- Alternating Current Field Measurements (Herman & Duff, 2011), (A. Raine, 1999)

but those have minimal use in diagnostics of bridges and mostly used for diagnostics of power machinery components.

8.2 Description

8.2.1 Functioning mode

- Electromagnetic Pulse Induction Methods – by means of covermeters – search head generates the magnetic field on the tested area. The disturbance caused by the presence of the metal produces local change in field strength which is detected by the meter. LED Screen shows directly the proximity and location of the bars (British Standards Institution, 1988) (Singapore Institute of Standards and Industrial Research, 1992).

This project has received funding from the European Union's Horizon 2020 research and innovation programme under grant agreement No 958171.

- Magnetic Memory Method (MMM) – magnetic field is introduced in vicinity of prestressed or post tensioned steel and variations of the field due to loss of rebars cross-section from corrosion or fracture are monitored (Simon X Yang, 2018) (Karel Pospisil, 2021).

Details on the phenomena of magnetization can be found in (D.C., 1955) (Craik D.J., 1970) (Vlasov V., 2004)

- Magnetic Flux Leakage Method (MFL) - powerful magnet used to magnetize the conductive material under test. If there are defects such as corrosion or material loss — the magnetic field colloquially speaking - “leaks”. Probes incorporate a magnetic detector placed between the poles of the magnet where it can detect the leakage field. During inspection, a magnetic circuit of sorts forms between the part and the probe. The magnetic field induced in the part saturates it until it can no longer hold any more flux. The flux overflows and leaks out of the pipe wall and strategically placed sensors can accurately measure the three-dimensional vector of the leakage field. Probe have three sensors to accurately measure spatial components of the signal (Bhagi, 2012) (Maierhofer, 2010).

- Pulsed Eddy Current Response (PEC) - application of step voltage to a conductor, magnetic field develops around it. This field changes in intensity as the current alternates. If brought close to the first field, another conductor will have a current induced in it. If there are any flaws in the material then the eddy current will distort. The first conductor is an eddy current probe and the second is the test material. Secondary field is then detected by a sensing device, which typically can be either a magnetic sensor or a coil. The output signal of the sensing device is then passed to the next stage to be conditioned and processed where eventually features are extracted. Sensing devices can broadly be categorised into two different types, namely induction coils and magnetic sensors (Lebrun B, 1997). (Ian Eddy, 2020) (Maierhofer, 2010).

8.2.2 Types

- Electromagnetic Pulse Induction Methods – applied in covermeter and advanced covermeters (e.g. Profometers) with directional heads; search heads can be aligned parallel or perpendicular to the bar axis.

- Magnetic Memory Method (MMM) – applied in different monitoring instruments such as electromagnetic crack indicator, magnetometric stress concentration meter.

- Magnetic Flux Leakage Method (MFL) – computerized system such as scanner is a designed to detect, size and map under corrosion; applied influx meter.

- Pulsed Eddy Current Response (PEC) – applied in an assembled system with various equipment, components, and accessories including coil, direct current power supply, oscilloscope, function generator, amplifier.

8.2.3 Process/event to be detected or monitored

- Electromagnetic Pulse Induction Methods – maximum response on the surface of concrete during scanning with search head of covermeter.

- Magnetic Memory Method (MMM) – variations of the magnetic field due to loss of section from corrosion or fracture are monitored. Change of the magnetic susceptibility of a material when subjected to a mechanical stress, dependence of the magnetic field strength on the distance of the probe from the beginning of the measurement.

- Magnetic Flux Leakage Method (MFL) - variations of the magnetic field – sensors measure variations of the field due to the presence of flaws.

- Pulsed Eddy Current Response (PEC) – transient voltage response in time (s), the relationship between the diameter of rebar and long-time decay slope.

This project has received funding from the European Union’s Horizon 2020 research and innovation programme under grant agreement No 958171.

8.2.4 Physical quantity to be measured (e.g. actions, displacements, deformations, dynamic structural properties, material properties including mechanical, electrical and chemical properties, relative displacements of the two sides of a crack, etc.).

- Electromagnetic Pulse Induction Methods – the diameter of cover [mm]; diameter of rebar [mm].
- Magnetic Memory Method (MMM) – the change of the magnetic susceptibility of a material when subjected to mechanical stress, magnetic permeability is measured [μ].
- Magnetic Flux Leakage Method (MFL) – the change of voltage in the measuring coils.
- Pulsed Eddy Current Response (PEC) - determination of reduced diameter of rebar due to corrosion process when compared to original diameter, independent of rebar depth into concrete structure.

8.2.5 Induced damage to the structure during the measurement

No damage.

8.2.6 General characteristics

8.2.6.1 Measurement type (static or dynamic, local or global, short-term or continuous, etc.)

Magnetic methods can be either passive or active. For corrosion detection purposes rather addressed for local measurements. Pulse Induction methods are designed for short- term measurements, while others can be used in both ways – continuous or short-term.

8.2.6.2 Measurement range

- Electromagnetic Pulse Induction methods:
  - nominal diameter of the rebars: 13 mm and less up to 38 mm,
  - distance between rebars: within 75 mm,
  - distance on the structure: 3 m or more,
  - cover range: depends on the manufacturer of covermeter used- from 5 to 185 mm.
- Metal Magnetic Memory Method:
  - range of the magnetic field measured: - 2000 T to + 2000 T.
- Magnetic Flux Leakage Method:
  - range for the material thicknesses up to 10 mm – losses up to 20% detected,
  - range for the material thicknesses up to 13 mm – losses up to 40% detected.
- Pulsed Eddy Current Response (PEC):
  - range of the magnetic field measured: 10−15 T up to around 100 mT.

8.2.6.3 Measurement accuracy

- Electromagnetic Pulse Induction Methods:
  - location: within ±10 mm or ± 1.0% of distance between centres of rebars,
  - cover depth: within 5+ actual value of cover depth × 0.1 in mm,
  - rebar diameter: ±2.5 mm.
- Metal Magnetic Memory Method:
  - depends on the systems configuration, calibration and type of sensors used.

This project has received funding from the European Union's Horizon 2020 research and innovation programme under grant agreement No 958171.

- Magnetic Flux Leakage Method:
  - depends on the systems configuration, calibration, and type of sensors used.

- Pulsed Eddy Current Response (PEC):
  - depends on the systems configuration, calibration, and type of sensors used.
  - sensitivity to defects depends on eddy current density at defect location
  - able to detect surface cracks greater than 2.0 mm in length.

8.3 Background (evolution through the years)

The principles of eddy current testing were first laid out in 1831. Later on, there was the discovery that the properties of a coil would change when placed in contact with metals of different connectivity and permeability. The concept of Metal Magnetic Memory was first introduced in 1994 in archeological studies. MMM method has been developed in practical and theoretical aspects for 20 years. Until 2004 there are more than thirty guiding documents on the method (Dubov, 2012) (García-Martín, Gómez-Gil, & Vázquez-Sánchez, 2011) (Ghorbanpoor, 2000) (International Atomic Energy Agency, 2002).

8.4 Performance

8.4.1 General points of attention and requirements

8.4.1.1 Design criteria and requirements for the design of the survey

Detailed technical sketches should be prepared before the measurement. All information about the studied area, environmental conditions, and expected results should be documented and taken into the account in estimation.

8.4.1.2 Procedures for defining layout of the survey

Depends on the structure of understudies and the type of method used. The methods are complex therefore it is not easy to state one specific procedure.

8.4.1.3 Design constraints (e.g. related to the measurement principles of the monitoring technologies)

Not applicable.

8.4.1.4 Sensibility of measurements to environmental conditions.

To use magnetic methods the area of the test has to be separated from ferromagnetic steel elements that could influence the measurement disturbance. Hall sensors used in Magnetic Flux Leakage method are sensitive to changes in environmental conditions, which leads to thermal drifts. Pulsed Eddy Current inspection can be carried out at temperatures up to 550 °C, but the probe has to be shielded from the heat by a ceramic block. Temperature is an important test variable, particularly when eddy currents are used to establish a basic conductivity range.

8.4.2 Preparation

8.4.2.1 Procedures for calibration, initialisation, and post-installation verification

- Electromagnetic Pulse Induction methods:
  - accuracy is affected by the concrete composition. The same concrete sample that will be tested should be used to avoid influence of iron content in the cement and aggregate in composition. For covermeters calibration should be carried out regularly, with a sample of concrete at predefined distances of the rebars from the surface.

- MFL method:
  - for calibration there are used plates with diameter o 6 – 12 mm from the same material as tests sample.

This project has received funding from the European Union's Horizon 2020 research and innovation programme under grant agreement No 958171.

8.4.2.2 Procedures for estimating the component of measurement uncertainty resulting from calibration of the data acquisition system (calibration uncertainty)

As an example for metal magnetic memory method the measurement has to be performed at least four times in order to evaluate uncertainty. This can be also applied for other techniques for better estimation.

8.4.2.3 Requirements for data acquisition depending on measured physical quantity (e.g. based on the variation rate)

The adaptive wavelet denoising method and data smoothing arithmetic can be applied in testing the system.

8.4.3 Performance

8.4.3.1 Requirements and recommendations for maintenance during operation (in case of continuous maintenance)

In all methods regular calibration should be performed as well as control of the sensing range for magnetic field.

8.4.3.2 Criteria for the successive surveying campaigns for updating the sensors. The campaigns include: (i) Georeferenced frame, i.e. the global location on the bridge; (ii) Alignment of sensor data, relative alignment of the data collected in a surveying; (iii) Multi-temporal registration to previous campaigns; and (iv) Diagnostics.

Not applicable.

8.4.4 Reporting

The report from the survey should include: date, type of concrete used, place of test, environmental conditions, location of the tested areas, type of covermeter or other equipment used and last calibration performed, results, interpretation of results, conclusions.

8.4.5 Lifespan of the technology (if applied for continuous monitoring)

- Electromagnetic Pulse Induction Methods:

  Covermeters are not used continuous monitoring.

- Magnetic Memory Method (MMM)
- Magnetic Flux Leakage Method (MFL)
- Pulsed Eddy Current Response (PEC)

The technologies above can be used in real-time measurements that can be prolonged to a few hours, however are not used in continuous monitoring for a longer period.

8.5 Interpretation and validation of results

8.5.1 Expected output (Format, e.g. numbers in a .txt file)

- Electromagnetic Pulse Induction Methods - graphical distribution overview of the cover measurements on the digital display. Advanced covermeters: area scan with colors depicting the cover data in mm; the distance to and between reinforcing bars in mm;
- Magnetic Memory Method (MMM) – graphical data (direct or as gradient) in a form of so-called magnetograms.
- Magnetic Flux Leakage Method (MFL) - graphical data (direct or as gradient) in a form of so-called magnetograms.

This project has received funding from the European Union's Horizon 2020 research and innovation programme under grant agreement No 958171. © 2021

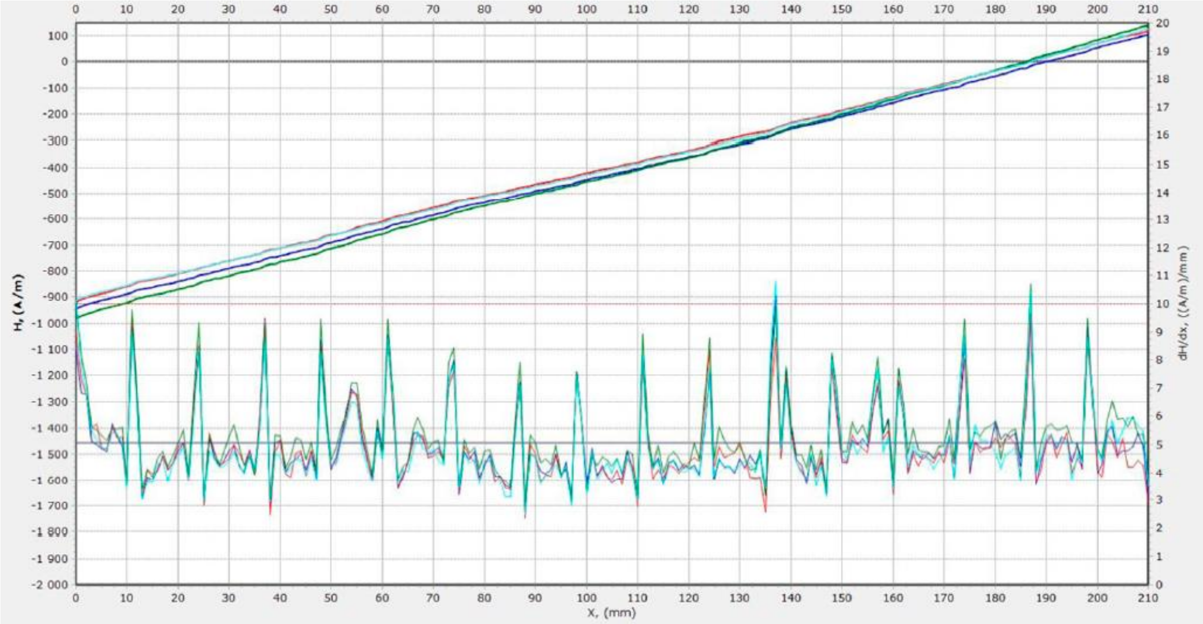

Figure 8.1 – The output of the undamaged reinforcing bar (Karel Pospisil, 2021)

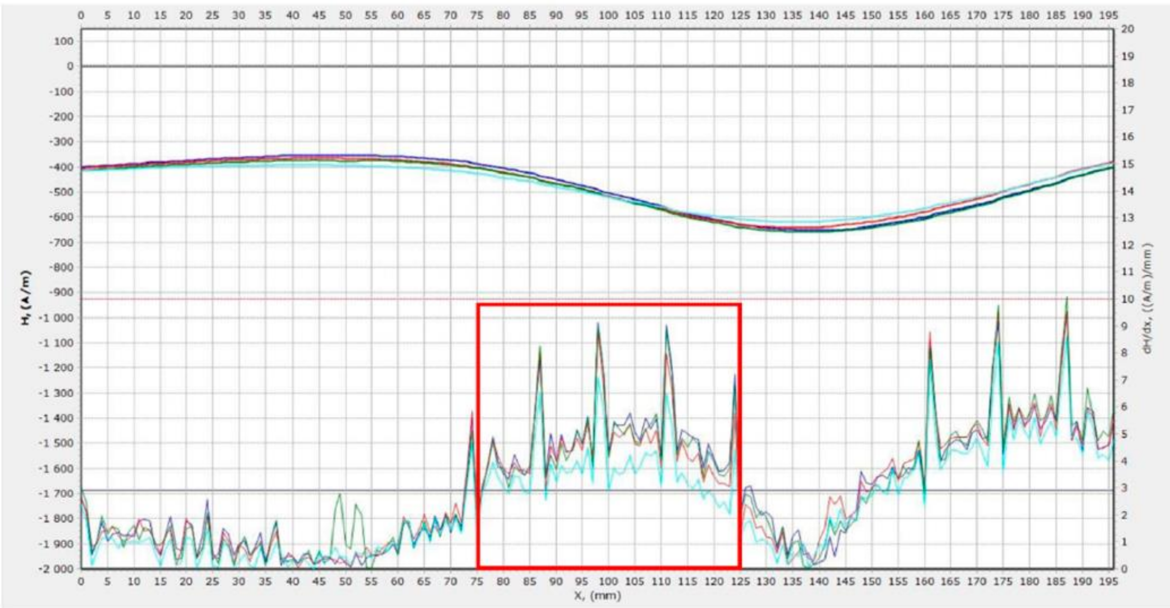

Figure 8.2 – The output of the damaged reinforcing bar. (Karel Pospisil, 2021)

- Pulsed Eddy Current Response (PEC) – graphical data of thickness correlated with the amount of time of decay of eddy currents.

8.5.2 Interpretation (e.g. each number of the file symbolizes the acceleration of a degree of freedom in the bridge)

- Electromagnetic Pulse Induction Methods – dimensions of the rebars, location in the structure, and cover depth.
- Magnetic Memory Method (MMM) – based on evaluation of magnetograms - determination of the zones with increased stress concentration, where is an increased probability of defects in the material structure; the size of the defects is related to the amplitude and shape of the magnetic signals.

This project has received funding from the European Union's Horizon 2020 research and innovation programme under grant agreement No 958171. © 2021

- Magnetic Flux Leakage Method (MFL) - corrosion maps of inspected areas; localization of defects and their parameters.
- Pulsed Eddy Current Response (PEC) - corrosion maps of inspected areas created automatically In the software; localization of defects and their parameters. The eddy current method relies on evaluating received eddy current signals containing information about the material characteristics. It is necessary to use applicable reference samples to properly inspect and analyze signals of interest. The reference samples used, therefore, must be made of similar materials with similar electrical and mechanical properties as those materials to be examined. This interpretation of eddy current signals to ascertain the integrity of the test parts, thus, depends largely on the selection and choice of suitable reference samples.

8.5.3 Validation

8.5.3.1 Specific methods used for validation of results depending on the technique

Numerical simulations for all experimental tests can be performed. Analytical methods utilizing Fourier superposition methods for modelling the crack detection, inverse Laplace transform. For validation of Pulsed Eddy Current experimental results Finite Element simulations can be applied or Ultrasonic Pulse Velocity tests.

8.5.3.2 Quantification of the error

Measurement errors on diameter of rebars should be determined by performing additional tests such as radar method (GPR) and by comparison of the results. Electromagnetic method can be also validated by use of half-cell potential method as well as ultrasonic tests with laser vibrometer.

8.5.3.3 Quantitative or qualitative evaluation

Both quantitative and qualitative analysis can be performed by means of electromagnetic methods.

8.5.4 Detection accuracy

- Electromagnetic Pulse Induction Methods:

The cover meters bar size measurements are typically only accurate to within +/- 20%.

- Magnetic Memory Method (MMM):

Detection of the future crack location and propagation direction on the test object with accuracy up to 1 mm as well as recording of the already formed cracks.

- Magnetic Flux Leakage Method (MFL) -

The probability of detection of pitting using the MFL is high within certain limits. With well-maintained equipment, trained and conscientious operators working on clean unpitted scanning surfaces on material thicknesses up to 10mm thick losses of 20% (sometimes as low as 10%) can be reliably detected. On less clean surfaces and on thicknesses up to 13mm 40% losses can be detected. Within these limits MFL is able to scan at speeds around 0.5m/sec with scan widths from 150mm to 450mm wide.

- Pulsed Eddy Current Response (PEC):

Accuracy of the PEC techniques may be improved through the use of newer types of magnetic sensors, such as the tunnelling magnetoresistance. Detection accuracy to the defects and other testing parameters can be modified by the design of the probe.

8.6 Advantages

- Electromagnetic Pulse Induction Methods:
  - fast and easy to operate
  - simple read-out of the results

This project has received funding from the European Union's Horizon 2020 research and innovation programme under grant agreement No 958171. © 2021

- not affected by environmental influences

- Magnetic Memory Method (MMM):
  - low-cost magnetoresistive sensors used
  - allows real-time monitoring
  - good sensitivity in wide range of magnetic field fluctuations
  - detection of early damages
- Magnetic Flux Leakage Method (MFL):
  - very powerful in scanning a large areas
  - efficient and easy operation
- Pulsed Eddy Current Response (PEC):
  - can be done without need for contact with the surface of the material
  - useful in situations where an object's surface is rough or inaccessible
  - does not require surface preparation or removing any insulation. It can be a quick and cost-effective solution for corrosion detection
  - possibility of location of the reinforcement and dimensions of the rebars with high accuracy
  - quality control of the cover of reinforcing bars after concrete placement
  - possibility of studying the elements for which no records or historical data are available
  - good sensitivity to pitting
  - high-speed inspection.

8.7 Disadvantages

- Electromagnetic Pulse Induction methods:
  - dependency on cover depths for minimum bar spacing detection
  - restricted detection range
- Magnetic Memory Method (MMM):
  - signals are prone to be easily interfered
  - low repeatability and reliability
- Magnetic Flux Leakage Method (MFL):
  - very poor for detecting axial cracks
  - dimensions of the defects are limited
- Pulsed Eddy Current Response (PEC):
  - impossible detection of small pitting
  - edge effect near metallic surfaces

8.8 Possibility of automatising the measurements

Advances of magnetic methods are mainly in development of novel systems, for future purposes of structural health monitoring in concrete (Yanhua Sun, 2017) .

The Pulsed Eddy Current instrument can be operated by remote control, e.g. for use in Remote Operated Vehicles (ROV's)..

This project has received funding from the European Union's Horizon 2020 research and innovation programme under grant agreement No 958171. © 2021

8.9 Barriers

Particular issues can be pointed out for Electromagnetic Pulse Induction methods:

- if other reinforcing bars, metal tie wires, bar supports are present in the area of tests the results will be affected
- if there is extensive corrosion and migration of the products, misleading results can be obtained
- if the reinforcing bars are closely packed the method is not suitable
- if rough surfaces are present the accuracy is reduced in significant way
- for rebars below 10 mm diameter the results are not reliable

It should be noted that MFL equipment is generally not intrinsically safe and should not be operated in a potentially explosive environment. MFL equipment generates strong magnetic fields and can present some hazards to the operators and electronic equipment. There can be a significant difference in the performance of individuals carrying out any MFL inspection. Thus it is important that their approach to MFL inspections follow the guidelines of the Recommended Practice document to ensure that the thoroughness, coverage and capability of the inspection are maximised.

8.10 Existing standards

- BS 1881: Testing concrete: Part 204 Recommendations on the use of electromagnetic covermeters: 1988, Dec. 1989.
- BS 1881 Part 5:1970: Testing Concrete. Methods of testing hardened concrete for other than strength. Determination of dynamic modulus of elasticity by electromagnetic method.
- BS 4408: pt. 1, Non-destructive methods of test for concrete-electromagnetic cover measuring devices", British Standards Institution, London.
- DIN 1045: Guideline Concrete, reinforced and prestressed concrete structures.
- GOST R 52081-2003: Nondestructive testing. Method of metal magnetic memory. The terms an definitions.
- GOST R 52005-2003: Nondestructive testing. Method of metal magnetic memory. General requirements.
- ST RWS 004-03: Nondestructive testing. Welded joints of equipment and constructions. Method of metal magnetic memory.
- ISO 24497-1:2020 Non-destructive testing — Metal magnetic memory — Part 1: Vocabulary and general requirements.

8.11 Applicability

8.11.1 Relevant knowledge fields

- Civil engineering:
    - pipelines,
    - bridges,
    - bricks,
    - vessels,
    - piping systems,
    - storage tanks.

This project has received funding from the European Union's Horizon 2020 research and innovation programme under grant agreement No 958171. © 2021

- Aerospace sector:
  - aircraft and spacecraft inspection,
  - jet engines and turbines.
- Railroad Industry:
  - integrity of railroad infrastructure.
- Offshore facilities:
  - oil and gas platforms inspection.
- Heat exchangers

8.11.2 Performance Indicators

Relate the surveying technology being studied with PIs from WP3, provided in the document of the TU1406 COST ACTION.

- cracks,
- corrosion of the reinforcement bars,
- loss of section,
- reinforcement bar failure/bending,
- bending,
- delamination

8.11.3 Type of structure

- bridges,
- tunnels.

8.11.4 Spatial scales addressed (whole structure vs specific asset elements)

Investigation with covermeters is performed mostly for structures that are available only from one side and in depicted areas. Other methods are suitable for rebar junctions, grinders. For assumptions on the whole structure additional non-destructive or destructive methods should be performed.

- water pipes,
- lighting conduits
- girders
- columns
- bridge slabs
- reinforced walls
- concrete slab soffits
- retaining walls
- welded joints

8.11.5 Materials

- concrete,

This project has received funding from the European Union's Horizon 2020 research and innovation programme under grant agreement No 958171.

- reinforced concrete,
- steel,
- silicate,
- ferromagnetic materials,
- polymer coatings.

8.12 Available knowledge

8.12.1 Reference projects

TRANSPORT2020+, PROJECT No. CK01000108: New approaches in the diagnosis of reinforcement of pre-stressed/ post-tensioned concrete bridge beam (Technological Agency of the Czech Republic).

8.12.2 Other

The covermeters are being under study in order to upgrade the equipment to perform tomography of rebars with 2D scanning. The recent advances in MFL technology are in automatic detection and sizing defects (Dubov, 2012).

One of the promising concepts in the area of magnetic methods is the iCAMM – Infrastructure Corrosion Assessment Magnetic Method, which is currently developed. Details can be found in - (M. Mosharfari, 2020) (M. Mosharafi, 2018) (S.B. Mahbaz, 2017).

Manufacturers:

ENERGODIAGNOSTYKA – Diagnostics with use of Metal Magnetic Memory Method

ZETEC – Eddy Current testing of Galvanized Steel: Best Practices.

ZETEC – Advanced Eddy Current Instruments for Eddy Current

Eddyfi Technologies – Magnetic Flux Leakage equipment and software/ Pulsed Eddy Current equipment/ Eddy Current Array equipment.

Rosen Group – Magnetic Flux Leakage solutions

Intertek – Non-destructive inspections with Magnetic Flux Leakage

8.13 Bibliography

•BS 1881 Part 5:1970: Testing Concrete. Methods of testing hardened concrete for other than strength. Determination of dynamic modulus of elasticity by electromagnetic method. (1970).

A. Raine, M. L. (1999, September 1). A review of the alternating current field measurement inspection technique. *Engineering*.

Bhagi, P. C. (2012). Magnetic Flux Leakage Technique: Basics. *Nondestructive Testing and Evaluation*, pp. 7-17.

British Standards Institution. (1988). *Testing concrete. Part 204, Recommendations on the use of electromagnetic covermeters.* London: British Standards Institution.

This project has received funding from the European Union's Horizon 2020 research and innovation programme under grant agreement No 958171.

BS 1881: Testing concrete: Part 204 Recommendations on the use of electromagnetic covermeters. . (1989, 12).

Craik D.J., W. M. (1970). Magnetization changes induced by stress in a constant applied field. *Phys. D Appl. Phys. vol 3 no 7*, pp. 1009-1016.

D. C. Hurley, K. H. (1992, January). Eddy Current Arrays for Defect Detection. *Review of Progress in Quantitative Nondestructive Evaluation*, pp. 1137-1144.

D.C., J. (1955). Theory of the magnetomechanical effect. . *Phys. D Appl. Phys. vol 28 no 8*, pp. 1537-1546.

Dai X W, L. R.-c.–3. (1990). Numerical simulation of pulsed eddy-current nondestructive testing phenomena. IEEE Transactions on Magnetics, 1990: 26(6): 3089–3096. *IEEE Transactions on Magnetics 26(6)*, pp. 3089-3096.

Drobiec, Ł., Jasinski, R., & Mazur, W. (2019). Accuracy of Eddy-Current and Radar Methods Used in Reinforcement Detection. Materials 2019, 12, 1168. *Materials 1168*.

Dubov, A. A. (2012). Development of a metal magnetic memory method. *Chemical and Petroleum Engineering Vol. 47*, pp. 837-839.

García-Martín, J., Gómez-Gil, J., & Vázquez-Sánchez, E. (2011). Non-Destructive Techniques Based on Eddy Current Testing. *Sensors*, pp. 2525–2565.

Géraldine Villain, R. D. (2015). Use of electromagnetic non-destructive techniques for monitoring water and chloride ingress into concrete. *Near Surface Geophysics 13(2068)*.

Ghorbanpoor, A. B. (2000). *Magnetic-Based NDE of Prestressed and Post-Tensioned Concrete Members: The MFL System.* Washington,: Federal Highway Administration,.

Herman, S. L., & Duff, J. R. (2011). *Alternating current fundamentals.* New York: Delmar Cengage Learning.

Hüblová, S. &. (2019). Experimental measurement of the diameter and cover depth of steel reinforcement using an electromagnetic concrete cover meter. *IOP Conference Series: Materials Science and Engineering 5*.

Ian Eddy, P. R. (2020). Pulsed Eddy Current Response to General Corrosion in Concrete Rebar. *Journal of Nondestructive Evaluation, Diagnostics and Prognostics of Engineering Systems, vol 3 no 4*, pp. 1-20. Retrieved from https://www.researchgate.net/publication/343118758_Pulsed_Eddy_Current_Response_to_General_Corrosion_in_Concrete_Rebar

International Atomic Energy Agency. (2002). *Guidebook on non-destructive testing of concrete structures. Training Course No.17.* Vienna: IAEA.

Karel Pospisil, M. M. (2021, 03). Diagnostics of Reinforcement Conditions in Concrete Structures by GPR, Impact-Echo Method and Metal Magnetic Memory Method. *Remote Sensing vol 13 no 5*. Retrieved from https://www.researchgate.net/publication/349805789_Diagnostics_of_Reinforcement_Conditions_in_Concrete_Structures_by_GPR_Impact-Echo_Method_and_Metal_Magnetic_Memory_Method

Lebrun B, J. Y.-C. (1997). Pulsed eddy current signal analysis: application to the experimental detection and characterization of deep flaws in highly conductive materials. *NDT E Int. 30(3)*, pp. 163-170.

M. Mosharafi, S. M. (2018). Simulation of real defect geometry and its detecion using passive magnetic inspection (PMI) method . *Applied Science 8(7), 1147*.

M. Mosharfari, S. M. (2020). Magnetic detection of corroded still rebar: Reality and simulations. *NDT &E International 110* .

This project has received funding from the European Union's Horizon 2020 research and innovation programme under grant agreement No 958171.

Maierhofer, C. (2010). *Non-destructive evaluation of reinforced concrete structures. Volume 2: Non-destructive testing methods.* Cambridghe: Woodhead Publishing Ltd. .

Pelkner, M., Pohl, R., Erthner, T., Stegemann, R., & Kreutzbruc, M. (2015). Eddy current testing with high-spatial resolution probes using MR arrays as receiver. *In: 7th International symposium on NDT in aerospace, Germany*. Bremen.

S.B. Mahbaz, M. D. (2017). Detecting defects in steel reinforcement using the passive magnetic inspection method. . *J Environ Eng Geophys 22 (2)* , pp. 153-166.

Simon X Yang, R. Z. (2018, 11). A STRESS DETECTION METHOD FOR REINFORCED CONCRETE STRUCTURE BASED ON METAL MAGNETIC MEMORY. *International Journal of Robotics and Automation, vol. 33 no 6*. Retrieved from https://www.researchgate.net/publication/328919583_A_stress_detection_method_for_reinforced_concrete_structure_based_on_metal_magnetic_memory

Singapore Institute of Standards and Industrial Research. (1992). *Testing concrete. Part B4, Recommendations on the use of electromagnetic covermeters.* Singapore : Singapore Institute of Standards and Industrial Research.

Vlasov V., D. A. (2004). Physical bases of the metal magnetic memory method. . *Moscow: ZAO Tisso*.

Yanhua Sun, S. L. (2017, January 3). Magnetic flux leakage structural health monitoring of concrete rebar using an open electromagnetic excitation technique. *Structural Health Monitoring 17(2)*, pp. 121-134.

This project has received funding from the European Union's Horizon 2020 research and innovation programme under grant agreement No 958171.

APPENDIX A9. Mechanical tests on cored samples

9.1 Goal(s)

9.1.1 Main objective

Quality control of produced concrete usually consists of few stages, such as production quality tests on fresh concrete, quality tests on hardened concrete, and tests performed on final structures. In the last case, which is important from the point of view of maintenance of bridges or tunnels, mechanical destructive test should be performed as a part of inspection in life cycle of the object. Mechanical tests performed on hardened concrete are a part of destructive surveying techniques used for characterization of concrete properties, such as compressive strength, that will affect the durability of the different structural elements of bridges or tunnels. In practical applications, it is necessary to combine different survey technologies in order to receive a more accurate and global view of the structural condition. Mechanical tests performed before construction in new bridge facilities will prevent potential failures in the future. In the case of existing ones, used as a complementary set of tests to other non-destructive or semi-destructive techniques (Francois, 2008) (Neville, 2000).

The methods described below are used in laboratory conditions play a very important role in a reliable assessment of the safety of constructions such as bridges or tunnels. The selection of the test methodology should take into account both the properties of the concrete itself, as well as the mechanism of its wear in the structure. Test methods should reflect the environmental and structural damaging effects as closely as possible.

9.2 Description

9.2.1 Functioning mode

The first step before the actual measurement in the laboratory involves samples collecting and preparation for all mechanical tests. Concrete samples are taken directly from structural elements of the object such as a bridge or tunnel in the form of drill cuttings from three different depths. The depth of the last borehole should correspond to the cover thickness of the bars armaments. Drilling locations are selected based on the visual assessment of the object. The most damaged or most exposed places should be considered first. Samples are also taken from places without visible damage as control tests. Drill cuttings are dried and sealed in the described containers and transported to the laboratory (Jarominiak, 1999).

Having this stage completed and documented following mechanical tests can be performed:

- *Compressive strength test* – samples of concrete are subjected to increasing load in a compression testing machine and the maximum load in which the sample failure occurs is detected (S.T. Yi, 2006) (Moczko, 2008)

This project has received funding from the European Union's Horizon 2020 research and innovation programme under grant agreement No 958171.

Figure 9.1 – Machine for compressive strength test

- *Fatigue test* – cured samples of concrete are placed in fatigue testing machine and subjected to pre-defined load and then unloaded to zero loads or loads in opposite direction; cycles are repeated until the end of the test; in general, there are many types of measurement, such as:
  - torsional fatigue testing,
  - rotating fatigue testing,
  - plane bending fatigue testing,
  - fatigue crack propagation testing,
  - simulated environment fatigue testing,

  As a result of the fact that there are different types of fatigue such as mechanical, creep, thermal, fretting, or corrosion (Gordon, 2011).

- *Torque test* - torque testing is a way of determining how an object will react when it is being turned - during normal operation or being twisted until it deliberately fails or breaks. Test is performed for steel anchors, which are used for fastenings in building materials (C. Jeng, 2019).

- *Tensile tests*:
  - *Split Cylinder test* – concrete cylindrical sample is placed horizontally in the testing machine and subjected to loading along the diameter, which results in lateral tensile stress and causes a splitting along with the sample,
  - *Uniaxial tensile test* – concrete sample is held by ends in the testing machine and disrupted, which cause uniaxial tensile stress,
  - *Flexure test* – in this case, the concrete beam is subjected to loading in four points until rupture occurs, because of tensile stresses induced in the material and after the modulus of rupture can be defined (Reichard, 2015) (Johannes Haufe, 2019).

This project has received funding from the European Union's Horizon 2020 research and innovation programme under grant agreement No 958171. © 2021

- *Abrasion resistance test* – generally there are four modes of measuring the abrasion resistance for concrete, from which rotating-cutter method is designed for drilled concrete samples:
  - *sand blasting – in this method abrasion is generated by sandblasting and based on the simulation of movement of the particles on the road surface in traffic,*
  - *underwater method – designed for hydraulic structures – in this method abrasive charges on the surface of the concrete sample are moved by water circulating with high speed which leads to abrasive effects,*
  - *rotating-cutter machine test for drilled samples,*
  - *abrasion resistance test of horizontal concrete surfaces* (Alexander, 1985) (Liu, 1981).

9.2.2 Types

- *Compression test:*

  Standard testing machine adjustable for the type of sample examined, which can be powered hydraulically or electromagnetically.

- *Fatigue tests:*

  performed with hydraulic test machines, consisting of a frame for the sample placement, load cell, grips, and testing software.

- *Torque test:*

  Torque Penetrometric test for in-situ purposes with a dynamometric torque wrench with display (0-30 Nm range and 0,5 Nm precision); with digital or analogic transducer; provided with a recording device to store the parameters measured during the test.

  Precision torque testers controlled by software.

- *Tensile tests:*

  machine consisting of steel frame, columns, and self-centering sample holder; load beam suspended with springs for adjustment to the sample.

- *Abrasion resistance test:*

  Rotating-cutter machine - testing machine consists of abrading cutter and drill press with lever, gear, spring system e abrading cutter when using the lever, gear and spring system of a drill press.

9.2.3 Process/event to be detected or monitored

- *Compression test* – a moment of failure of the sample under applied compressive load;

This project has received funding from the European Union's Horizon 2020 research and innovation programme under grant agreement No 958171.

- *Fatigue test* – fatigue cracks resulting from cyclic stresses applied to the sample; observation if a minimum number of cycles of fatigue loads there will be any partial or complete damage, such as visible transverse crack;
- *Torque test* –failure of the anchor if either the bolt or the grout shows any movement;
- *Tensile test*:
  - *Split Cylinder test* - splitting along diameter depending on the type of tensile test performed,
  - *Uniaxial tensile test* – breakage of the sample in the middle,
  - *Flexure test* – the crack of the sample due to force applied.

- *Abrasion resistance test* – determination of resistance to degradation of concrete when subjected to combine the action of impact and abrasion.

9.2.4 Physical quantity to be measured (e.g. actions, displacements, deformations, dynamic structural properties, material properties including mechanical, electrical and chemical properties, relative displacements of the two sides of a crack, etc.).

- Compression test – maximum load [N] at which failure of the sample has been registered.
- Fatigue test – force [N] needed to break the sample over a number of cycles of stress.
- Torque test – measurement of the maximum torque/rotational force resisted by the material; tension force in the bolt or screw as a function of the applied torque moment.
- Tensile test – force [N] needed to break the sample under load.
- Abrasion resistance test - average loss in mass [g] or depth of wear [mm].

9.2.5 Induced damage to the structure during the measurement

In all mechanical tests, there is damage induced to the structure since sample collection requires drilling into the structures.

9.2.6 General characteristics

9.2.6.1 Measurement type (static or dynamic, local or global, short-term or continuous, etc.)

Mechanical tests of concrete are considered static measurements for local applications in short-term intervals. However, for global estimations, there are used specific factors in calculations to reflect the strength of concrete in the whole structure and ensure safety and reliability of the data.

9.2.6.2 Measurement range

For each of the test range depends on the equipment used and its with accordance to technical specification of manufactures. For example universal strength testing machine range can be between 300 - 3000 kN or 400 - 4000 kN. For tensile test the constant load applied range can be between 1.2 MPa/min - 2.4 MPa/min.

This project has received funding from the European Union's Horizon 2020 research and innovation programme under grant agreement No 958171.

9.2.6.3 Measurement accuracy

Measurement accuracy of mechanical tests will be affected by the characteristics of concrete borehole samples such as porosity, discontinuities in concrete due to local air voids, presence of reinforcement, segregation of concrete components, aggregate grain size and diameter, length/diameter ratio. Important part is also the drilling process and direction. Instrument accuracy will also have influence on the final results, which depends on the force capacity and speed. Torque can be measured with automatic systems with +/- 0.5% accuracy. Tensile can be measured with ±0.5% of reading accuracy.

9.3 Background (evolution through the years)

Already in the 20th century, there was a need to monitor concrete workability to ensure the quality control of the concrete mixes and achieve expected strength and hardness. Since then a lot of test procedures have been developed for mix proportioning, research and field use (Eric P. Koehler, 2003). The majority of those did not find widespread acceptance, even though has been extensively developed. The main method used, even with increasing knowledge in concrete rheology, was the slump test. Modern concrete production has not limited only to monitoring concrete workability in the field. In 1998 National Ready Mixed Concrete Association identified the need for the characterization of high-performance concrete. However, even after 80 years of development, the industry is still facing problems with accurate, quick, and reliable mechanical testing methods (Eric P. Koehler, 2003) (Francois, 2008) (H.W. Fritz, 1990) (Malhorta, 1977).

In 2000 there was published norm EN 12504-1:2000, describing the methods of collecting the boreholes, their quality assessment, and measurement of the compression strength. In 2008 has been introduced the norm EN 1379:2008, which was directed at old, destroyed constructions for modernization, redesign (Michalak, 2016).

9.4 Performance

9.4.1 General points of attention and requirements

9.4.1.1 Design criteria and requirements for the design of the survey

For strength-mechanical analysis:

Criteria for sample collection – requirements are included in the standard EN12504-1:2000.

Testing machines must meet the requirements of the standard EN12390-4:1999.

For example in compression and bending strength following samples are used:

- for compression tests:
  - cubic samples 100, 150, 200, 300 mm,
  - cylindrical samples 100 x 200 mm or 150 x 300 mm.
- for bending strength tests:
  - cement bars 40 x 40 x 160 mm,
  - concrete beams 100 x 100 x 500 mm or 150 x 150 x 700 mm.

This project has received funding from the European Union's Horizon 2020 research and innovation programme under grant agreement No 958171.

In case of abrasion resistance measurement for drilled samples:

- cubic samples 100 × 100 × 100 mm on the base of ASTM C 944 (EN 12504 - Concrete testing in structures - Part 1: Core drilling - Cutting, evaluation and compressive strength testing, 2001).

9.4.1.2 Procedures for defining layout of the survey

The following steps should be considered when defining the layout of the survey:

- visual inspection of the structure,
- decision regarding the places of drilling,
- identification of the samples,
- preparation of the samples for further testing in the laboratory,
- calibration processes for selected test,
- performance of the measurement,
- documentation of the results and observations,
- validation of results,
- conclusions and preventive actions.

9.4.1.3 Design constraints (e.g. related to the measurement principles of the monitoring technologies)

Design issues are related mostly to sample collection from the specific parts of the bridge or other structures.

9.4.1.4 Sensibility of measurements to environmental conditions

The mechanical tests on cored samples are performed under controlled environmental conditions, therefore no significant factors should influencing the measurements.

9.4.2 Preparation

9.4.2.1 Procedures for calibration, initialisation, and post-installation verification

The operation of automatic presses for measuring concrete strength does not require qualified personnel. After connecting the device to the network, placing the test sample on the measuring table, there are a few steps to perform before initialization of the measurement:

- setting the test parameters - sample selection, rate of force increase) - the change is required only when the type of the tested sample changes,
- pressing start button on the control panel,
- wait for automatic control rate of force increase after reaching 1% of the range.

9.4.2.2 Procedures for estimating the component of measurement uncertainty resulting from calibration of the data acquisition system (calibration uncertainty)

No specific procedures. Some guidelines should be given by the manufacturer of the testing equipment.

This project has received funding from the European Union's Horizon 2020 research and innovation programme under grant agreement No 958171.

9.4.2.3 Requirements for data acquisition depending on measured physical quantity (e.g. based on the variation rate)

Not applicable.

9.4.3 Performance

9.4.3.1 Requirements and recommendations for maintenance during operation (in case of continuous maintenance)

Not applicable.

9.4.3.2 Criteria for the successive surveying campaigns for updating the sensors. The campaigns include: (i) Georeferenced frame, i.e. the global location on the bridge; (ii) Alignment of sensor data, relative alignment of the data collected in a surveying; (iii) Multi-temporal registration to previous campaigns; and (iv) Diagnostics.

Not applicable.

9.4.4 Reporting

Report from mechanical testing should include:

- date of the test,
- age of the concrete,
- composition of the concrete,
- conditions of curing and storage of the samples,
- identification of the samples, dimensions,
- measured quantities e.g. maximum load registered during compression test,
- observations e.g.

For abrasion test report should include also:

- sample dimensions,
- age of concrete,
- type of finish,
- concrete strength,
- applied surface treatment,
- time of abrasion and load used,
- average loss in grams.

9.4.5 Lifespan of the technology (if applied for continuous monitoring)

Mechanical tests can be repeated in different intervals of time, however, it is not possible to perform continuous monitoring.

This project has received funding from the European Union's Horizon 2020 research and innovation programme under grant agreement No 958171.

9.5 Interpretation and validation of results

9.5.1 Expected output (Format, e.g. numbers in a .txt file)

- Compression test – value of concrete strength calculated by dividing the maximum load [N] at failure by cross sectional area [mm2].
- Fatigue test - total number of load cycles to failure.
- Torque test – indication of load applied [N], maximum torque [N/m], maximum angle of twist.
- Tensile test – value of load [N] that caused sample failure; values can be exported to excel or on email address, depending on the software used.
- Abrasion resistance test – sample weight after the test [g], mass loss [g/%], average abrasion resistance and relative abrasion resistance value.

Software available on the market enables to present measurement data graphically and prepare customised test reports.

9.5.2 Interpretation (e.g. each number of the file symbolizes the acceleration of a degree of freedom in the bridge)

- Compression test – characteristic compressive strength is designated as a strength that will exceed 95% of the tested samples; characteristic strength for cubic sample, characteristic strength for cylindrical sample in [N/mm^2] is calculated.
- Fatigue test – fatigue limit is a stress level below which there would be no fatigue failure disregarding the number of load cycles the material is subjected to; plot an S-N diagram from which fatigue strength can be determined. Example is shown below:

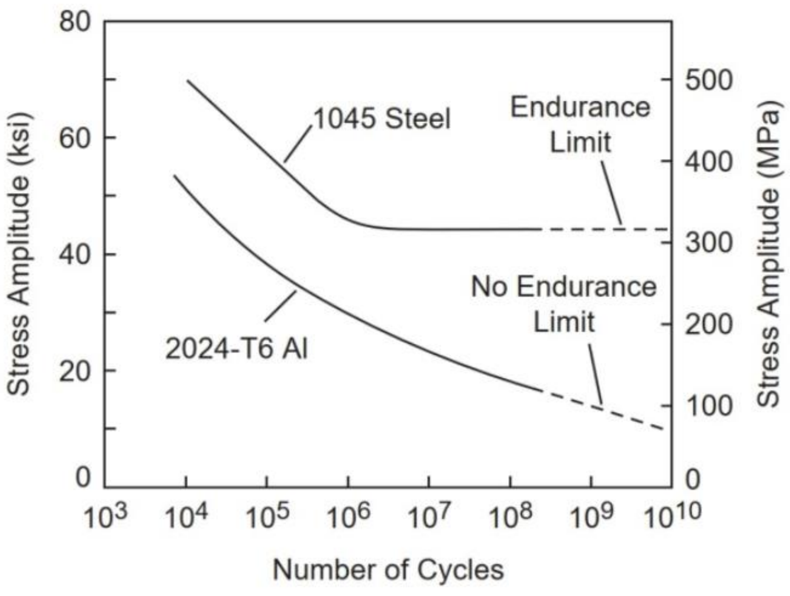

Figure 9.2 – Output from fatigue test

- Torque test – torsional strength and stiffness of the measuring element.

This project has received funding from the European Union's Horizon 2020 research and innovation programme under grant agreement No 958171. © 2021

- Tensile test – mean tensile splitting strength [N/mm^2], tensile strength is determined by dividing measured value of force by cross-sectional area.
- Abrasion resistance test – abrasion resistance resists mechanical wear, which means that the higher the value the better it is for the structure; Abrasion resistance is connected with compressive strength of concrete and strong concrete is more abrasion-resistant, so both of the tests can be correlated.

1.6.3 Validation

9.5.2.1 Specific methods used for validation of results depending on the technique

Converting the results of core drilling tests with different proportions of height to diameter should be based on reliable conversion factors.

9.5.2.2 Quantification of the error

Numerical analysis and simulations can be used for this matter.

9.5.2.3 Quantitative or qualitative evaluation

Both quantitative and qualitative analysis is possible with mechanical testing.

9.5.3 Detection accuracy

According to standard EN12504-1:2000, the accuracy and reproducibility of test results are not assessed.
Not applicable.

9.6 Advantages

Used core samples are qualitatively better material than those from the laboratory, because they contain all potential defects resulting from various technological and transport situations or climatic influence. Testing the strength of hardened concrete is particularly useful, because the quality of the concrete in structure depends to a large extent on this property. Based on the static strength tests it is possible to conclude if the analysed bridge structure can still transfer utility loads with accordance to norm.

9.7 Disadvantages

All methods induce damage to the structures which can cause risk during works and require repairs. In practical situation drilled sample taken may not be a good representation of the entire structure, which leads to inaccuracies and doubts.

This project has received funding from the European Union's Horizon 2020 research and innovation programme under grant agreement No 958171.

9.8 Possibility of automatising the measurements

Mechanical tests cannot be performed without the presence of the operator for now, however the measurements can be automated with use of most advanced equipment enabling reduce of the time needed to perform tests.

9.9 Barriers

There is a need to develop a base of correlation curves for various typical concrete groups and different dimensions to study degradation process in whole structures accurately.

9.10 Existing standards

- EN 12390-3:2001 Testing hardened concrete - Part 3: Compressive strength of test specimens
- EN 12390-1:2001 Testing hardened concrete - Part 1: Shape, dimensions and other requirements for specimens and moulds
- EN 12390-4:2001 Testing hardened concrete - Part 4: Compressive strength - Specification for testing machines
- EN 12504-1:2002 Testing concrete in structures
- ASTM C801-98 STM for Determining the Mechanical Properties of Hardened Concrete under Triaxial Load
- ASTM C900-94 STM for Pullout Strength of Hardened Concrete
- AS 1012.14-1991. Method of Testing Concrete - Method for securing and testing cores from hardened concrete for compressive strength
- BS 1881: pt. 4, “Methods of testing concrete for strength”, British Standards Institution, London
- BS 1881: Part 121: 1983 - Method for Determination of Static Modulus of Elasticity in Compression
- BS 1881: Part 120: 1983 - Method for Determination of Compressive Strength of Concrete Cores
- BS 1881: Part 116: 1983 - Method for Determination of Compressive Strength of Concrete Cubes
- ASTM C944 (2012), Standard test method for abrasion resistance of concrete or mortar surfaces by the rotating-cutter method, ASTM International, West Conshohocken, 5pp.

9.11 Applicability

9.11.1 Relevant knowledge fields

Civil engineering:

- quality control of concrete
- production quality of concrete

This project has received funding from the European Union’s Horizon 2020 research and innovation programme under grant agreement No 958171.

- historical building structural assessment

9.11.2 Performance Indicators

- rupture,
- deformation,
- holes,
- wire break,
- loss of section,
- obstruction/impeding,
- displacement,
- cracks,
- stirrup rupture,
- displacement,
- reinforcement bar failure/bending,
- tensioning force deficiency,
- prestressing cable,
- debonding,
- delamination.

9.11.3 Type of structure

- bridge,
- tunnel,
- road.

9.11.4 Spatial scales addressed (whole structure vs specific asset elements)

- steel-concrete spans,
- concrete bridge supports,
- abutments,
- bearings,
- pillars.

9.11.5 Materials

- concrete,
- steel,
- polymer,
- composite,
- silicate,

This project has received funding from the European Union's Horizon 2020 research and innovation programme under grant agreement No 958171.

- nanocomposite,
- metal,
- alloys.

9.12 Available knowledge

9.12.1 Reference projects

Not applicable.

9.12.2 Other

Bruker mechanical Testers

MATEST Compression Machines

MATEST Core Drilling Machines

MATEST Specimen Cutting Machines

MATEST Elastic Modulus Determination

Prescott Instruments Dynamic Testing

Central Road Research Institute Abrasion Testing Machine

9.13 Bibliography

Alexander, M. (1985). Towards standard test for abrasion resistance of concrete. Report on a limited number of test studied with a critical evaluation. *Materials and Structures 18, 106*, pp. 297-307.

C. Jeng, M. C. (2019). Torsion experiment and cracking-torque formulae of hollow presstresed concrete beams. . *Materials Science, Engineering Structures* .

EN 12504 - Concrete testing in structures - Part 1: Core drilling - Cutting, evaluation and compressive strength testing. (2001).

EN 13791:2007 Assessment of concrete compressive strength in structures or in structural elements. (2007).

Eric P. Koehler, D. W. (2003). *Summary of Concrete Workability Test Methods. (ICAR 105-1).* Aggregates Foundation for Technology, Research, and Education . Texas: International Center for Aggregates Research, The University of Texas at Austin.

Francois, D. (2008). *Structural Components - Mechanical Tests and Behavioral Laws.* John Wiley & Sons, Inc. .

Gordon, P. (2011). *Low cycle fatigue behaviour of concrete with recycled concrete aggregates.* Faculty of California Polytechnic State University.

H.W. Fritz, E. E. (1990). Mechanical Tests for Bituminous Mixes. Characterization, Design and Quality Control . *Proceedings of the Fourth International Symposium RILEM Technical Commitee 101-BAT* . Budapest: Chapman and Hall.

Indelicato, F. (1997). Estimate of concrete cube strength by means of different diameter cores: A statistical approach. *Materials and Structures vol. 30, no 4*, pp. 131-138.

This project has received funding from the European Union's Horizon 2020 research and innovation programme under grant agreement No 958171.

J.R. Del Viso, J. C. (2008). Shape and Size Effects on The Compressive Strength Of High Strength Concrete, Cement And Concrete Research 3 (2008) 386-395;. *Cement And Concrete Research 3* , 386-395.

Jarominiak, A. (1999). *Podstawy utrzymania mostów.* Oficyna Wydawnicza Politechniki Rzeszowskiej.

Johannes Haufe, A. V. (2019). Tensile strength of concrete exposed to sulfate attack. . *Materials Science, Cement and Concrete Research* .

Liu, T. C. (1981). Abrasion resistance of concrete. *ACI Journal*, pp. 341-350.

Malhorta, V. M. (1977). Concrete strength requirements - cores versus in-situ evaluation. *Journal of American Concrete Institute vol. 74, no 4*, pp. 163-172.

Michalak, E. (2016). Diagnostics of the concrete bridges in a view of European Union Norms. *Archives of Institute of Civil Engineering no. 21*.

Moczko, A. (2008). Ocena wytrzymałości betonu na ściskanie w konstrukcjach na podstawie badania odwiertów rdzeniowych w świetle nowej normy europejskiej. *Budownictwo, Technologie, Architektura*, pp. 50-55.

Neville, A. M. (2000). *Właściwości betonu.* Kraków: Polski Cement Sp. z o. o.,.

PN-EN 12390 - Część 3:2001 Badania betonu - Wytrzymałość na ściskanie. (2001).

Reichard, B. (2015). Uniaxial tensile testing technique to obtain softening response of ultra-high performance concrete under confining pressures. *Materials Science* .

S.T. Yi, E. Y. (2006). Effect Of Specimen Sizes, Specimen Shapes and Placement Directions on Compressive Strength of Concrete. . *Nuclear Engineering And Design 236*, pp. 115-127.

This project has received funding from the European Union's Horizon 2020 research and innovation programme under grant agreement No 958171. © 2021

APPENDIX A10. Microelectromechanical Systems (MEMs) - Accelerometers

10.1 Goal(s)

10.1.1 Main objective

MEMS sensors include a variety of transducers based on special micromachining of silicon. This allows to create sensor families having tunable features, according to the specific needs.
One application of MEMS sensors are accelerometers, that measure linear acceleration and allow the analysis of vibrations and structures dynamic behaviour.

10.2 Description

10.2.1 Types

There are several types of MEMS accelerometers, all provided as an Integrated Circuit with some conditioning electronics on a board. MEMS accelerometers differ in the following parameters values:

- Methodology of measure: in function of the embedded circuit and the methodology of measure MEMS accelerometers can be capacitive and thermal.
- Full Scale (FS): range of acceleration values that can be measured
- Bandwidth (BW): frequency range in which the MEMS sensor operates.
- Resolution: minimum detectable change in acceleration, expressed in [mg]
- Noise Density: parameter related to resolution and expressed in [mg/√Hz]; through noise density integration over the noise bandwidth, sensor resolution is obtained.
- Sensitivity: also known as gain, is the output change per unit of input acceleration.
- Connection types: the accelerometers can be linked to the acquisition system using wired or wireless connections.

MEMS accelerometer can both work along linear degrees of freedom or along rotation degrees of freedom.

10.2.2 Functioning mode

- Capacitive MEMs

MEMS accelerometers can measure acceleration along a single axis or three normal axes to give the acceleration vector. Their working principle is the same of all accelerometers, made of a single degree of freedom oscillating system, along each of the measurement axes. An external frame is rigidly connected to the body whose acceleration has to be known and the internal mass is suspended on springs. A relative displacement sensor detects the relative motion between the external frame (the accelerometer case) and the internal mass: this motion depends upon the inertia force acting on the

This project has received funding from the European Union's Horizon 2020 research and innovation programme under grant agreement No 958171.

mass, which, in turn, is related to the sensor absolute acceleration. The relative motion between the frame and the mass is detected by means of a number of differential capacitors created on the same accelerometer structure: their combination results in a measurable output.

Dealing with MEMS sensing element, the whole structure is miniaturized and made of silicon: the external frame, the internal mass and the supporting beams acting as springs are all made of silicon: also the sensing elements are a series of differential capacitances in a comb shape, worked on the same silicon structure.

- Functioning mode of thermal MEMS

Thermal convection based micro-electromechanical accelerometer is an acceleration sensor which is characterized by the lack of a solid proof mass. This feature confers to thermal mems a high shock survivability, a low cost fabrication and, at last, a convenient integration of the sensor with CMOS integrated circuit technology.

Thermal accelerometers sense acceleration by measuring the displacement of a fluid bubble present within a sealed cavity.

The operation of thermal inertial sensors is based on the natural convection of fluid. In figure 1(a) it is possible to observe a general structure of a single-axis thermal accelerometer, which consists of an electrical resistive heater, suspended at the centre of the cavity, and a pair of temperature sensors, which are placed symmetrically around the heater, while an outer cover encapsulates the fluid present in the cavity. The heat dissipation of the heater induces the formation of a hot thermal bubble of the fluid surrounding it. In steady, the temperature profile within the cavity remains symmetrical with respect to the heater, and the symmetrically placed temperature sensors detect identical temperatures. However, when an acceleration is applied, the temperature profile gets skewed due to physical displacement of the thermal bubble (figure 1(b)) and the temperature increases on one side of the heater and decreases at the other one

(figure 1(c)): the resultant differential temperature (ΔT) is proportional to the applied acceleration and is measured by the temperature sensors.

This project has received funding from the European Union's Horizon 2020 research and innovation programme under grant agreement No 958171.

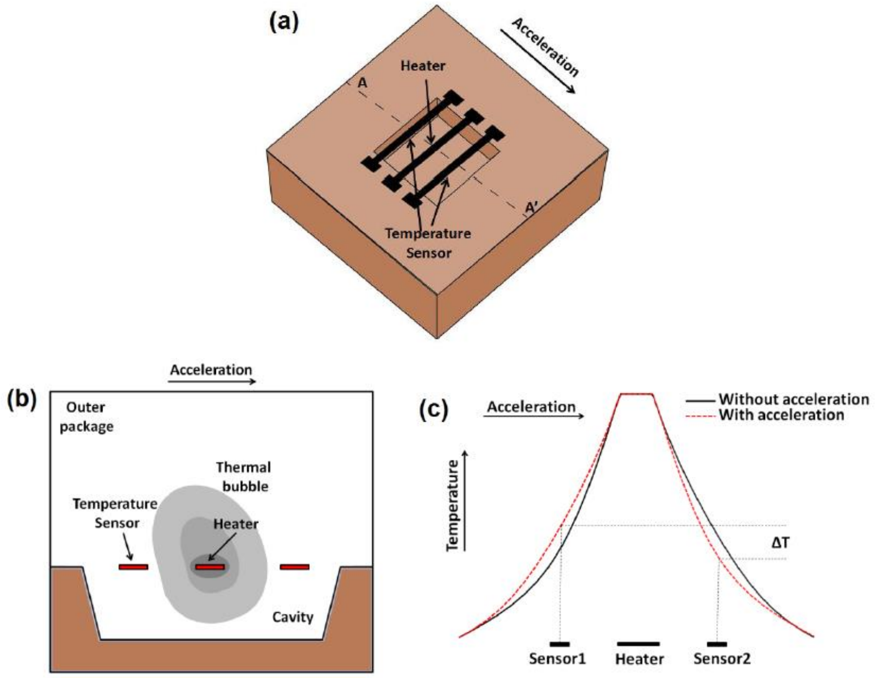

Figure 10.1 – (a) Schematic view of thermal accelerometer, (b) cross-sectional view along AA' line, and (c) temperature profile along AA'. (Rahul Mukherjee, 2017)

Simple geometries can be used for the accelerometer modelling: for instance, for the structure in figure 1(a), which has a centrally placed heater and working fluid enclosed by cavity and outer cover, the heater can be modelled as a cylindrical heat source and the outer cover as a larger cylinder at ambient temperature. Instead, a simplified model, as shown in figure 2(a), may consists of a spherical structure where the heater is a spherical source, and the outer cover is a larger sphere centring the heater and kept at ambient temperature.

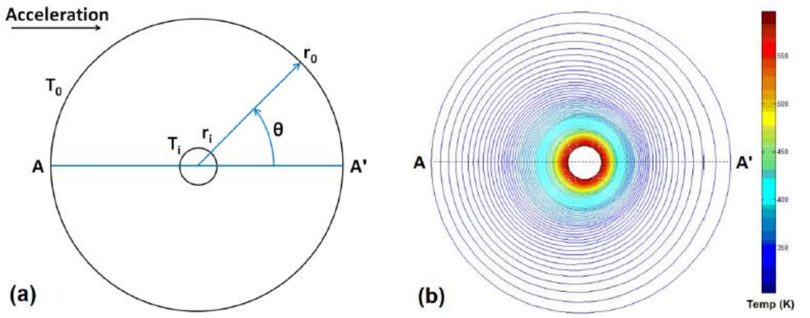

Figure 10.2 – (a) Simplified model of thermal accelerometer represented using concentric spheres. (b) Temperature contour plotted by solving the governing equations. (Rahul Mukherjee, 2017).

Here:

- r and θ are the radial distance and angle of the spherical coordinate system respectively;
- The inner sphere represents the heater with radius r_i and surface temperature T_i;
- the outer sphere represents the cavity wall surface having radius r_0 and wall temperature T_0 (where $T_i > T_0$);

This project has received funding from the European Union's Horizon 2020 research and innovation programme under grant agreement No 958171.

- AA' represents the vertical axis along midsection;
- $R = r_0/r_i$ is the ratio of the outer to inner sphere radius.

The concentric cylinder model is generally used for single-axis accelerometers, while concentric sphere for the dual axis ones. In three-axis accelerometers, the x and y-axes accelerations are applied in-plane, while the z-axis acceleration is applied out-of-plane and these too can be modelled with concentric spheres.

The governing equations predicting temperature profile of a thermal accelerometer device are based on the principle of conservation of mass, momentum and energy, but since the structure of a practical accelerometer is quite complex, it cannot be easily analysed by means of the analytical equations. To study its various performance parameters like temperature profile, numerical simulators are required to be used, like ANSYS, CoventorWare, and COMSOL Multiphysics.

For further information on thermal accelerometers in MEMS process and in CMOS-MEMS process, see (Rahul Mukherjee, 2017).

In conclusion, the advantages of thermal MEMS, include a superior shock survival, simplistic compact structure, low cost, wide measurement range, and integrability with CMOS integrated circuit technology.

In spite of the advantages, thermal inertial sensors in their present form have a sensitivity and frequency response that restricts the possible fields of application and, moreover, sensitivity and bandwidth improvement is still an active research area.

10.2.3 Process/event to be detected or monitored

According to their design and the related electronics, MEMS accelerometers can be used for low level accelerations typical of operational conditions, up to shocks. In most cases and applications their performances are fit for monitoring purposes: through a wide number of sensors properly placed on structures, their dynamic behaviour can be described (e.g. modal parameters, principal mode shapes, etc.). Besides, if a continuous monitoring system is adopted damages or geometry changes in time can be detected with respect to the initial state, i.e. when the monitoring system is installed. With a well-designed MEMS accelerometers network, part of a continuous SHM system, eventual anomalous vibrations, interesting few structural/non-structural elements or the whole structure, can be measured, helping in maintenance procedures.

10.2.4 Physical quantity to be measured (e.g. actions, displacements, deformations, dynamic structural properties, material properties including mechanical, electrical and chemical properties, relative displacements of the two sides of a crack, etc.).

The output, which can both be analog (voltage or current) or digital (usually in terms of number of least significant bits) is directly related to the quantity being measured, which is acceleration. In case this is

This project has received funding from the European Union's Horizon 2020 research and innovation programme under grant agreement No 958171.

linear the output can be expressed in m/s2, or multiples of gravity (in g). In case of rotational acceleration the measurement units are typically rad/s2.

10.2.5 Induced damage to the structure during the measurement

No damage induced.

10.2.6 General characteristics

10.2.6.1 Measurement type (static or dynamic, local or global, short-term or continuous, etc.)

The design of MEMS accelerometers makes them g-sensitive, this means that their lower bound can extend to 0 Hz, which means capability to measure static or quasi static quantities. Therefore, they are suitable to measure tilt, as the projection of gravity along the measurement axis.

Their natural use is for dynamic acceleration measurements: each sensor can cover a point measurement over a single axis or three axes. Sensors can be considered alone, providing the evolution in time about the dynamics of a single point, or many of them can be evaluated together to perform more advanced dynamic approaches like modal analysis.

MEMS accelerometers can be employed for both short-term and continuous testing; besides, they can be used to describe the behavior of both local structural elements and the global structure.

10.2.6.2 Measurement range

As accelerometers work below resonance, the MEMS accelerometer performances depend upon the natural frequency of the silicon structure, which can be designed to reach bandwidths from some hundreds of Hertz up to some thousands, for sure redundant for monitoring applications, mainly requiring low-frequency ranges and low full scales.

The full scale can also be adjusted thanks to specific electronic hardware: full scale for the MEMS commonly adopted in monitoring applications can range from fractions of gravity up to some g, even if it is not so uncommon to have full scales of several hundred g, for specific applications, not related to monitoring.

10.2.6.3 Measurement accuracy

MEMS accelerometers have a measurement accuracy changeable based on multiple variables: setted sensors parameters (sampling frequency, FS, resolution, sensitivity, etc.), signal to noise ratio, energy of the input excitation, fixing type of the board in the sensor case.

Indeed, MEMS accelerometers can provide an analog output, though these are not so common today, or an already digitized output; they require a power supply typically in the range 0-5 V and also the output is within the mentioned range; this bias requires careful attention in case the output signal undergoes integration or other mathematical calculations.

This project has received funding from the European Union's Horizon 2020 research and innovation programme under grant agreement No 958171.

Other issues specific of SHM applications are related to the board, acting as a dynamic system between the vibrating body and the sensor itself: care must be devoted to ensure that the vibration to be measured is properly transmitted to the sensor without attenuation of amplification.

Often MEMS accelerometers already have on-board temperature sensors to help compensating temperature drifts.

The main feature making these sensors different from quartz accelerometers for similar applications, apart from the sensitivity to gravity, is the signal to noise ratio, which is still about one order of magnitude higher in case of common MEMS accelerometer: while with robust input all accelerometers are expected to show similar performances, in case of operational measurements, with a very low input excitation, the MEMS accelerometer response can be buried in the background noise: this also warns against the attempt to couple MEMS accelerometers to A/D converters with a high number of bits, to avoid any resource waste.

The noise floor is often declared in terms of power spectral density in a given frequency band. A comparison in terms of noise floor between a MEMS triaxial accelerometer (continuous lines) and a piezoelectric triaxial accelerometer (dashed lines) is given in the figure below, showing how main frequencies are well identifiable in both sensors types, even if an higher noise floor characterise the MEMS ones.

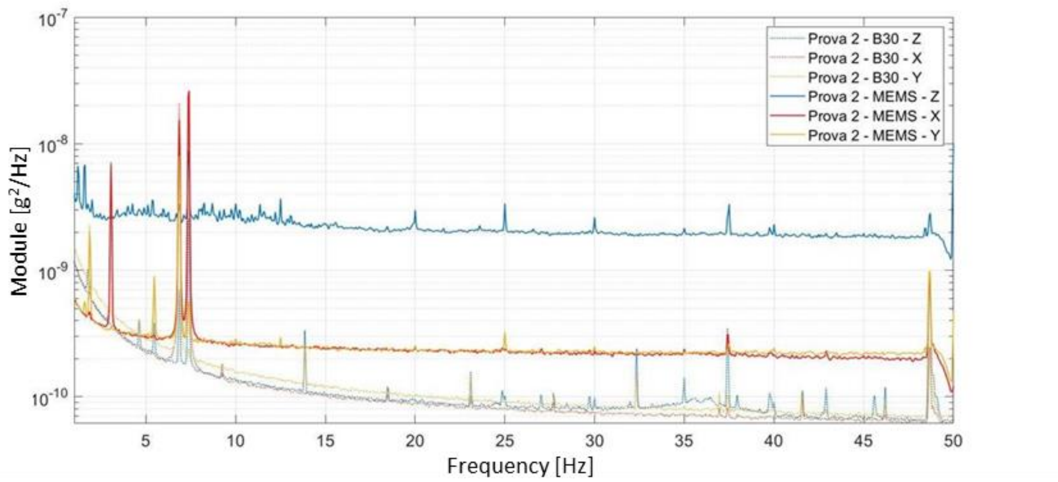

Figure 10.3 – Comparison in terms of noise floor between a MEMS triaxial accelerometer and a piezoelectric triaxial accelerometers

10.3 Background (evolution through the years)

In the second half of the 1950s, first papers regarding MEMS technology were published (C.S. Smith, 1954), describing piezoresistive effects in silicon and germanium. First MEMS applications are related to silicon pressure sensors, which commercialization started in the USA at the end of the 1960s. The technology development was very fast, thanks to improvements in silicon processing and in micromachining. Small, rugged and inexpensive devices with always increasing performance were produced, ranging in different categories: accelerometers, strain gauges, pressure sensors,

This project has received funding from the European Union's Horizon 2020 research and innovation programme under grant agreement No 958171.

microphones, gyroscopes, etc. Fields of application of the technology, as consequence, increased through the years: MEMS sensors are applied in the automotive, medical, aerospace, automation industry. Accelerometers technology is continuously evolving and for instance - advanced surface micromachining techniques developed allow to sense in one, two or three axes. Through the improved performance, their market is expanding and it is expected to grow rapidly in the future.

10.4 Performance

10.4.1 General points of attention and requirements

10.4.1.1 Design criteria and requirements for the design of the survey

Sensors layout should be carefully designed according to the phenomenon to be analysed and/or monitored. It would be advisable to have one sensor on each key node of the structure and on each relevant structural element. For example, if a modal analysis wants to be performed, sensors numbers and position must be properly chosen so that all structure principal mode shapes can be derived.

Another key point regards sensors parameters (full scale, sampling frequency, resolution, etc.), that should be adequately set according to the structure type, the desired measure and the frequency range of interest.

Moreover, if signals coming from different sensors should be combined in post-processing analysis, their synchronization must be guaranteed.

10.4.1.2 Procedures for defining layout of the survey

No information available.

10.4.1.3 Design constraints (e.g. related to the measurement principles of the monitoring technologies)

No information available.

10.4.1.4 Sensibility of measurements to environmental conditions

MEMS accelerometers measurements can be influenced by environmental conditions, especially by temperature and during long-term/continuous testing. For this reason, it is advisable having an on-board temperature sensor, so that eventual temperature drift can be compensated.

10.4.2 Preparation

10.4.2.1 Procedures for calibration, initialisation, and post-installation verification

Standards for accelerometers calibration are illustrated in ISO 160063 (“Methods for the calibration of vibration and shock transducers”), including 8 parts regarding calibration procedures (i.e. Part 1, Part 11, Part 12, Part 13, Part 15, Part 21, Part 22, Part 41). For each method, the description of scopes and implementation steps is given, as well as specifications about apparatus requirements, variation ranges of measured quantities (frequency, acceleration amplitude, etc.), measurement uncertainties

This project has received funding from the European Union’s Horizon 2020 research and innovation programme under grant agreement No 958171.

(divided into random and systemic) and recommendation for laboratory ambient conditions (temperature, humidity, etc.). Calibration procedure can provide several information about accelerometers characteristics, such as sensitivity, frequency response, resonant frequency, linearity, transverse sensitivity, etc.
Calibration methods can be divided in two different categories: absolute methods and relative methods. Absolute methods include tests in which sensors are subjected to a known input; some examples are:

- Gravity inversion test: each MEMS accelerometer axis is rotated of 180° along gravity direction, experimenting known acceleration of +1g and -1g.

Figure 10.4 – Accelerometers absolute calibration methods - Gravity inversion test

- Drop test: accelerometer is dropped in gravity direction from different heights. The acceleration during the sensor free-fall is measured and compared with the expected g value, evaluating its sensitivity.

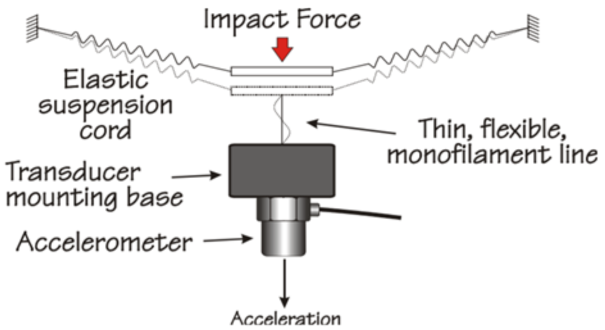

Figure 10.5 – Accelerometers absolute calibration methods - Drop test

- Gravimetric test
- Calibration by laser interferometry

Relative methods, instead, calibrate the accelerometer to be tested by comparing its output with a reference sensor, previously calibrated, when they're subjected to the same input acceleration. Characteristics of the reference sensor and of the exciter must be carefully chosen according to the test to be performed; in this regard, some recommendations are given in ISO 16063 Part 21 and Part 22, about vibration and shock calibration, respectively, by comparison to a reference transducer. Among relative calibration methods, the more commonly used are:

This project has received funding from the European Union's Horizon 2020 research and innovation programme under grant agreement No 958171.

- Back-to-back method: reference and tested accelerometer are mounted “back-to-back” and subjected to the same acceleration imposed by an exciter. These methods are used both for vibration calibration and shock calibration. In the first case, a vibration exciter is set to different frequencies and acceleration levels; the reference accelerometer can be both internal and external to exciter. In case of shock calibration, instead, coupled sensors are subjected to shock pulse, measuring the ratio between peaks acceleration to get sensitivity and event duration.

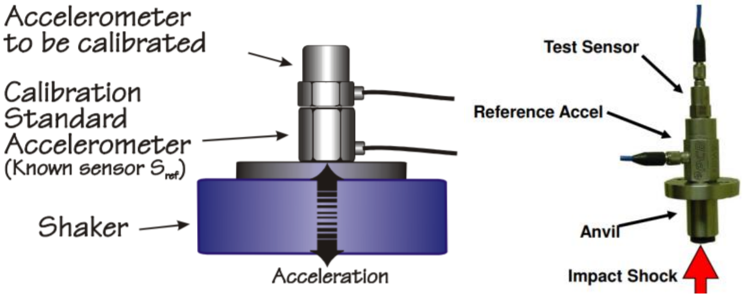

Figure 10.6 – Accelerometers relative calibration methods – back-to-back method

- Handheld shaker: easy to perform and quick test. The shaker has an internal reference accelerometer and provides a fixed g force via a built-in servo-stabilization.
- Portable vibration calibrator

10.4.2.2 Procedures for estimating the component of measurement uncertainty resulting from calibration of the data acquisition system (calibration uncertainty)

Some recommendations are given in ISO 160063 (vibration calibration of rectilinear accelerometers (with or without amplifier) to obtain magnitude and phase of the complex sensitivity.

10.4.2.3 Requirements for data acquisition depending on measured physical quantity (e.g. based on the variation rate)

No specific guidelines available.

10.4.3 Performance

10.4.3.1 Requirements and recommendations for maintenance during operation (in case of continuous maintenance)

Not applicable.

10.4.4 Reporting

No information available.

10.4.5 Lifespan of the technology (if applied for continuous monitoring)

Lifespan up to 5 years.

This project has received funding from the European Union’s Horizon 2020 research and innovation programme under grant agreement No 958171.

10.5 Interpretation and validation of results

10.5.1 Expected output (Format, e.g. numbers in a .txt file)

MEMS accelerometers output are accelerations, expressed in a measure of gravity (g) or in LSB (Least Significant Bit). Output length for each second of acquisition changes based on the set sampling frequency.

10.5.2 Interpretation (e.g. each number of the file symbolizes the acceleration of a degree of freedom in the bridge)

MEMS accelerometers output consists in a measure of acceleration, along one or three axes. Based on sensors settings (e.g. sampling frequency) data quantity can be highly variable.

10.5.3 Validation

Not applicable.

10.5.3.1 Specific methods used for validation of results depending on the technique

10.5.3.2 Quantification of the error

10.5.3.3 Quantitative or qualitative evaluation

10.5.4 Detection accuracy

Not applicable.

10.6 Advantages

MEMS accelerometer main advantages are:

- Low-cost technology
- Applicable in a continuous SHM system
- Easy transportation and installation
- Small size
- Depending on the application, sensors can be set with different parameters

10.7 Disadvantages

Not suitable when operational applications are characterized by low level inputs, due to their noise floor.

10.8 Possibility of automatising the measurements

A sensors network made by MEMS can be automatised by means of a gateway that manages sensors acquisition. In this way, sensors acquisition can depend on different rules: it can be continuous in time, limited to predefined intervals in a journey, etc.

10.9 Barriers

No information available.

This project has received funding from the European Union's Horizon 2020 research and innovation programme under grant agreement No 958171.

10.10 Existing standards

No information available.

10.11 Applicability

10.11.1 Relevant knowledge fields

- Civil Engineering and Structural Health Monitoring
- Automotive Application
- Industrial Application
- Medical Application

10.11.2 Performance Indicators

- Frequency
- Vibrations/oscillations
- Prestressing cable failure
- Reinforcement bar failure/bending
- Tensioning force deficiency
- Loss of section

10.11.3 Type of structure

- Bridges
- Buildings
- Towers
- Transmission towers
- Windmills

10.11.4 Spatial scales addressed (whole structure vs specific asset elements)

10.11.5 Materials

10.12 Available knowledge

10.12.1 Reference projects

10.12.2 Other

10.13 Bibliography

SMARTEC SA Branko Glisic, Daniele Inaudi. (2007). *Sensing tape for easy integration of optical fiber sensors in composite structures.* Manno, Switzerland : SMARTEC SA.

This project has received funding from the European Union's Horizon 2020 research and innovation programme under grant agreement No 958171.

A. Grosso, D. I. (January de 2001). Monitoring of bridges and concrete structures with Fibre Optic Sensors in Europe. *IABSE Symposium, Seoul 2001: Cable-Supported Bridges - Challenging Technical Limits*.

Alexis Mendez, T. G. (2012). Overview of fiber optic sensors for NDT applications. *IV NDT Panamerican Conference Buenos Aires*. Buenos Aires. Obtenido de https://www.researchgate.net/publication/228340034_Overview_of_fiber_optic_sensors_for_NDT_applications

Andrea Del Groso, K. B. (2001). *IABSE Symposium Report: Monitoring of bridges and concrete structures with Fibre optic sensors in Europe*. International Association for Bridge and Structural Engineering.

Andrea del Grosso, K. B. (2001). *Monitoring of Bridges and Concrete Structures with Fibre Optic Sensors in Europe*. IABSE Symposium Report .

BAUMER. (10 de 12 de 2021). *BAUMER* . Obtenido de Passion for sensors : https://www.baumer.com/medias/__secure__/Baumer_Fiber-optic-sensors-to-detect-liquid-levels-and-leakage-of-fluids_EN_0610_AR.pdf?mediaPK=8837757272094

D. Inaudi, S. V. (1999, February 12-13). SOFO: Structural Monitoring with Fiber Optic Sensors . *FIB, Monitoring and Safety Evaluation of Existing Concrete Structures*.

David Krohn, T. M. (2014). *Fiber Optic Sensors Fundamentals and Applications* . Washington: SPIE PRESS .

Fidanboylu, K. E. (2009). Fiber Optic Sensors and their applications. *5th Intenrational Advanced Technologies Symposium* . Karabuk: Fauniversity .

Glisic, B. (2000). Fibre optic sensors and behaviour in concrete at early age . *PhD thesis*. Switzerland: Laboratory of Stress Analysis (IMAC) Swiss Federal Institute of Technology .

H.Hartog, A. (2017). An Introduction to Distributed Optical Fibre Sensors. In A. H.Hartog, *An Introduction to Distributed Optical Fibre Sensors* (pp. 115-128). Boca Raton, United States: CRC Press Taylor & Francis Group.

Instytut Maszyn Przepływowych im. Roberta Szewalskiego PAN. (2011, March). Specyfikacja Istotnych warunków zamówienia (SIWZ). *Dostawa czujników światłowodowych i przetworników* . Gdańsk , Polska .

J. Biliszczuk, W. B. (2009). System monitorowania mostu w Puławach. *Mosty 4* , págs. 12-17.

Jose Luis Santos, F. F. (2015). *Handbook of Optical Sensors*. Boca Raton: CRC Press Taylor & Francis Group.

KEYENCE. (2021, 11 30). *Fibre optic sensors FS-N40 Series*. Retrieved from Digital Fibre optic Sensor: https://www.keyence.co.uk/products/sensor/fiber-optic/fs-n40/downloads/

This project has received funding from the European Union's Horizon 2020 research and innovation programme under grant agreement No 958171. © 2021

Łukasz Bednarski, R. S. (2015). Wybrane zagadnienia monitorowania konstrukcji. *XXX Jubileuszowe Ogólnopolskie Warsztaty Pracy Projektanta Konstrukcji* (págs. 28-30). Szczyrk : Politechnika Krakowska, Akademia Górniczo-Hutnicza.

Mathew kautzman, B. J. (2018). Calibration and testing of distributed fiber optic sensors for detection of high energy radiation . *Journal of Directed Energy* .

Measures, R. M. (2001). *Structural Monitoring with Fiber Optic Technology* . Ontario: Institute of Aerospace Studies .

Mei, Y. (2018, August). Error analysis for distributed fibre optic sensing tehcnology based on Brillouin scattering. USA: University of Cambridge, Department of Philosophy .

Narodowe Centurm Badań i Rozwoju, Politechnika Rzeszowska, . (08 de 12 de 2021). *OptiDeck*. Obtenido de Inteligentny system pomostowy z kompozytów polimerowych do budowy i modernizacji drogowych obiektów mostowych: https://optideck.prz.edu.pl/

NERVE-SENSORS. (2021, 11 30). *NERVE SENSORS Epsilon Rebar strain sensor*. Retrieved 11 30, 2021, from NERVE SENSORS: www.nerve-sensors.com

R. B. Figuera, C. J. (2021). *Development of Advanced Fibre Optic Sensors to Monitor the Durability of Concrete and Reinforced Concrete Structures - SolSensors.* Universidade do Minho, INESC-TEC and Engiprojects, Lda.

Rafał Sieńko, Ł. B. (2016). Monitorowanie obiektów budowlanych w sąsiedztwie budowy . *Geoinzynieria* , págs. 60-65.

Rahul Mukherjee, J. B. (2017). A review of Micromachined Thermal Accelerometers. *Journal of Micromechanics and Microengineering*.

Romaniuk, R. S. (2001). *Miernictwo Światłowodowe Wydanie II Uzupełnione.* Warszawa: Instytut Systemów elektronicznych Politechnika Warszawska.

Samuel Vurpillot, D. I.-M. (1996, April 22). Smart Structures and Materials vol. 2719. *Bridge Monitoring by fiber optic deformation sensors: design, emplacemnet and results*. San Diego , USA: Society of Photo-Optical Instrumentation Engineers.

SHM SYSTEMS. (7 de 12 de 2021). *SHM Systems Projects*. Recuperado el 7 de 12 de 2021, de SHM Systems: https://www.shmsystem.pl/projects/

SMARTEC SA, Branko Glisic, Daniele Posenato, Daniele Inaudi. (2007, May). Integrity monitoring of old steel bridge using fiber optic distributed sensors based on Brillouin scattering. *Proceedings of SPIE.* The International Society for Optical Engineering. doi:10.1117/12.716055

T. H. Nguyen, T. V. (2014, February). Fluorescence based fibre optic pH sensor for the pH 10–13 range suitable for corrosion monitoring in concrete structures. *Sensors and Actuators B Chemical 191*, pp. 498-507.

This project has received funding from the European Union's Horizon 2020 research and innovation programme under grant agreement No 958171.

Tomasz Siwowski, R. S. (2017, May). System monitorowania mostów kompozytowych z wykorzystaniem światłowodowych czujników odkształceń. *PROJECT COM-BRIDGE, DEMONSTRATOR+*, (pp. 50-53).

Udd, E. (2006). *Fiber Optic Sensors And Introduction for Engineers and Scientists.* New Jersey : John Wiley & Sons, Inc. .

W. Barcik, R. S. (2012). System monitorowania konstrukcji Mostu Rędzińskiego we Wrocławiu. *Mosty 2*, págs. 56-62.

This project has received funding from the European Union's Horizon 2020 research and innovation programme under grant agreement No 958171.

APPENDIX A11. Microelectromechanical Systems (MEMs) - Clinometers

11.1 Goal(s)

11.1.1 Main objective

MEMS sensors include a variety of transducers based on special micromachining of silicon. This allows to create sensor families having tunable features, according to the specific needs.

One application of MEMS sensors are Clinometers. They derive from MEMS accelerometers and measure the inclination with respect to the horizontal axis. For this reason, they are useful to analyse structures static behaviour.

11.2 Description

11.2.1 Functioning mode

MEMS Clinometers measure acceleration along a single axis or two normal axes to give the acceleration vector.

MEMS Clinometers are g sensitive: pitch or roll cause a change in the projection of gravity along the sensitive axis.

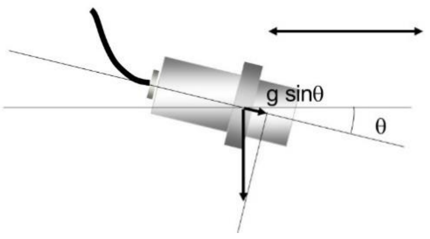

Figure 11.1 – Clearance hole mounting (SIEMENS , 2021)

As a fraction of gravity is sensed, MEMS clinometers only work for rotations around axes lying in the horizontal plane, while rotations around a vertical axis do not produce any measurable change.

The output is proportional to sinθ, where θ is the angle between the sensing axis and the horizontal plane: this means that the output is not linear and that sensitivity changes according to the same angle θ the clinometer is sensing. Some facts are easily noted:

- For small rotations around θ=0 deg the calibration curve can be linearized and the maximum sensitivity is achieved
- For angles close to θ=90 deg the sensitivity (proportional to cosθ) tends towards 0 and linearization is not really possible as the calibration curve rate of change is higher than around zero.

This project has received funding from the European Union's Horizon 2020 research and innovation programme under grant agreement No 958171.

11.2.2 Types

There are several types of MEMS clinometers, all provided as an Integrated Circuit with some conditioning electronics on a board. MEMS clinometers differ in parameters settings values, such as:

- Full Scale (FS): range of acceleration values that can be measured
- Resolution: minimum detectable change in acceleration, expressed in [mg]
- Sensitivity: also known as gain, is the output change per unit of input acceleration.

MEMS clinometers can be single axis or dual axis.

11.2.3 Process/event to be detected or monitored

MEMS clinometers are useful to analyse structures static behaviour. Through pitch and roll measurements they allow the detection of structures elements deformations, highlighting the appearance of eventual damage process, of brittle or plastic nature.

11.2.4 Physical quantity to be measured (e.g. actions, displacements, deformations, dynamic structural properties, material properties including mechanical, electrical and chemical properties, relative displacements of the two sides of a crack, etc.).

MEMS clinometers, returning tilt, can be used to measure structures deformations and relative displacements between different structural elements.

11.2.5 Induced damage to the structure during the measurement

No damage induced.

11.2.6 General characteristics

11.2.6.1 Measurement type (static or dynamic, local or global, short-term or continuous, etc.)

The design of MEMS accelerometers makes them g-sensitive, this means that their lower bound can extend to 0 Hz, which means capability to measure static or quasi static quantities. Therefore, they are suitable to measure tilt, as the projection of gravity along the measurement axis.

MEMS clinometers can be employed for both short-term and continuous testing; besides, they can be used to describe the behavior of both local structural elements and the global structure.

11.2.6.2 Measurement range

As accelerometers work below resonance, the MEMS accelerometer performances depend upon the natural frequency of the silicon structure, which can be designed to reach bandwidths from some hundreds of Hertz up to some thousands, for sure redundant for monitoring applications, mainly requiring low frequency ranges and low full scales.

This project has received funding from the European Union’s Horizon 2020 research and innovation programme under grant agreement No 958171.

The full scale can also be adjusted thanks to a specific electronic hardware: full scale for the MEMS commonly adopted in monitoring applications can range from fractions of gravity up to some g, even if it is not so uncommon to have full scales of several hundred g, for specific applications, not related to monitoring.

11.2.6.3 Measurement accuracy

MEMS accelerometers can provide an analog output, though these are not so common today, or an already digitized output; they require a power supply typically in the range 0-5 V and also the output is within the mentioned range.

Clinometers have a measurement accuracy changeable based on their setted parameters (FS, etc.). Maximum sensitivity is achieved for low angle, around the horizontal axis.

The measurement can be affected by errors due to temperature drifts; for compensating this error it is advisable to have an on-board temperature sensor in the clinometer case itself.

11.3 Background (evolution through the years)

In the second half of the 1950s, the first papers regarding MEMS technology were published (C.S. Smith, 1954), describing piezoresistive effects in silicon and germanium. First MEMS applications are related to silicon pressure sensors, which commercialization started in the USA at the end of the 1960s. The technology development was very fast, thanks to improvements in silicon processing and in micromachining. Small, rugged and inexpensive devices with always increasing performance were produced, ranging in different categories: accelerometers, strain gauges, pressure sensors, microphones, gyroscopes, etc. Fields of application of the technology, as consequence, increased through the years: MEMS sensors are applied in the automotive, medical, aerospace, automation industry. Accelerometers technology is continuously evolving, advanced surface micromachining techniques allow them to sense in one, two or three axes and thanks to always improved performance, their market is expanding and it is expected to grow rapidly in the future.

11.4 Performance

11.4.1 General points of attention and requirements

11.4.1.1 Design criteria and requirements for the design of the survey

11.4.1.2 Procedures for defining layout of the survey

11.4.1.3 Design constraints (e.g. related to the measurement principles of the monitoring technologies)

Sensors layout should be carefully designed according to the phenomenon to be analysed and/or monitored. It would be advisable to have one sensor on each key node of the structure and on each relevant structural element, so that any deformation of the structure can be detected.

This project has received funding from the European Union's Horizon 2020 research and innovation programme under grant agreement No 958171.

11.4.1.4 Sensibility of measurements to environmental conditions

MEMS accelerometers measurements can be influenced by environmental conditions, especially by temperature and during long-term/continuous testing. For this reason, it is advisable having an on-board temperature sensor, so that eventual temperature drift can be compensated.

11.4.2 Preparation

11.4.2.1 Procedures for calibration, initialisation, and post-installation verification

MEMS clinometers calibration aim to obtain sensors sensitivity at different tilts. Procedure usually consists in rotating the device through a known set of angles and measuring the acceleration output given by the sensor. Through a subsequent analysis, comparing sensor and theorical measure, the calibration curve is obtained.

11.4.2.2 Procedures for estimating the component of measurement uncertainty resulting from calibration of the data acquisition system (calibration uncertainty)

No applicable.

11.4.2.3 Requirements for data acquisition depending on measured physical quantity (e.g. based on the variation rate)

No applicable.

11.4.3 Performance

11.4.3.1 Requirements and recommendations for maintenance during operation (in case of continuous maintenance)

No applicable.

11.4.4 Reporting

11.4.5 Lifespan of the technology (if applied for continuous monitoring)

MEMS lifespan can vary between 2 and 5 years.

11.5 Interpretation and validation of results

11.5.1 Expected output (Format, e.g. numbers in a .txt file)

MEMS clinometers output are accelerations, expressed in a measure of gravity (g) or, if the measures are already calibrated, in degrees.

11.5.2 Interpretation (e.g. each number of the file symbolizes the acceleration of a degree of freedom in the bridge)

MEMS accelerometers output consists in a measure of tilt, along one or two axis.

This project has received funding from the European Union's Horizon 2020 research and innovation programme under grant agreement No 958171.

11.5.3 Validation

No applicable.

11.5.3.1 Specific methods used for validation of results depending on the technique

11.5.3.2 Quantification of the error

11.5.3.3 Quantitative or qualitative evaluation

11.5.4 Detection accuracy

11.6 Advantages

MEMS accelerometer main advantages are:

- Low-cost technology.
- Applicable in a continuous SHM system.
- Easy transportation and installation
- Small size
- Depending on the application, sensors can be set with different parameters.

11.7 Disadvantages

- High measurement accuracy only around small angles.
- Only rotations around axis laying in the horizontal plane can be measured.

11.8 Possibility of automatising the measurements

A sensors network made by MEMS can be automatised by means of a gateway that manages sensors acquisition. In this way, sensors acquisition can depend on different rules: it can be continuous in time, limited to predefined intervals in a journey, etc.

11.9 Barriers

11.10 Existing standards

11.11 Applicability

11.11.1 Relevant knowledge fields

- Civil Engineering and Structural Health Monitoring
- Automotive Application
- Industrial Application
- Medical Application

This project has received funding from the European Union's Horizon 2020 research and innovation programme under grant agreement No 958171.

11.11.2 Performance Indicators

Relate the surveying technology being studied with PIs from WP3, provided in the document of the TU1406 COST ACTION.

- Deformation
- Loss of section
- Reinforcement bar failure/bending

11.11.3 Type of structure

- Bridges
- Tunnels

11.11.4 Spatial scales addressed (whole structure vs specific asset elements)

11.11.5 Materials

11.12 Available knowledge

11.12.1 Reference projects

11.12.2 Other

11.13 Bibliography

SMARTEC SA Branko Glisic, Daniele Inaudi. (2007). *Sensing tape for easy integration of optical fiber sensors in composite structures.* Manno, Switzerland : SMARTEC SA.

A. Grosso, D. I. (2001, January). Monitoring of bridges and concrete structures with Fibre Optic Sensors in Europe. *IABSE Symposium, Seoul 2001: Cable-Supported Bridges - Challenging Technical Limits*.

Alexis Mendez, T. G. (2012). Overview of fiber optic sensors for NDT applications. *IV NDT Panamerican Conference Buenos Aires.* Buenos Aires. Retrieved from https://www.researchgate.net/publication/228340034_Overview_of_fiber_optic_sensors_for_NDT_applications

Andrea Del Groso, K. B. (2001). *IABSE Symposium Report: Monitoring of bridges and concrete structures with Fibre optic sensors in Europe.* International Association for Bridge and Structural Engineering.

Andrea del Grosso, K. B. (2001). *Monitoring of Bridges and Concrete Structures with Fibre Optic Sensors in Europe.* IABSE Symposium Report .

BAUMER. (2021, 12 10). *BAUMER* . Retrieved from Passion for sensors : https://www.baumer.com/medias/__secure__/Baumer_Fiber-optic-sensors-to-detect-liquid-levels-and-leakage-of-fluids_EN_0610_AR.pdf?mediaPK=8837757272094

D. Inaudi, S. V. (1999, February 12-13). SOFO: Structural Monitoring with Fiber Optic Sensors . *FIB, Monitoring and Safety Evaluation of Existing Concrete Structures*.

David Krohn, T. M. (2014). *Fiber Optic Sensors Fundamentals and Applications* . Washington: SPIE PRESS .

This project has received funding from the European Union's Horizon 2020 research and innovation programme under grant agreement No 958171.

Fidanboylu, K. E. (2009). Fiber Optic Sensors and their applications. *5th Intenrational Advanced Technologies Symposium* . Karabuk: Fauniversity .

Glisic, B. (2000). Fibre optic sensors and behaviour in concrete at early age . *PhD thesis*. Switzerland: Laboratory of Stress Analysis (IMAC) Swiss Federal Institute of Technology .

H.Hartog, A. (2017). An Introduction to Distributed Optical Fibre Sensors. In A. H.Hartog, *An Introduction to Distributed Optical Fibre Sensors* (pp. 115-128). Boca Raton, United States: CRC Press Taylor & Francis Group.

Instytut Maszyn Przepływowych im. Roberta Szewalskiego PAN. (2011, March). Specyfikacja Istotnych warunków zamówienia (SIWZ). *Dostawa czujników światłowodowych i przetworników* . Gdańsk , Polska .

J. Biliszczuk, W. B. (2009). System monitorowania mostu w Puławach. *Mosty 4* , pp. 12-17.

Jose Luis Santos, F. F. (2015). *Handbook of Optical Sensors.* Boca Raton: CRC Press Taylor & Francis Group.

KEYENCE. (2021, 11 30). *Fibre optic sensors FS-N40 Series*. Retrieved from Digital Fibre optic Sensor: https://www.keyence.co.uk/products/sensor/fiber-optic/fs-n40/downloads/

Łukasz Bednarski, R. S. (2015). Wybrane zagadnienia monitorowania konstrukcji. *XXX Jubileuszowe Ogólnopolskie Warsztaty Pracy Projektanta Konstrukcji* (pp. 28-30). Szczyrk : Politechnika Krakowska, Akademia Górniczo-Hutnicza.

Mathew kautzman, B. J. (2018). Calibration and testing of distributed fiber optic sensors for detection of high energy radiation . *Journal of Directed Energy* .

Measures, R. M. (2001). *Structural Monitoring with Fiber Optic Technology* . Ontario: Institute of Aerospace Studies .

Mei, Y. (2018, August). Error analysis for distributed fibre optic sensing tehcnology based on Brillouin scattering. USA: University of Cambridge, Department of Philosophy .

Narodowe Centurm Badań i Rozwoju, Politechnika Rzeszowska, . (2021, 12 08). *OptiDeck*. Retrieved from Inteligentny system pomostowy z kompozytów polimerowych do budowy i modernizacji drogowych obiektów mostowych: https://optideck.prz.edu.pl/

NERVE-SENSORS. (2021, 11 30). *NERVE SENSORS Epsilon Rebar strain sensor*. Retrieved 11 30, 2021, from NERVE SENSORS: www.nerve-sensors.com

R. B. Figuera, C. J. (2021). *Development of Advanced Fibre Optic Sensors to Monitor the Durability of Concrete and Reinforced Concrete Structures - SolSensors.* Universidade do Minho, INESC-TEC and Engiprojects, Lda.

Rafał Sieńko, Ł. B. (2016). Monitorowanie obiektów budowlanych w sąsiedztwie budowy . *Geoinzynieria* , pp. 60-65.

Romaniuk, R. S. (2001). *Miernictwo Światłowodowe Wydanie II Uzupełnione.* Warszawa: Instytut Systemów elektronicznych Politechnika Warszawska.

Samuel Vurpillot, D. I.-M. (1996, April 22). Smart Structures and Materials vol. 2719. *Bridge Monitoring by fiber optic deformation sensors: design, emplacemnet and results*. San Diego , USA: Society of Photo-Optical Instrumentation Engineers.

SHM SYSTEMS. (2021, 12 7). *SHM Systems Projects*. Retrieved 12 7, 2021, from SHM Systems: https://www.shmsystem.pl/projects/

This project has received funding from the European Union's Horizon 2020 research and innovation programme under grant agreement No 958171.

SIEMENS . (2021, 12 14). *SIEMENS Acoustic Sensors* . Retrieved from Siemens Operating Instructions SIT Trans AS100: https://adegis.com/media/asset/981b1fab3911f86718855fb811cc55a8ce6ece66f0e5f730aaf297fca9f45200.pdf

SMARTEC SA, Branko Glisic, Daniele Posenato, Daniele Inaudi. (2007, May). Integrity monitoring of old steel bridge using fiber optic distributed sensors based on Brillouin scattering. *Proceedings of SPIE.* The International Society for Optical Engineering. doi:10.1117/12.716055

T. H. Nguyen, T. V. (2014, February). Fluorescence based fibre optic pH sensor for the pH 10–13 range suitable for corrosion monitoring in concrete structures. *Sensors and Actuators B Chemical 191*, pp. 498-507.

Tomasz Siwowski, R. S. (2017, May). System monitorowania mostów kompozytowych z wykorzystaniem światłowodowych czujników odkształceń. *PROJECT COM-BRIDGE, DEMONSTRATOR+*, (pp. 50-53).

Udd, E. (2006). *Fiber Optic Sensors And Introduction for Engineers and Scientists.* New Jersey : John Wiley & Sons, Inc. .

W. Barcik, R. S. (2012). System monitorowania konstrukcji Mostu Rędzińskiego we Wrocławiu. *Mosty 2*, pp. 56-62.

This project has received funding from the European Union's Horizon 2020 research and innovation programme under grant agreement No 958171.

APPENDIX A12. Qualitative Chemical Methods

12.1 Goal(s)

12.1.1 Main objective

Chemical methods based on pH determination are widely used for inspection of the carbonation front depth, and determination of whether the standard pH of concrete has been changed under environmental conditions. The carbonation of concrete consists of many physicochemical changes due to the constant influence of the carbon dioxide from the air as well as in the indoor atmosphere of building structures. The carbonation process has a complicated effect on concrete properties and leads to a decrease of the alkalinity resulting in a loss of protective properties against the reinforcement. From the point of view of diagnostic tests for bridge structures it is crucial to use pH indicators to analyse analyze of the carbonation process and assessment of the natural ability of concrete to protect the reinforcement against corrosion – eventually to prevent the risk of degradation of the entire structure (Grzegorz Bajorek, 2014) (Jaroszyńska-Wolińska, 2011).

12.2 Description

12.2.1 Functioning mode

- *pH indicators* – methods used for pH determination work on the principle of visual observation of the changes of colors on the sample after subjecting to a specific indicator. For concrete structure applications indicators are used in a form of spray, such as phenolphthalein, thymolphthalein, or universal indicator. Used compounds are widely known in various industries, so this methods are well established (J. Hulimka, 2020).
- *Uranyl-Acetate Treatment* – method base on the use of uranyl acetate solution and UV light source for inspection of concrete structures to determine presence of gel in the composition, associated with observation of the change of color under UV light in areas subjected to Alkali-Aggregate reaction; uranyl acetate solution is applied from a plastic squeeze bottle or spray.
- *Half-cell potential* – method base on the measurement of potential detected at the electrode of a half cell in an electrochemical cell. reinforcing concrete, an electrode forms one half of the cell and the reinforcing steels in the concrete form the other half cell Registered data are used for evaluation of corrosion probability and potential vulnerability to corrosion;
- *Electrical resistivity tomography* – calculates the distribution of electrical resistivity from a large number of resistance measurements made from electrodes on a concrete sample; the procedure is repeated using different current patterns, and the three-dimensional conductivity distribution is reconstructed from data set corresponding to multiple current applications. Available modes of, measurements are apparent resistivity mode, resistance mode, voltage mode, and battery voltage mode.

This project has received funding from the European Union's Horizon 2020 research and innovation programme under grant agreement No 958171.

- *Infrared Spectroscopy* – measures the change in the dipole moment of molecules due to irradiation with light at frequencies that trigger transitions between vibrational energy levels of molecules. The two most common modes are:
  - Transmission mode,
  - Attenuated Total Reflexion mode.

Details on electrical resistivity tomography and infrared spectroscopy functioning modes can be found in (Lataste, 2003) (Karhunen K. S., 2010) (Buettner, 1996) (Ghosh, 1974) (Hughes, 1995).

12.2.2 Types

- *pH indicators*:
  - Phenolphthalein test (Deep Purple indicator) – spraying indicator, which is an alcohol solution of phenolphthalein, changing color at pH values higher than 8,
  - Thymolphthalein test – spraying indicator with a solution of thymolphthalein, changing the colour to navy blue when pH is higher than 9 (Reis, 2019),
  - Rainbow test for pH determination; spraying indicator which is used for pH changes in the range of 5 to 13.
- *Uranyl-Acetate Treatment* – powdered indicator is used as a source of ultraviolet of short wavelength. Uranyl acetate solution is applied from plastic bottle or sprayer.
- *Half-cell potentials method* – for reinforced concrete samples, half-cell electrodes are made
- *Electrical resistivity tomography* - two types of electrodes are usually used in this method:
  - wet electrodes – the wet sponge is submerged in the solution of copper - sulphate and placed in the copper cylinder covered by a plastic casing; sponge is attached to the concrete surface and current is applied to the copper cylinders; springs are used to push the electrodes to the concrete surface,
  - gel electrodes – steel electrodes with non-polarizing electrode gel between steel and concrete; there is used for example KIT4 Electrical impedance Tomography Measurement System designed by the University of Eastern Finland; two types of electrodes can be used – wet and gel electrodes which are designed for measurement with concrete samples; systems can be designed for 2D imaging or 3D imaging with 60 or 120 channels.

Example parameters of the Electrical Resistivity Tomograph are shown below:

This project has received funding from the European Union's Horizon 2020 research and innovation programme under grant agreement No 958171.

Input Gain Ranging	Automatic; 0.08, 0.4, 2, 10 V
Maximum Output Current	2.5 Amps
Maximum Output Voltage	475 Volts 950 V peak to peak
Maximum Output Power	250 Watts
Power Supply	12 V
Input Impedance	~10^9 Ohm
Electrodes	Simple Metal Electrodes
Input (Receiver) Voltage Range	+/- 10 V, 1000 V Common Mode
Analogue to Digital Conversion	24 Bit A to D converters per channel
Measurement Precision	0.05% Typical
IP Measurement	User Selectable 35 Custom Windows
Power-Line Rejection	60 Hz / 50 Hz
SP Compensation	Proprietary High-Order Polynomial
Waveform	Square: On+, Off, On-, Off (Time Domain) or On+, On- (Frequency Domain)
Operation Frequency	Programmable From 1/64 Hz to 13.5 Hz
Signal Processing	Continuous Stacking Over Integration Window
Stacking	Maximum Stacks 256
Noise Reporting	As Standard Deviation
Noise Rejection	Proprietary Rejection of Electrode Noise
Multi-Channel	8 Independent Receiver Channels
Memory & Data Storage	MicroSD Card
Data Transmission	RS-232C or USB or Direct Read of MicroSD Card
User Controls	Laptop Computer Software Interface
Receiver Weight	Approximately 19 kg (Multiplexer = 12 kg)
Dimensions	47 cm X 36 cm X 31 cm

Figure 12.1 – The DAS-1 system from ERTLab Studio (ERTLab Studio)

- *Infrared Spectroscopy* – the IR spectrophotometer consist of the radiation source, the chamber for sample, photometer, monochromator, and detector. The optical system of the IR spectrophotometer is in the form of a series of mirrors guiding the proper course of the radiation beam. Prisms or diffraction gratings are used as the monochromator. As a prism material must be permeable to IR radiation - the most common are sodium chloride NaCl or potassium bromide KBr crystals (Grzegorz Bajorek, 2014).

12.2.3 Process/event to be detected or monitored

- *pH indicators* – pH evaluation based on the visual inspection of the cross-section of sample and colours revealed by indicator used; localization of the corrosion centre and depth of carbonation process; estimation of the service life if penetration of the carbonation front is high.
- *Uranyl-Acetate Treatment* – change of the colour on the sample due to presence of gel associated with alkali-aggregate reaction or no change, which excludes the influence of alkali-aggregate reaction in potential degradation at the time of inspection; early stage of cracking.
- *Half-cell potentials method – determination* of the probability of corrosion within the rebar based on half-cell potential changes within the sample.
- *Electrical resistivity tomography* – crack detection, localization of rebars (KImmo Karhunen, 2010).
- *Infrared Spectroscopy* – monitoring of carbonates formation.

This project has received funding from the European Union's Horizon 2020 research and innovation programme under grant agreement No 958171.

12.2.4 Physical quantity to be measured (e.g. actions, displacements, deformations, dynamic structural properties, material properties including mechanical, electrical and chemical properties, relative displacements of the two sides of a crack, etc.).

- *pH indicators* - no quantity is measured directly during the test, only visual assessment.
- *Uranyl-Acetate Treatment* - no quantity is measured directly during the test, only visual assessment.
- *Half-cell potential method – the* potential difference between both electrodes, rate of dissolution of the anode, spacing between rebars, cover diameter
- *Electrical resistivity tomography* - conductivity [µS/cm] distribution, voltages are measured between several electrode pairs.
- *Infrared Spectroscopy* – absorption level [%] vs wavenumber [cm^{-1}].

12.2.5 Induced damage to the structure during the measurement

Samples for pH determination should be taken as newly cut out form or freshly broken piece of concrete from different depths of the structure. There is also a possibility of examination and application of indicators directly on the fresh fracture or forgings of the structure, without additional damage. In other methods there is a need to collect the sample as a drilled part of the structure so the damage is induced in the preparation stage.

12.2.6 General characteristics

12.2.6.1 Measurement type (static or dynamic, local or global, short-term or continuous, etc.)

- *pH indicators - local investigation within at least five different points of the inspected area, short-term.*
- *Uranyl-Acetate Treatment - local investigation within at least five different points of the inspected area, short-term.*
- *Half-cell potentials method – local investigation which can be performed short-term, changes of the potential are dynamic, however there is only registered a value at specific time and location.*
- *Electrical resistivity tomography – local and short-term measurement, geometrically continuous.*
- *Infrared Spectroscopy – local and short-term measurement.*

12.2.6.2 Measurement range

- *pH indicators* - with deep purple test pH can be measured in a range of 8.5 to 9.5. For thymolphthalein test the pH upper limit is 10. Rainbow test can be used in a range of 5 to 13.
- *Uranyl-Acetate Treatment* – not applicable;

This project has received funding from the European Union's Horizon 2020 research and innovation programme under grant agreement No 958171. © 2021

- *Half-cell potentials method* – range depends on the conditions of the sample, for example for humid and chloride free concrete sample potential values can be measured within range -200 to +100 mV, while for dry concrete within 0 to + 200 mV; also depends on the size of the rebar:

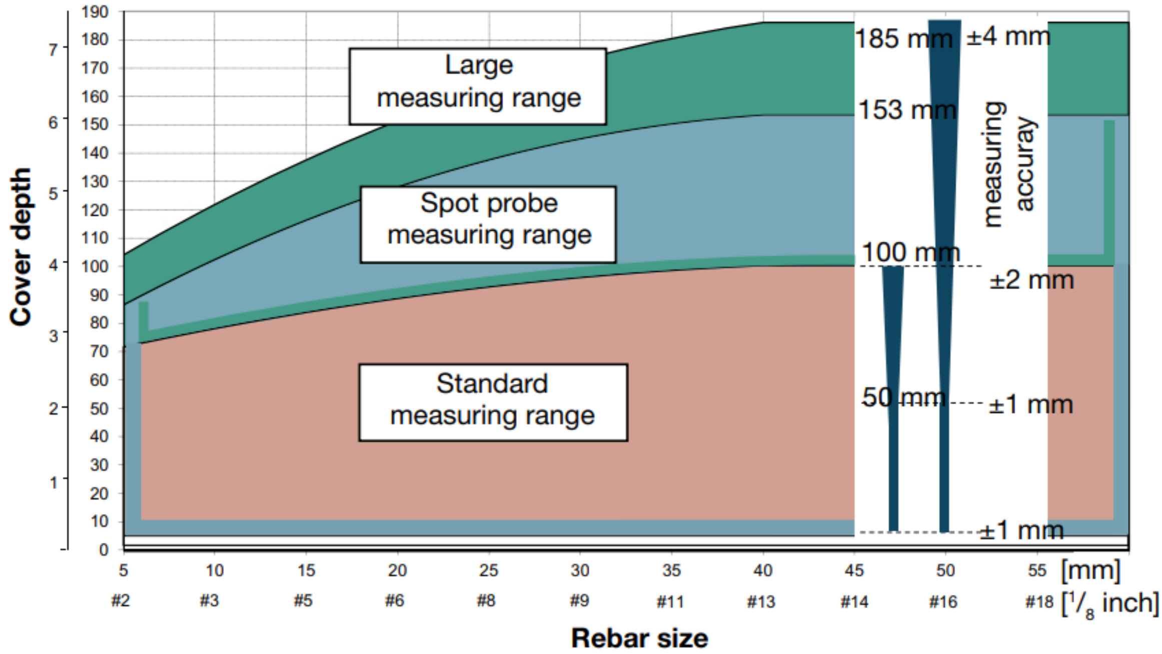

Figure 12.2 – Measuring ranges and accuracy (Hammond Concrete Services).

- *Electrical resistivity tomography* - depending on the instruments used, resistance can be measured within range: 400 kΩ – 0,1 mΩ and voltage within 0 - 500V;
- *Infrared Spectroscopy* – spectra is registered within the wavelength range of 2,500 to 16,000 nm.

12.2.6.3 Measurement accuracy

- *pH indicators* - depth of the carbonated surface should can be measured with an accuracy of 1 mm.
- *Uranyl-Acetate Treatment* – used only as an estimation technique, accuracy is not recorded.
- *Half-cell potentials method* – please see measurement range section and the resolution is given on the diagram below:

This project has received funding from the European Union's Horizon 2020 research and innovation programme under grant agreement No 958171.

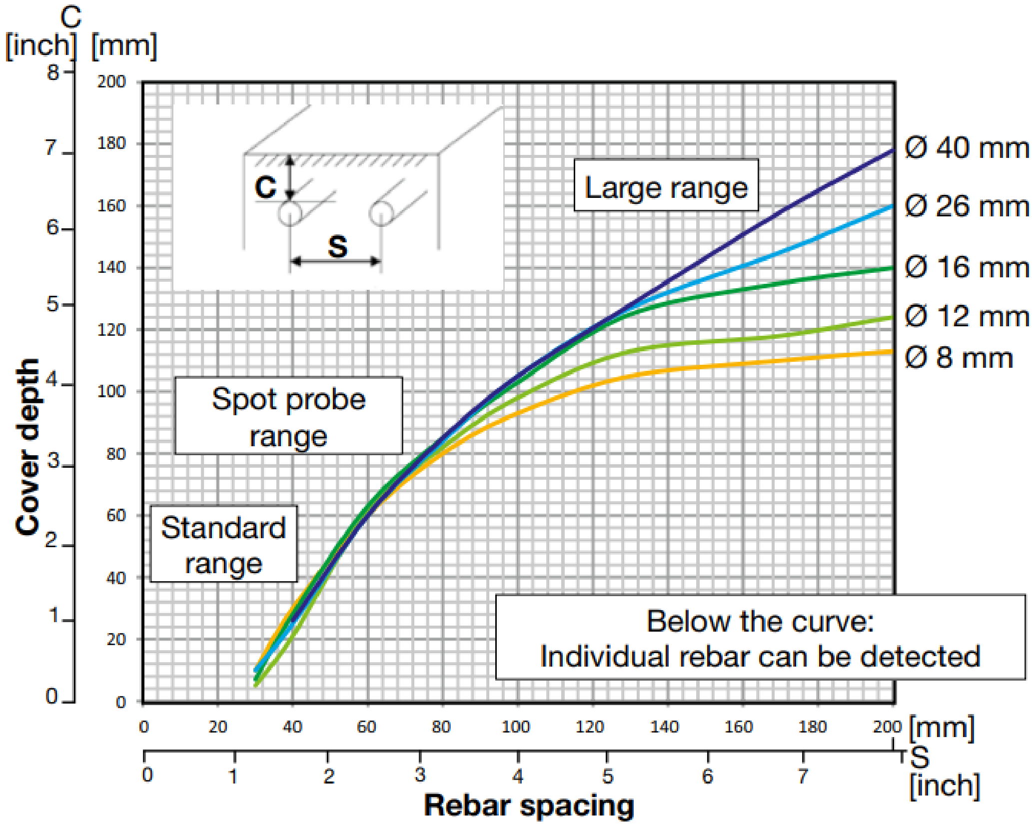

Figure 12.3 – Measurement resolution (Hammond Concrete Services)

- *Electrical resistivity tomography – depends on the equipment used.*
- *Infrared Spectroscopy - depends on the equipment used.*

12.3 Background (evolution through the years)

Rainbow test has been created by Germann Instruments in Denmark. In 1991 the pH value has been correlated with the depth of carbonation process. Electrical resistivity tomography was developed in the same time as electrical impedance tomography in 1978. Theoretical and practical aspects of both ethod has been developed since 1980 (Buettner, 1996).

12.4 Performance

12.4.1 General points of attention and requirements

12.4.1.1 Design criteria and requirements for the design of the survey

- *pH indicators* – surface of concrete should be cleaned and smoothed before test.
- *Uranyl-Acetate Treatment* - grinding wheel or electric drill is used to grind off surface layer of concrete and rinsed with tap water; protective eye wear and rubber gloves have to be used. Concrete surface should be investigated in a darkened room or, when in the field, through viewing openings in a box that prevents light from reflecting on the concrete surface.

This project has received funding from the European Union's Horizon 2020 research and innovation programme under grant agreement No 958171. © 2021

12.4.1.2 Procedures for defining layout of the survey

- *Half-cell potentials method* - the survey procedure is firstly to locate the steel and determine the bar spacing using a covermeter. The cover concrete is removed locally over a suitable bar and an electrical connection made to the steel. It is necessary to check that the steel is electrically continuous by measuring the resistance between two widely separated points. The reinforcing bar is then connected to the half-cell via a digital voltmeter. For details please refer to (The Concrete Society, 2000)
- *Electrical resistivity tomography* – survey planning can be found for example in manufacturer manual - (Geostudi Astier srl and Multi-Phase Technologies LLC, 2006).

12.4.1.3 Design constraints (e.g. related to the measurement principles of the monitoring technologies)

- *Infrared Spectroscopy* - One common problem will be the appearance of two strong bands around 2300-2400 cm-1 (usually out-of-phase). These are CO stretches caused by the ionization of air in the machine. This can be eliminated by purging the instrument with nitrogen gas for 2-3 hours, but the people in charge must know about the problem to fix it.

12.4.1.4 Sensibility of measurements to environmental conditions

Electrical resistivity tomography and Infrared Spectroscopy measurements are performed in reproducible environment in controlled laboratorial conditions, therefore the measurements are not influenced by them.

12.4.2 Preparation

12.4.2.1 Procedures for calibration, initialisation, and post-installation verification

- *Electrical resistivity tomography* – calibration is performed digitally by microprocessor which is basing on the correction factors stored in memory; correction factors are determined during periodical calibration performed by authorized service centres of manufacturer of the instrument.

12.4.2.2 Procedures for estimating the component of measurement uncertainty resulting from calibration of the data acquisition system (calibration uncertainty)

No specific guidelines.

12.4.2.3 Requirements for data acquisition depending on measured physical quantity (e.g. based on the variation rate)

No specific guidelines.

This project has received funding from the European Union's Horizon 2020 research and innovation programme under grant agreement No 958171.

12.4.3 Performance

12.4.3.1 Requirements and recommendations for maintenance during operation (in case of continuous maintenance)

Not applicable. Regular calibration checks over the life of the equipment are a requirement of quality management procedures, e.g. ISO 9000, and other similar standards.

12.4.3.2 Criteria for the successive surveying campaigns for updating the sensors. The campaigns include: (i) Georeferenced frame, i.e. the global location on the bridge; (ii) Alignment of sensor data, relative alignment of the data collected in a surveying; (iii) Multi-temporal registration to previous campaigns; and (iv) Diagnostics.

Not applicable.

12.4.4 Reporting

- *pH indicators* - the report should include description of the samples, sampling depth/area, pH values and photo documentation of the pH profile changes, date of measurements, indication of the substances used as pH indicators.
- *Uranyl-Acetate Treatment* - the report should include description of the samples, sampling depth/area, photo documentation of the observations, date of measurements, indication of the substance used.
- *Half-cell potentials method*
- *Electrical resistivity tomography*
- *Infrared Spectroscopy*

For these methods, reports are usually given automatically by the software used.

12.4.5 Lifespan of the technology (if applied for continuous monitoring)

pH tests are not used in the continuous monitoring. The measurements can be repeatedly performed over time to monitor the progress of carbonation process, but it requires the procedure to be repeated with samples from the same areas. The same applies for other methods.

12.5 Interpretation and validation of results

12.5.1 Expected output (Format, e.g. numbers in a .txt file)

- *pH indicators – visual observation* - graphical representation of pH changes on the surface of a sample;
- *Uranyl-Acetate Treatment* - the presence of gel visible in UV light as a yellow/ green fluorescent glow;
- *Half-cell potentials method* – potential values as a number; display of a spacing between rebars and change of cover depth:

This project has received funding from the European Union's Horizon 2020 research and innovation programme under grant agreement No 958171.

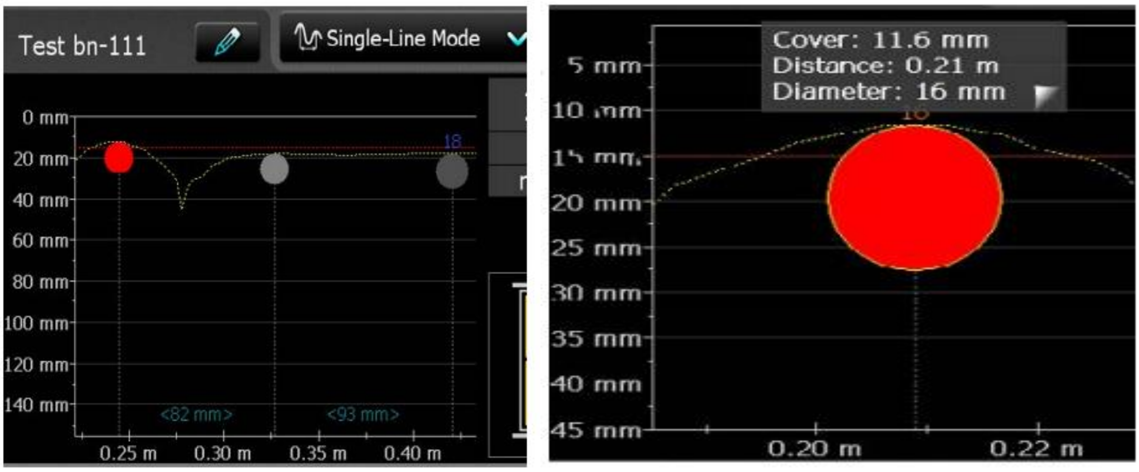

Figure 12.4 – Output of the half-cell profometer measurement (Hammond Concrete Services)

- *Electrical resistivity tomography* – map of the conductivity reconstruction, for example:

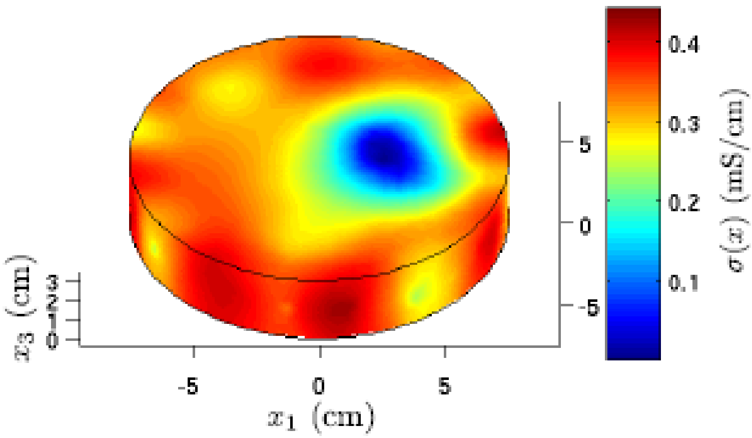

Figure 12.5 – Conductivity reconstruction map

- *Infrared Spectroscopy* - plot of absorbance vs wavenumber cm^{-1};

This project has received funding from the European Union's Horizon 2020 research and innovation programme under grant agreement No 958171.

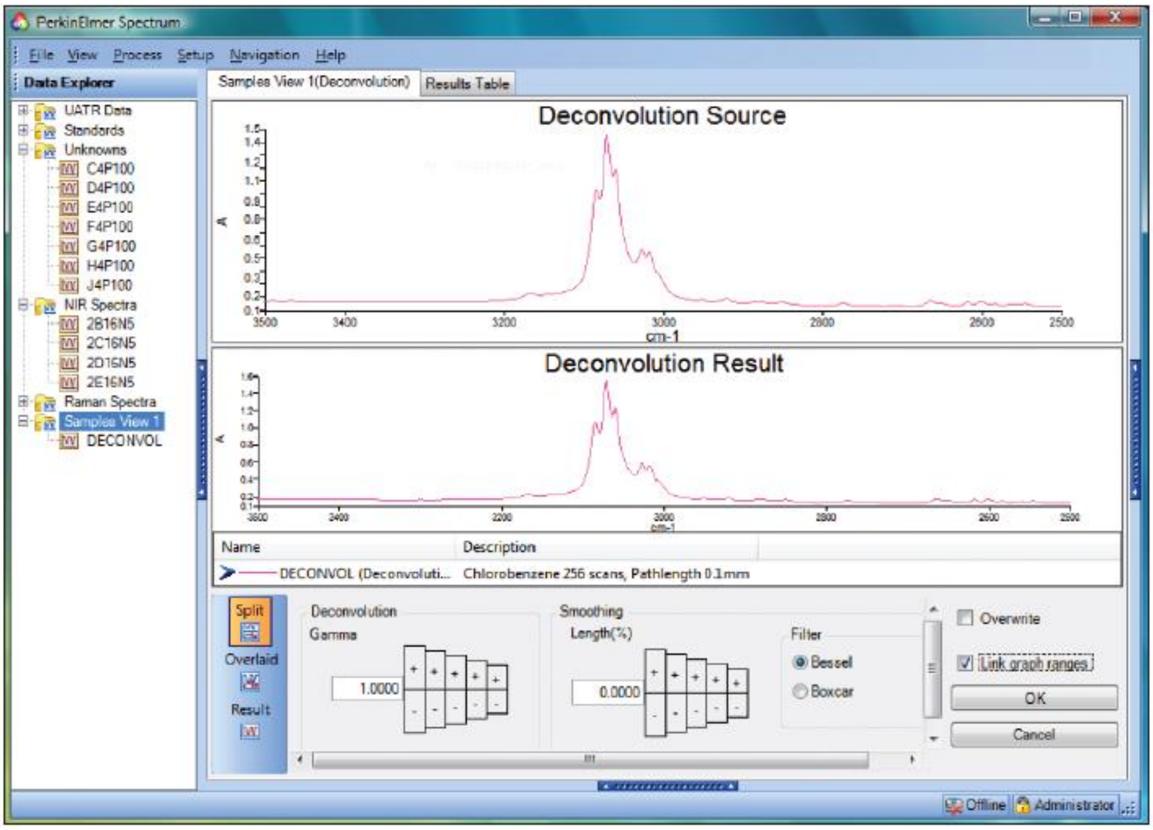

Figure 12.6 – The Output of IR Spectrometer (Perkin Elmer , 2011-2015)

12.5.2 Interpretation (e.g. each number of the file symbolizes the acceleration of a degree of freedom in the bridge)

- *pH indicators – visual observation* - comparing the colours on the samples with the scale, which is enclosed to the used indicator, it is possible to determine approximate pH level. For the phenolphthalein test, the red color should be considered the boundary of the concrete carbonization zone, which corresponds to a pH value of 8.5. If phenolphthalein becomes colorless, the concrete is carbonated.

  In the case of Rainbow Test, concrete with a navy blue or purple color, which corresponds to a pH value of 11-13, should be considered completely safe for the reinforcement. The transition of the color palette from violet to green should be considered the boundary of the carbonized zone, which corresponds to pH value 9-10. The change of the color palette from green to yellow and possibly orange indicates an advanced corrosion process.

  If carbonation depth is above 25 mm that can be associated with corrosion which requires monitoring.

- *Uranyl-Acetate Treatment* - presence of the gel in the sample may indicate progressing alkali-aggregate reaction in the concrete structure.
- *Half-cell potentials method* – relationship between the measured values of potential and the corrosion probability is described in the standard ASTM C876*:*

This project has received funding from the European Union's Horizon 2020 research and innovation programme under grant agreement No 958171. © 2021

- value below - 350 is associated with more than 90% probability of the steel corrosion,
- value between -350 and +200 is associated with uncertain corrosion activity, which should be confirmed with other methods,
- value higher than – 200 is associated with low probability of steel corrosion activity.

- *Electrical resistivity tomography* - from the tomographic output it is possible to determine the orientation of the crack, size of the crack as well as contrast between steel and concrete inside the sample, however for correct interpretation it is necessary to apply mathematical model, for example: complete electron model, basing on Maxwell's equations. Size of cracks can be evaluated visually from photographs.
- *Infrared Spectroscopy* - absorption characteristics provide information about the molecular structure of the sample.

12.5.3 Validation

12.5.3.1 Specific methods used for validation of results depending on the technique

- *pH indicators* - porosity test of concrete can be additionally performed as well as compressive strength tests, since for concrete with a lower compression strength the process of carbonation is progressing faster;
- *Uranyl-Acetate Treatment* - other non-destructive or destructive techniques can be used for validation of the result;
- *Half-cell potentials method* - other non-destructive or destructive techniques can be used for validation of the result or theoretical models;
- *Electrical resistivity tomography* – measurements are validated by numerical methods such as finite difference or finite-element method;
- *Infrared Spectroscopy – validation can be performed with other destructive or non-destructive techniques and with other spectroscopic methods such as NMR, UV/VIS.*

12.5.3.2 Quantification of the error

- *pH indicators* - not applicable.
- *Uranyl-Acetate Treatment* – not applicable.
- *Half-cell potentials method* – in modern equipment calculated automatically.
- *Electrical resistivity tomography* – noise errors are calculated automatically and displayed as a percentage of reading.
- *Infrared Spectroscopy* – usually calculated automatically in the software of spectrometer.

This project has received funding from the European Union's Horizon 2020 research and innovation programme under grant agreement No 958171.

12.5.3.3 Quantitative or qualitative evaluation

All methods are used in qualitative evaluation. In some cases electrical resistivity tomography and infrared spectroscopy can be used for quantitative evaluation under certain conditions, however it is not a common approach for concrete structures investigation.

12.5.4 Detection accuracy

- *pH indicators* - depth of the carbonated surface should can be measured with an accuracy of 1 mm; depth of the carbonation front can be determined with an accuracy of ±10% to ±15 %.
- *Uranyl-Acetate Treatment* – depends on the operator.
- *Half-cell potentials method* - survey results a probabilistic assessment of the risk of corrosion of rebars correlated with potential measured at the concrete surface, detection accuracy can be very

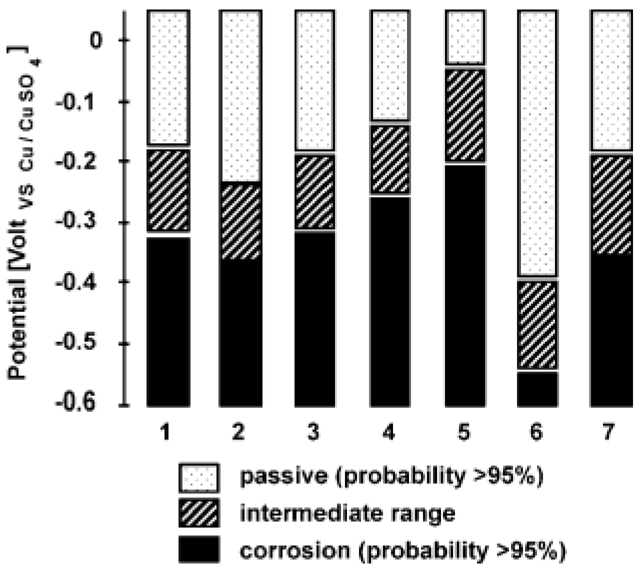

Figure 12.7 – Potential ranges indicating active and passive areas (B. Elsener, 2003)

- *Electrical resistivity tomography* - total accuracy is calculated and displayed automatically in the software.
- *Infrared Spectroscopy* – depends on the experience of the operator in interpretation of the resulting spectra.

12.6 Advantages

- *pH indicators:*
  - easy feasible,
  - no specific training required,
  - measurements can be performed in laboratory or on the construction site,

This project has received funding from the European Union's Horizon 2020 research and innovation programme under grant agreement No 958171.

- easy to repeat.

- *Uranyl-Acetate Treatment:*
  - high contrast between damaged and not damaged areas,
  - easy to repeat.
- *Half-cell potentials method:*
  - widely known technology,
  - not expensive equipment.
- *Electrical resistivity tomography:*
  - enables creation of internal maps of the structure.
- *Infrared Spectroscopy:*
  - accurate and precise,
  - enables identification of the structure of unknown sample if complied with other spectroscopic techniques.
  - small amount of sampling material needed.

12.7 Disadvantages

- *pH indicators:*
  - limited measurement precision.
- *Uranyl-Acetate Treatment:*
  - requires the use of a UV light source to fluoresce the gel
  - in field analysis where bright sunlight may be difficult to adjust viewing of the concrete under UV light
  - uranyl ion is nonspecific, will associate with other cations in concrete leading to false positives
  - concrete exposed to uranyl acetate is contaminated and must be disposed with specific procedures.
- *Half-cell potentials method:*
  - not enough accurate
  - difficult to repeat.
- *Electrical resistivity tomography:*
  - requires knowledge on the computational and numerical methods.
- *Infrared Spectroscopy:*
  - requires very good expierience in interpretation of the IR-spectra
  - requires training on the use of IR-spectrometer
  - not easy to perform
  - requires expensive equipment

This project has received funding from the European Union's Horizon 2020 research and innovation programme under grant agreement No 958171.

12.8 Possibility of automatizing the measurements

The indicators methods are simplified, used in in-situ tests, consist only of spraying on fresh concrete breakthrough the appropriate indicator and reading the pH value from the available range. No consideration on automatization are taking place, since this methods are only used as a, on-site, simple method of estimation of pH and there is no need of that. However some more accurate methods can displace the following approach in the future.

12.9 Barriers

- *pH indicators - in* case of phenolphthalein and thymolphthalein test, these are sensitive only to the selected pH. It is not possible to assess the distribution of the carbonated surface on tested cross-section using these two tests.
- *Infrared Spectroscopy* – althought it is used in different areas also as quantitative method - for concrete inspection purposes should not be considered so. The intensity of certain IR bands can vary as a function of their content in the sample, it is difficult to make the relation between the intensity or the area of an IR band and a specific concentration. Traces of chemical compounds can be under-estimated or erased due to the high intensity of certain signals, for instance of silica or calcium carbonate. The presence of a large amount of capillary water into the hydrated sample can mask some of the chemical compounds.

12.10 Existing standards

- ASTM F710-11 Standard Practice for Preparing Concrete Floors to Receive Resilient Flooring – indicating method of surface pH measurement
- EN 14630:2006 Products and systems for the protection and repair of concrete structures - Test methods - Determination of carbonation depth in hardened concrete by the phenolphthalein method
- EN 1239-12:2020 Testing hardened concrete - Part 12: Determination of the carbonation resistance of concrete - Accelerated carbonation method
- ASTM C876 Standard Test Method for Corrosion Potentials of Uncoated Reinforcing Steel in Concrete
- ASTM C876-91 (2001). "Standard test method for half-cell potentials of uncoated reinforcing steel in concrete." ASTM Standards Developed by Subcommittee, Vol. 03.02, G.1.14, pp. 42.

12.11 Applicability

12.11.1 Relevant knowledge fields

- Civil engineering:
  - technical inspections of the concrete structures
  - facility renovations

This project has received funding from the European Union's Horizon 2020 research and innovation programme under grant agreement No 958171.

  - foundations maintenance
  - historical buildings presevations
  - evolution of moisture distributions in concrete structures.
- Medicine and pharmacology:
  - identification of substances
  - determination of progress of reactions
  - impurities detection.
- Material engineering:
  - degree of polymerization
  - characterization of micro- or nanostructured materials.
- Food industry:
  - concentration of compounds in food products
- Geophysics:
  - measurement of electrical resistance of soil
  - monitoring of water movement.

12.11.2 Performance Indicators

Relate the surveying technology being studied with PIs from WP3, provided in the document of the TU1406 COST ACTION.

- loss of section
- cracks
- obstruction/impeding
- displacement
- debonding
- delamination
- spalling
- reinforcement bar corrosion.

12.11.3 Type of structure

- Bridges
- tunnels

12.11.4 Spatial scales addressed (whole structure vs specific asset elements)

Inspection directed on elements of the structure near to the reinforcement for assessment of the corrosion risk. Half-cell potential method is useful in inspection of bridge decks, concrete piers and docks, foundations and tunnel lining.

This project has received funding from the European Union's Horizon 2020 research and innovation programme under grant agreement No 958171.

12.11.5 Materials

- aggregate
- concrete
- technical ceramic
- building lime
- slag
- cement
- gravel
- pigment
- ferroalloys.

12.12 Available knowledge

12.12.1 Reference projects

No reference projects.

12.12.2 Other

Manufacturers websites:

NDT James Instruments – Basic Half Cell Potential System for Locating Areas of Rebar Corrosion
NDT James Instruments – Basic Half Cell Potential System for Locating Areas of Rebar Corrosion Specification

Hammond Concrete Services – Elcometer 331

Hammond Concrete Services – Elcometer – covermeter manual

Hammond Concrete Services - Profometer Corrosion Half-Cell

Hammond Concrete Services – Profometer Corrosion Half Cell manual

12.13 Bibliography

A. Nadezhdin, D. A. (1988). The Effect of Deicing Chemicals on Reinforced Concrete. *Transportation Research Record*, pp. 31-37.

B. Elsener, C. A. (2003). RILEM TC 154-EMC: Half-cell potential measurement -Potential mapping on reinforced concrete structures. *Materials and Structures vl. 36*, 461-471.

Buettner, M. R. (1996). Electrical resistance tomography for imaging concrete structures. *Structural materials technology an NDT conference, San Diego.* San Diego.

Campbell, D. S. (1991). Detecting Carbonation.

Czarnecki L., W. P. (2008). Metody oceny przebiegu karbonatyzacji betonu . *Materiały II Sympozjum naukowo-techniczne Trwałość Betonu.* Górażdze Cement.

David Whiting, T. M. (1992). History of the Rapid Chloride Permeability Test. *Transportation Research Record*, pp. 55-62.

This project has received funding from the European Union's Horizon 2020 research and innovation programme under grant agreement No 958171.

Elcometer 331. Concrete Covermeter. Model SH • Model TH. (2006-2009). Copyright Elcometer Limited.

ERTLab Studio . (n.d.). The DAS-1 . USA .

Geostudi Astier srl and Multi-Phase Technologies LLC. (2006). 3D ELECTRICAL RESISTIVITY TOMOGRAPHY - INVERSION SOFTWARE_The ERTLab . *User Manual* . Retrieved from https://www.mptech3d.com/_files/ugd/bee905_dc4757cf25824c4e8afdea7cfb5f5d90.pdf

Ghosh, S. &. (1974). Absorption and reflection infrared spectra of major cement minerals, clinker, and cements. . *Journal of Materials Science, vol. 9* , pp. 1577-1584.

Grzegorz Bajorek, B. K.-H. (2014). Instrumentalne metody analiz chemicznych materiałów budowlanych w ujęciu normowym. *Scientific Works of Institute of Ceramics and Building Materials*, pp. 6-14.

Hammond Concrete Services . (n.d.). PM600-630 Profometer Manual . Switzerland.

Hemeda, S. (2013). Electrical Resistance Tomography (ERT) Subsurface Imaging for Non-destructive Testing and Survey in Historical Buildings Preservation. *Australian Journal of Basic and Applied Sciences*, pp. 344-357.

Hughes, T. M. (1995). Determining cement composition by Fourier Transform Infrared Spectroscopy. . *Advanced Cement Based Materials, 2*, pp. 91-104.

Izabela Wysocka, A. Z.-J. (2019). Korozja betonu. Badanie przebiegu korozji kwasowej beotnu cementowego i jego skażenie chlorkami. *Technologie Materiałów Budowlanych* (pp. 1-5). Gdańsk: Politechnika Gdańska.

J. Hulimka, M. K. (2020, January 3). Basic Chemical Tests of Concrete during Assessment of Structure Suitability - Discussion on Selected Industrial Structures . *Applied Science 12, 358*.

Jacek Hulimka, M. K. (2020, January 3). Basic Chemical Tests of Concrete during the Assessment of Structure Suitability—Discussion on Selected Industrial Structures. *Applied sciences*, pp. 1-16.

Jaroszyńska-Wolińska, J. (2011). *Chemia w laboratorium budownictwa.* Lublin: Politechnika Lubelska.

Jóźwiak, H. (2009). Możliwości wykorzystania metody jądrowego rezonansu magnetycznego w badaniach domieszek chemicznych w betonie. *Prace Instytutu Techniki Budowlanej* , pp. 3-13.

Juan Lizarazo-Marriagaa, P. C. (2009, October 15). Determination of the concrete chloride diffusion coefficient based on an electrochemical test and an optimization model. *Materials Chemistry and Physics*, pp. 536-543.

Karhunen, K. (2013). *Electrical Resistance.* Kuopio: University of Eastern Finland.

Karhunen, K. S. (2010). Electrical resistance tomography imaging of concrete. . *Cement and Concrete Research 40* , pp. 137-145.

KImmo Karhunen, A. S. (2010, 09). Electrical resistance tomography for assessment of cracks in concrete. *Aci Materials Journal*, pp. 523-531.

Lataste, J. S. (2003). Electrical resistivity measurement applied to cracking assessment on reinforced concrete structures in civil engineering. *NDT & E international, 36(6)*, pp. 383-394.

Nadejda V. Orlova, J. C. (1999). *The Study of Chloride Ion Migration in Reinforced Concrete Under Cathodic Protection.* Oregon: Oregon Department of Transportation.

This project has received funding from the European Union's Horizon 2020 research and innovation programme under grant agreement No 958171. © 2021

P. von der Hardt, H. R. (1981). *Neutron Radiography Handbook. Nuclear Science annd Technology*. London: D. Reidel Publishing Company.

Pasierb, B. (2015). Nmerical Evaluation of 2D Electrical Resistivity Tomography for subsoil Investigations. *Enviromental Engineering*, pp. 101-112.

Perkin Elmer . (2011-2015). Spectrum 10 Spectroscopy Software Product Brochure.

Philip J. Nixon, J. L. (2008). *The EU "Partner" Project - European Standards Tests to Prevent Alkali Reactions in Aggregates Final Results and Recommendations.* Trondheim: 13th International Conference on Alkali-Aggregate Reaction in Concrete (ICAAR).

Piotr Gwoździewicz, D. D. (2010). Wpływ dyfuzji jonów chlorkowych i procesu karbonatyzacji na trwałość żelbetowych obiektów mostowych. *Czasopismo Techniczne. Budownictwo*, pp. 11-23.

Proceq SA. (2016). Profometer. Operating Instructions. Proceq SA.

Reis, R. &. (2019). Using Thymolphthalein for Accelerated Carbonation Testing of High Volume Fly Ash Cementitious Blends. *Selected Papers of the 8th International RILEM PhD Workshop held in Marne-la-Vallée.*

Smith, D. (2006). The Development of a Rapid Test for Determining the Transport Properties of Concrete. New Brunswick: University of New Brunswick.

The Concrete Society. (2000, 08). Current Practice Sheet 120 - Half-cell potential surveys. *CONCRETE*.

This project has received funding from the European Union's Horizon 2020 research and innovation programme under grant agreement No 958171.

APPENDIX A13. Quantitative chemical methods

13.1 Goal(s)

13.1.1 Main objective

The concrete has to maintain adequate durability in the assumed environmental conditions with low maintenance expenditure for the designed operational time. During the use period, concrete structures are exposed to many environmental factors causing concrete degradation. From the projecting phase the main influence on the behaviour of concrete in real constructions is the initial composition, especially – type and quantity of cement, water/cement ratio, quality of aggregate, type and quantity of additives. Performance of concrete can be modified by reduction of the water quantity in the mixture or use of cement with mineral additives, limiting the capillary porosity of the grout cement on the structural scale. In global scale this influences directly the penetration depth of aggressive media and level of the diffusion of aggressive ions into the interior of the cement matrix . However there are many factors influencing the final performance of concrete in various environments and applications

Concrete subjected to the aggressive ions environment will corrode at different rates depending on the concentration of different salts. Main types of corrosion processes influenced by different salt concentrations are: chloride corrosion, sulphate corrosion and alkali-aggregate reaction corrosion. Chloride ions penetrate very fast into the deepest parts of the cement matrix, therefore the chloride corrosion proceeds quickly into the structure. Presence of the chloride ions lead to the reduction of pH and formation of the compounds which increase their volume and that can result in cracks and other deformations. Main problem arising from the chloride corrosion as well as for other mechanisms of this process is the corrosion of reinforced steel bars. The source of the chloride ions can be assigned to mine waters or sea waters, but most of all from defrosting detergents. The penetration level depends on the cycles of saturation, drying of the surface, freeze thaw.

Sulphate corrosion is one of the most dangerous type of the degradation process in the life cycle of the concrete structures. Sulphate ions presence is directly connected with influence of groundwater, sewage, fertilizers, industrial waste. In case of sulphate corrosion there are two types of propagation – external or internal. External attack occurs when concrete is subjected to the sulphate solutions and ions react with cement matrix forming gypsum or ettringite. This leads to the expansion inside the structure and cracking. Internal attack occurs when in the structure there is cement with high content of gypsum, which leads to excessive content of sulphates from the beginning. The problem also affects concrete subjected to thermal treatment.

Alkali-aggregate reaction corrosion is a destructive process resulting from the reaction of sodium and potassium hydroxides in the pores of the concrete with reactive silica from certain aggregates. Mostly affected types of are those reach in active silica and carbonate aggregates. The resulting sodium-potassium-calcium silica gel expands by absorbing water and the induced pressure causes cracking

This project has received funding from the European Union's Horizon 2020 research and innovation programme under grant agreement No 958171. © 2021

and damages inside the structure. This mechanism is especially dangerous for concretes used in road construction, for instance pavements or bridge elements. The alkaline reactivity of aggregates is a complex phenomenon, both in terms of the type of alkaline reactions and the variety of mineralogical, chemical and atmospheric factors influencing the progress of alkali-aggregate reaction.

For these purposes several chemical methods are used in order to quantitatively assess the rate of degradation processes due to mechanisms mentioned above, which can be generally divided into groups such as analytical and electrochemical methods. Those will be detailed below.

13.2 Description

13.2.1 Functioning mode

- Electroanalytical methods:
  - *Potentiometric titration* - method base on the potential difference between the indicator electrode and the reference electrode after adding portions of titration substance. Selected indicator electrode reacts to changes in the concentration of the analyte or the titration reagent (Climent, Viqueira, Vera, & López-Atalaya, 1999).
  - *Chloride Diffusion Test/ Ions migration in electrical field* – method base on accelerated movement of the chloride ions in concrete sample, induced by electrical field. Test is performed in two chambers with electrodes separated by concrete sample and the concentration changes of chlorides penetrating the cathode are monitored. Samples are usually cut in the form of 50 mm thick discs from 100 mm diameter cylinders and saturated in solution of NaOH. upstream reservoir is filled with NaOH and NaCl solution while the downstream reservoir is filled with NaOH solution only. Power supply is connected to the sample that the negative pole is attached to the upstream cell and the positive pole is attached to the downstream cell. Samples from the upstream and downstream reservoirs are taken periodically and analysed for chloride content (E Poulsen, 2014) (Zofia Szweda, 2012) (Nordtest, 1995) (Nadejda V. Orlova, 1999).
  - *Galvanostatic pulse technique* - current pulse is applied galvanostatically with the external counter electrode over the concrete surface and the resultant change in potential is detected; A current pulse is imposed on the reinforcement from a counter electrode placed on the concrete surface. A guard ring confines the current to an area A of the reinforcement below the central counter electrode. The applied current is usually in the range of 5 to 400 A and the typical pulse duration is 5 to 10 seconds. The reinforcement is polarized in the anodic direction compared to its free corrosion potential. The resulting change of the electrochemical potential of the reinforcement is recorded as a function of time using a reference electrode (Ag/AgCl). Modern equipment for the galvanostatic pulse technique can be also used in non-destructive testing directly on the tested area (S. Sathiyanarayanan, 2006) (Bertolini, 2013).

This project has received funding from the European Union's Horizon 2020 research and innovation programme under grant agreement No 958171. © 2021

- Analytical methods:
  - *Argentometric titration* – method allows the quantitative determination of a specific analyte dissolved in a sample based on a chemical reaction between the analyte and a titrant of known concentration. Precipitation of silver compounds is used to determine chloride content in the samples Argentometric titration is usually working in three modes – direct, back compensated or blank compensated mode (Bertolini, 2013).
  - *Gravimetric method* – method used for determination of sulfate ions content in concrete sample, basing on the reaction of sulfates with barium chloride in acidic solution; hardly soluble barium sulfate is precipitated and the content of vial is dried and weighed (Bertolini, 2013).
  - *Ion chromatography* – adequate chromatography columns and eluents are used for analyses of water - soluble anions and cations in concrete. Concrete samples are pre-processed and extracted with distilled water (Bertolini, 2013).

13.2.2 Types

- *Potentiometric titration* – modern titrators are fully automated in data collection and calibration, all setup is made on the interface through software application to the equipment; usually titrators consist of with an Ag/ AgCl electrode with AgCl coating. Apparatus and equipment used in potentiometric titration for concrete consist of chloride-ion selective electrode, pH/mV meter and compatible automatic temperature compensation probe, adjustable-volume digital pipette, glassware: beakers, graduated cylinders, magnetic stirrer and teflon-coated stirring bars;
- *Chloride Diffusion Test/ Ions migration in electrical field* - testing apparatus consists of an upstream and downstream reservoirs and an electrical power source.
- *Galvanostatic pulse technique - apparatus consists of battery and constant current source; stable current is applied - 1, 0.1 or 0.01 mA;* A pulse duration of between 45 to 180 seconds can be used with a sampling rate of 1000 Hz to collect the dynamic response data.
- *Argentometric titration – method can be generally divided into three commonly used types:*
  - *Mohr method* – yellow potassium chromate is used as an indicator in the titration of chloride ions with silver nitrate solution. In the beginning chloride ions will react with silver nitrate solution and form white precipitate of silver chloride. Endpoint is determined by chloride ions precipitation and if there is an excess - precipitation of red/brown silver chromate.
  - *Volhard method* - excess amount of silver nitrate is be added to the sample solution to react with the chloride ions and form white precipitate of silver chloride; unreacted silver ions are then titrated with a standard solution of potassium thiocyanate in the presence of ferric ammonium sulfate solution (which acts as an indicator; the free silver ions had been completely reacted with thiocyanate ions, the first excess thiocyanate ion will react with the ferric ions of the indicator to form the red ferrithiocyanate complex, indicating the endpoint;

This project has received funding from the European Union's Horizon 2020 research and innovation programme under grant agreement No 958171.

  - *Fajans method* – in this method an adsorption indicator such as dichlorofluorescein which is a weakly acidic dye that exists in ionized form in the solution. Colloidal silver chloride precipitates tends to adsorb silver ions or chloride ions which in excess in the solution.

- *Gravimetric method* – in general there are three different types of gravimetric analysis:
  - *precipitation gravimetry* – this type is applied for determination of sulfate ions in concrete sample; basing on the precipitation of the compound,
  - *volatilization gravimetry* – basing on the thermal or chemical energy to remove a volatile compound,
  - particulate gravimetry – basing on the separation of the analyte from the sample by filtration or extraction.

- *Ion chromatography* – typical modern chromatograph consists of single pump, conductivity detector, autosampler, eluent generator, cartridge, suppressor, analytical column, guard column; can be operated with various types of detection; sample processor processes samples from 500 µL to 500 ml; the sample transfer takes place by means of a peristaltic pump; There are two main types of ion chromatography:
  - *anion exchange chromatography,*
  - *cation exchange chromatography.*

13.2.3 Process/event to be detected or monitored

- *Potentiometric titration* - corrosion risk of rebars resulting from the influence of chlorides ions.
- *Chloride Diffusion Test/ Ions migration in electrical field - chloride penetration level,* capacity of concrete to resist chloride ions penetration.
- *Galvanostatic pulse technique* – detection of corrosion parameters of reinforcement ; dynamic response to a galvanostatic pulse.
- *Argentometric titration* – corrosion risk of rebars resulting from the influence of chlorides ions; observations of change of colour at the endpoint.
- *Gravimetric method* – expansion, cracking, strength loss and disintegraton of the concrete due to the presence of sulfate ions.
- *Ion chromatography* – detection and quantification of harmful ions and its influence on the structure integrity.

13.2.4 Physical quantity to be measured (e.g. actions, displacements, deformations, dynamic structural properties, material properties including mechanical, electrical and chemical properties, relative displacements of the two sides of a crack, etc.).

- *Potentiometric titration* - the potential or potential changes of the indicator electrode.
- *Chloride Diffusion Test/ Ions migration in electrical field* - concentration of the chloride ions in the sample.

This project has received funding from the European Union's Horizon 2020 research and innovation programme under grant agreement No 958171.

- *Galvanostatic pulse technique* - corrosion current density measurement, polarization resistance change [mV] in potential of the steel reinforcement in time [S].
- *Argentometric titration* – chloride ions concentration in concrete sample.
- *Gravimetric method* – sulfate ions concentrations in concrete sample.
- *Ion chromatography* – concentrations of the ions present in the aqueous phase of concrete.

13.2.5 Induced damage to the structure during the measurement

For the mentioned experimental methods it is necessary to collect samples in forms of bore-holes or powdered samples from the inspected area, which induce damage to the structure in both cases.

13.2.6 General characteristics

13.2.6.1 Measurement type (static or dynamic, local or global, short-term or continuous, etc.)

- *Potentiometric titration* - static, local and short-term measurement.
- *Chloride Diffusion Test/ Ions migration in electrical field* - static, local and short-term measurement.
- *Galvanostatic pulse technique* - static, local and short-term evaluation.
- *Argentometric titration* - static, local and short-term evaluation.
- *Gravimetric method* - static, local and short-term evaluation.
- *Ion chromatography* - static, local and short-term evaluation.

13.2.6.2 Measurement range

- *Potentiometric titration* - balance sensitive to 0.0001 gram with a minimum capacity of 100 grams and volume digital pipette, with a range of 0.200 to 1.000 mL are usually used.
- *Chloride Diffusion Test/ Ions migration in electrical field* – range (×10-12 m2/s).
- *Galvanostatic pulse technique* - the applied current is usually in the range of 5 to 400 A and the typical pulse duration is 5 to 10 seconds.
- *Argentometric titration* - automated precipitation titrators work in measuring range: ± 2000 mV / 0–14 pH.
- *Gravimetric method – not applicable.*
- *Ion chromatography – concentrations in range* - µg/l (sub ppb) to mg/l (ppm), *1 mg/mL (1000 ppm).*

13.2.6.3 Measurement accuracy

- *Potentiometric titration* - pH/mV meter, with accuracy of 0,1 mV.
- *Chloride Diffusion Test/ Ions migration in electrical field* – precision of the diffusion coefficient determination has been analysed In literature - (L. Tang, 2001).
- *Galvanostatic pulse technique* - potential is measured to an accuracy of ±5 mV with the Ag/AgCl electrode. The electrical resistance is estimated to be measured with an accuracy of ± 5 %.

This project has received funding from the European Union's Horizon 2020 research and innovation programme under grant agreement No 958171.

- *Argentometric titration* - titration can achieve a relative error of 0.1–0.2%. The principal limitation to accuracy is the difference between the end point and the equivalence point.
- *Gravimetric method* – up to 0,01 g, depends on the balance used.
- *Ion chromatography* - flow rate: Programmable Analytical: 0,001 – 10,000 ml/min.
  Flow Accuracy: ± 1,0 % 1,000 ml/ min
  Flow Precision: ± 0,1 % RSD 1,000 ml/min

13.3 Background (evolution through the years)

- *Potentiometric titration* - first potentiometric titration was performed in 1893 with mercurous solution and potassium chloride, bromide, iodide. There were used a mercury electrode with a mercury/mercurous nitrate reference electrode. Wilhelm Bottger developed the tool of potentiometric titration at Ostwald's Institute. Potentiometric titration was used to examine the differences in titration between strong and weak acids (E Poulsen, 2014) .
- *Galvanostatic pulse technique* - introduced in 1988 to when problems of the interpretation of corrosion risk of reinforcement occurred, in situations where half-cell potential method is applied in wet or polymer-modified concrete and access of oxygen is limited (Thomas Frølund, 2002) (D.W.Law, 2001).
- *Gravimetric method* - technique was used to determine the atomic mass of many elements in the periodic table (U.S. Dept. of the Interior, 1992).
- *Ion chromatography* - technique was introduced in 1850 study the adsorption of ammonium ions on soils. In 1947 the technique was used for separation of rare earth. Further the technique was extended to separate anions such as chlorides, fluorides, nitrates, and sulfates. Modern solutions offer improved sensitivity of detection and improvement in speed of analysis (R. Vedalakshmi, 2010)

13.4 Performance

13.4.1 General points of attention and requirements

13.4.1.1 Design criteria and requirements for the design of the survey

- Potentiometric titration – titrators are designed for laboratory use only, because there are requirements of the environment that should be fulfilled: ambient conditions, no powerful vibrations, no direct sunlight, no corrosive and explosive gas atmosphere, no magnetic fields; after configuration of the system there should be no leaks in any part of the titrator; usually 2,5 g powdered samples of concrete are used.
- *Galvanostatic pulse technique* - concrete slabs of dimension 1000 x 1000 x 150 mm can be used for testing.
- *Argentometric titration* - sample solutions have to be adjusted to near neutral pH, since at higher value, brown silver hydroxide precipitate may form and mask the endpoint.

This project has received funding from the European Union's Horizon 2020 research and innovation programme under grant agreement No 958171. © 2021

- Ion *chromatography* – liquid samples have to be filtered out for removal of sediments or other impurities present in the sample.

13.4.1.2 Procedures for defining layout of the survey

Detailed procedures for described method can be found in documents listed in paragraph 1.10 Existing Standards.

13.4.1.3 Design constraints (e.g. related to the measurement principles of the monitoring technologies)

Not applicable.

13.4.1.4 Sensibility of measurements to environmental conditions

Galvanostatic pulse measurements are very sensitive to temporal environmental conditions, hence conclusive interpretations of the test data can only be made when the site is tested over a long period of time that covers seasonal as well as daily variations in temperature and humidity. Titration measurements are sensitive to temperature changes. Environmental effects can be causes of systematic error, for example a change in lab temperature, changing the calibration of a balance or the volume of a flask.

13.4.2 Preparation

13.4.2.1 Procedures for calibration, initialisation, and post-installation verification

According with the documents and standards listed in paragraph 1.10 Existing standards and to manufacturer guidance and manuals.

13.4.2.2 Procedures for estimating the component of measurement uncertainty resulting from calibration of the data acquisition system (calibration uncertainty)

Usually, the uncertainty resulting from calibration can be evaluated by means of statistical methods.

13.4.2.3 Requirements for data acquisition depending on measured physical quantity (e.g. based on the variation rate)

Not applicable.

13.4.3 Performance

13.4.3.1 Requirements and recommendations for maintenance during operation (in case of continuous maintenance)

Not applicable.

13.4.3.2 Criteria for the successive surveying campaigns for updating the sensors. The campaigns include: (i) Georeferenced frame, i.e. the global location on the bridge; (ii) Alignment of sensor data, relative alignment of the data collected in a surveying; (iii) Multi-temporal registration to previous campaigns; and (iv) Diagnostics.

Not applicable

This project has received funding from the European Union's Horizon 2020 research and innovation programme under grant agreement No 958171. © 2021

13.4.4 Reporting

In all mentioned methods modern software enable to automatically create reports after series or single measurement. Potentiometric titration software, for example AT- Win provide tools for automatic reporting to MS Word format. Titration test report usually contain the following elements: name and surname of the person carrying out the analysis, date of analysis, reactions, all obtained titration results, calculated mean mass of Cl- ions in the original sample for each method, compare the results obtained and any possible comment of discrepancies between them as well differences in their accuracy.

Example of the data report for Argentometric titration is shown below:

Name and Surname:	**Argentometric titration of chloride ions content**						Date:
Volume of the volumetric flask used [cm^3]							
Capacity of the measuring pipette used [cm^3]							
Commensurability of the flask with the pipette							
Titre of the $AgNO_3$ solution used [M]:							
The titer of the used KSCN or NH_4SCN solution [M]							
M_{Cl}[g/mol]							
	Mohr Method						
Indicators							
Reactions							
Lp.	V	[cm^3]	Remarks	Average V	[cm^3]	mass	[g]
1.							
2.							
3.							
4.							
Average content of chloride ions Cl^-							

This project has received funding from the European Union's Horizon 2020 research and innovation programme under grant agreement No 958171. © 2021

Table 13-1 – Report for Argentometric Titration

13.4.5 Lifespan of the technology (if applied for continuous monitoring)

Quantitative analytical methods are not used for continuous monitoring.

13.5 Interpretation and validation of results

13.5.1 Expected output (Format, e.g. numbers in a .txt file)

- *Potentiometric titration – titration curves* - plot of change of the potential vs volume of the added titrant reagent [mL].
- *Chloride Diffusion Test/ Ions migration in electrical field - plot of* concentration changes of chlorides penetrating the cathode in time [s] – migration profile as shown below:

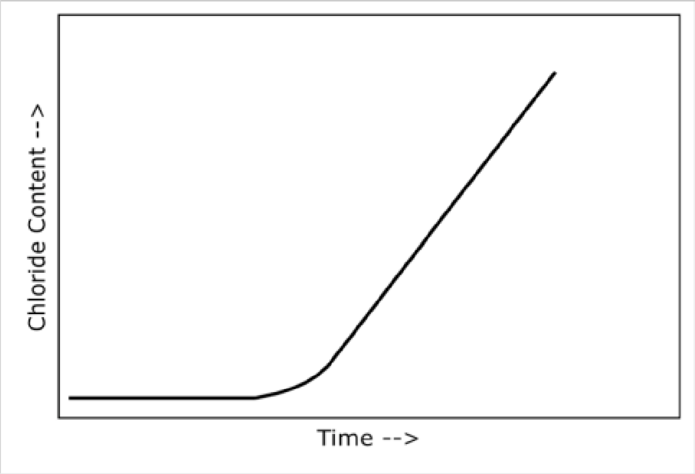

Figure 13.1 – Chloride Diffusion Test output

- *Galvanostatic pulse technique* – graph of the potential changes [mV] in time [s]; if used with 3D reporting software – 3D plot of the corrosion rates; below there is shown an example of the graph after application of the galvanostatic pulse:

This project has received funding from the European Union's Horizon 2020 research and innovation programme under grant agreement No 958171.

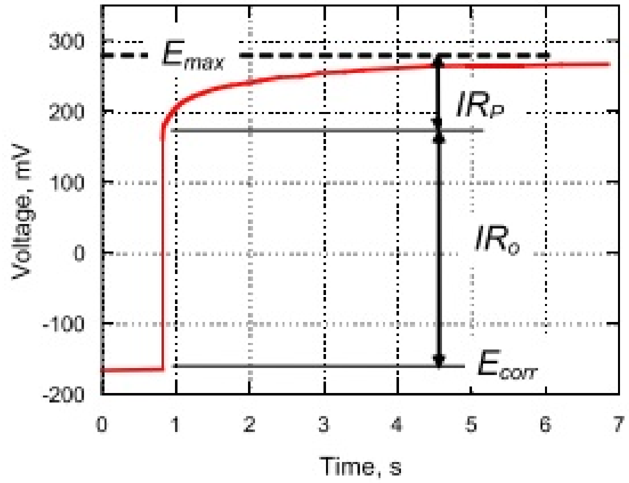

Figure 13.2 – Output of the galvanostatic measurement

- *Argentometric titration – titration curves* - plot of logarithm of concentration of [Ag+] ions vs. volume of Ag titrant added [mL].

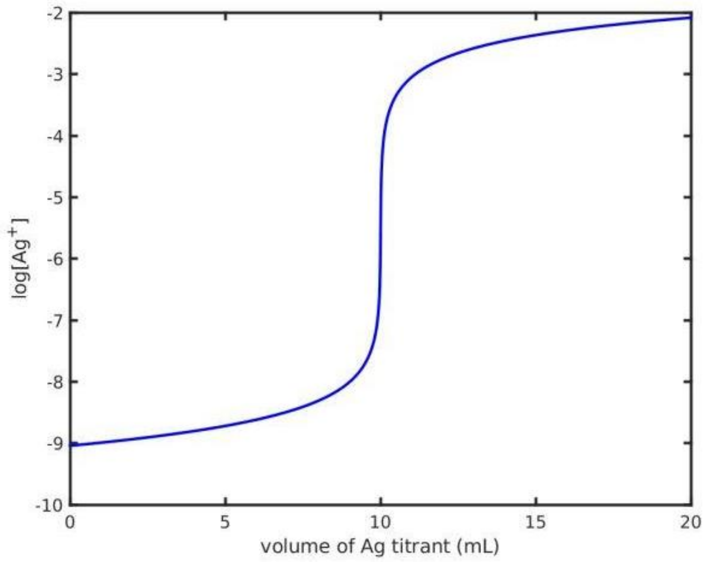

Figure 13.3 – Argentometric titration curve

- *Gravimetric method* – list of percentage content by sample weight of sulphate ions, mean values.
- *Ion chromatography* – the data is presented in a chromatogram - electrical conductivity versus time as the analyte passes through the system. Consists of several peaks corresponding to the different times in which components of the analyte emerge from the column, as shown below:

This project has received funding from the European Union's Horizon 2020 research and innovation programme under grant agreement No 958171.

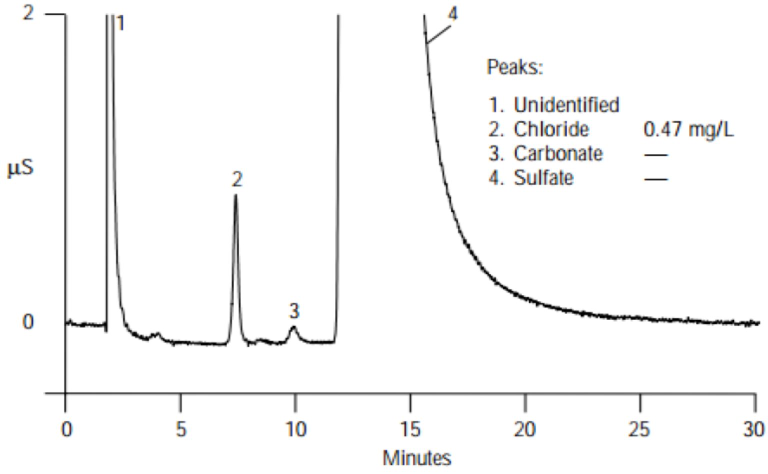

Figure 13.4 – Example of the chromatogram

13.5.2 Interpretation (e.g. each number of the file symbolizes the acceleration of a degree of freedom in the bridge)

- *Potentiometric titration* - concentration of a given analyte based on titration curves.
- *Chloride Diffusion Test/ Ions migration in electrical field* - concentration changes of chlorides penetrating the cathode are used for determination of diffusion coefficient.
- *Galvanostatic pulse technique* – the corrosion rate is linked with the magnitude of corrosion current density; this value can be calculated using the charge transfer resistance from acquired data; charge transfer resistance is measured by summation of the individual resistances of components associated with corrosion.
- *Argentometric titration* - in Volhard method for example - the concentration of chloride ion in the sample solution is determined by subtracting the titration findings of the moles of silver ions that reacted with the thiocyanate ions from the total moles of silver nitrate solution that added.
- *Gravimetric method* – quantified sulphates concentration across the thickness of tested concrete elements; collected data indicate penetration length over the sample thickness and concentrations in the cross-section; determination of the damage depth of the tested elements due to sulfates aggression.
- *Ion chromatography* – concentrations of the ions of interests are calculated automatically and given by the instrument.

13.5.3 Validation

13.5.3.1 Specific methods used for validation of results depending on the technique

- Potentiometric titration results of the potentiometric titration should be valuated with another instrumental technique such as ion chromatography.
- *Chloride Diffusion Test/ Ions migration in electrical field* - linear, Freundlich, and Langmuir isotherms are used to fit the relationship between the experimental data;

This project has received funding from the European Union's Horizon 2020 research and innovation programme under grant agreement No 958171. © 2021

- *Galvanostatic pulse technique, Argentometric titration, Gravimetric method, Ion chromatography*: Validation should be performed as for potentiometric method– with other analytic tools and the results should be analysed and compared.

13.5.3.2 Quantification of the error

Quantification of error is usually performed with use of statistical methods.

In titration methods:

- Random errors:

Random errors cause positive and negative deviations from the average value of a measurement. Random errors cancel by averaging, if the experiment is repeated many

times. Upon averaging many trials, random errors have an effect only on the precision of a measurement. Solution is to increase the number of replicates performed to obtain a more trustworthy mean value (Mettler Toledo International Inc. , 2015).

- Systematic errors:

Without any changes in the procedure, systematic errors are repeated if the experiment is repeated. Systematic errors have a biased effect on the final results. Systematic errors make the final result high or low, but not both. Instrument calibration errors are examples of systematic errors (Butler, 1963).

- Gross errors:

Blend of systematic and random errors.

Sources of the errors in titration methods are listed below:

This project has received funding from the European Union's Horizon 2020 research and innovation programme under grant agreement No 958171.

Area	Error
Primary standard	Impure, contaminated
	Inhomogeneous
	Unsuitable, no guaranteed primary standard quality
Sample size/balance	Balance not accurate, extant temperature gradient from titration vessel to balances
	Careless weighing, concentration too low or high, improper sampling, contaminated balance
Titration vessel	Electrostatically charged, contaminated
	Unsuitable
Dispensing unit	Leaky piston or burette tip, air in tubing system, 3-way stopcock leaking
	Tube connection not tight
Sample	Matrix effect from similar species
Solvent	Impure, poor solubilizing power, contaminated, wrong pH value or ionic strength
	Not stable
Titrant	Impure, contaminated, wrong pH value or ionic strength
	Decomposed, light-sensitive
	Very high or low concentration
Measurement	Contaminated sensor, blocked diaphragm, poor mixing of sample solution, excessive sensor response time, insufficient rinsing of sensor and stirrer
	Unsuitable sensor type, loose contact at connector, unfavorable arrangement of burette tip and sensor
Titration parameters	Unsuitable titration mode, titration rate too fast or too slow, unsuitable evaluation procedure
	Wrong measuring mode parameters
Temperature	Highly exothermic or endothermic reaction
	Temperature fluctuations
Environment	Changing, fluctuating, adverse conditions (humidity, temperature, UV light)

Figure 13.5 – Sources of errors in titration (Mettler Toledo International Inc. , 2015)

13.5.3.3 Quantitative or qualitative evaluation

Quantitative evaluation is performed by the methods listed.

13.5.4 Detection accuracy

With electrical resistance tomography it is possible to detect cracks with size below 1 mm.

In titration methods the values of repeatability and reproducibility can be determined following the standard ISO 5725-1981.

13.6 Advantages

- *Potentiometric titration:* can be performed even in the presence of a small amount of solute whose concentration is to be determined.
- *Chloride Diffusion Test/ Ions migration in electrical field:* fast and effective method to determine the corrosion resistance of reinforced concrete against chloride.
- *Galvanostatic pulse technique:* rapid evaluation.

This project has received funding from the European Union's Horizon 2020 research and innovation programme under grant agreement No 958171. © 2021

- *Argentometric titration*
  - very clear colour change at the end point of titration
  - feasible to automate the process
  - does not require specialized chemical knowledge.
  - provides fast and precise result of the analysis
- *Gravimetric method*
  - instrumental error is usually excluded
  - does not require a series of standards for calculation.
- *Ion chromatography*
  - accurate quantitative analysis
  - identification and quantification of low concentrations of ions in the sample
  - low maintenance costs and long-life of the apparatus used.

13.7 Disadvantages

- *Potentiometric titration*
  - variation in electrolyte pH alters the result of titration
  - electrolyte used in the reaction must be freshly prepared.
- Chloride Diffusion Test/ Ions migration in electrical field
  - simple to operate.
- Galvanostatic pulse technique
  - not possible to distinct between passive and actively corroding rebars.
- Argentometric titration
  - requires practice to achieve effective results
  - high background ionic level leads to errors.
- Gravimetric method
  - time consuming
  - small mistake during the measurement may affect the final result.
- Ion chromatography
  - only ions concentrations can be determined - complete salt-phases are determined by deduction

13.8 Possibility of automatising the measurements

Modern equipment for titration and chromatography is fully automatic in most cases, however the preparation stage of the samples and operations on the software cannot be omitted, which require presence of the qualified personnel.

Automating a titration analysis means more than simply having the titration and results calculation performed by automatic titrators. It must also include sample preparation steps and operator-

This project has received funding from the European Union's Horizon 2020 research and innovation programme under grant agreement No 958171.

independent sample series analysis. The main focus of automation is keeping actions throughout the process consistent to eliminate systematic, random, and even gross errors during routine tasks (Mettler Toledo International Inc. , 2015).

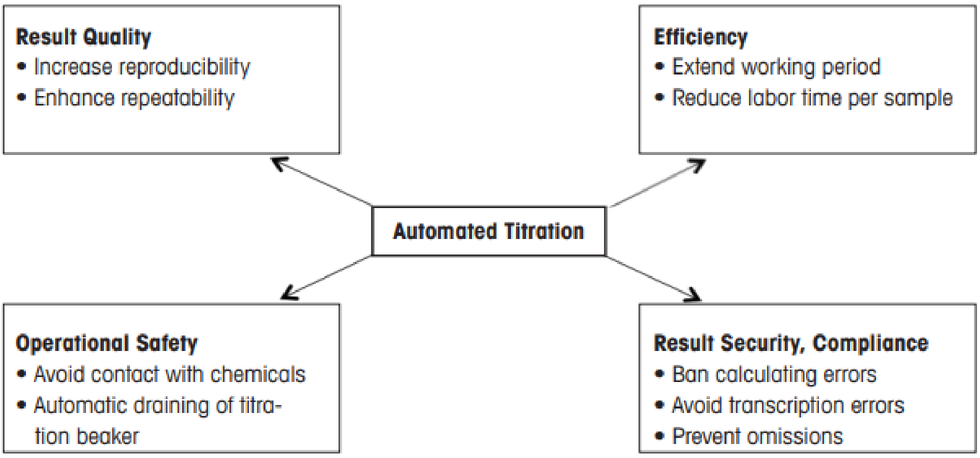

Figure 13.6 – Automated Titration benefits (Mettler Toledo International Inc. , 2015)

13.9 Barriers

Quantitative chemical analysis requires access to tested areas in order to collect representative samples from different structural elements. Analytical analysis is performed in the laboratory and thus requires additional time planned in advance if applied for periodic inspections.

13.10 Existing standards

- German Society for Non-destructive Testing Recommendations: Recommendations for Electrochemical Potential Measurement for Corrosion Detection in Reinforced Concrete Structures;
- AS 1012.20-1992, Method of Testing Concrete - Determination of chloride and sulfate in hardened concrete and concrete aggregates;
- PN-EN 14629:2008, Products and systems for the protection and repair of concrete structures -Test methods - Determination of chloride content in hardened concrete;
- PN-EN 1767:2008, Products and systems for the protection and repair of concrete structures - Test methods - Infrared analysis;
- ASTM C 1152, Test for nitric acid-soluble chloride content in concrete;
- ASTM C 1218, Test for water-soluble chloride content in concrete;
- ASTM D 4327, Standard Test Method for Anions in Water by Suppressed Ion Chromatography;
- PN-B-06714-46:1992 Kruszywa mineralne – Badania – Oznaczanie potencjalnej reaktywności alkalicznej metodą szybką;

This project has received funding from the European Union's Horizon 2020 research and innovation programme under grant agreement No 958171.

- ISO 5725–94, Precision of test methods - Determination of repeatability and reproducibility for a standard test method by inter-laboratory tests;
- ASTM C 1202, Chloride ion migration-diffusion test.

13.11 Applicability

13.11.1 Relevant knowledge fields

- *Civil engineering:*
  - corrosion diagnostics in concrete structures
  - underground anthropogenic objects diagnostics.
- *Geotechnics and Hydrotechnics:*
  - landlside risk assessment
  - mapping of slope deformations
  - slope stability monitoring
  - river dike stability
  - monitoring of processes in subsoil.
- *Environmental studies:*
  - ground water penetration
  - sources of contamination
  - determination of water chemistries in aquatic ecosystems
  - determination of chloride in sea water.
- *Welfare and public health:*
  - monitoring of lead in water for consumption
  - determination of sugar and salt content in foods
  - analysis of cyanide, ammonia etc. in water or wastewater.
- *Biology and medicine:*
  - water content in lyophilized vaccines
  - determination of plasma volume
  - determination of the active pharmaceutical ingredients
  - clinical diagnosis
  - monitoring of ions in body tissue, blood
  - analysis of metals
  - drug analysis
- *Material Engineering:*
  - nickel content in stainless steel
  - corrosion diagnostics
  - explosives analysis.
- *Food Industry*

This project has received funding from the European Union's Horizon 2020 research and innovation programme under grant agreement No 958171.

- detection of perchlorate vegetables, milk
- detection of sugars in alcoholic and non-alcoholic drinks
- detection of acids in drinks and beverages

- *Chemical Industry:*
  - detergents manufacturing
  - detection of different elements in fertilizers
  - paints analysis.
- *Textile industry*
- *Oil and gas industry*
  - determination of acid number in crude oil.

13.11.2 Performance Indicators

- loss of section
- cracks
- obstruction/impeding
- displacement
- debondingspalling

13.11.3 Type of structure

- reinforced concrete slabs of the load-bearing bridge structure
- abutments of the bridge
- cable-concrete girders
- slabs
- concrete beams

13.11.4 Spatial scales addressed (whole structure vs specific asset elements)

Chemical analysis is addressed for components of the reinforced structures particularly subjected to the corrosion.

13.11.5 Materials

- concrete
- reinforced concrete
- ceramics
- polymer
- composites
- biomolecules
- nanomaterials

This project has received funding from the European Union's Horizon 2020 research and innovation programme under grant agreement No 958171.

13.12 Available knowledge

13.12.1 Reference projects

- *PARTNER (2002-2006) – founded by the European Community:*

Objective – establishing a unified test procedure for evaluating the potential alkali – reactivity of aggregates across the different European economic and geological regions. Published by the Norwegian research institute SINTEF, Mannvit Engineering in Iceland, Verein Deutscher Zementwerke e.V in Germany, Associate - Building Research Establishment in England and SP Technical Research Institute of Sweden.

- RILEM TC 219 ACS Alcali-Aggregate Reactions in Concrete Structures Committee.

13.12.2 Other

GAMRY INSTRUMENTS – Pulse Voltammetry Software

13.13 Bibliography

Bertolini, L. (2013). *Corrosion of steel in concrete : prevention, diagnosis, repair.* Weinheim: Wiley-VCH.

Butler, J. N. (1963, February). Calculating titration errors. *J. Chem. Educ. 40, 2, 66, American Chemical Society and Division of Chemical Education, Inc.*

Climent, M. A., Viqueira, E., Vera, G. d., & López-Atalaya, M. M. (1999). Analysis of acid-soluble chloride in cement, mortar, and concrete by potentiometric titration without filtration steps. *Cement and Concrete Research, vol. 29 no 6*, pp. 893-898.

D.W.Law, S. ,. (2001, January). The use of galvanostatic pulse measurements to determine corrosion parameters. *British Corrosion Journal*, pp. 1-10.

E Poulsen, L. M. (2014). *Diffusion of Chloride in Concrete: Theory and Application.* . Boca Raton: FL : CRC Press.

Gerardo G. Clemeña, C. M. (2002). *An Alternative Potentiometric Method for Determining Chloride Content in Concrete Samples from Reinforced-Concrete bridges.* Charlottesville, Virginia: Virginia Transportation Research Council.

James A. Farny, B. K. (2007, July 21). Diagnosis and Control of Alkali-Aggregate Reactions in Concrete. *Portland Cement Association*, pp. 1-26.

Jóźwiak, H. (2009). Możliwości wykorzystania metody jądrowego rezonansu magnetycznego w badaniach domieszek chemicznych w betonie. *Prace Instytutu Techniki Budowlanej*, pp. 3-13.

K.D. Stanish, R. H. (1997). *Testing the Chloride Penetration Resistance of Concrete: A Literature Review.* Toronto, Ontario: University of Toronto.

L. Tang, H. E. (2001, 10). Precision of the Nordic test methods for measuring the chloride diffusion/migration coefficients of concrete. *Materials and Structures/Matériaux et Constructions, Vol. 34*, pp. 479-485.

Mettler Toledo International Inc. . (2015). *Titraion Guide* . Greifensee: Mettler Toledo .

This project has received funding from the European Union's Horizon 2020 research and innovation programme under grant agreement No 958171.

Nadejda V. Orlova, J. C. (1999). *The study of chloride ion migration in reinforced concrete under cathodic protection - Final Report (SPR 357).* Oregon : Oregon Department of Transportation.

Nordtest. (1995, November 22). *Concrete, hardened: Accelerated chloride penetration.* Retrieved from http://nordtest.info/images/documents/nt-methods/building/NT%20build%20443_Concrete,%20hardened_Accelerated%20chloride%20penetration_Nordtest%20Method.pdf

R. Vedalakshmi, L. B.-H. (2010, March 3). Reliability of Galvanostatic Pulse Technique in Assessing the Corrosion Rate of Rebar in Concrete Structures: Laboratory vs Field Studies. *KSCE Journal of Civil Engineering* , pp. 867-877.

S. Sathiyanarayanan, P. N. (2006, May 24). Corrosion monitoring of steel in concrete by galvanostatic pulse technique. *Cement & Concrete Composites*, pp. 630-637.

Shing, G. Y. (2014). *A comparision of three methods used for determining cholride in acid copper sulfate plating bath.* Kuala Lumpur: Faculty of Science University of Malaya .

Stark, D. (1991). *Handbook For The Identification Of Alkali Iica Reactivity In Highway Structures.* Washington: Strategic Highway Research Program National Research Council.

Thomas Frølund, F. M. (2002). Smart Structures: Determination of reinforcement corrosion rate by means of the galvanostatic pulse technique. *First International Conference on Bridge Maintenance, Safety and Management* (pp. 1-9). Barcelona: IABMAS.

U.S. Dept. of the Interior, B. o. (1992). *Concrete manual.* U.S. Dept. of the Interior, Bureau of Reclamation.

Zofia Szweda, A. Z. (2012). Wyznaczanie współczynnika dyfuzji chlorków w betonie na podstawie badań migracji jonów w polu elektrycznym. *Trwałość Budowli i Ochrona przed Korozją*, pp. 60-62.

This project has received funding from the European Union's Horizon 2020 research and innovation programme under grant agreement No 958171. © 2021

APPENDIX A14. Radiological and Nuclear Methods

14.1 Goal(s)

14.1.1 Main objective

Radiological methods are very popular for the non-destructive determination of defects, which are not visible to the naked eye in various types of structures. By means of industrial radiography, it is possible to detect and document fractures inside elements or ensure that there are no cracks in an object for quality control aspects. Radiological methods are also used for the assessment of reinforcement distribution in reinforced concrete structures. This group of methods is based on directing radiation from sources such as radioisotopes and X-ray generators against or through fresh or hardened concrete samples (in case of bridge maintenance purposes), taking advantage of the dependence of attenuation of radiation on material thickness and density. As a result, it is possible to obtain qualitative and quantitative Information about the object under study such as cracks dimensions, early signs of corrosion, microcracking progress. The durability of concrete can be quantified by certain characteristics such as porosity, sorptivity, and permeability. The quantification of neutron radiography images of concrete structures validates conventional measurements (Mitchell, 2003).

Nuclear methods are commonly used for the evaluation of the dampness and water absorption rate in different materials. Nuclear Magnetic Resonance and Neutron Radiography are really powerful in accurate detection on the smallest scale, but at the same time need a lot of technical practice and knowledge that requires specific training. For laboratory applications, NMR is used for the analysis of mixtures, analysis of molecular structures, dynamics of chemical reactions, determination of polymers conformations in fields such as food or pharmaceutical industry, or conservation of works of art. NMR techniques allow also to detection of free chloride molecules in the structure of concrete (Peyvandi, 2015) (Wang Y., 2017) (K. Schabowicz, 2016).

For industrial purposes both – radiological and nuclear methods are widely used in different areas for estimation of corrosion of aluminium components, water flow in plants, a study of nuclear fuels, combustion in engines. For civil engineering purposes, those are used for quantification of water movement in building materials.

14.2 Description

14.2.1 Functioning mode

- Computed X-ray/Gamma Tomography – reconstruction of a cross-sectional image from its projections; sample subjected to X-ray/gamma radiation at a given intensity. A detector registers the intensity of the ray received - sample revolves in front of the emitter and detector, emitting rays in all directions on the plane Another functioning mode consists of system with flat detector and conic beam of X-rays and in this case only the specimen has to revolve, relative displacement

This project has received funding from the European Union's Horizon 2020 research and innovation programme under grant agreement No 958171.

between detector and emitter is unnecessary; process is repeated for different sections of the sample and tri-dimensional information is being registered in the software (Wang Y., 2017) (Dewanckele J., 2014) (X. Wang, 2019).

- Neutron Radiography – objects bombarded with neutrons become radioactive and emit gamma radiation. In neutron radiography, imaging screen can retain their radioactivity and indirectly transfer the test object image to the radiographic film. Crucial parameters that can be controlled in this method are: neutron energy, exposure time, film type, L/D ratio source to target distance divided by beam diameter and type of conversion screen. Neutron radiographic imaging is a complex process, therefore in order to fully understand the methodology it is necessary to search for a detailed source of information such as - (Domanus, 1992) (Peng Zhang, 2011) (Dewanckele J., 2014).
- Nuclear Magnetic Resonance Spectroscopy - sample subjected to a magnetic field and pulses of radiofrequency radiation to induce precession of the nuclear spin; The electromagnetic signal is measured by electronic device in the system inside, which is then converted to an NMR spectrum by applying a Fourier transform. NMR Spectroscopy is a complex technology as Neutron Radiography - details on the method functioning can be found for example n (Lambert, 2004) (Peyvandi, 2015) (Mitchell, 2003)

14.2.2 Types

- Computed X-ray/Gamma Tomography - system composed of an emitter of X-ray radiation at a given intensity, a detector, computed radiography reader, cassettes with imaging plates and control station with monitors.
- Neutron Radiography – a system composed of the neutron beam, collimator, scintillator screen, mirror, and camera.
- Nuclear Magnetic Resonance Spectroscopy – solid-state, liquid-state NMR applied in continuous and pulsed wave spectrometers or Fourier –Transform spectrometers.

14.2.3 Process/event to be detected or monitored

- Computed X-ray/Gamma Tomography images to evaluate the structural integrity of concrete samples.
- Neutron Radiography – neutron flux density transmitting through the object, neutron flux density leaving the collimator, water absorption time.
- Nuclear Magnetic Resonance Spectroscopy – the electromagnetic response produced as the nuclei relax back to their equilibrium states (relaxation time), analysis of the spectra based on the ^{1}H nuclei associated with water.

This project has received funding from the European Union's Horizon 2020 research and innovation programme under grant agreement No 958171.

14.2.4 Physical quantity to be measured (e.g. actions, displacements, deformations, dynamic structural properties, material properties including mechanical, electrical and chemical properties, relative displacements of the two sides of a crack, etc.).

- Computed X-ray/Gamma Tomography – attenuation measurements, the density of each point of the specimen under study; composition, the structural integrity of concrete samples.
- Neutron Radiography – depth of water absorption.
- Nuclear Magnetic Resonance Spectroscopy – electromagnetic signal measured as a free induction decay, atomic/structural details within the material on spectra; dampness of the structure.

14.2.5 Induced damage to the structure during the measurement

Radioactive and nuclear methods are non-destructive without moving the structure.

14.2.6 General characteristics

14.2.6.1 Measurement type (static or dynamic, local or global, short-term or continuous, etc.)

- Computed X-ray/Gamma Tomography: local measurement, both short-term or continuous.
- Neutron Radiography: local measurement, both short-term or continuous.
- Nuclear Magnetic Resonance Spectroscopy: local both short-term or continuous

14.2.6.2 Measurement range

- Computed X-ray/Gamma Tomography:
  - structural changes detection at resolution down to hundred nanometres
- Neutron Radiography:
  - detection of the liquid channels in range of 100 – 200 μm
  - greyscale resolution of the camera – depends on the manufacturer e.g. 4096 gray level (12 bits)
- Nuclear Magnetic Resonance Spectroscopy:
  - frequency region 4 - 600 MHz
  - wavelength region: 75 - 0.5 m. field.

14.2.6.3 Measurement accuracy

- Computed X-ray/Gamma Tomography:
  - depends on the quality of an image – computerized tomography is capable of producing images of millimetre or submillimetre resolution
- Neutron Radiography
  - beam purity indicator (L/D ratio) is a determining factor in the sharpness of an image in a neutron radiograph
- Nuclear Magnetic Resonance Spectroscopy

This project has received funding from the European Union's Horizon 2020 research and innovation programme under grant agreement No 958171. © 2021

- affected by magnetic field fluctuation, quality of calibration process, and preparation of the sample

14.3 Background (evolution through the years)

At first, computer tomography has been widely used for medical purposes to detect pathologies on the internal organs. In 1980 computer tomography technique has been developed for use in geological surveys such as analysis of the internal microstructures of rocks. Since its first use in the medical field, the technique of computer tomography becomes popular in other areas such as palaeontology and engineering. Also, In 1980 high-resolution tomographic equipment has been introduced and named a micro CT scan. New sources of the radiation haves been then developed – gamma rays and synchrotron. For medical purposes, the equipment functioning mode is different than for industrial purposes. In the first case, the emitter and receptor revolve, while in the second case the specimen is moved and turned in system emitter-detector. CT method has been then applied in the asphalt mixtures technology for obtaining the geometry of the internal structure of the asphaltic mixtures to improve their properties. Recent advances in Tomography Imaging are the HRXCT – High-resolution X-ray Computed Tomography and micro-CT analysis in geosciences.
Neutron radiography has been used in industrial applications for at least fifty years until now as a non-destructive technique. Recent advances concern automatic systems for neutron inspection (Domanus, 1992) (Lister, 2004) (X. Wang, 2019).

14.4 Performance

14.4.1 General points of attention and requirements

14.4.1.1 Design criteria and requirements for the design of the survey

Necessary to comply with health and safety regulations taking into account the radiation during measurement. The assessment of the suitability of the method should be preceded with examination of material under studies – its thickness, type, geometry and types of defects to be expected.

14.4.1.2 Procedures for defining layout of the survey

For radiological surveys:

- selection of energy, type and source of the radiation,
- selection of the direction and method of exposure of the examined object,
- selection of photographic film and exposure time,
- time of irradiation exposure,
- method of developing of the photographic film,
- interpretations of radiograms,
- report from the survey.

This project has received funding from the European Union's Horizon 2020 research and innovation programme under grant agreement No 958171. © 2021

14.4.1.3 Design constraints (e.g. related to the measurement principles of the monitoring technologies)

In the case of the NMR method – NMR equipment used has a specific restriction on usage – laboratory organization for the stability of magnetic field and many others. This requires specific knowledge in the area of Nuclear Magnetic Spectroscopy and permission to work with NMR.

14.4.1.4 Sensibility of measurements to environmental conditions

The measurements are not influenced by environmental conditions.

14.4.2 Preparation

14.4.2.1 Procedures for calibration, initialisation, and post-installation verification

For NMR Spectroscopy the experimental set-up, initialization, and procedures of gradient shimming require ground knowledge and training in the use of NMR Spectroscopy. An example of the technical user guide can be found in - (Varian NMR Systems, Everett Schreiber, 2007). Anyhow it will vary on the type of spectrometer and manufacturer.

14.4.2.2 Procedures for estimating the component of measurement uncertainty resulting from calibration of the data acquisition system (calibration uncertainty)

14.4.2.3 Requirements for data acquisition depending on measured physical quantity (e.g. based on the variation rate)

Not applicable.

14.4.3 Performance

14.4.3.1 Requirements and recommendations for maintenance during operation (in case of continuous maintenance)

For NMR – magnetic field stability has to be verified in specified intervals of time or by observation of any abnormal signals on the spectrum, however, this requires great experience in analysis of NMR spectra.

14.4.3.2 Criteria for the successive surveying campaigns for updating the sensors. The campaigns include: (i) Georeferenced frame, i.e. the global location on the bridge; (ii) Alignment of sensor data, relative alignment of the data collected in a surveying; (iii) Multi-temporal registration to previous campaigns; and (iv) Diagnostics.

Not applicable.

14.4.4 Reporting

Reports include:

- *Computed X-ray/Gamma Tomography* – images of the samples with description.
- *Neutron Radiography* - images of the samples with description.
- *Nuclear Magnetic Resonance Spectroscopy* – analysis of the spectra of the sample.

This project has received funding from the European Union's Horizon 2020 research and innovation programme under grant agreement No 958171.

14.4.5 Lifespan of the technology

- *Computed X-ray/Gamma Tomography* – geometrically continuous monitoring in hours.
- *Neutron Radiography* – suitable for monitoring of long term changes of water content; starting from at least 240 minutes, neutron images can be taken automatically through time.
- *Nuclear Magnetic Resonance Spectroscopy* – continuous monitoring in days.

14.5 Interpretation and validation of results

14.5.1 Expected output (Format, e.g. numbers in a .txt file)

- *Computed X-ray/Gamma Tomography* – tri-dimensional image in a greyscale, where darker tones represent lower densities in the object.
- *Neutron Radiography* - time-dependent moisture distribution in a graphical form as a function of time; three-dimensional projection of the object in two dimensions, averaged over thickness along the path – radiograms.
- *Nuclear Magnetic Resonance Spectroscopy* – spectra with ^{1}H NMR relaxometry distribution; peaks on NMR spectra in a Lorentzian curve shape with parameters: amplitude [A], width at half height [Hz], and position in [Hz].

14.5.2 Interpretation (e.g. each number of the file symbolizes the acceleration of a degree of freedom in the bridge)

- *Computed X-ray/Gamma Tomography* - two-dimensional images of three-dimensional discontinuities are obtained; the images show the shape and size of the discontinuity in a plane perpendicular to the direction of radiation propagation; the difference in the degree of blackness of the radiographs in the place of the discontinuity image and outside this area (contrast) contains information about the dimensions of the discontinuity.
- *Neutron Radiography* – water penetration depth is obtained after post-processing of the data; the dampness of the structure; radiation attenuation can be related to the water content in a given material.
- *Nuclear Magnetic Resonance Spectroscopy* – correlation of the sample of interest with the signal intensity representing concentration; water mobility and pore size distribution can be assessed; relaxation time corresponds to molecular mobility and interatomic distance.

14.5.3 Validation

14.5.3.1 Specific methods used for validation of results depending on the technique

Comparison of the numerical results with the experimental data.

This project has received funding from the European Union's Horizon 2020 research and innovation programme under grant agreement No 958171.

14.5.3.2 Quantification of the error

For neutron radiography, additional tests should be carried out such as capillary suction tests in order to quantify the error.

14.5.3.3 Quantitative or qualitative evaluation

Quantitative analysis with the use of finite element methods (FEM and image-based finite elements methods. In NMR Spectroscopy after spectra processing – baseline correction, chemical shift calibration, removal of solvents and other contaminants – statistical methods are used for spectra analysis. Peaks are associated with for example Alkali-Silica Reaction and quantification.

14.5.4 Detection accuracy

The detection accuracy of radiological methods is affected by local temperature variations, presence, and concentration of dissolved salts in the pore solution as well as by the presence of metallic components close to the measurement point.

14.6 Advantages

- Computed X-ray/Gamma Tomography:
  - dimensionally accurate analysis,
  - vertical and horizontal overview of the specimen,
  - no interference in the structure of the investigated object,
  - analysis of the shape of a defect,
  - easily accessible source of radiation.
- Neutron Radiography:
  - possibility of imaging light elements.
- Nuclear Magnetic Resonance Spectroscopy:
  - very accurate and detailed technique,
  - advanced NMR techniques use portable magnets that are applied to the object of interest.

14.7 Disadvantages

- Computed X-ray/Gamma Tomography:
  - slow in case of use of X-ray radiation,
  - expensive for high power sources,
  - limited resolution.
- Neutron Radiography:
  - expensive for high power sources.
- Nuclear Magnetic Resonance Spectroscopy:
  - limited availability of the equipment,

This project has received funding from the European Union's Horizon 2020 research and innovation programme under grant agreement No 958171.

- high cost of tests,
- difficult to operate without training,
- equipment sensitive to environmental condition,
- difficult calibration process.

14.8 Possibility of automatising the measurements

NMR, Computed Tomography and Neutron Radiography work in an automated manner, however it is necessary to prepare the samples and control the process by an experience operator. Technical improvements focus on the ongoing optimization of standard imaging setups and development of the methods that go beyond the established 3D mapping. The main aim is to increase the potential of neutron imaging and widen the range of applications. Advances in neutron imaging consists of introducing new ways of achieving the image contrast and new neutron imaging concepts (M. Strobl, 2009).

14.9 Barriers

The main barrier in usefulness of the methods on a daily basis is the cost of the equipment. The presence of ionizing radiation forces strict rules during operation which limits radiological methods to laboratory inspections in many cases. In computed radiography that can be overcome with use of imaging plates, which are suitable for laboratory and mobile inspections under various environmental conditions.

14.10 Existing standards

- ASTM D2950-91 (1997) STM for Density of Bituminous Concrete in place by Nuclear Methods.
- BS 4408: pt. 3, 1970 Non-destructive methods of test for concrete-gamma radiography of concrete, British Standards Institution, London.
- TGL 21 100/01 Non-destructive testing of concrete buildings and structures – Guideline for the determination of the density with gamma rays.
- NDIS 1401-1992 Methods of radiographic examination for concrete constructions.

14.11 Applicability

14.11.1 Relevant knowledge fields

- Civil Engineering:
  - diagnostics of civil engineering structures,
  - high-performance concrete investigation,
  - fibre reinforced concrete investigation,
  - asphalt mixtures testing.
- Palaeontology:

This project has received funding from the European Union's Horizon 2020 research and innovation programme under grant agreement No 958171.

- ancient relics and heritage.
- Geotechnical engineering:
  - aspects of rocks and minerals.
- 3D Printing:
  - replicas.
- Automotive:
  - inspection of defects after manufacturing.
- Art conservation

14.11.2 Performance Indicators

- cracks,
- deteriorated mortar joints,
- delamination,
- displacement,
- loss of section,
- rupture,
- deformation,
- debonding.

14.11.3 Type of structure

- bridges,
- tunnels.

14.11.4 Spatial scales addressed (whole structure vs specific asset elements)

Radiological and nuclear methods are used especially in bridge components such as abutments, decks, beams, girders, cables, rivets, trusses, pins and hangars, paint, fenders, footings, foundations, and culverts.

- piers,
- rivets, bolts,
- welding joints,
- retaining walls,
- culverts,
- foundations.

14.11.5 Materials

- concrete,
- reinforced concrete,

This project has received funding from the European Union's Horizon 2020 research and innovation programme under grant agreement No 958171. © 2021

- steel,
- metals,
- composites,
- wood,
- polymers,
- ceramics.

14.12 Available knowledge

14.12.1 Reference projects

No reference projects.

14.12.2 Other

Phoenix Transforming Nuclear Technology – Neutron Radiography Training Description

Phoenix Transforming Nuclear Technology – Neutron Generators

14.13 Bibliography

Chen, M.-C. &.-C.-L.-Y. (2008). Radioactive methods for detecting concrete imperfections and steel locations. *Journal of the Chinese Institute of Engineers*, pp. 565-572.

Czabaj M.W., R. M. (2014). Numerical reconstruction of graphite/epoxy composite microstructure based on sub-micron resolution X-ray computed tomography. *Composites Science and Technology*, pp. 174-182.

Dewanckele J., D. K. (2014). Neutron radiography and X-ray computed tomography for quantifying watering and water uptake processes inside porous limestone used as building material. *Materials Characterization*, pp. 86-99.

Domanus, J. (1992). *Practical Neutron Radiography.* Springer Netherlands/Springer Science+Business Media Dordrecht.

Hu J., Q. Z. (2015). Influence of aggregate particles on mastic and air-voids in asphalt concrete. *Construction and Building Materials*, pp. 1-9.

J., R. (1989). The development of neutron radiography and its potential application in Malaysian industries. *Proceedings of the third world conference* (pp. 171-178). Osaka: Kluwer Academic Publishers.

John Rogers, A. A.-R. (2015). Evaluation of Measurement Accuracy in Neutron and X-ray Radiography. *Physics Procedia Volume 69*, pp. 366-373.

K. Schabowicz, Z. R.-N. (2016). Application of X-ray microtomography to quality assessment of fibre cement boards. *Construction and Building Materials*, pp. 182-188.

Lambert, J. B. (2004). *Nuclear Magnetic Resonance Spectroscopy: An Introduction to Princliples, Applications, and Experimental Methods.* . Upper Saddle River: Pearson Education.

This project has received funding from the European Union's Horizon 2020 research and innovation programme under grant agreement No 958171. © 2021

Lin Q., A.-K. Y. (2014). Quantification of sub-resolution porosity in carbon rocks by applying high-salinity contrast brine using X-ray microtomography differential imaging. *Materials Characterization*, pp. 150-160.

Lister, P. F. (2004). Applications of X-ray computed tomography in the wood products in industry. *16th World Conference on NDT*. Montreal.

M. Strobl, I. M. (2009 , November). Advances in neutron radiography and tomography. . *Journal of Physics. D: Applied Physics 42*.

Mitchell, T. (2003). *Radioactive/nuclear methods* .

Muhammad Rawi, M. Z. (2003). The Comparison of Neutron, Gamma and X-Ray Radiography Images for Materials Evaluation. *The 5th National Seminar on Non-Destructive Testing*, (pp. 58-63). Shah Alam.

Peng Zhang, F. H.-j. (2011, February 25). Neutron radiography, a powerful method to determine time-dependent moisturedistributions in concrete. *Nuclear Engineering and Design*, pp. 4758-4766. Retrieved from https://www.researchgate.net/publication/272163426_Neutron_Radiography_a_Powerful_Method_to_Determine_Time-dependent_Moisture_Distributions_in_Concrete

Peyvandi, A. (2015). Monitoring of Sulfate Attack in Concrete by Al27 and Si29 MAS NMR Spectroscopy. *Journal of Materials in Civil Engineering*.

Sencu RM, Y. Z. (2016). Generation of micro-scale finite element models from synchrotron X-ray CT images for multidirectional carbon fibre reinforced composites. *Composites: Part A.*, pp. 85-95.

Varian NMR Systems, Everett Schreiber. (2007). NMR Spectroscopy, User Guide, Varian NMR Systems. *Varian NMR spectrometer systems with VnmrJ 2.2C*. Retrieved from https://www.agilent.com/cs/library/usermanuals/public/0199934300c.pdf

Wang D., W. H. (2015). Evaluation of aggregate resistance to wear with Micro-Deval test in combination with aggregate imaging techniques. *Wear*, pp. 338-339, 288-296.

Wang Y., B. T. (2017). X-Ray computed tomography study of kink bands in unidirectional composites. *Composite Structures*, pp. 917-924.

Wells, J. M. (2004). On the future of 3-D visualization in non-medical industrial X-ray computed tomography. *16th World Conference on NDT*. Montreal.

X. Wang, Y. P. (2019, July 12). Pore Structure Damages in Cement-Based Materials by Mercury Intrusion: A Non-Destructive Assessment by X-ray Computed Tomography. *Materials*.

Zhang Y., V. W. (2015). Using high-resolution industrial CT scan to detect the distribution of rejuvenation products in porous asphalt concrete. *Construction and Building Materials*, pp. 1-10.

This project has received funding from the European Union's Horizon 2020 research and innovation programme under grant agreement No 958171.

APPENDIX A15. Satellite

15.1 Goal(s)

15.1.1 Main objective

Remote sensing is the term that encompasses the acquisition, among others, of satellite images, since the basis of this technique consists in collecting information about the object to be measured without making physical contact with it, in contrast to on-site observation.

The use of satellite images for monitoring in the different types of infrastructures (example bridges) responds to two great advantages, the great coverage that is achieved in a single analysis and the possibility of recovering historical data, through old images.

These virtues make its use more accessible, compared to jobs where on-site data is more difficult and expensive to obtain.

The satellites that are used to monitor the different infrastructures of the earth have the main objective the observation and mapping the earth's surface.

15.2 Description

The data acquisition by remote sensing, through the different satellites, could be by two types, depending on the signal source used to explore the object:

- Active: They generate their own radiation and receive it bounced. Most devices use microwaves because they are relatively immune to weather conditions. Active remote sensing is different in what it transmits (light and waves) and what it determines (for example distance, height, etc.).
- Passive: Receives radiation emitted or reflected by the earth. It depends on the natural energy (solar rays) that bounces off the target. For this reason, it only works in the correct light, if not, there will be nothing to reflect. Passive remote sensing uses multispectral or hyperspectral sensors that measure the amount acquired with multiple combining bands. Those combinations are different by the number of channels (wavelength and more). The scope of the bands includes spectra within and beyond human vision (IR, NIRS, TIRS, microwave, etc.).

15.2.1 Functioning mode

In order to capture the data, the different satellites employ whit electromagnetic waves, those could be (“Distintos tipos de sensores: sistemas fotográficos, ópticos y de microondas", n.d.):

1) Photographic ultraviolet: with λ between 0.3 to 0.4 μ. Only this portion can be captured with photographic emulsions; the rest are absorbed by the atmosphere and do not reach the earth's surface.

This project has received funding from the European Union’s Horizon 2020 research and innovation programme under grant agreement No 958171.

2) Visible: with λ from 0.4 to 0.7 µ. It is the operating range of most image-producing sensors and the best known, since it corresponds to the sensitivity of the human eye, thus facilitating the interpretation of images.

3) Photographic: with λ between 0.3 to 0.9 µ. It corresponds to the sensitivity ranges of the photographic films currently in use. It is located within the atmospheric window between 0.3 to 1.35 µ. It is the range used in multispectral photography.

4) Reflective region: with λ between 0.3 to 3 µ. It corresponds to the capture of radiation reflected by natural bodies at ordinary temperatures of the earth's surface.

5) Emissive region: with λ between 3 and 14 µ. In this region, the sensors capture the energy emitted by bodies as a function of their temperature. It is operated with thermal sensors. It is called I.R. thermal or emissive.

6) Reflective infrared: with λ between 0.7 to 3 µ. It is the region of the I.R. in which the reflected radiation is captured. Photographic systems and multispectral scanners operate there. Two subregions can be considered:

6.a) I.R. close with λ between 1.3 to 3 µ in which high sensitivity photographic emulsions operate and corresponds to an atmospheric window between U.V., the visible and the I.R.

6.b) I.R. medium with λ between 1.3 to 3µ. It is the region where there is the greatest influence of the absorption zones of electromagnetic radiation. The sensors must operate in two atmospheric windows that are between 1.5 to 1.8 µ and 2.0 to 2.4 µ of wavelengths.

7) optical region: with λ from 0.3 to 15 µ. It includes the entire application range of optical systems such as lenses, prisms, mirrors. Multispectral scavengers have the capacity to operate throughout this region.

8) Microwave: with λ between 0.3 to 300 cm. It corresponds to the side-sight radar (SLAR), the synthetic aperture radar (SAR), both active sensors, and the radiometer as a passive sensor.

Inside the class of the passive sensors are the Photographic, the Optical-electronic sensors, (that combine one focus similar to the photographic and one detection electronic system (Push Broom and Whisk Broom Sensors)), imaging and antenna spectrometers (Microwave radiometer). Referred to the sensor's actives, exist the LIDAR and the RADAR ("Plataformas, sensores y canales.", n.d.).

There are two optical-electronic system types ("Plataformas, sensores y canales.", n.d.):

- Whisk Broom are the most common in remote sensing. They have a movable mirror that oscillates perpendicular to the direction of the trajectory that allows to explore the swaths of land on both sides. Each movement of the mirror sends information from a different swath to the set of sensors.
- The Push Broom: eliminates the oscillating mirror because it has a chain with many detectors so that they cover the entire field of view of the sensor. This allows increasing the spatial

This project has received funding from the European Union's Horizon 2020 research and innovation programme under grant agreement No 958171.

resolution and reducing geometric errors because they eliminate the mobile and less robust part of the Whisk Broom, however they make a more complex calibration since it must be done for all the sensors at the same time to achieve a homogeneous behaviour.

In addition to the Push Broom and Whisk Broom, there is the microwave radiometer ("Plataformas, sensores y canales.", n.d.):

- The Microwave radiometer are composed of an antenna that functions as a receiver and amplifier element of the microwave signal (because it is too weak) and a detector. In this type of system, the spatial resolution is inversely proportional to the diameter of the antenna and directly proportional to the wavelength. Also, the spatial resolution is worse and should only be applied in global studies.

Finally, the satellites catch the information by two different ways in function of the position form the ("Plataformas, sensores y canales.", n.d.):

- Geosynchronous or geostationary: they are located on the Equator in an orbit 36000 km from the Earth. They always remain in the vertical of a certain point accompanying the Earth in its rotational movement.
- Heliosynchronous satellites move in generally circular and polar orbits (the plane of the orbit is parallel to the axis of rotation of the Earth) so that, taking advantage of the Earth's rotational motion, it can capture images of different points each time it passes through the same point in the orbit. These orbits are only possible between 300 and 1500 km high. The orbit is designed in such a way that the satellite always passes over the same point at the same local time.

In addition, depending on the orientation with which the sensor captures the images, a distinction is made between sensors of ("Plataformas, sensores y canales.", n.d.):

- Vertical orientation, typical for satellites of low or medium spatial resolution
- Oblique orientation, typical of radar
- Modifiable orientation appears on high resolution sensors. It allows maintaining a high spatial resolution and having a high temporal resolution as well. Images of the entire earth's surface are no longer taken systematically, but the sensor is oriented on request. The downside is that it is difficult to find images afterwards, since only those images that have been previously ordered are taken.

15.2.2 Types

From the observation of the electromagnetic spectrum, the remote sensing uses certain regions of the electromagnetic spectrum for different systems. Then, according to the type of energy that the systems capture, the sensors can be photographic, optical and microwave sensors.

Photographic systems are all those that capture images with cameras using photographic emulsions with a long-wave sensitivity of 0.3 to 0.9 µm (UV to IR). Optical systems are the sensors that work to

This project has received funding from the European Union's Horizon 2020 research and innovation programme under grant agreement No 958171.

capture images with long waves from 0.3 to 15 µm. Both systems capture the electromagnetic energy reflected or emitted by the ground, and the spectral response is recorded in the image.

The microwave system operates from 0.8 µm to 100 cm, the information or the content of each pixel of the images captured by the satellite is the result of the amount of beams of waves that return to the satellite, once they were emitted to Earth., the information is called backscatter. the study of them should have a big knowledge of the physic ("Distintos tipos de sensores: sistemas fotográficos, ópticos y de microondas", n.d.).

15.2.3 Process/event to be detected or monitored

In the optical-electronic system the by the optical components are decompose in several wavelengths. Each one is sent to in thar region of the spectrum that and converting in electric signal and finally in one numeric value. These values can convert in others values of radiance knowing the calibrate coefficients. The mission of the image spectrometers is to obtain images in a big number of spectral bands, for that obtain an almost continuous spectrum of radiation. The radar works for the band between 1mm and 1m. It works because artificial microwaves sent in a certain direction collide with targets and then the microwaves scatter. The scattered energy is received, amplified, and analysed to determine the location and properties of the targets, so it is possible to measure the time it takes for the radiation pulse to go and return, thanks to this the distance travelled can be known and generate a DTM. The radar could work in any weather condition, so it is a good option in cloudy areas ("Plataformas, sensores y canales.", n.d.).

15.2.4 Physical quantity to be measured

The resolution of the different satellites limits the monitoring of the infrastructure in the conservation evaluation in a general way, being impossible to detect structural problems in detail, in any case the objective is to detect changes over time, either for example movement mm/year (radar satellites) or visual changes of maximum 50 cm (optical satellites).

15.2.5 Induced damage to the structure during the measurement

As the images are taken remotely, this type of technique does not cause any damage during measurement.

15.2.6 General characteristics

15.2.6.1 Measurement type (static or dynamic, local or global, short-term or continuous, etc.)

The emission of radiation (emitted or reflected) from the earth's surface is a continuous phenomenon in 4 dimensions (space, time, wavelength, and radiance).

This project has received funding from the European Union's Horizon 2020 research and innovation programme under grant agreement No 958171.

15.2.6.2 Measurement range

Due to this great diversity of measurements between satellites, there is a wide measurement range for each type of data used.

15.2.6.3 Measurement accuracy

The above defines the four types of resolution used in remote sensing (“Distintos tipos de sensores: sistemas fotográficos, ópticos y de microondas", n.d.), (“Plataformas, sensores y canales.”, n.d.) and therefore the measurement accuracy:

- Spatial resolution (pixel size): For photographic sensors, the resolution depends on the photographic scale and the flight height. For the optical-electronic sensors it also depends on the flight height of the platform, the scanning speed (interpreted as reading) and the number of detectors. In antenna sensors such as radar, it depends on the aperture radius of the antenna, the flight height, and the wavelength at which they work.
- Spectral resolution (indicates the number and width of the spectrum regions for which the sensor collects data): Among the space sensors the lowest spectral resolution corresponds to the photographic systems that operate in the visible and the radar that operates in the microwaves.
- Radiometric resolution (number of intensity intervals that can be captured): In photographic systems, the radiometric resolution is indicated by the number of grey levels captured by the film. In electro-optical sensors, the spectral resolution is given by the number of values that correspond to the digital levels that the sensor transforms analog-digitally.
- Temporal resolution: is the time that elapses between capturing sequential images detecting the same area.

15.3 Background

Currently it is easy to access a large amount of data, but in the beginning access to satellite information was inaccessible or too expensive. So, the evolution has been at the origin of a scarcity of data (in which, for example, users were only able to have a single image available per year) to currently having an excess of data available.

The first satellite, providing images for earth observation, was launched in 1972 through the LandSat program by the United States.

Europe, through the European Union and the European Space Agency (ESA) launched the first satellite of the constellation, Sentinel 1A, in 2014 through its Copernicus earth observation program, which constantly offers free images, that is one of the most important sources of data, available for users for their various analyses.

This project has received funding from the European Union’s Horizon 2020 research and innovation programme under grant agreement No 958171.

In addition, other international agencies have launched their own satellites, enriching the availability of information on the earth.

Currently, the rapid development of electronics, and increasingly smaller and cheaper, but more powerful computing devices, allows the launching of small satellites or nanosatellites (from private companies) that, added to the images available in the past, represent an exponential increase in the availability of Earth observation images, so currently the challenge is knowing how to use all this available information in an effective and useful way (Pultarova, 2018).

15.4 Performance

15.4.1 General points of attention and requirements

15.4.1.1 Design criteria and requirements for the design of the survey

Does not apply.

15.4.1.2 Procedures for defining layout of the survey

Does not apply.

15.4.1.3 Design constraints (e.g. related to the measurement principles of the monitoring technologies)

To obtain the data or satellite images, it is necessary to analyze in advance what is the objective of the study to be carried out, depending on what it wants to measure it is better to use one type of satellite or another.

That is why it must be clear about the different resolutions that the different satellites on the market have, as well as the type of data capture (if they are optical or radar satellites, etc.).

Start from this first decision, it must be considered that the meteorological conditions of the earth affect the data capture. It is therefore necessary to review or filter the choice of the day of the image that is intended to be used.

Finally, it is necessary to know the different data sources, where the images can be downloaded for use, whether public or private.

15.4.1.4 Sensibility of measurements to environmental conditions.

To reduce distortion and other accuracy issues, consider the following factors (mapwaredev, 2020):

- Atmospheric conditions: Changes in the atmosphere, sun illumination, and viewing geometries during image capture can impact data accuracy, and result in distortions that can hinder automated information extraction and change detection processes. Humidity, water vapor, and light are common culprits for errors and distortion.
  When atmospheric conditions change, reference points can be obscured or lost, which impacts efforts to create accurate measurements from images. Differences in light temperature can lead to color changes that distort data quality, and make for unsightly inconsistencies that ruin the magic of 3D maps.

This project has received funding from the European Union's Horizon 2020 research and innovation programme under grant agreement No 958171.

- Altitude and reflectance: Light collected at high elevation goes through a larger column of air before it reaches the sensor. The result is surface reflectance, a phenomena which can diminish color quality and detail in images.
  The difference in reflectance near the surface and at top-of-atmosphere creates substantial changes in color, image resolution, and perspective that may need to be accounted for in normalization. Even on a small scale, variances in altitude between data sets should raise a red flag for cross-referencing and review.

15.4.2 Preparation

15.4.2.1 Procedures for calibration, initialization, and post-installation verification

Does not apply.

15.4.2.2 Procedures for estimating the component of measurement uncertainty resulting from calibration of the data acquisition system (calibration uncertainty)

Does not apply.

15.4.2.3 Requirements for data acquisition depending on measured physical quantity (e.g. based on the variation rate)

- Study of the environment in which the object / infrastructure is placed.
- Choice of the type of satellite image appropriate for the case study.
- Study of the number of images required for analysis.
- Analysis of the climatic conditions for the study area and discarding the satellite images of the day the image was taken and there were no good climatic conditions.
- Choice of the download platform, as well as the choice of programs to deal with them.

15.4.3 Performance

15.4.3.1 Requirements and recommendations for maintenance during operation (in case of continuous maintenance)

Since a user of the satellite data cannot carry out the maintenance work of the satellites or the image data sources, the best recommendation that can be given is the continuous verification of the availability of the product that is to be used, always considering the market images alternatives.

15.4.3.2 Criteria for the successive surveying campaigns for updating the sensors. The campaigns include: (i) Georeferenced frame, i.e. the global location on the bridge; (ii) Alignment of sensor data, relative alignment of the data collected in a surveying; (iii) Multi-temporal registration to previous campaigns; and (iv) Diagnostics.

Due to the great diversity of data sources and the different types of data, it is recommended to try to define an ontology in a "standardized" way as follows (Zotti & La Mantia, 2014) in Figure 15.1:

This project has received funding from the European Union's Horizon 2020 research and innovation programme under grant agreement No 958171. © 2021

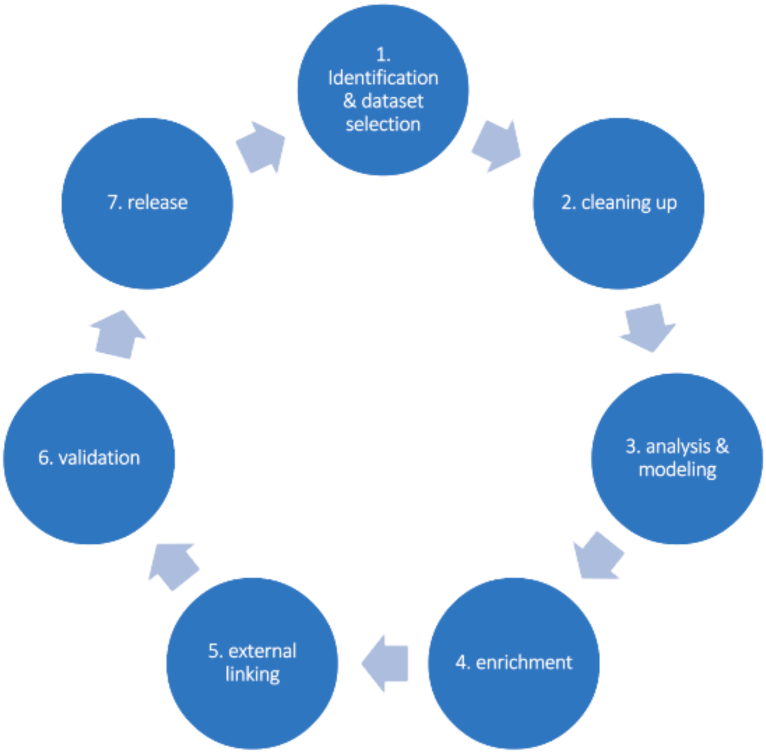

Figure 15.1 – LOD Life Cycle

15.4.4 Reporting

Does not apply.

15.4.5 Lifespan of the technology (if applied for continuous monitoring)

It is necessary to know the useful life in *Figure 15.2* of the different satellites that exist in the market.

This project has received funding from the European Union's Horizon 2020 research and innovation programme under grant agreement No 958171.

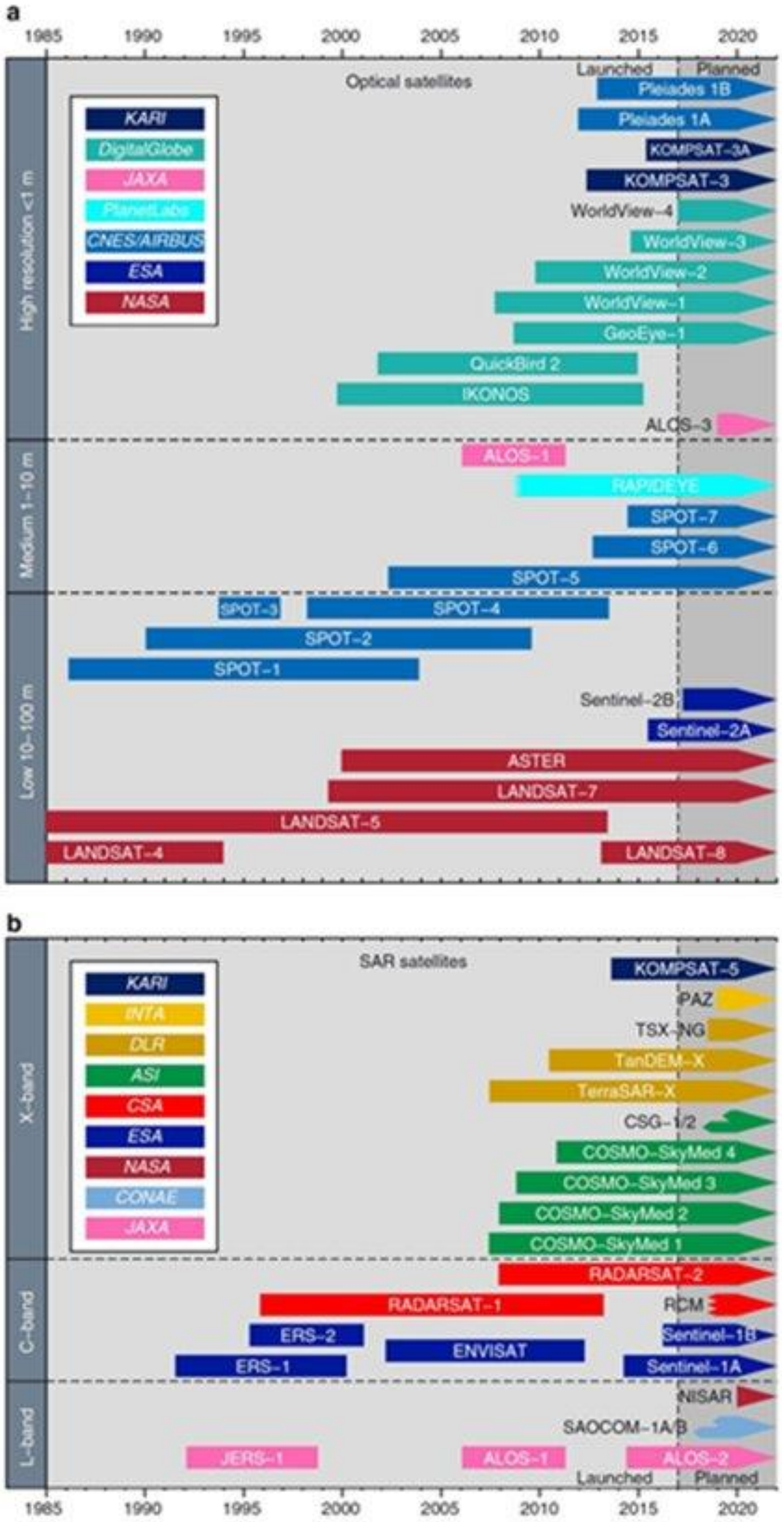

Figure 15.2 – Optical (a) and SAR (b) satellite timeline for major Earth Observing satellites with systematic and global coverage. Source: (Elliott, Walters, & Wright, 2016).

This project has received funding from the European Union's Horizon 2020 research and innovation programme under grant agreement No 958171.

Many of them extend their useful life but it is also possible to start the analysis with images from a satellite and that the analysis cannot be continued due to the lack of more images. In this sense, a good alternative is the combination of images from different satellites for analysis.

15.5 Interpretation and validation of results

15.5.1 Expected output (Format, e.g. numbers in a .txt file)

Due to the diversity of satellites, and their different uses and technologies, there is a great variety of file output formats, which are very difficult to unify. However, there are several commonly used files that can be considered standardized formats (NASA's Earth Science Data Systems (ESDS), n.d.), (Yang, 2006):

HDF5.Addresses some of the limitations and deficiencies in old versions of HDF to meet with the requirements of the current and anticipated computing systems and applications. The improvements in HDF5 include larger file size, more objects, multi-thread and parallel I/O, unified and flexible data models and interfaces, etc. Although inheriting the old version numbering, HDF5 is a new data format and is not back compatible with old versions of HDF. HDF5 consists of a software package for manipulating an HDF5 file, a file format specification describing low-level objects in a physical disk file, and a user's guide describing high-level objects as exposed by HDF5 APIs. 7.4.1 The Physical Layout of HDF5 At lowest level, an HDF5 file consists of the following components: a super block, B-tree nodes, object headers, a global heap, local heaps, and free space. The HDF5 file physical format is specified with three levels of information. Level-0 is file identification and definition information. Level-1 provides information about the infrastructure of an HDF5 file. Level-2 contains the actual data objects and the metadata about the data objects (NCSA, 2003c).

The National Imagery Transmission Format (NITF) is designed primarily by the National Geospatial-Intelligence Agency (NGA), formerly named National Imagery and Mapping Agency (NIMA) and is a component of the National Imagery Transmission Format Standard (NITFS). It is adopted by ISO as an international standard known as Basic Image Interchange Format (BIIF) (ISO/ IEC 12087-5). NITF is aimed primarily to be a comprehensive format that shares various kinds of imagery and associated data, including images, graphics, texts, geo- and non-geo-coordinate systems, and metadata, among diverse computing systems and user groups. The format is comprehensive in contents, implementable among different computer systems, extensible for additional data types, simple for pre- and post-processing, and minimal in terms of formatting overhead.

The Physical Layout of NITF. The top level NITF file structure includes a file header and one or more data segments which can be image, graphics, text, data extension, and reserved extension.

TIFF and GeoTIFF. The Tagged-Image File Format (TIFF) is designed for raster image data. It is primarily used to describe the unsigned integer type bi-level, gray scale, palette pseudo color, and

This project has received funding from the European Union's Horizon 2020 research and innovation programme under grant agreement No 958171.

three-band full color image data but can also be used to store other types of raster data. Although TIFF is not considered as a geospatial data format, its extension, GeoTIFF, which includes standardized definition of geolocation information, is one of the most popular formats for earth observing remote sensing data.

The TIFF physical layout includes four components: (1) an 8-byte TIFF header containing byte order, TIFF file identifier, and the offset address (in byte) of the first Image File Directory (IFD) in the file; (2) one or more IFDs, each containing the number of directory entries, a sequence of 12-byte directory entries, and the address of the next IFD; (3) directory entries each having a tag number indicating the meaning of the tag, a data type identifier, a data value count containing number of values included in this tag, and an offset containing the file address of the value or value array; and (4) the actual data of a tag. Because the offset is of 4-byte size, the actual value of a tag is directly put in the offset field if and only if there is only one value and the value fits into 4 bytes.

15.5.2 Interpretation (e.g. each number of the file symbolizes the acceleration of a degree of freedom in the bridge)

Depending on the analysis that one wants to make of the infrastructure, you must choose the type of satellite to use since the data will contain different information for the information of each pixel of the image, for example, the optical images have different information in its pixels to the radar image for the same study area or target.

For example in *Table 15-1*, the European agency has the Copernicus program that has a constellation of satellites called Sentinel. To monitor infrastructures with the Copernicus program, only Sentinel-1 (radar images) or Sentinel-2 (optical images) are usually used.

	Sentinel-1	**Sentinel-2**
Launch A-unit/B-unit	2013/18 months after A-unit	2013/18 months after A-unit
Design lifetime per unit	7.25 yrs (consumables for 12 yrs)	7.25 yrs (consumables for 12 yrs)
Orbit	Sun-sync, 693 km/incl. 98.18/LTAN 18:00	Sun-sync, 786 km/LTDN: 10:30
Instrument	C-band SAR	MSI (multi-spectral-instrument)
Coverage	Global/20 min per orbit	All land surfaces and coastal waters + full med. sea between: − 56 and + 84° latitude, 40 min imaging per orbit

This project has received funding from the European Union's Horizon 2020 research and innovation programme under grant agreement No 958171.

Revisit	12 days (6 days for A- and B-units)	10 days (5 days for A- and B-units)
Spatial resolution/swath width	Strip mode: 5 × 5m/80 km interferometric wide-swath mode: 5 × 20m/250 km (standard mode) extra-wide-swath mode: 20 × 40 m/400 km wave mode: 5 × 5m/20 × 20 km	Depending on spectral band 10–20–60 m/290 km
Spectral coverage/resolution	5.405 GHz — VV + VH, HH + HV	13 spectral bands: 443 nm–2190 nm (incl. 3 bands at 60 m for atmos. corr.)
Radiometric resolution/accuracy	1 dB (3 s)	12 bit/ < 5%

Table 15-1 – Example of 2 types of infrastructure monitoring satellite (instrument characteristics). Source: (Berger, Moreno, Johannessen, Levelt, & Hanssen, 2012)

These characteristics mean that, for example, for monitoring with Sentinel-2 is usually used only to visually detect the effects of collapse, whereas for Sentinel-1 is usually used to constantly monitor the movement-displacement of the infrastructure surface.

15.5.3 Validation

15.5.3.1 Specific methods used for validation of results depending on the technique

Different technical approaches have been developed in the Earth Observation (EO) communities to address the validation problem which results in a large variety of methods as well as terminology, in the following shows the generic structure of the comparison part within a validation process (Loew, y otros, 2017) in *Figure 15.3*:

This project has received funding from the European Union's Horizon 2020 research and innovation programme under grant agreement No 958171.

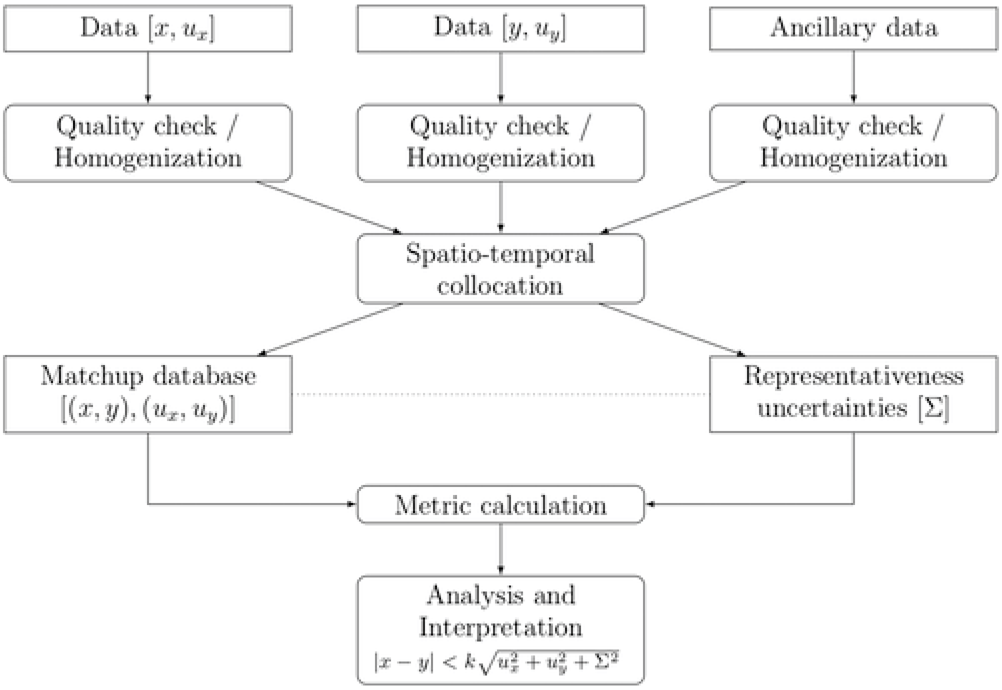

Figure 15.3. Schematic overview of the general validation process. Source: (Loew, y otros, 2017)

15.5.3.2 Quantification of the error

It is important to clarify here what exactly is understood by the terms “error” and “measurement uncertainty” are often used interchangeably within the scientific community. The VIM defines the measurement uncertainty as a nonnegative parameter describing the dispersion of the quantity values attributed to a measurand. The measurement error on the other hand is the difference between the measured value and the true value, i.e., a single draw from the probability density function (PDF) determined by the measurement uncertainty. The measurement error can contain both a random and a systematic component. While the former averages out over multiple measurements, the latter does not. Uncertainties in the reference and EO measurements are derived from a consideration of the calibration chain in each system and the statistical properties of outputs of the measurement system (Loew, y otros, 2017).

15.5.3.3 Quantitative or qualitative evaluation

The CAL-VAL process in *Figure 15.4* starts already before the launch of the platform because it's the unique opportunity where can directly calibrate and characterize physically the satellite, After the launch continues this process directly to obtain Level 1 and 2 data reliable and calibrate. The CAL-VAL of one mission includes the sensor calibration, verify the algorithm, the geophysical data validation and the intercomparison with other missions, all of this going to the uncertainties quantification. This process can be better through the comparison of multiple independent sources so that confidence is generated in the veracity of the data (Sterckx, y otros, 2020).

This project has received funding from the European Union’s Horizon 2020 research and innovation programme under grant agreement No 958171.

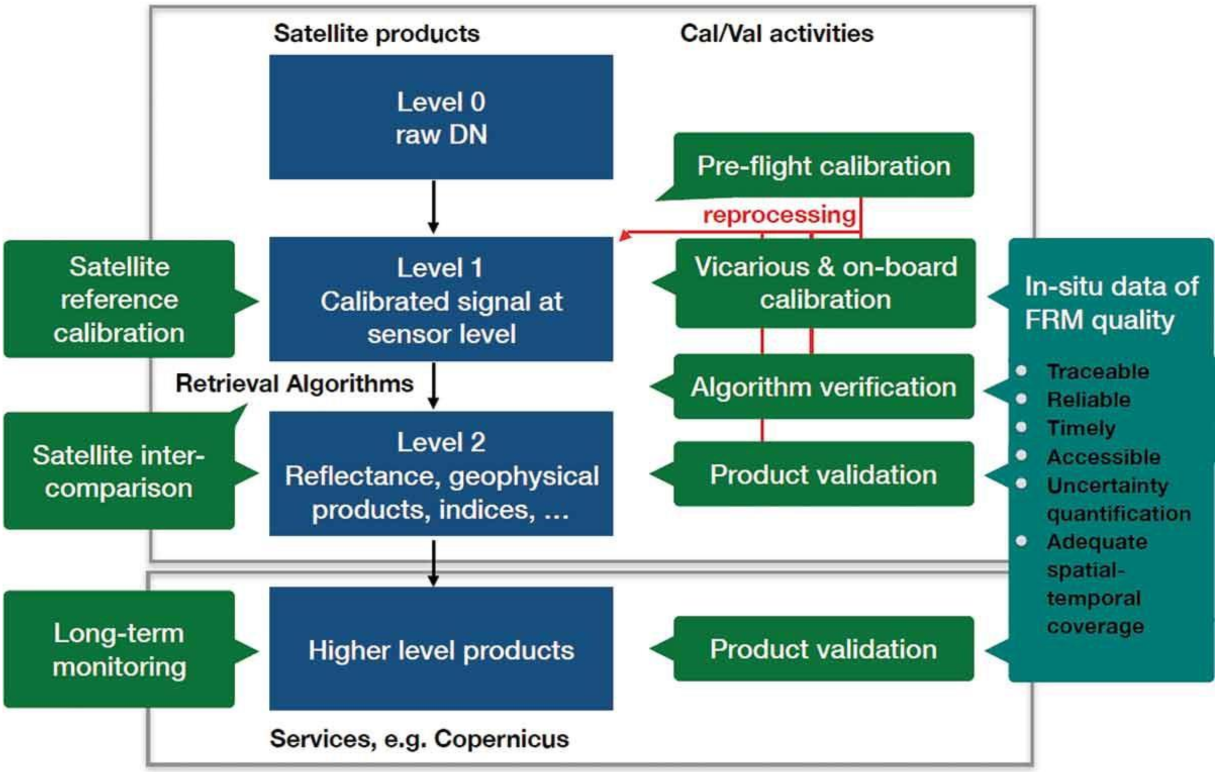

Figure 15.4. Steps necessary for comprehensive Cal/Val activities for satellite missions. Source: (Sterckx, y otros, 2020)

15.5.4 Detection accuracy

In addition to the factor's mentioned in section 16.4.1.4 (Atmospheric conditions and Altitude and reflectance), there are others that can trigger incorrect satellite images (mapwaredev, 2020):

- Documented metadata for cross-referencing

Many data errors come from sources that are difficult to pinpoint — momentary glitches in connectivity, inconsistencies in light or other atmospheric distortions in remote sensing.

- False accuracy is a problem. Good data practices involve regularly layering and cross-referencing data sets against existing data to pinpoint errors and ensure accuracy.

In addition to these factors, the precision is determined by the resolution of the images, since the more pixels (resolution) an image has, the more detailed it is (Setyawan, 2019) in *Table 15-2*.

Resolution Satellite	Approximate Accuracy of Satellite
0.31 m	< 5.0 m

This project has received funding from the European Union's Horizon 2020 research and innovation programme under grant agreement No 958171. © 2021

0.41 m	3.0 m
0.55 m	23 m
0.82 m	9 m
1.50 m	35 m
0.40 m	7.8 m
0.50 m	9.5 m

Table 15-2. Approximate relationship between Resolution Satellite Accuracy of Satellite. Source: (Setyawan, 2019)

However, the precision of an image is not directly related to the resolution and is specified less often (and less clearly) than the resolution of an image (Setyawan, 2019).

15.6 Advantages

The use of satellite images offers a series of advantages over other technologies such as:

Wide geographical and temporal coverage of the study area.

Access to free information depends on the resolution you want to reach.

Possibility, depending on the satellite employee, to obtain images under any climatic and geographical conditions and therefore high accessibility of information.

Easy to complement or combine with other on-site techniques.

15.7 Disadvantages

High-resolution images often come at a high price.

The satellite images require a large storage capacity, as well as, to process them a great demand for computational performance.

Need for experts for its use and interpretation.

Depending on the type of satellite image and weather conditions, certain images may not be valid for use.

This project has received funding from the European Union's Horizon 2020 research and innovation programme under grant agreement No 958171.

15.8 Possibility of automatising the measurements

In the conception of the operation of all satellites, a periodic automation of data collection is already established, an exception of data capture at express request (such as natural disasters).

Satellite	Sensor	Spatial Resolution	Temporal Resolution	Free or Charge
Landsat	MSS+TM (Landsat-5) ETM+ (Landsat-7) OLI (Landsat-8)	30 m	16 days	Free
Terra/Aqua	MODIS	250–1000 m	1–2 days	Free
HJ-1A/B	CCD1/2	30 m	2–4 days	Free
SPOT	HRV (SPOT1~3) VGT (SPOT-4) HRG/HRS/VGT (SPOT-5)	1 km	1 day	Charge
Sentinel-2	MSI	10–20 m	5 days	Free
Sentinel-1	SAR	5–40 m	12 days	Free
COSMO-SkyMed	SAR	3–15 m	16 days	Charge
TerraSAR-X	SAR	3–10 m	11 days	Charge
ENVISAT	ASAR	20–500 m	35 days	Free
RADARSAT-1	SAR	10–100 m	24 days	Charge
RADARSAT-2	SAR	3–100 m	24 days	Charge
ALOS-2	PALSAR-2	25 m	14 days	Charge

Figure 15.5 – Automatization of data collection from the main satellites

For the automation of downloading images by the user, there are numerous tools and freely accessible codes to put it into operation (example: Google Earth Engine, DIAS, USGS Earth Explorer, etc)

15.9 Barriers

The resolution of the images has a limit, in which certain infrastructure monitoring jobs require overcoming them, making their use unfeasible.
Certain satellites are restricted for the civil use of their images.

This project has received funding from the European Union's Horizon 2020 research and innovation programme under grant agreement No 958171.

15.10 Existing standards

Since the 1990s, many national and international organizations have participated in the development of spatial data and information infrastructures for facilitating the sharing of spatial data and information among broad geospatial data producers and consumers and for supporting geospatial applications in multiple disciplines. Since remote sensing is one of the major methods for acquiring geospatial data, remote sensing standards are always one of the core standards for construction of any spatial data infrastructure.

For example:

- The National Spatial Data Infrastructure (NSDI) initiative of the United States is using the remote sensing standards discussed in this encyclopaedia entry for the construction of NSDI (FGDC 2004).
- Internationally, the intergovernmental Group on Earth Observations (GEO) is leading a worldwide effort to build a Global Earth Observation System of Systems (GEOSS).

According to the principle of information engineering, the remote sensing standards can be classified into four general categories based on the subject a standard tries to address: Data, Processes, Organizations and technology (Di, 2017).

15.11 Applicability

15.11.1 Relevant knowledge fields

The purpose of the analysis will be linked to the sensor available on board the satellite. Each satellite has one or more instruments that allow obtaining conventional optical images, radar data, presence of pollutants, temperatures, etc.

That is why, focused on the monitoring of infrastructures, the following topics can be considered as the fields of action of satellites:

- Civil Engineering
- Geosciences
- Civil and environmental protection
- Climate change
- Archaeology
- Urbanism

15.11.2 Performance Indicators

Cracks

Obstruction/ impending

Crushing

This project has received funding from the European Union's Horizon 2020 research and innovation programme under grant agreement No 958171.

Debonding

Holes

rupture

holes

Displacement

Deformation

15.11.3 Type of structure

Bridges, roads, railways, buildings, docks or ports, airports, etc.

15.11.4 Spatial scales addressed (whole structure vs specific asset elements)

Infrastructure monitoring is more efficient and advisable for big study areas since this is where this technology is really advantageous compared to other types of on-site technologies.

15.11.5 Materials

Environment in general

15.12 Available knowledge

15.12.1 Reference projects

SIRMA:

Strengthening infrastructure risk management in the Atlantic Area

15.12.2 Other

https://skygeo.com/ → Radar images for mining, energy, civil engineering, underground gas storage

https://kartenspace.com/ → satellite monitoring for LINEAR INFRASTRUCTURES, AGRICULTURE FIELDS, MINES, LOGISTIC CENTRES, FOREST, NATURAL DISASTERS, CITIES, OCEANS & PORTS

https://www.orbitaleos.com/ → satellite monitoring for Urban Planning, Deforestation, Infrastructure Monitoring, Gas Leaks, Catastrophe Claims, Power Lines and others.

http://dares.tech/ → Radar images for Mining, Infrastructure, Oil and Gas

https://site.tre-altamira.com/ → Radar images for Mining, Oil and Gas, civil engineering, geohazards

https://satsense.com/ → Radar images for Residential & Commercial Properties, Insurance, Infrastructure and Geotechnical

This project has received funding from the European Union's Horizon 2020 research and innovation programme under grant agreement No 958171.

15.13Bibliography

(n.d.). Retrieved junio 24, 2021, from http://www.bibliotecacpa.org.ar/greenstone/collect/facagr/index/assoc/HASH42bc.dir/doc.pdf

SMARTEC SA Branko Glisic, Daniele Inaudi. (2007). *Sensing tape for easy integration of optical fiber sensors in composite structures.* Manno, Switzerland : SMARTEC SA.

"Plataformas, sensores y canales.". (n.d.). Retrieved Junio 24, 2021, from https://www.um.es/geograf/sigmur/teledet/tema03.pdf

27892, I. (2010). Vacuum technology - Turbomolecular pumps - Measurement of rapid shutdown torque. *Technical Committee of Vacuum technology*, 16.

A. Grosso, D. I. (2001, January). Monitoring of bridges and concrete structures with Fibre Optic Sensors in Europe. *IABSE Symposium, Seoul 2001: Cable-Supported Bridges - Challenging Technical Limits*.

AASHTO. (2004). *AASHTO R 37-04. Standard Practice for Application of Ground Penetrating Radar (GPR) to Highways.* Washington, DC, USA: American Association of State and Highway Transportation Officials.

Achievement Standard 91610. (n.d.). *Developing a conceptual design considering fitness for purpose in the broadest sense.* Retrieved from https://es.calameo.com/read/003415039afdc4054de72

ACI. (1998). *ACI 228.2R-98 (Reapproved 2004). Nondestructive Test Methods for Evaluation of Concrete in Structures.* Farmington Hills, MI, USA: American Concrete Institute.

Ahlborn, T. (2010). An Evaluation of Commercially Available Remote Sensors for Assessing Highway Bridge Condition. *Michigan Tech Transportation Institute*, 73.

Alexis Mendez, T. G. (2012). Overview of fiber optic sensors for NDT applications. *IV NDT Panamerican Conference Buenos Aires.* Buenos Aires. Retrieved from https://www.researchgate.net/publication/228340034_Overview_of_fiber_optic_sensors_for_NDT_applications

American Society for Photogrammetry & Remote Sensing. (2013). LAS SPECIFICATION VERSION 1.4 – R13.

Andrea Del Groso, K. B. (2001). *IABSE Symposium Report: Monitoring of bridges and concrete structures with Fibre optic sensors in Europe.* International Association for Bridge and Structural Engineering.

Andrea del Grosso, K. B. (2001). *Monitoring of Bridges and Concrete Structures with Fibre Optic Sensors in Europe.* IABSE Symposium Report .

Annan. (2023).

Annan, P. (2003). *GPR Principles, Procedures & Applications.* Mississauga, ON, Canada: Sensors and Software Inc.

Annan, P. (2003). *GPR Principles, Procedures & Applications.* Mississauga, ON, Canada: Sensors and Software Inc.

Annan, P. (n.d.). *GPR* .

Asteris, P., & Plevris, V. (2015, 7). Handbook of research on seismic assessment and rehabilitation of historic structures. *Handbook of Research on Seismic Assessment and Rehabilitation of Historic Structures*, 1-867.

This project has received funding from the European Union's Horizon 2020 research and innovation programme under grant agreement No 958171.

ASTM. (2004). *Standard Test Method for Determining the Thickness of Bound Pavement Layers Using Short-Pulse Radar; Non-destructive testing of pavement structures; ASTM D4748.* West Conshohocken, PA, USA: ASTM.

ASTM. (2015). *ASTM D6087-08(2015)e1. In Standard Test Method for Evaluating Asphalt-Covered Concrete Bridge Decks Using Ground Penetrating Radar*. West Conshohocken, PA, USA: ASTM.

B10. (2008). *Document B10—Recommendation for Nondestructive Testing of Civil Engineering Structures by GPR.* Berlin, Germany: German Society for Non-Destructive Testing (DGZfP).

Balado, J., Díaz-Vilariño, L., Arias, P., & Lorenzo, H. (2019, 2). Point clouds for direct pedestrian pathfinding in urban environments. *ISPRS Journal of Photogrammetry and Remote Sensing, 148*, 184-196.

Balaguer, C., Montero, R., Victores, J., Martínez, S., & Jardón, A. (2014). Towards fully automated tunnel inspection: A survey and future trends. *Proceedings of the 31st International Symposium on Automation and Robotics in Construction and Mining.* Sydney, Australia.

Barr, S. H. (2009). Bridging the valley of death: Lessons learned from 14 years of commercialization of technology education. *Academy of management learning & education, 8*(3), 370-388.

BASt. (2007). *BASt-Report B55. Examination of GPR in Combination with Magnetic Techniques for the Determination of Moisture and Salinity of Concrete Bridge Decks with Asphalt Cover*. Bundesanstalt für Straßenwesen: Federal Highway Research Institute.

BAUMER. (2021, 12 10). *BAUMER* . Retrieved from Passion for sensors : https://www.baumer.com/medias/__secure__/Baumer_Fiber-optic-sensors-to-detect-liquid-levels-and-leakage-of-fluids_EN_0610_AR.pdf?mediaPK=8837757272094

Bazovsky, I. (2004). *Reliability theory and practice.* Courier Corporation.

Benedetto, A., & Pajewski, L. (2015). *Civil Engineering Applications of Ground Penetrating Radar*. New York, NY, USA: Springer International.

Berger, M., Moreno, J., Johannessen, J., Levelt, P., & Hanssen, R. (2012). ESA's sentinel missions in support of Earth system science. *Remote Sensing of Environment, 120*, 84-90.

Bertolino, M., & Tanzi, T. (2020). Towards 3D Simulation for Disaster Intervention Robot Behaviour Assessment. *Adv. Radio Sci., 18*, 23–32.

BIN File Extension - What is .bin and how to open? - ReviverSoft. (2021, 12 17). Retrieved from https://www.reviversoft.com/file-extensions/bin

Chang, R. (2004). IEEE Intelligent TranSPOrtation Systems. *San Diego, USA, October 3-6*, 971.

Chen, S., Truong-Hong, L., Laefer, D., & Mangina, E. (2018). Automated Bridge Deck Evaluation through UAV Derived Point Cloud. *undefined*.

Conde, B., Del Pozo, S., Riveiro, B., & González-Aguilera, D. (2016, 6). Automatic mapping of moisture affectation in exposed concrete structures by fusing different wavelength remote sensors. *Structural Control and Health Monitoring, 23*(6), 923-937. Retrieved from https://onlinelibrary.wiley.com/doi/full/10.1002/stc.1814

This project has received funding from the European Union's Horizon 2020 research and innovation programme under grant agreement No 958171.

D. Inaudi, S. V. (1999, February 12-13). SOFO: Structural Monitoring with Fiber Optic Sensors . *FIB, Monitoring and Safety Evaluation of Existing Concrete Structures*.

Daniels , D. J. (2004). *Ground Penetrating Radar*. London, UK: The institution of Electrical Engineers.

David Krohn, T. M. (2014). *Fiber Optic Sensors Fundamentals and Applications* . Washington: SPIE PRESS .

Di, L. (2017). Standards, Critical Evaluation of Remote Sensing. *Encyclopedia of GIS, Springer International Publishing*, 2187–2196.

Digital technologies can enhance climate resilience of critical infrastructure – infrastructuResilience. (2021, 12 17). Retrieved from http://www.infrastructuresilience.com/lake-polyfytos-bridge/

DMRB3.1.7. (2006). *Department for Transport, Highway Agency. DMRB 3.1.7.: Design Manual for Roads and Bridges, Advice Notes on the Non-Destructive Testing of Highway Structures—Advice Note 3.5 BA 86/2006: Ground Penetrating Radar (GPR).* Birmingham, UK: Department for Transport, Highway Agency.

DMRB7.3.2. (2008). *DMRB 7.3.2.: Design Manual for Roads and Bridges, Data for Pavement Assessment—Annex 6 HD 29/2008: Ground-Penetrating Radar (GPR).* Birmingham, UK: Highway Agency.

Elliott, J., Walters, R., & Wright, T. (2016). The role of space-based observation in understanding and responding to active tectonics and earthquakes. *Nature communications, 7*(1), 1-16.

Fidanboylu, K. E. (2009). Fiber Optic Sensors and their applications. *5th Intenrational Advanced Technologies Symposium* . Karabuk: Fauniversity .

Filgueira, A., González-Jorge, H., Lagüela, S., Díaz-Vilariño, L., & Arias, P. (2017, 1). Quantifying the influence of rain in LiDAR performance. *Measurement, 95*, 143-148.

Garcia-Fernandez, M., Alvarez-Lopez, Y., & Las Heras, F. (2019). Autonomous airborne 3D SAR imaging system for subsurface sensing: UWB-GPR on board a UAV for landmine and IED detection. *Remote Sens., 11*(2357).

Garcia-Fernandez, M., Alvarez-Lopez, Y., & Las Heras, F. (2019). Autonomous airborne 3D SAR imaging system for subsurface sensing: UWB-GPR on board a UAV for landmine and IED detection. *Remote Sens, 11*(2357).

Gibb, S., La, H., Le, T., Nguyen, L., Schmid, R., & Pham, H. (2018). Nondestructive evaluation sensor fusion with autonomous robotic system for civil infrastructure inspection. *J. Field Robot., 35*, 988–1004.

Glisic, B. (2000). Fibre optic sensors and behaviour in concrete at early age . *PhD thesis*. Switzerland: Laboratory of Stress Analysis (IMAC) Swiss Federal Institute of Technology .

H.Hartog, A. (2017). An Introduction to Distributed Optical Fibre Sensors. In A. H.Hartog, *An Introduction to Distributed Optical Fibre Sensors* (pp. 115-128). Boca Raton, United States: CRC Press Taylor & Francis Group.

Héder, M. (2017). From NASA to EU: the evolution of the TRL scale in Public Sector Innovation. *The Innovation Journal, 22*(2), 1-23.

Howlader, M., Sattar, T., & Dudley, S. (2016). Development of a Wall Climbing Robotic Ground Penetrating Radar System for Inspection of Vertical Concrete Structures. *Int. J. Mech. Mechatron. Eng., 10*, 1382–1388.

This project has received funding from the European Union's Horizon 2020 research and innovation programme under grant agreement No 958171.

Hugener, C. M. (2014). *"Fit-for-purpose" infrastructure strategy. How companies can manage increasing IT demands.* Retrieved from https://www.strategyand.pwc.com/gx/en/insights/2014/fit-for-purpose-infrastructure-strategy/strategyand-fit-for-purpose-infrastructure-strategy.pdf

Hugenschmidt, J., Kalogeropoulos, A., Soldovieri, F., & Prisco, G. (2010). Processing strategies for high-resolution GPR concrete inspections. *NDT E Int., 43*, 334–342.

Hugenschmidt, J., Kalogeropoulos, A., Soldovieri, F., & Prisco, G. (2010). Processing strategies for high-resolution GPR concrete inspections. *NDT E Int., 43*, 334–342.

Hülsenbeck. (1926). *Germany Patent No. 489434.*

Instytut Maszyn Przepływowych im. Roberta Szewalskiego PAN. (2011, March). Specyfikacja Istotnych warunków zamówienia (SIWZ). *Dostawa czujników światłowodowych i przetworników* . Gdańsk , Polska .

ISO 11352. (2021). Water quality — Estimation of measurement uncertainty based on validation and quality control data. *Technical Committee of Physical, chemical and biochemical methods*, 26.

ISO 12718. (2019). Non-destructive testing - Eddy current testing - Vocabulary. *Technical Committee of Eddy current testing*, 39.

ISO 13372. (2012). Condition monitoring and diagnostics of machines - Vocabulary. *Technical Committee of Condition monitoring and diagnostics of machine systems*, 15.

ISO 13822. (2010). Bases for design of structures - Assessment of existing structures. *Technical Committee of Reliability of structures*.

ISO 17123. (2014). *Optics and optical instruments - Field procedures for testing geodetic and surveying instruments - Part 1: Theory.* Technical Committee of Geodetic and surveying instruments.

ISO 19159. (2014). *Geographic information - Calibration and validation of remote sensing imagery sensors and data - Part 1: Optical sensors.* Technical Committee of Geographic information.

ISO 19262. (2015). Photography — Archiving Systems — Vocabulary. *Technical Committee of Photography*, 44.

ISO 19345. (2019). Petroleum and natural gas industry - Pipeline transportation systems - Pipeline integrity management specification . *Technical Committee of Pipeline transportation systems*, 108.

ISO 1998. (1998). Petroleum industry — Terminology — Part 1: Raw materials and products. *Technical Committee of Petroleum and related products, fuels and lubricants from natural or synthetic sources*.

ISO 23907. (2019). Sharps injury protection - Requirements and test methods - Part 2: Reusable sharps containers. *Technical Committee of devices for administration of medicinal products and catheters*, 17.

ISO 27892. (2010). Vacuum technology - Turbomolecular pumps - Measurement of rapid shutdown torque. *Technical Committee of Vacuum technology*, 16.

ISO 3534. (2006). Statistics - Vocabulary and symbols - Part 1: General statistical terms and terms used in probability. *Applications of statistical methods*, 105.

ISO 7078. (2020). *Buildings and civil engineering works - Procedures for setting out, measurement and surveying - Vocabulary.* Technical Committee of Terminology and harmonization of languages.

This project has received funding from the European Union's Horizon 2020 research and innovation programme under grant agreement No 958171. © 2021

ISO 7078. (2020). Buildings and civil engineering works — Procedures for setting out, measurement and surveying — Vocabulary. *Technical Committee of Terminology and harmonization of languages*, 34.

ISO 9001:2015. (n.d.). *Quality management systems — Requirements*.

ISO 99. (2007). International vocabulary of metrology - Basic and general concepts and associated terms (VIM). *Technical Committee of Management Board*, 92.

J Carr, J. (1993). Sensors & Circuits: Sensors, Transducers, & Supporting Circuits for Electronic Instrumentation Measurement and Control. *Prentice Hall*.

J. Biliszczuk, W. B. (2009). System monitorowania mostu w Puławach. *Mosty 4* , pp. 12-17.

Jafarov, E., Parsekian, A., Schaefer, K., Liu, L., Chen, A., Panda, S., & Zhang, T. (2017). Estimating active layer thickness and volumetric water content from ground penetrating radar measurements in Barrow, Alaska. *Geoscience Data Journal*, *4(2)*, 72-79.

Jiang, H., Li, Q., Jiao, Q., Wang, X., & Wu, L. (2018, 9). Extraction of Wall Cracks on Earthquake-Damaged Buildings Based on TLS Point Clouds. *IEEE Journal of Selected Topics in Applied Earth Observations and Remote Sensing, 11*(9), 3088-3096.

Jo, H. C., Kim, J., Lee, K., Sohn, H.-G., & Lim, Y. M. (2018). Non-contact strain measurement for laterally loaded steel plate using LiDAR point cloud displacement data. *Sensors and Actuators A: Physical, 283*, 362-374.

Jol, H. M. (2009). *Ground Penetrating Radar: Theory and Applications.* Amsterdam, The Netherlands: Elsevier Science.

Jose Luis Santos, F. F. (2015). *Handbook of Optical Sensors.* Boca Raton: CRC Press Taylor & Francis Group.

Kang, D., Lee, H., Park, H., & Lee, I. (2007, 9). Computing Method for Estimating Strain and Stress of Steel Beams Using Terrestrial Laser Scanning and FEM. *Key Engineering Materials, 347*, 517-522. Retrieved from https://www.scientific.net/KEM.347.517

Kazi, A., Sausthanmath, A., Meena, S., Gurlahosur, S., & Kulkarni, U. (2020, 1). Detection of holes in 3D architectural models using shape classification based Bubblegum algorithm. *Procedia Computer Science, 167*, 1684-1695.

KEYENCE. (2021, 11 30). *Fibre optic sensors FS-N40 Series*. Retrieved from Digital Fibre optic Sensor: https://www.keyence.co.uk/products/sensor/fiber-optic/fs-n40/downloads/

Khatereh, V. (2012). Evaluation of commercially available remote sensors for highway bridge condition assessment. *ournal of Bridge Engineering*, 10.

Laefer, D. F., Gannon, J., & Deely, E. (2010). Reliability of crack detection methods for baseline condition assessments. *Journal of Infrastructure Systems, 16*(2), 129-137.

Laefer, D. F., Truong-Hong, L., Carr, H., & Singh, M. (2014). Crack detection limits in unit based masonry with terrestrial laser scanning. *Ndt & E International, 62*, 66-76.

Leimbach, G., & Löwy, H. (1910). *Germany Patent No. 237944.*

Leimbach, G., & Löwy, H. (1910). *Germany Patent No. 246836.*

Li, Q., & Cheng, X. (2018, 4). DAMAGE DETECTION FOR HISTORICAL ARCHITECTURES BASED ON TLS INTENSITY DATA. *The International Archives of the Photogrammetry, Remote Sensing and Spatial Information Sciences, XLII-3*(3), 915-921. Retrieved from https://doi.org/10.5194/isprs-archives-XLII-3-915-2018

This project has received funding from the European Union's Horizon 2020 research and innovation programme under grant agreement No 958171. © 2021

Linford, N., Linford, P., Martin, L., & Payne, A. (2010). Stepped frequency ground-penetrating radar survey with a multi-element array antenna: Results from field application on archaeological sites. *Archaeological Prospection*.

LINK, L., G, C., & J, C. (1981). AIRBORNE LASER SYSTEMS USE IN TERRAIN MAPPING.

Loew, A., Bell, W., Brocca, L., Bulgin, C., Burdanowitz, J., Calbet, X., & Verhoelst, T. (2017). Validation practices for satellite-based Earth observation data across communities. *Reviews of Geophysics, 55*(3), 779-817.

Łukasz Bednarski, R. S. (2015). Wybrane zagadnienia monitorowania konstrukcji. *XXX Jubileuszowe Ogólnopolskie Warsztaty Pracy Projektanta Konstrukcji* (pp. 28-30). Szczyrk : Politechnika Krakowska, Akademia Górniczo-Hutnicza.

mapwaredev. (2020, Jun 4). *Understanding Errors and Distortion in Remote Sensing*. Retrieved Jun 24, 2021, from https://mapware.ai/blog/understanding-errors-and-distortion-in-remote-sensing/

Mathew kautzman, B. J. (2018). Calibration and testing of distributed fiber optic sensors for detection of high energy radiation . *Journal of Directed Energy* .

ME91/16. (2016). *ME91/16: Methodologies for the Use of Ground-Penetrating Radar in Pavement Condition Surveys.* Brussels, Belgium: Belgian Road 445 Research Centre.

Measures, R. M. (2001). *Structural Monitoring with Fiber Optic Technology* . Ontario: Institute of Aerospace Studies .

Mei, Y. (2018, August). Error analysis for distributed fibre optic sensing tehcnology based on Brillouin scattering. USA: University of Cambridge, Department of Philosophy .

Narodowe Centurm Badań i Rozwoju, Politechnika Rzeszowska, . (2021, 12 08). *OptiDeck*. Retrieved from Inteligentny system pomostowy z kompozytów polimerowych do budowy i modernizacji drogowych obiektów mostowych: https://optideck.prz.edu.pl/

NASA's Earth Science Data Systems (ESDS). (n.d.). Retrieved Junio 24, 2021, from Standards and Practices: https://earthdata.nasa.gov/esdis/esco/standards-and-references#deprecated

NCHRP. (2017). *NCHRP Research Report 848. In Inspection Guidelines for Bridge Post-Tensioning and Stay Cable Systems Using NDE Methods.* Washington, DC, USA: TRB's National Cooperative Highway Research Program.

NERVE-SENSORS. (2021, 11 30). *NERVE SENSORS Epsilon Rebar strain sensor*. Retrieved 11 30, 2021, from NERVE SENSORS: www.nerve-sensors.com

Nolan, J. (n.d.). *Analysis of measuring and monitoring requirements in ISO 9001:2015*. Retrieved from 9001 Academy: https://advisera.com/9001academy/knowledgebase/analysis-of-measuring-and-monitoring-requirements-in-iso-90012015/

Pajewski, L., Fontul, S., & Solla, M. (2019). Ground-penetrating radar for the evaluation and monitoring of transport infrastructures. In *Innovation in Near-Surface Geophysics. Instrumentation, Application, and Data Processing Methods.* Amsterdam, The Netherlands: Elsevier.

Pajewski, L., Fontul, S., & Solla, M. (2019). Ground-penetrating radar for the evaluation and monitoring of transport infrastructures. In *Innovation in Near-Surface Geophysics. Instrumentation, Application, and Data Processing Methods.* Amsterdam, The Netherlands: Elsevier.

This project has received funding from the European Union's Horizon 2020 research and innovation programme under grant agreement No 958171.

Pajewski, L., Vrtunski, M., Bugarinovic, Ž., Ristic, A., Govedarica, M., Van der Wielen, A., . . . al., e. (2018). GPR system performance compliance according to COST Action TU1208 guidelines. *Ground Penetrating Radar, 1*, 104–122.

Park, H. (2020). Convolutional neural network-based safety evaluation method for structures with dynamic responses. *xpert Systems with Applications*, 14.

Park, H. S., Lee, H., Adeli, H., & Lee, I. (2007). A new approach for health monitoring of structures: terrestrial laser scanning. *Computer-Aided Civil and Infrastructure Engineering, 22*(1), 19-30.

Paulus, S., Eichert, T., Goldbach, H., & Kuhlmann, H. (2014, 2). Limits of Active Laser Triangulation as an Instrument for High Precision Plant Imaging. *Sensors 2014, Vol. 14, Pages 2489-2509, 14*(2), 2489-2509. Retrieved from https://www.mdpi.com/1424-8220/14/2/2489/htm

Persico, R., Provenzano, A., Trela, C., Sato, M., Takahashi, K., Arcone, S., . . . S. Ebihara, K. W. (2015). *Recommendations for the safety of people and instruments in ground-penetrating radar and near-surface geophysical prospecting.* European Association of Geoscientists and Engineers, EAGE Publications.

Plati, C., Loizos, A., & Gkyrtis, K. (2020). Assessment of modern roadways using non-destructive geophysical surveying techniques. *Surveys in Geophysics, 41*, 395-430.

Puente, I., González-Jorge, H., Riveiro, B., & Arias, P. (2013, 2). Accuracy verification of the Lynx Mobile Mapper system. *Optics & Laser Technology, 45*(1), 578-586.

Pultarova, T. (2018, December). *The Evolution Of Earth Observation*. Retrieved Oct 22, 2021, from The Evolution Of Earth Observation: https://www.ingenia.org.uk/ingenia/issue-77/the-evolution-of-earth-observation

Qiang, L. (2013). Research on Data Correlation in Structural Health Monitoring System. *Advanced Materials Research*, 11.

R. B. Figuera, C. J. (2021). *Development of Advanced Fibre Optic Sensors to Monitor the Durability of Concrete and Reinforced Concrete Structures - SolSensors.* Universidade do Minho, INESC-TEC and Engiprojects, Lda.

Retrieved from http://www.eurosdr.net/

Radoi, A. (2021). Static and Dynamic Structural Health. *Romanian Journal of Transport Infraestructure*, 16.

Rafał Sieńko, Ł. B. (2016). Monitorowanie obiektów budowlanych w sąsiedztwie budowy . *Geoinzynieria* , pp. 60-65.

Regtien, P. (20014). *Measurement science for engineers.* Elsevier.

RIEGL - RIEGL Laser Measurement Systems. (2021, 12 17). Retrieved from http://www.riegl.com/

Riveiro, B., DeJong, M., & Conde, B. (2016, 12). Automated processing of large point clouds for structural health monitoring of masonry arch bridges. *Automation in Construction, 72*, 258-268.

Riveiro, B., González-Jorge, H., Conde, B., & Puente, I. (2016, 4). Laser Scanning Technology: Fundamentals, Principles and Applications in Infrastructure. *Non-Destructive Techniques for the Evaluation of Structures and Infrastructure*, 53-80. Retrieved from https://www.taylorfrancis.com/chapters/edit/10.1201/b19024-12/laser-scanning-technology-fundamentals-principles-applications-infrastructure-riveiro-gonzález-jorge-conde-puente

This project has received funding from the European Union's Horizon 2020 research and innovation programme under grant agreement No 958171.

Romaniuk, R. S. (2001). *Miernictwo Światłowodowe Wydanie II Uzupełnione.* Warszawa: Instytut Systemów elektronicznych Politechnika Warszawska.

Rücker, W. (2006). Guideline for Structural Health Monitoring. *Federal Institute of Materials Research and Testing*, 63.

Saarenketo, T. (2012). *Recommendations for guidelines for the use of GPR in asphalt air voids content measurement. Mara Nord Project; Europeiska Unionen.* Brussels, Belgium.

Saarenketo, T., Maijala, P., & Leppäl¨, A. (2011). *Recommendations for Guidelines for the Use of GPR in Bridge Deck Surveys.* Publications of Mara Nord Project.

Samuel Vurpillot, D. I.-M. (1996, April 22). Smart Structures and Materials vol. 2719. *Bridge Monitoring by fiber optic deformation sensors: design, emplacemnet and results*. San Diego , USA: Society of Photo-Optical Instrumentation Engineers.

Sánchez, A., Riveiro, B., Puente, I., Conde, B., Mendes, N., Cabaleiro, M., & Lourenço, P. (2019). Parameterization of Structural Faults in Large Historical Constructions for Further Structural Modelling Thanks to Laser Scanning Technology and Computer Vision Algorithms. *RILEM Bookseries, 18*, 351-359. Retrieved from https://link.springer.com/chapter/10.1007/978-3-319-99441-3_37

Sanchez-Rodríguez, A., Riveiro, B., Conde, B., & Soilán, M. (2018, 3). Detection of structural faults in piers of masonry arch bridges through automated processing of laser scanning data. *Structural Control and Health Monitoring, 25*(3), e2126. Retrieved from https://onlinelibrary.wiley.com/doi/full/10.1002/stc.2126

SBRCURnet. (2015). *Kennispaper: Slimme constructies voor slim beheer en onderhoud – praktijkcases.* Delft, The Netherlands.

Semyon, G. (2018). *Evaluating Measurement Accuracy: A Practical Approach.* Springer.

Setyawan, E. (2019, August 12). *Intermap*. Retrieved Dec 15, 2021, from Satellite Imagery: Resolution vs. Accuracy: https://www.intermap.com/blog/satellite-imagery-resolution-vs.-accuracy

SHM SYSTEMS. (2021, 12 7). *SHM Systems Projects*. Retrieved 12 7, 2021, from SHM Systems: https://www.shmsystem.pl/projects/

SHRP. (2013). *SHRP 2- report S2-R06A-RR-1. In Nondestructive Testing to Identify Concrete Bridge Deck Deterioration.* Washington, DC, USA: Transportation Research Board.

Simi, A., Manacorda, G., Miniati, M., Bracciali, S., & Buonaccorsi, A. (2010). Underground asset mapping with dualfrequency dual-polarized GPR massive array. *Proceedings 13rd International Conference on Ground-Penetrating Radar*, (pp. 1001-1005). Lecce, Italy.

SMARTEC SA, Branko Glisic, Daniele Posenato, Daniele Inaudi. (2007, May). Integrity monitoring of old steel bridge using fiber optic distributed sensors based on Brillouin scattering. *Proceedings of SPIE.* The International Society for Optical Engineering. doi:10.1117/12.716055

Soilán, M., Riveiro, B., Sánchez-Rodríguez, A., & Arias, P. (2018, 2). Safety assessment on pedestrian crossing environments using MLS data. *Accident; analysis and prevention, 111*, 328-337. Retrieved from https://pubmed.ncbi.nlm.nih.gov/29272790/

Soilán, M., Sánchez-Rodríguez, A., Del Río-Barral, P., Perez-Collazo, C., Arias, P., & Riveiro, B. (2019, 9). Review of Laser Scanning Technologies and Their Applications

This project has received funding from the European Union's Horizon 2020 research and innovation programme under grant agreement No 958171. © 2021

for Road and Railway Infrastructure Monitoring. *Infrastructures 2019, Vol. 4, Page 58, 4*(4), 58. Retrieved from https://www.mdpi.com/2412-3811/4/4/58/htm

Solla, M., González-Jorge, H., Lorenzo, H., & Arias, P. (2013). Uncertainty evaluation of the 1 GHz GPR antenna for the estimation of concrete asphalt thickness. *Measurement, 46*, 3032–3040.

Solla, M., Lorenzo, H., & Pérez-Gracia, V. (2016). Ground Penetrating Radar: Fundamentals, Methodologies and Applications in Structures and Infrastructures. In B. Riveiro, & M. Solla, *Non-Destructive Techniques for the Evaluation of Structures and Infrastructures.* EH Leiden, The Netherlands: CRC Press/Balkema.

Solla, M., Lorenzo, H., & Pérez-Gracia, V. (2016). Ground Penetrating Radar: Fundamentals, Methodologies and Applications in Structures and Infrastructures. In B. Riveiro, & M. Solla, *Non-Destructive Techniques for the Evaluation of Structures and Infrastructures.* EH Leiden, The Netherlands: CRC Press/Balkema.

Solla, M., Pérez-Gracia, V., & Fontul, S. (2021). A review of GPR application on transport infrastructures: troubleshooting and best practices. *Remote Sensing, 13*(672).

Sterckx, S., Brown, I., Kääb, A., Krol, M., Morrow, R., Veefkind, P., & Thorne, P. (2020). Towards a European Cal/Val service for earth observation. *International Journal of Remote Sensing, 41*(12), 4496-4511.

Stryk, J., Matula, R., Pospíšil, K., Dérobert, X., Simonin, J., & Alani, A. (2017). Comparative measurements of ground penetrating radars used for road and bridge diagnostics in the Czech Republic and France. *Constr. Build. Mater., 154*, 1199–1206.

Surry, D. W. (n.d.).

Surry, D., & Stanfield, A. (2008). Performance technology. In J. M. Spector, *The Foundations of Instructional Technology.* M. K. Barbour & M. Orey.

T. H. Nguyen, T. V. (2014, February). Fluorescence based fibre optic pH sensor for the pH 10–13 range suitable for corrosion monitoring in concrete structures. *Sensors and Actuators B Chemical 191*, pp. 498-507.

Technology Readiness Level (TRL). (n.d.). Retrieved from HORIZON 2020 – WORK PROGRAMME 2014-2015.

Tomasz Siwowski, R. S. (2017, May). System monitorowania mostów kompozytowych z wykorzystaniem światłowodowych czujników odkształceń. *PROJECT COM-BRIDGE, DEMONSTRATOR+*, (pp. 50-53).

Tzinis, I. (2012). *Technology Readiness Level*. (NASA) Retrieved from National Aeronautics and Space Administration (NASA): https://www.nasa.gov/directorates/heo/scan/engineering/technology/technology_readiness_level

Udd, E. (2006). *Fiber Optic Sensors And Introduction for Engineers and Scientists.* New Jersey : John Wiley & Sons, Inc. .

USGS. (n.d.). Lidar Base Specification. Retrieved from moz-extension://d5b2584d-3b96-42e7-ab74-19371b183693/enhanced-reader.html?openApp&pdf=https%3A%2F%2Fpubs.usgs.gov%2Ftm%2F11b4%2Fpdf%2Ftm11-B4.pdf

W. Barcik, R. S. (2012). System monitorowania konstrukcji Mostu Rędzińskiego we Wrocławiu. *Mosty 2*, pp. 56-62.

This project has received funding from the European Union's Horizon 2020 research and innovation programme under grant agreement No 958171.

Wai-Lok Lai, W., Dérobert, X., & Annan, P. (2018). A Review of Ground Penetrating Radar Application in Civil Engineering: A 30-Year Journey from Locating and Testing to Imaging and Diagnosis. *NDT E Int.*, *96*, 58–78.

Wu, H., Ao, X., Chen, Z., Liu, C., Xu, Z., & Yu, P. (2019). Concrete spalling detection for metro tunnel from point cloud based on roughness descriptor. *Journal of Sensors, 2019*.

Wu, K., Rodriguez, G., Zajc, M., Jacquemin, E., Clément, M., De Coster, A., & Lambot, S. (2019). A new drone-borne GPR for soil moisture mapping. *Remote Sens. Environ., 235*(111456).

Xie, F., Lai, W., & Dérobert, X. (2021). GPR uncertainty modelling and analysis of object depth based on constrained least squares. *Measurement*(109799).

Xie, X., Chen, Y., & Zhou, B. (2016). Data processing of backfill grouting detected by GPR in shield tunnel and research on equipment of GPR antenna. *Proceedings of the 16th International Conference on Ground Penetrating Radar.* Hong Kong, China.

Yang, W. (2006). A review of remote sensing data formats for earth system observations. *Earth Science Satellite Remote Sensing*, 120-145.

Yangí, L., Yang, G., Liu, Z., Chang, Y., Jiang, B., Awad, Y., & Xiao, J. (2018). Wall-climbing robot for visual and GPR inspection. *Proceedings of the 2018 13th IEEE Conference on Industrial Electronics and Applications (ICIEA)*, (pp. 1004–1009). Wuhan, China.

Yoon, J., Sagong, M., Lee, J., & Lee, K. (2009, 3). Feature extraction of a concrete tunnel liner from 3D laser scanning data. *NDT & E International*, *42*(2), 97-105.

Zan, Y., Su, G., & Li, Z. (2016). A Train-mounted GPR System for Fast and Efficient Monitoring of Tunnel Health Conditions. *Proceedings of the 16th International Conference on Ground Penetrating Radar.* Hong Kong, China.

Zhou, Y., Wang, S., Mei, X., Yin, W., Lin, C., Hu, Q., & Mao, Q. (2017). Railway tunnel clearance inspection method based on 3D point cloud from mobile laser scanning. *Sensors*, *17*(9).

Zotti, M., & La Mantia, C. (2014). "Open data from earth observation: From big data to linked open data, through INSPIRE". *Journal of e-Learning and Knowledge Society, 10*(2).

This project has received funding from the European Union's Horizon 2020 research and innovation programme under grant agreement No 958171.

APPENDIX A16. Surface measurements

16.1 Goal(s)

16.1.1 Main objective

Bridge infrastructure monitoring technologies are crucial for predicting the effects of the damages and preventing potential accidents. The advantages of the multi-scale data collection cannot be disregarded for future infrastructure maintenance purposes, especially the possibility of real-time data storage, remote control of facilities from different locations, and enabling and sharing research results on a large scale. However, multi-scale data collection requires a specific system configuration and operational knowledge of a professional level. In addition, it requires significant financial expenses on the equipment, power supplies, training, and maintenance over time and under different environmental conditions.

Surface measurements can be used on concrete samples or concrete structures directly on the facility. Mostly used techniques are Schmidt hammer test, Windsor probe test or pull-out test, which enable to identify of important quality characteristics of different structural elements of bridges such as compressive strength and hardness of selected elements. If performed regularly, prevent the degradation processes to expand and accelerate and thus allow the implementation of appropriate preventive steps.

16.2 Description

16.2.1 Functioning mode

- *Schmidt hammer test/Rebound test* – a hammer is pushed against a concrete sample and its body is allowed to move away from the concrete until the handle connects the hammer mass to the plunger. The plunger is placed perpendicularly to the surface of concrete and the body is slowly pushed towards the concrete. This movement extends the spring which holds the mass to the body. In the maximum extension of the spring – the latch releases, mass is pushed by the spring. Then the mass hits the shoulder of the plunger and rebounds. Slide indicator goes with hammer mass and stops at the maximum distance after rebounding. The plunger is locked, and the rebound number can be read from the scale of the tool.
- *Windsor probe test/Penetration test* – usually the system consists of a digital measuring unit with a memory for data storage, probes and charges; the suitable probe is loaded into the driver, the driver is placed on the actuating template and fired, probe is located at the corners of a fixed triangle. By the electronic device, there are few parameters selected such as type of concrete, units, aggregate hardness. Every three individual tests are averaged automatically, and the results can be read from the screen.

This project has received funding from the European Union's Horizon 2020 research and innovation programme under grant agreement No 958171.

- *Pull-out test* – before the measurement a metal anchor is concreted in the inspected area and then extracted to estimate the resistance in the tested place; the equipment is then pulled to the designated stress load; The anchor is concreted in the structure and expanded in a specially cut hole. During the measurement, the anchors are pulled out of the concrete by a hydraulic actuator, which presses against the concrete surface through a stop ring. Two functioning modes can be highlighted:
  - *LOK-test – when the anchors are pre-concreted during concreting the structure, used for new constructions.*
  - *CAPO-test – when the anchors are placed into the drilled measurement holes in existing constructions.*

16.2.2 Types

- *Schmidt Hammer test* – from the point of view of the measured sample Schmidt hammers can be divided into two categories:
  - *hammer type N – used in case of walls and other structural elements with thickness more than 10 mm,*
  - *hammer type L – used in case of materials with lower thickness, which are subjected to damage due to brittleness; there are other impact parameters than in N-type.*

Figure 16.1 – Schmidt Hammer

From the point of view of advancement of the equipment and measured range of resistance to pressure there are several different models of Schmidt hammers, depending on the manufacturer, however there are ones suitable for almost full range of the spectrum, or specifically for one range with following subdivision:

- *for fresh, low-strength concrete – 1-5 MPa, 5-10 MPa.*
- *normal concrete – 10-30 MPa, 30-70 MPa.*
- *high-strength concrete – 70 – 100 MPa.*

Modern advanced Schmidt hammers offer web-based functionalities and mobile applications, which enables to share the results quickly, also offers automatic angle correction to eliminates the errors during operation (Screening Eagle) (H., 2009) (Szilágyi, Borosnyói i Zsigovics, 2011).

This project has received funding from the European Union's Horizon 2020 research and innovation programme under grant agreement No 958171.

- *Windsor probe test* – depending on the application there are two types of equipment used:
  - *Windsor system with a probe for lightweight, low density concrete.*
  - *Windsor system with a probe for standard mix designs*

From the point of view of probe material used there are two common ones:

  - *silver probes for high performance concrete with strength up to 110 MPa.*
  - *golden probes for concretes with strength below 110 MPa.*

Probes are consumable and can be used one time only.

There are also two power settings available usually:

  - *low power*
  - *standard power*

- *Pull-out test* – usually the system consists of a hydraulic jack, pressure gauge for precise readings over a wide load range, bearing ring and pull-out inserts – contained in a carrying case. There are different adapters for different fixings and tests available. The load can be applied mechanically or hydraulically. Hydraulic systems are used for high loads (H., 2009).

16.2.3 Process/event to be detected or monitored

- *Schmidt Hammer test* – change of the hardness of the surface in different intervals of time, due to changes in surface hardness, surface of the concrete can be mapped, and corrosion can be detected.
- *Windsor probe test* – change of concrete compressive strength of a structure by driving a probe into the concrete with a known amount of force; monitoring of the strength for rehabilitation as concrete ages.
- *Pull-out test* – change of compressive strength in the structure and monitoring of potential strength and durability problems.

16.2.4 Physical quantity to be measured (e.g. actions, displacements, deformations, dynamic structural properties, material properties including mechanical, electrical and chemical properties, relative displacements of the two sides of a crack, etc.).

- *Schmidt Hammer test – average* rebound value R; compressive strength; hardness value.
- *Windsor probe test* – compressive strength; hardness value.
- *Pull-out test* - force [kN] required to pull a shaped steel rod out of the hardened concrete.

16.2.5 Induced damage to the structure during the measurement

- *Schmidt Hammer test* – during on-site measurements usually there are no damages to the structure or slight scratches, under laboratory conditions, it is necessary to prepare the samples by drilling holes in inspected areas.

This project has received funding from the European Union's Horizon 2020 research and innovation programme under grant agreement No 958171.

- *Windsor probe test* – during on-site measurements after the penetration at least 8 mm holes are present in the structure, under laboratory conditions it is necessary to prepare the samples by drilling holes in the inspected area.
- *Pull-out test* – after the penetration leaves at least 8 mm holes in the structure, involves breaking the concrete, under laboratory conditions it is necessary to prepare the samples by drilling holes in the inspected area.

16.2.6 General characteristics

16.2.6.1 Measurement type (static or dynamic, local or global, short-term or continuous, etc.)

- *Schmidt Hammer test* – static and local measurement; short-term.
- *Windsor probe test* – static and local measurement; short-term.
- *Pull-out test* – static and local measurement; short-term.

16.2.6.2 Measurement range

- *Schmidt Hammer test:* 10 – 70 MPa for resistance to pressure.
- *Windsor probe test:* 10 – 70 MPa depending on the mixture of concrete.
- *Pull-out test: 5 – 130 MPa; load range: 0 – 255 kN.*

16.2.6.3 Measurement accuracy

- Schmidt Hammer test: 2.2 +/– 0.1 J for impact energy.
- *Windsor probe test:* compressive strength above 3.62 MPa can be detected.
- *Pull-out test: load is applied with 0.2 – 0.5 kN accuracy.*

16.3 Background (evolution through the years)

The Schmidt hammer for concrete testing was developed by Ernst O. Schmidt and introduced to the market in early 1950. It is the most widely used measuring device for quick, non-destructive assessment of the condition of a concrete structure. Its use expanded over the years of testing. In 1938 there were first publications about in-place testing of concrete by pull-out tests in the Soviet Union. In 1970 pull-out test was widespread and used as a standard practice. The Windsor Probe test was developed in 1960 between the New York Port Authority and the Windsor Machine Company (Grimmelsman, 1999) (Karaś, O badaniach betonu mostów metodami „pull-off" i „pull-out", 2004) (Ł. Drobiec, 2010).

This project has received funding from the European Union's Horizon 2020 research and innovation programme under grant agreement No 958171. © 2021

16.4 Performance

16.4.1 General points of attention and requirements

16.4.1.1 Design criteria and requirements for the design of the survey

- *Schmidt Hammer test* – rough surfaces do not give reliable results and should be avoided – the surface of the measured area (or sample) should be smooth; If the test is carried out on the sample any movement caused by the impact of the hammer will result in a reduction in the rebound number. In such cases, the member has to be rigidly held. The rebound numbers are lower for well-cured air-dried samples than for the same ones tested after being soaked in water and tested in the saturated surface dried conditions.

- *Windsor probe test* – in order to measure correctly and to avoid damaging the surface on which the measurement is carried out, it is recommended to use special frames to relieve the structure from the load; to obtain accurate results, it is necessary to know the hardness of the aggregate – in situations in which there is no historical data about the mixture of concrete used there are procedures to obtain the hardness value such as performing Mohs' test; In order to get a good reading,

  - maximum spacing between probes = 175 mm
  - minimum spacing between probes = 100 mm
  - minimum spacing between concrete and the edge of a concrete surface = 100 mm

- *Pull-out test* - The test should be preceded by the location of the reinforcement, the removal of corroded concrete of corroded concrete and the smoothening of the surface. The axis of the anchor must be at least 100 mm from the edges and corners of the element and 50 mm from the reinforcement inserts. On a single element, tests are performed in at least 5 measurement places.

16.4.1.2 Procedures for defining layout of the survey

- *Schmidt Hammer test*
- *Windsor probe test*
- *Pull-out test*

For all the methods above the layout out of the survey should be considered with use of available standards and the availability to reach specific parts of the construction by the operator.

16.4.1.3 Design constraints (e.g. related to the measurement principles of the monitoring technologies)

- *Pull-out test* - The method is not applicable to concretes on lightweight aggregates and to concretes with aggregate grain size not exceeding 38 mm.

This project has received funding from the European Union's Horizon 2020 research and innovation programme under grant agreement No 958171.

16.4.1.4 Sensibility of measurements to environmental conditions

In case of Schmidt hammer, Windsor Probe and pull-out test there are no major environmental conditions that will directly influence the measurements, preferably tests should be performed at temperatures between 10°C and 50°C . However it should be noted that the equipment itself can be sensitive to environmental conditions and should not be subjected to water, very high temperature and immersed in water,

16.4.2 Preparation

16.4.2.1 Procedures for calibration, initialisation, and post-installation verification

- *Schmidt Hammer test* – hammer should be calibrated using a calibration test anvil supplied by the manufacturer. Twelve readings should be taken, eliminating the highest and lowest, and taking the average of the ten remaining.
- *Windsor probe test* – according with the manufacturer manual, usually serviced and calibrated on annual basis
- *Pull-out test* – calibration should be done at least once a year; recalibration should be made whenever there is a doubt on accuracy of the measurement. Procedure of calibration is given in ASTM C 900.

16.4.2.2 Procedures for estimating the component of measurement uncertainty resulting from calibration of the data acquisition system (calibration uncertainty)

Not applicable.

16.4.2.3 Requirements for data acquisition depending on measured physical quantity (e.g. based on the variation rate)

Not applicable.

16.4.3 Performance

16.4.3.1 Requirements and recommendations for maintenance during operation (in case of continuous maintenance)

Not applicable for continuous measurements. Rebound hammers require periodic servicing and verification as well as Windsor probe equipment and machine for pull-out test.

16.4.4 Reporting

- *Schmidt Hammer test* – example of the report has been shown below; also reports can be automatically created by phone applications in advanced hammers technology.

REPORT FROM REBOUND TEST	**Operator:….**

This project has received funding from the European Union's Horizon 2020 research and innovation programme under grant agreement No 958171.

Date of the inspection: .... Model of the hammer and type: .... Object/Structure identification: .... Element of the construction: .... Age of concrete:													**Standard rebound average value on steel anvil:** …………………… **(80+/-2)**
	Degree	**1**	**2**	**3**	**4**	**5**	**6**	**7**	**8**	**9**	**10**	**Average**	**Standard deviation**
1	0º												
2	0º												
3	0º												
4	0º												

Table 16-1 – Report after Schmidt hammer testing

- *Windsor probe test* – data from the tests are stored in the memory and can be transferred on the computer.

REPORT FROM WINDSOR PROBE TEST	**Operator:….**
Date of the inspection:...................... Model of the system and type of probe :............... Object/Structure identification:……………… Element of the construction:……………………… Age of concrete:........................	

This project has received funding from the European Union's Horizon 2020 research and innovation programme under grant agreement No 958171.

Type of concrete...........						
	Tested Area	**Aggregate**	**Mohs Number**	**Cure days**	**Probe Certification Number**	**Compressive Strength**
1						
2						
3						

Table 16-2 – Report after Windsor Probe test.

- *Pull-out test* - example of the report has been shown below:

REPORT FROM PULL-OUT TEST		**Operator:….**
Date of the inspection:...................... Model of the device:............... Object/Structure identification:……………… Element of the construction:……………………… Age of concrete:........................		
Concrete type and identification of the sample	Pull out result	**Strength**

This project has received funding from the European Union's Horizon 2020 research and innovation programme under grant agreement No 958171. © 2021

Table 16-3 – Report for pull-out test.

16.4.5 Lifespan of the technology

- *Schmidt Hammer test* – does not offer continuous measurement.
- *Windsor probe test* – does not offer continuous measurement.
- *Pull-out test* – does not offer continuous measurement.

16.5 Interpretation and validation of results

16.5.1 Expected output (Format, e.g. numbers in a .txt file)

- *Schmidt Hammer test* – list of numbers with rebound values; in advanced Schmidt hammers the results can be storage, evaluated in phone application (e.g. Schmidt App) and exported as txt, Excel file etc..
- *Windsor probe test* – list of numbers with compressive strength values.
- *Pull-out test* – force value needed to pull out the steel anchor for selected tested areas.

16.5.2 Interpretation (e.g. each number of the file symbolizes the acceleration of a degree of freedom in the bridge)

- *Schmidt Hammer test* – for surfaces that are subjected to damage processes such as corrosion and carbonation the rebound number will be significantly higher than for the non-affected surfaces. For estimation of the compressive strength correlation curves are used, usually added by manufacturer to the manual which show the relationship between the rebound number and compressive strength. However, in advance equipment data are evaluated automatically. Example of the correlation curves is shown below:

This project has received funding from the European Union's Horizon 2020 research and innovation programme under grant agreement No 958171. © 2021

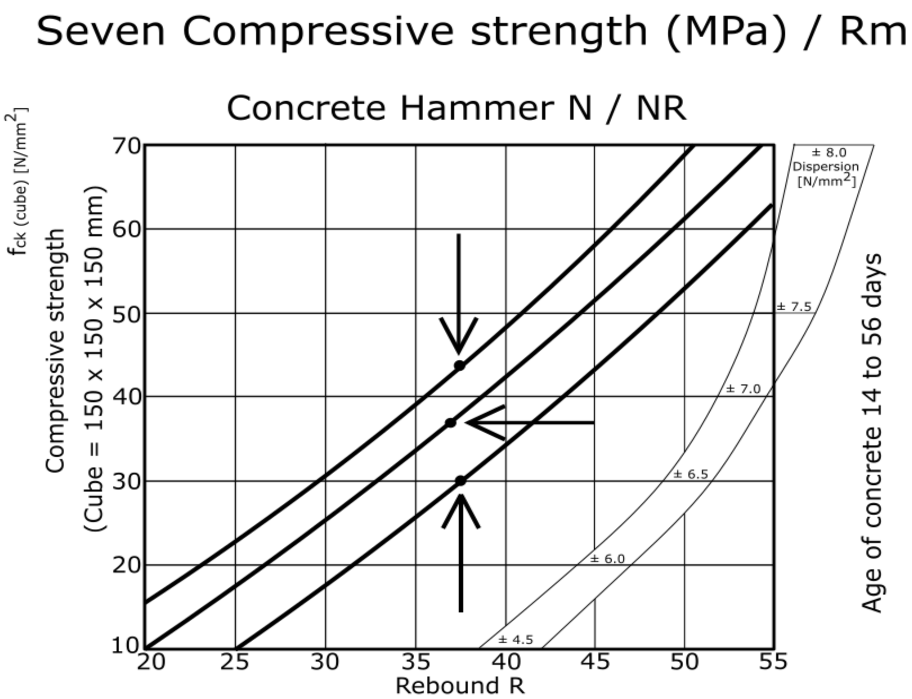

Figure 16.2 – Correlation curves for Schmidt hammer

- *Windsor probe test* – based on the surface hardness of a concrete element – hardness is used to estimate concrete strength. The penetration resistance of concrete is computed by measuring the exposed length of probes driven into concrete. In order to estimate concrete strength, it is necessary to establish a relationship between penetration resistance and concrete strength. Relationship must be established for a given test apparatus, using similar concrete materials and mixture proportions as in the structure. Statistical methods can be used for developing and using the strength relationship.

This project has received funding from the European Union's Horizon 2020 research and innovation programme under grant agreement No 958171.

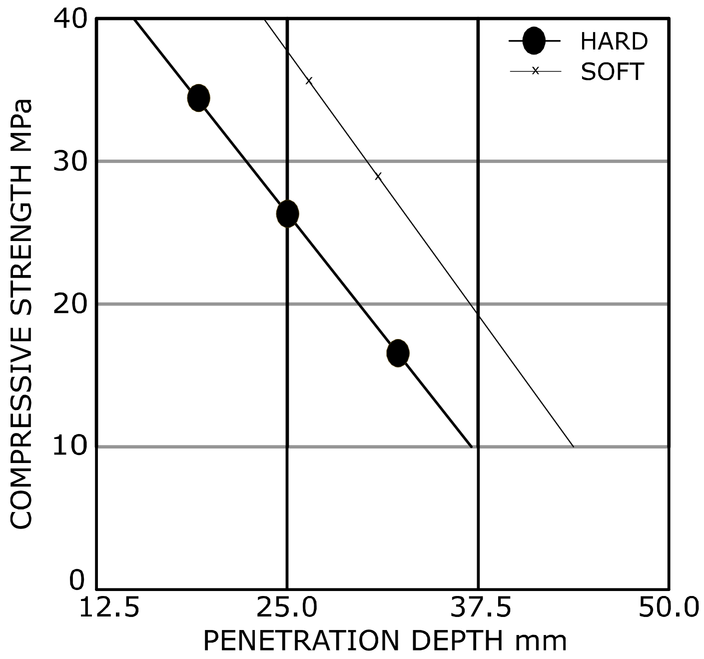

Figure 16.3 – Correlation curves for Windsor probe test

- *Pull-out test* – value of force generated by the test is then used to determine the strength parameters of concrete through calibration curves or correlation of the test with other non-destructive testing methods. The individual pull-out test results are converted to equivalent values of compressive strength using the previously established correlation. The mean and standard deviation of the set of pull-out test results are determined.

16.5.3 Validation

16.5.3.1 Specific methods used for validation of results depending on the technique

Evaluation of the rebound value include taking average of 8-10 rebound numbers, eliminating values which are too high or too low and the compressive strength is read off with use of the selected conversion curve, usually supplied by the manufacturer with a tool. Validation of the conversion curves is performed on the standard concrete made from Portland or bleat furnace slag cement with sand gravel with smooth surface at age in days: 14-56.

16.5.3.2 Quantification of the error

Standard deviation can be calculated.

16.5.3.3 Quantitative or qualitative evaluation

Qualitative evaluation of surface hardness and compressive strength.

This project has received funding from the European Union's Horizon 2020 research and innovation programme under grant agreement No 958171.

16.5.4 Detection accuracy

- *Schmidt Hammer test* – only a test used for estimating the strength of concrete in structure, detection depends on the type of hammer used – there are basic hammers with analogue screens or automatic ones which show greater accuracy by eliminating the error of reading by the operator; reliable in determining whether the exploitation of the structure would still be safe, but it is not used for determination if it is not safe already. In this case additional surveys should be carried out with other techniques.
- *Windsor probe test* – depends on the type of system configuration used, however useful in assessing the quality and relative strengths of concrete; equally accurate at obtained results on horizontal or vertical surfaces if the probe is at right angles to the tested surface.
- *Pull-out test* - method can be more than twice as accurate in comparison with non-destructive surveys.

16.6 Advantages

- *Schmidt Hammer test:*
  - rapid testing,
  - inexpensive equipment.
- *Windsor probe test:*
  - can be used as substitute of core tests,
  - light, standard and high-weight concrete strength can be tested,
  - high-precision,
  - fast and economical,
  - no accidental discharge,
  - not complicated maintenance.
- *Pull-out test:*
  - good performance on new and old structures,
  - easy to install.

16.7 Disadvantages

- *Schmidt Hammer test:*
  - estimation of the values only.
  - can generate misleading results.
- *Windsor probe test:*
  - leaves holes in concrete, where the probe penetrated,
  - damaged area has to be repaired usually,
  - can cause minor cracking.

This project has received funding from the European Union's Horizon 2020 research and innovation programme under grant agreement No 958171.

- *Pull-out test:*
  - destructive for the structure
  - does not measure the interior strength of the concrete.
  - large number of tests needed in different parts of the construction for accurate results.

16.8 Possibility of automatising the measurements

Measurement with Schmidt Hammer and Windsor Probe are automatic, however it is not possible to eliminate the presence of the operator to perform the test for now.

16.9 Barriers

No major barriers.

16.10 Existing standards

- *Schmidt Hammer test:*
  - EN 12 504-2, ENV 206 Europe
  - BS 1881: Part 202: 1986 - Recommendations for Surface Hardness Testing by Rebound Hammer
  - ASTM C805-97 STM for Rebound Number of Hardened Concrete, USA
  - ISO/DIS 8045 Concrete, hardened - Determination of rebound number using rebound hammer
  - BS 4408: pt. 4, BS 1881: part 202, Non-destructive methods of test for concrete - surface hardness methods British Standards Institution, Great Britain
  - DIN 1048, part 2 Germany
  - NFP 18-417, France
  - B 15-225, Belgium
  - JGJ/T 23-2011, China
- *Windsor probe test:*
  - ASTM C 803-82, STM for Penetration Resistance of Hardened Concrete
  - BS 4408: pt. 4, Non-destructive methods of test for concrete - surface hardness methods British Standards Institution, London
  - AS 1012.18-1996. Method of Testing Concrete - Determination of setting time of fresh concrete, mortar and grout by penetration resistance
  - ACI 228.1R-03: In-Place Methods to Estimate Concrete Strength
- *Pull-out test:*
  - ASTM C900-94 STM for Pullout Strength of Hardened Concrete
  - ISO/DIS 8046 Concrete, hardened - Determination of pull-out strength

This project has received funding from the European Union’s Horizon 2020 research and innovation programme under grant agreement No 958171.

16.11 Applicability

16.11.1 Relevant knowledge fields

- Civil engineering:
    - formwork removal,
    - rock testing,
    - profiles testing,
    - railways,
    - commercial buildings,
    - airports.

16.11.2 Performance Indicators

- deformation,
- rupture,
- loss of section,
- cracks,
- holes,
- displacement,
- reinforcement bar failure/bending,
- tensioning force deficiency,
- debonding.

16.11.3 Type of structure

- concrete bridges,
- masonry bridges,
- tunnels.

16.11.4 Spatial scales addressed (whole structure vs specific asset elements)

Surface measurements are not designed in a way for specific assets, however it is possible to study various element of a bridges and other facilities. Methods are not suitable for drawing conclusions about whole structure. Most commonly used for parts of bridge like: beams, slabs, columns, piers, abutment walls.

16.11.5 Materials

- concrete,
- steel,
- composites,
- rock,

This project has received funding from the European Union's Horizon 2020 research and innovation programme under grant agreement No 958171.

- paper,
- mortar,
- sand.

16.12 Available knowledge

16.12.1 Reference projects

No reference projects.

16.12.2 Other

Manufacturers (Schmidt hammer):

Gilson Company, Inc.

Humboldt Construction Materials Testing Equipment

NDT JAMES INSTRUMENTS - Windsor Probe System

16.13 Bibliography

Flaga, K. (1970). Wpływ wielkości elementów próbnych na ocenę wytrzymałości betonu metodą sklerometryczną. *Inżynieria i budownictwo*, pp. 395-399.

Grimmelsman, A. E. (1999, July). The role of NDE in bridge health monitoring in Nondestructive Evaluation of Bridges and Highways III. *Proceedings of SPIE*, pp. 2-15.

H., W. (2009). Advanced NDT Methods for Quality Assurance of concrete Structures. *NDTCE'09, Non-Destructive Testing in Civil Engineering* . Nantes.

Hannachi S., G. M. (2012). Application of the Combined Method for Evaluating the Compressive Strength of Concrete on Site. *Open Journal of Civil Engineering*, pp. 16-21.

J. K. Kim, C. Y. (2009). Effect of carbona-tion on the rebound number and compressive strength of concrete. *Cement and Concrete Composites* , pp. 139-144.

Karaś, S. (2004). O badaniach betonu mostów metodami „pull-off" i „pull-out". *Inżynieria i Budownictwo, nr 7*, pp. 359-369.

Karaś, S. (2011). Ocena wytrzymałości betonu według normy PN-EN 13791. *Drogownictwo, nr 2*, pp. 42-48.

Ł. Drobiec, R. J. (2010). *Diagnostyka konstrukcji żelbetowych. Metodologia, badania polowe, badania laboratoryjne betonu i stali. Tom 1*. Warszawa: Wydawnictwo Naukowe PWN.

Runkiewicz, L. (1983). Ocena wytrzymałości betonu w konstrukcji za pomocą sklerometrów Schmidta. ITB, Warszawa. *Instytut Techniki Budowlanej Warszawa*.

Runkiewicz, L. (1991). Wpływ wybranych czynników na wyniki badań sklerometrycznych betonu. *Prace Naukowe Instytutu Techniki Budowlanej, Warszawa*.

Samarin A., D. R. (1984). Determination of in situ concrete strength: rapidly and confidently by nondestructive testing. *ACI SP-82*.

This project has received funding from the European Union's Horizon 2020 research and innovation programme under grant agreement No 958171. © 2021

Screening Eagle. (n.d.). *The Original Schmidt Hammer.* Retrieved from https://www.screeningeagle.com/en/product-family/schmidt-rebound-hammers

Szilágyi, K., Borosnyói, A., & Zsigovics. (2011). Rebound surface hardness of concrete: introduction of an empirical consti-tutive model. *Construction and Building Materials*, pp. 2480–2487.

This project has received funding from the European Union's Horizon 2020 research and innovation programme under grant agreement No 958171.

APPENDIX A17. Water penetration test/ Permeability test

17.1 Goal(s)

17.1.1 Main objective

The main objective of the water penetration test in bridges or tunnels diagnostics is the determination of resistance or durability of concrete extracted from elements of structure exposed to the water flow. The water permeability tests are the best for evaluating concrete durability under hydrostatic pressure and as a good indicator of its quality. The application in durability assessment of concrete elements of the existing structures is growing. The permeability test should be considered as an essential one to evaluate the case whereby concrete is subjected to hydrostatic pressure.

17.2 Description

17.2.1 Functioning mode

Pressurized water acts on the surface of the hardened concrete at a constant pressure of 500 (± 50) KPa, usually for a period of 72 hours. After the test, the sample should be immediately split in the plane of water penetration and the contour of the wetted area should be marked. The apparatus consists of a robust steel frame with clamping system, incorporating the hydraulic circuit, valves, gauge to check the water pressure and measuring transparent burettes mounted on top of the apparatus. The clamping system is adjusted for cube or prismatic specimens up to 200 mm side and cylinders up to 300 mm height.

After the pressure has been applied, the specimen should be split in half, perpendicularly to the face on which the water pressure was applied. When splitting the specimen, and during the examination, the face of specimen exposed to the water pressure should be placed on the bottom. As soon as the split face has dried to such an extent that the water penetration front can be clearly seen, the water front on the specimen can be marked (Gwizdak, 2015) (A. M. Neville, Properties of Concrete, 2012) (I. L. Tyler, 1961).

This project has received funding from the European Union's Horizon 2020 research and innovation programme under grant agreement No 958171.

Figure 17.1 – Pressured permeability tester

17.2.2 Types

Water penetration test can be distinguished into two types:

- performed on the samples in laboratory – in a test chamber with water pipe ensuring continuous flow and homogeneous water coverage and air pressure applied,
- performed on the built walls in the construction site conditions – in a test chamber with a box format and internal dimensions 160 mm x 340 m and no air pressure is used.

17.2.3 Process/event to be detected or monitored

Depth of the penetration of water after observation of the fracture structure after splitting the sample. The wet area is darker.

17.2.4 Physical quantity to be measured (e.g. actions, displacements, deformations, dynamic structural properties, material properties including mechanical, electrical and chemical properties, relative displacements of the two sides of a crack, etc.).

Measurement of the maximum range of water penetration from the surface. Maximum average depth for examined samples (Z. Kledyński, 2005).

17.2.5 Induced damage to the structure during the measurement

For diagnostics of existing civil engineering structures it is necessary to collect samples from the structure in a borehole form, therefore the method is destructive.

This project has received funding from the European Union's Horizon 2020 research and innovation programme under grant agreement No 958171.

17.2.6 General characteristics

17.2.6.1 Measurement type (static or dynamic, local or global, short-term or continuous, etc.)

Uncomplicated method of determination of the resistance to water penetration suitable for concrete structures such as bridges and tunnels and in general concrete elements. Measurement is static, local and short term – up to 72 hours.

17.2.6.2 Measurement range

Not applicable.

17.2.6.3 Measurement accuracy

Penetration from the surface should be measured with 1 mm accuracy (PN-EN 206+A2:2021-08 , 2021).

17.3 Background (evolution through the years)

Historically tests on water penetration have been performed on windows by exposing them to rain and additional pressure.

The ASTM E1105 (Standard Test Method for Field Determination of Water Penetration of Installed Exterior Windows, Skylights, Doors, and Curtain Walls, by Uniform or Cyclic Static Air Pressure Difference) test procedure was specifically written for field testing and as a component to the quality assurance and commissioning process of a building enclosure. ASTM E1105 uses a calibrated spray rack to simulate rain from the outside and a negative pressure chamber inside to simulate wind. The procedure describes how to test with either a constant or a fluctuating interior pressure.

Another standard – ASTM E331 has been established in 1967. Further development consisted of transition from manual to automatic methods of testing. ASTM E514 M-20 Standard Test Method for Water Penetration and Leakage Through Masonry subjected to wind-driven rain. Has been introduced in 1990. US Army published in 1992 a procedure for determining the permeability of concrete subjected to water pressure (1,38 MPa) with a code - COE CRD-C 48-92 as a Handbook for Concrete and Cement Standard Test Method for water permeability of Concrete. (G. J. R. Von der Meulen, 1969). (ACI 201.2R-1992, 1994) (Young, 1988) (Ritchie, 1974).

The ASTM C1601-10 Standard Test Method for Field Determination of Water Penetration of Masonry Wall Surfaces has been introduced in 2010 to determine criteria for water penetration resistance of masonry wall.

This project has received funding from the European Union's Horizon 2020 research and innovation programme under grant agreement No 958171.

17.4 Performance

17.4.1 General points of attention and requirements

17.4.1.1 Design criteria and requirements for the design of the survey

Water pressure must not be exerted on the obliterated, smoothed surface of the extracted concrete sample. When fresh concrete sample is tested it is recommended that the pressure should be applied on the surface, which was in contact with the form.

For the samples extracted from the existing structures the area of the sample to be subjected to water pressure must be cleaned with a steel brush. The depth of water penetration inside the sample decreases with the age of the samples (EN 12390-8:2019).

17.4.1.2 Procedures for defining layout of the survey

No specific guidelines.

17.4.1.3 Design constraints (e.g. related to the measurement principles of the monitoring technologies)

In order to extract samples there should be safe access to the part of the existing concrete structure to avoid any risk. The sample at the time of testing must be at least 28 days old in case if fresh concrete is being examined.

17.4.1.4 Sensibility of measurements to environmental conditions.

When the surface of the material is obscured due to atmospheric soiling or biological growth and presence of hygroscopic salts within the interior the permeability of concrete will be affected. Formation of a weathering crust from mineralogical changes on the exposed surface will affect water permeability measurements.

17.4.2 Preparation

17.4.2.1 Procedures for calibration, initialisation, and post-installation verification

Cubic, cylindrical and rectangular samples can be used for the tests, provided that the minimum size of the area over which the water pressure is applied is not less than 150 mm. The diameter of the pressurized area is 75 mm. The water pressure can be exerted from above or below. Samples in the process of testing have to remain without any outer coating and the test itself is to be conducted in laboratorial conditions at a temperature of 20 ± 2ºC and air humidity greater than 50%.

17.4.2.2 Procedures for estimating the component of measurement uncertainty resulting from calibration of the data acquisition system (calibration uncertainty)

Not applicable.

This project has received funding from the European Union's Horizon 2020 research and innovation programme under grant agreement No 958171.

17.4.2.3 Requirements for data acquisition depending on measured physical quantity (e.g. based on the variation rate)

Not applicable.

17.4.3 Performance

17.4.3.1 Requirements and recommendations for maintenance during operation (in case of continuous maintenance)

Not applicable.

17.4.3.2 Criteria for the successive surveying campaigns for updating the sensors. The campaigns include: (i) Georeferenced frame, i.e. the global location on the bridge; (ii) Alignment of sensor data, relative alignment of the data collected in a surveying; (iii) Multi-temporal registration to previous campaigns; and (iv) Diagnostics.

Not applicable.

17.4.4 Reporting

An identification of sample should be included in the report, the direction of the supply of water in relation to the formation of the sample (perpendicular or in parallel), date, maximal penetration depth in mm, leak outline/cross section.

17.4.5 Lifespan of the technology

Water penetration test is not used in continuous monitoring.

17.5 Interpretation and validation of results

17.5.1 Expected output (Format, e.g. numbers in a .txt file)

Cross-section of the drenched area of the split sample; the maximum depth of penetration, expressed in mm after different days period.

17.5.2 Interpretation (e.g. each number of the file symbolizes the acceleration of a degree of freedom in the bridge)

Cross section shows the image of dampness for different samples, which can be compared for different concrete classes. Values present the maximum depth of water penetration in concrete samples.
If the water penetration depth is below 50 mm concrete is classified as impermeable and if below 30 mm as impermeable in corrosion conditions (A. M. Neville, Properties of Concrete, 2012).

17.5.3 Validation

17.5.3.1 Specific methods used for validation of results depending on the technique

The water penetration test can be coupled with observation on Scanning Electron Microscope to observe how the penetrated water behave inside the sample.

This project has received funding from the European Union's Horizon 2020 research and innovation programme under grant agreement No 958171.

17.5.3.2 Quantification of the error

The test should be carried out on at least 3 samples to identify and reject any outliers (testing in accordance with the standard on a single sample does not provide such opportunities and may lead to a possible disqualification of a concrete batch that meets the requirements).

17.5.3.3 Quantitative or qualitative evaluation

Both quantitative and qualitative evaluation.

17.5.4 Detection accuracy

The water penetration depth should be detected with accuracy to 1 mm.
Not applicable.

17.6 Advantages

Method can be performed with use of apparatus for testing water permeability with automatic control, which allows testing several samples simultaneously. Possibility of automatic testing in different research cycles as well as pressure reading directly from the pressure gauge, automatic water supply simplifies the procedures.

17.7 Disadvantages

Guidelines for performance of test do not specify precise age of the sample at which the test should begin, nor the cut-off age of concrete that can be tested. This fact indicates on the possibility of different result for this property.

17.8 Possibility of automatising the measurements

On the market there are available fully automatic apparatuses for cubic concrete specimens, where the water permeated through the test specimen is directly collected and measured. Each sample cell includes pressure control manometer and the apparatuses are supplied with an automatic pump.

17.9 Barriers

No specific barriers to be included.

17.10 Existing standards

- EN 12390-8:2019, Testing hardened concrete - Part 8: Depth of penetration of water under pressure
- PN-EN 206+A2:2021-08, Concrete – requirements, properties, production and compliance
- 1.11.3 ASTM C1601 – 11 Standard Test Method for Field Determination of Water Penetration of Masonry Wall Surfaces
- DIN 1048 - Testing concrete; testing of hardened concrete (specimens prepared in mould)

This project has received funding from the European Union's Horizon 2020 research and innovation programme under grant agreement No 958171. © 2021

- DIN 1045-2 - Concrete, reinforced and prestressed concrete structures - Part 2: Concrete - Specification, performance, production and conformity - Application rules for DIN EN 2061.

17.11 Applicability

17.11.1 Relevant knowledge fields

- Industry:
  - control of blasting process,
  - quality control in production of anti-corrosion coatings,
- Civil Engineering:
  - water penetration of masonry wall surfaces.

17.11.2 Performance Indicators

- holes
- loss of section
- rupture
- deformation
- displacement
- cracks
- wire break
- tensioning force deficiency.

17.11.3 Type of structure

- bridges
- curtain walls
- tunnels.

17.11.4 Spatial scales addressed (whole structure vs specific asset elements)

Water penetration test can be useful when used for the samples collected from the places particularly vulnerable to corrosion and chemical attack.

17.11.5 Materials

- concrete
- reinforced concrete
- polymers
- composites
- wood

This project has received funding from the European Union's Horizon 2020 research and innovation programme under grant agreement No 958171.

17.12 Available knowledge

17.12.1 Reference projects

Not reference projects

17.12.2 Other

CONTROL Groups

MATEST Automatic Concrete Permeability Apparatus

17.13 Bibliography

A. M. Neville, T. R. (2012). *Properties of Concrete.* Pearson.

A. M. Neville, T. R. (2012). *Properties of Concrete.* Pearson.

ACI 201.2R-1992. (1994). *Guide to durable concrete, ACI Manual of Concrete Practice Part 1: Materials and General Properties of Concrete.* Detroit, Michigan.

Dany Smyl, F. G.-G. (n.d.). Modelling water absorption .

EN 12390-8:2019. (n.d.). *Testing hardened concrete - Part 8: Depth of penetration of water under pressure*.

G. J. R. Von der Meulen, J. v. (1969). A Permeability - Testing Apparatus for Concrete. *Journal of the PCA Research and Development Laboratories* , 121-123.

Gwizdak, M. (2015). Badanie wodoszczelności betonu – porównanie metod badawczych. *Praca dyplomowa inżynierska*. Poliecthnika Rzeszowska.

I. L. Tyler, B. E. (1961). A Proposed Simple Test Method for Determining the Permeability of Concrete. *Journal of the PCA Research and Development Laboratories*, 2-7.

PN-EN 12390-8:2019-08 . (2019, 08 02). *Concrete tests - Part 8: Penetration depth of water under pressure*.

PN-EN 206+A2:2021-08 . (2021, 08 16). *Concrete - Requirements, properties, production and compliance*.

Ritchie, T. (1974). *Water Penetration Tests of Hollow Brick Walls.*

Young, J. F. (1988). *ACI SP-108: A review of pore structure of cement paste and concrete and its influence on permeability* . Detroit, Michigan .

Z. Kledyński, E. K. (2005). Ocena wodoszczelności betonu studium porównawcze norm polskich i europejskich. Wpływ warunków przygotowania próbek na ocenę wodoszczelności betonu. *Cement Wapno Beton 4*, 215-227.

This project has received funding from the European Union's Horizon 2020 research and innovation programme under grant agreement No 958171.

APPENDIX A18. Water resistance/Absorption test

18.1 Goal(s)

18.1.1 Main objective

Concrete structures are exposed to different weather conditions, soil, water and deicing agents. Crucial contribution to the deterioration processes in bridges or tunnels is assigned to water influence. Water works not only by reacting directly to reinforced concrete structure materials, but mainly by activating the chemicals present in the environment causing chemical reactions to progress. Water resistance measurement test is used as a characterization of durability of concrete elements and durability of the surface protections.

Measurement of water resistance allows to determine the space of pores and absorption rate in the concrete and should not be mistaken with a water penetration test since absorption and permeability values can be uncorrelated with each other.

Method of water absorption is widely used in determination of the effectiveness of hydrophobic surface agents used in securing building materials from the influence of water (Krzywobłocka-Laurów, 2007).

18.2 Description

18.2.1 Functioning mode

In water absorption test, the cut out samples from the structure are dried in an oven for a specified time and temperature (usually 70±5)°C and then placed in a desiccator to cool. Immediately upon cooling the specimens are weighed. The material is then emerged in water at agreed upon conditions, often 23°C for 24 hours. After that time samples are removed, patted dry with a lint free cloth, and weighed. Sorption depends on both the capillary pressure and effective porosity. Capillary pressure is related to the pore size and effective porosity refers to the pore space in the capillary and gel pores. In addition, different pore size leads to different capillary pressure, and capillary pressure of concrete can be calculated by the average pore size (Neville, 2000) (Krzywobłocka-Laurów, 2007).

18.2.2 Types

Water absorption test can be divided in four types:

- in laboratory:
    - internal water absorption observed – sample of concrete is fully submerged into water:

This project has received funding from the European Union's Horizon 2020 research and innovation programme under grant agreement No 958171.

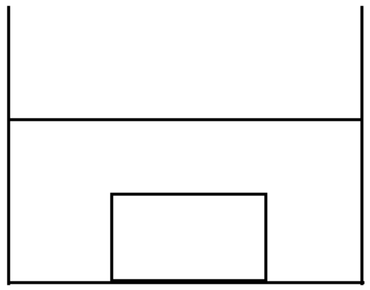

Figure 18.1 – Internal water absorption test

- surface water absorption observed – sample of concrete is placed on the support creating a contact surface with water (ISO 16535:2019-08):

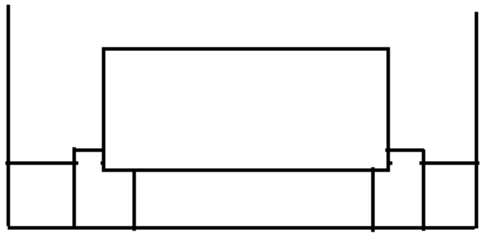

Figure 18.2 – Surface water absorption test

- on-site:
  - measurement of the vertical transport of water and resistance to wind-driven rain penetration with an apparatus mounted on the surface under low pressure:

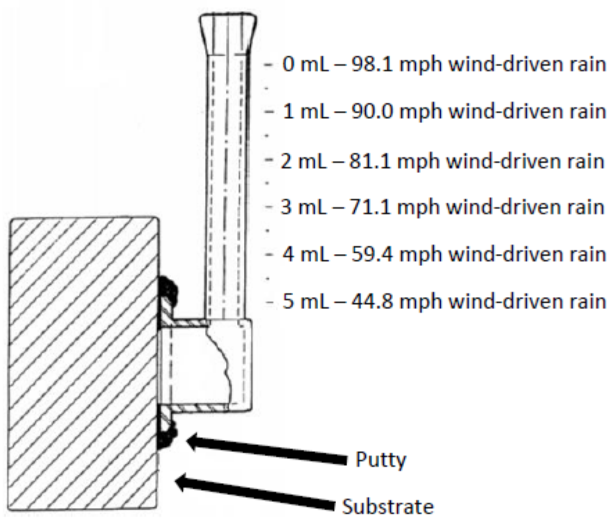

Figure 18.3 – Vertical transport of water (Frances Gale, PROSOCO , 2020)

  - measurement of the horizontal transport of water and resistance to wind-driven rain penetration with an apparatus mounted on the surface under low pressure:

This project has received funding from the European Union's Horizon 2020 research and innovation programme under grant agreement No 958171.

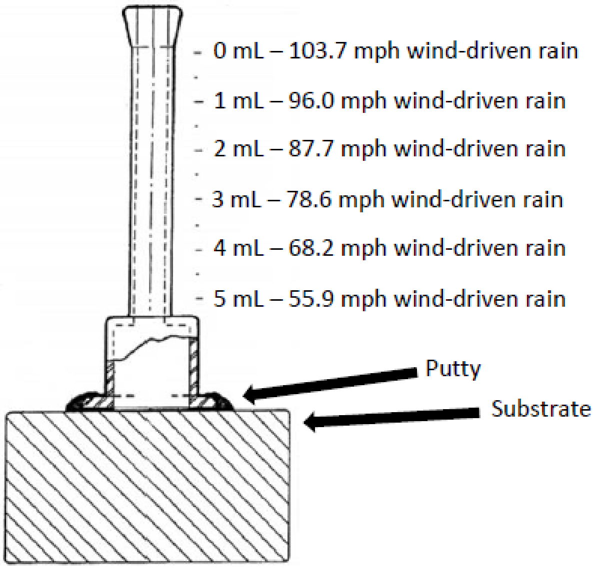

Figure 18.4 – Horizontal transport of water (Frances Gale, PROSOCO , 2020)

18.2.3 Process/event to be detected or monitored

The test is used to detect increase in the mass of a specimen resulting from absorption of water as a function of time when only one surface of the specimen is exposed to water.

In case of on-site measurements the volume of water absorbed by a material within specified time period is detected.

18.2.4 Physical quantity to be measured (e.g. actions, displacements, deformations, dynamic structural properties, material properties including mechanical, electrical and chemical properties, relative displacements of the two sides of a crack, etc.).

Physical quantity measured is an increase of the mass of the sample or volume of water absorbed due to the capillary absorption of water on the surface or through the volume as a function of time.

18.2.5 Induced damage to the structure during the measurement

Damage is induced during initial stage when drilling in the structure to collect the samples.

In – case of on-site measurement no damage is induced or minor damage in process of mounting the measurement tubes.

18.2.6 General characteristics

18.2.6.1 Measurement type (static or dynamic, local or global, short-term or continuous, etc.)

Water absorption testing is a static and local measurement. Used in short-term investigation, which can be repeated in specified intervals of time.

18.2.6.2 Measurement range

Not applicable.

This project has received funding from the European Union's Horizon 2020 research and innovation programme under grant agreement No 958171. © 2021

18.2.6.3 Measurement accuracy

Depends on the balance used for measuring the weight of the sample. Samples should be weighted with 0,01 mm accuracy and their dimensions defined with 1 mm accuracy.

18.3 Background (evolution through the years)

In general the water absorption test has been widely used in different industries and fields such as geology, material sciences, textiles etc. to test rate of absorption of water when the desired properties must be maintained due to different requirements (Parrott, 1992) (S. Kartal, 2007) (International Society for Rock Mechanics. Commission on Standardization of Laboratory and Field Tests. Committee on Laboratory Tests, 1979) (McNeil, Bennett i Leininger, 1963).
In civil engineering most of the works concerning the water absorption test were focused on the effectiveness of the surface protection systems for concrete. In 2000 there was introduced polish norm concerning the products used for thermal insulation, defining the test procedure for determination of the water absorption during long-term immersion (PN-EN 12087:2000, 2021).
Current norm concerning the absorption test was introduced in 2019 - ISO 16535:2019-08, which includes two types of absorption test, equipment and procedures. It is used for thermal insulation products. Two methods are given in this document:
- method 1: Partial immersion;
- method 2: Complete immersion.
Water absorption with prolonged partial immersion is intended to simulate water absorption caused by prolonged exposure to water (ISO 16535:2019-08).

18.4 Performance

18.4.1 General points of attention and requirements

18.4.1.1 Design criteria and requirements for the design of the survey

Depending on the material the samples collected should have different dimensions:

- concrete - cubic samples 100 mm x 100 mm,
- stone – cubic samples 70 mm x 70 mm or 50 mm 50 mm,
- cement-lime – bars 40 mm x 40 mm x 160 mm.

18.4.1.2 Procedures for defining layout of the survey

General survey layout for test performed in laboratory will consist of:

- collection of the sample from the place of interest, depending on the material – choice of the dimensions of the samples,
- drying of the samples and cooling to ambient temperature (20°C),
- measurement of the dimensions of the samples,
- placement of the samples in the cuvette with water an registering the hour,

This project has received funding from the European Union's Horizon 2020 research and innovation programme under grant agreement No 958171. © 2021

- covering the cuvette with foil to avoid evaporation from the samples,
- after specified intervals – removing the samples, delicate drying and weighting directly after taking out,
- inserting the sample again in the cuvette until next weighting period or removal of the sample,
- determination of the mass change and water absorption rate from the formula,
- conclusions.

18.4.1.3 Design constraints (e.g. related to the measurement principles of the monitoring technologies)

To receive reliable results the test should be performed under repeatable and controlled conditions.

18.4.1.4 Sensibility of measurements to environmental conditions

The measurement of water resistance of concrete is performed in a controlled environment, however the conditions to which the whole structure has been subjected during lifetime and therefore the sample drilled out will affect the results. From such factors one can mention: high humidity levels (which leads to pH level increase and temperature inside concrete), leaks, inadequate landscaping grade, poor drainage,

18.4.2 Preparation

18.4.2.1 Procedures for calibration, initialisation, and post-installation verification

Water absorption test does not require any specific calibration process or post-installation verification since there are no electronic devices used, except the balance.

18.4.2.2 Procedures for estimating the component of measurement uncertainty resulting from calibration of the data acquisition system (calibration uncertainty)

No specific procedures. The weight should be calibrated as usual. Samples should be dried to constant weight, which means that the differences between two weighting between 24 h it’s not higher than 0,1% of the weight.

18.4.2.3 Requirements for data acquisition depending on measured physical quantity (e.g. based on the variation rate)

No specific requirements.

18.4.3 Performance

18.4.3.1 Requirements and recommendations for maintenance during operation (in case of continuous maintenance)

Not applicable. In this case no continuous maintenance is required.

18.4.3.2 Criteria for the successive surveying campaigns for updating the sensors. The campaigns include: (i) Georeferenced frame, i.e. the global location on the bridge; (ii) Alignment of sensor data, relative alignment of the data collected in a surveying; (iii) Multi-temporal registration to previous campaigns; and (iv) Diagnostics.

Not applicable.

This project has received funding from the European Union’s Horizon 2020 research and innovation programme under grant agreement No 958171.

18.4.4 Reporting

Example of the report table after water resistance test is shown below:

Sample identification	Dimensions	Concrete composition (if known)	Temperature of drying	Duration of drying	Weight after drying	Soaking time	Weight after soaking	Absorptivity [%]
1								
2								
3								

Table 18-1. Example of the water absorption test report

18.4.5 Lifespan of the technology (if applied for continuous monitoring)

Water resistance test is not used as for continuous monitoring.

18.5 Interpretation and validation of results

18.5.1 Expected output (Format, e.g. numbers in a .txt file)

Final output of the test is the calculated absorption coefficient as a number for an element on the basis of mass of the sample after soaking time.

18.5.2 Interpretation (e.g. each number of the file symbolizes the acceleration of a degree of freedom in the bridge)

Water absorption is expressed as increase in weight in percentage or a volume absorbed.

Percent Water Absorption = [(Wet weight - Dry weight)/ Dry weight] x 100

The lower the absorption, the better the result.

18.5.3 Validation

18.5.3.1 Specific methods used for validation of results depending on the technique

The water resistance test can be coupled with observation on Scanning Electron Microscope.

18.5.3.2 Quantification of the error

Standard deviation methodology can be applied.

18.5.3.3 Quantitative or qualitative evaluation

Both quantitative and qualitative analysis possible. Numerical methods are used for modelling ingress of moisture in concrete, which is essential for quantitative estimation of the service life of concrete structures (D. Smyl, 2016).

18.5.4 Detection accuracy

Accuracy of the absorption level determination is affected by the preparation stage and the accuracy of balance used.

18.6 Advantages

- simple to perform
- no specific qualifications needed for the operator.

This project has received funding from the European Union's Horizon 2020 research and innovation programme under grant agreement No 958171.

- can be performed on-site and in laboratory

18.7 Disadvantages

- does not account for any type of reactive process that ties up water
- assumes that all the weight gain is due to water
- short duration of submersion compared to what might happen in long term conditions.

18.8 Possibility of automatizing the measurements

Water resistance test may be partially automatized in such a manner that samples will be placed and taken out by a programmed equipment and the time of immersion will be designed in automatic software, however full procedure has to be supervised, taking into account the process of collecting the samples and decisions making.

18.9 Barriers

The periods of time designed for the test depends on the porosity of the material under studies.

18.10 Existing standards

- BS 1881: Part 122: 1983 - Method for Determination of Water Absorption.
- ASTM C 642-90, Standard Test Method for Density, Absorption, and Voids in Hardened Concrete.
- PN-EN 772-11:2011 Masonry test methods - Part 11: Determination of water absorption of aggregate concrete, artificial stone and natural stone masonry caused by capillary rise and initial water absorption of ceramic masonry elements.
- PN-EN ISO 16535:2019-08 Thermal insulation products in construction - Determination of water absorption during long-term immersion.
- RILEM Test Method – Test No. 11.4. Measurement of water absorption under low pressure.

18.11 Applicability

18.11.1 Relevant knowledge fields

- Industry:
  - pulp and paper quality control,
  - powder testing,
  - thermal-insulating materials testing,
- Geotechnics:
  - soil absorption testing.

18.11.2 Performance Indicators

- spalling

This project has received funding from the European Union's Horizon 2020 research and innovation programme under grant agreement No 958171.

- cracks.

18.11.3 Type of structure

- pavement slubs,
- curbs
- bricks

18.11.4 Spatial scales addressed (whole structure vs specific asset elements)

There are no specific asset elements for testing. However method is useful in testing bricks, which absorbs water and release air.

18.11.5 Materials

- concrete
- polymer
- aggregate
- paper.

18.12 Available knowledge

18.12.1 Reference projects

Not reference projects.

18.12.2 Other

BOSMAL – water resistance tests

18.13 Bibliography

ASTM C 642-90, Standard Test Method for Density, Absorption, and Voids in Hardened Concrete. (n.d.).

BS 1881: Part 122: 1983 - Method for Determination of Water Absorption. (n.d.).

D. Smyl, F. G.-G. (2016). Modelling water absorption in concrete and mortar with distributed damage . *Cnstruction and Building Materials vol. 125*, pp. 438-449.

Dias, W. (2000). Reduction of concrete sorptivity with age through carbonation. *Cement and Concrete Research vol. 30, no. 8*, pp. 1255-1261.

Frances Gale, PROSOCO . (2020). *RILEM Test Method No.11.4. Measurement of water absorption under low pressure* . Lawrence : RILEM Technical Committee.

G. D. Schutter, K. (2004). Evaluation of water absorption of concrete as a measure for resistance against carbonation and chloride migration. *Materials and Structures vol. 37 no. 273*, pp. 591-596.

Hall, C. (1989). Water sorptivity of mortars and concretes: a review. *Magazine of Concrete Research vol. 41, no. 147*, pp. 51-61.

International Society for Rock Mechanics. Commission on Standardization of Laboratory and Field Tests. Committee on Laboratory Tests. (1979). *Suggested methods for*

This project has received funding from the European Union's Horizon 2020 research and innovation programme under grant agreement No 958171.

determining water content, porosity, density, absorption and related properties and swelling and slake-durability index properties. Pergamon .

ISO 16535:2019-08. (n.d.).

Kelham, S. (1988). A water absorption test for concrete. *Magazine of Concrete Research vol. 40, no. 143*, 106-110.

Krzywobłocka-Laurów, R. (2007). Water reppellent treatment of building products . *Prace Instytutu Techniki Budowlanej vol. 36 no.1*, pp. 17-46.

McNeil, D. W., Bennett, B., & Leininger, R. I. (1963). *MECHANISM OF WATER ABSORPTION IN GLASS REINFORCED PLASTICS.* BATTELLE MEMORIAL INST COLUMBUS OH.

Monteiro, P. K. (2006). *Concrete: Microstructure, Properties and Materials.* NewYork: McGraw-Hill.

Monteiro, P. K. (2014). *Concrete: Microsturcture, Properties and Materials, Chapter 11.5.* McGraw-Hill Education.

Neville, A. M. (2000). *Właściwości betonu.* Kraków: Polski Cement Sp. z o. o.,.

Parrott, L. J. (1992). Water absorption in cover concrete. *Materials and structures*, 284-292.

PN-EN 12087:2000. (2021, 12 13). Retrieved from https://sklep.pkn.pl/pn-en-12087-2000p.html

Reda Taha, M. M.-D. (2001). Sorptivity: a reliable measurement for surface absorption of masonry brick units. *Materials and Structures, RILEM*.

S. Kartal, W. H. (2007, 10 1). Water absorption of boron-treated and heat-modified wood. . *Journal of wood science vol. 53 no. 5*, pp. 454-457.

This project has received funding from the European Union's Horizon 2020 research and innovation programme under grant agreement No 958171.

APPENDIX A19. Weight in Motion Systems (WIM-Systems)

19.1 Goal(s)

19.1.1 Main objective

The infrastructure of bridges can be damaged under loads of vehicles. For this reason Weight in Motion (WIM) systems are utilized for traffic data collection and prevention of the overload of the structures. The vehicles with load above the maximum tolerance contribute to the deterioration of the roads and bridges thus, there is a huge need to control the overload on the infrastructure with accurate scales. On the European Union level, there are no uniform regulations since the technology is quite new, especially for advanced WIM systems measuring during normal traffic flow and not used in every country.

However, there are many attempts on the standardization and analysis of the WIM systems technology, data analysis, legal issues in different countries as can be found in other projects such as the REMOVE project for enforcement or the WAVE project for improving the accuracy and performance of Weigh-in-Motion (WIM) technology (Rooke, 2005) (Bernard Jacob, 2001)

The perspectives of WIM systems technology are giving huge possibilities in global monitoring of the bridge structures with the understanding that uniform standards across the European Union need to be established.

19.2 Description

19.2.1 Functioning Mode

A WIM system implements the process of weighing a moving road vehicle by first measuring the dynamic (varying with time), a vertically-downward component of the tire force from each wheel on the vehicle as the vehicle passes on a smooth road surface over specially-designed sensors. Then, the characteristics of these measured tire forces—along with other measured or calculated parameters such as speed and longitudinal position of the vehicle in the traffic lane are used to estimate the gross-vehicle weight and the portion of that weight carried by each wheel, axle, and axle group of a corresponding static vehicle (P. Burnos J. G., 2007).

WIM systems consist of:

- WIM sensors embedded in the roadway surface or placed under/on the bridge deck for detection of the exceeded weight, classification of the vehicles. Typically used sensors are: bending plates, load cells, quartz piezo sensors, polymer piezo sensors, and strain gauge strip sensors.
- Electronics which are needed for the control of the system functions and to provide vehicles records,

This project has received funding from the European Union's Horizon 2020 research and innovation programme under grant agreement No 958171.

- Infrastructure such as junction boxes, directional bore, cabinet, poles, conduit needed to connect parts of the system,
- Support devices, mainly power supply which can be A/C, solar or wind needed to run the system,
- Software and hardware to process, analyze, format, and report the data collected during the measurements,
- Communication devices including a cellular modem or telephone jacks.

WIM controller is placed on the roadside cabinet for convenient access to the interface.

19.2.2 Types

There are six main types of WIM systems depending on the application and technology:

- Static weighing - the static weighing of road vehicles has an important relationship to WIM. The static weighing results are, in most cases, used as the reference values when testing and calibrating a WIM system. Static weighing systems are in many countries around the world legally approved for direct enforcement or trade applications.
- High-Speed Weight-in-Motion systems – the weighing is carried out in the open traffic lanes at normal speed and under free-flow conditions. The measurements are affected by the vehicle dynamics that depend on a combination of the geometry of the road, the driving behavior of the driver, and the reaction of the vehicle suspension on the influences mentioned previously. More and less accurate systems are also available.
- Low-Speed Weight-in-Motion systems - the weighing takes place in a dedicated controlled area, mostly outside the main traffic lane, on a flat and smooth platform (generally made of concrete) that is longer than 30 m. In the weighing area, the velocity and transverse movement of the passing vehicles are controlled to eliminate the dynamic effects of the vehicle
- Bridge Weight-in-Motion systems - a dynamic weighing system where the sensors are attached to the soffit (bottom side of beams or deck) of a bridge, viaduct, or culvert. The sensors typically measure strains due to the bending of the bridge caused by the passing vehicles. In addition to the same vehicle information as provided by the pavement WIM systems, the B-WIM systems can also collect valuable data about structure behaviour that can be used for safety assessment of the bridge
- Dynamic On-Board WIM (OBW) systems are fitted to vehicles, rather than to the infrastructure. An OBW system will constantly measure the weight, axle, and wheel loads of the vehicle while it is moving. The measured weight data of the moving vehicle may be combined with location (GPS) data and stored. Used to manage heavy vehicle operation and to monitor compliance to access certain parts of the road network.
- Rail Weight-in-Motion systems – the dynamic weighing of rail vehicles to determine the weight of wagons to collect revenue from shipping companies and to ensure any shortfalls or leakage of

This project has received funding from the European Union's Horizon 2020 research and innovation programme under grant agreement No 958171.

goods upon arrival at the depot (European Cooperation in Science and Technology , 1999) (Kwon, 2016).

19.2.3 Process/event to be detected or monitored

The main purpose of the use of WIM monitoring systems for bridges is the detection of overloading of the structure and thus, any induced damages through service-life of the bridge.

19.2.4 Physical quantity to be measured (e.g. actions, displacements, deformations, dynamic structural properties, material properties including mechanical, electrical, and chemical properties, relative displacements of the two sides of a crack, etc.).

The most important physical quantities measured by WIM sensors are:

- weight of the vehicles (estimation)
- axle group loads, axle loads, wheel loads of the passing vehicles
- tire impact forces
- strain forces
- velocity of the vehicles

Process of measurement of dynamic tire forces of a moving vehicle on a road.

19.2.5 Induced damage to the structure during the measurement

No damage is induced during the measurement.

19.2.6 General characteristics

19.2.6.1 Measurement type (static or dynamic, local or global, short-term or continuous, etc.)

WIM systems measurements are dynamic, global, and both short-term or continuous, depending on the target application and purpose.

19.2.6.2 Measurement range

The operating range for each measured parameter is displayed in the WIM display and the test reports. Ranges for temperature, humidity, speed, number of axles per vehicle, axle spacing, vehicle length, axle load, and gross vehicle weight are given, as well as electromagnetic and mechanical conditions.

19.2.6.3 Measurement accuracy

Measurement accuracy is a varying parameter, depending on the type of system used, type of structure for which the system is applied, decisions regarding the choice of the conditions, as well as the type of sensors used and their configuration.

Commercially available WIM system performance (for example - produced by Kistler) has the following specification:

- Gross vehicle weight - +/- 10%
- Velocity - +/- 5%

This project has received funding from the European Union's Horizon 2020 research and innovation programme under grant agreement No 958171.

- Axle distances +/- 10 cm
- Vehicle length +/- 50 cm

19.3 Background (evolution through the years)

WIM systems were invented in 1950 by Clyde Lee. Historically were used mostly for the collection of the large samples of data for vehicle loads – for pavement design. Bending plates were among the first sensors used for weighing. New technologies of WIM sensors were developed such as wire, strip and bar sensors, capacitive, piezo-electric (ceramic, then polymer, and then quartz), and then - fiber optics. Bridge WIM was also introduced in the US in the late 70s and then developed in Europe in the 90s. In 1970 and 1980, data were used for bridge design and bridge assessment, mainly in fatigue, but also to estimate the extreme loads and load effects. WIM data were also used for traffic monitoring and statistics on road freight transport (P. Burnos J. G., 2007) (D. Walker, 2012).

19.4 Performance

19.4.1 General points of attention and requirements

19.4.1.1 Design criteria and requirements for the design of the survey

General requirements for the WIM-System are focused on the road selection, characteristics of the pavement, and environmental conditions. One of the major factors to be considered is the road type and its geometry (longitudinal and transverse slope, radius of curvature). Parts of the road areas that should be avoided such as traffic lights, toll stations in order to register vehicles at the uniform speed on the measurement path. For the bridges there are also additional criteria that have to be considered such as bridge type, span length, traffic intensity and evenness of the pavement before and on the facility. Sensors are crucial elements of the entire measuring system, their properties largely influence the entire weighing system. The most popular sensors for wheel or axle loads of vehicles are: quartz, plate - strain gauge, capacitive and polymer sensors. It has to be noted that sensors have to be used in a range of temperature from – 20°C to + 60°and humidity range from 0 to 90%. Sensors should be resistant to water and salt in areas where snow is present. In case of sensors supported by the pavement their performance is affected by modulus of bituminous pavement, which depends on the temperature as well. This dependence affects directly the lifespan of the sensors as well as accuracy of their responses. Since sensors are mounted on the places where heavy loads are going through, therefore must be resistant to mechanical pressure under crossing vehicles. In cold areas also under vehicles such as snow-clearing devices and studded tires. Installation of the WIM system requires considering additional components such as – electricity supply for sensors and software operation Before deciding to install WIM system it is important to consider additional facilities such as electricity supply for sensors, the communication link to connect station for remote monitoring. For the purposes

This project has received funding from the European Union's Horizon 2020 research and innovation programme under grant agreement No 958171. © 2021

of further maintenance, it is useful to have a parking area close to the system station (Federal Highway Administration (FHWA), McLean, 2012).

19.4.1.2 Procedures for defining the layout of the survey

For example standard test plans to check the accuracy of the system are given in COST 323 Appendix 1. This can be helpful in planning and defining the layout of the survey for future purposes. The main convenient test plan for major WIM systems configurations requires the use of four lorries on the real traffic flow on a given structure. Decisions on the types of vehicles used should be based on the most common types registered in the traffic flow. The procedure consists of 110 runs within one or two consecutive days in the same environmental conditions (temperature, humidity, etc.). The runs can be also split for different loads – full and half loaded concerning proportions in traffic flow. Test plan level of confidence is fixed at 95%. Additionally, after 110 runs there are performed at least six abnormal runs for purpose of detection of any unexpected responses. The reference weights of the vehicles passed by are assessed in comparison with static weights registered.

19.4.1.3 Design constraints (e.g. related to the measurement principles of the monitoring technologies)

Bridge WIM Systems can be applied to the great majority of bridges, as long as the distance between the two furthest points that affect the measurement is less than 40 m.

19.4.1.4 Sensibility of the measurements to environmental conditions

Measurements are sensitive to pavement surface temperature, air temperature, humidity, wind direction, precipitation intensity. The most important factor is the temperature, which directly affects parameters such as vertical deflection and stiffness modulus and influence the accuracy of weighting results. Other conditions include: direction and strength of the wind, the icing on the road surface, water film. (P. Burnos J. G., 2021)

As a result WIM systems may be subjected to uncontrolled changes, affected by various climatic conditions.

19.4.2 Preparation

19.4.2.1 Procedures for calibration, initialization, and post-installation verification

There are at least four calibration methods depending on the sensor used and measured quantity.

- First method is a static calibration used for sensors such as piezo quartz crystal bars and fibre optics sensors and is suitable for low-speed WIM systems with good quality pavement sites when weight measurements will be carried out. Calibration masses of various intensities are placed on the scale, in this case, sensor and the relation between them and the system measurement is established. For Bridge-WIM systems there should be used additionally a two or three axle rigid lorry, which has to be weighed – empty and full. If more lorries are used, the accuracy can be improved.

This project has received funding from the European Union's Horizon 2020 research and innovation programme under grant agreement No 958171.

- Another procedure requires use of shock or pressure variation devices such as a Falling Weight Deflectometer or a Piezodyn. In this case calibration is not dependent on the pavement profile, speed, load or calibration vehicle characteristics. However the traffic lane has to be closed during the calibration which is a problem on highways or bridges with high traffic flow. On the other hand, this procedure can be used when WIM system is configured for measurement of the impact forces only.
- Third method require use of pre-weighed calibration lorries for measurement of the instantaneous axle impact forces. This is the most common, simple and direct calibration path for all kinds of WIM Systems. Consists of series of measurements along the WIM system with pre-weighed vehicles, performed for few days with repeatable environmental conditions – homogenous temperature and climate conditions. Traffic flow does not have to be stopped in this case.
- Another method requires use of instrumented calibration lorries for measurement of the instantaneous axle impact forces. Especially convenient for the multiple sensor arrays. The main issue of this type of calibration is the cost of the instrumented lorries and also the need to have skilled technicians on the site with specific knowledge on the operating mode. Method base on the fitting of WIM records to on-board measured impact forces for the same axis or wheel with at least three load cases, different speed levels, repeated subsequently (Kwon, 2016).

It is also possible to perform automatic self-calibration by fitting statistics recorded and computed by WIM System to target values. The procedure of self-calibration is usually designed by the supplier of the system so details depends on the equipment used and configuration of the systems. This type of calibration should be agreed with the supplier prior to the initial set-up and well documented for future reference.

Initialisation of the system should be performed by the manufacturer, prior to the tests based on the agreement between user and supplier. Usually initial test for High Speed WIM Systems consist of eight runs at different speeds, for example:

- 4 runs at 75km/h (average target vehicle velocity)
- 2 runs at 60km/h
- 2 runs at 90 km/h

19.4.2.2 Procedures for estimating the component of measurement uncertainty resulting from calibration of the data acquisition system (calibration uncertainty)

The calibration is the basis for the verification, the process of checking if the performance of a measurement system lies within its specifications or not, and the adjustment of the system, by means of varying the offset and/or the gain in the software, in order to keep the performance within the specification.

This project has received funding from the European Union's Horizon 2020 research and innovation programme under grant agreement No 958171.

19.4.2.3 Requirements for data acquisition depending on measured physical quantity (e.g. based on the variation rate)

Not applicable.

19.4.3 Performance

19.4.3.1 Requirements and recommendations for maintenance during operation (in case of continuous maintenance)

Mainly there are three processes to be performed during the service-life of the WIM systems. The sensors and the pavement surrounding the sensors should be visually inspected, without interference in the traffic flow, to find any external damages and prevent further internal deterioration in specified intervals of time. Sensors maintenance depends on the type and configuration used, however any moving parts that can be covered with dust or other dirt should be also checked and cleaned. Calibration has to be repeated in specified periods of time and compared with the data obtained during first documented, initial calibration. Also in case of any discrepancies or suspicious responses registered at any given time to make adjustments to the system. Another important issue is the data quality control, mainly consisting of checks over stability of the system parts, electronics as well as reliability and reproducibility of the results.

19.4.4 Reporting

Recorded data are considered for further analysis. In reports there are marked any abnormal runs with a validation codes given by the system.

Standard report include:

- system manufacturer,
- period of test,
- date and time,
- test conditions,
- location,
- lane number,
- number of test vehicles,
- vehicle types,
- velocity [km/h],
- the gross weight, axle loads by axle rank or group of axle loads measured in motion,
- static references values of these weights and loads.

This project has received funding from the European Union's Horizon 2020 research and innovation programme under grant agreement No 958171.

19.4.5 Lifespan of the technology

No reliable information on the average performance of the bridge WIM Systems at the moment can be provided. WIM systems offer continuous monitoring for at least 7 years when properly maintained/calibrated.

19.5 Interpretation and validation of results

19.5.1 Expected output (Format, e.g. numbers in a .txt file)

Data are displayed on the interface of WIM System or in a form of report when exported. Thus expected output consist of:

- gross vehicle weight,
- axle group loads, axle loads, wheel loads of the passing vehicles,
- vehicle record (depending on the system configuration and application), consisting of: identification (registration) number, date and time
- location: road number, direction, traffic lane,
- number of axles and axle distances,
- total vehicle length and/or wheel base,
- vehicle classification,
- vehicle speed.

For some configurations of the system also additional data can be exported:

- single/double tyre detection
- lateral position of the vehicle
- tyre pressure distribution
- calibration coefficient of the WIM sensors
- error code (to validate or eliminate measurements)

If the system is connected with other sensors or devices output will also include:

- height/width of the vehicle
- overview picture of the vehicle
- picture of the licence plate or registration number
- picture of dangerous goods identification shield
- code of dangerous goods shield
- temperature of the pavement or bridge, at one or several locations;
- deflection of the pavement

This project has received funding from the European Union's Horizon 2020 research and innovation programme under grant agreement No 958171.

19.5.2 Interpretation (e.g. each number of the file symbolizes the acceleration of a degree of freedom in the bridge)

Test results are analysed with accordance to the COST323 specification. For gross vehicle weights there are defined probabilities of lying within a percentage range of static values. Estimated weights are then used to check which accuracy class has been achieved and whether it meets the weighting criteria for a given road. Data collected in short period of time, for instance in hours are used for real time traffic information and management, while data collected through weeks/years are used for maintenance of the roads or bridges, statistics and operation.

19.5.3 Validation

19.5.3.1 Specific methods used for validation of results depending on the technique

No specific guidelines – validation of the results can be performed for example by designed for this purpose Excel workbooks, which are compliant with ASTM E 1318-09. Specification of this files is given on the website of International Society of Weight in Motion. However this approach should be treated only as a recommendation, not as a standard methodology. Third party software to automate and perform data validation checks.

19.5.3.2 Quantification of the error

The relative error with respect to the weights and static loads are calculated for each measurement of the different sub-populations in following manner:

$$\frac{W_{measured(dynamic)} - W_{reference(static)}}{W_{reference(static)}}$$

Mean and standard deviation of the relative error is calculated with standard mathematical methods.

19.5.3.3 Quantitative or qualitative evaluation

Both quantitative and qualitative evaluation can be performed. Evaluation of the tolerances and accuracy class of the tested data can be done with analytical formulas such as parabolic linear or tri-linear formula.

19.5.4 Detection accuracy

To achieve the highest weighing accuracy sensors should be installed on the road of the best category. The accuracy is referred to the static loads and weights mostly, for impact forces applied by the wheels/axles on the pavement and sensors. There are specified several accuracy classes, predefined for weight estimations by WIM systems. These classes are fully presented in the standard COST 323. Accuracy is affected by the calibration process in the initial phase and during service life and should not be assessed on the aggregated data. Specific tolerances are given for a load from:

- single axle,
- group of axles.

This project has received funding from the European Union's Horizon 2020 research and innovation programme under grant agreement No 958171. © 2021

For bridge WIM systems accuracy tolerances specified for a group of axles in the COST 323 are not applicable. Accuracy classes mentioned in the European WIM Specification are derived by a statistical approach explained further in Appendix 1 paragraph 8.2 and applied for most of the WIM systems with specified confidence intervals.

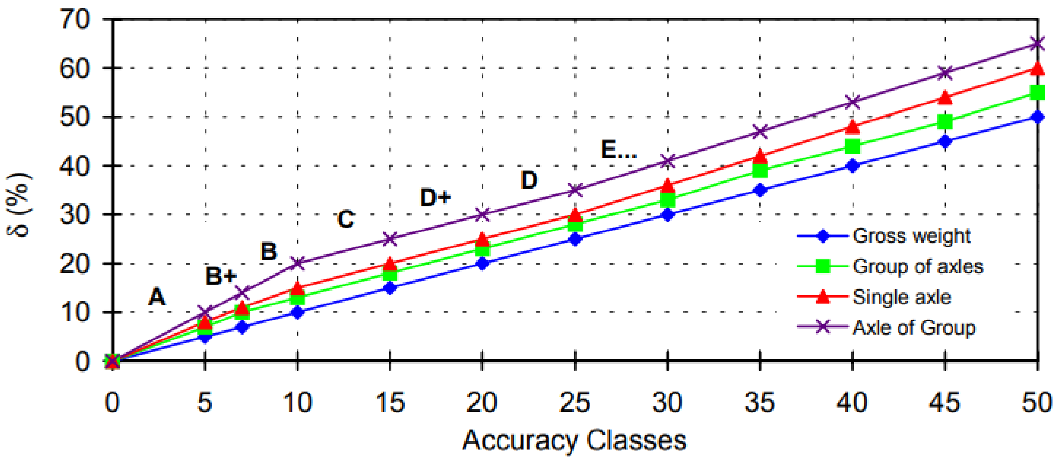

Figure 19.1 – Accuracy class tolerances according to COST 323

Accuracy levels depend on the requirements, depending on the applicability, for instance for legal purposes 90-95% will be required, while for infrastructure on the level 80-90%. However, accuracy levels can be adjusted depending on the final user's needs.

19.6 Advantages

- Automated non-stop traffic data collection
- Optimized infrastructure and maintenance planning
- Tracking of special transports
- Reliable calculation of remaining bridge lifetime:
- Reduced risk: early detection and continuous monitoring of critical structures
- Longer bridge lifetimes: overloaded vehicles are prevented from crossing the bridge
- Improved traffic safety
- Structural health monitoring: monitoring changes in a bridge's structural behavior - faults are detected at an early stage

19.7 Disadvantages

- Lack of standardization
- Costs of the equipment,
- Costs of the maintenance of the system
- Legal issues

This project has received funding from the European Union's Horizon 2020 research and innovation programme under grant agreement No 958171. © 2021

- Depending on the systems – problems generated with the closing of the traffic flow

19.8 Possibility of automatising the measurements

WIM Systems are complex monitoring systems, which already work in an automatized manners. In Germany, in 2000-2002 there was finalized European Union project on the topic of: Technologies for Optimising the Precision of MS-WIM of Road Transports to Improve Overload Control and European Procedures for Enforcement, which aimed in improvement of the technologies for higher traffic safety (Cordis Europa , 2002). Future considerations of the development of WIM Systems mostly include use of new technologies and increase of the accuracy of existing systems,

19.9 Barriers

The main barrier in the application of WIM systems is the lack of standardization and uniformity in traffic management solutions across the European Union and the availability of the technology in different countries. Throughout the European Union, there is a high level of disparity in how the issue of overloading is dealt with, both in terms of the legal basis, enforcement, and technical and functional applications. Incidental use of WiM technology currently in the EU is another operational barrier as well as issues regarding acceptance by the Road Transport Industry in different countries.

19.10 Existing standards

- COST 323 Post-proceedings of the Second European Conference on weigh-in-motion of road vehicles, Lisbon, 14th to 16th September 1998.
- ASTM E1318-09 Standard Specification for Highway Weigh-In-Motion (WIM) Systems with User Requirements and Test Methods is a primary WIM standard.
- ASTM E867 - 06(2020) Standard Terminology Relating to Vehicle-Pavement Systems
- NMi International WIM Standard: Specification and Test Procedures for Weigh-in-Motion Systems, NMi Certin, Dordrecht, Netherlands, 2016.
- The OIML R-134 [OIML, 2004] from the International Organisation for Legal Metrology, the recommendation for ‘Automatic Instruments for weighing road vehicles in motion’ for use in enforcement for low-speed weighing.

19.11 Applicability

19.11.1 Relevant knowledge fields

WIM systems technology is used for specific applications:

- statistic in traffic loading – planning and design of future road networks,
- analysis of transport flows,
- collection of evidence for Government policy,
- achievement of compliance with loading regulations

This project has received funding from the European Union’s Horizon 2020 research and innovation programme under grant agreement No 958171. © 2021

- tolling by weight – fair toll prices
- industrial applications at ports and logistic centers,
- rail track and maintenance.

19.11.2 Performance Indicators

- overloading

19.11.3 Type of structure

- bridge
- railway
- road

19.11.4 Spatial scales addressed (whole structure vs specific asset elements)

WIM systems are designed for whole structure monitoring such as bridges, highways, motorways, or railways.

19.11.5 Materials

- concrete,
- steel.

19.12 Available knowledge

19.12.1 Reference projects

WAVE project:

- WAVE (2001a), Multiple sensor WIM, Report of Work Package 1.1, WAVE, ed. D. Cebon, University of Cambridge.
- WAVE (2001b), Bridge WIM, Report of Work Package 1.2, WAVE, ed. E.J. O'Brien, University College Dublin.
- WAVE (2001c), A Data Quality Assurance System for the European WIM Database, Report of Work Package 2, WAVE, ed. R. Henny, Rijkswaterstraat, Delft.
- WAVE (2001d), Durability of WIM system in cold climates, Report of Work Package 3.1, WAVE, ed. B. Hallström, SNRA, Borlange.
- WAVE (2001e), Calibration of WIM systems, Report of Work Package 3.2, WAVE, ed. M. Huhtala, VTT, Helsinki.
- WAVE (2001f), Fibre Optic WIM systems, Report of Work Package 4, WAVE, ed. J-M.Caussignac, LCPC, Paris.

REMOVE project: (Rooke, 2005)

- REMOVE: Final Report
- REMOVE: Application Terms utilized in Vehicle Weighing

This project has received funding from the European Union's Horizon 2020 research and innovation programme under grant agreement No 958171. © 2021

- REMOVE: WP4 - Cost Benefit Analysis
- REMOVE: WP3 - Future Enforcement Strategy
- REMOVE: WP2 - Technical Issues
- REMOVE: WP1 - Legal Issues

BRIDGEMON PROJECT: (Cordis Europa , 2015)

- WP1 – Improved Bridge-WIM algorithms
- WP2 - General Overview
- WP3 - Structural Health Monitoring of Railway Bridges

TOP TRIAL: (Cordis Europa , 2002)

- Milestones:

  - Realisation, operation and evaluation of WIM trial
  - Improvement of accuracy of truck load measurement
  - Recommendation for European code of praxis for enforcement

  Major milestones will be:

  MS1: Trial concept and specification

  MS2: Pre algorithms, test site hand-over, press conference, web page

  MS 3: Information exchange platform, workshop

  MS 4: End of trial period, accuracy improvement and evaluation report, CBA report, draft code of practice for enforcement

  MS 5: WIM enforcement workshop, video, project finalisation, final report

19.12.2 Other

Manufacturers websites:

KISTLER

CROSS-TRAFIC

CAMEA

INTERCOMP

International Society for Weight in Motion in Switzerland:

ISWIM

European Roads Police Network:

TISPOL/ROADPOL

19.13 Bibliography

This project has received funding from the European Union's Horizon 2020 research and innovation programme under grant agreement No 958171.

Bernard Jacob, E. O. (2001). *WAVE - Weight-in-Motion of Axles and Vehicles for Europe project Executive Summary* . Cambridge, Helsinki, Delft, Dublin, Borlange, Paris: European RTD project RO-96-SC, 403.

Burnos P., G. J. (2011). Road traffic parameters measuring system with variable structure. *Metrology and Measurement Systems vol. 18 no 4* , 659-666.

Cordis Europa . (2002). *Technologies for Optimising the Precision of MS-WIM of Road Transports to Improve Automatic Overload Control and European Procedures for Enforcement*. Retrieved from https://cordis.europa.eu/project/id/IST-1999-20868/de

Cordis Europa . (2015, August 11). *Final Report Summary - BRIDGEMON*. Retrieved from Cordis Europa : https://cordis.europa.eu/project/id/315629/reporting/it

D. Walker, O. S. (2012). Findings from LTPP SPS WIM Systems Validation Study. *Proceedings of the 6th International Conference on Weight-in-Motion* . Dallas, Texas : International Society for Weigh-In-Motion.

European Cooperation in Science and Technology . (1999). *COST Action 323: Weight-in-Motion of Road Vehicles* . Paris : European Cooperation in Science and Technology .

Federal Highway Administration (FHWA), McLean. (2012). *LTPP Field Operations Guide for SPS WIM Sites Version 1.0. Draft.* Federal Highway Administration.

Kwon, T. M. (2016). *Weight-Pad- Based Portable Weight-in-Motion System User Manual. Report No. MN/RC 2016-07.* . Duluth : University of Minnesota .

Ossowski R. L., B. P. (2015). Weighing vehicles in motion. The present state and prospects of wigh in Motion systems application for law enforcement . *Metrology and Measurement Systems vol. 1*, 40-45.

P. Burnos, J. G. (2007). Accurate weighing of moving vehicles . *Metrology and Measurement Systems vol. 14 no 4* , 508-516.

P. Burnos, J. G. (2007). Measurements of Road Traffic Parameters Using Inductive Loops and Piezoelectric Sensors. *Metrology and Measurement Systems vol. 14, no 2* , 187-203.

P. Burnos, J. G. (2021). High Accuracy Weigh-In-Motion Systems for Direct Enforcement . *Sensors 21 (8046).*

P., B. (2014). Weighing vehicles in motion, Part 3: Pressure sensors applied in Weigh in Motion (WIM) systems. *Drogownictwo 9*, pp. 275-279.

Rooke, A. (2005). *PROJECT REMOVE Final Report.* European Comission: TREN-03-ST-S07.30766.

This project has received funding from the European Union's Horizon 2020 research and innovation programme under grant agreement No 958171.